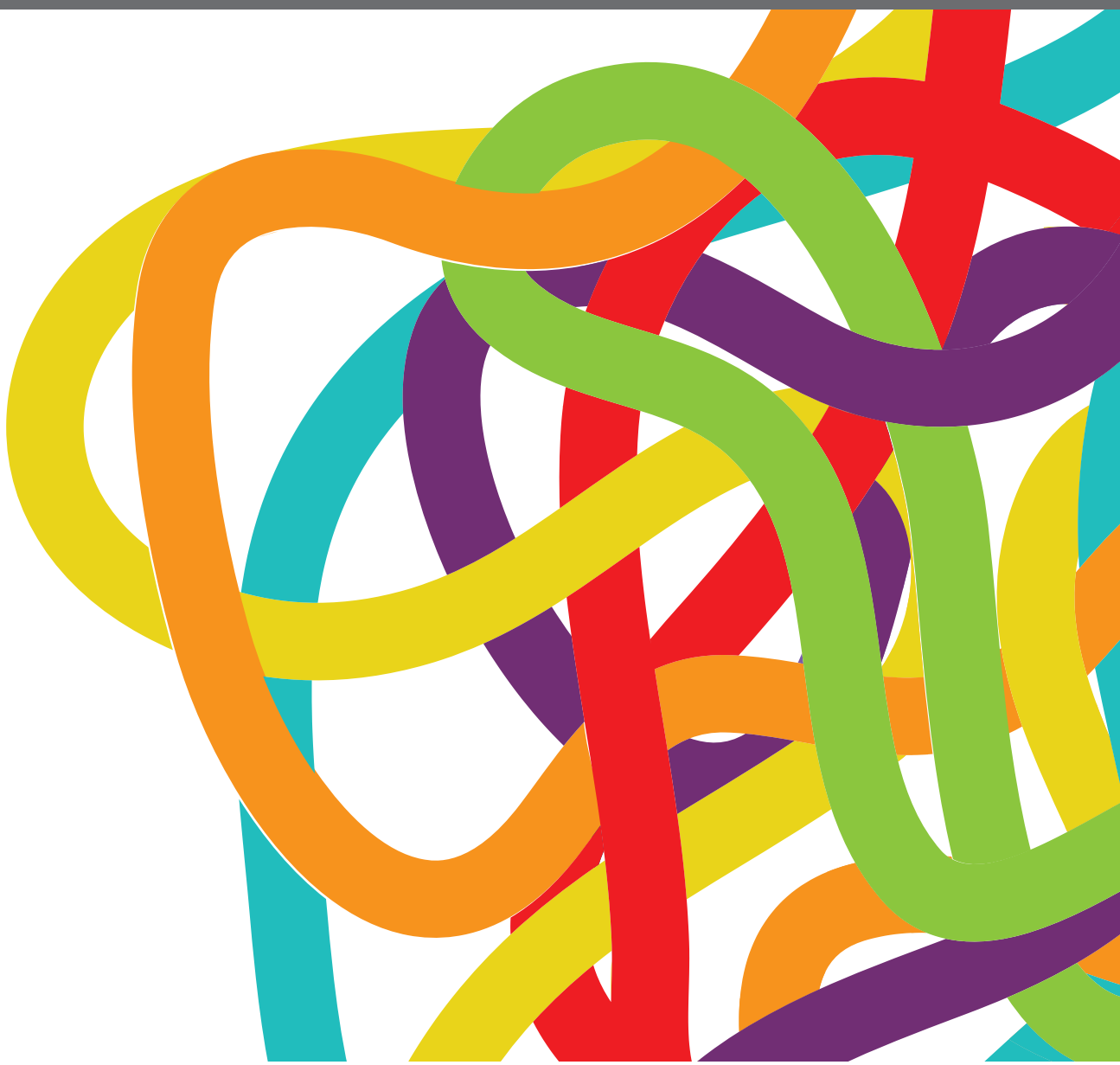
WOMEN IN SKIN CANCER: 2021

EDITED BY: Sapna Patel
PUBLISHED IN: Frontiers in Oncology



frontiers Research Topics

Frontiers eBook Copyright Statement

The copyright in the text of individual articles in this eBook is the property of their respective authors or their respective institutions or funders. The copyright in graphics and images within each article may be subject to copyright of other parties. In both cases this is subject to a license granted to Frontiers.

The compilation of articles constituting this eBook is the property of Frontiers.

Each article within this eBook, and the eBook itself, are published under the most recent version of the Creative Commons CC-BY licence. The version current at the date of publication of this eBook is CC-BY 4.0. If the CC-BY licence is updated, the licence granted by Frontiers is automatically updated to the new version.

When exercising any right under the CC-BY licence, Frontiers must be attributed as the original publisher of the article or eBook, as applicable.

Authors have the responsibility of ensuring that any graphics or other materials which are the property of others may be included in the CC-BY licence, but this should be checked before relying on the CC-BY licence to reproduce those materials. Any copyright notices relating to those materials must be complied with.

Copyright and source acknowledgement notices may not be removed and must be displayed in any copy, derivative work or partial copy which includes the elements in question.

All copyright, and all rights therein, are protected by national and international copyright laws. The above represents a summary only. For further information please read Frontiers' Conditions for Website Use and Copyright Statement, and the applicable CC-BY licence.

ISSN 1664-8714
ISBN 978-2-83250-870-1
DOI 10.3389/978-2-83250-870-1

About Frontiers

Frontiers is more than just an open-access publisher of scholarly articles: it is a pioneering approach to the world of academia, radically improving the way scholarly research is managed. The grand vision of Frontiers is a world where all people have an equal opportunity to seek, share and generate knowledge. Frontiers provides immediate and permanent online open access to all its publications, but this alone is not enough to realize our grand goals.

Frontiers Journal Series

The Frontiers Journal Series is a multi-tier and interdisciplinary set of open-access, online journals, promising a paradigm shift from the current review, selection and dissemination processes in academic publishing. All Frontiers journals are driven by researchers for researchers; therefore, they constitute a service to the scholarly community. At the same time, the Frontiers Journal Series operates on a revolutionary invention, the tiered publishing system, initially addressing specific communities of scholars, and gradually climbing up to broader public understanding, thus serving the interests of the lay society, too.

Dedication to Quality

Each Frontiers article is a landmark of the highest quality, thanks to genuinely collaborative interactions between authors and review editors, who include some of the world's best academicians. Research must be certified by peers before entering a stream of knowledge that may eventually reach the public - and shape society; therefore, Frontiers only applies the most rigorous and unbiased reviews.
Frontiers revolutionizes research publishing by freely delivering the most outstanding research, evaluated with no bias from both the academic and social point of view. By applying the most advanced information technologies, Frontiers is catapulting scholarly publishing into a new generation.

What are Frontiers Research Topics?

Frontiers Research Topics are very popular trademarks of the Frontiers Journals Series: they are collections of at least ten articles, all centered on a particular subject. With their unique mix of varied contributions from Original Research to Review Articles, Frontiers Research Topics unify the most influential researchers, the latest key findings and historical advances in a hot research area! Find out more on how to host your own Frontiers Research Topic or contribute to one as an author by contacting the Frontiers Editorial Office: frontiersin.org/about/contact

WOMEN IN SKIN CANCER: 2021

Topic Editor:
Sapna Patel, University of Texas MD Anderson Cancer Center, United States

Citation: Patel, S., ed. (2022). Women in Skin Cancer: 2021.
Lausanne: Frontiers Media SA. doi: 10.3389/978-2-83250-870-1

Table of Contents

06 ***An Immunometabolic Shift Modulates Cytotoxic Lymphocyte Activation During Melanoma Progression in TRPA1 Channel Null Mice***
Maria Fernanda Forni, Omar Alberto Domínguez-Amorocho, Leonardo Vinícius Monteiro de Assis, Gabriela Sarti Kinker, Maria Nathalia Moraes, Ana Maria de Lauro Castrucci and Niels Olsen Saraiva Câmara

20 ***Early Exanthema Upon Vemurafenib Plus Cobimetinib Is Associated With a Favorable Treatment Outcome in Metastatic Melanoma: A Retrospective Multicenter DeCOG Study***
Katharina C. Kähler, Ralf Gutzmer, Friedegrund Meier, Lisa Zimmer, Markus Heppt, Anja Gesierich, Kai-Martin Thoms, Jochen Utikal, Jessica C. Hassel, Carmen Loquai, Claudia Pföhler, Lucie Heinzerling, Martin Kaatz, Daniela Göppner, Annette Pflugfelder, Ann-Sophie Bohne, Imke Satzger, Lydia Reinhardt, Jan-Malte Placke, Dirk Schadendorf and Selma Ugurel

31 ***PI3K Promotes Basal Cell Carcinoma Growth Through Kinase-Induced p21 Degradation***
Rachel Y. Chow, Ung Seop Jeon, Taylor M. Levee, Gurleen Kaur, Daniel P. Cedeno, Linda T. Doan and Scott X. Atwood

41 ***Real Life Clinical Management and Survival in Advanced Cutaneous Melanoma: The Italian Clinical National Melanoma Registry Experience***
Anna Crispo, Maria Teresa Corradin, Erika Giulioni, Antonella Vecchiato, Paolo Del Fiore, Paola Queirolo, Francesco Spagnolo, Vito Vanella, Corrado Caracò, Giulio Tosti, Elisabetta Pennacchioli, Giuseppe Giudice, Eleonora Nacchiero, Pietro Quaglino, Simone Ribero, Monica Giordano, Desire Marussi, Stefania Barruscotti, Michele Guida, Vincenzo De Giorgi, Marcella Occelli, Federica Grosso, Giuseppe Cairo, Alessandro Gatti, Daniela Massa, Laura Atzori, Nicola Calvani, Tommaso Fabrizio, Giuseppe Mastrangelo, Federica Toffolutti, Egidio Celentano, Mario Budroni, Sara Gandini, Carlo Riccardo Rossi, Alessandro Testori, Giuseppe Palmieri, Paolo A. Ascierto and the Clinical National Melanoma Registry Study Group at the Italian Melanoma Intergroup

50 ***Overall Survival of Patients With Unresectable or Metastatic BRAF V600-Mutant Acral/Cutaneous Melanoma Administered Dabrafenib Plus Trametinib: Long-Term Follow-Up of a Multicenter, Single-Arm Phase IIa Trial***
Lili Mao, Ya Ding, Xue Bai, Xinan Sheng, Jie Dai, Zhihong Chi, Chuanliang Cui, Yan Kong, Yun Fan, Yanjun Xu, Xuan Wang, Bixia Tang, Bin Lian, Xieqiao Yan, Siming Li, Li Zhou, Xiaoting Wei, Caili Li, Jun Guo, Xiaoshi Zhang and Lu Si

59 ***Prognostic and Clinicopathological Value of Ki-67 in Melanoma: A Meta-Analysis***
Qixin Liu, Ziheng Peng, Liangfang Shen and Lin Shen

67 ***Digital Quantification of Tumor PD-L1 Predicts Outcome of PD-1-Based Immune Checkpoint Therapy in Metastatic Melanoma***
Jan-Malte Placke, Camille Soun, Jenny Bottek, Rudolf Herbst, Patrick Terheyden, Jochen Utikal, Claudia Pföhler, Jens Ulrich, Alexander Kreuter, Christiane Pfeiffer, Peter Mohr, Ralf Gutzmer, Friedegund Meier, Edgar Dippel, Michael Weichenthal, Lisa Zimmer, Elisabeth Livingstone, Jürgen C. Becker, Georg Lodde, Antje Sucker, Klaus Griewank, Susanne Horn, Eva Hadaschik, Alexander Roesch, Dirk Schadendorf, Daniel Robert Engel and Selma Ugurel

78 ***Grade 4 Neutropenia Secondary to Immune Checkpoint Inhibition — A Descriptive Observational Retrospective Multicenter Analysis***
Anne Zaremba, Rafaela Kramer, Viola De Temple, Stefanie Bertram, Martin Salzmann, Anja Gesierich, Lydia Reinhardt, Barouyr Baroudjian, Michael M. Sachse, Gunhild Mechtersheimer, Douglas B. Johnson, Alison M. Weppler, Lavinia Spain, Carmen Loquai, Milena Dudda, Claudia Pföhler, Adriana Hepner, Georgina V. Long, Alexander M. Menzies, Matteo S. Carlino, Céleste Lebbé, Tomohiro Enokida, Makoto Tahara, Paul J. Bröckelmann, Thomas Eigentler, Katharina C. Kähler, Ralf Gutzmer, Carola Berking, Selma Ugurel, Nadine Stadtler, Antje Sucker, Jürgen C. Becker, Elisabeth Livingstone, Friedegund Meier, Jessica C. Hassel, Dirk Schadendorf, Maher Hanoun, Lucie Heinzerling and Lisa Zimmer

91 ***Prognosis for Cutaneous Melanoma by Clinical and Pathological Profile: A Population-Based Study***
Alessandra Buja, Andrea Bardin, Giovanni Damiani, Manuel Zorzi, Chiara De Toni, Riccardo Fusinato, Romina Spina, Antonella Vecchiato, Paolo Del Fiore, Simone Mocellin, Vincenzo Baldo, Massimo Rugge and Carlo Riccardo Rossi

99 ***Profile of Basal Cell Carcinoma Mutations and Copy Number Alterations - Focus on Gene-Associated Noncoding Variants***
Paulina Maria Nawrocka, Paulina Galka-Marciniak, Martyna Olga Urbanek-Trzeciak, Ilamathi M-Thirusenthilarasan, Natalia Szostak, Anna Philips, Laura Susok, Michael Sand and Piotr Kozlowski

119 ***Predictive Performance of Serum S100B* Versus *LDH in Melanoma Patients: A Systematic Review and Meta-Analysis***
Eszter Anna Janka, Tünde Várvölgyi, Zoltán Sipos, Alexandra Soós, Péter Hegyi, Szabolcs Kiss, Fanni Dembrovszky, Dezső Csupor, Patrik Kéringer, Dániel Pécsi, Margit Solymár and Gabriella Emri

130 ***Immune Checkpoint Inhibitor Induced Pericarditis and Encephalitis in a Patient Treated With Ipilimumab and Nivolumab for Metastatic Melanoma: A Case Report and Review of the Literature***
Jorja Braden and Jenny H. Lee

134 ***Vitamin D Enhances Anticancer Properties of Cediranib, a VEGFR Inhibitor, by Modulation of VEGFR2 Expression in Melanoma Cells***
Anna Piotrowska, Fernando Pereira Beserra, Justyna Marta Wierzbicka, Joanna Irena Nowak and Michał Aleksander Żmijewski

148 ***Predictive Values of Pathological and Clinical Risk Factors for Positivity of Sentinel Lymph Node Biopsy in Thin Melanoma: A Systematic Review and Meta-Analysis***
Hanzi Huang, Ziyao Fu, Jiang Ji, Jiuzuo Huang and Xiao Long

158 ***Immune Checkpoint Inhibitor-Induced Hypophysitis and Patterns of Loss of Pituitary Function***
Shlomit Jessel, Sarah A. Weiss, Matthew Austin, Amit Mahajan, Katrina Etts, Lin Zhang, Lilach Aizenbud, Ana Luisa Perdigoto, Michael Hurwitz, Mario Sznol, Kevan C. Herold and Harriet M. Kluger

168 ***Non-Melanoma Skin Cancers and Other Cutaneous Manifestations in Bone Marrow Failure Syndromes and Rare DNA Repair Disorders***
Jennie Vagher, Amanda Gammon, Wendy Kohlmann and Joanne Jeter

184 ***Considerations for Germline Testing in Melanoma: Updates in Behavioral Change and Pancreatic Surveillance for Carriers of* CDKN2A *Pathogenic Variants***
Kristen Pauley, Ambreen Khan, Wendy Kohlmann and Joanne Jeter

191 ***Second Primary Malignancies in Patients With Melanoma Subtypes: Analysis of 120,299 Patients From the SEER Database (2000-2016)***
Asad Loya, Dan S. Gombos and Sapna P. Patel

200 ***Case Report: Delayed Onset Multi-Organ Toxicities in a Melanoma Patient Achieving Complete Response to BRAF/MEK Inhibition***
Hannah M. Knochelmann, Michael Brandon Ware, Aditya Rali, Susanne Linderman, Jessica G. Shantha, David H. Lawson, Melinda Yushak, Robert Swerlick, Chrystal M. Paulos, Steven Yeh and Ragini Kudchadkar

209 ***Cancer Progression Gene Expression Profiling Identifies the Urokinase Plasminogen Activator Receptor as a Biomarker of Metastasis in Cutaneous Squamous Cell Carcinoma***
Elahe Minaei, Simon A. Mueller, Bruce Ashford, Amarinder Singh Thind, Jenny Mitchell, Jay R. Perry, Benjamin Genenger, Jonathan R. Clark, Ruta Gupta and Marie Ranson

225 ***Outcomes From Cytotoxic Chemotherapy Following Progression on Immunotherapy in Metastatic Melanoma: An Institutional Case-Series***
Elizabeth M. Gaughan and Bethany J. Horton

231 ***Neurotropic Cutaneous Malignancies: Case Report on Keratinocyte Derived Malignancies of the Head and Neck With Perineural Invasion***
Grace Sora Ahn, Brian Hinds, Frederic Kolb, Amy K. Reisenauer, Seaver L. Soon, Ali R. Sepahdari, Kathryn B. Bollin and Soo J. Park

239 ***Circulating Tumor DNA Testing Supports Rapid Therapeutic Decision-Making in Metastatic Melanoma: A Case Report***
Tapas Ranjan Behera, Jung Min Song, Jennifer Ko, Donald Eicher, Joshua Arbesman, Brian Gastman, Daniel H. Farkas and Pauline Funchain

244 ***Treatment Related Toxicities With Combination BRAF and MEK Inhibitor Therapy in Resected Stage III Melanoma***
Morgan Homan, Govind Warrier, Christopher D. Lao, Sarah Yentz, Shawna Kraft and Leslie A. Fecher

frontiers in Oncology

ORIGINAL RESEARCH
published: 10 May 2021
doi: 10.3389/fonc.2021.667715

An Immunometabolic Shift Modulates Cytotoxic Lymphocyte Activation During Melanoma Progression in TRPA1 Channel Null Mice

Maria Fernanda Forni[1†‡], *Omar Alberto Domínguez-Amorocho*[1‡], *Leonardo Vinícius Monteiro de Assis*[2†‡], *Gabriela Sarti Kinker*[3], *Maria Nathalia Moraes*[4], *Ana Maria de Lauro Castrucci*[2,5‡§] *and Niels Olsen Saraiva Câmara*[1*‡§]

[1] Laboratory of Transplantation Immunobiology, Institute of Biomedical Sciences, University of São Paulo, São Paulo, Brazil, [2] Laboratory of Comparative Physiology of Pigmentation, Department of Physiology, Institute of Biosciences, University of São Paulo, São Paulo, Brazil, [3] Laboratory of Translational Immuno-Oncology A. C. Camargo Cancer Center – International Research Center, São Paulo, Brazil, [4] Laboratory of Neurobiology, Department of Physiology and Biophysics, Institute of Biomedical Sciences, University of São Paulo, São Paulo, Brazil, [5] Department of Biology, University of Virginia, Charlottesville, VA, United States

Melanoma skin cancer is extremely aggressive with increasing incidence and mortality. Among the emerging therapeutic targets in the treatment of cancer, the family of transient receptor potential channels (TRPs) has been reported as a possible pharmacological target. Specifically, the ankyrin subfamily, representing TRPA1 channels, can act as a pro-inflammatory hub. These channels have already been implicated in the control of intracellular metabolism in several cell models, but little is known about their role in immune cells, and how it could affect tumor progression in a process known as immune surveillance. Here, we investigated the participation of the TRPA1 channel in the immune response against melanoma tumor progression in a mouse model. Using *Trpa1*$^{+/+}$ and *Trpa1*$^{-/-}$ animals, we evaluated tumor progression using murine B16-F10 cells and assessed isolated CD8+ T cells for respiratory and cytotoxic functions. Tumor growth was significantly reduced in *Trpa1*$^{-/-}$ animals. We observed an increase in the frequency of circulating lymphocytes. Using a dataset of CD8+ T cells isolated from metastatic melanoma patients, we found that *TRPA1* reduction correlates with several immunological pathways. Naïve CD8+ T cells from *Trpa1*$^{+/+}$ and *Trpa1*$^{-/-}$ animals showed different mitochondrial respiration and glycolysis profiles. However, under CD3/CD28 costimulatory conditions, the absence of TRPA1 led to an even more extensive metabolic shift, probably linked to a greater *in vitro* killling ability of *Trpa1*$^{-/-}$ CD8+ T cells. Therefore, these data demonstrate an unprecedented role of TRPA1 channel in the metabolism control of the immune system cells during carcinogenesis.

Keywords: TRPA1 channel, melanoma, immunometabolism, CD8+ T cells, metabolic shift

OPEN ACCESS

Edited by:
Samisubbu Naidu, Indiana University, United States

Reviewed by:
Chandra K. Singh, University of Wisconsin-Madison, United States
Gagan Chhabra, University of Wisconsin-Madison, United States

****Correspondence:***
Niels Olsen Saraiva Câmara
niels@icb.usp.br

†Present Address:
Maria Fernanda Forni, Horsley Lab, Department of Molecular, Cellular and Developmental Biology, Yale University, New Haven, CT, United States
Leonardo Vinícius Monteiro de Assis, Institute of Neurobiology, Center for Brain, Behavior, and Metabolism, University of Lübeck, Lübeck, Germany

‡These authors have contributed equally to this work

§These authors have contributed equally to this work and share senior authorship

Specialty section:
This article was submitted to Skin Cancer, a section of the journal Frontiers in Oncology

Received: *27 February 2021*
Accepted: *21 April 2021*
Published: *10 May 2021*

INTRODUCTION

Melanocytes are key players in skin biology since they produce a pigment, melanin, that protects the skin against the deleterious effects of UV radiation and visible light (1, 2). However, the uncontrolled and deregulated proliferation of melanocytes may result in cutaneous, mucosal, or uveal melanoma. Cutaneous melanoma (CM) is the most aggressive and treatment-resistant skin cancer (3, 4), being responsible for the majority of deaths, thus imposing a massive economic burden on the health system (3–5).

The interaction of cancer cells with cells and molecules or metabolites in tissues, also known as tumor microenvironment, plays an important role in cancer progression (6). Among these components, immune cells are responsible for the immune surveillance (7–9). They are directly involved in the tumor microenvironment and may favor or halt cancer development (10). During early stages of cancer, effector immune cells efficiently eliminate immunogenic cancer cells; however, selected cancer cells that survive, can progress, and evolve to clinically detectable tumors, through several cellular mechanisms that lead to evasion or inactivation of immune cells (10).

Due to this fact, new pharmacological targets for melanoma treatment are greatly needed. Among these new players, transient receptor potential (TRP) channels have received some attention as putative targets for pain and diabetes treatment, skin, central nervous and cardiovascular disorders [reviewed in (11–15)]. TRP channels are divided into six subfamilies, among them, TRPA ("A" for ankyrin) (16). Several *in vitro* and *in vivo* studies have shown the involvement of TRPC, TRPV, and TRPM family in many cancer models. However, the clinical and therapeutic value of TRP channels is still elusive (17).

Recently, it became evident that activation, growth and proliferation, engagement of effector functions, and homeostasis of immune cells are intimately linked and dependent on dynamic changes in cellular metabolism (18). This is even more evident in the tumor microenvironment where the competition for nutrients conditioning metabolic reprogramming can impact T cell activation and function (19–21). Moreover, even though TRPA1 has been associated with the control of growth, survival, and activation of neutrophils, macrophages, B and T cells, the roles of this channel upon the metabolic regulation of T lymphocyte activation remain unclear, especially in the tumor microenvironment (22, 23).

In an attempt to fill this gap, in this study we sought to evaluate the contribution of TRPA1 for the metabolic activation of the immune system and its impact on the carcinogenic process in a murine model of melanoma cancer. Through the usage of intact cell metabolic evaluation and flow cytometry, we demonstrated that the lack of TRPA1 in CD8+ T cells leads to increased respiratory response and glycolysis that culminates with T cell activation and enhanced killing activity. This study provides a novel evidence that TRPA1 could represent an important modulator of immune cells and a putative new pharmacological target in melanoma treatment.

MATERIAL AND METHODS

In Vivo Procedures

All experimental procedures were performed according to Brazilian legislation approved by the Committee for Animal Use (CEUA IB/USP, number 255/2016, 14th of June 2016). Experiments were performed on B6;129 (*Trpa1*$^{+/+}$) male mice, which is the result of 129 SvWT crossing with C57BL/6J, both provided by the Institute of Biomedical Sciences vivarium, University of São Paulo, originally acquired from Jackson Laboratories and on *Trpa1*$^{-/-}$ male mice in a mix background (B6;129), also acquired from Jackson Laboratories (B6;129P-Trpa1^{tm1Kykw}/J, 003770). Three to eight month-old *Trpa1*$^{+/+}$ and *Trpa1*$^{-/-}$ animals were used. Mouse genotypes were confirmed according to the instructions provided by Jackson Laboratories.

Mice were kept under a 12:12 light/dark cycle (800 – 1000 lux white LED light, ranging from 420 to 750 nm) at controlled temperature (22 ± 2°C). Lights were on at 7 a.m. and off at 7 p.m. Mice were subcutaneously inoculated in the right flank with $2x10^6$ B16-F10 cells (kindly donated by Prof. Roger Chammas, Faculty of Medicine, University of São Paulo) in 100 µL of phosphate buffered saline (PBS). Control animals were injected with the same volume of PBS. Then, mice were single housed for the entire experiment. Animals were euthanized with CO_2, 22 days after inoculation, and death was assured by cervical dislocation. After euthanasia every animal was visually inspected and no metastasis was found, as previously demonstrated (24). The organs and blood were harvested and immediately processed or stored at -80°C as described below.

Mouse Weight, Food Consumption, and Tumor Volume

All the following parameters were assessed every 3 to 4 days at the same time of the day (from 2 to 3 p.m.). Mouse weight values were expressed in grams. On the 22nd day, tumor was resected and weighed. Food consumption was assessed by measuring the initial and every 3 to 4 days the weight of ration pellets and expressed in grams. Tumor volume (mm^3) was evaluated from the 13th day onwards, measuring length, width, and height with a caliper rule, and calculated following the formula: π/6 x length x width x height (25). Before the 13th day tumor growth was considered negligible due to the absence of visible growth, and thus, plotted as zero.

Gene Expression

Small fragments of tumor were homogenized in TRIzol (Thermo Fisher Scientific, USA) and total RNA was extracted and purified according to the kit manufacturer's instructions (Direct-zol™ RNA MiniPrep, Zymo Research, USA). RNA concentration (OD_{260}) was determined in a spectrophotometer (Nanodrop, USA), and 1 µg was subject to reverse transcription with SuperScript III Reverse Transcriptase, random hexamer primers and other reagents, according to the manufacturer's instructions (Thermo Fisher Scientific, USA), as described

previously (26). To evaluate gene expression, 25 ng of cDNA per well were subject to quantitative PCR (qPCR) using species-specific primers (**Table 1**) spanning introns, based on sequences obtained from GenBank (http://www.ncbi.nlm.nih.gov/genbank), designed by Primer Blast (http://www.ncbi.nlm.nih.gov/genbank) and synthesized by IDT (Integrated DNA Technologies, USA) or Exxtend (Brazil). *Rpl37a* RNA was used to normalize gene expression values, which has been previously shown to be an adequate housekeeping gene in melanoma tumor samples (24). Reactions were carried out using BioRad iQ™ SYBR® Green Supermix (Bio-Rad Laboratories, USA) with the following conditions in iQ5 thermocycler (Bio-Rad Laboratories, USA): 3 min at 95°C, followed by 45 cycles of 15 s at 95°C, 30 s at 60°C, and 80 cycles of 10 s at 55°C with a gradual rise of 0.5°C. Negative controls with no templates were routinely included. Gene expression was quantified according to the $2^{\Delta\Delta Ct}$ method (27). ΔC_t was determined by subtracting the normalizer C_t from the C_t of the gene of interest at the same time point, both corresponding to the average of duplicates of the same cDNA sample. The mean value obtained from control mice was subtracted from all other values, obtaining the $\Delta\Delta C_t$, which was used as a negative exponential of base 2 ($2^{-\Delta\Delta Ct}$). The log values were obtained from a minimal of three animals of at least two independent experiments. Data are shown as the mean ± SD.

Hematological Analyses

After euthanasia, blood was collected by cardiac puncture in EDTA (10.25 mg/mL) collection tubes and immediately processed. Analyses were performed on an automated hematology analyzer (BC-2800Vet, Mindray, USA) using mouse-specific algorithms and parameters.

Flow Cytometry

Tumor was dissected and filtered through a cell strainer (100 μm, Corning, USA) in PBS. Red blood cells (RBC) were lysed using ACK (Ammonium-Chloride-Potassium) RBC Lysing Buffer (0.15 M NH_4Cl, 10.0 mM $KHCO_3$, 0.1 mM Na_2 EDTA), and the B16-F10 and immune infiltrating cells were kept in PBS. One million cells per well were stained in a round bottom 96 well plate using a two-step staining protocol. First, cells were stained with a live/dead dye (Fixable aqua 405 nm, Invitrogen, USA) at 4°C for 20 min, cells were washed, and 100 μL final volume of a solution containing surface antibodies diluted in staining buffer (1% fetal bovine serum, FBS, 1 mM EDTA, and 0.02% NaN_3 in PBS) were added into each well. After 30 min at 4°C, the samples were washed (2X) and resuspended in staining buffer until acquisition. The following antibodies were used: PerCP-Cy5.5 Anti-Mouse CD80 (Clone 16-10A1 Cat no. 194722), APC-Cy7 anti-Mouse F4/80 (Clone BM8 Cat no. 123118), FITC Anti-Mouse CD206 (Clone C068C2 Cat no.141704), from Biolegend, USA, and PE-Cy7 anti-mouse CD86 (Clone GL1 Cat no. 560582) from BD, USA. Samples were assessed with a FACSCanto II cell analyzer (Becton Dickinson, USA) using DiVA 8 acquisition software and FlowJo 5 V10 (Becton Dickinson, USA) data analysis software.

Cell Isolation and Culture

All experiments using live cells were performed with murine splenic CD8+ T cells isolated with the Mouse CD8+ T Cell Isolation Kit (MACS Miltenyi Biotech, USA). Following isolation, cells were resuspended at 1×10^6 cells/mL in T cell culture medium: RPMI 1640 medium (Thermo Fisher, USA)

TABLE 1 | List of primers used (300 nM) in the manuscript, and the corresponding access numbers.

Gene	Forward Sequence 5' – 3'	Reverse Sequence 5' – 3'
Rpl37a NM_009084.4	GCATGAAAACAGTGGCCGGT	AGGGTCACACAGTATGTCTCAAAA
Il-1-β NM_008361	GCAACTGTTCCTGAACTCAACT	ATCTTTTGGGGTCCGTCAACT
Il-6 NM_010559	CCTGAGACTCAAGCAGAAATGG	AGAAGGAAGGTCGGCTTCAGT
Il-10 NM_010548	GCTCTTACTGACTGGCATGAG	CGCAGCTCTAGGAGCATGTG
Il-12 NM_008351.2	CTGTGCCTTGGTAGCATCTATG	GCAGAGTCTCGCCATTATGATTC
Prf1 NM_011073	AGCACAAGTTCGTGCCAGG	GCGTCTCTCATTAGGGAGTTTTT
Gzmf NM_010374	GCTGGGGGAGAACATCCATC	TGTCCTGTTTAGCCCATAGGT
TGF-β NM_009367	CTTCGACGTGACAGACGCT	GCAGGGGCAGTGTAAACTTATT
Tnf-α NM_009396	AGGAGGAGTCTGCGAAGAAGA	GGCAGTGGACCATCTAACTCG
Ifn-γ NM_008337.4	ATGAACGCTACACACTGCATC	CCATCCTTTTGCCAGTTCCTC

containing 10% FBS, 1X Glutamax (Life Technologies, USA), 1 mM sodium pyruvate, 0.1% β-mercaptoethanol, and 100 U/mL penicillin/ 100 μg/mL streptomycin (Gibco, USA). Cells were kept on ice, counted in a hemocytometer, and evaluated for viability using Trypan Blue (Gibco, USA) and immediately analyzed in the Seahorse experiment.

Seahorse High Resolution Live Cell Respirometry

The oxygen consumption rate (OCR) and the extracellular acidification rate (ECAR) were recorded using a Seahorse XFe96 Analyzer (Agilent, USA). CD8+ T cells were freshly isolated and resuspended in Agilent XF Assay Medium supplemented with 25 mM glucose, 1 mM sodium pyruvate, and 2 mM L-glutamine. Cells (0.2×10^6 cells/well) were then plated on Seahorse assay plates coated with poly-D-lysine (Sigma Aldrich, USA) and let to rest at room temperature in the hood for 30 min. During the assay, cells were kept in the same medium and exposed to 1 μM oligomycin, 1.5 μM carbonyl cyanide p-trifluoromethoxyphenylhydrazone (FCCP), 100 nM rotenone and 1 μM antimycin A, purchased from Sigma-Aldrich, USA, as indicated in the figures. Alternatively, a mix of phorbol myristate acetate (5 ng/mL, PMA) and ionomycin (1 μM), purchased from Sigma-Aldrich, USA, were used in the injections during the experiments. For some of the experiments, the seahorse plate was also coated with 2 μg/mL mouse anti-CD3 (Clone 145-2C11 Cat no. 553058) and 10 μg/mL mouse anti-CD28 (Clone 37.51 Cat no. 553294), both from Becton, Dickinson, USA, for 24 h, and washed twice with PBS before plating the cells.

CD8+ T Cell Purification and *In Vitro* Cytotoxic T Lymphocyte (CTL) Assay

Splenocytes collected from *Trpa1*$^{+/+}$ and *Trpa1*$^{-/-}$ mice were stained with fluorochrome-conjugated antibodies FITC anti-mouse CD4 (Clone RM4-5 Cat no. 100509, Biolegend, USA), PER-CP anti-mouse F4/80 (Clone BM8 Cat no. 123126, Biolegend, USA), APC anti-mouse CD19 (Clone 1D3 Cat no. 550992, BD, USA), PE anti-mouse CD105 (Clone MJ7/18 Cat no. 12-1051-82, eBioscience, USA), and BV421 anti-mouse CD11c (Clone HL3 Cat no. 562783 BD, USA) and sorted to obtain a purified and enriched CD8+ T cell population using a FACS (FACS Aria II Cell sorter, BD Biosciences). Meanwhile, B16-F10 WT cells cultured in RPMI 1640 medium (Atena, Brazil) with 10% FBS, to be used as target cells, were stained with a cell tracking marker (1 μL of dye per 10^6 cells, Cell TraceCellTrace™ Violet Cell Proliferation Kit, Invitrogen, USA) following the manufacturer's instructions. For *in vitro* stimulation, sorted CD8+ T cells (effector cells) were co-cultured on plate-bound anti-CD3 (2 μg/mL) (Clone 145-2C11 Cat no. 553058) and mouse anti-CD28 (10 μg/mL) (Clone 37.51 Cat no. 553294) with B16-F10 stained cells in a ratio of 5 CD8+ cells to 1 B16-F10 cell, and incubated at 37°C with 5% CO_2 for 4 h (28, 29). Finally, co-cultured cells were stained using the two-step protocol using the following dye and fluorescent antibody: live/dead dye (Fixable aqua 405 nm, Invitrogen, USA) and APC anti mouse CD8 (Clone 53-6.7 Cat no. MCD0805, Invitrogen, USA), according to the staining method previously described. Samples were assessed with a FACSCanto II cell analyzer (Becton Dickinson, USA) using DiVA 8 acquisition software and FlowJo 5 V10 (Becton Dickinson, USA) data analysis software.

CD8 T RNA-Seq Data Analysis

Data were retrieved from the Gene Expression Omnibus [accession GSE141465 (30)] using GEOquery and Biobase Bioconductor R packages (http://www.bioconductor.org/). In Parrot's study (30), CD8+ T cells were sorted from metastatic melanomas (n = 8) expanded and stimulated or not for 6 h with plate-bound anti-CD3 (1 μg/mL). Gene expression of paired unstimulated/stimulated T CD8 samples was quantified using Illumina HumanHT-12 V4.0 Expression Beadchip arrays. Data were processed using quantile normalization and log2-transformed. For analysis, we first grouped CD8+ T samples according to their expression of *Trpa1* in basal conditions (unstimulated). Next, we evaluated the impact of CD3 activation in low *Trpa1* and high *Trpa1* samples and computed the log2 (fold change) in gene expression for each group separately (log2FClow and log2FChigh). For gene set enrichment analysis (GSEA), we ranked genes by comparing their differential expression upon CD3 activation in high *Trpa1* vs. low *Trpa1* samples (log2FChigh - log2FClow). GSEA was performed using the desktop application v.4.0.3 (31) and the Reactome (32), KEGG (33) and HALLMARK databases (34). Enrichment scores (ES) were calculated based on a weighted Kolmogorov–Smirnov-like statistic and normalized (NES) to account for gene set size. p-values corresponding to each NES were calculated using 1,000 gene set permutations and corrected for multiple comparisons with the false discovery rate (FDR) procedure. Differences were considered statistically significant for adjusted p-values (FDR q) < 0.05.

The Cancer Genome Atlas (TCGA) RNA-Seq Data Analysis

TCGA RNA-seq and clinical data from 473 melanomas (35) were downloaded from the UCSC XENA Browser (36). Data were generated using the Illumina HiSeq 2000 RNA sequencing platform and quantified with RSEM. Estimated counts were upper quartile normalized and $\log_2$(normalized counts + 1). Estimation of the abundance of different immune cell types was calculated with CIBERSORT and the LM22 reference signature matrix, using the absolute mode, B-mode batch correction, disabled quantile normalization, and 100 permutations (37). One sample presented a p > 0.05 and was removed from the analysis.

Statistical Analysis

Body weight, food intake, and tumor volume were analyzed by Two-Way ANOVA followed by Bonferroni's post-test. Hematological analysis, flow cytometry, and gene expression assays were analyzed by unpaired Student's *t*-test. For Seahorse data analysis, the area under the curve was calculated and the data were analyzed with One-Way ANOVA followed by Tukey

for the comparison of more than two groups or with unpaired Student's *t*-test for two group comparison. In all scenarios, $p < 0.05$ was established to reject the null hypothesis. GraphPad Prism 7.0 was used for all statistical analyses (USA).

RESULTS

Melanoma Progression Is Delayed in *Trpa1*$^{-/-}$ Mice

The modulation of immune cells by metabolism has become one of the hallmarks of immune function. Although presenting a clear role in metabolic regulation (22), the influence of TRPA1 channel family on immunometabolic alterations during cancer progression has not been fully elucidated. In order to fill this gap, we used a model in which *Trpa1*$^{+/+}$ and *Trpa1*$^{-/-}$ mice were inoculated with B16-F10 melanoma cells to understand CD8+ T activation and tumor progression.

We first evaluated the weight of tumor-bearing mice along the experiment and no temporal differences within each genotype were found. Interestingly, at all experimental time points, we found that *Trpa1*$^{-/-}$ animals were heavier than their wild-type counterparts (**Figure 1A**); however, such difference in weight was not associated with increased food intake (**Figure 1B**).

Despite the subtle differences in mice weight, a considerable difference in tumor growth could be observed. After inoculation with B16-F10 cells, the tumor was visible from the 13th day onwards in both *Trpa1*$^{+/+}$ and *Trpa1*$^{-/-}$ mice. On the 17th day, we found a reduction trend in tumor volume in *Trpa1*$^{-/-}$ compared to *Trpa1*$^{+/+}$ animals. On the 22nd day, the difference became even more evident and statistically significant, i.e., the tumor volume and weight were significantly reduced in *Trpa1*$^{-/-}$ mice compared to *Trpa1*$^{+/+}$ animals (**Figures 1C, D**). In order to verify if these striking differences in melanoma progression could be related to a difference in immune surveillance, we evaluated the circulating pool of immune cells in these two genotypes in the absence or presence of the tumor.

The Pool of Circulating Lymphocytes Is Higher in *Trpa1*$^{-/-}$ Mice

To determine the relative levels of circulating immune cells in the *Trpa1*$^{+/+}$ and *Trpa1*$^{-/-}$ mice, we used an automated hemocytometer to evaluate the main cellular components of the circulating blood after tumor inoculation (**Figures 2A–J**). The total number of circulating white blood cells (WBC) was lower in the mutant mice as compared to the wild type animals, suggesting a higher level of recruitment to the tumor microenvironment (**Figure 2A**). The main striking difference between these groups was not associated with total number (**Figure 2B**), but with the overall higher percentage of circulating lymphocytes (**Figure 2C**) and smaller absolute number (**Figure 2D**), but not frequency (**Figure 2E**), of monocytes in *Trpa1*$^{-/-}$ mice. No difference of granulocytes, red blood cells (RBC), and hemoglobin was found between *Trpa1*$^{-/-}$ and wild type mice (**Figures 2F–I**). The differences (**Figures 2B–G**) became even more evident when the relative abundance of lymphocytes, monocytes, and granulocytes was plotted in a percentage image, as observed in **Figure 2J**.

Interestingly, healthy animals that were not submitted to PBS or melanoma cell inoculation, did not show any differences in lymphocyte, monocyte, granulocyte, RBC absolute number and percentage, and hemoglobin levels between the genotypes (**Supplementary Figure 1**).

Since the animals of the cohort were not injected with PBS and did not suffer the same experimental manipulation of the tumor-inoculated mice, we did not compare tumor inoculated with non-PBS injected animals. Our data, therefore, suggest that the differences seen in tumor inoculated mice are due to the presence of tumor cells.

There Are No Significant Differences in Pro- and Anti-Inflammatory Populations of Tumor Associated Macrophages Between *Trpa1*$^{+/+}$ and *Trpa1*$^{-/-}$ Mice

As one of the most well-established mechanisms of tumor development is the growth benefits generated by tumor-

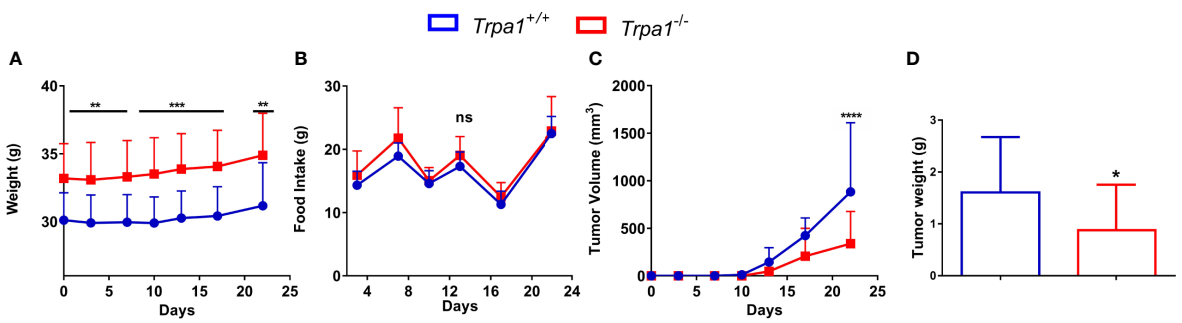


FIGURE 1 | Evaluation of body weight, food intake, and tumor volume of *Trpa1*$^{+/+}$ or *Trpa1*$^{-/-}$ mice. Values are shown as mean (n = 13 for *Trpa1*$^{+/+}$ and n=18 for *Trpa1*$^{-/-}$) ± SD. All temporal analyses were carried out using Two-Way ANOVA followed by Bonferroni post-test. Tumor weight was calculated using unpaired Student's *t*-test. **(A)** Animal weight; **(B)** Food intake; **(C)** Tumor volume; **(D)** Tumor weight. *p < 0.05; **p < 0.01; ***p < 0.001; ****p < 0.0001; ns, not significant, at each time point between genotypes.

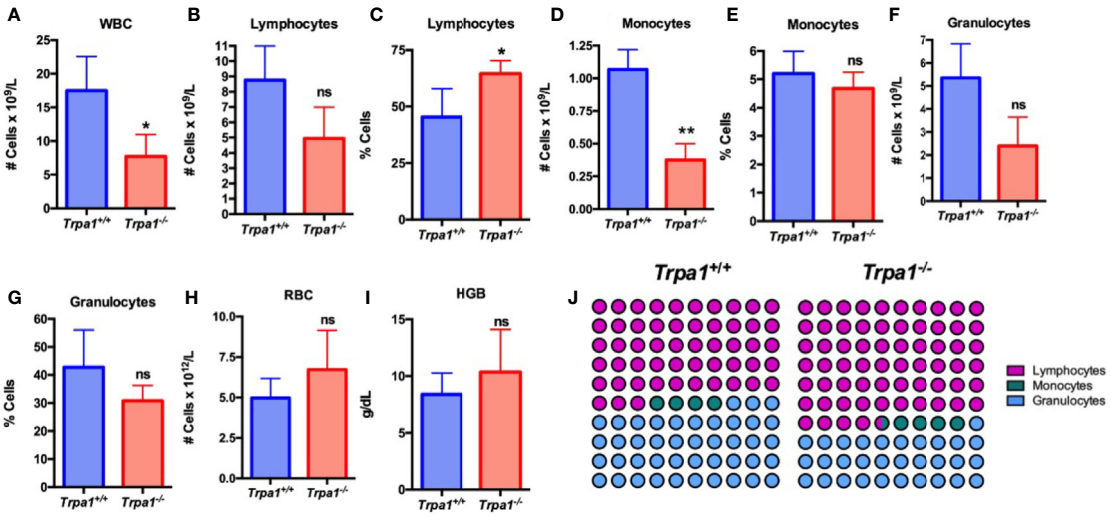


FIGURE 2 | Blood analysis of *Trpa1*$^{+/+}$ or *Trpa1*$^{-/-}$ mice on the 22nd day after B16-F10 cell inoculation. **(A)** White blood cells; **(B, C)** Absolute number and percentage of lymphocytes; **(D, E)** Absolute number and percentage of monocytes; **(F, G)** Absolute number and percentage of granulocytes; **(H)** Red blood cells; **(I)** Hemoglobin; **(J)** Representative percentage of lymphocytes, granulocytes, and monocytes. Values are shown as mean (n = 3 for *Trpa1*$^{+/+}$ and n=4 for *Trpa1*$^{-/-}$) ± SD. *p < 0.05; **p < 0.01; ns, not significant. Statistical analyses were performed by Student's *t*-test between the genotypes.

associated macrophages (TAM), and knowing that these cells can originate from monocyte recruitment and differentiation, we sought to investigate if there were differences in the relative abundance of TAMs between *Trpa1*$^{+/+}$ and *Trpa1*$^{-/-}$ mice.

To evaluate TAM frequency, present in tumor microenvironment, we dissociated the tumor mass and stroma on the 22nd day after inoculation and determine the main population expressing the surface marker F4/80 (total macrophages) by flow cytometry, observing no significant differences between *Trpa1*$^{+/+}$ and *Trpa1*$^{-/-}$ inoculated mice (**Figures 3A, B**). Moreover, when this population was further subdivided into CD80+ pro-inflammatory CD206+ resolving/anti-inflammatory macrophages, we observed a slight increase in some *Trpa1*$^{+/+}$ mice, but this was also not significant (**Figures 3A, B**).

Since differences in TAM populations did not seem to account for the delayed tumor progression in *Trpa1*$^{-/-}$ mice, we further investigated if this might be due to the difference observed in circulating lymphocytes.

There Are Striking Differences on CD8+ T Lymphocyte Abundance and Activation in Tumor Microenvironment Between *Trpa1*$^{+/+}$ and *Trpa1*$^{-/-}$ Mice

We initially analyzed human T lymphocytes using a public available transcriptome dataset of the tumor infiltrating CD8+ T cells isolated from patients with metastatic melanoma, which were obtained through cell sorting, expanded *in vitro*, and stimulated with CD3+ for 6 h (30). CD8+ T cells were stratified into high and low *TRPA1* expression and gene enrichment analysis was performed using KEGG, Reactome, and GSEA datasets. Interestingly, we observed a negative correlation of *TRPA1* transcripts with several immune system-related datasets such as IL-2, IL-6, inflammatory response, cytokine and cytokine receptor interaction, interleukin signaling, and several others (**Figure 4A**). Therefore, CD8+ T cells displaying lower levels of *TRPA1* correlate with several immune system pathways associated with increased immune system activation. Furthermore, using the dataset of cutaneous melanoma from the TCGA, we implemented the Cibersoft algorithm, which is used to estimate the frequency of different immune system cells in the tumor bulk. In *TRPA1* low primary melanoma increased frequency of activated natural killer, resting dendritic, and eosinophils were found compared to *TRPA1* high tumors (**Supplementary Figure 2A**). However, in metastatic melanoma differential frequency of immune system cells were less prominent. Only CD4+ naïve T and mast resting cells were in higher and lower frequency, respectively, in *TRPA1* low metastatic tumors compared to *TRPA1* high ones (**Supplementary Figure 2B**). These data suggest that *TRPA1* likely plays a more complex role in tumor microenvironment in melanoma cancer.

We then analyzed the relative abundance of T lymphocytes in the tumor microenvironment. Using flow cytometry, we found out that the frequencies of CD3+CD4+ lymphocytes, B cells, and natural killers (NKs) were not significantly different between the two genotypes in both spleen and tumor stroma (**Supplementary Figures 3** and **4**). A distinct pattern was observed for CD3+CD8+ lymphocytes (CD8+ T), that presented significantly lower levels in the *Trpa1*$^{-/-}$ group (**Figure 4B**). These cells display important effector functions

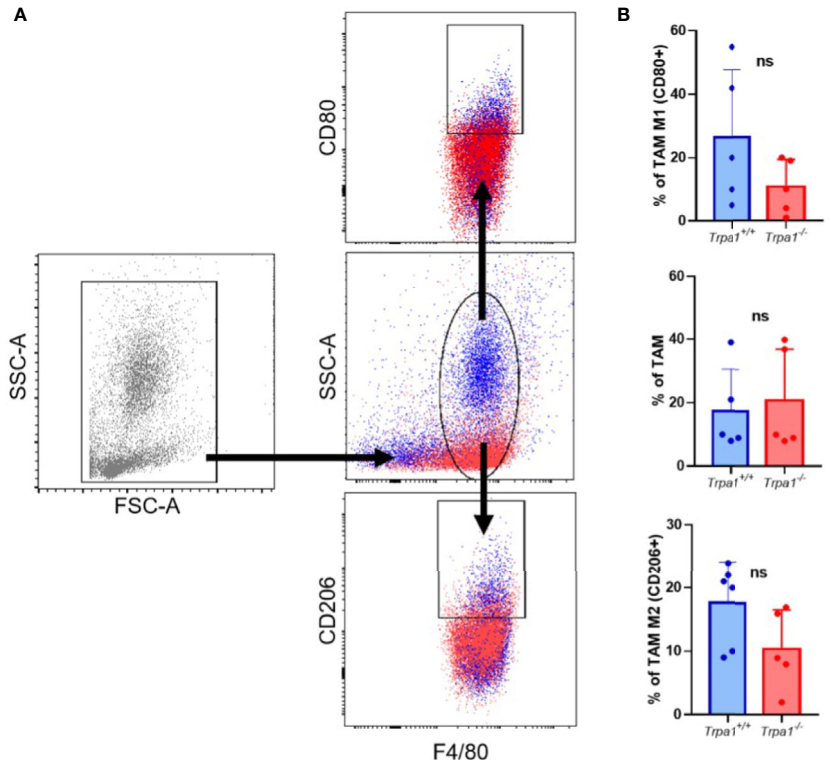


FIGURE 3 | Evaluation of tumor-associated macrophages (TAM) from *Trpa1*$^{+/+}$ or *Trpa1*$^{-/-}$ mice. **(A)** Gating strategy for the definition of TAM populations; **(B)** Analysis of frequency of TAM in tumors. Subpopulations of M1 and M2 TAM were analyzed. Values are presented as the mean (n = 5) ± SD of the frequency (%) in each group. ns, not significant.

after recognizing dysfunctional somatic cells such as tumor cells, and release the cytotoxins perforin, granzyme, and granulysin. It is important to stress that after activation the CD8+ T cytotoxic cells also undergo programmed cell death due to their intrinsic effector function, so a lower frequency of this population, as observed in the *Trpa1*$^{-/-}$ group, actually suggests that these cells are more active in the tumor site in these animals.

Through the action of perforin, granzyme enter the target cell and its serine protease activity triggers the caspase cascade leading to apoptosis. The relative levels of both perforin (**Figure 4C**, *Prf1*) and granzyme (**Figure 4D**, *Gsmf*) observed in the tumor stroma were highly upregulated in the *Trpa1*$^{-/-}$ group, supporting the fact that in this group the CD8+ T cytotoxic effector function was more prevalent that in the wild type group. We also found increased expression of *Il-1β, Il-6*, and *Ifn- γ* in tumor stroma from *Trpa1*$^{-/-}$ group compared to wild type animals (**Supplementary Figure 5**).

Recently it has been reported that TRPA1 can modulate the metabolism in mammals (14, 38) and this became clearer as one of the GSEA pathways associated with TRPA1 relates to oxidative metabolism in humans (**Figure 4A**). Knowing that this is a regulatory hub for cytotoxic lymphocyte response during tumor onset and development, we decided to evaluate the metabolism of these cells in *in vitro* experiments.

TRPA1 Modulates Both Glycolysis and the Oxidative Metabolism of CD8+ Cytotoxic T Lymphocytes Upon Stimulus

To investigate the possible role of TRPA1 channel in modulating the metabolic phenotype displayed by CD8+ T lymphocytes, we isolated fresh unstimulated cells from the spleen of the *Trpa1*$^{-/-}$ and wild type animals and assessed their extracellular acidification rate (ECAR) and oxygen consumption rate (OCR) as a proxy of glycolysis and oxidative metabolism, respectively.

When unstimulated CD8+ T lymphocytes from *Trpa1*$^{-/-}$ and *Trpa1*$^{+/+}$ mice were compared, we observed a slight increase in the resting state of OCR, although not statistically significant, in the overall number of the knockout cells (**Figure 5A**). This suggests that at the resting/non activated state these groups present comparable levels of oxidative metabolism. A remarkable difference can be observed when these two groups were stimulated with a cocktail of ionomycin and phorbol ester, PMA, simulating the signaling transduction elicited in the immunological synapsis with an antigen-presenting cell. With activating stimuli, the *Trpa1*$^{-/-}$ group displayed almost immediately a significant increase in their oxygen consumption (**Figure 5B**) that was significantly higher than the one from the *Trpa1*$^{+/+}$ group, as can be seen in the quantification of the area under the curves (**Figure 5C**). The increased level of oxidative

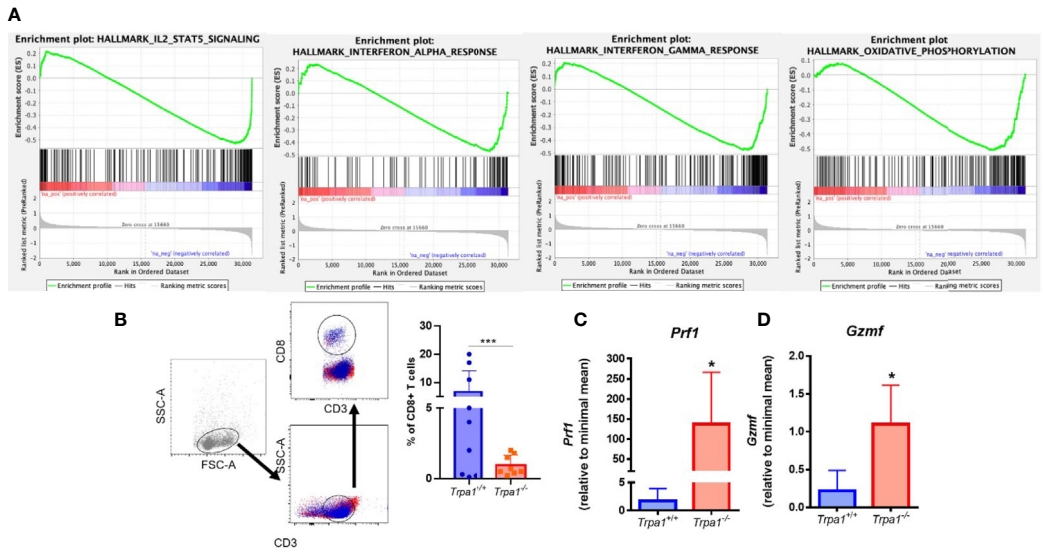


FIGURE 4 | **(A)** Analysis of transcriptome data of T CD8+ cells sorted from human patient tumors. We used GSEA to compare the changes in gene expression induced by CD3 activation in *TRPA1* low and high cells. FDR-adjusted p values < 0.05 were considered statistically significant. IL-2 and Stat1 NES: -2,05246 and FDR: 1,00e-06; Oxidative phosphorylation NES: -1,9378266 and FDR 1,00e-06; IF gamma response NES: -1,8219428 and FDR 4,22e-04; IF alpha response NES: -1,6389698 and FDR 3,92e-03; **(B)** Gating strategy for the definition of CD8+ T cell populations and analysis of frequency of infiltrating CD8 T cells in tumors from *Trpa1*$^{+/+}$or *Trpa1*$^{-/-}$ mice. **(C, D)** Bulk tumor mRNA isolation and qRT-PCR analysis 22 days after subcutaneous inoculation of B16-F10 cell inoculation; **(C)** Perforin mRNA relative levels; **(D)** Granzyme mRNA relative levels. Statistical analyses were performed by Student's *t*-test. Values are presented as the mean (n = 9) ± SD of the frequency (%) in each group. *p < 0.05; ***p < 0.001.

metabolism could mean a better metabolic activation capacity towards consuming energetic substrates in the mitochondria along with a higher rate of ATP production.

Moreover, upon determining the lactate production using the extracellular acidification rate as a proxy for glycolysis, we observed that in the non-stimulated condition the *Trpa1*$^{-/-}$ group already displayed significantly higher ECAR levels than the wild type animals, and upon stimulation this was even more evident (**Figure 5D**), suggesting that these cells are capable of a more robust bioenergetic shift towards allocating energetic reserves during activation.

Based on these data, we went on to fully characterize the resting and stimulated metabolic states in these cells using a series of drugs commonly used to evaluate the behavior of the mitochondrial ATP synthase and electron transport chain and the associated parameters.

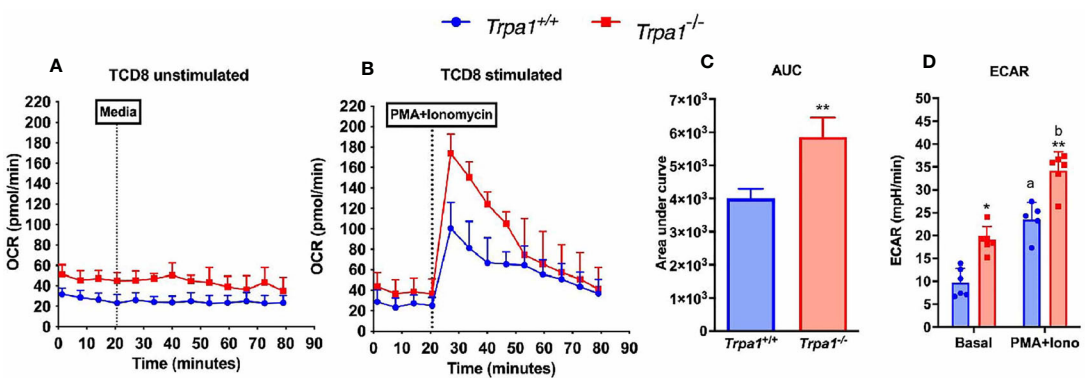


FIGURE 5 | Metabolic parameters from spleen-derived *Trpa1*$^{+/+}$ or *Trpa1*$^{-/-}$ T CD8 lymphocytes. **(A)** Basal unstimulated levels of oxygen consumption rate (OCR) of freshly isolated T CD8 cells; **(B)** OCR levels of T CD8 exposed to a cocktail with ionomycin and PMA compared to the basal rate; **(C)** Area under the curves of B; **(D)** Extracellular acidification rates (ECAR) for both non-stimulated and stimulated cells from the two groups. Values are presented as the mean (n = 8) ± SD of each group. Statistical analyses were performed by Student's *t*-test in C and by One Way ANOVA followed by Tukey in **(D)** Each well contained 100,000 cells. *p < 0.05; **p < 0.01 between genotypes. Difference between the different conditions within the same genotype is represented by letters a ≠ b, p < 0.05.

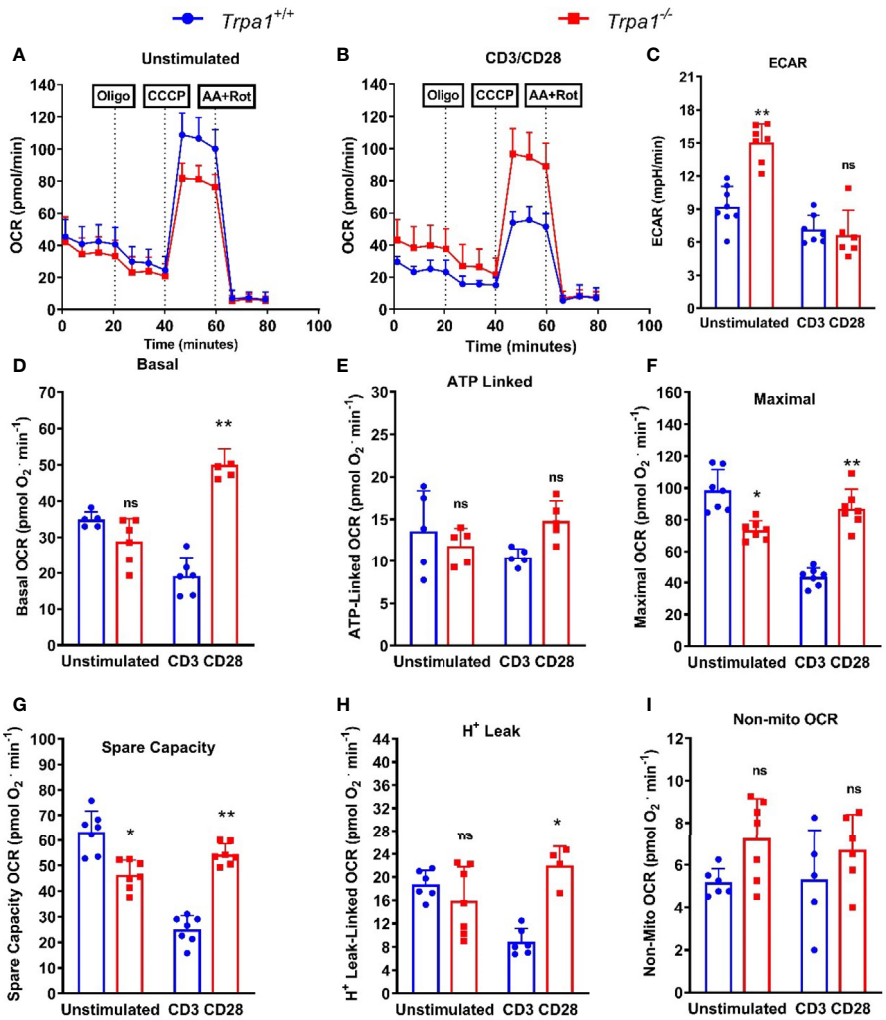


FIGURE 6 | Mitochondrial metabolic evaluation from spleen-derived *Trpa1*$^{+/+}$or *Trpa1*$^{-/-}$ T CD8 lymphocytes under CD3/CD28 activation. **(A)** Traces obtained from unstimulated *Trpa1*$^{+/+}$or *Trpa1*$^{-/-}$ T CD8 cells after injections of oligomycin (ATP synthase inhibitor), CCCP (uncoupler) and antimycin A plus rotenone (Complex III and I inhibitors); **(B)** Same as in A but cells were stimulated for 30 min using immobilized CD3/CD28; **(C)** Extracellular acidification rate (ECAR) from unstimulated and stimulated cells; **(D)** Basal respiration; **(E)** ATP-linked oxygen consumption rate; **(F)** Maximal oxygen consumption rate; **(G)** Spare capacity (difference between maximal and basal respiration); **(H)** Proton-leak linked oxygen consumption rate; **(I)** Non-mitochondrial respiration (this part is subtracted from all the other respiration rates shown in **D–H**). Values are presented as the mean (n = 8) ± SD of each group. *p < 0.05; **p < 0.01. One-Way ANOVA analysis followed by Tukey was performed to evaluate differences between conditions and genotypes.

The Lack of TRPA1 Dramatically Increases the Maximal Mitochondrial Respiration of CD8+ T Cytotoxic Lymphocytes Upon Stimulus Impacting Spare Respiratory Capacity Along With Glycolysis

To examine whether there were differences in the metabolism of CD8+ T lymphocytes from *Trpa1*$^{-/-}$ and *Trpa1*$^{+/+}$ mice, we isolated and immobilized these cells for intact cell respiration using the Seahorse technology. We observed (**Figure 6A**) that the oxygen consumption rates between these two groups did not display significant differences when these cells were in the non-stimulated basal condition. This result contrasts to what was observed after a 30 min-long stimulation with anti-CD3+ and CD28+ antibodies (**Figure 6B**). The first intriguing observation is that only non-stimulated CD8+ T cells from *Trpa1*$^{-/-}$ mice presented increased levels of ECAR indicating that this group exhibits a predisposition to higher glycolytic rates (**Figure 6C**). As this has been directly associated with the cytotoxic function of these cells *in vitro*, it is interesting to speculate that maybe this poises these cells with an advantage in the capacity to be activated when dealing with the tumor progression.

We next examined the basal respiration, or the consumption of oxygen by the cell mitochondrial network under basal condition using only culture medium. Under this condition the basal respiration of *Trpa1*$^{-/-}$ cells was slightly lower than of their *Trpa1*$^{+/+}$ counterparts, but when activated these cells go on to

fully display increased basal respiration. These data suggest that their oxidative metabolism is upregulated most probably to generate more ATP and or precursors necessary for their killing activity (**Figure 6D**).

To further characterize the metabolic response in these two groups, we used a treatment comprising the injection of oligomycin, that inhibits the ATP synthase, and we could observe that there were no significant differences in the ATP-linked oxygen consumption between the two groups (**Figure 6E**), suggesting that the majority of the ATP that fuels the difference response of these CD8+ T cells is most likely derived from the substrate level generation found in glycolysis. Next, we characterized the mitochondrial maximal and spare respiratory capacity using an uncoupler drug (CCCP) that dissociates the flux of electrons from the oxygen consumption in the mitochondria leading to maximal rates in the OCR. Our first observation is that both maximal, as well as spare respiratory capacity, presented a similar behavior (**Figures 6F, G**, respectively). The levels of maximal respiration in non-activated *Trpa1*$^{-/-}$ CD8+ T cells were slightly, but significantly, lower than of their wildtype counterparts but this pattern inverted after CD3/CD28 co-stimulation, as the knockout group presented a significantly higher maximal oxygen consumption (**Figure 6F**). This, coupled with higher levels of glycolysis displayed by these cells, allows for a substantial glycolytic shift without losing mitochondrial activity which is advantageous *per se*. The same can be observed for the spare respiratory capacity (**Figure 6G**), which in general correlates with better physiological responses in cells exposed to metabolic challenges. The same could be observed for the proton leak (**Figure 6H**) that relates to their uncoupled state. These data suggest that *Trpa1*$^{-/-}$ CD8+ T cells would be in better conditions to modulate their metabolism when facing the activation stimuli. We also evaluated the levels of non-mitochondrial respiration by adding inhibitors of the mitochondrial complexes I and III (rotenone and antimycin A, respectively), but could not observe any significant differences in this activity (**Figure 6I**).

Taken altogether, these data suggest that *Trpa1*$^{-/-}$ CD8+ T lymphocytes can modulate their metabolism in a more prominent way when activated. Subsequently, we investigated whether this metabolic plasticity would entail these cells with a more proficient killing activity.

TRPA1 Impacts the Cytotoxic Response Proficiency of CD8+ T Lymphocytes

To evaluate the metabolic plasticity and efficiency of these cells to undergo an increased oxidative response while also ramping up the glycolysis, we sorted CD8+ T cells from the spleen of *Trpa1*$^{+/+}$ and *Trpa1*$^{-/-}$ mice, stimulated these cells with immobilized CD3+ and CD28+ antibodies for 30 min and then exposed them to B16-F10 melanoma cells in a 5:1 ratio (5 tumor cells to 1 CD8+ T cell). Four hours later, the number of dead tumor cells was quantified by using the loss of membrane integrity and covalently protein binding flow cytometry coupled with discrimination and exclusion of the lymphocytes through CD8+ T staining (**Figures 7A–D**).

Using this approach, we did not find any difference in cytotoxic activity of CD8+ T cells from either *Trpa1*$^{+/+}$ or *Trpa1*$^{-/-}$ mice in the unstimulated scenario; however, upon stimulation with CD3/CD28 antibodies, there was an increase in cytotoxic activity of *Trpa1*$^{-/-}$ CD8+ T cells compared to wild type cells (**Figure 7E**). Collectively these data show that the increased metabolic capacity displayed by *Trpa1*$^{-/-}$ CD8+ T cells directly translates into a better cytotoxic performance.

DISCUSSION

Tumors promote a major disturbance to tissue homeostasis: They create energetic and substrate demanding environments that impact on metabolism and function of the stroma and infiltrating immune cells. Nutrient competition is at bay as the unrestrained cell growth seen in cancer is often supported by aerobic glycolysis, the same metabolic pathway needed to fuel optimal effector functions in many immune cells (18). The demand for nutrients, essential metabolites, and oxygen imposed by proliferative cancer cells creates harsh environmental conditions in which immune cells must navigate and adapt. How tumor and immune cells share or compete for resources in this microenvironment, and how such relationships regulate antitumor immunity are pressing questions to address.

At the forefront of these mechanisms, how immune cell metabolism, and thus immune cell function, is altered by the tumor microenvironment, is a question of utmost interest and importance. To address this question, we evaluated the participation of the TRPA1 channel in the immune response against melanoma tumor progression in a model of murine melanoma. Recently, Antoniazzi and colleagues (39) showed that tumor growth, through injection of B16-F10 cells in the mouse paw, is not different between *Trpa1*$^{+/+}$ and *Trpa1*$^{-/-}$ genotypes, which contrasts with our results. However, we highlight some methodological differences that impair the comparison between that study and our data presented here: 1) In (39) a *Trpa1*$^{-/-}$ mice in C57 background was used while we used knockouts in B6;129 background along with its appropriate control; 2) we injected $2x10^6$ B16-F10 cells in the right flank while Antoniazzi and coworkers (39) inoculated $2x10^5$ cells in the paw. Nonetheless, using *Trpa1*$^{+/+}$ and *Trpa1*$^{-/-}$ animals, we followed tumor progression using B16-F10 cells and assessed isolated CD8 + T cells for respiratory and cytotoxic function with an in depth look on how immunometabolism contributes to cell function during cancer progression.

Cytotoxic CD8+ T lymphocytes (CTL) play an essential role in providing effective antigen-specific immunity against tumors. CTL recognizes tumor-associated antigens presented on major histocompatibility complex class I (MHCI) by their expressed T cell receptor (TCR) and destroys target tumor cells through different mechanisms. This includes release of granules containing perforin and granzymes and inducing FasL-mediated apoptosis. However, to achieve long-lasting anti-tumor immunity, it is necessary to establish memory CD8+

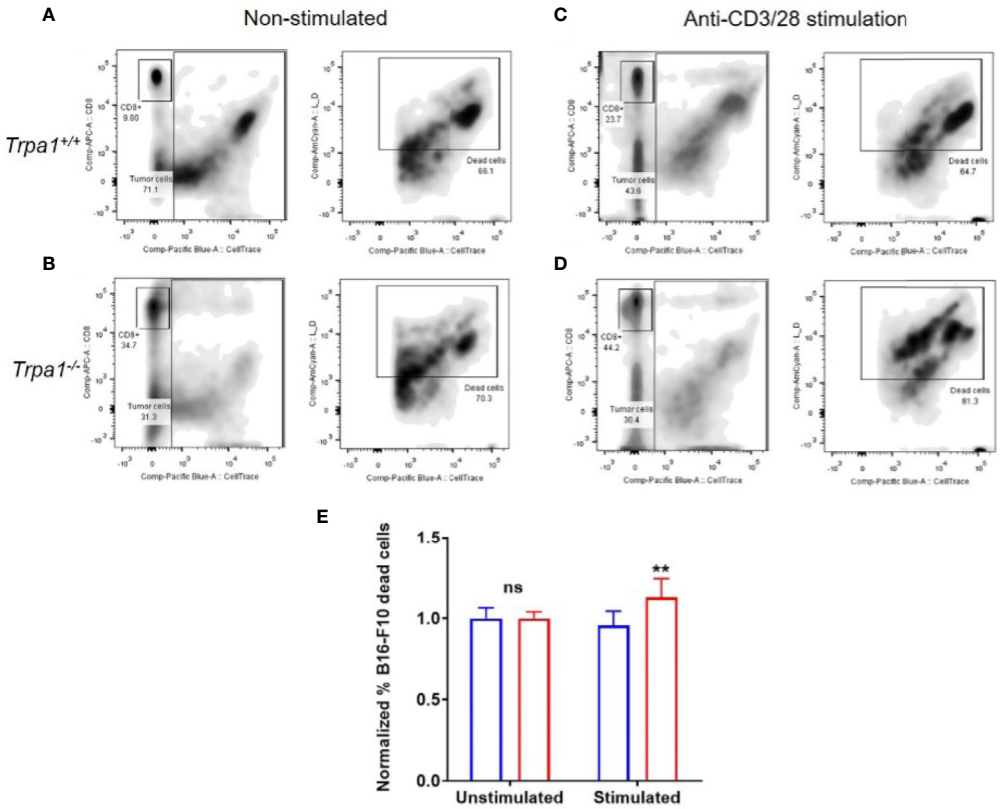


FIGURE 7 | Killing capacity of CD8$^+$ cells from *Trpa1*$^{+/+}$ and *Trpa1*$^{-/-}$ mice co-cultured with B16-F10 cells. A and B) Representative assessment of B16-F10 cell killing by CD8$^+$ T cells from *Trpa1*$^{+/+}$ **(A)** and *Trpa1*$^{-/-}$ **(B)** mice under non stimulated conditions. C and D) Representative assessment of B16-F10 cell killing by CD8$^+$ T cells from *Trpa1*$^{+/+}$ **(C)** and *Trpa1*$^{-/-}$ **(D)** mice under CD3/CD28 stimulation. **(E)** Normalized frequency of B16-F10 cell death by CD8$^+$ T cells from *Trpa1*$^{+/+}$ and *Trpa1*$^{-/-}$ mice; values are presented as the mean (n = 3 and 6 for unstimulated and stimulated group, respectively) ± SD. Statistical analyses were performed by Student's *t*-test. **p < 0.01, ns, not significant.

T cell responses (40, 41). CTL populations have been classified by several surface markers and distinguished by their functions and residency, along with their effector cytokine production. Naïve CTL cells possess strong proliferative potential after antigen stimulation and resist terminal differentiation and exhaustion when compared with memory T cells which can rapidly produce multiple functional molecules after restimulation to control the tumor progression (42, 43).

While naive CD8+ T cells have relatively low energetic requirements, effector T cells present an increased demand for energy and biosynthetic precursors to support proliferation and effector function. Signaling in T cells through the TCR receptor and co-stimulatory molecules (such as CD28 and cytokine receptors) leads to the activation of immunological pathways which are accompanied by a profound alteration in the cellular metabolism to support their proliferation and effector function (44).

The TRPA family contains only one member, TRPA1, in vertebrates. This ion channel is best known in sensory neurons as a sensor for environmental irritants, inflammatory pain, and itching, but it has a diverse tissue distribution and plays different roles in a variety of non-neuronal cells (45). The constitutive expression of TRPA1 mRNA and protein in mouse and human primary CD4+ T cells controls CD4+ T cell activation and pro-inflammatory responses in models of colitis (45). In a recent study, Sahoo and colleagues reported TRPA1 expression in murine and human T CD3+ cells. Interestingly, TRPA1 inhibition prevents CD25 and CD69 expression and tumor necrosis factor (TNF), interferon γ (IFN-γ), and interleukin 2 (IL-2) secretion by stimulated T cells (46). Although not providing the data in the manuscript, the authors stated that inhibition of TRPA1 prevented T cell activation of CD4+ and CD8+ (46). Such findings seem to be in contradiction to our data since the lack of TRPA1 in our experimental model augmented T cell activity with a metabolic shift and increased cytotoxicity activity. However, it should be stressed that the mentioned study used BALB/c mice while we used B6;129 animals and no cytotoxicity assay was performed in that study (46). In addition, the lack of TRPA1 could lead to a compensatory mechanism, which would ultimately lead to increased T cell response. As TRP channels, including TRPA1, are known to form heterodimers especially with TRPV1 (47), a putative

compensation between TRP channels could affect our results and prompts for future investigation.

Research over the past decade shows the critical role of TRPA1 as a sensor of inflammation throughout the body [as summarized in (11)]. In this review the authors draw attention to the fact that there is an increasing appreciation of the role that chronic inflammation plays in tumorigenesis and of the presence of inflammation in the tumor microenvironment. A possible unknown role of TRPA1 that may contribute to the pathogenesis of cancer and other inflammatory diseases is its role in modulating the metabolism of CD8+ T cells. If true, this could serve as the mechanistic explanation as to why we observed such a great degree of delay in tumor progression in *Trpa1* $^{-/-}$ mice inoculated with melanoma cells. Moreover, it could also explain why the relative composition of the circulating and local immune cells differ so drastically in the presence and absence of this channel. And finally, more importantly, it could suggest that *Trpa1*$^{+/+}$ and *Trpa1*$^{-/-}$ CD8+ T cells would express a completely different metabolic landscape, which was one of our objectives.

Initially described as a "Warburg-like" effect (48), current knowledge states that the activation of T cells does not lead to a complete switch from mitochondrial respiration toward aerobic glycolysis. Indeed, mitochondrial oxidation plays an important role in CD8+ T cell activation, as evidenced by the deleterious effects that inhibiting mitochondrial function has on T cell differentiation (44).

During cancer progression both tumor and immune cells are in active competition for nutritional resources due to limited availability of glucose, amino acids, fatty acids and oxygen within the tumor microenvironment. Thus, a better glycolytic and oxidative metabolic capacity displayed by the *Trpa1*$^{-/-}$ CD8+ T lymphocytes could translate into a more effective clonal expansion capacity of CD8+ effector T cells, since they both rely on the coexistence of robust bioenergetic catabolism and concomitant anabolism (49).

In vitro activated mouse CD8+ T cells exhibit both higher ECAR and OCR compared with naïve T cells, indicating that both glycolysis and oxidative phosphorylation, respectively, can be engaged to meet important increased metabolic demands upon T cell activation (50). Moreover, mitochondrial oxidation is a hallmark of CD8+ T memory cell development (51). In an *in vitro* study, van der Windt and colleagues (51) have shown that memory CD8+ T cells possessed substantial mitochondrial spare respiratory capacity. They found that interleukin-15 (IL-15), a cytokine critical for CD8+ memory T cells, regulates oxidative metabolism by promoting mitochondrial biogenesis and expression of carnitine palmitoyl transferase (CPT1a), a metabolic enzyme that controls the rate-limiting step to mitochondrial fatty acid oxidation.

The development and optimal function of anticancer memory CD8+ T cells rely on efficient fatty acid oxidation and can be boosted by inhibiting glycolysis, as at least in part, this effect stems from metabolic reprogramming involving increased oxidative phosphorylation (49). This resonates with our finding showing increased oxygen consumption rates in activated *Trpa1*$^{-/-}$ CD8+ T lymphocytes.

Another interesting finding supporting our data has been recently published pertaining the roles of interleukin 2 (IL-2) and IL-21 in T CD8 cells (52), cytokines that shape CD8+ T cell differentiation. IL-2 drives terminal differentiation, generating cells that are poorly effective against tumors, while IL-21 promotes stem cell memory T cells. The authors describe that the exposure to IL-2 promoted effector-like metabolism and aerobic glycolysis, robustly inducing lactate dehydrogenase (LDH) and lactate production, whereas IL-21 elicited a state dependent on mitochondrial oxidative phosphorylation. Even more interesting, the transient inhibition of LDH in these cells enhanced the generation of memory cells capable of triggering robust antitumor responses after adoptive transfer, thus showing how important the oxidative metabolism for effector function is. Accordingly, we found that *Trpa1*$^{-/-}$ CD8+ T cells were more effective in killing tumor cells *in vitro* and *in vivo*, which highlights the importance of these immunometabolic modulatory changes exerted to immune cell function. Corroborating our experimental data, we discovered that *TRPA1* is negatively correlated with several immunological related pathways in CD8+ T cells isolated from metastatic melanoma patients. Thus, reduced *TRPA1* expression in CD8+ T cells is associated with increased immune system activation, as it has been demonstrated in our *in vitro* and *in vivo* mouse experiments.

Finally, it is known that tumor-infiltrating CD8+ T cells undergo metabolic exhaustion in the nutrient and oxygen-deprived tumor microenvironment (48). Thus, reprograming CD8+ T cell metabolism may provide important therapeutic strategies for cancer treatment. Indeed, the adoptive transfer of memory CD8+ T cells with sustained metabolic fitness may yield better antitumor protection in both mouse model and the clinic (50). Here we show that *Trpa1*$^{-/-}$ CD8+ T cells display an impressive capacity of metabolic shift with enhanced killing activity that slows down tumor progression *in vivo*. It should be mentioned that our study used one melanoma cell line (B16-F10). It is unclear whether the described events in this study would also happen in different murine and human melanoma cell lines, which is a matter of further investigation. It is an open question the role of TRPA1 channel in CD8+ T cells in a metastatic cancer model, and further studies are necessary. Moreover, we decided to study male mice to avoid confounding factors of the female gender such as estrous cycle-dependent changes in tumor development. Therefore, our findings cannot be extrapolated to females, which may be another limitation of our study. Nevertheless, our data have opened a new venue to explore this ion channel as a target for immune cell-based therapies. We hope that our findings spark a deeper investigation of TRPA1 and other TRP channels in cancer development. Within this line, our data suggest that TRPA1 could be an important player in modulating T-dependent responses in the tumor microenviroment. The modulatory role of TRPA1 channel may also affect other types of immune system and healthy cells in the tumor microenviroment, and therefore, may result in exciting putative pharmacological targets in melanoma treatment.

DATA AVAILABILITY STATEMENT

The original contributions presented in the study are included in the article/**Supplementary Material**. Further inquiries can be directed to the corresponding author.

ETHICS STATEMENT

All experimental procedures were performed according to Brazilian legislation approved by the Committee for Animal Use (CEUA IB/USP, number 255/2016, 14th of June 2016).

AUTHOR CONTRIBUTIONS

MF, LA, OD-A, NC, and AC conceptualized the study and the original hypothesis. LA together with MM collected data for mice weight, food intake, and tumor volume. MF, LA, and OD-A performed experiments, analyzed the data. GK researched the bioinformatic data together with LA. LA, MF, and OD-A wrote together the first draft of the manuscript. AC and NC supervised the study, ensuring rigorous data quality control, and contributed to the discussion, and critically revised the manuscript. All authors contributed to the article and approved the submitted version.

FUNDING

AC's lab is supported by the Sao Paulo Research Foundation (FAPESP, 2017/24615-5, and 2018/14728-0) and by the National Council of Technological and Scientific Development (CNPq 303078/2019-7). NC's lab is supported by FAPESP (2017/05264-7). MM is a Young Investigator of FAPESP (2017/26651-9). LA and OD-A are fellows of FAPESP (2018/16511-8 and 2017/16711-4, respectively). MF is supported by a fellowship of the Pew Latin American Fellow Program in the Biomedical Sciences from Pew Charitable Trusts.

ACKNOWLEDGMENTS

The authors thank Renata Alves dos Santos for providing excellent care of the mice.

SUPPLEMENTARY MATERIAL

The Supplementary Material for this article can be found online at: https://www.frontiersin.org/articles/10.3389/fonc.2021.667715/full#supplementary-material

REFERENCES

1. Sklar LR, Almutawa F, Lim HW, Hamzavi I. Effects of Ultraviolet Radiation, Visible Light, and Infrared Radiation on Erythema and Pigmentation: A Review. *Photochem Photobiol Sci* (2013) 12(1):54–64. doi: 10.1039/c2pp25152c
2. Fajuyigbe D, Young AR. The Impact of Skin Colour on Human Photobiological Responses. *Pigment Cell Melanoma Res* (2016) 29(6):607–18. doi: 10.1111/pcmr.12511
3. Matthews NH, Li WQ, Qureshi AA, Weinstock MA, Cho E. Epidemiology of Melanoma. In: WH Ward, JM Farma, editors. *Cutaneous Melanoma: Etiology and Therapy*. Brisbane (AU: Codon Publications The Authors (2017).
4. Siegel RL, Miller KD, Jemal A. Cancer Statistics, 2018. *CA Cancer J Clin* (2018) 68(1):7–30. doi: 10.3322/caac.21442
5. Guy GP Jr, Machlin SR, Ekwueme DU, Yabroff KR. Prevalence and Costs of Skin Cancer Treatment in the U.S., 2002-2006 and 2007-2011. *Am J Prev Med* (2015) 48(2):183–7. doi: 10.1016/j.amepre.2014.08.036
6. Hanahan D, Weinberg RA. Hallmarks of Cancer: The Next Generation. *Cell* (2011) 144(5):646–74. doi: 10.1016/j.cell.2011.02.013
7. Balkwill FR, Capasso M, Hagemann T. The Tumor Microenvironment At a Glance. *J Cell Sci* (2012) 125(Pt 23):5591–6. doi: 10.1242/jcs.116392
8. Fang H, Declerck YA. Targeting the Tumor Microenvironment: From Understanding Pathways to Effective Clinical Trials. *Cancer Res* (2013) 73(16):4965–77. doi: 10.1158/0008-5472.CAN-13-0661
9. Wu T, Dai Y. Tumor Microenvironment and Therapeutic Response. *Cancer Lett* (2017) 387:61–8. doi: 10.1016/j.canlet.2016.01.043
10. Gonzalez H, Hagerling C, Werb Z. Roles of the Immune System in Cancer: From Tumor Initiation to Metastatic Progression. *Genes Dev* (2018) 32(19-20):1267–84. doi: 10.1101/gad.314617.118
11. Bautista DM, Pellegrino M, Tsunozaki M. TRPA1: A Hatekeeper for Inflammation. *Annu Rev Physiol* (2013) 75:181–200. doi: 10.1146/annurev-physiol-030212-183811
12. Kaneko Y, Szallasi A. Transient Receptor Potential (TRP) Channels: A Clinical Perspective. *Brit J Pharmacol* (2014) 171(10):2474–507. doi: 10.1111/bph.12414
13. Yue Z, Xie J, Yu AS, Stock J, Du J, Yue L. Role of TRP Channels in the Cardiovascular System. *Am J Physiol Heart Circ Physiol* (2015) 308(3):H157–82. doi: 10.1152/ajpheart.00457.2014
14. Dhakal S, Lee Y. Transient Receptor Potential Channels and Metabolism. *Mol Cells* (2019) 42(8):569–78. doi: 10.14348/molcells.2019.0007
15. Falcon D, Galeano-Otero I, Calderon-Sanchez E, Del Toro R, Martin-Bornez M, Rosado JA, et al. TRP Channels: Current Perspectives in the Adverse Cardiac Remodeling. *Front Physiol* (2019) 10:159. doi: 10.3389/fphys.2019.00159
16. Minke B. The History of the Drosophila TRP Channel: The Birth of a New Channel Superfamily. *J Neurogenet* (2010) 24(4):216–33. doi: 10.3109/01677063.2010.514369
17. Santoni G, Maggi F, Morelli MB, Santoni M, Marinelli O. Transient Receptor Potential Cation Channels in Cancer Therapy. *Med Sci (Basel)* (2019) 7(12):1–23. doi: 10.3390/medsci7120108
18. Buck MD, Sowell RT, Kaech SM, Pearce EL. Metabolic Instruction of Immunity. *Cell* (2017) 169(4):570–86. doi: 10.1016/j.cell.2017.04.004
19. Chang CH, Qiu J, O'Sullivan D, Buck MD, Noguchi T, Curtis JD, et al. Metabolic Competition in the Tumor Microenvironment is a Driver of Cancer Progression. *Cell* (2015) 162(6):1229–41. doi: 10.1016/j.cell.2015.08.016
20. Gupta S, Roy A, Dwarakanath BS. Metabolic Cooperation and Competition in the Tumor Microenvironment: Implications for Therapy. *Front Oncol* (2017) 7:68. doi: 10.3389/fonc.2017.00068
21. Kedia-Mehta N, Finlay DK. Competition for Nutrients and its Role in Controlling Immune Responses. *Nat Commun* (2019) 10(1):2123. doi: 10.1038/s41467-019-10015-4
22. Fernandes ES, Fernandes MA, Keeble JE. The Functions of TRPA1 and TRPV1: Moving Away From Sensory Nerves. *Br J Pharmacol* (2012) 166(2):510–21. doi: 10.1111/j.1476-5381.2012.01851.x
23. Parenti A, De Logu F, Geppetti P, Benemei S. What is the Evidence for the Role of TRP Channels in Inflammatory and Immune Cells? *Br J Pharmacol* (2016) 173(6):953–69. doi: 10.1111/bph.13392
24. de Assis LVM, Moraes MN, Magalhaes-Marques KK, Kinker GS, da Silveira Cruz-Machado S, Castrucci AML. Non-Metastatic Cutaneous Melanoma

Induces Chronodisruption in Central and Peripheral Circadian Clocks. *Int J Mol Sci* (2018) 19(4):1–24. doi: 10.3390/ijms19041065
25. Tomayko MM, Reynolds CP. Determination of Subcutaneous Tumor Size in Athymic (Nude) Mice. *Cancer Chemother Pharmacol* (1989) 24(3):148–54. doi: 10.1007/BF00300234
26. de Assis LV, Moraes MN, da Silveira Cruz-Machado S, Castrucci AM. The Effect of White Light on Normal and Malignant Murine Melanocytes: A Link Between Opsins, Clock Genes, and Melanogenesis. *Biochim Biophys Acta* (2016) 1863(6 Pt A):1119–33. doi: 10.1016/j.bbamcr.2016.03.001
27. Livak KJ, Schmittgen TD. Analysis of Relative Gene Expression Data Using Real-Time Quantitative PCR and the 2(-Delta Delta C(T)) Method. *Methods* (2001) 25(4):402–8. doi: 10.1006/meth.2001.1262
28. Tau GZ, Cowan SN, Weisburg J, Braunstein NS, Rothman PB. Regulation of IFN-gamma Signaling is Essential for the Cytotoxic Activity of CD8(+) T Cells. *J Immunol* (2001) 167(10):5574–82. doi: 10.4049/jimmunol.167.10.5574
29. Nguyen HH, Kim T, Song SY, Park S, Cho HH, Jung SH, et al. Naive CD8(+) T Cell Derived Tumor-Specific Cytotoxic Effectors as a Potential Remedy for Overcoming TGF-beta Immunosuppression in the Tumor Microenvironment. *Sci Rep* (2016) 6:28208. doi: 10.1038/srep28208
30. Parrot T, Oger R, Allard M, Desfrancois J, Raingeard de la Bletiere D, Coutolleau A, et al. Transcriptomic Features of Tumour-Infiltrating CD4 (low)CD8(high) Double Positive Alphabeta T Cells in Melanoma. *Sci Rep* (2020) 10(1):5900. doi: 10.1038/s41598-020-62664-x
31. Subramanian A, Tamayo P, Mootha VK, Mukherjee S, Ebert BL, Gillette MA, et al. Gene Set Enrichment Analysis: A Knowledge-Based Approach for Interpreting Genome-Wide Expression Profiles. *Proc Natl Acad Sci USA* (2005) 102(43):15545–50. doi: 10.1073/pnas.0506580102
32. Croft D, O'Kelly G, Wu G, Haw R, Gillespie M, Matthews L, et al. Reactome: A Database of Reactions, Pathways and Biological Processes. *Nucleic Acids Res* (2011) 39(Database issue):D691–7. doi: 10.1093/nar/gkq1018
33. Kanehisa M, Goto S. KEGG: Kyoto Encyclopedia of Genes and Genomes. *Nucleic Acids Res* (2000) 28(1):27–30.
34. Liberzon A, Birger C, Thorvaldsdóttir H, Ghandi M, Mesirov JP, Tamayo P. The Molecular Signatures Database (MsigDB) Hallmark Gene Set Collection. *Cell Syst* (2015) 1(6):417–25. doi: 10.1016/j.cels.2015.12.004
35. Cancer Genome Atlas N. Genomic Classification of Cutaneous Melanoma. *Cell* (2015) 161(7):1681–96. doi: 10.1016/j.cell.2015.05.044
36. Goldman MJ, Craft B, Hastie M, Repečka K, McDade F, Kamath A, et al. Visualizing and Interpreting Cancer Genomics Data Via the Xena Platform. *Nat Biotechnol* (2020) 38(6):675–8. doi: 10.1038/s41587-020-0546-8
37. Newman AM, Steen CB, Liu CL, Gentles AJ, Chaudhuri AA, Scherer F, et al. Determining Cell Type Abundance and Expression From Bulk Tissues With Digital Cytometry. *Nat Biotechnol* (2019) 37(7):773–82. doi: 10.1038/s41587-019-0114-2
38. Uchida K, Dezaki K, Yoneshiro T, Watanabe T, Yamazaki J, Saito M, et al. Involvement of Thermosensitive TRP Channels in Energy Metabolism. *J Physiol Sci* (2017) 67(5):549–60. doi: 10.1007/s12576-017-0552-x
39. Antoniazzi CTD, Nassini R, Rigo FK, Milioli AM, Bellinaso F, Camponogara C, et al. Transient Receptor Potential Ankyrin 1 (TRPA1) Plays a Critical Role in a Mouse Model of Cancer Pain. *Int J Cancer* (2019) 144(2):355–65. doi: 10.1002/ijc.31911
40. Fu C, Jiang A. Dendritic Cells and CD8 T Cell Immunity in Tumor Microenvironment. *Front Immunol* (2018) 9:3059. doi: 10.3389/fimmu.2018.03059
41. Reading JL, Galvez-Cancino F, Swanton C, Lladser A, Peggs KS, Quezada SA. The Function and Dysfunction of Memory CD8(+) T Cells in Tumor Immunity. *Immunol Rev* (2018) 283(1):194–212. doi: 10.1111/imr.12657
42. Jameson SC, Masopust D. Understanding Subset Diversity in T Cell Memory. *Immunity* (2018) 48(2):214–26. doi: 10.1016/j.immuni.2018.02.010
43. Ando M, Ito M, Srirat T, Kondo T, Yoshimura A. Memory T Cell, Exhaustion, and Tumor Immunity. *Immunol Med* (2020) 43(1):1–9. doi: 10.1080/25785826.2019.1698261
44. Raud B, McGuire PJ, Jones RG, Sparwasser T, Berod L. Fatty Acid Metabolism in CD8(+) T Cell Memory: Challenging Current Concepts. *Immunol Rev* (2018) 283(1):213–31. doi: 10.1111/imr.12655
45. Bertin S, Raz E. Transient Receptor Potential (TRP) Channels in T Cells. *Semin Immunopathol* (2016) 38(3):309–19. doi: 10.1007/s00281-015-0535-z
46. Sahoo SS, Majhi RK, Tiwari A, Acharya T, Kumar PS, Saha S, et al. Transient Receptor Potential Ankyrin1 Channel is Endogenously Expressed in T Cells and is Involved in Immune Functions. *Biosci Rep* (2019) 39(9):1–16. doi: 10.1042/BSR20191437
47. Fischer MJ, Balasuriya D, Jeggle P, Goetze TA, McNaughton PA, Reeh PW, et al. Direct Evidence for Functional TRPV1/TRPA1 Heteromers. *Pflugers Arch* (2014) 466(12):2229–41. doi: 10.1007/s00424-014-1497-z
48. Kouidhi S, Elgaaied AB, Chouaib S. Impact of Metabolism on T-Cell Differentiation and Function and Cross Talk With Tumor Microenvironment. *Front Immunol* (2017) 8:270. doi: 10.3389/fimmu.2017.00270
49. Bantug GR, Galluzzi L, Kroemer G, Hess C. The Spectrum of T Cell Metabolism in Health and Disease. *Nat Rev Immunol* (2018) 18(1):19–34. doi: 10.1038/nri.2017.99
50. Zhang L, Romero P. Metabolic Control of CD8(+) T Cell Fate Decisions and Antitumor Immunity. *Trends Mol Med* (2018) 24(1):30–48. doi: 10.1016/j.molmed.2017.11.005
51. van der Windt GJ, Everts B, Chang CH, Curtis JD, Freitas TC, Amiel E, et al. Mitochondrial Respiratory Capacity is a Critical Regulator of CD8+ T Cell Memory Development. *Immunity* (2012) 36(1):68–78. doi: 10.1016/j.immuni.2011.12.007
52. Hermans D, Gautam S, García-Cañaveras JC, Gromer D, Mitra S, Spolski R, et al. Lactate Dehydrogenase Inhibition Synergizes With IL-21 to Promote CD8+ T Cell Stemness and Antitumor Immunity. *Proc Natl Acad Sci USA* (2020) 117(11):6047–55. doi: 10.1073/pnas.1920413117

Conflict of Interest: The authors declare that the research was conducted in the absence of any commercial or financial relationships that could be construed as a potential conflict of interest.

Citation: *Forni MF, Domínguez-Amorocho OA, de Assis LVM, Kinker GS, Moraes MN, Castrucci AML and Câmara NOS (2021) An Immunometabolic Shift Modulates Cytotoxic Lymphocyte Activation During Melanoma Progression in TRPA1 Channel Null Mice.*
Front. Oncol. 11:667715. doi: 10.3389/fonc.2021.667715

Copyright © 2021 Forni, Domínguez-Amorocho, de Assis, Kinker, Moraes, Castrucci and Câmara. This is an open-access article distributed under the terms of the Creative Commons Attribution License (CC BY). The use, distribution or reproduction in other forums is permitted, provided the original author(s) and the copyright owner(s) are credited and that the original publication in this journal is cited, in accordance with accepted academic practice. No use, distribution or reproduction is permitted which does not comply with these terms.

frontiers in Oncology

ORIGINAL RESEARCH
published: 24 May 2021
doi: 10.3389/fonc.2021.672172

Early Exanthema Upon Vemurafenib Plus Cobimetinib Is Associated With a Favorable Treatment Outcome in Metastatic Melanoma: A Retrospective Multicenter DeCOG Study

Katharina C. Kähler[1], Ralf Gutzmer[2], Friedegrund Meier[3,4], Lisa Zimmer[5], Markus Heppt[6], Anja Gesierich[7], Kai-Martin Thoms[8], Jochen Utikal[9,10], Jessica C. Hassel[11], Carmen Loquai[12], Claudia Pföhler[13], Lucie Heinzerling[6,14], Martin Kaatz[15], Daniela Göppner[16], Annette Pflugfelder[17], Ann-Sophie Bohne[1], Imke Satzger[2], Lydia Reinhardt[3,4], Jan-Malte Placke[5], Dirk Schadendorf[5] and Selma Ugurel[5]*

[1] Department of Dermatology, University Hospital Schleswig-Holstein (UKSH), Kiel, Germany, [2] Department of Dermatology, University Hospital Hannover, Hannover, Germany, [3] Skin Cancer Center, National Center for Tumor Diseases, University Cancer Centre Dresden, Dresden, Germany, [4] Department of Dermatology, TU Dresden, University Hospital Carl Gustav Carus, Dresden, Germany, [5] Department of Dermatology, University Hospital Essen, German Cancer Consortium (DKTK), Essen, Germany, [6] Department of Dermatology, Universitätsklinikum Erlangen, Friedrich-Alexander University Erlangen-Nürnberg, Erlangen, Germany, [7] Department of Dermatology, University Hospital Würzburg, Würzburg, Germany, [8] Department of Dermatology, University Medical Center Göttingen, Göttingen, Germany, [9] Skin Cancer Unit, German Cancer Research Center (DKFZ), Heidelberg, Germany, [10] Department of Dermatology, Venereology and Allergology, University Medical Center Mannheim, Ruprecht-Karl University of Heidelberg, Mannheim, Germany, [11] Department of Dermatology, University Hospital Heidelberg, Heidelberg, Germany, [12] Department of Dermatology, University Hospital Mainz, Mainz, Germany, [13] Department of Dermatology, University Hospital Homburg, Homburg, Germany, [14] Department of Dermatology and Allergology, Ludwig-Maximilian University, München, Germany, [15] Department of Dermatology, SRH Waldklinikum, Gera, Germany, [16] Department of Dermatology, University Hospital Giessen, Gießen, Germany, [17] Department of Dermatology, University Hospital Tübingen, Tübingen, Germany

OPEN ACCESS

Edited by:
Colette Pameijer, Pennsylvania State University, United States

Reviewed by:
Gagan Chhabra, University of Wisconsin-Madison, United States
Xiu-Qiong Fu, Hong Kong Baptist University, China

***Correspondence:**
Katharina C. Kähler
kkaehler@dermatology.uni-kiel.de

Specialty section:
This article was submitted to Skin Cancer, a section of the journal Frontiers in Oncology

Received: *25 February 2021*
Accepted: *26 April 2021*
Published: *24 May 2021*

Citation:
Kähler KC, Gutzmer R, Meier F, Zimmer L, Heppt M, Gesierich A, Thoms K-M, Utikal J, Hassel JC, Loquai C, Pföhler C, Heinzerling L, Kaatz M, Göppner D, Pflugfelder A, Bohne A-S, Satzger I, Reinhardt L, Placke J-M, Schadendorf D and Ugurel S (2021) Early Exanthema Upon Vemurafenib Plus Cobimetinib Is Associated With a Favorable Treatment Outcome in Metastatic Melanoma: A Retrospective Multicenter DeCOG Study. Front. Oncol. 11:672172. doi: 10.3389/fonc.2021.672172

Background: The combination of BRAF and MEK inhibitors has become standard of care in the treatment of metastatic BRAF V600-mutated melanoma. Clinical factors for an early prediction of tumor response are rare. The present study investigated the association between the development of an early exanthema induced by vemurafenib or vemurafenib plus cobimetinib and therapy outcome.

Methods: This multicenter retrospective study included patients with BRAF V600-mutated irresectable AJCC-v8 stage IIIC/D to IV metastatic melanoma who received treatment with vemurafenib (VEM) or vemurafenib plus cobimetinib (COBIVEM). The development of an early exanthema within six weeks after therapy start and its grading according to CTCAEv4.0 criteria was correlated to therapy outcome in terms of best overall response, progression-free (PFS), and overall survival (OS).

Results: A total of 422 patients from 16 centers were included (VEM, n=299; COBIVEM, n=123). 20.4% of VEM and 43.1% of COBIVEM patients developed an early exanthema.

In the VEM cohort, objective responders (CR/PR) more frequently presented with an early exanthema than non-responders (SD/PD); 59.0% versus 38.7%; p=0.0027. However, median PFS and OS did not differ between VEM patients with or without an early exanthema (PFS, 6.9 versus 6.0 months, p=0.65; OS, 11.0 versus 12.4 months, p=0.69). In the COBIVEM cohort, 66.0% of objective responders had an early exanthema compared to 54.3% of non-responders (p=0.031). Median survival times were significantly longer for patients who developed an early exanthema compared to patients who did not (PFS, 9.7 versus 5.6 months, p=0.013; OS, not reached versus 11.6 months, p=0.0061). COBIVEM patients with a mild early exanthema (CTCAEv4.0 grade 1-2) had a superior survival outcome as compared to COBIVEM patients with a severe (CTCAEv4.0 grade 3-4) or non early exanthema, respectively (p=0.047). This might be caused by the fact that 23.6% of patients with severe exanthema underwent a dose reduction or discontinuation of COBIVEM compared to only 8.9% of patients with mild exanthema.

Conclusions: The development of an early exanthema within 6 weeks after treatment start indicates a favorable therapy outcome upon vemurafenib plus cobimetinib. Patients presenting with an early exanthema should therefore be treated with adequate supportive measures to provide that patients can stay on treatment.

Keywords: melanoma, vemurafenib, cobimetinib, BRAF/MEK inhibition, skin toxicity, therapy outcome

INTRODUCTION

Melanoma patients treated with BRAF and MEK inhibitors frequently develop an exanthema, also referred to as "skin rash" by non-dermatologists. This exanthema is typically characterized by inflammatory macules and papules but may also present with pustules or urticae. Its first signs commonly show within the first four to six weeks after therapy start. In the pivotal COBRIM trial the incidence of a skin rash upon monotherapy with vemurafenib was reported to be around 67.5% and during combination therapy with vemurafenib/cobimetinib the incidence was slightly higher with 72.5% (1). However, the term "skin rash" covers a variety of cutaneous side effects and thus cannot be equated with exanthema. Studies of EGFR inhibitors demonstrated an association of skin rash development with an improved therapy outcome in various cancer entities including colorectal carcinoma, head-and-neck squamous cell carcinoma, non-small cell lung cancer, prostate cancer, gastro-esophageal cancer, pancreatic adenocarcinoma and cutaneous squamous cell carcinoma (2, 3). Thus, in these cancer entities patients presenting with a skin rash under EGFR inhibitor therapy are encouraged to continue this treatment with the prospect of an increased probability of a favorable treatment outcome. For BRAF and MEK inhibition in metastatic melanoma, so far, no correlation has been reported between treatment efficacy and outcome and the occurrence of cutaneous side effects.

The present study was aimed to investigate the frequency and severity of an early exanthema upon BRAF and MEK inhibition with vemurafenib alone or combined with cobimetinib and its association with therapy outcome in patients with metastatic melanoma.

PATIENTS AND METHODS

This multicenter retrospective study was initiated by the Dermatologic Cooperative Oncology Group (DeCOG), and undertaken with Ethics Committee approval (Hannover University Medical School, 1612-2012). Patients were identified for study inclusion at clinical centers of the DeCOG based on the following eligibility criteria: histologically proven diagnosis of melanoma, unresectable metastatic disease in stage III or IV following the American Joint Committee on Cancer version 8 (AJCCv8) criteria (4), detection of a BRAF V600 mutation in the tumor tissue, treatment with vemurafenib as a single agent (VEM) or as the combination of cobimetinib plus vemurafenib (COBIVEM) within a time frame of June 01, 2012 and April 30, 2018, either as per clinical trial or *via* prescription, and availability of follow-up data after treatment start including adverse events, response and survival. The patients were identified at the centers *via* their digital hospital information systems or by chart review, and the requested data were extracted from the respective patient files.

Data Collection

The requested data were collected on standardized electronic case report forms and merged in one central database for analysis. The data comprised patient demographics, BRAF V600 mutation subtype, sites of metastasis, overall performance status (OPS) graded by Eastern Cooperative Oncology Group (ECOG) criteria, and serum LDH activity, all at onset of VEM or COBIVEM therapy. For categorization of metastatic sites, we used the AJCCv8 M category by grouping by localization of metastases regardless of serum LDH activity. The used groups were (a) metastases to skin and/or lymph nodes (skin/LN), (b) metastases to the lung (lung),

(c) metastases to other organs (other organs), and (d) metastases to the brain (brain). Data on other systemic treatments received by the patients before VEM or COBIVEM were recorded as previous treatments. This pre-treatment was categorized into (a) regimens containing immune checkpoint inhibitors (checkpoint inhibition), and (b) regimens containing kinase inhibitors (BRAF/MEK inhibition). Collected data on the course and outcome of VEM or COBIVEM therapy included therapy duration, best response following RECIST criteria (5) categorizing into complete response (CR), partial response (PR), stable disease (SD), and progressive disease (PD), as well as progression-free (PFS) and overall survival (OS). Patients were grouped into either objective responders (CR +PR) or non-responders (SD+PD). An exanthema presenting within the first six weeks after start of VEM or COBIVEM therapy was considered as an early exanthema, regardless of its morphology (macular, papular, pustular, urticae). The severity of the exanthema was graded according to CTCAEv4.0 (grade 1, <10% body surface area (BSA); grade 2, 10-30% BSA; grade 3, 30-100% BSA; grade 4, 100% BSA and/or severe reduction of general condition; grade 5, death) (6).

Statistical Analysis

Data analysis was performed between January 01 and March 31, 2019. Survival (PFS, OS) was calculated from onset of VEM or COBIVEM until death or disease progression, respectively. If no such event occurred, the date of last patient contact was used as survival end point (censored observation). Survival curves, hazard ratios, and median survival times were calculated using the Kaplan–Meier method for censored failure time data. The log-rank test was used for comparison of survival probabilities between groups. Differences between groups were calculated using Fisher's exact test or Chi square test. P<0.05 was considered statistically significant.

RESULTS

Patient Characteristics and Early Exanthema

Data were collected of 422 patients at 16 clinical cancer centers in Germany. In total, 299 patients received VEM, 123 patients received COBIVEM. The patient flow is shown in **Figure 1**; detailed patient characteristics are presented in **Tables 1**, **2**. An early exanthema occurring within the first 6 weeks after start of therapy occurred in 61 VEM patients (20.4%) (CTCAE grade 1, 62.3%; grade 2, 22.9%; grade 3, 11.4%; and grade 4, 3.2%) and in 53 COBIVEM patients (43.1%) (CTCAE grade 1, 28.3%; grade 2, 22.6%; grade 3, 45.2%; and grade 4, 3.7%). Representative patients from both cohorts are demonstrated in **Figure 2**. In the VEM cohort, most patient characteristics at therapy start were balanced between groups with and without occurrence of an early exanthema, besides patients' sex with females more often represented within the group of patients developing early exanthema than males (p=0.043; **Table 1**). In the COBIVEM cohort, the overall performance status at therapy start differed significantly between groups with and without occurrence of an early exanthema with patients presenting at ECOG 0 being strongly over-represented in the group developing an early exanthema (p=0.0058; **Table 2**). Age or LDH were not identified to be an influencing factor for the incidence of early exanthema (p= 0.11, **Table 2**).

VEM and COBIVEM Therapy and Outcome

All patients started with the initial doses of 960 mg vemurafenib orally b.i.d. (VEM) or vemurafenib 960 mg orally b.i.d. plus cobimetinib 60 mg orally once daily (COBIVEM). Due to the occurrence of an early exanthema, 32.7% of VEM patients and 26.8% of COBIVEM patients had a dose reduction, and 11.4% of VEM and 5.7% of COBIVEM patients had a therapy discontinuation. At database closure on September 30, 2019, the median follow-up time was 21.6 months. 48.2% of the VEM patients and 30.1% of the COBIVEM patients had died. Of the patients alive, 27.4% were still on VEM treatment, and 30.8% on COBIVEM treatment.

As best overall response, 4.0% of VEM patients achieved a CR, 53.8% achieved a PR, 22.1% showed a SD, and 15.7% revealed a disease progression. 4.3% of the patients were not evaluable for treatment response due to other reasons. Patients presenting an early exanthema upon VEM revealed a superior therapy response with an objective response rate (CR+PR) of 59.0% in patients showing an early exanthema versus 38.7% in patients without this cutaneous reaction (p=0.0027; **Table 1**). In the patient cohort treated with COBIVEM, 10.6% of patients achieved a CR, 48.8% achieved a PR, 18.7% showed a SD, and 14.6% revealed disease progression. 7.3% of the patients were not evaluable for therapy response. Here again, patients showing an early exanthema upon treatment had a higher objective response rate than patients who did not (66.0% versus 54.3%; p=0.031; **Table 2**).

With regard to survival after therapy start, for patients treated with VEM median PFS and OS were not significantly different for patients with or without an early exanthema (6.9 versus 6.0 months, p=0.65; 11.0 versus 12.4 months, p=0.69 respectively, **Figures 3A, B**). Additionally, the respective Kaplan-Meier survival curves were almost identical in shape and were crossing each other repeatedly. In contrast, for patients treated with COBIVEM survival after therapy start was significantly better in patients presenting an early exanthema. Median PFS and OS were significantly prolonged in patients showing an early exanthema versus patients who did not (PFS, 9.7 versus 5.6 months, p=0.013; OS, not reached versus 11.6 months, p=0.0061; **Figures 4A, B**). With regard to the severity of the early exanthema, patients who developed a mild exanthema (CTCAE grade 1-2) had a superior outcome in terms of PFS and OS compared to patients who developed a severe (CTCAE grade 3-4) exanthema or patients who developed no exanthema (p=0.047, **Figures 4C, D**).

DISCUSSION

Vemurafenib is a selective inhibitor of V600-mutated BRAF, and was the first-in-class mitogen-activated protein (MAP) kinase

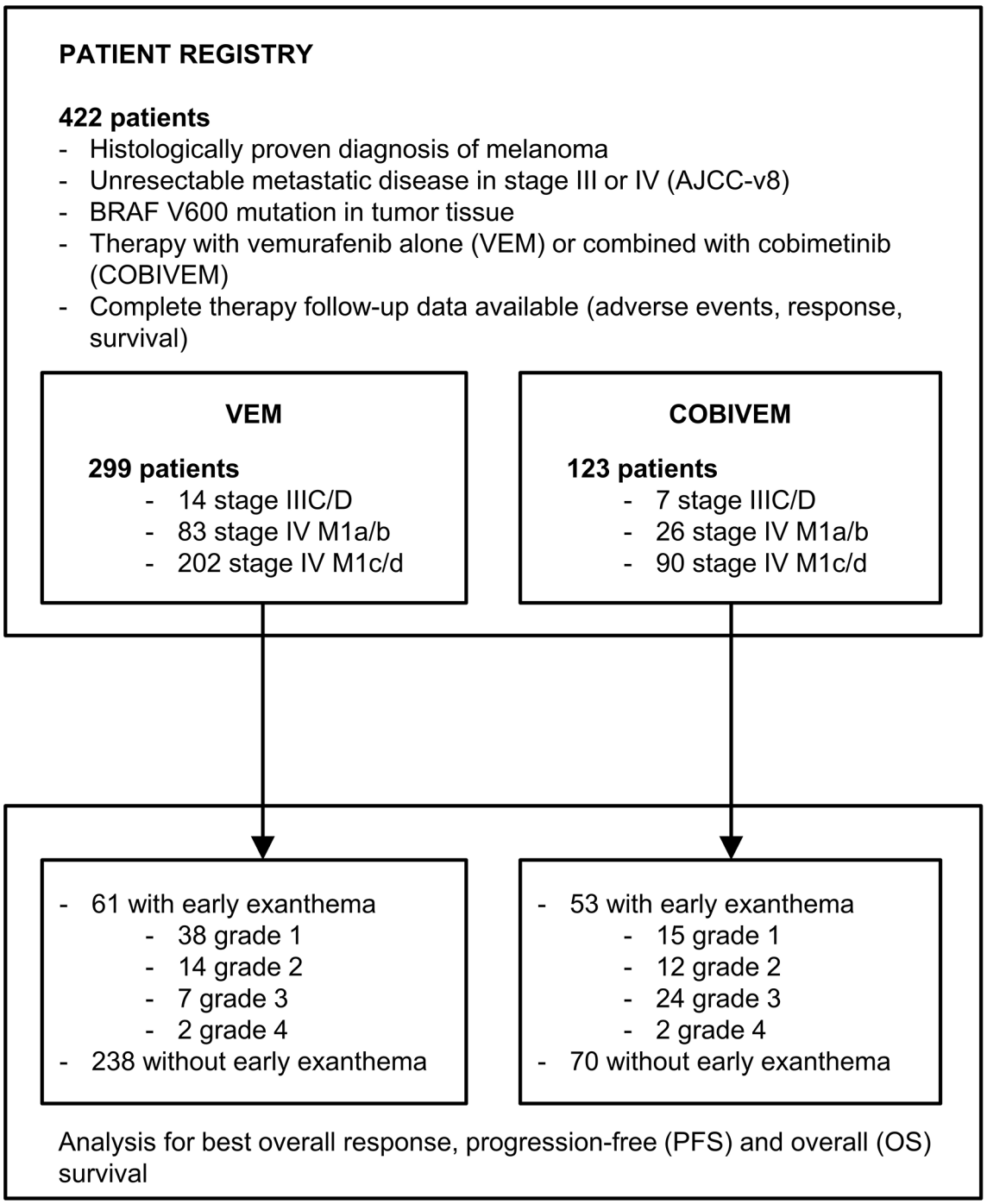


FIGURE 1 | Schematic presentation of the study patient flow into patient registry. Patient inclusion criteria and grading of the early exanthemas was performed according to CTCAEv4.0 (grade 1, <10% body surface area (BSA); grade 2, 10-30% BSA; grade 3, 30-100% BSA; grade 4, 100% BSA and/or severe reduction of general condition).

pathway inhibitor approved for the treatment of melanoma (7). Subsequently, the combination therapy of vemurafenib together with the MEK inhibitor cobimetinib was approved for metastatic melanoma due to the significant prolongation of survival times shown by clinical trial data (1, 8). Nevertheless, predictive markers of the treatment outcome of either vemurafenib monotherapy or vemurafenib plus cobimetinib combination therapy are rare and most often characterized by low

TABLE 1 | Patients treated with vemurafenib (VEM).

	Total n=299 (100%)	Early exanthema n=61 (100%)	No early exanthema n=238 (100%)	P-value	Relative risk
Patient characteristics at therapy start					
Sex					
male	164 (54.8%)	26 (42.6%)	138 (58.0%)		
female	135 (45.2%)	35 (57.4%)	100 (42.0%)	**0.043**	1.64
Age at treatment onset					
≤65 years	199 (66.6%)	39 (63.9%)	160 (67.2%)		
>65 years	100 (33.4%)	22 (36.1%)	78 (32.8%)	0.65	1.12
Localisation of primary					
skin	248 (82.9%)	50 (82.0%)	198 (83.2%)		
occult (MUP)	51 (17.1%)	11 (18.0%)	40 (16.8%)	0.85	1.07
Pre-treatment in stage III/IV					
no	169 (56.5%)	30 (49.2%)	139 (58.4%)		
yes	130 (43.5%)	31 (50.8%)	99 (41.6%)	0.25	1.34
BRAF/MEK inhibition	0 (0.0%)	0 (0.0%)	0 (0.0%)		
checkpoint inhibition	25 (8.4%)	6 (9.8%)	19 (8.0%)		
chemotherapy	127 (42.5%)	30 (49.2%)	87 (36.6%)		
Serum LDH					
normal (≤ULN)	150 (50.2%)	30 (49.2%)	120 (50.4%)		
elevated (>ULN)	149 (49.8%)	31 (50.8%)	118 (49.6%)	0.89	1.04
OPS (ECOG)					
0	177 (59.2%)	39 (63.9%)	138 (58.0%)		
≥1	110 (36.8%)	15 (24.6%)	95 (39.9%)	0.088	0.62
not specified	12 (4.0%)	7 (11.5%)	5 (2.1%)		
Stage (sites of metastasis)					
IIIC/D (skin/LN)	14 (4.7%)	8 (13.1%)	6 (2.5%)		
IV M1a (skin/LN)	46 (15.4%)	6 (9.8%)	40 (16.8%)		
IV M1b (lung)	37 (12.4%)	4 (6.6%)	33 (13.9%)		
IV M1c/d (other organ/brain)	202 (67.6%)	43 (70.5%)	159 (66.8%)	0.15	
BRAF V600 mutation status					
V600E	169 (56.5%)	34 (55.7%)	135 (56.7%)		
V600K	24 (8.0%)	5 (8.2%)	19 (8.0%)		
V600D	1 (0.3%)	0 (0.0%)	1 (0.4%)		
not further specified	105 (35.1%)	22 (36.1%)	83 (34.9%)	0.96	
Therapy outcome					
Best overall response					
CR	12 (4.0%)	3 (4.9%)	9 (3.8%)		
PR	161 (53.8%)	33 (54.1%)	128 (53.8%)		
SD	66 (22.1%)	15 (24.6%)	51 (21.4%)		
PD	47 (15.7%)	6 (9.8%)	41 (17.2%)		
NE	13 (4.3%)	4 (6.6%)	9 (3.8%)		
objective response (CR + PR)	128 (42.8%)	36 (59.0%)	92 (38.7%)	**0.0027**	**2.12**
Disease progression	207 (69.2%)	47 (77.0%)	160 (67.2%)		
Median PFS	6.3 months	6.9 months	6.0 months	0.65	HR=1.08
Death	144 (48.2%)	33 (54.1%)	111 (46.6%)		
Median OS	12.0 months	11.0 months	12.4 months	0.69	HR=1.09

The given patient characteristics refer to the start of vemurafenib (VEM) therapy. Percentages are given per column. Stage categories refer to the AJCCv8 classification system. Pre-treatment describes systemic therapies received by the patient for inoperable stage III or IV disease (non-adjuvant) prior to VEM therapy. Patient groups with and without early exanthema were compared by Fisher's exact test or Chi square test; results are given by p-values, relative risks or hazard ratios. MUP, melanoma of unknown primary; LDH, lactate dehydrogenase; ULN, upper limit of normal; OPS, overall performance status; CR, complete response; PR, partial response; SD, stable disease; PD, progressive disease; NE, not evaluable.
Bold means statistically significant.

specificity. Elevated serum LDH, as well as multiple organ involvement by metastases were shown to be associated with a less favorable treatment outcome of BRAF/MEK inhibition (9). However, these parameters are likewise associated with a poor treatment outcome upon immune checkpoint inhibition (10). Thus, other biomarkers associated with treatment outcome are urgently required to indicate a patient's individual probability to benefit from vemurafenib/cobimetinib therapy. Optimally, these markers are detectable immediately before treatment start. However, biomarkers which become evident shortly after treatment start like cutaneous adverse events may also be of great help.

So far, only one retrospective analysis showed a possible correlation between the cutaneous side effects panniculitis and vitiligo-like lesions and the treatment outcome upon the BRAF plus MEK inhibitor combination dabrafenib and trametinib (11). Another retrospective case series showed a correlation between different cutaneous and extra-cutaneous adverse events including vitiligo, erythema nodosum, uveitis and keratitis sicca and the treatment outcome upon BRAF inhibitors either administered alone or in combination with MEK inhibitors (12). However, all these adverse events were reported in patients under BRAF/MEK inhibition, but at low frequencies and thus are of

TABLE 2 | Patients treated with cobimetinib plus vemurafenib (COBIVEM).

	Total n=123 (100%)	Early exanthema n=53 (100%)	No early exanthema n=70 (100%)	P-value	Relative risk
Patient characteristics at therapy start					
Sex					
male	69 (56.1%)	27 (50.9%)	42 (60.0%)		
female	54 (43.9%)	26 (49.1%)	28 (40.0%)	0.36	1.23
Age at treatment onset					
≤65 years	88 (71.5%)	42 (79.2%)	46 (65.7%)		
>65 years	35 (28.5%)	11 (20.8%)	24 (34.3%)	0.11	0.66
Localisation of primary					
skin	108 (87.8%)	47 (88.7%)	61 (87.1%)		
occult (MUP)	15 (12.2%)	6 (11.3%)	9 (12.9%)	1.0	0.92
Pre-treatment in stage III/IV					
no	55 (44.7%)	24 (45.3%)	31 (44.3%)		
yes	68 (55.3%)	29 (54.7%)	39 (55.7%)	1.0	0.98
BRAF/MEK inhibition	43 (34.9%)	12 (22.6%)	31 (44.3%)		
checkpoint inhibition	44 (35.8%)	17 (32.1%)	27 (38.6%)	0.36	1.38
Serum LDH					
normal (≤ULN)	72 (58.5%)	31 (58.5%)	41 (58.6%)		
elevated (>ULN)	51 (41.5%)	22 (41.5%)	29 (41.4%)	1.0	1.0
OPS (ECOG)					
0	83 (67.5%)	42 (79.2%)	41 (58.6%)		
≥1	38 (30.9%)	9 (17.0%)	29 (41.4%)	**0.0058**	0.47
not specified	2 (1.6%)	2 (3.8%)	0 (0.0%)		
Stage (sites of metastasis)					
IIIC/D (skin/LN)	7 (5.7%)	1 (1.9%)	6 (8.6%)		
IV M1a (skin/LN)	13 (10.6%)	7 (13.2%)	6 (8.6%)		
IV M1b (lung)	13 (10.6%)	8 (15.1%)	5 (7.1%)		
IV M1c/d (other organ/brain)	90 (73.1%)	37 (69.8%)	53 (75.7%)	0.18	
BRAF V600 mutation status					
V600E	92 (74.8%)	39 (73.6%)	53 (75.7%)		
V600K	15 (12.2%)	6 (11.3%)	9 (12.9%)		
V600R	2 (1.6%)	1 (1.9%)	1 (1.4%)		
V600D	1 (0.8%)	1 (1.9%)	0 (0.0%)		
K601E	1 (0.8%)	0 (0.0%)	1 (1.4%)		
not further specified	12 (9.8%)	6 (11.3%)	6 (8.6%)	0.79	
Therapy outcome					
Best overall response					
CR	13 (10.6%)	8 (15.1%)	5 (7.1%)		
PR	60 (48.8%)	27 (50.9%)	33 (47.1%)		
SD	23 (18.7%)	8 (15.1%)	15 (21.4%)		
PD	18 (14.6%)	3 (5.7%)	15 (21.4%)		
NE	9 (7.3%)	7 (13.2%)	2 (2.9%)		
objective response (CR + PR)	73 (59.3%)	35 (66.0%)	38 (54.3%)	**0.031**	1.79
Disease progression	77 (62.6%)	30 (56.6%)	47 (67.1%)		
Median PFS	7.3 months	9.7 months	5.6 months	**0.013**	HR=0.55
Death	37 (30.1%)	7 (13.2%)	30 (42.9%)		
Median OS	not reached	not reached	11.6 months	**0.0061**	HR=0.39

The given patient characteristics refer to the start of cobimetinib plus vemurafenib (COBIVEM) therapy. Percentages are given per column. Stage categories refer to the AJCCv8 classification system. Pre-treatment describes systemic therapies received by the patient for inoperable stage III or IV disease (non-adjuvant) prior to COBIVEM therapy. Patient groups with and without early exanthema were compared by Fisher's exact test or Chi square test; results are given by p-values, relative risks or hazard ratios. MUP, melanoma of unknown primary; LDH, lactate dehydrogenase; ULN, upper limit of normal; OPS, overall performance status; CR, complete response; PR, partial response; SD, stable disease; PD, progressive disease; NE, not evaluable.

Bold means statistically significant.

little use as predictive markers of treatment response in the majority of patients treated with BRAF/MEK inhibitors.

In contrast, exanthema is a common adverse event in patients treated with BRAF/MEK inhibitors (13). In clinical trials, 15.7% of patients treated with encorafenib/binimetinib developed a low grade rash/maculopapular rash (high grade 1%). Additional 3.1% showed an acneiform exanthem (high grade 0%). 27.7% of patients treated with dabarafenib/trametinib developed a low grade rash/maculopapular rash (high grade 1.5%). Additional 6.6% showed an acneiform exanthema (high grade 0%). The combination of vemurafenib/cobimetinib induced in 56.3% of patients a low grade rash/maculopapular rash (high grade 12.6%). Additional 13.8% showed an acneiform exanthema (high grade 2.4%). Important to acknowledge is the fact, that non-dermatologists do not differentiate between the common term rash and the specific characteristics of e.g. a maculopapular

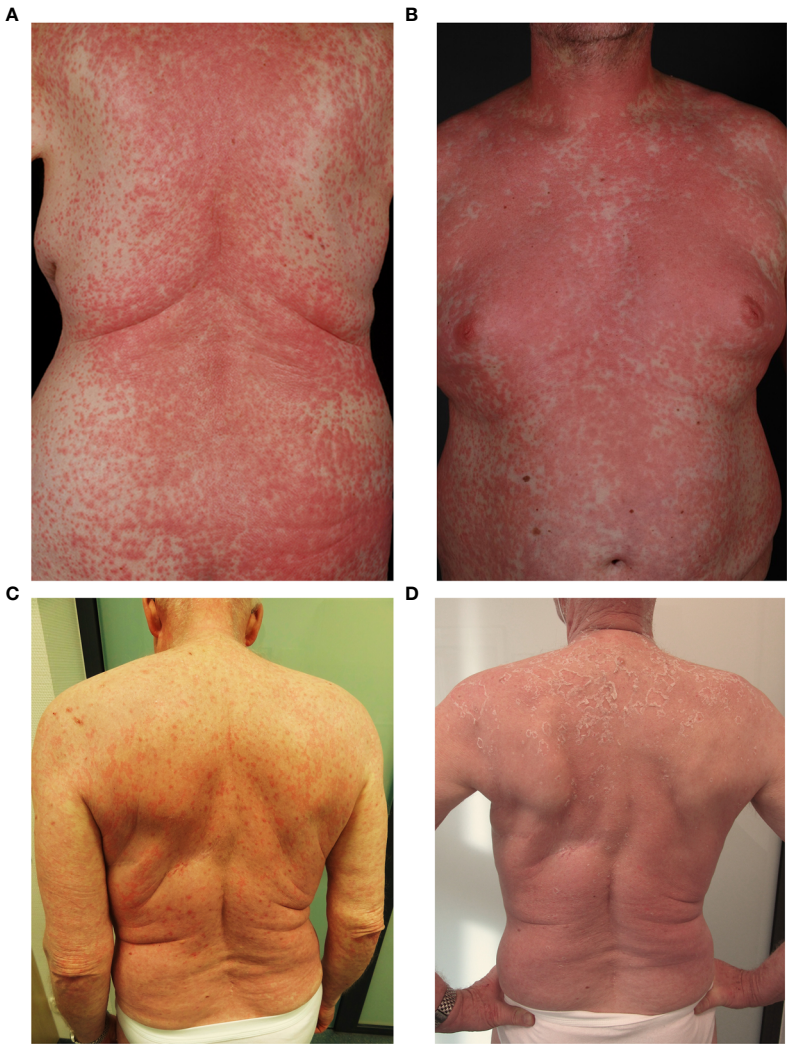


FIGURE 2 | Representative patients from the study cohorts showing an early exanthema defined as onset within 6 weeks upon start of vemurafenib **(A)** or vemurafenib plus cobimetinib **(B)**, both grade 4 according to CTCAEv4.0. **(C)** Exanthem during vemurafenib and cobimetinib **(D)** follow-up after 4 weeks of topical and systemic steroids.

exanthema or acneiform exanthema (13). Additionally, in clinical trials the onset of exanthema is not specified, so the reported incidence of exanthema does not give further information about the rate of early exanthemas within the first weeks of treatment initiation. Moreover, an exanthema develops early during treatment, most often within the first four to six weeks of treatment, and is easily detectable by an inspection of the patient's skin (13). These advantages render the detection of an early exanthema as a useful indicator of a favorable treatment outcome.

Interestingly, in the VEM cohort, females were more often represented within the group of patients developing early exanthema than males (p=0.043; **Table 1**). This has also been demonstrated to be a known risk factor for rash induced by BRAF/MEK inhibitors in the metaanalysis of Hopkins et al. (14).

This early exanthema is usually treated by a dose reduction of the BRAF/MEK inhibitors in combination with topical steroids and only in rare, severe cases with systemic steroids. Due to their early exanthema, 32.7% of VEM patients and 26.8% of COBIVEM patients needed a dose reduction.

Indeed, in our study we found that the occurrence of an exanthema within the first six weeks of treatment was significantly associated with an improved response rate and a prolonged survival in terms of PFS and OS in patients treated with COBIVEM. In patients treated with VEM, the development of an early exanthema was correlated with an improved objective response, but did not show an association to an improved survival.

Possible reasons for this differential impact on survival remain to be elucidated. First it should be mentioned that the early exanthema during COBIVEM and other BRAF/MEK

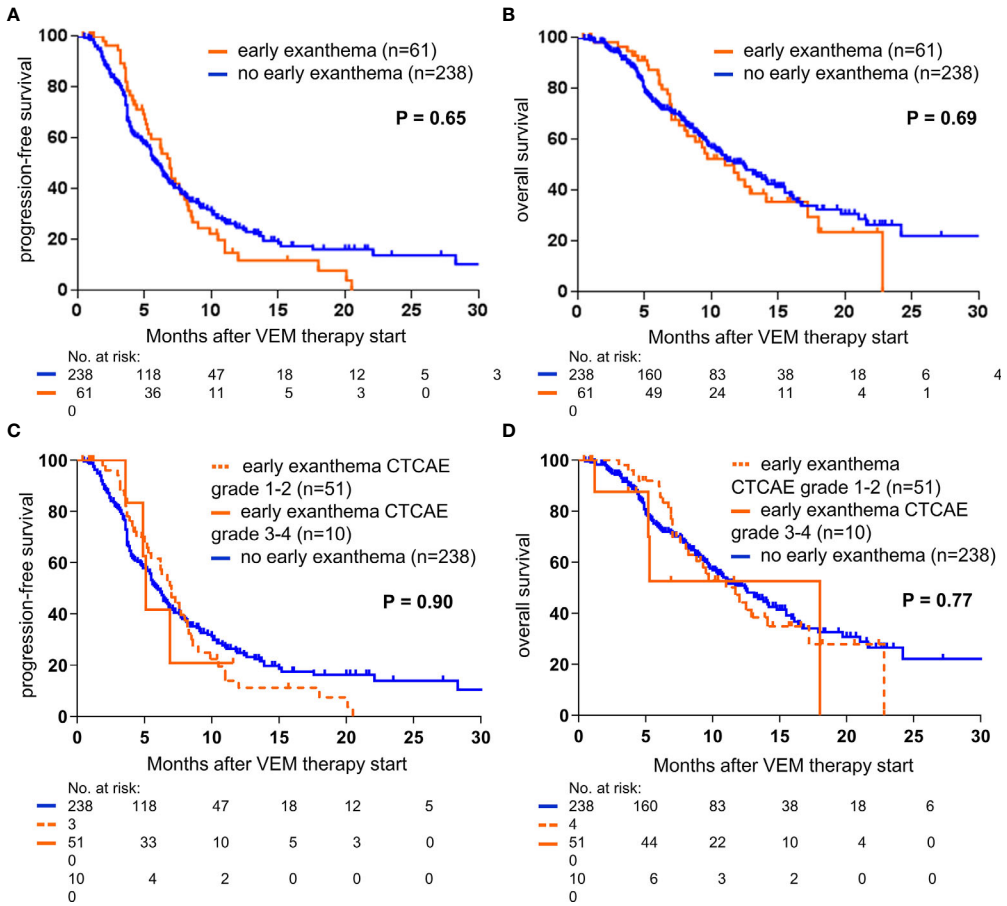


FIGURE 3 | Kaplan-Meier curves showing the probability of progression-free **(A, C)**, and overall survival **(B, D)**, of metastatic melanoma patients treated with vemurafenib (VEM; n=299). Survival curves are displayed for patients with or without presentation of early exanthema upon treatment. Censored observations are indicated by vertical bars. P-values were calculated using the log rank test.

combination therapies has to be differentiated from the acneiform rash induced specifically by MEK inhibitor monotherapies. This acneiform rash commonly occurs later during treatment, most often between week 6 and 12 after treatment start, and has a well-defined causal mechanism (13). The early exanthema developing within the first six weeks of COBIVEM treatment might be induced by the immune activation described for MEK inhibition therapies. It has been demonstrated that COBIVEM as well as dabrafenib plus trametinib therapy induces a type I interferon response in keratinocytes which acts proinflammatory and antineoplastically (15). In histopathology analysis, a slight basal layer vacuolization, dermal edema and a superficial dermal perivascular lymphocyte and eosinophil infiltrate was described (16). Also, it has been demonstrated that a pre-treatment with MEK inhibitors enhances immune responses, tumor-infiltrating T cells, and an immune-stimulating tumor microenvironment (17).

Interestingly, patients developing a mild exanthema revealed a stronger benefit from COBIVEM therapy than patients with a severe exanthema or patients without any exanthema. This finding might be explained by the fact that of the patients who developed a severe exanthema, 18.7% underwent a dose reduction of COBIVEM and 4.9% completely discontinued the treatment, compared to only 8.1% of patients who developed a mild exanthema that needed a dose reduction and 0.8% that discontinued the treatment. In contrast, it has been shown that dose reductions of BRAF/MEK inhibitors due to early toxicity in the first 28 days are significantly associated with improved survival, progression free survival and response (18, 19). However, following our present results, patients developing an early exanthema upon COBIVEM are patients with a high probability of a favorable therapy outcome and should thus be supported to continue treatment with COBIVEM. This support can be provided by an adequate therapeutic management of the exanthema, e.g. by the use of topical corticosteroids and/or anti-pruritics.

In conclusion, our results indicate that the development of an early exanthema upon BRAF/MEK inhibition with COBIVEM is a surrogate marker of a favorable therapy outcome in metastatic melanoma patients. Thus, patients presenting with an early exanthema under COBIVEM therapy should be treated with

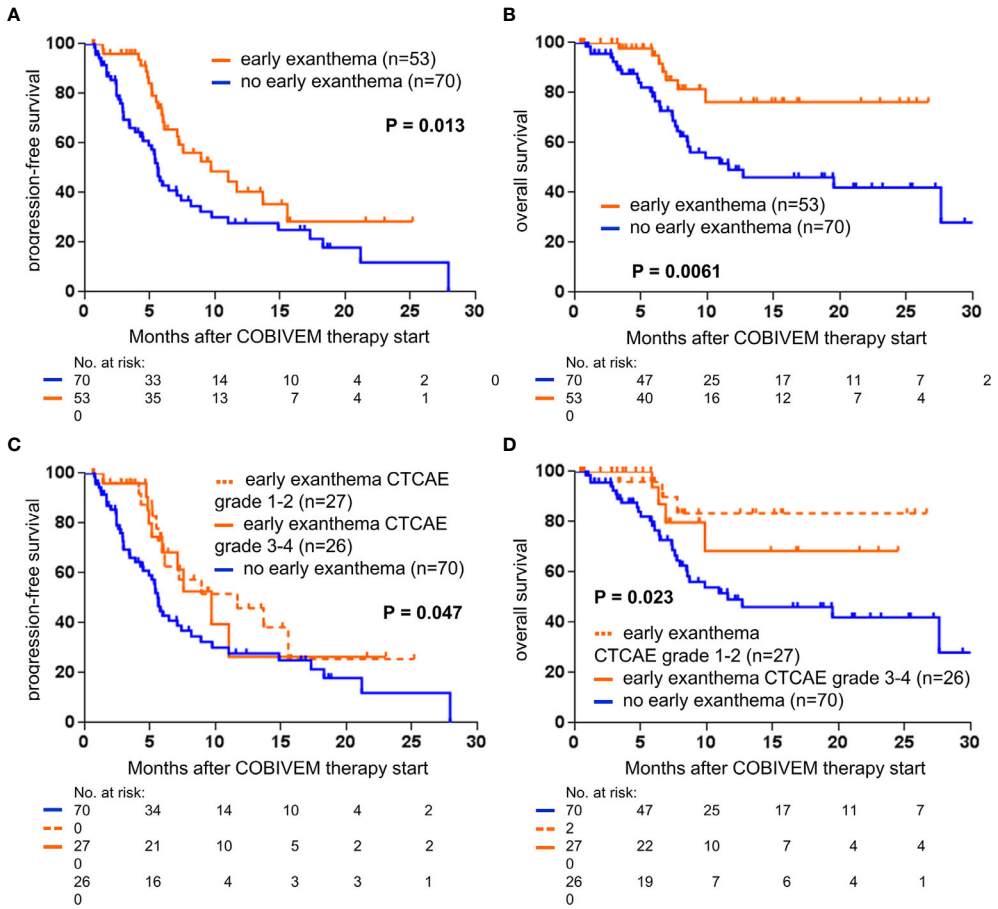


FIGURE 4 | Kaplan-Meier curves showing the probability of progression-free **(A, C)** and overall survival **(B, D)** of metastatic melanoma patients treated with vemurafenib plus cobimetinib (COBIVEM; n=123). Survival curves are displayed for patients with or without presentation of early exanthema upon treatment. Censored observations are indicated by vertical bars. P-values were calculated using the log rank test.

adequate supportive measures to provide that patients can stay on treatment. As a limitation, our findings result from a retrospective analysis and should therefore be confirmed in prospective clinical trials or registries.

DATA AVAILABILITY STATEMENT

The original contributions presented in the study are included in the article/supplementary material. Further inquiries can be directed to the corresponding author.

ETHICS STATEMENT

The studies involving human participants were reviewed and approved by Ethics Committee approval (Hannover University Medical School, 1612-2012). Written informed consent for participation was not required for this study in accordance with the national legislation and the institutional requirements.

AUTHOR CONTRIBUTIONS

SU and KK contributed to conception and design of the study. All authors contributed to the acquisition pf data. SU organized the database. SU and KK performed the statistical analysis. KK wrote the first draft of the manuscript. SU and KK wrote sections of the manuscript. All authors contributed to the article and approved the submitted version.

FUNDING

This study was performed within the network of study centers of the German Dermatologic Cooperative Oncology Group (DeCOG). This research did not receive any specific grant from funding agencies in the public, commercial, or not-for-profit sectors.

ACKNOWLEDGMENTS

We wish to thank all patients participating in this study, as well as their families and caregivers.

REFERENCES

1. Dréno B, Ribas A, Larkin J, Ascierto PA, Hauschild A, Thomas L, et al. Incidence, Course, and Management of Toxicities Associated With Cobimetinib in Combination With Vemurafenib in the coBRIM Study. *Ann Oncol* (2017) 28(5):1137–44. doi: 10.1093/annonc/mdx040
2. Abdel-Rahman O, Fouad M. Correlation of Cetuximab-Induced Skin Rash and Outcomes of Solid Tumor Patients Treated With Cetuximab: A Systematic Review and Meta-Analysis. *Crit Rev Oncol Hematol* (2015) 93 (2):127–35. doi: 10.1016/j.critrevonc.2014.07.005
3. Sonnenblick A, de Azambuja E, Agbor-Tarh D, Bradbury I, Campbell C, Huang Y, et al. Lapatinib-Related Rash and Breast Cancer Outcome in the ALTTO Phase III Randomized Trial. *J Natl Cancer Inst* (2016) 108(8):djw037. doi: 10.1093/jnci/djw037
4. Gershenwald JE, Scolyer RA, Hess KR, Sondak VK, Long GV, Ross MI, et al. For Members of the American Joint Committee on Cancer Melanoma Expert Panel and the International Melanoma Database and Discovery Platform. Melanoma Staging: Evidence-based Changes in the American Joint Committee on Cancer Eighth Edition Cancer Staging Manual. *CA Cancer J Clin* (2017) 67(6):472–92. doi: 10.3322/caac.21409
5. Therasse P, Arbuck SG, Eisenhauer EA, Wanders J, Kaplan RS, Rubinstein L, et al. New Guidelines to Evaluate the Response to Treatment in Solid Tumors. European Organization for Research and Treatment of Cancer, National Cancer Institute of the United States, National Cancer Institute of Canada. *J Natl Cancer Inst* (2000) 92(3):205–16. doi: 10.1093/jnci/92.3.205
6. National Cancer Institute Enterprise Vocabulary Services. *Criteria for Adverse Events (Ctcae)* . Available at: https://evs.nci.nih.gov/ftp1/CTCAE/CTCAE_4.03/CTCAE_4.03_2010-06-14_QuickReference_5x7.pdf (Accessed May 14, 2020).
7. Chapman PB, Hauschild A, Robert C, Haanen JB, Ascierto P, Larkin J, et al. Brim-3 Study Group. Improved Survival With Vemurafenib in Melanoma With BRAF V600E Mutation. *N Engl J Med* (2011) 364(26):2507–16. doi: 10.1056/NEJMoa1103782
8. Ascierto PA, McArthur GA, Dréno B, Atkinson V, Liszkay G, Di Giacomo AM, et al. Cobimetinib Combined With Vemurafenib in Advanced BRAF (V600)-mutant Melanoma (coBRIM): Updated Efficacy Results From a Randomised, Double-Blind, Phase 3 Trial. *Lancet Oncol* (2016) 17(9):1248–60. doi: 10.1016/S1470-2045(16)30122-X
9. Petrelli F, Ardito R, Merelli B, Lonati V, Cabiddu M, Seghezzi S, et al. Prognostic and Predictive Role of Elevated Lactate Dehydrogenase in Patients With Melanoma Treated With Immunotherapy and BRAF Inhibitors: A Systematic Review and Meta-Analysis. *Melanoma Res* (2019) 29(1):1–12. doi: 10.1097/CMR.0000000000000520
10. Hodi FS, Chiarion-Sileni V, Gonzalez R, Grob JJ, Rutkowski P, Cowey CL, et al. Nivolumab Plus Ipilimumab or Nivolumab Alone Versus Ipilimumab Alone in Advanced Melanoma (CheckMate 067): 4-Year Outcomes of a Multicentre, Randomised, Phase 3 Trial. *Lancet Oncol* (2018) 19(11):1480–92. doi: 10.1016/S1470-2045(18)30700-9
11. Consoli F, Manganoni AM, Grisanti S, Petrelli F, Venturini M, Rangoni G, et al. Panniculitis and Vitiligo Occurring During BRAF and MEK Inhibitors Combination in Advanced Melanoma Patients: Potential Predictive Role of Treatment Efficacy. *PloS One* (2019) 14(4):e0214884. doi: 10.1371/journal.pone.0214884
12. Ben-Betzalel G, Baruch EN, Boursi B, Steinberg-Silman Y, Asher N, Shapira-Frommer R, et al. Possible Immune Adverse Events as Predictors of Durable Response to BRAF Inhibitors in Patients With BRAF V600-Mutant Metastatic Melanoma. *Eur J Cancer* (2018) 101:229–35. doi: 10.1016/j.ejca.2018.06.030
13. Heinzerling L, Eigentler TK, Fluck M, Hassel JC, Heller-Schenck D, Leipe J, et al. Tolerability of BRAF/MEK Inhibitor Combinations: Adverse Event Evaluation and Management. *ESMO Open* (2019) 4(3):e000491. doi: 10.1136/esmoopen-2019-000491
14. Hopkins AM, Rathod AD, Rowland A, Kichenadasse G, Sorich MJ. Risk Factors for Severe Rash With Use of Vemurafenib Alone or in Combination With Cobimetinib for Advanced Melanoma: Pooled Analysis of Clinical Trials. *BMC Cancer* (2020) 20:157. doi: 10.1186/s12885-020-6659-0
15. Lulli D, Carbone ML, Pastore S. The MEK Inhibitors Trametinib and Cobimetinib Induce a Type I Interferon Response in Human Keratinocytes. *Int J Mol Sci* (2017) 18(10):2227. doi: 10.3390/ijms18102227
16. Naqash AR, File DM, Ziemer CM, Whang YE, Landman P, Googe PB, et al. Cutaneous Adverse Reactions in B-RAF Positive Metastatic Melanoma Following Sequential Treatment With B-RAF/MEK Inhibitors and Immune Checkpoint Blockade or Vice Versa. A Single-Institutional Case-Series. *J Immunother Cancer* (2019) 7(1):4. doi: 10.1186/s40425-018-0475-y
17. Kuske M, Westphal D, Wehner R, Schmitz M, Beissert S, Praetorius C, et al. Immunomodulatory Effects of BRAF and MEK Inhibitors: Implications for Melanoma Therapy. *Pharmacol Res* (2018) 136:151–9. doi: 10.1016/j.phrs.2018.08.019
18. Hopkins AM, Van Dyk M, Rowland A, Sorich MJ. Effect of Early Adverse Events on Response and Survival Outcomes of Advanced Melanoma Patients Treated With Vemurafenib or Vemurafenib Plus Cobimetinib: A Pooled Analysis of Clinical Trial Data. *Pigment Cell Melanoma Res* (2019) 32(4):576–83. doi: 10.1111/pcmr.12773
19. Lewis K, Hauschild A, Larkin J, Ribas A, Flaherty KT, McArthur GA, et al. Effect of Concomitant Dosing With Acid-Reducing Agents and Vemurafenib Dose on Survival in Patients With $BRAF^{V600}$ Mutation-Positive Metastatic Melanoma Treated With Vemurafenib ± Cobimetinib. *Eur J Cancer* (2019) 116:45–55. doi: 10.1016/j.ejca.2019.05.002

Conflict of Interest: KK has served as consultant or/and has received honoraria from Amgen, Roche, Bristol Myers Squibb, Merck Sharp and Dohme, Pierre Fabre, and Novartis, and received travel support from Amgen, Merck Sharp and Dohme, Bristol Myers Squibb, Amgen, Pierre Fabre, Medac, and Novartis. RG received honoraria for lectures and advisory boards, research support and meeting support from Almirall Hermal, Amgen, Astra Zeneca, Bristol Myers Squibb, Leo, Merck Serono, Merck Sharp and Dohme, Pierre Fabre, Roche, Sanofi Genzyme, Regeneron, Sun Pharma, Takeda, Pfizer, Novartis, Johnson&Johnson, 4SC, and Incyte. FM has received travel support or/and speaker's fees or/and advisor's honoraria by Novartis, Roche, BMS, MSD and Pierre Fabre, and research funding from Novartis and Roche. LZ has served as consultant and/or has received honoraria from Roche, Bristol Myers Squibb, Merck Sharp and Dohme, Novartis, Pierre Fabre, and Sanofi, and received travel support from Bristol Myers Squibb, Merck Sharp and Dohme, Amgen, Pierre Fabre, and Novartis. MH has received consultant and/or speaker honoraria form Bristol Myers Squibb, Novartis, Merck Sharp and Dohme, Sanofi, Roche and travel support from Novartis, and Bristol Myers Squibb. AG reports speakers honoraria from Bristol Myers Squibb, Merck Sharp and Dohme, and Roche, advisory board honoraria from Bristol Myers Squibb, Novartis, Merck Sharp and Dohme, Pierre Fabre, Pfizer, Roche and Sanofi Genzyme, and travel support from Bristol Myers Squibb, Merck Sharp and Dohme, Novartis, and Roche. K-MT received honoraria for lectures and advisory boards from Bristol-Myers Squibb, Roche, Novartis, Merck Sharp and Dohme, Pierre Fabre, LEO, Galderma, AbbVie, La Roche-Posay and Candela, and travel support from Bristol-Myers Squibb, Roche, Novartis, Merck Sharp and Dohme, Pierre Fabre, LEO, and Candela. JU is on the advisory board or has received honoraria and travel support from Amgen, Bristol Myers Squibb, GSK, LeoPharma, Merck Sharp and Dohme, Novartis, Pierre Fabre, Roche, Sanofi outside the submitted work. JH reports speakers honoraria from Bristol Myers Squibb, Novartis, Merck Sharp and Dohme, and Roche, advisory board honoraria from Merck Sharp and Dohme, Pierre Fabre, Sunpharma and Sanofi Genzyme, and travel support from Bristol Myers Squibb, and Pierre Fabre. CL declares speakers and advisory board honoraria and travel support from Bristol Myers Squibb, Merck Sharp and Dohme, Merck Serono, Novartis, Roche, Amgen, Pierre Fabre, and Sun Pharma. CP received speaker or consultant honoraria and travel support from Novartis, Bristol Myers Squibb, Roche, Merck Serono, Merck Sharp and Dohme, Celgene, AbbVie, and LEO. LH received grants from Novartis, and has received speaker or consultant fees personal fees from Amgen, Bristol Myers Squibb, Merck Sharp and Dohme, Roche, Curevac, Pierre Fabre, Roche, Novartis, and Sanofi. MK has received grants from Bristol Myers Squibb, Merck Sharp and Dohme, Leo, Novartis, and Roche.

DG declares speakers and advisory honoraria as well as travel support from Bristol Myers Squibb, Novartis, Pierre Fabre, Sanofi Genzyme, Amgen, Galderma, Janssen, and Roche.

DS declares advisory board and speakers honoraria from Roche, Novartis, Bristol-Myers-Squibb, MSD, Merck-Serono, Sanofi, Nektar, Amgen, Hexal, InFlaRx, Array, Pierre Fabre, Immunocore, Philogen Sun Pharma, Regeneron, and Ultimovacs, as well as grant and travel support from Roche, Novartis, Bristol-Myers-Squibb, MSD, Merck-Serono, and Sanofi. SU declares research support

from Bristol Myers Squibb, and Merck Serono, speakers and advisory board honoraria from Bristol Myers Squibb, Merck Sharp and Dohme, Merck Serono, Novartis and Roche, and travel support from Bristol Myers Squibb, Merck Sharp, and Dohme.

The remaining authors declare that the research was conducted in the absence of any commercial or financial relationships that could be construed as a potential conflict of interest.

Copyright © 2021 Kähler, Gutzmer, Meier, Zimmer, Heppt, Gesierich, Thoms, Utikal, Hassel, Loquai, Pföhler, Heinzerling, Kaatz, Göppner, Pflugfelder, Bohne, Satzger, Reinhardt, Placke, Schadendorf and Ugurel. This is an open-access article distributed under the terms of the Creative Commons Attribution License (CC BY). The use, distribution or reproduction in other forums is permitted, provided the original author(s) and the copyright owner(s) are credited and that the original publication in this journal is cited, in accordance with accepted academic practice. No use, distribution or reproduction is permitted which does not comply with these terms.

frontiers in Oncology

ORIGINAL RESEARCH
published: 29 June 2021
doi: 10.3389/fonc.2021.668247

PI3K Promotes Basal Cell Carcinoma Growth Through Kinase-Induced p21 Degradation

Rachel Y. Chow[1], *Ung Seop Jeon*[1], *Taylor M. Levee*[1], *Gurleen Kaur*[1], *Daniel P. Cedeno*[1], *Linda T. Doan*[2] *and Scott X. Atwood*[1,2,3]*

[1] Department of Developmental and Cell Biology, University of California, Irvine, Irvine, CA, United States, [2] Department of Dermatology, University of California, Irvine, Irvine, CA, United States, [3] Chao Family Comprehensive Cancer Center, University of California, Irvine, Irvine, CA, United States

Basal cell carcinoma (BCC) is a locally invasive epithelial cancer that is primarily driven by the Hedgehog (HH) pathway. Advanced BCCs are a critical subset of BCCs that frequently acquire resistance to Smoothened (SMO) inhibitors and identifying pathways that bypass SMO could provide alternative treatments for patients with advanced or metastatic BCC. Here, we use a combination of RNA-sequencing analysis of advanced human BCC tumor-normal pairs and immunostaining of human and mouse BCC samples to identify a PI3K pathway expression signature in BCC. Pharmacological inhibition of PI3K activity in BCC cells significantly reduces cell proliferation and HH signaling. However, treatment of *Ptch1*$^{fl/fl}$; *Gli1-Cre*^{ERT2} mouse BCCs with the PI3K inhibitor BKM120 results in a reduction of tumor cell growth with no significant effect on HH signaling. Downstream PI3K components aPKC and Akt1 showed a reduction in active protein, whereas their substrate, cyclin-dependent kinase inhibitor p21, showed a concomitant increase in protein stability. Our results suggest that PI3K promotes BCC tumor growth by kinase-induced p21 degradation without altering HH signaling.

Keywords: basal cell carcinoma, hedgehog, PI3K - AKT pathway, p21, atypical PKCι

OPEN ACCESS

Edited by:
Todd Ridky,
University of Pennsylvania,
United States

Reviewed by:
Kenneth Y. Tsai,
Moffitt Cancer Center, United States
Jennifer Yunyan Zhang,
Duke University, United States

***Correspondence:**
Scott X. Atwood
satwood@uci.edu

Specialty section:
This article was submitted to Skin Cancer, a section of the journal Frontiers in Oncology

Received: *15 February 2021*
Accepted: *14 June 2021*
Published: *29 June 2021*

Citation:
Chow RY, Jeon US, Levee TM, Kaur G, Cedeno DP, Doan LT and Atwood SX (2021) PI3K Promotes Basal Cell Carcinoma Growth Through Kinase-Induced p21 Degradation. Front. Oncol. 11:668247. doi: 10.3389/fonc.2021.668247

INTRODUCTION

The Hedgehog (HH) pathway is an evolutionarily conserved signaling pathway that plays an essential role in vertebrate embryogenesis and adult tissue homeostasis (1). Aberrant activation of the HH pathway results in uncontrolled proliferation and differentiation that leads to tumorigenesis in various tissues, with medulloblastoma (2, 3), rhabdomyosarcoma (4), and basal cell carcinoma (BCC) (5) commonly displaying mutations in HH pathway components. BCC is a locally invasive epithelial cancer that represents the most prevalent cancer in the United States, with more than four million cases estimated each year (6). While most cases of BCC are characterized by low mortality and metastasis that can be easily excised (7), advanced BCCs display elevated invasiveness, metastasis, and mortality (8). As the initiation and progression of BCCs predominantly depend on deregulation of the canonical HH pathway *via* activation of the seven-pass transmembrane protein Smoothened (SMO) (9), such dependency has led to the development of vismodegib and other SMO inhibitors for the treatment of locally advanced and metastatic BCCs (10). Yet, despite vismodegib demonstrating feasibility and efficacy in clinical trials against HH-driven

medulloblastoma (11, 12), it has failed to achieve adequate success in treating advanced BCCs with 57% of patients displaying inherent resistance to the treatment (13) and 21% of treated patients developing secondary resistance after 56 weeks (14). Thus, it is vital to elucidate the mechanisms by which resistant BCCs evade SMO inhibition, as well as develop alternative therapeutic strategies that would effectively undermine such mechanisms.

In the normal vertebrate cell state, ion-driven cholesterol transporter Patched1 (PTCH1) actively depletes cholesterol from the membrane of the primary cilium and thus inhibits the cholesterol-dependent activation of SMO (15). This inhibition allows Suppressor of Fused homolog (SUFU) to sequester the Glioma-associated oncogene (GLI) transcription factors (16) and facilitate their post-translational proteolytic processing into repressor forms (17). The canonical HH pathway signaling initiates with the binding of HH ligands to PTCH1, which inhibits its activity and allows the activation of SMO *via* cholesterylation (18, 19). Activated SMO in turn induces the disassociation of the SUFU-GLI complex and facilitates the nuclear localization of the activator forms of GLI (20), which results in the expression of HH target genes. Uncontrolled activation of the HH pathway in BCC patients has been observed to occur primarily through inactivating mutations in PTCH1 (73%) or activating mutations in SMO (20%) (21). Yet, inspection of BCC patients with inherent and secondary resistance to vismodegib has revealed that the majority of mutations are within the SMO gene and either incite constitutive activity or deter inhibitor binding (22). Current efforts to circumvent BCC chemoresistance are focused on perturbing the oncogenic activity of GLI, either through directly inhibiting the GLI proteins or inhibiting the molecules that modulate GLI activity (23). Recent studies have demonstrated the potency of inhibiting GLI (24), DYRK1B (25), HDAC1 (26), BRD4 (27), MLK1 (28), and aPKC (29) in attenuating resistant BCCs in preclinical studies.

Recently, various studies have highlighted the critical interconnections between the HH pathway and other signaling pathways in promoting the persistence and chemoresistance of cancer. In BCC, progression and therapeutic resistance have been linked with molecular crosstalk between the HH pathway and other developmental signaling pathways such as WNT (30), Notch (31), TGF-β (32), and RAS/MAPK (33) pathways. The phosphoinositide 3-kinase (PI3K) pathway is another developmental signaling pathway that has been demonstrated to interact with the HH pathway in colon (34), pancreatic, and ovarian carcinomas (35). In addition, the PI3K pathway functions in therapeutic resistance against SMO inhibitors in medulloblastoma (36) and esophageal adenocarcinoma (37). Combinatory inhibition of both PI3K and HH signaling pathways in preclinical studies on medulloblastoma have demonstrated favorable efficacy in attenuating SMO inhibitor-resistant tumors (36), although the effects on other HH-mediated cancers like BCC remains to be determined.

The canonical PI3K pathway initiates with the activation of PI3K by receptor tyrosine kinases, which subsequently activates AKT *via* phosphorylation facilitated by phosphoinositides (38). Activated AKT in turn phosphorylates and regulates the activities of a wide array of signaling proteins that are associated with proliferation and differentiation of the cell (39). The PI3K/AKT pathway has been shown to interact with the HH pathway through multiple mechanisms that are largely independent of canonical HH signaling, with components of the PI3K/AKT pathway coinciding primarily upstream of GLI (40). In embryonic fibroblasts, upregulation of the PI3K/AKT pathway signaling promotes HH signaling by antagonizing the inhibitory function of PKA on GLI2 (41). Additionally, upregulation of the PI3K/AKT pathway signaling has been shown to promote HH signaling and tumor cell proliferation in esophageal (42) and breast cancers (43). However, the PI3K/AKT pathway has been shown to promote tumor cell growth with no effect on GLI1 activity in neuroblastomas (44), suggesting that PI3K/AKT either operates in parallel to or downstream of the HH pathway in this context. Thus, variation in how PI3K/AKT operates with respect to HH signaling confounds our ability to generally apply its function across distinct cancers.

Here, we demonstrate that the PI3K pathway signaling is upregulated in bulk-level RNA-sequencing data of 14 matched tumor-normal pairs. Human and mouse BCC tumors show a significant increase in PI3K protein expression, and PI3K is essential for both BCC tumor cell growth and HH signaling. However, our data shows disparate results between BCC cells and *in vivo* tumors, where PI3K inhibition has no effect on GLI1 activity despite suppressing tumor growth. Finally, we show that PI3K likely functions in BCC tumors by promoting aPKC- and AKT1-depedent degradation of cyclin-dependent kinase inhibitor p21 to maintain cell cycle progression. Our results suggest that the PI3K pathway functions in parallel to or downstream of the HH pathway to promote BCC tumor growth.

MATERIALS AND METHODS

Ethics Statement

Human clinical studies were approved by the Ethics Committee of the University of California, Irvine. All human studies were performed in strict adherence to the Institutional Review Board (IRB) guidelines of the University of California, Irvine (2009–7083).

Data Availability Statement

The data that supports the findings of this study are available in GEO at http://www.ncbi.nlm.nih.gov/geo/query/acc.cgi?acc-GSE58375, reference number GSE58375.

RNA-Sequencing Analysis

RNA-sequencing data were obtained from patient-matched advanced human BCC patients (22). RNA-sequencing data were aligned as previously described (22). The NCBI Reference Sequence databases were used as reference annotations to calculate the values of reads per kilobase of transcript per million mapped reads for known transcripts (RPKM). RPKM values were then log2-transformed, and heat map analysis was

used to visualize the differential gene expression. Pathway enrichment terms from the RNA sequencing data were obtained using Enrichr (45).

Human Samples

Written informed consent was obtained for all archived human samples and was reviewed by the University of California, Irvine IRB. Human normal epidermis and BCC samples were collected from the UC Irvine Medical Center. Paraffinized samples were sectioned with a rotary microtome (Leica RM2155) at 7 μm for analysis. Samples were deparaffinized as described by Abcam, and antigen retrieval was performed using Tris-EDTA buffer (10 nM Tris base, 1 mM EDTA, 0.05% Tween-20, pH 9.0) at 60°C overnight.

Cell Culture

ASZ001 cells (46) were grown in 154CF medium (Life Technologies) containing 2% Fetal Bovine Serum (FBS; Life Technologies) chelated overnight with Chelex® 100 Resin (Bio-Rad), 1% Penicillin-Streptomycin (P/S; Life Technologies), and 0.07 mM $CaCl_2$. NIH3T3 cells (ATCC, CRL-1658) were grown in DMEM medium (Life Technologies) containing 10% FBS and 1% Penicillin-Streptomycin.

RT-qPCR

ASZ001 cells at confluence were serum-starved with dimethyl sulfoxide (DMSO; Fisher Scientific) or varying concentrations of LY294002 (1 μM, 5 μM, 25 μM, and 100 μM; Fisher Scientific) or BKM120 (250 nM, 1.25 μM, 6.25 μM, and 31.25 μM; Fisher Scientific) for 24 hours. RNA was purified using Direct-zol RNA MiniPrep Plus (Zymo Research). Quantitative real-time polymerase chain reaction (RT-qPCR) was performed using the iTaq Universal SYBR Green 1-Step Kit (Bio-Rad) on the StepOnePlus Real-time PCR System (Applied BioSystem) using primers for *Gli1* (forward: 5'-GCAGGTG TGAGGCC AGGTAG TGACGA TG-3', reverse: 5'-CGCGGG CAGCAC TGAGGA CTTGTC-3') and *Gapdh* (forward: 5'-AATGAA TACGGC TACAGC AACAGG GTG-3', reverse: 5'-AATTGT GAGGGA GATGCT CAGTGT TGGG-3'). Fold change in *Gli1* mRNA expression was measured using ΔΔCt analysis with *Gapdh* as an internal control. Experiments were run in triplicates and were repeated three times.

MTT Assay

ASZ001 cells were seeded at 2000 cells/well into 96-well plates. After 48 hours, cells were treated with DMSO or varying concentrations of LY294002 (1 μM, 5 μM, 25 μM, and 100 μM) or BKM120 (250 nM, 1.25 μM, 6.25 μM, and 31.25 μM) for 2, 4, and 6 days. Growth assays were performed with MTT (Sigma-Aldrich) per manufacturer's protocol. Plates were analyzed using the BioTek uQuant MQX200 Microplate Reader (BioTek). Experiments were run in 6 wells and were repeated three times.

Mice

All mice were housed under standard conditions, and animal care was in compliance with the protocols approved by the Institutional Animal Care and Use Committee (IACUC) at the University of California, Irvine. *Ptch1$^{fl/fl}$; Gli1-Cre^{ERT2}* mice were administered with 100 μL of 10 mg/mL tamoxifen (Sigma) intraperitoneally for three consecutive days at six weeks of age. After five weeks when BCC microtumors have developed, mice were treated with 100 μL of DMSO or BKM120 (10 mg/kg) intraperitoneally for seven consecutive days. At the end of treatment, mice were euthanized and collected for their back skin. Collected skin samples were fixed with 4% paraformaldehyde (PFA; Electron Microscopy Sciences) for 30 minutes at room temperature, washed with DPBS (Life Technologies), immersed in 30% sucrose at 4°C overnight, and frozen in Tissue-Tek OCT Compound (Sakura Finetek). Samples were then cryo-sectioned using the CryoStar NX50 Cryostat (Thermo Fisher Scientific) at 14 μm for analysis. Five mice were used for each treatment condition.

Microtumor Assessment

Skin sections were stained with hematoxylin and eosin (H&E; Richard-Allan Scientific) per standardized protocol. Stained sections were imaged at 200x magnification using the AmScope microscope with the AmScope MU500B digital camera. Tumor sizes were measured using ImageJ. BCC tumors display characteristic features such as peripheral basal palisading and are connected to the upper and lower bulge of the hair follicle, but not the infundibulum or matrix cells of anagen hair follicles. Microtumors were assessed as the total tumor size per square area. More than 50 tumors were measured from each of the five mice. Palpable macrotumors do not form in this genetic background unless additional genetic insults occur.

Immunofluorescence

Skin sections were blocked using 10% Bovine Serum Albumin (BSA; Fisher Scientific) and 0.1% Triton X-100 (Fisher Scientific) in DPBS for 1 hour at room temperature. Sections were immunostained per standardized protocol using the following antibody dilutions: rabbit anti-PI3K (1:100, Abcam, ab40776), rabbit anti-GLI1 (1:500, Santa Cruz Biotechnology, sc-20687), rabbit anti-p-T304 GLI1 (1:200) (47), rabbit anti-AKT (1:400, Cell Signaling, 4691S), rabbit anti-p-T308 AKT (1:400, Cell Signaling, 13038S), rabbit anti-p21 (1:250, Cell Signaling, 2947S), and rabbit anti-p-T145 p21 (1:250, GeneTex, GTX32376). Sections were mounted in Prolong Diamond AntiFade Mountant with DAPI (Invitrogen). Immunostained sections were imaged using the Zeiss LSM700 confocal microscope (Zeiss) with 63x oil immersion objective. Pixel intensities were measured and averaged over five distinct tumors for each skin section using ImageJ. Images were arranged using ImageJ and Adobe Illustrator.

Statistics

Statistical analyses were done with two-tailed t-test or one-way and two-way ANOVA using GraphPad Prism.

RESULTS

PI3K/AKT Pathway Is Upregulated in Advanced BCC Tumors

To assess alternative pathways that may drive BCC tumor growth, we reanalyzed our bulk-level RNA-sequencing (RNA-seq) data of 14 matched tumor-normal pairs of advanced and

SMO inhibitor-resistant BCC samples (22, 48). Differential gene expression analysis across the 14 tumor-normal pairs identified 1602 genes that were upregulated by two-fold or more in the resistant BCC tumors compared to their normal skin counterparts (48). Database analysis of the upregulated genes with the Kyoto Encyclopedia of Genes and Genomes (KEGG) showed the expected upregulation of the cell cycle, HH pathway, and BCC-associated genes (**Figure 1A**, **Supplementary Data 1**). Another term that was significantly enriched was the PI3K/AKT pathway (**Figure 1A** and **Supplementary Data 1**). Analogously, Kinase Enrichment Analysis (KEA) (49) linked many of the upregulated genes with kinases that are closely associated with PI3K/AKT signaling, such as MAPK, AKT, GSK3β, CSNK, S6K, and PRKCB (**Figure 1B** and **Supplementary Data 1**). Close analysis of the PI3K pathway gene expression showed many components and downstream targets significantly upregulated in most tumors, including GRB2, PLCG1, and RPS6KA1 (**Figure 1C** and **Supplementary Data 2**).

PIK3CA Is Upregulated in Human and Mouse BCC Tumors

To validate whether PI3K pathway upregulation in BCC tumors is consistent at the protein level, we measured the expression of the catalytic subunit PIK3CA in human nodular BCC tumors and normal epidermis using immunofluorescence staining. We observed that tumors displayed significantly enhanced expression of PIK3CA compared to normal epidermis (**Figures 2A, B**). To analyze Pik3ca expression in mice, we utilized a *Ptch1*$^{fl/fl}$; *Gli1-Cre*^{ERT2} mouse model in which BCC microtumors arise from the hair follicle, secondary hair germ, and the touch dome in the interfollicular epidermis (50). BCC tumors were grown for five weeks post-Cre induction and formed predominantly from the hair follicle regions. Similar to our observations in human BCC tumors, we also observed a significant increase in Pik3ca expression in mouse BCC tumors compared to both normal epithelium and the hair follicle (**Figures 2C, D**). Together, these results suggest that PI3K pathway activity is upregulated in human and mouse BCC tumors.

Inhibition of PI3K Suppresses Growth and Hh Signaling in BCC Cells *In Vitro*

To assess whether upregulation of the PI3K pathway signaling affects growth and HH signaling in BCCs, we assayed ASZ001 mouse BCC cells with two PI3K inhibitors, BKM120 and LY294002. BKM120 acts as an allosteric inhibitor of PI3K (51) while LY294002 acts as an ATP-competitive inhibitor (52). Treatment of ASZ001 cells with BKM120 and LY294002 both significantly decreased HH signaling as assayed by *Gli1* mRNA expression (**Figure 3A**). Additionally, treatment of ASZ001 cells with BKM120 and LY294002 both resulted in complementary and dose-dependent reduction of tumor cell growth over time (**Figures 3B, C**). A significant increase in Casp3-mediated apoptosis was also observed upon BKM120 inhibition, with the proliferation marker Mki67 trending downward (**Figures 3D–F**). Together, these results show that the PI3K pathway promotes BCC cell growth upstream of the HH pathway.

Inhibition of PI3K Suppresses Growth but Not Hh Signaling in BCC Tumors *In Vivo*

To evaluate whether inhibition of PI3K can serve as an effective therapeutic strategy in attenuating BCC tumors, we generated

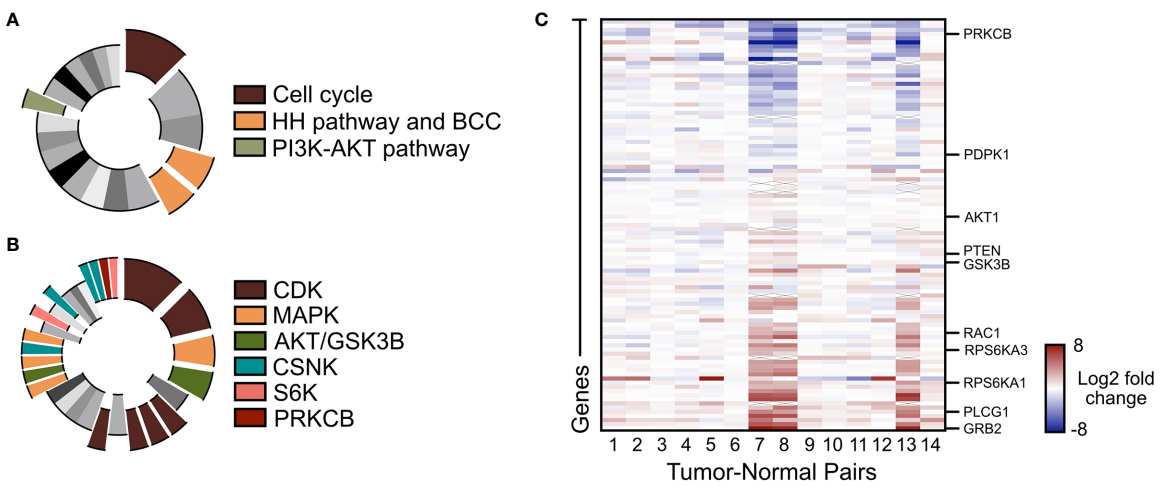


FIGURE 1 | PI3K/AKT pathway is upregulated in advanced BCC tumors. **(A)** KEGG analysis of the upregulated genes in advance BCC tumors highlighting the significant indicated terms. Cell cycle, p = 3.10 x 10^{-8}; BCC, p = 1.03 x 10^{-4}; HH signaling pathway, p = 2.49 x 10^{-4}; PI3K-AKT signaling pathway, p = 0.00675. **(B)** Kinase Enrichment Analysis of differentially expressed genes showing significant kinases as indicated. In descending significance to color codes: CDK2, p = 4.80 x 10^{-12}; CDK1, p = 1.13 x 10^{-8}; MAPK14, p = 2.59 x 10^{-6}; GSK3B, p = 5.42 x 10^{-6}; CDK15, p = 3.88 x 10^{-4}; CDK14, p = 4.39 x 10^{-4}; CDK18, p = 4.94 x 10^{-4}; CDK11A, p = 6.23 x 10^{-4}; MAPK1, p = 0.00460; AKT1, p = 0.00534; MAP3K10, p = 0.00641; CSNK2A1, p = 0.00796; MAPK9, p = 0.00828; RPS6KA5, p = 0.0123; CSNK2A2, p = 0.0165; CSNK1E, p = 0.0268; CSNK1D, p = 0.0275; PRKCB, p = 0.0281; RPS6KA1, p = 0.0332. **(C)** Heat map of the differentially expressed PI3K pathway genes in advanced human BCCs compared to patient-matched normal skin. X mark, absence of data.

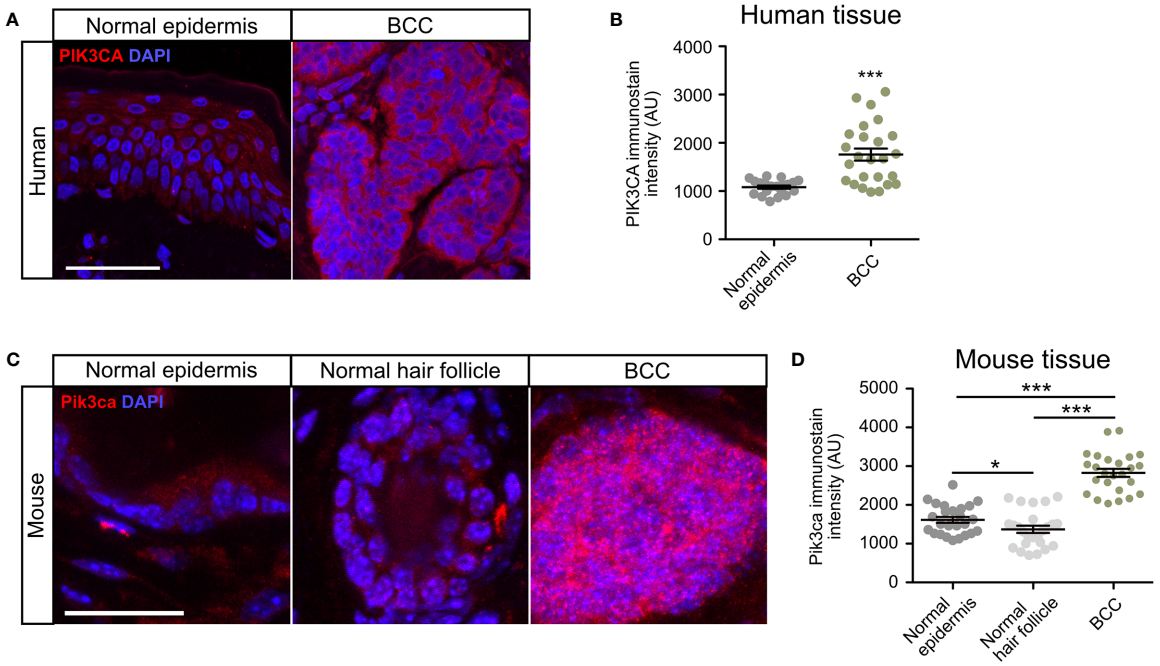


FIGURE 2 | PIK3CA is upregulated in human and mouse BCC tumors. **(A)** Immunofluorescence staining of PI3KCA (red) and DAPI counterstain (blue) in human normal epidermis and nodular BCC tumors. Scale bar, 50 μm. **(B)** Quantification of PI3KCA immunofluorescence intensity (five points of measurement per sample, n=4 samples). AU, arbitrary unit. Error bar, SEM. **(C)** Immunofluorescence staining of Pi3kca (red) and DAPI counterstain (blue) in mouse normal epithelium, normal hair follicle, and BCC tumors. Scale bar, 25 μm. **(D)** Quantification of Pi3kca immunofluorescence intensity (five points of measurement per animal, n = 5 mice). AU, arbitrary unit. Error bar, SEM. Significance was determined by unpaired two-tailed *t* test. *p < 0.05; ***p < 0.001.

BCC tumors in the *Ptch1*$^{fl/fl}$; *Gli1-Cre*^{ERT2} mouse model and intraperitoneally injected either DMSO or 10 mg/kg of BKM120 daily for seven days. Histological staining of the dorsal skin of BKM120-treated mice showed a significant reduction in total tumor size compared to DMSO controls (**Figures 4A, B**). Interestingly, Gli1 protein expression was not altered in BKM120-treated mice (**Figures 4C, D**), suggesting that the PI3K operates downstream or in parallel to the HH pathway *in vivo*, a result that is similar to Mtor inhibition (48). The discrepancy between our *in vitro* and *in vivo* results may indicate that the tumor microenvironment alters how the PI3K pathway functions in relation to the HH pathway.

To further define how the PI3K pathway functions *in vivo*, we assayed that status of aPKC, a Gli1 kinase that is necessary for high sustained Gli1 activity (29). Atypical PKCs are activated downstream of PI3K by Pdk1-dependent phosphorylation at T410 in a variety of cell types (53, 54). While we observed a slight increase in total aPKC immunostaining in BKM120-treated mouse BCC tumors, phosphorylation at T410 was significantly reduced (**Figures 4C, D**), indicating suppressed kinase activity. Although aPKC phosphorylates and activates Gli1 at residue T304 (29), we observed no change in p-T304 Gli1 expression (**Figures 4C, D**), reinforcing the possibility of PI3K's role outside of HH signaling and suggesting that aPKC likely exerts its effects on another substrate. Akt1 is also activated downstream of PI3K by Pdk1-dependent phosphorylation at T308 (55), and we found a significant reduction in both total and p-T308 Akt1 expression in BKM120-treated mouse BCC tumors (**Figures 4E, F**). As both aPKC and Akt1 facilitate the degradation of cyclin-dependent kinase inhibitor p21 by phosphorylating T145 (56–58), we assayed p21 protein expression and found a substantial increase in p21 stability and a corresponding decrease in p21 phosphorylation (**Figures 4E, F**). Altogether, our data suggests PI3K likely facilitates BCC tumor growth by promoting cell cycle progression through aPKC- and Akt1-mediated p21 degradation.

DISCUSSION

PI3K appears to operate at distinct levels within the HH pathway depending on context. For instance, upregulation of the PI3K/AKT pathway promotes HH signaling in embryonic fibroblasts (41), esophageal cancer (42), and breast cancer (43). Alternatively, the PI3K/AKT pathway promotes tumor cell growth independent of GLI1 activity in neuroblastomas (44), suggesting that PI3K/AKT either operates in parallel to or downstream of the HH pathway in this context. Our results show HH signaling is dependent on PI3K signaling in BCC cells grown in culture, but not in BCC tumors. This discrepancy between cell culture and three-dimensional (3D) growth conditions is a relatively common phenomenon and has been

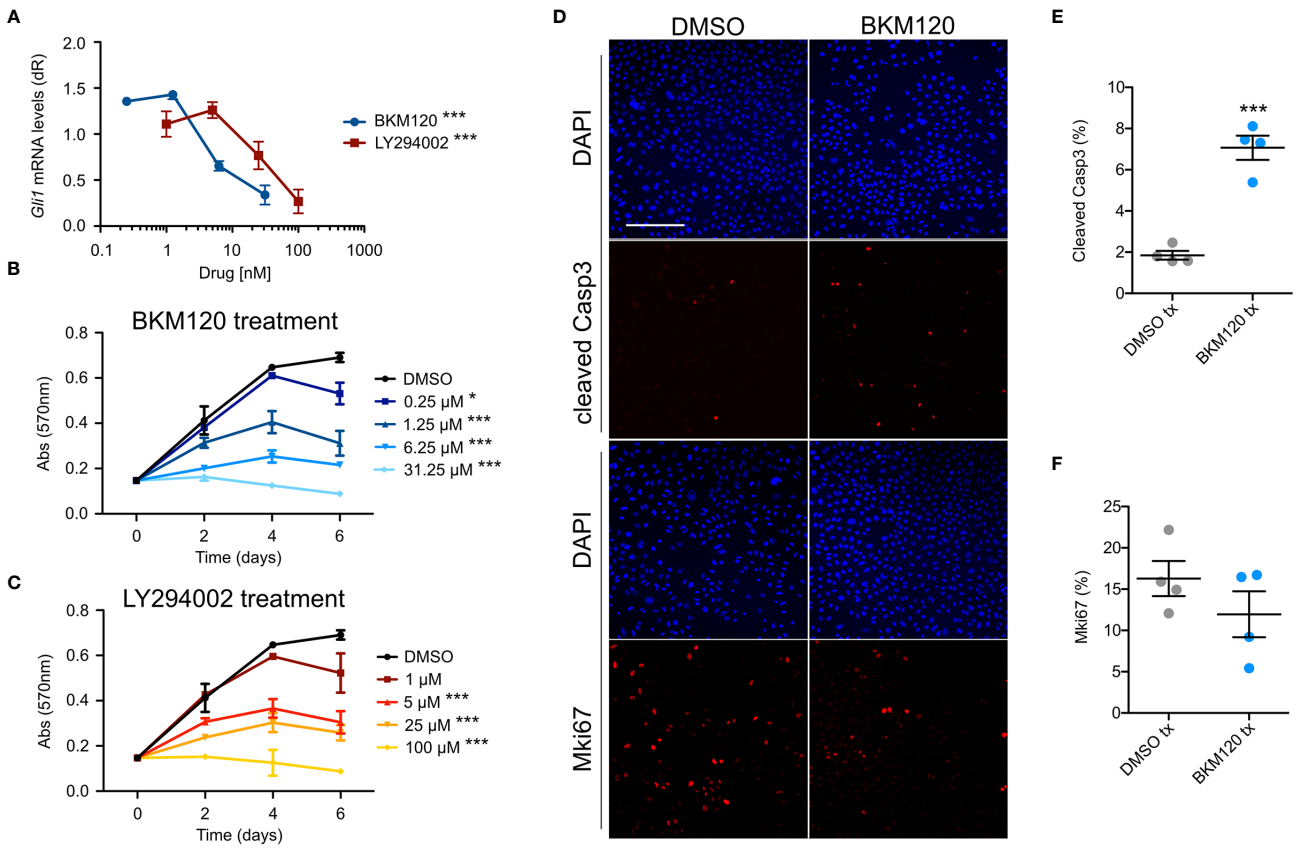


FIGURE 3 | Inhibition of PI3K suppresses BCC cell growth and HH signaling. **(A)** *Gli1* mRNA expression in ASZ001 cells treated with DMSO or varying concentrations of BKM120 or LY294002 (n = 3 experiments). dR, delta reporter gene normalized to passive reference dye. Error bar, SEM. Significance was determined by one-way ANOVA test. ***P < 0.001. **(B, C)** MTT assay of ASZ001 cells treated with DMSO or varying concentrations of **(B)** BKM120 or **(C)** LY294002 (n = 3 experiments). Abs, absorbance. Error bar, SEM. Significance was determined by two-way ANOVA test. *p < 0.05; ***p < 0.001. **(D)** Immunofluorescence staining of the indicated markers in ASZ001 cells treated with DMSO or BKM120. Scale bar, 200 µm. **(E)** Quantification of cleaved Casp3 signal (n = 4 experiments). **(F)** Quantification of Mki67 signal (n = 4 experiments). Error bars, SEM. Significance was determined by unpaired two-tailed *t* test. ***p < 0.001.

shown for the AKT-MTOR pathway, where inhibition of AKT resulted in elevated ERK signaling in cell culture but reduced signaling in 3D culture (59). Why this occurs in our system remains unclear, but one explanation could be that BCC tumors receive an abundance of signals from the surrounding niche that are absent in cell culture and can compensate for the loss of PI3K signaling to maintain HH pathway activation. Another possibility could be that higher *in vivo* dosage of drug could eventually suppress HH signaling, although the current dosage is able to inhibit tumor growth. Nevertheless, PI3K likely operates downstream or in parallel to the HH pathway in BCC, similar to our results for MTOR in *Ptch1*$^{fl/fl}$; *Gli1-Cre*^{ERT2} BCCs (48) and consistent with models where MTOR acts downstream of the HH pathway in *Ptch1*$^{+/-}$/*SKH-1* BCCs (60).

p21 is a potent universal cyclin-dependent kinase inhibitor that is activated downstream of p53 upon DNA damage or other cellular stresses and promotes G1 cell cycle arrest, which can lead to senescence or apoptosis (61). When p53 is present, p21 and p53 can act together to help correct DNA damage and preserve genome stability. However, when p53 is disrupted, p21 can promote genomic instability and escape from senescence (62). p21 degradation is facilitated by aPKC- and AKT1-dependent phosphorylation at T145 (56–58). As aPKC and AKT1 are both overexpressed in BCC and are required for tumor growth (29, 63), our results suggest that BCCs activate both kinases downstream of PI3K to promote cell cycle progression and continued tumor growth. PI3K inhibition significantly suppresses aPKC and Akt1 activity, likely leading to enhanced p21 stability, suppression of proliferation, and enhanced apoptosis.

Targeting the PI3K pathway in the clinic may be a viable option for BCC patients. In addition to the present study showing BKM120 efficacy on *Ptch1*$^{fl/fl}$; *Gli1-Cre*^{ERT2} BCCs, inhibition of the PI3K/AKT/MTOR pathway has been shown to suppress irradiated *Ptch1*$^{+/-}$; *Krt14*^{CreER2}; *p53*$^{fl/fl}$ BCCs with XL765, but not XL147 or GDC-0941 (64). In addition, suppressing MTOR activity using everolimus can suppress *Ptch1*$^{fl/fl}$; *Gli1-Cre*^{ERT2} BCCs through an aPKC-dependent process (48) and has been used in the clinic for compassionate treatment of BCCs in elderly patients who refused

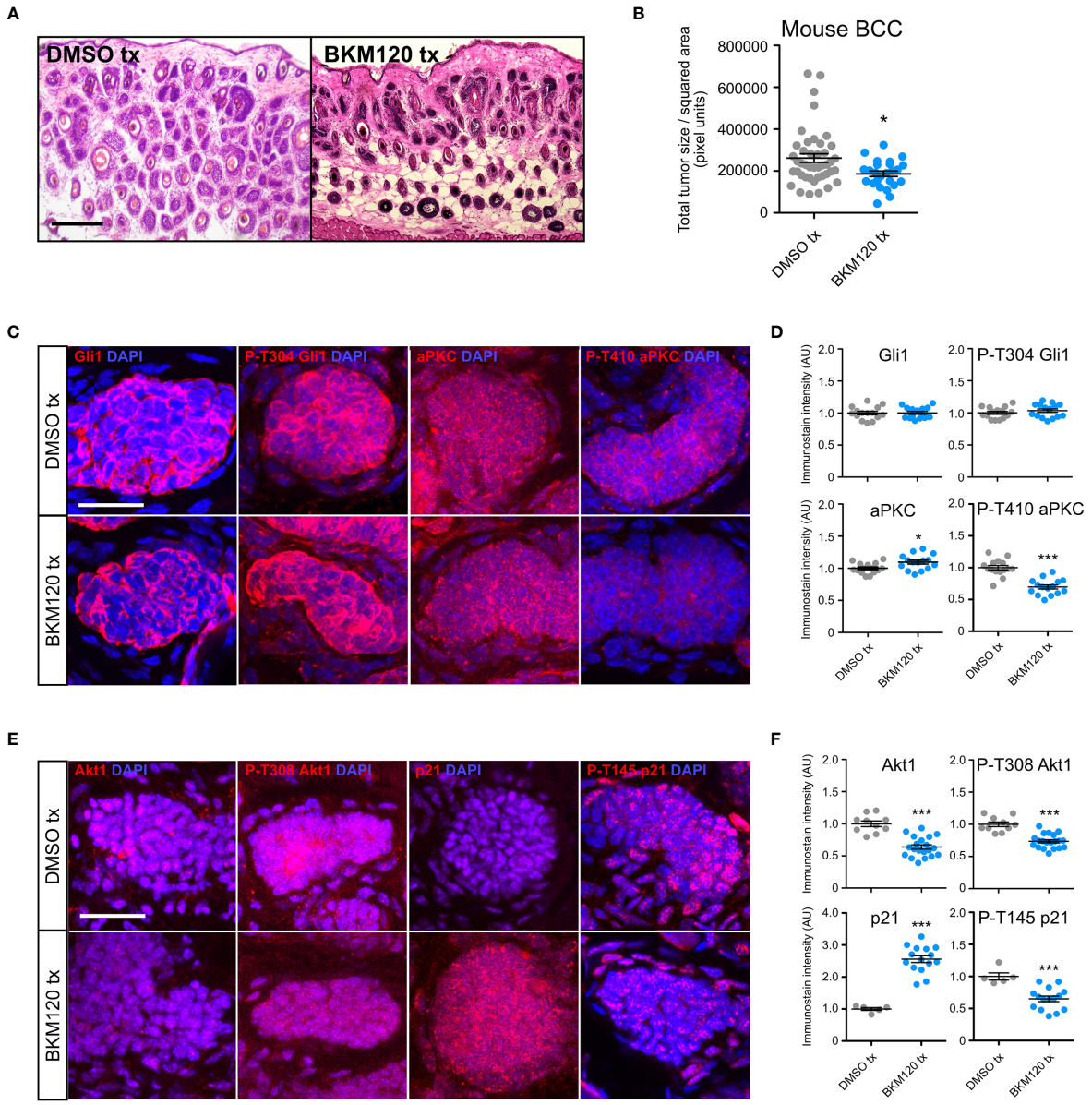


FIGURE 4 | PI3K inhibition suppresses murine BCC growth and stabilizes p21. **(A)** Hematoxylin and eosin staining of dorsal back skin collected from *Ptch*$^{fl/fl}$; *Gli1-Cre*^{ERT2} mice treated with DMSO or BKM120. Tx, treatment. Scale bar, 50 µm. **(B)** Quantification of total tumor size per square area (n>250 tumors from 5 mice). Tx, treatment. **(C)** Immunofluorescence staining of indicated markers (red) and DAPI counterstain (blue) in *Ptch1*$^{fl/fl}$; *Gli1-Cre*^{ERT2} tumors treated with DMSO or BKM120. Scale bar, 25 µm. **(D)** Quantification of immunofluorescence intensity of indicated markers (five points of measurement per animal, n=3 mice). AU, arbitrary unit. **(E)** Immunofluorescence staining of indicated markers (red) and DAPI counterstain (blue) in *Ptch1*$^{fl/fl}$; *Gli1-Cre*^{ERT2} tumors treated with DMSO or BKM120. Scale bar, 25 µm. **(F)** Quantification of immunofluorescence intensity of indicated markers (five points of measurement per animal, n=3 mice). Error bars, SEM. Significance was determined by unpaired two-tailed *t* test. *p < 0.05; ***p < 0.001.

surgery and did not respond to alternative treatments (65). Combination therapy may also be crucial to treat advanced BCC patients. For instance, PI3K/MTOR inhibition can delay therapeutic resistance against SMO inhibitors in mouse models of cancer, including BKM120 cotreatment in HH-driven medulloblastoma (36) or cotreatment with the MTOR inhibitor RAD-001 in esophageal adenocarcinoma (37). In addition, SMO inhibitor-resistant mouse medulloblastoma are still sensitive to PI3K inhibition (66) and combination therapy with the GLI inhibitor GANT61 and PI3K/MTOR inhibitor PI103 synergistically inhibited tumors in a HH-driven rhabdomyosarcoma mouse model (67). Altogether, PI3K pathway-targeted therapies, solely or in combination with HH pathway inhibitors, may broaden our repository for treating advanced and SMO inhibitor-resistant BCCs.

DATA AVAILABILITY STATEMENT

Publicly available datasets were analyzed in this study. This data can be found here: The data that supports the findings of this study are available in GEO at http://www.ncbi.nlm.nih.gov/geo/query/acc.cgi?acc-GSE58375, reference number GSE58375.

ETHICS STATEMENT

The animal study was reviewed and approved by Institutional Animal Care and Use Committee (IACUC) at the University of California, Irvine.

AUTHOR CONTRIBUTIONS

SA and RC conceived the project. SA supervised research. RC performed experiments. UJ, TL, GK, and DC quantified and immunostained tumor data. LD collected and annotated human clinical samples SA, UJ, and RC wrote the manuscript. All authors contributed to the article and approved the submitted version.

FUNDING

The work is funded by NIH grant R01CA237563 (SXA) and ACS Research Scholar Award RSG-19-089-01-DDC (SA).

ACKNOWLEDGMENTS

We would like to thank Sunny Wong for the *Ptch1*$^{fl/fl}$; *Gli1-Cre*^{ERT2} mice. The authors wish to acknowledge the support of the Chao Family Comprehensive Cancer Center Optical Biology Core Shared Resource, supported by the National Cancer Institute of the NIH under award number P30CA062203.

SUPPLEMENTARY MATERIAL

The Supplementary Material for this article can be found online at: https://www.frontiersin.org/articles/10.3389/fonc.2021.668247/full#supplementary-material

REFERENCES

1. Armas-López L, Zúñiga J, Arrieta O, Ávila-Moreno F. The Hedgehog-GLI Pathway in Embryonic Development and Cancer: Implications for Pulmonary Oncology Therapy. *Oncotarget* (2017) 8(36):60684–703. doi: 10.18632/oncotarget.19527
2. Taylor MD, Liu L, Raffel C, Hui CC, Mainprize TG, Zhang X, et al. Mutations in SUFU Predispose to Medulloblastoma. *Nat Genet* (2002) 31(3):306–10. doi: 10.1038/ng916
3. Raffel C, Jenkins RB, Frederick L, Hebrink D, Alderete B, Fults DW, et al. Sporadic Medulloblastomas Contain PTCH Mutations. *Cancer Res* (1997) 47 (5):842–5.
4. Tostar U, Malm CJ, Meis-Kindblom JM, Kindblom LG, Toftgård R, Undén AB. Deregulation of the Hedgehog Pathway: A Possible Role for the PTCH and SUFU Genes in Human Rhabdomyoma and Rhabdomyosarcoma Development. *J Pathol* (2006) 208(1):17–25. doi: 10.1002/path.1882
5. Reifenberger J, Wolter M, Knobbe CB, Köhler B, Schönicke A, Scharwächter C, et al. Somatic Mutations in PTCH, Smoh, SUFUH, and TP53 Genes in Sporadic Basal Cell Carcinomas. *Br J Dermatol* (2005) 152(1):43–51. doi: 10.1111/j.1365-2133.2005.06353.x
6. Nguyen TTL, Tarapore E, Atwood SX. "Common Skin Diseases – Skin Cancer". In: *Imaging Technologies and Transdermal Delivery in Skin Disorders*. Weinheim, Germany: Wiley (2019). doi: 10.1002/9783527814633.ch5
7. Kauvar AN, Cronin T Jr, Roenigk R, Hruza G, Bennett R. Consensus for Nonmelanoma Skin Cancer Treatment: Basal Cell Carcinoma, Including a Cost Analysis of Treatment Methods. *Dermatologic Surg* (2015) 41(5):550–71. doi: 10.1097/DSS.0000000000000296
8. Lear JT, Corner C, Dziewulski P, Fife K, Ross GL, Varma S, et al. Challenges and New Horizons in the Management of Advanced Basal Cell Carcinoma: A UK Perspective. *Br J Cancer* (2014) 1111(8):1476–81. doi: 10.1038/bjc.2014.270
9. Pietrobono S, Gagliardi S, Stecca B. Non-Canonical Hedgehog Signaling Pathway in Cancer. Activation of GLI Transcription Factors Beyond Smoothened. *Front Genet* (2019) 10:556. doi: 10.3389/fgene.2019.00556
10. Von Hoff DD, LoRusso PM, Rudin CM, Reddy JC, Yauch RL, Tibes R, et al. Inhibition of the Hedgehog Pathway in Advanced Basal-Cell Carcinoma. *New Engl J Med* (2009) 361(12):1164–72. doi: 10.1056/NEJMoa0905360
11. Gajjar A, Stewart CF, Ellison DW, Kaste S, Kun LE, Packer RJ, et al. Phase I Study of Vismodegib in Children With Recurrent or Refractory Medulloblastoma; a Pediatric Brain Tumor Consortium Study. *Clin Cancer Res* (2013) 19(22):6305–12. doi: 10.1158/1078-0432.CCR-13-1425
12. Robinson GW, Orr BA, Wu G, Gururangan S, Lin T, Qaddoumi I, et al. Vismodegib Exerts Targeted Efficacy Against Recurrent Sonic Hedgehog-Subgroup Medulloblastomas: Results From Phase Ii Pediatric Brain Tumor Consortium Studies Pbtc-025B and PBTC-032. *J Clin Oncol* (2015) 33 (24):2646–54. doi: 10.1200/JCO.2014.60.1591
13. Sekulic A, Migden MR, Oro AE, Dirix L, Lewis KD, Hainsworth JD, et al. Efficacy and Safety of Vismodegib in Advanced Basal-Cell Carcinoma. *New Engl J Med* (2012) 366(23):2171–9. doi: 10.1056/NEJMoa1113713
14. Chang AL, Oro AE. Initial Assessment of Tumor Regrowth After Vismodegib in Advanced Basal Cell Carcinoma. *Achieves Dermatol* (2012) 148(11):1324–5. doi: 10.1001/archdermatol.2012.2354
15. Zhang Y, Bulkley DP, Xin Y, Roberts KJ, Asarnow DE, Sharma A, et al. Structural Basis for Cholesterol Transport-Like Activity of the Hedgehog Receptor Patched. *Cell* (2018) 175(5):1352–64. doi: 10.1016/j.cell.2018.10.026
16. Humke EW, Dorn KV, Milenkovic L, Scott MP, Rohatgi R. The Output of Hedgehog Signaling Is Controlled by the Dynamic Association Between Suppressor of Fused and Gli Proteins. *Genes Dev* (2010) 24(7):670–82. doi: 10.1101/gad.1902910
17. Wang B, Fallon JF, Beachy BA. Hedgehog-Regulated Processing of Gli3 Produces an Anterior/Posterior Repressor Gradient in the Developing Vertebrate Limb. *Cell* (2000) 100(4):423–34. doi: 10.1016/s0092-8674(00)80678-9
18. Xiao X, Tang JJ, Peng C, Wang Y, Fu L, Qiu ZP, et al. Cholesterol Modification of Smoothened Is Required for Hedgehog Signaling. *Mol Cell* (2017) 66 (1):154–62. doi: 10.1016/j.molcel.2017.02.015
19. Deshpande I, Liang J, Hedeen D, Roberts KJ, Zhang Y, Ha B, et al. Smoothened Stimulation by Membrane Sterols Drives Hedgehog Pathway Activity. *Nature* (2019) 571(7764):284–8. doi: 10.1038/s41586-019-1355-4
20. Tukachinsky H, Lopez LV, Salic A. A Mechanism for Vertebrate Hedgehog Signaling: Recruitment to Cilia and Disassociation of SuFu-Gli Protein Complexes. *J Cell Biol* (2010) 191(2):415–28. doi: 10.1083/jcb.201004108
21. Bonilla X, Parmentier L, King B, Bezrukov F, Kaya G, Zoete V, et al. Genomic Analysis Identifies New Drivers and Progression Pathways in Skin Basal Cell Carcinoma. *Nat Genet* (2016) 48(4):398–406. doi: 10.1038/ng.3525
22. Atwood SX, Sarin KY, Whitson RJ, Li JR, Kim G, Rezaee M, et al. Smoothened Variants Explain the Majority of Drug Resistance in Basal Cell Carcinoma. *Cancer* (2015) 27(3):342–53. doi: 10.1016/j.ccell.2015.02.002
23. Peer E, Tesanovic S, Aberger F. Next-Generation Hedgehog/GLI Pathway Inhibitors for Cancer Therapy. *Cancers* (2019) 11(4):538. doi: 10.3390/cancers11040538
24. Kim J, Aftab BT, Tang JY, Kim D, Lee AH, Rezaee M, et al. Itraconazole and Arsenic Trioxide Inhibit Hedgehog Pathway Activation and Tumor Growth

Associated With Acquired Resistance to Smoothened Antagonists. *Cancer Cell* (2013) 23(1):23–4. doi: 10.1016/j.ccr.2012.11.017
25. Gruber W, Hutzinger M, Elmer DP, Parigger T, Sternberg C, Cegielkowski L, et al. DYRK1B as Therapeutic Target in Hedgehog/GLI-dependent Cancer Cells With Smoothened Inhibitor Resistance. *Oncotarget* (2016) 7(6):7134–48. doi: 10.18632/oncotarget.6910
26. Gruber W, Peer E, Elmer DP, Sternberg C, Tesanovic S, Del Burgo P, et al. Targeting Class I Histone Deacetylases by the Novel Small Molecule Inhibitor 4SC-202 Blocks Oncogenic Hedgehog-GLI Signaling and Overcomes Smoothened Inhibitor Resistance. *Int J Cancer* (2018) 142(5):968–75. doi: 10.1002/ijc.31117
27. Tang Y, Gholamin S, Schubert S, Willardson MI, Lee A, Bandopadhayay P, et al. Epigenetic Targeting of Hedgehog Pathway Transcriptional Output Through BET Bromodomain Inhibition. *Nat Med* (2014) 20(7):732–40. doi: 10.1038/nm.3613
28. Whitson RJ, Lee A, Urman NM, Mirza A, Yao CY, Brown AS, et al. Noncanonical Hedgehog Pathway Activation Through SRF-MKL1 Promotes Drug Resistance in Basal Cell Carcinoma. *Nat Med* (2018) 24 (3):271–81. doi: 10.1038/nm.4476
29. Atwood SX, Li M, Lee A, Tang JY, Oro AE. GLI Activation by Atypical Protein Kinase C ι/λ Regulates the Growth of Basal Cell Carcinoma. *Nature* (2013) 494(7438):484–8. doi: 10.1038/nature11889
30. Yang SH, Andl T, Grachtchouk V, Wang A, Liu J, Syu LJ, et al. Pathological Responses to Oncogenic Hedgehog Signaling in Skin are Dependent on Canonical Wnt/beta3-catenin Signaling. *Nat Genet* (2008) 40(9):1130–5. doi: 10.1038/ng.192
31. Eberl M, Mangelberger D, Swanson JB, Verhaegen ME, Harms PW, Frohm ML, et al. Tumor Architecture and Notch Signaling Modulates Drug Response in Basal Cell Carcinoma. *Cancer Cell* (2018) 33(2):229–43. doi: 10.1016/j.ccell.2017.12.015
32. Yao CD, Haensel D, Gaddam S, Patel T, Atwood SX, Sarin KY, et al. AP-1 and TGFβ Cooperatively Drives Non-Canonical Hedgehog Signaling in Resistant Basal Cell Carcinoma. *Nat Commun* (2020) 11(1):5079. doi: 10.1038/s41467-020-18762-5
33. Zhao X, Ponomaryov T, Ornell KJ, Zhou P, Dabral SK, Pak E, et al. Ras/Mapk Activation Drives Resistance to Smo Inhibition, Metastasis, and Tumor Evolution in Shh Pathway-Dependent Tumors. *Cancer Res* (2015) 75 (17):3623–35. doi: 10.1158/0008-5472.CAN-14-2999-T
34. Cai X, Yu K, Zhang L, Li Y, Li Q, Yang Z, et al. Synergistic Inhibition of Colon Carcinoma Cell Growth by Hedgehog-Gli1 Inhibitor Arsenic Trioxide and Phosphoinositide 3-Kinase Inhibitor LY294002. *Onco Targets Ther* (2015) 8:877–83. doi: 10.2147/OTT.S71034
35. Singh R, Dhanyamraju PK, Lauth M. DYRK1B Blocks Canonical and Promotes Non-Canonical Hedgehog Signaling Through Activation of the mTOR/AKT Pathway. *Oncotarget* (2017) 8(1):833–45. doi: 10.18632/oncotarget.13662
36. Buonamici S, Williams J, Morrissey M, Wang A, Guo R, Vattay A, et al. Interfering With Resistance to Smoothened Antagonists by Inhibition of the PI3K Pathway in Medulloblastoma. *Sci Trans Med* (2010) 2(51):51ra70. doi: 10.1126/scitranslmed.3001599
37. Wang Y, Ding Q, Yen CJ, Xia W, Izzo JG, Lang JY, et al. The Crosstalk of mTOR/S6K1 and Hedgehog Pathways. *Cancer Cell* (2012) 21(3):374–87. doi: 10.1016/j.ccr.2011.12.028
38. Vanhaesebroeck B, Guillermet-Guibert J, Graupera M, Bilanges B. The Emerging Mechanisms of Isoform-Specific PI3K Signaling. *Nat Rev Mol Cell Biol* (2010) 11(5):329–41. doi: 10.1038/nrm2882
39. Engelman JA, Luo J, Cantley LC. The Evolution of Phosphatidylinositol 3-Kinases as Regulators of Growth and Metabolism. *Nat Rev Genet* (2006) 7 (8):606–19. doi: 10.1038/nrg1879
40. Brechbiel J, Miller-Moslin K, Adjei AA. Crosstalk Between Hedgehog and Other Signaling Pathways as a Basis for Combination Therapies in Cancer. *Cancer Treat Rev* (2014) 40(6):750–9. doi: 10.1016/j.ctrv.2014.02.003
41. Riobó NA, Lu K, Ai X, Haines GM, Emerson CP Jr. Phosphoinositide 3-Kinase and Akt are Essential for Sonic Hedgehog Signaling. *PNAS USA* (2006) 103(12):4505–10. doi: 10.1073/pnas.0504337103
42. Wei L, Xu Z. Cross-Signaling Among Phosphoinositide-3 Kinase, Mitogen-Activated Protein Kinase and Sonic Hedgehog Pathways Exists in Esophageal Cancer. *Int J Cancer* (2011) 129(2):275–84. doi: 10.1002/ijc.25673
43. Ramaswamy B, Lu Y, Teng KY, Nuovo G, Li X, Shapiro CL, et al. Hedgehog Signaling is a Novel Therapeutic Target in Tamoxifen-Resistant Breast Cancer Aberrantly Activated by PI3K/AKT Pathway. *Cancer Res* (2012) 72(19):5048–59. doi: 10.1158/0008-5472.CAN-12-1248
44. Diao Y, Rahman MF, Villegas VE, Wickström M, Johnsen JI, Zaphiropoulos PG. The Impact of S6K1 Kinase on Neuroblastoma Cell Proliferation Is Independent of GLI1 Signaling. *BMC Cancer* (2014) 14:600. doi: 10.1186/1471-2407-14-600
45. Kuleshov MV, Jones MR, Rouillard AD, Fernandez NF, Duan Q, Wang Z, et al. Enrichr: A Comprehensive Gene Set Enrichment Analysis Web Server 2016 Update. *Nucleic Acids Res* (2016) 44(W1):W90–7. doi: 10.1093/nar/gkw377
46. So PL, Langston AW, Daniallinia N, Herbert JL, Fujimoto MA, Khaimskiy Y, et al. Long-Term Establishment, Characterization, and Manipulation of Cell Lines From Mouse Basal Cell Carcinoma Tumors. *Exp Dermatol* (2006) 15 (9):742–50. doi: 10.1111/j.1600-0625.2006.00465.x
47. Drummond ML, Li M, Tarapore E, Nguyen TTL, Barouni BJ, Cruz S, et al. Actin Polymerization Controls Cilia-Mediated Signaling. *J Cell Biol* (2018) 217(9):3255–66. doi: 10.1083/jcb.201703196
48. Chow R, Levee TM, Kaur G, Cedeno DP, Doan LT, Atwood SX. MTOR Promotes Basal Cell Carcinoma Growth Through Atypical PKC. *Exp Dermatol* (2020) 30(3):358–66. doi: 10.1111/exd.14255
49. Lachmann A, Ma'ayan A. KEA: Kinase Enrichment Analysis. *Bioinformatics* (2009) 25(5):684–6. doi: 10.1093/bioinformatics/btp026
50. Peterson SC, Eberl M, Vagnozzi AN, Belkadi A, Veniaminova NA, Verhaegen ME, et al. Basal Cell Carcinoma Preferentially Arises From Stem Cells Within Hair Follicle and Mechanosensory Niches. *Cell Stem Cell* (2015) 16(4):400–12. doi: 10.1016/j.stem.2015.02.006
51. Burger MT, Pecchi S, Wagman A, Ni ZJ, Knapp M, Hendrickson T, et al. Identification of NVP-BKM120 as a Potent, Selective, Orally Bioavailable Class I Pi3 Kinase Inhibitor for Treating Cancer. *Cell Stem Cell* (2011) 16 (4):400–12. doi: 10.1021/ml200156t
52. Walker EH, Pacold ME, Perisic O, Stephens L, Hawkins PT, Wymann MP, et al. Structural Determinants of Phosphoinositide 3-Kinase Inhibition by Wortmannin, LY294002, Quercetin, Myricetin, and Staurosporine. *Mol Cell* (2000) 6(4):909–19. doi: 10.1016/s1097-2765(05)00089-4
53. Chou MM, Hou W, Johnson J, Graham LK, Lee MH, Chen CS, et al. Regulation of Protein Kinase C Zeta by PI 3-Kinase and PDK-1. *Curr Biol* (1998) 8(19):1069–77. doi: 10.1016/s0960-9822(98)70444-0
54. Le Good JA, Ziegler WH, Parekh DB, Alessi DR, Cohen P, Parker PJ. Protein Kinase C Isotypes Controlled by Phosphoinositide 3-Kinase Through the Protein Kinase PDK1. *Science* (1998) 281(5385):2042–5. doi: 10.1126/science.281.5385.2042
55. Alessi DR, James SR, Downes CP, Holmes AB, Gaffney PR, Reese CB, et al. Characterization of a 3-Phosphoinositide-Dependent Protein Kinase Which Phosphorylates and Activates Protein Kinase Balpha. *Curr Biol* (1997) 7 (4):261–9. doi: 10.1016/s0960-9822(06)00122-9
56. Rössig L, Jadidi AS, Urbich C, Badorff C, Zeiher AM, Dimmeler S. Akt-Dependent Phosphorylation of p21(Cip1) Regulations PCNA Binding and Proliferation of Endothelial Cells. *Mol Cell Biol* (2001) 21(16):5644–57. doi: 10.1128/MCB.21.16.5644-5657.2001
57. Zhou BP, Liao Y, Xia W, Spohn B, Lee MH, Hung MC. Cytoplasmic Localization of p21Cip1/WAF1 by Akt-Induced Phosphorylation in HER-2/neu-overexpressing Cells. *Nat Cell Biol* (2001) 3(3):245–52. doi: 10.1038/35060032
58. Scott MT, Ingram A, Ball KL. PDK1-Dependent Activation of Atypical PKC Leads to Degradation of the p21 Tumour Modifier Protein. *EMBO J* (2002) 21 (24):6771–80. doi: 10.1093/emboj/cdf684
59. Riedl A, Schlederer M, Pudelko K, Stadler M, Walter S, Unterleuthner D, et al. Comparison of Cancer Cells in 2D vs 3D Culture Reveals Differences in AKT-mTOR-S6K Signaling and Drug Responses. *J Cell Signaling* (2017) 130 (1):203–18. doi: 10.1242/jcs.188102
60. Kim AL, Back JH, Chaudhary SC, Zhu Y, Athar M, Bickers DR. Sox9 Transcriptionally Regulates Mtor-Induced Proliferation of Basal Cell Carcinomas. *J Invest Dermatol* (2018) 138(8):1716–25. doi: 10.1016/j.jid.2018.01.040

61. Georgakilas AG, Martin OA, Bonner WM. P21: A Two-Faced Genomic Guardian. *Trends Mol Med* (2017) 23(4):310–19. doi: 10.1016/j.molmed.2017.02.001
62. Galanos P, Vougas K, Walter D, Polyzos A, Maya-Mendoza A, Haagensen EJ, et al. Chronic p53-Independent p21 Expression Causes Genomic Instability by Deregulating Replication Licensing. *Nat Cell Biol* (2016) 18(7):777–89. doi: 10.1038/ncb3378
63. Kim AL, Back JH, Zhu Y, Tang X, Yardley NP, Kim KJ, et al. Akt1 Activation is Obligatory for Spontaneous Bcc Tumor Growth in a Murine Model That Mimics Some Features of Basal Cell Nevus Syndrome. *Cancer Prev Res* (2016) 9(10):794–802. doi: 10.1158/1940-6207.CAPR-16-0066
64. So PL, Wang GY, Wang K, Chuang M, Chiueh VC, Kenny PA, et al. Pi3k-AKT Signaling Is a Downstream Effector of Retinoid Prevention of Murine Basal Cell Carcinogenesis. *Cancer Prev Res* (2014) 7(4):407–17. doi: 10.1158/1940-6207.CAPR-13-0304
65. Eibenschutz L, Colombo D, Catricalà C. Everolimus for Compassionate Use in Multiple Basal Cell Carcinomas. *Case Rep Dermatol Med* (2013) 2013:604301. doi: 10.1155/2013/604301
66. Dijkgraaf GJ, Alicke B, Weinmann L, Januario T, West K, Modrusan Z, et al. Small Molecule Inhibition of GDC-0449 Refractory Smoothened Mutants and Downstream Mechanisms of Drug Resistance. *Cancer Res* (2011) 71(2):435–44. doi: 10.1158/0008-5472.CAN-10-2876
67. Graab U, Hahn H, Fulda S. Identification of a Novel Synergistic Lethality of Combined Inhibition of Hedgehog and PI3K Signaling in Rhabdomyosarcoma. *Oncotarget* (2015) 6(11):8722–35. doi: 10.18632/Oncotarget.2726

Disclaimer: The content is solely the responsibility of the authors and does not necessarily represent the official views of the NIH.

Conflict of Interest: The authors declare that the research was conducted in the absence of any commercial or financial relationships that could be construed as a potential conflict of interest.

Copyright © 2021 Chow, Jeon, Levee, Kaur, Cedeno, Doan and Atwood. This is an open-access article distributed under the terms of the Creative Commons Attribution License (CC BY). The use, distribution or reproduction in other forums is permitted, provided the original author(s) and the copyright owner(s) are credited and that the original publication in this journal is cited, in accordance with accepted academic practice. No use, distribution or reproduction is permitted which does not comply with these terms.

frontiers in Oncology

ORIGINAL RESEARCH
published: 08 July 2021
doi: 10.3389/fonc.2021.672797

Real Life Clinical Management and Survival in Advanced Cutaneous Melanoma: The Italian Clinical National Melanoma Registry Experience

Anna Crispo[1], Maria Teresa Corradin[2], Erika Giulioni[2], Antonella Vecchiato[3], Paolo Del Fiore[3], Paola Queirolo[4,5], Francesco Spagnolo[4], Vito Vanella[1], Corrado Caracò[1], Giulio Tosti[5], Elisabetta Pennacchioli[5], Giuseppe Giudice[6], Eleonora Nacchiero[6], Pietro Quaglino[7], Simone Ribero[7], Monica Giordano[8], Desire Marussi[8], Stefania Barruscotti[9], Michele Guida[10], Vincenzo De Giorgi[11], OccelliMarcella[12], Federica Grosso[13], Giuseppe Cairo[14], Alessandro Gatti[15], Daniela Massa[16], Laura Atzori[17], Nicola Calvani[18], Tommaso Fabrizio[19], Giuseppe Mastrangelo[20], Federica Toffolutti[21], Egidio Celentano[1], Mario Budroni[22], Sara Gandini[5], Carlo Riccardo Rossi[3,20], Alessandro Testori[9], Giuseppe Palmieri[23], Paolo A. Ascierto[1] and the Clinical National Melanoma Registry Study Group at the Italian Melanoma Intergroup*

[1] Istituto Nazionale Tumori IRCCS Fondazione G. Pascale, Napoli, Italy, [2] Dermatology Department, Azienda Sanitaria Friuli Occidentale, Pordenone, Italy, [3] Istituto Oncologico Veneto IOV - IRCCS, Padova, Italy, [4] IRCCS Ospedale Policlinico San Martino, Genova, Italy, [5] Istituto Europeo di Oncologia - IRCCS, Milano, Italy, [6] Plastic and Reconstructive Surgery Department, Università degli Studi di Bari Aldo Moro, Bari, Italy, [7] Clinica Dermatologica, Dipartimento di Scienze Mediche, Università di Torino, Torino, Italy, [8] Oncology Department, Ospedale Sant'Anna di Como, Como, Italy, [9] Fondazione I.R.C.C.S. Policlinico San Matteo, Pavia, Italy, [10] IRCCS Istituto Tumori "Giovanni Paolo II", Bari, Italy, [11] Dermatology Department, Università di Firenze, Firenze, Italy, [12] Oncology Department, Azienda ospedaliera Santa Croce e Carle, Cuneo, Italy, [13] Mesothelioma Unit, Azienda Ospedaliera SS Antonio e Biagio e Cesare Arrigo, Alessandria, Italy, [14] Oncology Department, ospedale "Vito Fazzi" di Lecce, Lecce, Italy, [15] ULSS 2 Marca Trevigiana Ospedale Ca' Foncello Treviso, Treviso, Italy, [16] Gruppo melanoma e tumori rari, Oncology Department, PO A Businco ARNAS G. Brotzu, Cagliari, Italy, [17] Dermatology Clinic, Department Medical Sciences and Public Health, University of Cagliari, Cagliari, Italy, [18] Oncology Department, Presidio Ospedaliero "Senatore Antonio Perrino", Brindisi, Italy, [19] IRCCS Centro di Riferimento Oncologico Basilicata, Rionero in Vulture, Italy, [20] Dermatology Clinic, Università degli studi di Padova, Padova, Italy, [21] Centro di Riferimento Oncologico di Aviano (CRO) IRCCS, Aviano (PN), Italy, [22] Registro Tumori Provincia di Sassari, Azienda Ospedaliera Universitaria Sassari, Sassari, Italy, [23] Istituto di Ricerca Genetica e Biomedica, CNR, Sassari, Italy

Background: Cutaneous melanoma (CM) is one of the most aggressive types of skin cancer. Currently, innovative approaches such as target therapies and immunotherapies have been introduced in clinical practice. Data of clinical trials and real life studies that evaluate the outcomes of these therapeutic associations are necessary to establish their clinical utility. The aim of this study is to investigate the types of oncological treatments employed in the real-life clinical management of patients with advanced CM in several Italian centers, which are part of the Clinical National Melanoma Registry (CNMR).

Methods: Melanoma-specific survival and overall survival were calculated. Multivariate Cox regression models were used to estimate the hazard ratios adjusting for confounders and other prognostic factors.

OPEN ACCESS

Edited by:
Xunwei Wu,
Shandong University, China

Reviewed by:
Xinan Sheng,
Peking University Cancer Hospital, China
Jinfeng Wu,
Fudan University, China

****Correspondence:***
Paolo A. Ascierto
paolo.ascierto@gmail.com;
p.ascierto@istitutotumori.na.it

Specialty section:
This article was submitted to Skin Cancer, a section of the journal Frontiers in Oncology

Received: *04 March 2021*
Accepted: *22 June 2021*
Published: *08 July 2021*

Citation:
Crispo A, Corradin MT, Giulioni E, Vecchiato A, Del Fiore P, Queirolo P, Spagnolo F, Vanella V, Caracò C, Tosti G, Pennacchioli E, Giudice G, Nacchiero E, Quaglino P, Ribero S, Giordano M, Marussi D, Barruscotti S, Guida M, De Giorgi V, Occelli M, Grosso F, Cairo G, Gatti A, Massa D, Atzori L, Calvani N, Fabrizio T, Mastrangelo G, Toffolutti F, Celentano E, Budroni M, Gandini S, Rossi CR, Testori A, Palmieri G, Ascierto PA and the Clinical National Melanoma Registry Study Group at the Italian Melanoma Intergroup (2021) Real Life Clinical Management and Survival in Advanced Cutaneous Melanoma: The Italian Clinical National Melanoma Registry Experience. Front. Oncol. 11:672797. doi: 10.3389/fonc.2021.672797

Results: The median follow-up time was 36 months (range 1.2-185.1). 787 CM were included in the analysis with completed information about therapies. All types of immunotherapy showed a significant improved survival compared with all other therapies (p=0.001). 75% was the highest reduction of death reached by anti-PD-1 (HR=0.25), globally immunotherapy was significantly associated with improved survival, either for anti-CTLA4 monotherapy or combined with anti-PD-1 (HR=0.47 and 0.26, respectively) and BRAFI+MEKI (HR=0.62).

Conclusions: The nivolumab/pembrolizumab in combination of ipilimumab and the addition of ant-MEK to the BRAFi can be considered the best therapies to improve survival in a real-world-population. The CNMR can complement clinical registries with the intent of improving cancer management and standardizing cancer treatment.

Keywords: medical record systems, cutaneous melanoma, survival analysis, immunotherapy, ipilimumab

INTRODUCTION

Cutaneous melanoma (CM) is one of the most aggressive types of skin cancer. The incidence of CM has increased in Europe over the last years, and cohort studies suggest that the increasing trend of incidence will continue for at least the next 2 decades (1–3) Mortality rates have also increased in the last decades, especially in men, despite a clear decrease of Breslow tumor thickness in the USA and Europe (1, 4). In the USA, the raw mortality rates per 100,000 inhabitants per year increased from 2.8 to 3.1, with an estimate of 10,130 deaths from melanoma in 2016 (they were 8,650 in 2009) (1). In Italy, 12,300 new cases and over 2,000 deaths were estimated in 2019 (5, 6).

Surgery is currently the golden standard for patients with early stage CM, who represent only part of the global cases. The treatment of patients with advanced stage CM is more complex, as for decades no chemotherapy regimens have been found effective in prolonging survival. Currently, innovative approaches such as target therapies and immunotherapies have been introduced in clinical practice for the treatment of metastatic CM. Target therapies are based on the use of drugs targeting specific genetic alterations in candidate genes, blocking specific pathways implicated in the oncogenesis of melanoma (7). BRAF mutations represent currently the main molecular targets for melanoma treatment, as they involve approximately 50% of the cases, and identify patients who may benefit from treatment with BRAF inhibitors, like vemurafenib or dabrafenib (8–10). Recently, the combination of BRAFi drugs with MEK inhibitors showed improved oncological outcomes in comparison to monotherapies (70% one-year and 50% two-years survival), with a better safety profile (11–13).

Immuno-therapy enhances the immune system's T-cell response and indirectly affects cancer cells by stimulating the patient's immune system (14). Ipilimumab, a monoclonal antibody that blocks the activity of the CTLA-4, has shown a long-term survival in about 20% of the patients treated (15–17). Programmed death 1 (PD1) is a membrane receptor of tumor cells (its main ligand is PD-L1) that represents a powerful brake to the immune system's response and the target of specific inhibitors (nivolumab and pembrolizumab). Recently they have been introduced into clinical practice, as they were shown more effective than ipilimumab in terms of overall survival (OS) and toxicity (18, 19). Recent studies showed that the combination of anti-CTLA-4 and anti-PD-1 is more effective than monotherapy, but a higher incidence of high-grade adverse events was found (20). Combinations of targeted therapies and immunotherapies are currently investigated; the advantage of such combinations is that more than one anti-tumoral mechanism are employed against CM. Data of clinical trials and real life studies that evaluate the outcomes of these therapeutic associations are necessary to establish their clinical utility.

The aim of this study is to investigate the types of oncological treatments employed in the real-life clinical management of patients with advanced CM in several Italian centers which are part of the Clinical National Melanoma Registry (CNMR), and the oncological outcomes obtained.

MATERIALS AND METHODS

Patients and Data Collection

CNMR is the first clinical registry established in Italy in 2010. It collects data from a wide network of melanoma centers throughout the country with the aim to carry out clinical and therapeutic evaluations investigating geographical and policy differences and instruments for planning specific health interventions in different populations and areas, in order to optimize the clinical management and survival of CM patients. CNMR collects data of patients with a histologically confirmed diagnosis of primary CM treated in 38 Italian institutions (hospitals, research institutes, ecc.) participating in the network, as previously described (21). The AJCC7 staging was used. For the purposes of the present study, data of consecutive patients enrolled from January 2011 to December 2018 were considered (CNMR established in 2010 but the first year was spent for administrative approvement and ethical committee in each centers).

A diagram of the CNMR's organizational structure can be found in **Figure 1**.

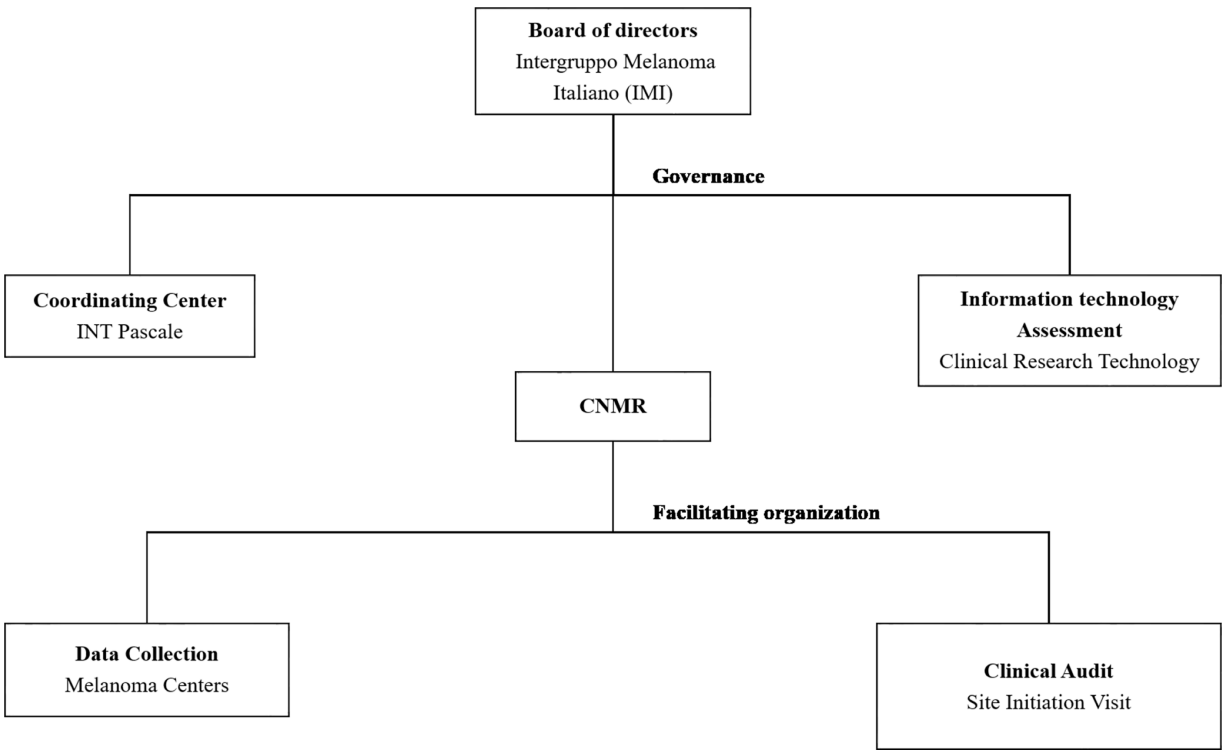


FIGURE 1 | Integrated management of CNMR. Two main complementary approaches are considered—Governance and Facilitating organization.

Data were collected *via* an electronic Case Report Form (eCRF), which was developed by the Clinical Research Technology S.r.l. group (Salerno, Italy) on its clinical platform 'eClinical'. 'eClinical' assigned an identification (ID) number to all the patients screened. The quality of the electronic data was verified through onsite clinical visits, undertaken periodically during the study. The eCRF was designed to collect information on sociodemographic, clinical, pathological and treatment variables. The first treatment was registered in all cases: local therapy (radiotherapy and electro-chemotherapy), systemic chemotherapy (platinum salts, dacarbazine, fotemustine), targeted therapy (BRAFi: vemurafenib/dabrafenib; BRAFI+MEKI: cobimetinib/trametinib), and immunotherapy (anti-CTLA4: ipilimumab, anti-PD-1: nivolumab/pembrolizumab; and anti-CTLA4 + anti-PD-1). Further information regarding the date of diagnosis, the duration of therapy, the date of the last follow-up, and the clinical status of the patients were also registered. Eligible patients for the survival analysis had histologically confirmed, unresectable stage III or stage IV metastatic melanoma (stage IIIB-IV) with an Eastern Cooperative Oncology Group (ECOG) performance status 0 or 3, and known BRAF mutation status.

Statistical Analysis

Descriptive statistics for the categorical data were reported. Pearson's Chi-squared was used to compare categorical variables. All patients were followed until 31 December 2018 or until the date of last visit, or death, whichever came first.

Melanoma-specific survival (MSS) was calculated from the date of initial adjuvant treatment to death for the disease and Overall survival (OS) until date of death from any cause. Patients who did not die were censored for OS on the last visit date available in the database. When the date of diagnosis was antecedent the beginning of the Melanoma Registry or the initial diagnosis was an early melanoma we considered the MSSurvival from the date of initial adjuvant treatment.

Kaplan-Meier curves and medians of OS and 95% CI are presented overall and by immunotherapy and target treatments. The Log-rank test compared curves by treatments (immunotherapy: anti-CTLA4, an-ti-PD-1 *vs.* no immunotherapy and no target therapy; BRAF: BRAFi, BRAFI+MEKI *vs.* no immunotherapy and no target therapy). Univariate and multivariable Cox regression models were used to estimate the hazard ratios adjusting for confounders and other prognostic factors.

All statistical tests were two-sided. P-values < 0.05 were considered significant. Statistical analyses were performed using statistical software SAS (version 9.02 for Windows), and Statistical Package for Social Science (SPSS) version 25 (SPSS inc., Chicago IL, USA).

RESULTS

Patients characteristics, sex, age, LDH, stage, BRAF execution and mutational status were reported in **Table 1**.

TABLE 1 | Tumor characteristics for Advanced Stage (IIIB-IIIC unresectable, IV).

	ADVANCED STAGE IIIB-IIIC (*unresectable*), IV N=787
Gender*	
Male	*476 (60)*
Female	*307 (39)*
missing	*4 (1)*
Age	
≤60 yrs	*355 (45)*
>60 yrs	*432 (55)*
BMI	
<25	315 (40)
≥25	386 (49)
missing	86 (11)
LDH	
Normal	479 (61)
Abnormal	43 (5)
Unknown	265 (34)
Initial Stage	
In situ	98 (12)
Stage I-II	297 (38)
Stage III	291 (37)
Stage IV	101 (13)
BRAF executed	
No	120 (15)
Yes	594 (76)
Not applicable	73 (9)
BRAF mutational status	
Mutant	322 (54)
Wild Type	269 (45.5)
unknown	3 (0.5)
Mutant	
BRAF V600	56 (17.4)
BRAF V600E	208 (64.6)
BRAF V600K	34 (10.6)
Other	24 (7.5)
Year BRAF executed	
<2013	498 (63)
≥2013	289 (37)

**4 patients did not report the gender.*

Regarding to stage 12% had an initial diagnosis of "in situ", 38% had an early diagnosis (IA-IIC), 37% stage III and 13% had a confirmed advanced melanoma stage (IV). 76% was the percentage of BRAF executed in our sample and the incidence of BRAF mutations was slightly greater than 50% and 65% reported a BRAF V600E mutation most cases were analyzed after the year 2013 when target therapies were diffusely employed in clinical practice; in addition, more cases among those analyzed harbored stage IV tumors rather than stage IIIB-IIIC melanomas.

The median follow-up time was 36 months (range 1.2-185.1). Observed patients and percentage according to type of treatment were reported in **Table 2**; total death events (for all causes and deaths for the diseases) were reported and median Melanoma-specific survival (MSS) were calculated. As first line of treatment (choice), 41% of patients (n=319) received immunotherapy, 36% received BRAF-targeted therapies (n=285), 35% received chemotherapy (n=275) and 35% received local therapy (electrochemotherapy) (n=275). In details, among immunotherapy: 62% received ipilimumab (anti-CTLA4), 25% nivolumab/pebrolizumab (anti PD1), 13% the two combined. Among BRAF therapy: 69% received BRAFi as monotherapy (vemurafenib/dabrafenib), about 31% received BRAFi+MEK combination treatment (vemurafenib/dabrafenib + cobimetinib/trametinib).

In the entire cohort the median overall melanoma-specific survival was 47 months (95% CI: 41-53), the lowest median survival was detected by patients treated by chemotherapy (33 months, 95% CI 27-38) as first option. Among immunotherapy the MSS globally was 50 months (95% CI 43-57), it varied from 47 months (95% CI 37-56) for ipilimumab (anti-CTLA4) to 70 months (95% CI 39-101) for nivolumab/pebrolizumab (anti-PD-1). Targeted therapy globally produced MSS of 44 months (95% CI 38-50), it varied from 40 months (95% CI 34-45) for BRAFi to 55 months (95% CI 49-61) for BRAFi+MEK (see **Table 3**).

Immunotherapy showed an improved survival compared with all other therapies (Chemotherapy, Local therapy and no targeted therapy) (p=0.001) (**Figure 2A**); for Ipilimumab and combined target therapy compared with all other therapies a slight significance were observed (p=0.05) (see **Figure 2B**). The highest survival (70 months; 95% CI 45-96) was reached by patients treated with Nivolumab/Pembrolizumab compared with combined target therapy and all other therapies (p=0.001) (see **Figure 2C**); Immunotherapy across strata showed an improved survival for anti-PD-1 and combined anti-PD-1 + anti-CTLA4 compared with Ipilimumab and all other therapies (p<0.0001) (see **Figure 2D**). The treatment-sequence did not show any significant difference (Immuno in 1st and Target in 2nd *vs.* Target in 1st and Immuno in 2nd line) (p=0.5) (see **Figure 2E**). A significant difference was observed between BRAF *vs*. BRAF with the addition of Cobimetinid/Trametinib (anti-MEK) (p=0.03) (see **Figure 2F**).

Multivariate Cox model hazard ratios were reported in **Table 4**: a significant increased risk of death was observed for abnormal LDH compared to normal (HR=1.94 95% CI 1.23-3.06); among the Target therapy a significant protective effect was observed for target therapy with the addition of Cobimetinid/Trametinib (BRAFI+MEKI) (HR=0.63 95% CI 0.42-0.94). All immunotherapy categories were significantly associated with a reduction of death: anti-PD-1 HR=0.25 (95% CI 0.15-0.43), anti-CTLA4 HR=0.47 (95% CI 0.33-0.67) and combined anti-PD-1+ anti-CTLA4 HR=0.26 (95% CI 0.15-0.47), respectively. The treatment-sequence was not associated to the risk of death (p=0.3).

DISCUSSION

In this study, we examined data of advanced melanoma in the Italian Clinical National Melanoma Registry (CNMR). CNMR does not have the typical aim of cancer registries to estimate incidence data, but as a clinical registry may collect data from the real world experience which is different from that coming from clinical studies which included selected patients (22, 23). Indeed, much of the existing research on advanced melanoma patients has been conducted in clinical trials settings among patients who meet stringent inclusion and exclusion criteria.

The analysis of the 787 patients from the advanced cohort showed some interesting results. As first, looking at the advanced patients' characteristics, a good percentage of them come from the initial stages more than from the high risk conditions.

TABLE 2 | Distribution of therapies and combined therapies in the cohort of advanced melanoma patients.

Indicator	Advanced Melanoma: IIIB-IIIC (unresectable), IV	
	Observed patients (n)	*(%)*
Patients eligible for analysis	787	(100)
Patients with at least one local treatment	275	(35)
No local treatment	512	
Patients with at least one chemotherapy	275	(35)
No chemotherapy	512	
Patients with at least one immunotherapy	319	(41)
Immunotherapy: ANTI-PD-1 (Nivolumab/Pebrolizumab)	*80 (25.1)*	
Immunotherapy: ANTI-CTLA4 (Ipilimumab)	*198 (62.1)*	
Immunotherapy: ANTI-PD-1 + ANTI-CTLA4	*41 (12.8)*	
No immunotherapy	468	
Patients with at least one target therapy (BRAFi, BRAFI+MEKI)	285	(36)
BRAFi: vemurafenib/dabrafenib	*198 (69.5)*	
BRAFI+MEKI: cobimetinib/trametinib	*87 (30.5)*	
No target therapy	502	
Numebr of Line-therapies		
Linel°	*233 (29.6)*	
Line I°+II°	*238 (30.2)*	
Linel°+II°+III°	*316 (40.2)*	

Indeed, 50% of advanced melanoma had an initial diagnosis of early stage that then developed into advanced one.

Unfortunately, the BRAF mutational status was not evaluated in all patients; indeed, the BRAF status has been documented in as much as 76% of these patients. An important consideration is that the CNMR collected data from December 2011 and the most important drug in the field of melanoma, like BRAF inhibitors, anti-CTLA4, anti-PD-1 were approved in the following years. Specifically ipilimumab was the first treatment to be approved, on February 2013, by AIFA (The Italian Medicines Agency). Vemurafenib and dabrafenib received approval on May 2013 and on October 2014 respectively as monotherapy, and on September 2016 and on January 2017 in combination with cobimetinib and trametinib respectively. Pembrolizumab was approved on May 2016 while nivolumab on 24 March 2016 (24). Moreover, the possibility to ask for the BRAF mutational status was probably related only to the centers which were participating to clinical studies or expanded access programs with such drugs.

Study strengths include a large sample size, many treatment options reported (immunotherapy such as anti-PD-1 or combination of anti-PD-1 and anti-CTLA-4, or targeted therapies) and this is the first study investigating oncological treatments in a real-life clinical settings in advanced melanoma in several Italian centers. Study limitations include a lack of information like the metastatic site and the collection of therapy data was not completely reported, therefore the evaluation of the combined treatment (chemotherapy and immunotherapy/chemotherapy and targeted therapy) was not possible.

Concerning the OS, with some limitations due to the time of data collection (before the approval and the use of anti-PD-1 and BRAF/MEK inhibitors, and the small number of patients considered), there are still some interesting findings. It is evident that the new therapies available had an important impact on the survival of these patients. Indeed, patients who practiced immunotherapy or target therapy performed better in terms of median survival than those who practiced local therapy and/or chemotherapy, considered for a long time the only standard of treatment for metastatic melanoma. The addition of the MEK inhibitor to the BRAF inhibitor significantly improved patient OS.

TABLE 3 | Results of the performance indicators on the quality of metastatic melanoma care – Univariate Analysis.

Long-term outcomes	Advanced Melanoma:IIIB-IIIC (unresectable), IV	
	Events[1] (n) DOD/DEAD	**Median MSS (95% CI)**
Melanoma-specific Survival (MSS) overall	314/353	*47 (41-53)*
Melanoma-specific Survival (MSS) of pts. with local treatment	132/147	*42 (35-48)*
Melanoma-specific Survival (MSS) of pts. with chemotherapy	151/163	*33 (27-38)*
Melanoma-specific Survival (MSS) of pts. with immunotherapy	126/137	*50 (43-57)*
***MSS* Immunotherapy: ANTI-PD-1 (Nivolumab/Pebrolizumab)**	17/18	*70 (39-101)*
***MSS* Immunotherapy: ANTI-CTLA4 (Ipilimumab)**	94/104	*47 (37-56)*
***MSS* Immunotherapy: ANTI-PD-1+ANTI-CTLA4**	15/15	*58 (26-90)*
***Melanoma-specific Survival (MSS) of pts. with* target therapy**	129/147	*44 (38-50)*
***MSS* BRAFi: vemurafenib/dabrafenib**	91/107	*40 (34-45)*
***MSS* BRAFI+MEKI: cobimetinib/trametinib**	38/40	*55 (49-61)*

[1]*Event: number of deaths of the disease (DOD)/number of deaths for all causes (DEAD).*

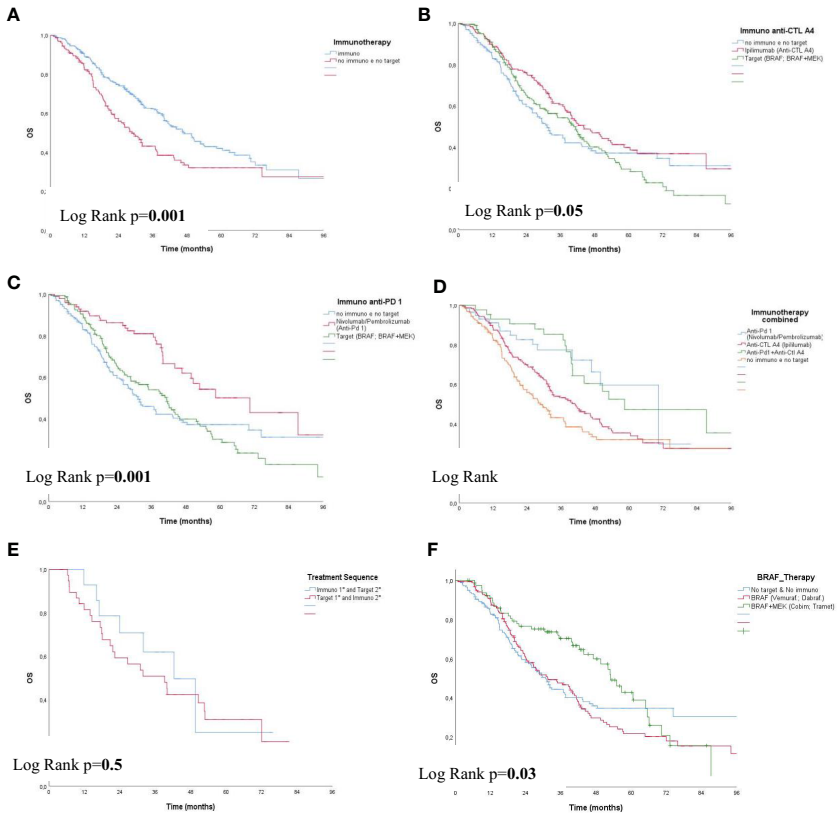


FIGURE 2 | Overall Survival (OS) in patients with IIIB-IIIC (UNRESECTABLE), IV by Therapy **(A–F)**. **(A)** Overall Survival (OS) Immunotherapy, **(B)** OS Immunotherapy: ANTI-CTL A4, **(C)** OS Immuno: ANTI-PD 1, **(D)** OS Immuno: ANTI-PD 1; ANTI-CTLA4; ANTI PD 1+ANTI-CTL A4, **(E)** OS Treatment Sequence:Immuno 1st, 2nd; Target 1st, 2nd; Target 1st & Immuno 2nd **(F)** OS BRAF *vs.* BRAFI+MEKI.

It seems that the greater advantage in terms of OS is in those patients who have performed immunotherapy lines, even compared to those who have performed target therapies. This finding could be explained by the fact that many patients received BRAF inhibitor therapy as single agent (69,5%), and only a minority had benefit from the addition of the MEK inhibitor. Indeed, we learned that disease progression during therapy with the BRAF inhibitor alone was often rapid and unresponsive to subsequent treatments (25); with the addition of MEK inhibitors, the fast progression from target therapy was reduced (26).

The data on the combination nivolumab + ipilimumab also appears intriguing, especially in terms of long survival; however, the low number of patients does not allow us to give definitive conclusions.

The correlation between survival and the LDH value is also consistent with the literature data. Analyzing the LDH values, there is an increased risk of death for patients with high LDH, compared to those with normal LDH, especially in the group of patients who received immunotherapy (HR = 2.45, p = 0.01)

We found that immunotherapy allows better results in terms of overall survival in patients with advanced melanoma, however in our analysis there is no statistically significant benefit of the treatment-sequence variable (Immuno in 1st and Target in 2nd *vs.* Target in 1st and Immuno in 2nd line). In consideration of the retrospective analysis, the small number of patients who started with anti-PD-1, and the lack of patients who received the dual MAPK blockade, definitive conclusions cannot be made.

At the moment several combination studies of target and immunotherapies as well as protocols to establish the best sequential therapy are ongoing (27). Our study has several limitations. In fact, most patients received chemotherapy as a first systemic treatment for advanced disease, because more effective drugs such as BRAF/MEK inhibitors, anti-CTLA4 and anti-PD-1 inhibitors were approved subsequently in different years. In addition, many centers did not test all patients for BRAF, especially at the beginning.

CONCLUSIONS

Finally, this study shows that immunotherapy improves survival in advanced melanoma in a real-world population. The CNMR represents a set of data useful not only to plan the appropriate prevention measures but to better understand the effectiveness of

TABLE 4 | Multivariate Cox regression models for death.

Parameter/Category	Adjusted Multivariate Analysis‡		
	HR	95% CI	p
Gender			
Female	1†		
Male	1.121	0.898-1.398	0.314
Age			
≤60	1†		
>60	1.192	0.961-1.478	0.109
Area of enrollment in Italy[3]			
Center/South	1†		
North	0.981	0.778-1.238	0.873
Year BRAF executed[4]			
<2013	1†		
≥2013	1.06	0.837-1.355	0.609
LDH			
Normal	1.0†		
Abnormal	1.95	1.24-3.01	0.004
Unknown	0.97	0.95-1.53	0.09
Target therapy			
No Target and No Immuno therapy	1.0†		
BRAF	1.14	0.85-1.53	0.4
BRAFI+MEKI	0.623	0.42-0.94	0.02
Immunotherapy			
No Immuno and No Target therapy	1.0†		
ANTI-PD-1 (Nivolumab/Pebrolizumab)	0.25	0.147-0.43	<0.0001
ANTI-CTLA4 (Ipilimumab)	0.47	0.33-0.67	<0.0001
ANTI-PD-1+ ANTI-CTLA4	0.26	0.15-0.47	<0.0001
Treatment Sequence			
Immuno 1st and Target 2nd	1.0†		
Target 1st and Immuno 2nd	1.64	0.65-4.12	0.3

†*Reference category;* ‡*Multivariate Cox model adjusted for gender (male, female); age (≤60, >60); geographical area (North, Central-South);Year BRAF executed (≤2013, >2013); N. @ of therapies (1, 2, ≥3); Other therapies: Chemotherapy; Local and systemic therapy whenever.*

anti-cancer treatments in a large unselected population from a real world experience. Furthermore, qualified data is essential and it is important that this information is constantly updated in order to maintain high levels of evidence.

The nivolumab/pembrolizumab and the combination of ipilimumab can be considered the best therapy to improve survival in a real-world-population. The CNMR can complement clinical registries with the intent of improving cancer management and standardizing cancer treatment.

DATA AVAILABILITY STATEMENT

The datasets presented in this study can be found in online repositories. The names of the repository/repositories and accession number(s) can be found below: http://imi.cr-technology.com/cnmr.

ETHICS STATEMENT

CNMR was approved by ethical committee of Istituto Nazionale dei Tumori Fondazione G. Pascale, protocol n.10/10, prot. CEI 537/10. The patients/participants provided their written informed consent to participate in this study.

CNMR GROUP

Maddalena Cespa, Fondazione I.R.C.C.S. Policlinico San Matteo Clinica Dermatologica, Pavia: **Rosachiara Forcignanò**, Azienda Ospedaliera Vito Fazzi, U.O. Di Oncologia, Lecce; **Gianmichele Moise**, Azienda Per I Servizi Sanitari N°2 Isontina Ospedale Di Gorizia Dipartimento Di Medicina , S.O.S. Di Dermatologia – Gorizia; **Maria Concetta Fargnoli**, Presidio Ospedaliero San Salvatore, U.O.S. Di Dermatologia Generale Ed Oncologica, L'Aquila; **Caterina Ferreli**, Università Degli Studi Di Cagliari - Azienda Ospedaliero Universitaria, Clinica Dermatologica, Cagliari; **Maria Grimaldi**, Istituto Nazionale dei Tumori Fondazione G. Pascale Napoli; **Guido Zannetti**, Azienda Ospedaliero-Universitaria Di Bologna Policlinico S. Orsola -Malpighi, Chirurgia Plastica, Bologna; **Saverio Cinieri**, Presidio Ospedaliero Antonio Perrino, U.O.C. Di Oncologia E Breast Unit, Brindisi; **Giusto Trevisan**, Ospedale Maggiore, Azienda Ospedaliera Universitaria Di Trieste, Clinica Dermatologica ,4° Piano (Palazzina Infettivi), Trieste; **Ignazio Stanganelli**, Ospedale S.Maria Delle Croci - Usl Di Ravenna, Centro Di Dermatologia Oncologica CPO/IRST, Ravenna; **Giovanna Moretti**, Azienda Ospedaliera Ospedali Riuniti Papardo-Piemonte S.C. Dermatologia Messina; **Francesca Bruder**, Ospedale Oncologico, Dipartimento Melanoma E Tumori Rari 5° Piano, Cagliari; **Luca Bianchi**, Azienda Ospedaliera Universitaria Policlinico Tor Vergata U.O.C. Dermatologia,

Roma; **Maria Teresa Fierro**, A.O.U. Città Della Salute E Della Scienza - P.O. San Lazzaro, S.C. Dermatolgia Torino; **Luigi Mascheroni**, Humanitas - Casa Di Cura San Pio X S.R.L., Chirurgia GeneraleMilano; **Salvatore Asero**, Azienda Ospedaliera Di Rilievo Nazionale E Di Alta Specializzazione Garibaldi-Nesima, U.O. Di Chirurgia Oncologica - Dip. Oncologia, Catania; **Caterina Catricalà**, Istituto Dermatologico San Gallicano IRCCS – IFO, UOC di Dermatologia Oncologica - Dipartimento Clinico-Sperimentale Di Dermatologia Oncologica Roma; **Stefania Staibano**, Azienda Ospedaliera Universitaria Federico II di Napoli, Scienze Biomorfologiche e Funzionali-Sezione Di Anatomia Patologica, Napoli; **Gaetana Rinaldi**, Azienda Ospedaliera Universitaria Policlinico `Paolo Giaccone`, Dipartimento Di Oncologia - U.O.C. Oncologia Medica, Palermo; **Riccardo Pellicano**, IRCCS Casa Sollievo Della Sofferenza, U.O.C. Dermatologia, San Giovanni Rotondo; **Laura Milesi**, Azienda Ospedaliera Papa Giovanni XXIII, USC Oncologia Medica, Bergamo; **Marilena Visini**, A.O. Di Lecco Presidio Ospedaliero Alessandro Manzoni, Oncologia Medica, Lecco; **Franco Di Filippo**, Istituto Nazionale Tumori Regina Elena IRCCS – IFO, Chirurgia Generale A, Roma; **Leonardo Zichichi**, Azienda Sanitaria Provinciale - Presidio Ospedaliero Di Trapani, U.O. C. Dermatologia, Casa Santa – Erice; **Maria Antonietta Pizzichetta**, Centro Di Riferimento Oncologico, Istituto Nazionale Tumori, Divisione Di Oncologia Medica C, Aviano; **Carmelo Iacono**, Azienda Ospedaliera Sanitaria 7 Ragusa - Ospedale Maria Paternò Arezzo, Dipartimento Di Oncologia, Ragusa; **Massimo Guidoboni**, I.R.S.T. Istituto Scientifico Romagnolo Per Lo Studio E La Cura Dei Tumori U.O. Immunoterapia E Terapia Cellulare Somatica, Meldola; **Giovanni Sanna**, Azienda Ospedaliero-Universitaria Di Sassari, Servizio Di Medicina Nucleare U.O. Di Oncologia Medica, Sassari; **Michele Maio**, Azienda Ospedaliera Universitaria Senese Ospedale Le Scotte U.O.C. Immunoterapia Oncologica, Siena; Michele Del Vecchio, Fondazione I.R.C.C.S. Istituto Nazionale Dei Tumori, S.C. Medicina Oncologica 1, Milano; **Lucia Lospalluti**, Azienda Sanitaria Locale BA - Ospedale Di Venere, U.O. Dermatologia, Carbonara Di Bari; **Rosanna Barbati**, Asl Roma C - Ospedale S.Eugenio , U.O. Dermatologia, Roma; **Leonardi Vita**, ARNAS Civico Palermo; **Annamaria Pollio**, Ospedale "A. Cardarelli" – Campobasso, U.O.C. di Anatomia Patologica; **Carlo Riberti**, Istituto di Chirurgia Plastica presso l'Arcispedale Sant'Anna, Ferrara.

AUTHOR CONTRIBUTIONS

Conceptualization, AC, GP, AT, and PA. Methodology, AC, VV, MB, SG, GP, and PA. Software, AC, and SG. Validation, AC, MC, AV, PF, PQ, FS, VV, CC, GT, GM, EC, MB, SG, AT, GP, and PA. Formal analysis, AC, VV, and SG. Investigation, MC, EG, AV, PF, PQ, FS, VV, CC, GT, EP, GG, EN, PQ, SR, MiG, DaM, SB, MoG, VG, MO, FG, GC, AG, DeM, LA, NC, TF, GM, FT, EC, MB, SG, CR, AT, and PA. Resources AC, VV, MB, SG, GP, and PA. Data curation, AC, VV, GP, and SG. Writing—original draft preparation, AC, MC, AV, PF, PQ, FS, VV, CC, GT, GM, EC, MB, SG, AT, GP, and PA. Writing—review and editing, AC, VV, GT, GM, EC, MB, SG, AT, GP, and PA. Visualization, AC, VV, SG, GP, and PA. Supervision, AC, VV, MB, SG, GP, and PA. Project administration, AC, VV, MB, SG, GP, and PA. Funding acquisition, CR, AT, and PA. All authors contributed to the article and approved the submitted version.

FUNDING

This research was funded by grants received from Bristol Myers Squibb (New York, NY, USA), GlaxoSmithKline (Brentford, UK) and Pierre Fabre Pharma. The funders were not involved in the study design, collection, analysis, interpretation of data, the writing of this article or the decision to submit it for publication.

ACKNOWLEDGMENTS

We would like to express our special thanks to Dr. Maurizio Montella († May 2, 2019) for his long-term contribution to the study and for his ideas and support of this current manuscript. The authors would like to thank the Intergruppo Melanoma Italiano (IMI), the Clinical Research Technology (CRT) and Dr. Giuseppe Porciello for graphical assistance.

REFERENCES

1. Bray F, Ferlay J, Soerjomataram I, Siegel RL, Torre LA, Jemal A. Global Cancer Statistics 2018: GLOBOCAN Estimates of Incidence and Mortality Worldwide for 36 Cancers in 185 Countries. *CA Cancer J Clin* (2018) 68 (6):394–424. doi: 10.3322/caac.21492
2. Hollestein LM, de Vries E, Nijsten T. Trends of Cutaneous Squamous Cell Carcinoma in the Netherlands: Increased Incidence Rates, But Stable Relative Survival and Mortality 1989-2008. *Eur J Cancer* (2012) 48:2046–53. doi: 10.1016/j.ejca.2012.01.003
3. de Vries E, Bray FI, Coebergh JW, Parkin DM. Changing Epidemiology of Malignant Cutaneous Melanoma in Europe 1953-1997: Rising Trends in Incidence and Mortality But Recent Stabilizations in Western Europe and Decreases in Scandinavia. *Int J Cancer* (2003) 107:119–26. doi: 10.1002/ijc.11360
4. Garbe C, Leiter U. Melanoma Epidemiology and Treands. *Clin Dermatol* (2009) 27:3–9. doi: 10.1016/j.clindermatol.2008.09.001
5. Crocetti E, Mallone S, Robsahm TE, Gavin A, Agius D, Ardanaz E, et al. Survival of Patients With Skin Melanoma in Europe Increases Further: Results of the EUROCARE-5 Study. *Eur J Cancer* (2015) 51(15):2179–90. doi: 10.1016/j.ejca.2015.07.039
6. Cossu A, Casula M, Cerasaccio R, Lissia A, Colombino M, Sini MC, et al. Epidemiology and Genetic Susceptibility of Malignant Melanoma in North Sardinia, Italy. *Eur J Cancer Prev* (2017) 26(3):263–7. doi: 10.1097/CEJ.0000000000000223
7. Ascierto PA and AIRTum Working Group and Working Group. In: *AssociazioneItaliana di Oncologia Medica, Associazione Italiana Registri Tumori, ed. I numeri del cancro in Italia*. (2018) p. 131–41.
8. Sini MC, Doneddu V, Paliogiannis P, Casula M, Colombino M, Manca A, et al. Genetic Alterations in Main Candidate Genes During Melanoma Progression. *Oncotarget* (2018) 9(9):8531–41. doi: 10.18632/oncotarget.23989
9. Palmieri G, Ombra M, Colombino M, Casula M, Sini M, Manca A, et al. Multiple Molecular Pathways in Melanomagenesis: Characterization of Therapeutic Targets. *Front Oncol* (2015) 5:183. doi: 10.3389/fonc.2015.00183
10. Chapman PB, Hauschild A, Robert C, Haanen JB, Ascierto PA, Larkin J, et al. Improved Survival With Vemurafenib in Melanoma With BRAF V600E Mutation. *N Engl J Med* (2011) J364(26):2507–16. doi: 10.1056/NEJMoa1103782

11. Hauschild A, Grob JJ, Demidov LV, Jouary T, Gutzmer R, Millward M, et al. Dabrafenib in BRAF-Mutated Metastatic Melanoma: A Multicentre, Open-Label, Phase 3 Randomised Controlled Trial. *Lancet* (2012) 380(9839):358–65. doi: 10.1016/S0140-6736(12)60868-X
12. Long GV, Flaherty KT, Stroyavskiy D, Gogas H, Levchenko, de Braud F, et al. Dabrafenib Plus Trametinib *Versus* Dabrafenib Monotherapy in Patients With Metastatic BRAFV600E/K-Mutant Melanoma: Long-Term Survival and Safety Analysis of a Phase 3 Study. *Ann Oncol* (2017) 28(7):1631–9. doi: 10.1093/annonc/mdx176
13. Robert C, Grob JJ, Stroyakovskiy D, Karaszewska B, Hauschild A, Levchenko E, et al. Five-Year Outcomes With Dabrafenib Plus Trametinib in Metastatic Melanoma. *N Engl J Med* (2019) 381(7):626–36. doi: 10.1056/NEJMoa1904059
14. Larkin J, Ascierto PA, Dréno B, Atkinson V, Liszkay G, Maio M, et al. Combined Vemurafenib and Cobimetinib in BRAF-Mutated Melanoma. *N Engl J Med* (2014) 371(20):1867–76. doi: 10.1056/NEJMoa1408868
15. Topalian SL, Stephen-Hodi F, Brahmer JR, Gettinger SN, Smith DC, McDermott DF, et al. Safety, Activity, and Immune Correlates of Anti-PD-1 Antibody in Cancer. *N Engl J Med* (2012) 366(26):2443–54. doi: 10.1056/NEJMoa1200690
16. Hodi FS, O'Day SJ, McDermott DF, Weber RW, Sosman JA, Haaner JB, et al. Improved Survival With Ipilimumab in Patients With Metastatic Melanoma. *N Engl J Med* (2010) 363(8):711–23. doi: 10.1056/NEJMoa1003466
17. Schadendorf D, Hodi FS, Robert C, Weber JS, Margolin K, Hamid O, et al. Pooled Analysis of Long-Term Survival Data From Phase II and Phase III Trials of Ipilimumab in Unresectable or Metastatic Melanoma. *J Clin Oncol* (2015) 33(17):1889–94. doi: 10.1200/JCO.2014.56.2736
18. Ascierto PA, Del Vecchio M, Robert C, Mackiewicz A, Chiarion-Sileni V, Arance A, et al. Ipilimumab 10 Mg/Kg *Versus* Ipilimumab 3 Mg/Kg in Patients With Unresectable or Metastatic Melanoma: A Randomised, Double-Blind, Multicentre, Phase 3 Trial. *Lancet Oncol* (2017) 18(5):611–22. doi: 10.1016/S1470-2045(17)30231-0
19. Schachter J, Ribas A, Long GV, Arance A, Grob JJ, Montier L, et al. Pembrolizumab *Versus* Ipilimumab for Advanced Melanoma: Final Overall Survival Results of a Multicentre, Randomised, Open-Label Phase 3 Study (KEYNOTE-006). *Lancet* (2017) 390(10105):1853–62. doi: 10.1016/S0140-6736(17)31601-X
20. Robert C, Long GV, Brady B, Dutriaux C, Maio M, Montier L, et al. Nivolumab in Previously Untreated Melanoma Without BRAF Mutation. *N Engl J Med* (2015) 372(4):320–30. doi: 10.1056/NEJMoa1412082
21. Larkin J, Chiarion-Sileni V, Gonzalez R, Grob JJ, Rutkowski P, Lao CD, et al. Five-Year Survival With Combined Nivolumab and Ipilimumab in Advanced Melanoma. *N Engl J Med* (2019) 381(16):1535–46. doi: 10.1056/NEJMoa1910836
22. Gandini S, Montella M, Ayala F, Benedetto L, Rossi CR, Vecchiato A, et al. Sun Exposure and Melanoma Prognostic Factors. *Oncol Lett* (2016) 4):2706–14. doi: 10.3892/ol.2016.4292
23. Jochems A, Schouwenburg MG, Leeneman B, Franken MG, van den Eertwegh AJ, Haanen JB, et al. Dutch Melanoma Treatment Registry: Quality Assurance in the Care of Patients With Metastatic Melanoma in the Netherlands. *Eur J Cancer* (2017) 72:156–65. doi: 10.1016/j.ejca.2016.11.021
24. Cowey CL, Liu FX, Boyd M, Aguilar KM, Krepler C. Real-World Treatment Patterns and Clinical Outcomes Among Patients With Advanced Melanoma: A Retrospective, Community Oncology-Based Cohort Study (A STROBE-Compliant Article). *Med (Baltimore)* (2019) 98(28):e16328. doi: 10.1097/MD.0000000000016328
25. *AIFA (Regime Di Rimborsabilita' E Prezzo Di Vendita Del Medicinale Nivolumab) - Autorizzata Con Procedura Centralizzata Europea Dalla Commissione Europea*. Gazzetta Ufficiale della Repubblica Italia n. 70 24-03-2016.
26. Pavlick AC, Fecher L, Ascierto PA, Sullivan RJ. Frontline Therapy for BRAF-Mutated Metastatic Melanoma: How Do You Choose, and Is There One Correct Answer? *Am Soc Clin Oncol Educ Book* (2019) 39:564–71. doi: 10.1200/EDBK_243071
27. Ascierto PA, Simeone E, Grimaldi AM, Curvietto M, Esposito E, Palmieri G, et al. Do BRAF Inhibitors Select for Populations With Different Disease Progression Kinetics? *J Transl Med* (2013) 11:61. doi: 10.1186/1479-5876-11-61

Conflict of Interest: PA has/had a consultant/advisory role for Bristol Myers Squibb, Roche-Genentech, Merck Sharp & Dohme, Novartis, Array, Merck Serono, Pierre-Fabre, Incyte, Medimmune, AstraZeneca, Syndax, Sun Pharma, Sanofi, Idera, Ultimovacs, Sandoz, Immunocore, 4SC, Alkermes, Italfarmaco, Nektar, Boehringer-Ingelheim, Eisai, Regeneron, Daiichi Sankyo, Oncosec, Pfizer. He also received research funding from Bristol Myers Squibb, Roche-Genentech, Array and travel support from MSD.

The remaining authors declare that the research was conducted in the absence of any commercial or financial relationships that could be construed as a potential conflict of interest.

Copyright © 2021 Crispo, Corradin, Giulioni, Vecchiato, Del Fiore, Queirolo, Spagnolo, Vanella, Caracò, Tosti, Pennacchioli, Giudice, Nacchiero, Quaglino, Ribero, Giordano, Marussi, Barruscotti, Guida, De Giorgi, Occelli, Grosso, Cairo, Gatti, Massa, Atzori, Calvani, Fabrizio, Mastrangelo, Toffolutti, Celentano, Budroni, Gandini, Rossi, Testori, Palmieri, Ascierto and the Clinical National Melanoma Registry Study Group at the Italian Melanoma Intergroup. This is an open-access article distributed under the terms of the Creative Commons Attribution License (CC BY). The use, distribution or reproduction in other forums is permitted, provided the original author(s) and the copyright owner(s) are credited and that the original publication in this journal is cited, in accordance with accepted academic practice. No use, distribution or reproduction is permitted which does not comply with these terms.

frontiers in Oncology

ORIGINAL RESEARCH
published: 24 August 2021
doi: 10.3389/fonc.2021.720044

Overall Survival of Patients With Unresectable or Metastatic BRAF V600-Mutant Acral/Cutaneous Melanoma Administered Dabrafenib Plus Trametinib: Long-Term Follow-Up of a Multicenter, Single-Arm Phase IIa Trial

Lili Mao[1†], Ya Ding[2†], Xue Bai[1], Xinan Sheng[3], Jie Dai[1], Zhihong Chi[1], Chuanliang Cui[1], Yan Kong[1], Yun Fan[4], Yanjun Xu[4], Xuan Wang[1], Bixia Tang[1], Bin Lian[1], Xieqiao Yan[3], Siming Li[3], Li Zhou[3], Xiaoting Wei[1], Caili Li[1], Jun Guo[1], Xiaoshi Zhang[2] and Lu Si[1*]*

[1] Key Laboratory of Carcinogenesis and Translational Research (Ministry of Education/Beijing), Department of Melanoma, Peking University Cancer Hospital & Institute, Beijing, China, [2] Department of Biotherapy, State Key Laboratory of Oncology in South China, Collaborative Innovation Center for Cancer Medicine, Sun Yat-Sen University Cancer Center, Guangzhou, China, [3] Key Laboratory of Carcinogenesis and Translational Research (Ministry of Education/Beijing), Department of Genitourinary Oncology, Peking University Cancer Hospital & Institute, Beijing, China, [4] Cancer Hospital of the University of Chinese Academy of Sciences (Zhejiang Cancer Hospital), Institute of Cancer and Basic Medicine (IBMC), Chinese Academy of Sciences, Hangzhou, China

Objectives: To examine the long-term survival outcome of dabrafenib in combination with trametinib in Chinese patients with unresectable or metastatic acral/cutaneous melanoma with BRAF-V600 mutation and to explore potential predictors of effectiveness.

Methods: This was a long-term follow-up of Chinese patients with unresectable or metastatic BRAF V600-mutant acral/cutaneous melanoma administered dabrafenib (150 mg twice daily) plus trametinib (2 mg once daily) in an open-label, multicenter, single-arm, phase IIa study (NCT02083354). Efficacy endpoints included objective response rate (ORR), duration of response (DOR), progression-free survival (PFS), and overall survival (OS). The impacts of baseline characteristics on PFS and OS were analyzed.

Results: A total of sixty patients were included. The median age was 48 years, and 24 patients (40.0%) were male. Totally 12 individuals (20.0%) had acral melanoma, and 45 (75.0%) had failed previous systemic therapy. Up to July 2020, the median duration of follow-up was 37.0 (95% confidence interval [CI] 29.1-44.9) months. The updated ORR was 71.7% (95%CI 60.3%-83.1%). The 3-year OS rate was 28.8% (95%CI 19.1-43.6%) in the overall population, and 35.7% (95%CI 15.5–82.4%) in acral melanoma patients.

OPEN ACCESS

Edited by:
Joshua Arbesman,
Cleveland Clinic, United States

Reviewed by:
Camelia Quek,
Melanoma Institute Australia, Australia
Jianming Zhang,
Shanghai Jiao Tong University, China

***Correspondence:**
Lu Si
silu15_silu@126.com
Xiaoshi Zhang
zhangxsh@sysucc.org.cn

†These authors have contributed equally to this work

Specialty section:
This article was submitted to Skin Cancer, a section of the journal Frontiers in Oncology

Received: *03 June 2021*
Accepted: *03 August 2021*
Published: *24 August 2021*

Citation:
Mao L, Ding Y, Bai X, Sheng X, Dai J, Chi Z, Cui C, Kong Y, Fan Y, Xu Y, Wang X, Tang B, Lian B, Yan X, Li S, Zhou L, Wei X, Li C, Guo J, Zhang X and Si L (2021) Overall Survival of Patients With Unresectable or Metastatic BRAF V600-Mutant Acral/Cutaneous Melanoma Administered Dabrafenib Plus Trametinib: Long-Term Follow-Up of a Multicenter, Single-Arm Phase IIa Trial. Front. Oncol. 11:720044. doi: 10.3389/fonc.2021.720044

The median DOR was 7.5 months (95%CI 4.5 to 10.5). Baseline normal lactic dehydrogenase (LDH), metastatic organ sites<3 and complete response to combination therapy with dabrafenib plus trametinib were associated with improved PFS and OS.

Conclusion: Dabrafenib combined with trametinib confer long-term survival in Chinese patients with BRAF V600-mutant, unresectable or metastatic acral/cutaneous melanoma.

Clinical Trial Registration: https://clinicaltrials.gov/ct2/show/NCT02083354, identifier NCT02083354.

Keywords: melanoma, dabrafenib, trametinib, BRAF, acral melanoma

INTRODUCTION

Although the incidence of melanoma is only 0.9 per 100,000 persons in China, it has been increasing for the past 20 years (1). Most melanoma cases are in locally advanced stage at the time of diagnosis, with some eventually developing metastatic disease, which results in poor prognosis (2, 3). BRAF mutations play a critical role in melanoma initiation and progression, and about 25% of all Chinese melanoma patients harbor BRAF mutations (4). BRAF mutation rate varies by anatomic type. Indeed, BRAF mutations were reported in 50% cutaneous melanoma and 15% acral melanoma cases; the latter is the most common subtype in Chinese melanoma patients (3, 4).

Major strides have been made in the treatment of advanced melanoma with BRAF mutation in recent years. Compared with chemotherapy, BRAF inhibitors have significantly improved the survival of BRAF mutant patients (5, 6). In addition, the combination of BRAF and MEK inhibitors circumvents the drug resistance caused by mitogen-activated protein kinase (MAPK) pathway reactivation when BRAF inhibitors are used alone, without increasing the overall toxicity (7–11). Although PD-1 blockade was effective regardless of the patient's BRAF mutation status in some trials (12, 13), existing data demonstrated an ORR of 15% in Chinese BRAF V600-mutant melanoma patients treated with pembrolizumab (14).

A recent phase IIa trial evaluated the efficacy and safety of dabrafenib plus trametinib in 77 East Asian patients with unresectable or metastatic BRAF V600-mutant cutaneous melanoma, including 61 (79.2%) from China's mainland. The preliminary results of this trial demonstrated an ORR of 61.0% and a median progression-free survival (PFS) of 7.9 months (15). However, the median follow-up time was 8.3 months in the above report at the time of data cutoff (February 23, 2018), and median overall survival (OS) was not reached due to the relatively short follow-up. Therefore, overall survival in Chinese patients with unresectable or metastatic BRAF V600-mutant melanoma administered the dabrafenib plus trametinib regimen remains unknown.

Here, we report updated the ORR, PFS and OS of patients treated with dabrafenib plus trametinib in this phase IIa study in China's mainland, including the data of acral melanoma cases. We also provide an analysis of factors that might be associated with derived long-term benefit from this combination therapy.

METHODS

Study Design and Participants

The original study was an open-label, multicenter, single-arm, phase IIa trial (ClinicalTrials.gov, NCT02083354) conducted in East Asia (China's mainland, Hong Kong, Taiwan, Korea, and Thailand) (15). Chinese mainland melanoma patients, treated in Peking University Cancer Hospital, Sun Yat-Sen University Cancer Hospital, and Zhejiang Cancer Hospital between March 2014 and November 2017, were included in the present analysis.

Briefly, eligible patients were ≥18 years of age, with histopathologically confirmed stage IIIc (unresectable) or IV (metastatic) melanoma, BRAF V600 mutation according to the central reference laboratory, at least one measurable lesion according to Response Evaluation Criteria in Solid Tumors (RECIST) version 1.1 (16), Eastern Cooperative Oncology Group (ECOG) performance status of 0 or 1, and adequate organ function. Individuals with primary mucosal or ocular melanoma were excluded. The study was conducted in accordance with the Declaration of Helsinki and Good Clinical Practice, and approved by the ethics committee of each participating center. Written informed consent was obtained from each patient.

Treatment

Patients received dabrafenib at 150 mg twice daily plus trametinib at 2 mg once daily by oral administration until disease progression (PD), death, unacceptable toxicity, withdrawal of consent, or discontinuation for any reason. Dose modifications were allowed for the management of adverse events (AEs).

Endpoints

Patients were followed up every 28 days. The primary endpoint was ORR. Tumor response was assessed by an investigator according to RECIST 1.1 at baseline, every 8 weeks until week 56, and then every 12 weeks until disease progression or death. Secondary endpoints included PFS, OS, and the duration of response (DOR). Post-hoc defined endpoints included time to response (TTR) and post progression survival (PPS). AEs were recorded and graded according to the National Cancer Institute Common Terminology Criteria for Adverse Events, version 4.0, during the study period (17).

Statistical Analysis

Statistical analysis was performed with SPSS 22.0 (IBM, Armonk, NY, USA) or GraphPad Prism version 8.0 (GraphPad Software). The Clopper–Pearson method was used to calculate the 95% confidence interval (CI) of the ORR. ORRs were compared by the chi-square test. Progression-free survival and overall survival were estimated by the Kaplan–Meier method, and compared by the log-rank test. P<0.05 was considered statistically significant.

RESULTS

Baseline Characteristics of the Participants

A total of 61 patients were enrolled in this study, and one withdrew consent before treatment. In the 60 patients included in this analysis, the median age was 48 years (range, 26-76 years), and 24 (40.0%) individuals were male. Twelve (20.0%) patients had melanomas at acral sites. Thirty-seven (61.7%) exhibited normal lactic dehydrogenase (LDH) amounts. Forty-one (68.3%) had visceral disease, including 14 (23.3%) with liver metastasis and 4 (6.7%) with central nervous system metastases. Thirty-five (58.3%) patients had ≥3 organ sites with metastasis at baseline. Fifteen cases (25.0%) were treatment-naïve, while forty-five (75.0%) received at least one line of therapy. Nine (15.0%) patients had prior immunotherapy including PD-1 inhibitor with or without CTLA-4 inhibitor (**Table 1**).

TABLE 1 | Baseline characteristics of the participants.

Characteristics	Number (%)
Median age (range)	48.0 (26.0 - 76.0)
Male	24 (40.0)
ECOG performance status	
0	20 (33.3)
1	40 (66.7)
Primary site	
Acral	12 (20.0)
Trunk	32 (53.3)
Limb	4 (6.7)
Head & Neck	5 (8.3)
Unknown	7 (11.7)
Tumor stage at screening	
Unresectable stage IIIc	2 (3.3)
Stage IV	
M1a	10 (16.7)
M1b	14 (23.3)
M1c	31 (51.7)
Unknown	3 (5.0)
LDH	
≤ULN	37 (61.7)
>ULN	23 (38.3)
Lines of previous therapies	
0	15 (25.0)
1	19 (31.7)
2	19 (31.7)
3	6 (10.0)
4	1 (1.7)
Previous immunotherapy	
PD-1 inhibitor only	6 (10.0)
CTLA-4 inhibitor only	2 (3.3)
Both	1 (1.7)
Number of organ sites with metastasis	
1	12 (20.0)
2	13 (21.7)
≥3	35 (58.3)

Data are number (%), unless otherwise indicated. ECOG, Eastern Cooperative Oncology Group; CSD, chronically sun-damaged cutaneous melanoma; LDH, lactic dehydrogenase; ULN, upper limit of normal; PD-1, programmed cell death protein-1; CTLA-4, cytotoxic T lymphocyte associate protein-4.

Efficacy

CR, PR and stable disease (SD) were achieved in 5 (8.3%), 38 (63.3%) and 17 (28.3%) patients, respectively. Overall, the ORR was 71.7% (43/60). Among the 15 treatment-naïve patients examined, the objective response rate was 86.7%. In patients with ≥1 previous therapy (n=45), the objective response rate was 66.7%. The response rates were 83.3% in the acral melanoma subgroup and 70.8% in the non-acral subgroup. Notably, acral melanomas also exhibited high response to combination therapy (**Table 2**). There was no significant difference in ORR among patients with different lines of prior therapy, primary sites, LDH levels or metastatic organ sites (**Table S1 in the Supplementary Appendix**).

At data cut-off, the median follow-up time was 37.0 months (95%CI 29.1–44.9). In the overall population, median PFS and 3 year-PFS rates were 9.3 month (95%CI 8.4–10.3) and 11.1% (95%CI 3.3–18.9%), respectively (**Figure 1**). Three year-PFS rates were 20.0% (95%CI 7.3–55.0%) and 8.9% (95%CI 3.5-22.7) in treatment-naïve and pretreated patients, respectively. Ten of the 12 patients with acral melanoma progressed in 2 years, and maximum PFS time was less than the landmark timepoint. Patients with non-acral melanoma had a 3 year-PFS rate of 10% (95%CI 4.2–23.8%). Patients with normal baseline lactate dehydrogenase levels had a 3-year PFS rate of 18.9% (95%CI 9.7-36.9%), *versus* 0% in patients with elevated lactate dehydrogenase levels. Patients with metastatic organ sites <3 had a 3-year PFS rate of 24% (95%CI 11.9-48.2%), *versus* 2.9% (95%CI 4 to 19.7%) in patients with ≥3 sites (**Figure S1 in the Supplementary Appendix**).

Median OS and 3-year OS rate were 17.6 (95%CI 13.1–22.1) months and 28.8% (95%CI 19.1-43.6%), respectively (**Figure 2**). Three year-OS rate was 44.5% (95%CI 23.2-85.4%) in treatment-naïve patients, *versus* 24.2% (95%CI 14.4-40.7%) in pretreated patients. In patients with acral melanoma and non-acral melanoma, 3-year OS rates were 35.7% (95%CI 15.5–82.4%) and 27% (95%CI 16.8–43.7%), respectively. Patients with normal baseline lactate dehydrogenase levels had a 3-year OS rate of 40.8% (95%CI 27.3-61.1%), *versus* 9.3% (95%CI 2.5-34.8%) in those with elevated lactate dehydrogenase levels at baseline. Patients with metastatic organ sites<3 had a 3-year OS rate of 53.1% (95%CI 36.0-78.1%), *versus* 11.9% (95%CI 4.8-29.9%) in those with ≥ 3 sites (**Figure S2 in the Supplementary Appendix**).

There were no significant differences in PFS and OS among subgroups based on lines of previous therapies or primary sites. Normal LDH levels and metastatic organ sites<3 were associated with improved PFS and OS (**Figures S1 and S2 in the Supplementary Appendix**).

The median DOR was 7.5 months (95%CI 4.5-10.5) in the overall population. In patients with best response of CR or PR,

TABLE 2 | Tumor response and ORR by subgroups.

Response	Number (%)
Type of response	
Complete response (n=60)	5 (8.3)
Partial response (n=60)	38 (63.3)
Stable disease (n=60)	17 (28.3)
Progression disease	0
Objective response rate (n=60)	43 (71.7)
Previous therapy	
Naïve (n=15)	13 (86.7)
Treated (n=45)	30 (66.7)
Primary site	
Acral (n=12)	9 (83.3)
Non-acral (n=48)	34 (70.8)
LDH	
Normal (n=37)	27 (73.0)
Elevated (n=23)	16 (69.6)
Organ sites	
<3 (n=25)	21 (84.0)
≥3 (n=35)	22 (62.9)

Data are number (%), unless otherwise indicated. LDH, lactic dehydrogenase.

the median TTR was 1.9 months. **Figure 3** presents the DOR of each patient who achieved CR or PR.

Post-Treatment and Survival After Disease Progression

At the time of this analysis, a total of 53 events of disease progression were noted. Median survival after disease progression in the overall population was 7.1 months (95%CI 4.2–10.0). Twenty-four of the 53 (45.2%) patients received subsequent anti-tumor therapies, including chemotherapy (12/53, 22.6%), immune checkpoint inhibitors (14/53, 26.4%), angiogenesis inhibitors (14/53, 26.4%), BRAF with or without MEK inhibitor re-challenge (8/53, 15.1%), and radiation therapy (2/53, 3.8%) (**Table S3 in the Supplementary Appendix**). Patients (n=10) administered a PD-1 inhibitor after disease progression post-treatment with dabrafenib plus trametinib achieved a median post progression survival (PPS) of 17.6 months (95%CI 16.9–28.3) (**Figure S3 in the Supplementary Appendix**). Eight patients received re-challenge therapy with BRAF with or without MEK inhibitors; one achieved PR and six

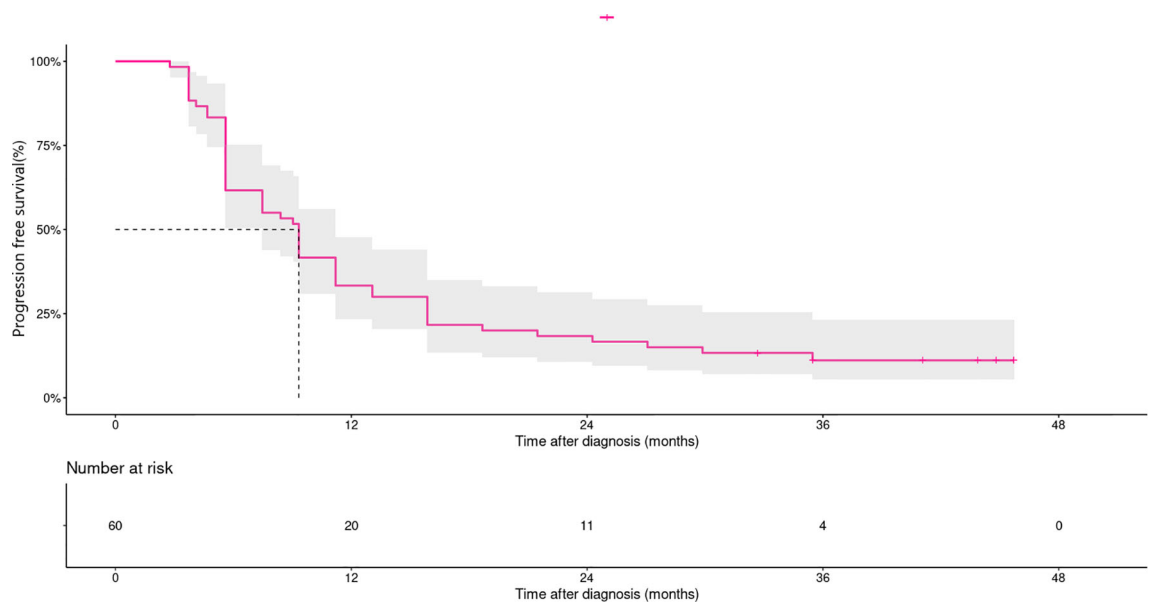


FIGURE 1 | Kaplan–Meier curves for progression-free survival in patients treated with dabrafenib and trametinib (n=60). Median PFS and 3 year-PFS rates were 9.3 month (95% CI, 8.4–10.3) and 11.1% (95% CI, 3.3–18.9%), respectively.

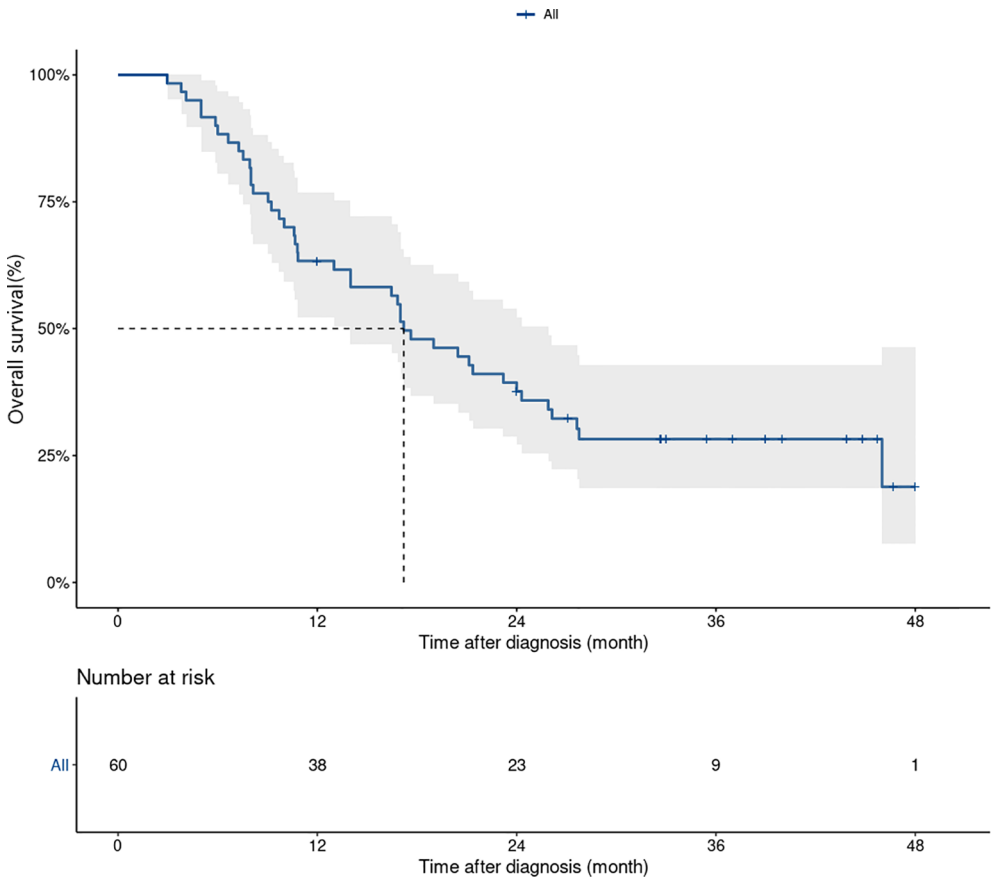


FIGURE 2 | Kaplan–Meier curves for overall survival in patients treated with dabrafenib and trametinib (n=60). Median OS and 3 years OS rate were 17.6 (95% CI, 13.1–22.1) month and 28.8% (95% CI, 19.1-43.6%), respectively.

had tumor shrinkage, of whom three were alive until the last follow-up (median PPS of 40.4 months).

Characteristics of the Patients Who Achieved CR or OS >3 Years

Five patients achieved CR, including 2 females and 3 males; four patients had normal LDH levels (126–164 U/L), and one had elevated LDH (330 U/L). Two patients were treatment naïve, and 3 were chemotherapy-treated. None of these patients underwent immunotherapy previously. All the 5 patients were M1a/b, and only 1 had visceral disease (lung); median baseline tumor size (BTS) was 20 mm (range, 15-34 mm; BTS was quantified as the sum of the longest dimensions of all measurable baseline target lesions). The detailed data of individuals who achieved CR are shown in **Table S4 in the Supplementary Appendix**. Patients who achieved CR had better survival (PFS, not available (NA); OS, NA) compared with those who achieved PR [PFS, 9.3 months (95%CI 8.9–9.8); OS, 21.4 months (95%CI 13.8–28.9)] or SD [PFS, 5.6 months (95%CI 4.3–6.9); OS, 10.6 months (95% CI 3.8–17.4)] (P<0.05) (**Figure S4 in the Supplementary Appendix**).

A total of 9 patients had OS beyond 3 years. Their median age was 42 years (range, 29-66), and they included 4 males. Eight patients had normal LDH, 1 had primary melanoma located in the acral area, 7 had metastatic organ sites<3, and four had previous immunotherapy before enrollment. Three male patients achieved complete response, and 6 patients achieved a partial response as best overall response. At the time of this analysis, 3 male patients were still on treatment, and four patients received subsequent anti-tumor therapies, of whom two achieved CR after subsequent chemotherapy. **Table S4 in the Supplementary Appendix** shows the detailed features of patients with OS >3 years.

Adverse Events

Treatment-related AE occurred in 53 patients (53/60, 88.3%). The most common AEs were pyrexia (31/60, 51.7%), anemia (25/60, 41.7%) and neutropenia (23/60, 38.3%). Ten of the sixty (13.3%) patients had dose reduction because of treatment-related AEs, including hypertension (one patient), elevated ALT/AST (one patient), and fever/chills (eight patients). Four of the sixty (6.7%) cases discontinued treatment due to treatment-related AEs, including pigment epithelial detachment (one patient), interstitial lung disease (one patient), fever/chills (one patient), and ejection fraction decrease (one patient). With an additional 28 months of follow-up since the last analysis, no new safety issues were reported.

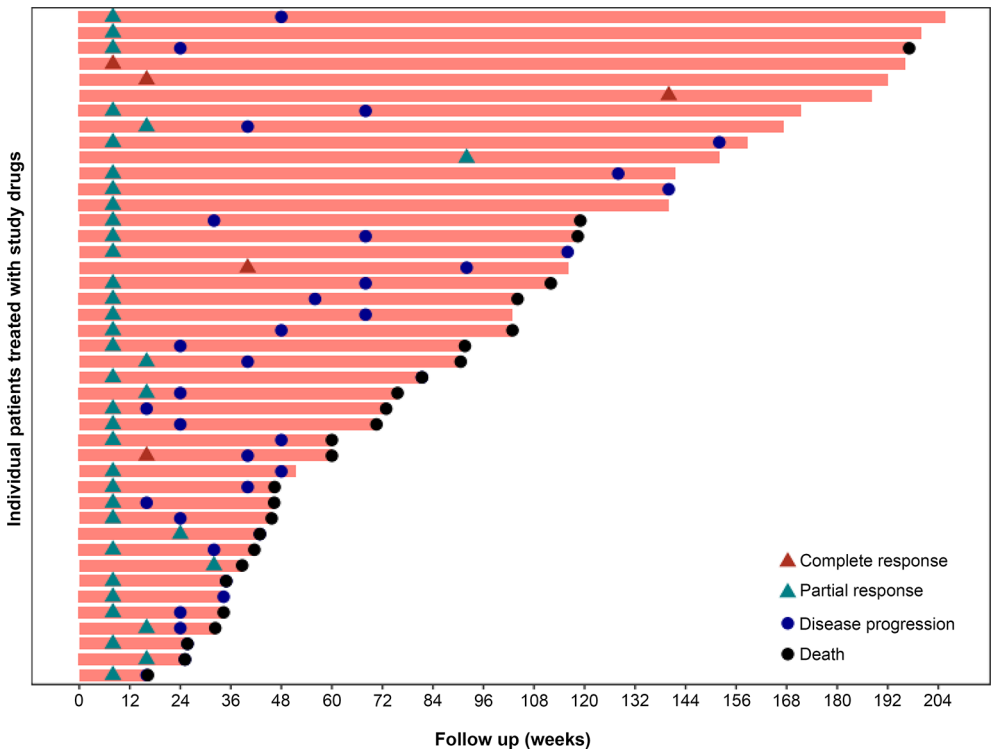


FIGURE 3 | Time to response and duration of study treatment. A total of 43 of the 60 patients had a response, including 5 patients with CR and 38 patients with PR. In the 43 patients with best response of CR or PR, the median TTR was 1.9 months.

DISCUSSION

This 3-year analysis showed that in Chinese patients with unresectable or metastatic BRAF V600-mutant melanoma, median OS and 3-year OS rate were 17.6 months and 23%, respectively, after treatment with dabrafenib plus trametinib. These data, which represent the longest follow-up of dabrafenib plus trametinib in Chinese melanoma patients to date, confirm the durable antitumor activity and safety of D+T in advanced and metastatic acral/cutaneous melanoma.

The safety profile of D+T in patients with melanoma has been established partly in a previous report (15); with continued follow-up, no new safety signals have been identified in this study.

Notably, 3-year PFS and OS rates in patients administered first-line treatment with dabrafenib plus trametinib were 22% and 44%, respectively. These results were consistent to 3-year landmark analysis results observed in a randomized, double-blinded, phase III Combi-D trial (18), which compared the combination of dabrafenib and trametinib to dabrafenib monotherapy as first-line therapy in patients with unresectable or metastatic BRAF V600E/K mutation-positive cutaneous melanoma. These data suggested that Chinese patients have similar clinical benefit as the Caucasian counterparts after treatment with first line dabrafenib and trametinib combination therapy for metastatic melanoma. There was a trend towards better ORR or survival outcomes in patients administered first line treatment compared with pretreated patients, although there was no significant difference.

Acral melanoma is the most common subtype in the Chinese population (19, 20), with lower incidence of BRAF mutations than cutaneous melanoma (4). In this study, 12 acral melanoma patients (20%) were enrolled. Acral melanoma is considered to be more aggressive with worse prognosis compared with cutaneous melanoma (21, 22). It is thought to be largely resistant to immunotherapy (14, 20, 23, 24). The present analysis demonstrated that acral melanoma patients could achieve favorable ORR, although median PFS and median OS were slightly lower in the acral subgroup compared with non-acral cases; 3-year PFS and OS rates in patients with acral melanoma were similar to those of cutaneous melanoma cases. Therefore, the BRAFi+MEKi combination might be the preferred strategy for the acral melanoma subtype with BRAF V600 mutation.

Multivariate analysis of baseline factors demonstrated that LDH levels and the number of metastatic sites were significantly associated with PFS and OS, corroborating previous randomized trials in Caucasian melanoma patients (9, 25, 26).

A recently published retrospective study demonstrated the clinical efficacy and safety of a combination therapy consisting of BRAF and MEK inhibitors (dabrafenib plus trametinib) in Japanese patients with unresectable or metastatic BRAF V600-mutant cutaneous melanoma (27). Of note, these patients had an ORR of 72.3%, a median PFS of 12 months and a median OS of

23 months. These findings confirmed that melanoma patients could achieve a favorable response and durable survival benefit with dabrafenib plus trametinib in East-Asian patients.

Regarding secondary endpoints, median PFS (9.3 months) achieved with dabrafenib and trametinib in this trial was similar to survival outcomes of the phase II BRF113220 trial (9, 28), as well as the phase III Combi-D trial with combination-targeted therapy (7). While median OS (17.6 months) seemed shorter than in the abovementioned trials (25.0 months), the differences in post-trial therapies were limited.

In the five-year outcome analysis of COMBI-v and COMBI-d trials evaluating 563 patients administered dabrafenib plus trametinib, CR occurred in 109 patients (19%) and was associated with improved long-term outcome, with an OS rate of 71% (95%CI 62 to 79) at 5 years (29). In the five cases who achieved CR in this study, lines of previous therapies were no more than two, no patients had prior immunotherapy, and metastatic organ sites were all under three. The four patients without visceral disease had longer PFS and OS, and neither death nor disease progression occurred in three of them. Therefore, patients with fewer lines of previous therapy, no previous immunotherapy, fewer metastatic organ sites and no visceral disease might gain more survival benefits from the combined regimen. Furthermore, while analyzing survival in patients with different tumor response in this trial, optimal outcomes were observed in individuals who achieved CR, confirming previous analyses (25, 26).

Nine cases had overall survival longer than 3 years, of whom 5 were progression free at the time of analysis. Longer OS may be attributed to longer PFS, fewer previous therapies, small baseline tumor size, less metastatic organ sites, and better response.

After disease progression post-treatment with dabrafenib plus trametinib, post progression survival (PPS) in the whole population was 7.1 months. Ten patients who were switched to PD-1 inhibitors achieved a PPS of 17.6 months, while BRAF re-challenge also conferred clinical benefit to a subgroup of patients. The further treatment choice for progression after combination therapy needs further investigation for confirmation. Overall survival may be affected by subsequent treatment after administration of dabrafenib plus trametinib; however, without strict response assessment and data collection beyond the clinical-trial setting, the correlation between PPS and OS remains unclear. Furthermore, there is an unmet need for optimal treatments to overcome resistance to BRAF and MEK inhibitors. Given the breakthrough of immunotherapy in melanoma, immune checkpoint inhibitors combined with targeted drugs might be an option for selected patients (28–30).

The present study had some limitations. First, this was a subgroup analysis of a phase IIa trial (15). The sample size of this study might be inadequate, and the subgroup analysis was underpowered. Secondly, no control group was set for direct comparisons. Thirdly, the original study classified patients according to histological subtype (i.e., three patients had acral lentiginous melanoma) (15), while in the present study, patients were classified according to the involved primary site (i.e., 12 patients had acral melanoma). The discrepant numbers of patients with acral melanoma in both studies could be ascribed to different classification methods. Nevertheless, dabrafenib plus trametinib demonstrated preliminary clinical benefit in acral melanoma cases with BRAF V600 mutations. Large-scale clinical trials of dabrafenib plus trametinib with multicenter design are required to substantiate the present findings. As the effect of dabrafenib plus trametinib in mucosal melanoma is unknown, it deserves further investigation.

In conclusion, this analysis confirms the durable and robust antitumor activity and safety of dabrafenib combined with trametinib in Chinese patients with BRAF V600 mutation-positive melanoma, including acral melanoma patients. The efficacy of dabrafenib plus trametinib in a Chinese population was favorable, corroborating previous studies in Caucasian populations.

DATA AVAILABILITY STATEMENT

The raw data supporting the conclusions of this article will be made available by the authors, without undue reservation.

ETHICS STATEMENT

The studies involving human participants were reviewed and approved by Ethics Committee of Beijing Cancer Hospital. The patients/participants provided their written informed consent to participate in this study.

AUTHOR CONTRIBUTIONS

JG and LS conceived of the presented idea. XZ, YD, YF, and YX contributed to data acquisition. LM and XB conducted the analyses and wrote the paper. The remaining authors contributed to collecting the data and finalizing this paper. LS is the guarantor for the article who accepts full responsibility for the work and/or the conduct of the study, had access to the data, and oversaw the decision to publish. All authors contributed to the article and approved the submitted version.

FUNDING

The current work was supported by GlaxoSmithKline (GSK) in 2014. Dabrafenib and trametinib are assets of Novartis AG as of March 2, 2015. The study sponsorship has been transferred from GSK to Novartis in all participating countries except China. The funder was not involved in the study design, collection, analysis, interpretation of data, the writing of this article or the decision to submit it for publication.

SUPPLEMENTARY MATERIAL

The Supplementary Material for this article can be found online at: https://www.frontiersin.org/articles/10.3389/fonc.2021.720044/full#supplementary-material

REFERENCES

1. Wu Y, Wang Y, Wang L, Yin P, Lin Y, Zhou M. Burden of Melanoma in China, 1990-2017: Findings From the 2017 Global Burden of Disease Study. *Int J Cancer* (2020) 147:692–701. doi: 10.1002/ijc.32764
2. Gao TW, Sun DJ, Li CY, He H, Li Q, Liu YS, et al. Retrospective Analysis of 1905 Patients With Skin Cancer From Two General Hospitals in Western China From 1981 to 2000. *Beijing Da Xue Xue Bao Yi Xue Ban* (2004) 36:469–72.
3. Chi Z, Li S, Sheng X, Si L, Cui C, Han M, et al. Clinical Presentation, Histology, and Prognoses of Malignant Melanoma in Ethnic Chinese: A Study of 522 Consecutive Cases. *BMC Cancer* (2011) 11:85. doi: 10.1186/1471-2407-11-85
4. Si L, Kong Y, Xu X, Flaherty KT, Sheng X, Cui C, et al. Prevalence of BRAF V600E Mutation in Chinese Melanoma Patients: Large Scale Analysis of BRAF and NRAS Mutations in a 432-Case Cohort. *Eur J Cancer* (2012) 48:94–100. doi: 10.1016/j.ejca.2011.06.056
5. Chapman PB, Hauschild A, Robert C, Haanen JB, Ascierto P, Larkin J, et al. Improved Survival With Vemurafenib in Melanoma With BRAF V600E Mutation. *N Engl J Med* (2011) 364:2507–16. doi: 10.1056/NEJMoa1103782
6. Hauschild A, Grob JJ, Demidov LV, Jouary T, Gutzmer R, Millward M, et al. Dabrafenib in BRAF-Mutated Metastatic Melanoma: A Multicentre, Open-Label, Phase 3 Randomised Controlled Trial. *Lancet* (2012) 380:358–65. doi: 10.1016/S0140-6736(12)60868-X
7. Long GV, Stroyakovskiy D, Gogas H, Levchenko E, de Braud F, Larkin J, et al. Combined BRAF and MEK Inhibition *Versus* BRAF Inhibition Alone in Melanoma. *N Engl J Med* (2014) 371:1877–88. doi: 10.1056/NEJMoa1406037
8. Long GV, Weber JS, Infante JR, Kim KB, Daud A, Gonzalez R, et al. Overall Survival and Durable Responses in Patients With BRAF V600-Mutant Metastatic Melanoma Receiving Dabrafenib Combined With Trametinib. *J Clin Oncol* (2016) 34:871–8. doi: 10.1200/JCO.2015.62.9345
9. Long GV, Eroglu Z, Infante J, Patel S, Daud A, Johnson DB, et al. Long-Term Outcomes in Patients With BRAF V600-Mutant Metastatic Melanoma Who Received Dabrafenib Combined With Trametinib. *J Clin Oncol* (2018) 36:667–73. doi: 10.1200/JCO.2017.74.1025
10. Robert C, Grob JJ, Stroyakovskiy D, Karaszewska B, Hauschild A, Levchenko E, et al. Five-Year Outcomes With Dabrafenib Plus Trametinib in Metastatic Melanoma. *N Engl J Med* (2019) 381:626–36. doi: 10.1056/NEJMoa1904059
11. Dummer R, Ascierto PA, Gogas HJ, Arance A, Mandala M, Liszkay G, et al. Encorafenib Plus Binimetinib *Versus* Vemurafenib or Encorafenib in Patients With BRAF-Mutant Melanoma (COLUMBUS): A Multicentre, Open-Label, Randomised Phase 3 Trial. *Lancet Oncol* (2018) 19:603–15. doi: 10.1016/S1470-2045(18)30142-6
12. Wolchok JD, Chiarion-Sileni V, Gonzalez R, Rutkowski P, Grob JJ, Cowey CL, et al. Overall Survival With Combined Nivolumab and Ipilimumab in Advanced Melanoma. *N Engl J Med* (2017) 377:1345–56. doi: 10.1056/NEJMoa1709684
13. Puzanov I, Ribas A, Robert C, Schachter J, Nyakas M, Daud A, et al. Association of BRAF V600E/K Mutation Status and Prior BRAF/MEK Inhibition With Pembrolizumab Outcomes in Advanced Melanoma: Pooled Analysis of 3 Clinical Trials. *JAMA Oncol* (2020) 6:1256–64. doi: 10.1001/jamaoncol.2020.2288
14. Si L, Zhang X, Shu Y, Pan H, Wu D, Liu J, et al. A Phase Ib Study of Pembrolizumab as Second-Line Therapy for Chinese Patients With Advanced or Metastatic Melanoma (KEYNOTE-151). *Transl Oncol* (2019) 12:828–35. doi: 10.1016/j.tranon.2019.02.007
15. Si L, Zhang X, Shin SJ, Fan Y, Lin CC, Kim TM, et al. Open-Label, Phase IIa Study of Dabrafenib Plus Trametinib in East Asian Patients With Advanced BRAF V600-Mutant Cutaneous Melanoma. *Eur J Cancer* (2020) 135:31–8. doi: 10.1016/j.ejca.2020.04.044
16. Schwartz LH, Litiere S, de Vries E, Ford R, Gwyther S, Mandrekar S, et al. RECIST 1.1-Update and Clarification: From the RECIST Committee. *Eur J Cancer* (2016) 62:132–7. doi: 10.1016/j.ejca.2016.03.081
17. National Institutes of Health. *Common Terminology Criteria for Adverse Events (CTCAE)*. Available at: https://ctep.cancer.gov/protocolDevelopment/electronic_applications/ctc.htmlhttps://ctep.cancer.gov/protocolDevelopment/electronic_applications/ctc.html (Accessed June 9, 2020).
18. Long GV, Flaherty KT, Stroyakovskiy D, Gogas H, Levchenko E, de Braud F, et al. Dabrafenib Plus Trametinib *Versus* Dabrafenib Monotherapy in Patients With Metastatic BRAF V600E/K-Mutant Melanoma: Long-Term Survival and Safety Analysis of a Phase 3 Study. *Ann Oncol* (2017) 28:1631–9. doi: 10.1093/annonc/mdx176
19. Nakamura Y, Namikawa K, Yoshino K, Yoshikawa S, Uchi H, Goto K, et al. Anti-PD1 Checkpoint Inhibitor Therapy in Acral Melanoma: A Multicenter Study of 193 Japanese Patients. *Ann Oncol* (2020) 31:1198–206. doi: 10.1016/j.annonc.2020.05.031
20. Ribas A, Hamid O, Daud A, Hodi FS, Wolchok JD, Kefford R, et al. Association of Pembrolizumab With Tumor Response and Survival Among Patients With Advanced Melanoma. *JAMA* (2016) 315:1600–9. doi: 10.1001/jama.2016.4059
21. Ravaioli GM, Dika E, Lambertini M, Chessa MA, Fanti PA, Patrizi A. Acral Melanoma: Correlating the Clinical Presentation to the Mutational Status. *G Ital Dermatol Venereol* (2019) 154:567–72. doi: 10.23736/S0392-0488.18.05791-7
22. Bello DM, Chou JF, Panageas KS, Brady MS, Coit DG, Carvajal RD, et al. Prognosis of Acral Melanoma: A Series of 281 Patients. *Ann Surg Oncol* (2013) 20:3618–25. doi: 10.1245/s10434-013-3089-0
23. Tang B, Chi Z, Chen Y, Liu X, Wu D, Chen J, et al. Safety, Efficacy, and Biomarker Analysis of Toripalimab in Previously Treated Advanced Melanoma: Results of the POLARIS-01 Multicenter Phase II Trial. *Clin Cancer Res* (2020) 26:4250–9. doi: 10.1158/1078-0432.CCR-19-3922
24. Schadendorf D, Long GV, Stroiakovski D, Karaszewska B, Hauschild A, Levchenko E, et al. Three-Year Pooled Analysis of Factors Associated With Clinical Outcomes Across Dabrafenib and Trametinib Combination Therapy Phase 3 Randomised Trials. *Eur J Cancer* (2017) 82:45–55. doi: 10.1016/j.ejca.2017.05.033
25. Long GV, Grob JJ, Nathan P, Ribas A, Robert C, Schadendorf D, et al. Factors Predictive of Response, Disease Progression, and Overall Survival After Dabrafenib and Trametinib Combination Treatment: A Pooled Analysis of Individual Patient Data From Randomised Trials. *Lancet Oncol* (2016) 17:1743–54. doi: 10.1016/S1470-2045(16)30578-2
26. Takahashi A, Namikawa K, Nakano E, Yamazaki N. Real-World Efficacy and Safety Data for Dabrafenib and Trametinib Combination Therapy in Japanese Patients With BRAF V600 Mutation-Positive Advanced Melanoma. *J Dermatol* (2020) 47:257–64. doi: 10.1111/1346-8138.15204
27. Flaherty KT, Infante JR, Daud A, Gonzalez R, Kefford RF, Sosman J, et al. Combined BRAF and MEK Inhibition in Melanoma With BRAF V600 Mutations. *N Engl J Med* (2012) 367:1694–703. doi: 10.1056/NEJMoa1210093
28. Gutzmer R, Stroyakovskiy D, Gogas H, Robert C, Lewis K, Protsenko S, et al. Atezolizumab, Vemurafenib, and Cobimetinib as First-Line Treatment for Unresectable Advanced BRAF(V600) Mutation-Positive Melanoma (IMspire150): Primary Analysis of the Randomised, Double-Blind, Placebo-Controlled, Phase 3 Trial. *Lancet* (2020) 395:1835–44. doi: 10.1016/S0140-6736(20)30934-X
29. Nathan P, Dummer R, Long GV, Ascierto PA, Tawbi HA, Robert C, et al. LBA43 Spartalizumab Plus Dabrafenib and Trametinib (Sparta-DabTram) in Patients (Pts) With Previously Untreated BRAF V600–Mutant Unresectable or Metastatic Melanoma: Results From the Randomized Part 3 of the Phase III COMBI-I Trial. *Ann Oncol* (2020) 31:S1172. doi: 10.1016/j.annonc.2020.08.2273
30. Ribas A, Lawrence D, Atkinson V, Agarwal S, Miller WHJr, Carlino MS, et al. Combined BRAF and MEK Inhibition With PD-1 Blockade Immunotherapy in BRAF-Mutant Melanoma. *Nat Med* (2019) 25:936–40. doi: 10.1038/s41591-019-0476-5

Conflict of Interest: LS has received speaker honoraria from MSD, Roche, Novartis, Shanghai Junshi Biosciences and OrienGene. Xiaoshi Zhang has consulting roles in MSD, Roche, Novartis, Shanghai Junshi. JG has consulting or advisory roles in MSD, Roche, Pfizer, Bayer, Novartis, Simcere Pharmaceutical Group, Shanghai Junshi Biosciences and OrienGene.

The remaining authors declare that the research was conducted in the absence of any commercial or financial relationships that could be construed as a potential conflict of interest.

Publisher's Note: All claims expressed in this article are solely those of the authors and do not necessarily represent those of their affiliated organizations, or those of the publisher, the editors and the reviewers. Any product that may be evaluated in

this article, or claim that may be made by its manufacturer, is not guaranteed or endorsed by the publisher.

Copyright © 2021 Mao, Ding, Bai, Sheng, Dai, Chi, Cui, Kong, Fan, Xu, Wang, Tang, Lian, Yan, Li, Zhou, Wei, Li, Guo, Zhang and Si. This is an open-access article distributed under the terms of the Creative Commons Attribution License (CC BY). The use, distribution or reproduction in other forums is permitted, provided the original author(s) and the copyright owner(s) are credited and that the original publication in this journal is cited, in accordance with accepted academic practice. No use, distribution or reproduction is permitted which does not comply with these terms.

frontiers in Oncology

SYSTEMATIC REVIEW
published: 08 September 2021
doi: 10.3389/fonc.2021.737760

Prognostic and Clinicopathological Value of Ki-67 in Melanoma: A Meta-Analysis

Qixin Liu[1†], *Ziheng Peng*[2†], *Liangfang Shen*[1] *and Lin Shen*[1*]

[1] Department of Oncology, Xiangya Hospital, Central South University, Changsha, China, [2] Department of Gastroenterology, Xiangya Hospital, Central South University, Changsha, China

Background: The prognostic and clinicopathological value of Ki-67 in melanoma is controversial. The purpose of this meta-analysis was to determine the prognostic role of Ki-67 in melanoma patients.

Materials and Methods: The PubMed, Cochrane Library, Web of Science, and Embase databases were searched systematically up to April 9, 2021. We calculated the pooled hazard ratios (HRs) and 95% confidence intervals (CIs) to determine the relationship between Ki-67 overexpression and survival outcomes. We also calculated the combined odds ratios (ORs) and 95% CIs to determine the relationship between Ki-67 expression levels and clinicopathologic parameters. All data were statistically analyzed by Stata 11.0.

Results: A total of 10 studies involving 929 patients were included in our meta-analysis. The pooled HR showed that Ki-67 overexpression was connected with poor overall survival rates (HR=2.92, 95% CI=2.17-3.91, p<0.000). However, there was no correlation between Ki-67 overexpression and the PFS (HR=0.999, 95% CI =0.958-1.041, P =0.958; I2 = 21.80%, P =0.258) or RFS (HR=1.14, 95% CI = 0.42-3.11, P =0.993; I2 = 85.00%, P =0.01) rates. Ki-67 expression levels were associated with tumor thickness, but not sex, location, ulceration or vascular invasion.

Conclusion: Ki-67 is a useful poor prognostic indicator for melanoma patients.

Keywords: melanoma, Ki-67, prognosis, clinicopathology, meta-analysis

OPEN ACCESS

Edited by:
Gil Bar-Sela,
Ha'Emek Medical Center, Israel

Reviewed by:
Olga Vornicova,
Ha'Emek Medical Center, Israel
Judit Krausz,
Ha'Emek Medical Center, Israel

***Correspondence:**
Lin Shen
sl168898@gmail.com

[†]*These authors have contributed equally to this work and share first authorship*

Specialty section:
This article was submitted to Skin Cancer, a section of the journal Frontiers in Oncology

Received: *07 July 2021*
Accepted: *13 August 2021*
Published: *08 September 2021*

Citation:
Liu Q, Peng Z, Shen L and Shen L (2021) Prognostic and Clinicopathological Value of Ki-67 in Melanoma: A Meta-Analysis. Front. Oncol. 11:737760. doi: 10.3389/fonc.2021.737760

1 INTRODUCTION

Melanoma is a diffuse neuroendocrine tumor originating from the neural crest that mainly occurs in the skin and mucosa. The global number of melanoma cases increased from 232,000 in 2012 to 351,880 in 2015, and 62,000 patients died from melanoma in 2015. As the most common cutaneous malignant tumour, melanoma has the characteristics of high malignancy levels, increasing morbidity and mortality rates, and extremely high treatment costs (1). Ethnicity, sun exposure, alcohol consumption, vitamin D deficiency, obesity and exposure to chemicals such as oil and pesticides have all been cited as causes of melanoma (2). With the continuing rise in morbidity, melanoma has become a challenging public health problem worldwide, especially in New Zealand, Australia, Norway, Sweden, and the Netherlands (3). Moreover, melanoma is projected to become the second most common cancer in the United States by 2040 (4). The global incidence of melanoma has increased observably in recent years; however, some emerging therapies, such as

immune checkpoint inhibitors, have led to a significant decline in melanoma patient mortality rates (5).

As a nuclear protein expressed in proliferating mammalian cells, Ki-67 controls gene expression by organizing heterochromatin spatially (6). Immunohistochemical (IHC) staining is usually used to detect Ki-67, and the expression level of Ki-67 is related to cell proliferation activity, disease progression and cancer recurrence (7). Some studies have shown that Ki-67 is one of the prognostic indices of multiple solid tumors, such as nasopharyngeal carcinoma (8), stage I non-small cell lung cancer (9), gastrointestinal stromal tumour (10), and gliomas (11), resected triple-negative breast cancer (12), colorectal cancer (13), hepatocellular carcinoma (14), and thyroid cancer (15). Previous studies have shown an association between Ki-67 expression and melanoma patient prognosis, but the results have been contradictory (16–25). Some studies show that high Ki-67 expression is an indicator of worse prognosis (16–22, 25), while other studies suggest that high Ki-67 expression predicts favorable prognosis (23, 24). Therefore, we conducted this meta-analysis to accurately determine the prognostic and clinicopathological significance of Ki-67 in melanoma patients to optimize treatment strategies.

2 MATERIALS AND METHODS

This meta-analysis was conducted on the basis of the Preferred Reporting Items for Systematic Reviews and Meta-Analyses statement (26).

2.1 Search Strategy

The PubMed, Cochrane Library, Web of Science, and Embase databases were searched systematically up to April 9, 2021. Because the data in this study were extracted from previous studies, ethical approval and patient consent were not required. The search terms were as follows: (melanoma or malignant melanoma or melanocytoma) and (Ki67 or Ki-67 or MIB-1 or MIB1).

2.2 Inclusion and Exclusion Criteria

The inclusion criteria were as follows: (1) histopathology confirmed the diagnosis of melanoma; (2) the expression of Ki-67 in tissues was detected by immunohistochemistry (IHC); (3) at least one survival outcome was reported, such as the overall survival (OS), progression-free survival (PFS), or relapse-free survival (RFS) rate with hazard ratio (HR) and 95% confidence interval (CI); and (4) studies were published in English or Chinese.

The exclusion criteria were as follows: (1) reviews, letters, case reports, expertise public opinion and conference abstracts; (2) studies on tumor cell lines and animal models; (3) duplicate studies or duplicate data; and (4) studies that did not provide necessary and complete data.

2.3 Data Extraction and Quality Assessment

Two independent researchers read the eligible studies and extracted basic information independently; any differences were settled through repeated discussion. The following information was extracted: author, country or region, sample size, sex, age, study type, Ki-67%, AJCC stage, Clark level, follow-up and HRs and 95% CIs of OS, PFS, and RFS rates. Some HRs and 95% CIs could be obtained directly from the studies, while others were calculated from the survival curves. The quality of the selected articles was assessed using the Newcastle Ottawa Scale (NOS) criteria (27). NOS scores range from 0 to 9, and studies with a score of 6 are considered high-quality studies; otherwise, they are considered low-quality studies.

2.4 Statistical Analysis

The statistical analysis was conducted by Stata SE11.0. The HR and 95% CI were used to estimate the relationship between the Ki-67 value and survival outcomes, including the OS, PFS and RFS rates. ORs (odds ratios) and 95% CIs were used to evaluate the relationship between the Ki-67 value and the clinical characteristics of the melanoma patients, such as sex and location and tumor ulceration, thickness, and vascular invasion. We performed subgroup analyses, as shown in **Table 4**, by stratifying the combined data according to region (Europe and America *versus* Asian), patients (≥100 *versus* <100), median age (≥50 years *versus* <50 years), study type (prospective *versus* retrospective), Ki-67% (≥25% *versus* <25%), and follow-up time (>=48 months *versus* <48 months). Cochran's Q statistic and I^2 statistic were used to quantify the heterogeneity among the studies. The random-effects model was applied when the heterogeneity was significant (I^2> 50%); otherwise, a fixed-effects model used. Begg's test was performed to assess potential publication bias. A p-value <0.05 was considered statistically significant.

3 RESULTS

3.1 Search Result and Research Characteristics

The flow chart of the article retrieval process is presented in **Figure 1**. A total of 693 records were found through an initial search. After deleting 61 duplicate records, 632 studies were screened by title and abstract. Subsequently, 602 studies were excluded because they were review articles, meta-analyses, case reports, conference abstracts or basic medical research reports. Then, a comprehensive assessment of the eligibility of 51 full-text articles was conducted, of which 41 studies were excluded for reasons such as lack of complete data and patient overlap between two studies. Finally, 10 studies were included in this meta-analysis, and the detailed characteristics of these included studies are shown in **Tables 1**, **2**. All the studies were conducted mainly in Europe and America, four of which were conducted in the United States (17–19, 24), one in Portugal, one in Spain, one in Israel, one in Poland, two in Norway, and one in Germany. The sample sizes ranged from 30 to 202, and the total number of patients was 929. Nine studies reported patient sex, nine studies reported age, five studies reported AJCC stage, and three studies reported Clark level. Ki-67 values were determined by immunohistochemistry (IHC) in all studies, with cut-off values ranging from 5% to 40%. Of all the studies, eight were retrospective studies, and two were prospective studies. The NOS scores ranged from 6 to 8, with a median value of 7. The follow-up period of the studies ranged from 19.2 months to 151 months.

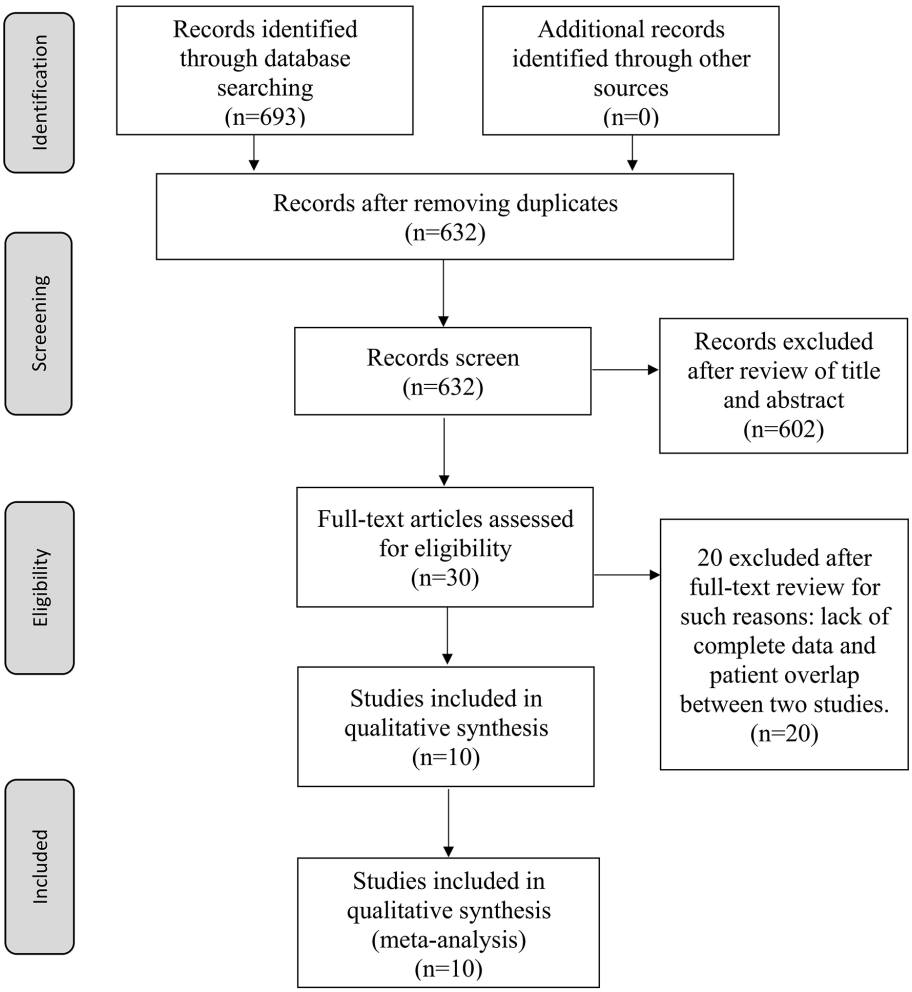


FIGURE 1 | Flow diagram of reviewing and selecting studies.

TABLE 1 | Characteristics of the included studies.

Author	Country	Patients	Duratin	Study type	NOS score	ki-67	HR and 95% CI	Survival analysis
Rui et al. (16)	Portugal	82	1990-1996	Retrospective	8	14%	Calculated	OS
Stefan et al. (17)	American&Spain	66	1991-2016	Retrospective	7	10%	Reported	PFS
Ting et al. (18)	American	114	2002-2008	Prospective	7	25%	Reported	OS
Eric M et al. (19)	American	68	2002-2015	Prospective	6	25%	Reported	OS;RFS
O Ben-Izhak et al. (20)	Israel	30	NA	Retrospective	7	40%	Calculated	OS
Oddbjørn et al. (21)	Norway	202	1981-1997	Retrospective	8	16%	Reported	OS
ALEKSANDER et al. (22)	Poland	93	1983-1991	Retrospective	7	20%	Calculated	OS
Vivi Ann et al. (23)	Norway	47	NA	Retrospective	7	5%	Reported	RFS
Nicholas et al. (24)	American	66	1991-2013	Retrospective	7	10%	Reported	PFS
Philipp et al. (25)	Germany	161	1980-2008	Retrospective	7	20%	Reported	OS

CI, confidence interval; HR, hazard ratio; OS, overall survival; PFS, progression-free survival; RFS, relapse-free survival. NA, not available.

3.2 Association Between Ki-67 Expression and OS, PFS and RFS Rates

The prognostic value of Ki-67 for the OS rate was reported in seven studies (16, 18–22, 25), and two studies each reported the prognostic value of Ki-67 for PFS (17, 24) and RFS (19, 23) rates. As shown in **Figure 2** and **Table 3**, we used a fixed-effects model because of nonsignificant heterogeneity (I2 = 27.30%, p=0.22), and the results showed that high Ki-67 expression predicted poor

TABLE 2 | Characteristics of patients enrolled in these studies.

Author	Patients	Gender M/F	Age(years)	AJCC Stage	Anatomic site	Ulceration	Follow-up (months)	Relapse& Metastasis
Rui et al. (16)	82	22/60	NA	I-III	Axial 38; Extremities 46	51/82	37.5 [1-103]	24/82
Stefan et al. (17)	66	42/24	70 [38-95]	NA	Axial 55; Extremities 11	NA	62 [0.5-229]	20/66
Ting et al. (18)	114	63/51	57 [15-92]	I-IV	Axial 57; Extremities 36	32/114	19.2	NA
Eric M et al. (19)	68	40/28	65.4 [26.2-87.4]	II-III	Axial 32; Extremities 36	48/68	31.2	40/68
O Ben-Izhak et al. (20)	30	10/20	16 [1-140]	NA	NA	30/30	16[1-140]	4/30
Oddbjørn et al. (21)	202	90/112	64.4	I-IV	Axial 106; Extremities 95	83/202	76[13-210]	NA
ALEKSANDER et al. (22)	93	35/58	48 [17-78]	I-III	Axial 44; Extremities 49	63/93	44.7[2-116]	50/93
Vivi Ann et al. (23)	47	NA	54 [19-88]	NA	NA	NA	151[26-172]	NA
Nicholas et al. (24)	66	44/22	71 [34-97]	NA	Axial 60; Extremities 6	NA	49[2-268]	37/66
Philipp et al. (25)	161	69/92	55 [22-89]	I-II	NA	NA	122[8-328]	NA

AJCC, American Joint Committee on Cancer; F, female; M, male; NA, not available.

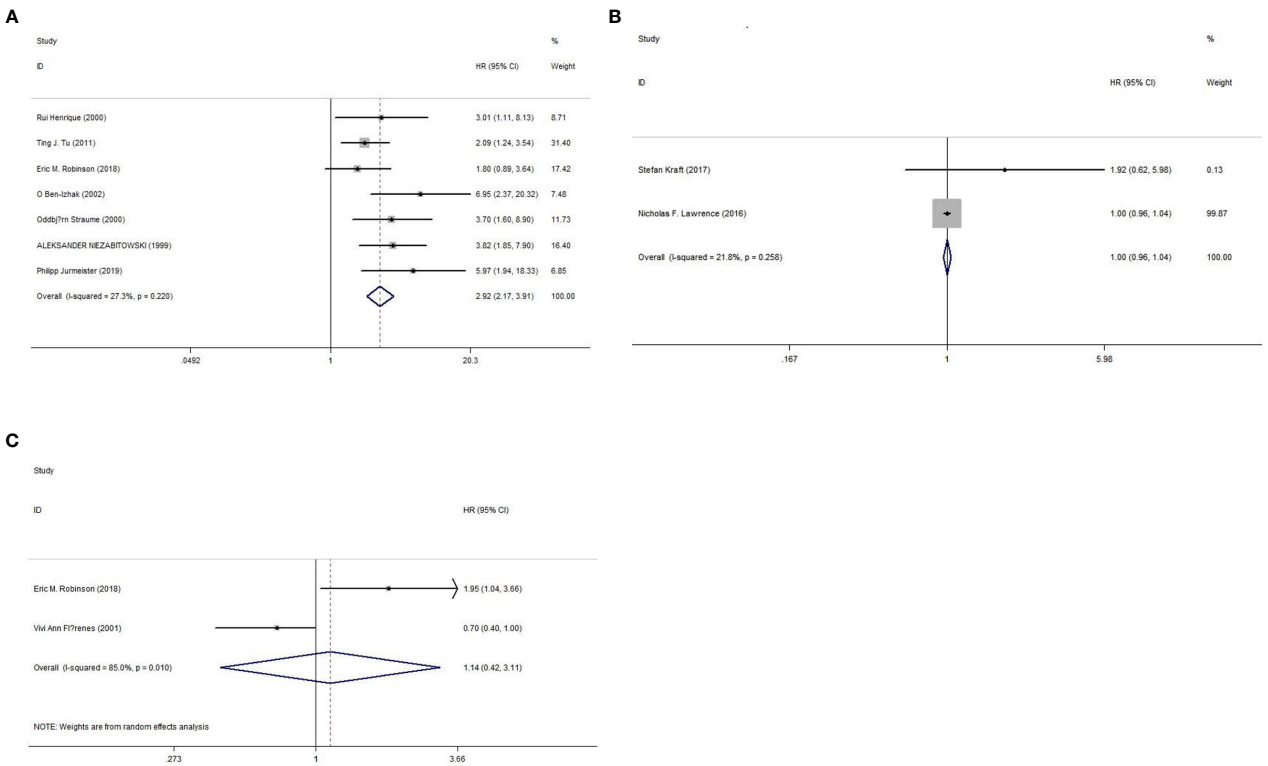


FIGURE 2 | Forest plot of OS, PFS, and RFS. **(A)** Meta-analysis of Ki-67 expression and OS. **(B)** Meta-analysis of Ki-67 expression and PFS. **(C)** Meta-analysis of Ki-67 expression and RFS.

OS outcomes (HR=2.92, 95% CI=2.17-3.91, p<0.000). However, there was no significant correlation between high expression of Ki-67 and PFS (HR=0.999, 95% CI =0.958-1.041, P =0.958; I2 = 21.80%, P =0.258) or RFS (HR=1.14, 95% CI = 0.42-3.11, P =0.993; I2 = 85.00%, P =0.01) rates. In addition, we also performed subgroup analysis by region, patients, median age, study type, Ki-67% and follow-up length. As shown in **Table 4**, the OS rate of melanoma patients did not differ between the European, American and Asian populations, between sample sizes greater than or less than 100, between patients with a median age below 50 years and those over 50 years, between retrospective and prospective studies, between Ki-67 values greater than or less than 25%, and between follow-up times greater than or less than 48 months. However, only two studies were included in the PFS and RFS survival analysis, so no subgroup analysis was performed in this study.

TABLE 3 | Summary of the meta-analysis of Ki-67 expression and OS, PFS, RFS.

Outcome	Studies	HR	P-value	95% CI	Heterogeneity		Effects model
					I2(%)	P-value	
OS	7	2.92	0.000	[2.17-3.91]	27.30%	0.22	Fixed
PFS	2	0.999	0.958	[0.958-1.041]	21.80%	0.258	Fixed
RFS	2	1.14	0.993	[0.42-3.11]	85.00%	0.01	Random

TABLE 4 | Subgroup analysis of pooled HR for melanoma patients with Ki-67 overexpression.

Group factors	Subgroup	Studies	Overall survival		95% CI	Heterogeneity		Effects model
			Pooled HR	P-value		I2(%)	P	
All	All	7	2.92	0.000	[2.17-3.91]	27.30%	0.22	Fixed
region	Europe and America	6	2.72	0.000	[2.00-3.69]	9.80%	0.353	Fixed
	Asia	1	6.95	0.0004	[2.37-20.32]	NA	NA	NA
patients	>=100	3	2.759	0.000	[1.821-4.182]	40.10%	0.188	Fixed
	<100	4	3.084	0.000	[2.035-4.673]	37.20%	0.189	Fixed
median age	>=50	4	2.471	0.000	[1.727-3.535]	31.60%	0.223	Fixed
	<50	2	4.608	0.000	[2.525-8.409]	0.00%	0.366	Fixed
study type	prospective	2	1.982	0.001	[1.301-3.018]	0.00%	0.739	Fixed
	retrospective	5	4.219	0.000	[2.798-6.362]	0.00%	0.773	Fixed
ki-67%	>=25%	3	2.6	0.004	[1.361-4.969]	57.00%	0.1843	Random
	<25%	4	3.873	0.000	[2.483-6.042]	0.00%	0.843	Fixed
follow-up	>=48	2	4.413	0.000	[2.232-8.725]	0.00%	0.508	Fixed
	<48	4	2.408	0.000	[1.711-3.389]	0.00%	0.443	Fixed

NA, not available.

3.3 Relationships Between Ki-67 Expression and Clinicopathologic Parameters

We investigated the relationship between the expression of Ki-67 and multiple clinicopathological factors, such as sex, location, ulceration, thickness and vascular invasion. As shown in **Table 5**, Ki-67 overexpression was associated with thickness >4.0 mm (OR=3.09, 95% CI=1.34-7.10, P=0.008; I^2 = 0.00%, p=0.351). However, Ki-67 overexpression was not significantly correlated with sex (OR=1.65, 95% CI=0.84-3.25, p=0.149), location (OR=1.43, 95% CI=0.67-3.09, p=0.357), ulceration (OR=5.08, 95% CI=0.73-35.37, p=0.100) or vascular invasion (OR=1.13, 95% CI=0.32-4.00, p=0.855).

3.4 Sensitivity Analysis

To assess the stability of the results, a sensitivity analysis for sequence deletion was performed for each study. We only conducted sensitivity analysis for OS outcomes because only 2 studies reported the PFS and RFS rates. As shown in **Figure 3**, the results showed that no separate study significantly affected the overall HR, which suggested that the results of this meta-analysis are reliable.

3.5 Publication Bias

Begg's test was performed to evaluate publication bias. As shown in **Figure 4**, the funnel plot did not indicate publication bias in the OS outcome (P=0.072). However, both PFS and RFS outcomes were only included in two studies, so it was unnecessary to determine whether there was publication bias in the PFS and RFS analysis.

4 DISCUSSION

Currently, the association between ki-67 expression levels and prognosis in melanoma patients is not clear. In this study, we integrated 10 clinical studies to determine the prognostic value of Ki-67 expression in melanoma patients. The results showed that Ki-67 expression was connected with different survival

TABLE 5 | The relationships between Ki-67 expression and clinicopathologic parameters.

Variables	Studies	OR	P-value	95% CI	Heterogeneity		Effects model
					I2(%)	P	
Gender (male *versus* female)	3	1.65	0.149	[0.84-3.25]	19.60%	0.288	Fixed
Location (head and neck *versus* others)	2	1.43	0.357	[0.67-3.09]	4.80%	0.305	Fixed
Ulceration (present *versus* absent)	2	5.08	0.100	[0.73-35.37]	65.10%	0.09	Random
Thickness (mm) (>4.0 *versus* <=4.0)	2	3.09	0.008	[1.34-7.10]	0.00%	0.351	Fixed
Vascular invasion (present *versus* absent)	2	1.13	0.855	[0.32-4.00]	0.00%	0.328	Fixed

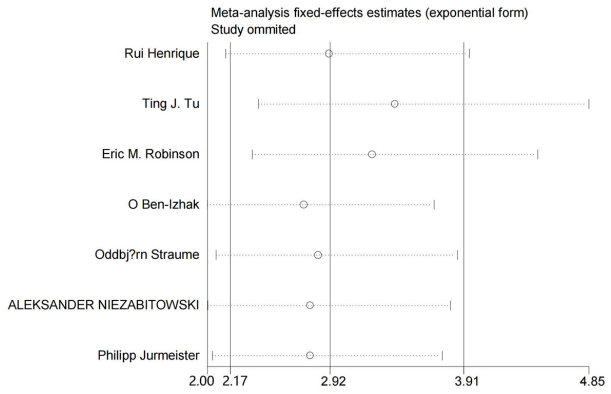


FIGURE 3 | Sensitivity analysis for OS.

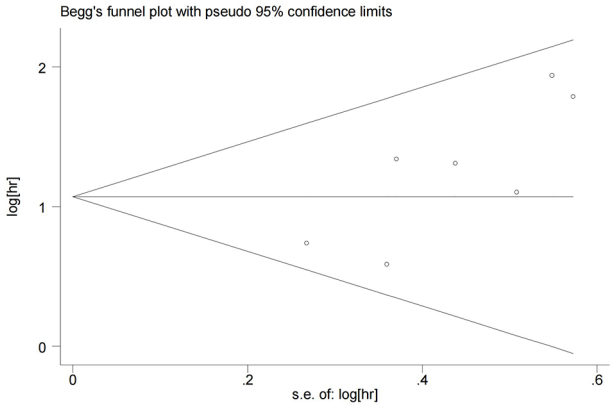


FIGURE 4 | Funnel plots for detecting publication bias of the association between Ki-67 expression level and overall survival of melanoma.

endpoints,including OS, PFS and RFS rate, suggesting that Ki-67 could be used as a valuable index in the prognostication of patients with melanoma. The pooled data also showed that high expression of Ki-67 was associated with melanoma thickness but not with sex, location, ulceration, or vascular invasion. In addition, subgroup analyses indicated that a high level of Ki-67 expression was related to poor OS outcomes in melanoma patients regardless of region, patients, median age of the patients, study type, cut-off of Ki-67% and length of follow-up. Taken together, this is the first study to reveal that high Ki-67 expression is associated with poor prognosis in melanoma patients by using meta-analysis approach.

As the best marker to evaluate cell proliferation, Ki-67 is expressed in all active stages of the cell cycle, including G1, S, G2 and mitosis (28). Therefore, the higher the expression level of KI-67, the faster the tumor growth and the larger the tumor volume will be, leading to the worse prognosis of patients. KI-67 has been proved to be an prognostic index for multiple solid tumors, for example, high ki-67 expression is closely associated with poor OS and DFS (Disease Free Survival) in lung adenocarcinoma (29). A meta-analysis including 8 studies showed that high ki-67 expression was associated with poor OS, PFS, and DMFS (distant metastasis-free survival) in patients with nasopharyngeal carcinoma (8). In hepatocellular carcinoma, high expression of KI-67 has been associated with poor DFS, RFS, and OS (14). Qiu et al. reported that Ki-67 overexpression was correlated with poor OS in patients with ovarian cancer (30). In our study, we revealed that the high expression of KI-67 was closely associated with poor OS in melanoma patients, which is consistent with the conclusion of other solid tumors. However, the reasons why Ki-67 is not related to PFS and RFS may be as follows. First, there are only two studies including PFS and RFS, so there is maybe some bias in the conclusion. Second, high expression of KI-67 may indeed be unrelated to poor PFS and RFS, but the current research data are insufficient, and we expect more data to confirm this conclusion in the future.

Previous studies have shown that the expression level of KI-67 is closely related to the tumor size, such as bladder cancer (31), hepatocellular carcinoma (14), and gastric cancer (32). In our study, we found the relationship between high expression of Ki-67 and melanoma thickness. Thus, the previous findings of the correlations of Ki-67 expression and tomor size in various solid cancers are in accordance with the present study.A recent study showed that melanoma tumor thickness is strongly associated with poor 5-year OS (33). Therefore, the high expression of KI-67 indicates the poor prognosis of melanoma patients, which may be related to tumor thickness. However, a study examining the relationship between ki-67 expression and patient prognosis in thick melanoma (≥4 mm) showed that KI-67 remains an index of poor prognosis in melanoma (19). Therefore, we believe that Ki-67 is still a marker of poor prognosis in melanoma patients even after removing the effect of tumor thickness. Furthermore, ki-67 expression was strongly associated with increased Breslow thickness, Clark level, ulceration, lymphovascular invasion, number of mitosis, and pT stage (34). However, pooled data of this study showed that high ki-67 expression was independent of gender, location, ulceration, or vascular invasion, which may account for the limited sample size of this study.

The advantages of our study are as follows. First, this is the first study to use a meta-analysis to demonstrate that Ki-67 overexpression is a predictor of poor prognosis in melanoma patients. Second, we did a through search to find the best fitting studies, and finally a total of 10 previours studies were included in our meta-analysis. Third, the expression level of KI-67 in the 10 eligible studies included was detected by IHC, which ensured the reliability of the results. Finally, only high quality English literature is included in this study to reduce errors and ensure the authenticity of research conclusions.

However, there are several limitations in our meta-analysis. First, both the number of studies and the total sample size were small. Second, the cut-off point for Ki-67 positivity was different among the included studies, which may have led to heterogeneity. Third, clinical data from Asian and African countries are scarce. Therefore, we need more data from other region groups to determine the influence of region on the study results. Forth, different types of melanomas behave differently, having

different molecular signitures and Ki67 proliferation index may have different impacts in those types of melanomas. Finally, as with all meta analysis,it cannot correct some of the bias in the included original studies, and some of the studies which were included in this article were too small for statistical analysis. Therefore, we need more comprehensive designs and large-scale clinical trials for further investigation.

Despite some limitations, our meta-analysis conclusively indicates that Ki-67 overexpression is associated with worse OS rates in melanoma patients. Ki-67 can be used as an important reference marker when evaluating the survival outcomes and prognoses of melanoma patients. Therefore, our study can provide some reference for clinicians in the formulation of melanoma diagnosis and treatment plan, rational allocation of medical resources and preliminary judgment of patient prognosis. There are some shortcomings in our study; thus, we look forward to the completion of more prospective multicentric clinical studies with reasonable designs and on larger scales to verify and supplement our conclusions.

DATA AVAILABILITY STATEMENT

The original contributions presented in the study are included in the article/supplementary material. Further inquiries can be directed to the corresponding author.

AUTHOR CONTRIBUTIONS

QL, ZP, and LSe conceived and designed the study. QL and ZP performed the analysis, prepared the figures and tables and wrote the main manuscript. LFS reviewed and revised the manuscript. All authors contributed to the article and approved the submitted version.

ACKNOWLEDGMENTS

Throughout the writing of this dissertation I have received a great deal of support and assistance. I would first like to thank my supervisor, LFS, whose expertise was invaluable in formulating the research questions and methodology. Your insightful feedback pushed me to sharpen my thinking and brought my work to a higher level. Without his enlightening instruction, impressive kindness and patience, I could not have completed my thesis. I would particularly like to acknowledge my teammates, ZP and LS, for their wonderful collaboration and patient support. In addition, I would like to thank my parents for their wise counsel and sympathetic ear. You are always there for me. Finally, I would like to thank the Xiangya Hospital of Central South University for its cultivation of me. This platform with a good academic atmosphere has deeply influenced my thinking on scientific research.

REFERENCES

1. Guy GP Jr, Thomas CC, Thompson T, Watson M, Massetti GM, Richardson LC, et al. Vital Signs: Melanoma Incidence and Mortality Trends and Projections - United States, 1982-2030. *MMWR Morb Mortal Wkly Rep* (2015) 64:591–6.
2. Bolick NL, Geller AC. Epidemiology of Melanoma. *Hematol Oncol Clin North Am* (2021) 35:57–72. doi: 10.1016/j.hoc.2020.08.011
3. Karimkhani C, Green AC, Nijsten T, Weinstock MA, Dellavalle RP, Naghavi M, et al. The Global Burden of Melanoma: Results From the Global Burden of Disease Study 2015. *Br J Dermatol* (2017) 177:134–40. doi: 10.1111/bjd.15510
4. Rahib L, Wehner MR, Matrisian LM, Nead KT. Estimated Projection of US Cancer Incidence and Death to 2040. *JAMA Netw Open* (2021) 4:e214708. doi: 10.1001/jamanetworkopen.2021.4708
5. Siegel RL, Miller KD, Jemal A. Cancer Statistics, 2020. *CA Cancer J Clin* (2020) 70:7–30. doi: 10.3322/caac.21590
6. Sobecki M, Mrouj K, Camasses A, Parisis N, Nicolas E, Lleres D, et al. The Cell Proliferation Antigen Ki-67 Organises Heterochromatin. *Elife* (2016) 5: e13722. doi: 10.7554/eLife.13722
7. Menon SS, Guruvayoorappan C, Sakthivel KM, Rasmi RR. Ki-67 Protein as a Tumour Proliferation Marker. *Clin Chim Acta* (2019) 491:39–45. doi: 10.1016/j.cca.2019.01.011
8. Shi Z, Jiang W, Chen X, Xu M, Wang X, Zha D. Prognostic and Clinicopathological Value of Ki-67 Expression in Patients With Nasopharyngeal Carcinoma: A Meta-Analysis. *Ther Adv Med Oncol* (2020) 12:1758835920951346. doi: 10.1177/1758835920951346
9. Xu J, Liu P, Da J, Hao J, Peng W, Sun G. Prognostic Value of Ki-67 in Stage I Non-Small-Cell Lung Cancer: A Meta-Analysis Involving 1931 Patients. *Pathol Res Pract* (2019) 215:855–60. doi: 10.1016/j.prp.2019.02.020
10. Pyo JS, Kang G, Sohn JH. Ki-67 Labeling Index can be Used as a Prognostic Marker in Gastrointestinal Stromal Tumor: A Systematic Review and Meta-Analysis. *Int J Biol Markers* (2016) 31:e204–10. doi: 10.5301/jbm.5000183
11. Chen WJ, He DS, Tang RX, Ren FH, Chen G. Ki-67 is a Valuable Prognostic Factor in Gliomas: Evidence From a Systematic Review and Meta-Analysis. *Asian Pac J Cancer Prev* (2015) 16:411–20. doi: 10.7314/apjcp.2015.16.2.411
12. Wu Q, Ma G, Deng Y, Luo W, Zhao Y, Li W, et al. Prognostic Value of Ki-67 in Patients With Resected Triple-Negative Breast Cancer: A Meta-Analysis. *Front Oncol* (2019) 9:2019.01068. doi: 10.3389/fonc.2019.01068
13. Li J, Liu ZY, Yu HB, Qu XS, Xue Q, Yu HT, et al. The Association Between Ki-67 Expression and the Clinical Pathological Characteristics of Colorectal Cancer: A Protocol for a Systematic Review and Meta-Analysis. *Med (Baltimore)* (2020) 99:e19996. doi: 10.1097/MD.0000000000019996
14. Luo Y, Ren F, Liu Y, Shi Z, Tan Z, Xiong H, et al. Clinicopathological and Prognostic Significance of High Ki-67 Labeling Index in Hepatocellular Carcinoma Patients: A Meta-Analysis. *Int J Clin Exp Med* (2015) 8:10235–47.
15. Pan DH, Wen DY, Luo YH, Chen G, Yang H, Chen JQ, et al. The Diagnostic and Prognostic Values of Ki-67/MIB-1 Expression in Thyroid Cancer: A Meta-Analysis With 6,051 Cases. *Onco Targets Ther* (2017) 10:3261–76. doi: 10.2147/OTT.S135593
16. Henrique R, Azevedo R, Bento MJ, Domingues JC, Silva C, Jeronimo C. Prognostic Value of Ki-67 Expression in Localized Cutaneous Malignant Melanoma. *J Am Acad Dermatol* (2000) 43:991–1000. doi: 10.1067/mjd.2000.109282
17. Kraft S, Fernandez-Figueras MT, Richarz NA, Flaherty KT, Hoang MP. PDL1 Expression in Desmoplastic Melanoma Is Associated With Tumor Aggressiveness and Progression. *J Am Acad Dermatol* (2017) 77:534–42. doi: 10.1016/j.jaad.2017.05.007
18. Tu TJ, Ma MW, Monni S, Rose AE, Yee H, Darvishian F, et al. A High Proliferative Index of Recurrent Melanoma Is Associated With Worse Survival. *Oncology* (2011) 80:181–7. doi: 10.1159/000328518
19. Robinson EM, Rosenbaum BE, Zhang Y, Rogers R, Tchack J, Berman RS, et al. Association Between Ki-67 Expression and Clinical Outcomes Among Patients With Clinically Node-Negative, Thick Primary Melanoma Who Underwent Nodal Staging. *J Surg Oncol* (2018) 118:150–6. doi: 10.1002/jso.25111
20. Ben-Izhak O, Bar-Chana M, Sussman L, Dobiner V, Sandbank J, Cagnano M, et al. Ki67 Antigen and PCNA Proliferation Markers Predict Survival in

Anorectal Malignant Melanoma. *Histopathology* (2002) 41:519–25. doi: 10.1046/j.1365-2559.2002.01444.x
21. Straume O, Sviland L, Akslen LA. Loss of Nuclear P16 Protein Expression Correlates With Increased Tumor Cell Proliferation (Ki-67) and Poor Prognosis in Patients With Vertical Growth Phase Melanoma. *Clin Cancer Res* (2000) 6:1845–53.
22. Niezabitowski A, Czajecki K, Rys J, Kruczak A, Gruchala A, Wasilewska A, et al. Prognostic Evaluation of Cutaneous Malignant Melanoma: A Clinicopathologic and Immunohistochemical Study. *J Surg Oncol* (1999) 70:150–60. doi: 10.1002/(sici)1096-9098(199903)70:3<150::aid-jso2>3.0.co;2-z
23. Florenes VA, Maelandsmo GM, Faye R, Nesland JM, Holm R. Cyclin a Expression in Superficial Spreading Malignant Melanomas Correlates With Clinical Outcome. *J Pathol* (2001) 195:530–6. doi: 10.1002/path.1007
24. Lawrence NF, Hammond MR, Frederick DT, Su Y, Dias-Santagata D, Deng A, et al. Ki-67, P53, and P16 Expression, and G691S RET Polymorphism in Desmoplastic Melanoma (DM): A Clinicopathologic Analysis of Predictors of Outcome. *J Am Acad Dermatol* (2016) 75:595–602. doi: 10.1016/j.jaad.2016.04.059
25. Jurmeister P, Bockmayr M, Treese C, Stein U, Lenze D, Johrens K, et al. Immunohistochemical Analysis of Bcl-2, Nuclear S100A4, MITF and Ki67 for Risk Stratification of Early-Stage Melanoma - A Combined IHC Score for Melanoma Risk Stratification. *J Dtsch Dermatol Ges* (2019) 17:800–8. doi: 10.1111/ddg.13917
26. Moher D, Liberati A, Tetzlaff J, Altman DG, Group P. Preferred Reporting Items for Systematic Reviews and Meta-Analyses: The PRISMA Statement. *BMJ* (2009) 339:b2535. doi: 10.1136/bmj.b2535
27. Stang A. Critical Evaluation of the Newcastle-Ottawa Scale for the Assessment of the Quality of Nonrandomized Studies in Meta-Analyses. *Eur J Epidemiol.* (2010) 25:603–5. doi: 10.1007/s10654-010-9491-z
28. Sobecki M, Mrouj K, Colinge J, Gerbe F, Jay P, Krasinska L, et al. Cell-Cycle Regulation Accounts for Variability in Ki-67 Expression Levels. *Cancer Res* (2017) 77:2722–34. doi: 10.1158/0008-5472.CAN-16-0707
29. Li Z, Li F, Pan C, He Z, Pan X, Zhu Q, et al. Tumor Cell Proliferation (Ki-67) Expression and Its Prognostic Significance in Histological Subtypes of Lung Adenocarcinoma. *Lung Cancer* (2021) 154:69–75. doi: 10.1016/j.lungcan.2021.02.009
30. Qiu D, Cai W, Zhang Z, Li H, Zhou D. High Ki-67 Expression is Significantly Associated With Poor Prognosis of Ovarian Cancer Patients: Evidence From a Meta-Analysis. *Arch Gynecol Obstet* (2019) 299:1415–27. doi: 10.1007/s00404-019-05082-3
31. Tian Y, Ma Z, Chen Z, Li M, Wu Z, Hong M, et al. Clinicopathological and Prognostic Value of Ki-67 Expression in Bladder Cancer: A Systematic Review and Meta-Analysis. *PloS One* (2016) 11:e0158891. doi: 10.1371/journal.pone.0158891
32. Liu G, Xiong D, Zeng J, Chen B, Huang Z. Clinicopathological and Prognostic Significance of Ki-67 Immunohistochemical Expression in Gastric Cancer: A Systematic Review and Meta-Analysis. *Onco Targets Ther* (2017) 10:4321–8. doi: 10.2147/OTT.S143089
33. Bian SX, Hwang L, Hwang J, Ragab O, In GK, Peng D, et al. Acral Lentiginous Melanoma-Population, Treatment, and Survival Using the NCDB From 2004 to 2015. *Pigment Cell Melanoma Res* (2021). doi: 10.1111/pcmr.12999
34. Udovicic-Gagula D, Ahmovic A, Bilalovic N, Doric M. Expression of Ki-67 and Estrogen Receptor Beta in Primary Cutaneous Melanoma as a Potential Indicator of Regional Lymph Node Positivity. *Appl Immunohistochem Mol Morphol* (2019) 27:27–32. doi: 10.1097/PAI.0000000000000530

Conflict of Interest: The authors declare that the research was conducted in the absence of any commercial or financial relationships that could be construed as a potential conflict of interest.

Publisher's Note: All claims expressed in this article are solely those of the authors and do not necessarily represent those of their affiliated organizations, or those of the publisher, the editors and the reviewers. Any product that may be evaluated in this article, or claim that may be made by its manufacturer, is not guaranteed or endorsed by the publisher.

Copyright © 2021 Liu, Peng, Shen and Shen. This is an open-access article distributed under the terms of the Creative Commons Attribution License (CC BY). The use, distribution or reproduction in other forums is permitted, provided the original author(s) and the copyright owner(s) are credited and that the original publication in this journal is cited, in accordance with accepted academic practice. No use, distribution or reproduction is permitted which does not comply with these terms.

frontiers in Oncology

ORIGINAL RESEARCH
published: 21 September 2021
doi: 10.3389/fonc.2021.741993

Digital Quantification of Tumor PD-L1 Predicts Outcome of PD-1-Based Immune Checkpoint Therapy in Metastatic Melanoma

Jan-Malte Placke[1†], Camille Soun[2†], Jenny Bottek[2], Rudolf Herbst[3], Patrick Terheyden[4], Jochen Utikal[5,6], Claudia Pföhler[7], Jens Ulrich[8], Alexander Kreuter[9], Christiane Pfeiffer[10], Peter Mohr[11], Ralf Gutzmer[12], Friedegund Meier[6,13], Edgar Dippel[14], Michael Weichenthal[15], Lisa Zimmer[1], Elisabeth Livingstone[1], Jürgen C. Becker[1,6,16], Georg Lodde[1], Antje Sucker[1], Klaus Griewank[1], Susanne Horn[1], Eva Hadaschik[1], Alexander Roesch[1,6], Dirk Schadendorf[1,6], Daniel Robert Engel[2] and Selma Ugurel[1]*

[1] Department of Dermatology, University Hospital Essen, University of Duisburg-Essen, Essen, Germany, [2] Institute of Experimental Immunology and Imaging, Department of Immunodynamics, University Hospital Essen, Essen, Germany, [3] Department of Dermatology, Medical Hospital, Erfurt, Germany, [4] Department of Dermatology, University of Lübeck, Lübeck, Germany, [5] Department of Dermatology, Venerology, and Allergology, University Medical Center, Ruprecht-Karls University of Heidelberg, Mannheim, Germany, [6] German Consortium of Translational Cancer Research (DKTK), German Cancer Research Center (DKFZ), Heidelberg, Germany, [7] Department of Dermatology, Saarland University Medical School, Homburg, Germany, [8] Department of Dermatology, Medical Hospital of Quedlinburg, Quedlinburg, Germany, [9] Department of Dermatology, Venereology, and Allergology, Helios St. Elisabeth Hospital Oberhausen, University of Witten-Herdecke, Oberhausen, Germany, [10] Department of Dermatology, Venereology, and Allergology University Ulm, Ulm, Germany, [11] Department of Dermatology, Elbe-Kliniken, Buxtehude, Germany, [12] Skin Cancer Center, Department of Dermatology, Hannover Medical School, Hannover, Germany, [13] Department of Dermatology, University Hospital Dresden, Dresden, Germany, [14] Hautklinik, Klinikum der Stadt Ludwigshafen am Rhein gGmbH, Ludwigshafen, Germany, [15] Department of Dermatology, University Hospital Kiel, Kiel, Germany, [16] Translationale Hautkrebsforschung, University Medicine Essen, University of Duisburg-Essen, Essen, Germany

Background: PD-1-based immune checkpoint blockade (ICB) is a highly effective therapy in metastatic melanoma. However, 40-60% of patients are primarily resistant, with valid predictive biomarkers currently missing. This study investigated the digitally quantified tumor PD-L1 expression for ICB therapy outcome prediction.

Patients and Methods: Tumor tissues taken prior to PD-1-based ICB for unresectable metastatic disease were collected within the prospective multicenter Tissue Registry in Melanoma (TRIM). PD-L1 expression (clone 28-8; cut-off=5%) was determined by digital and physician quantification, and correlated with therapy outcome (best overall response, BOR; progression-free survival, PFS; overall survival, OS).

Results: Tissue samples from 156 patients were analyzed (anti-PD-1, n=115; anti-CTLA-4+anti-PD-1, n=41). Patients with PD-L1-positive tumors showed an improved response compared to patients with PD-L1-negative tumors, by digital (BOR 50.5% *versus* 32.2%; p=0.026) and physician (BOR 54.2% *versus* 36.6%; p=0.032) quantification. Tumor PD-L1 positivity was associated with a prolonged PFS and OS by either digital (PFS, 9.9 *versus* 4.6 months, p=0.021; OS, not reached *versus* 13.0 months, p=0.001) or physician

OPEN ACCESS

Edited by:
Sander Bekeschus,
Leibniz Institute for Plasma Research and Technology e.V. (INP), Germany

Reviewed by:
Aurobind Vidyarthi,
Yale University, United States
Ramona Clemen,
Leibniz Institute for Plasma Research and Technology e.V. (INP), Germany
Woo Cheal Cho,
University of Texas MD Anderson Cancer Center, United States

***Correspondence:**
Jan-Malte Placke
jan-malte.placke@uk-essen.de

[†]These authors contributed equally to this work

Specialty section:
This article was submitted to Skin Cancer, a section of the journal Frontiers in Oncology

Received: 15 July 2021
Accepted: 02 September 2021
Published: 21 September 2021

Citation:
Placke J-M, Soun C, Bottek J, Herbst R, Terheyden P, Utikal J, Pföhler C, Ulrich J, Kreuter A, Pfeiffer C, Mohr P, Gutzmer R, Meier F, Dippel E, Weichenthal M, Zimmer L, Livingstone E, Becker JC, Lodde G, Sucker A, Griewank K, Horn S, Hadaschik E, Roesch A, Schadendorf D, Engel DR and Ugurel S (2021) Digital Quantification of Tumor PD-L1 Predicts Outcome of PD-1-Based Immune Checkpoint Therapy in Metastatic Melanoma. Front. Oncol. 11:741993. doi: 10.3389/fonc.2021.741993

(PFS, 10.6 *versus* 5.6 months, p=0.051; OS, not reached *versus* 15.6 months, p=0.011) quantification. Multivariable Cox regression revealed digital (PFS, HR=0.57, p=0.007; OS, HR=0.44, p=0.001) and physician (OS, HR=0.54, p=0.016) PD-L1 quantification as independent predictors of survival upon PD-1-based ICB. The combination of both methods identified a patient subgroup with particularly favorable therapy outcome (PFS, HR=0.53, p=0.011; OS, HR=0.47, p=0.008).

Conclusion: Pre-treatment tumor PD-L1 positivity predicted a favorable outcome of PD-1-based ICB in melanoma. Herein, digital quantification was not inferior to physician quantification, and should be further validated for clinical use.

Keywords: PD-L1 quantification, melanoma, immune checkpoint blockade therapy, response, survival

INTRODUCTION

The introduction of immune checkpoint blockade (ICB) therapy led to a tremendous survival improvement in patients with advanced metastatic melanoma (1–3). PD-1-based ICB therapies can be used alone or in combination with CTLA-4 inhibitors (4). Despite improved long-term survival in responders, up to 60% of melanoma patients are primary resistant to PD-1-based ICB and have significantly inferior survival as a consequence (5). Approximately 40% of melanomas have a targetable tumor BRAF-V600 mutation with inhibition of the mitogen-activated protein kinase (MAPK) pathway as a viable alternative treatment option to ICB (6). There is a high need for valid pre-treatment biomarkers that predict the response to ICB to enable an optimal treatment choice for advanced melanoma patients. Nonspecific blood-based biomarkers have been reported to predict ICB treatment outcome such as serum lactate dehydrogenase (LDH) activity, as well as blood counts of lymphocytes and eosinophils (7–10). Tumor tissue-based biomarkers described to be associated with PD-1-based ICB therapy outcome are the density of tumor-infiltrating lymphocytes and the expression of PD-L1 (11). In particular, the quantification of PD-L1 expression in tumor tissue is widely used in routine clinical diagnostics of various cancer types such as non-small cell lung carcinoma (NSCLC), renal cell carcinoma, Hodgkin's lymphoma, and colorectal carcinoma (12).

The role of tumor PD-L1 expression as a predictive biomarker in melanoma, however, is not clear, mainly because of the difficulties in evaluating melanomas with overall low PD-L1 expression and high melanin content (2, 13–15). Moreover, PD-L1 staining can be detected not only on the cell membrane but also intracellularly and shows high spatial heterogeneity, so its evaluation is associated with a high interobserver variability (16). In addition, it has already been shown that PD-L1 expression can differ greatly depending on the melanoma subtype and that melanoma subtypes respond differently to ICB (17). Whole-slide imaging and digital pathology have shown an improvement in the evaluation of the immunohistochemical tumor tissue stainings for HER2 and KI67 in breast cancer and for the Gleason classification in prostate cancer (18–20). In addition, a recent study demonstrated that a digital pathology algorithm can be helpful to the pathologist in the evaluation of tumor PD-L1 expression in melanin-bleached melanoma tissue samples. However, a correlation between digital PD-L1 quantification and therapy outcome has not been performed up to now (21).

The aim of the present study was to investigate digital PD-L1 quantification *versus* physician PD-L1 quantification in pre-treatment tumor tissue of melanoma patients as potential predictors of therapy outcome of a PD-1-based ICB.

PATIENTS AND METHODS

Patients and Tissues

Formalin-fixed, paraffin-embedded (FFPE) tumor tissue samples from patients diagnosed with melanoma were prospectively collected within the multicenter translational study Tissue Registry in Melanoma (TRIM; CA209-578) performed within the framework of the skin cancer registry ADOREG of the German Dermatologic Cooperative Oncology Group (DeCOG). Out of this cohort, patients were selected for the present analysis according to the following criteria: Histologically confirmed diagnosis of melanoma of the skin, mucosa, or unknown primary; tumor tissue specimen obtained for analysis prior to a PD-1-based ICB for unresectable stage III or IV (AJCCv8) (18) metastatic disease; complete documentation of therapy outcome and follow-up, and availability of consecutive tissue slides stained for PD-L1 and control IgG, comparable in size and quality. Best overall response (BOR) was determined according to RECIST version 1.1 (22). Progression-free (PFS) and overall (OS) survival were defined as time from therapy start until disease progression or death, respectively; if no such event occurred, the date of the last patient contact was used as endpoint of survival assessment (censored observation). The study was approved by the ethics committee of the University Duisburg-Essen (15-6566-BO).

PD-L1 Staining

The PD-L1 expression was assessed in FFPE tumor tissue specimens with the use of a rabbit monoclonal anti-human PD-L1 antibody (clone 28-8) and an analytically validated

automated immunohistochemical assay (PD-L1 IHC 28-8 pharmDx for Autostainer Link 48; Dako, Agilent Technologies, Santa Clara, CA, USA), as described previously (23). A consecutive tissue slide of the same specimen was prepared accordingly for each sample, stained with non-specific IgG and used as negative control. Hematoxylin was used as nuclear staining. For detailed visualization of morphological structures, an additional control tissue slide was stained with hematoxylin and eosin (H&E).

Quantification of PD-L1 Expression by the Physician

PD-L1 expression in tumor tissue was quantified as the percentage of live tumor cells that exhibited specific cell surface staining of any intensity in a section containing at least 100 evaluable tumor cells, with ≥5% defined as positive staining, as previously described (23). The cutoff >5% as the definition of PD-L1 positivity is recommended by the manufacturer of the assay and is the established standard in our department. This type of quantification of PD-L1 expression was performed by either pathologists or histopathologically experienced dermatologists or both using conventional bright field microscopy, and is referred to as "physician's quantification".

Quantification of PD-L1 Expression by a Digital Algorithm

The anti-PD-L1 stained slides and the negative control slides were digitized with the whole-slide scanner Aperio AT2 (Leica, Wetzlar, Germany) using a resolution of 20x. These digitized whole-slide images were used for the quantification of PD-L1 expression by a newly defined method based on a digital algorithm. This newly developed Java-based algorithm removes artifacts present on the tumor regions and quantifies the number of PD-L1 expressing cells. Corresponding tumor regions were manually selected as regions of interest on the anti-PD-L1-stained slide and the negative control slide; **Figures 1A, B**. Binary masks were generated by applying an intensity threshold for PD-L1 and melanin (brown) as well as hematoxylin (blue), **Figures 1C, D**. The binary masks were obtained by using various thresholding methods implemented by *Fiji* (https://imagej.net/Fiji), each best adapted to the type of signal. To generate the tissue masks (tumor and biopsy), the "Triangle" thresholding method was used. For the Melanin and PDL1 stainings,"MaxEntropy", and "Moments" for the cellular nucleus. These methods are part of the Auto-threshold algorithms of Fiji and were chosen based on their accuracy (24). The digitized image of the respective negative control staining was used to deduct the background signal (melanin). The binary

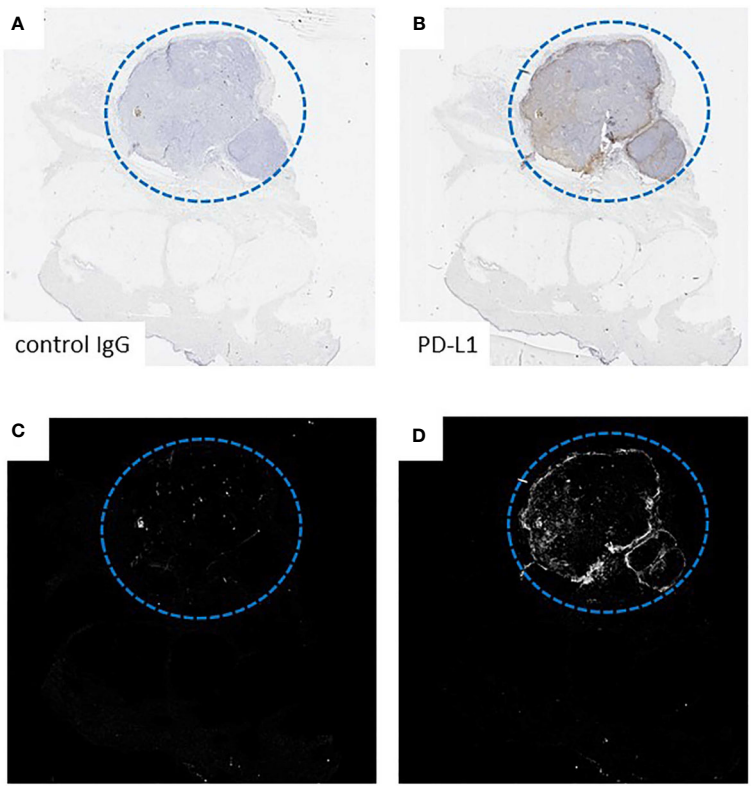


FIGURE 1 | Exemplary presentation of the functioning of the digital algorithm on the basis of a sample from the patient group. Digital quantification of PD-L1 expression demonstrated on representative tissue slides from a subcutaneous melanoma metastasis. **(A, B)** Manual selection of the tumor regions of interest on an anti-PD-L1-stained slide and a consecutive negative control IgG-stained slide. **(C, D)** Binary masks of **(A, B)**.

information for cellular and nuclear signals was co-registered and overlapping mask regions were used to extract the number of cells stained positive for PD-L1 (hematoxylin+/PD-L1+) or melanin (hematoxylin+/melanin+). In addition, the total number of cells (hematoxylin+) was determined to calculate the percentage of PD-L1+ cells relative to the total number of cells in the tumor area, with a percentage ≥5% defined as positive, similar to the physician evaluation. This method of PD-L1 quantification is referred to as "digital quantification". It should be noted here that the digital algorithm quantifies not only PD-L1 expression of tumor cells, but of all cells in the ROI, such as macrophages or lymphocytes as well.

Statistical Analysis

The survival endpoints (PFS and OS) were calculated using the Kaplan-Meier method for censored failure time data. The two-sided log-rank test was used to compare survival rates between groups. Multivariable analyses were performed using the Cox proportional hazards model. Known prognostic and predictive parameters of metastatic melanoma were included as covariates: age (≤65 *versus* >65 years), sex (male *versus* female), disease stage (III *versus* IV), location of primary (skin *versus* others), M category of metastasis (M1a/b *versus* M1c/d), LDH serum activity (elevated *versus* normal), therapy type (anti-PD-1 monotherapy *versus* anti-PD-1 plus anti-CTLA-4), BRAF mutation status (mutation *versus* wild type), and PD-L1 expression (positive *versus* negative). The correlation analysis was performed using the Pearson's correlation coefficient. Best overall response (BOR) was calculated by chi-square test. $P<0.05$ was considered statistically significant. Survival analysis was performed with SPSS (Version 25, IBM, Armonk, NY, USA) and Graphpad Prism (Version 9, GraphPad Software, CA, USA).

RESULTS

Patient Characteristics and Study Flow

Of the patients participated in/were registered in the TRIM project, 388 patients started an anti-PD-1-based ICB therapy between February 2014 and July 2019 and 156 patients met the above mentioned selection criteria for the present study; **Figure 2**. The tumor tissue specimens examined for PD-L1

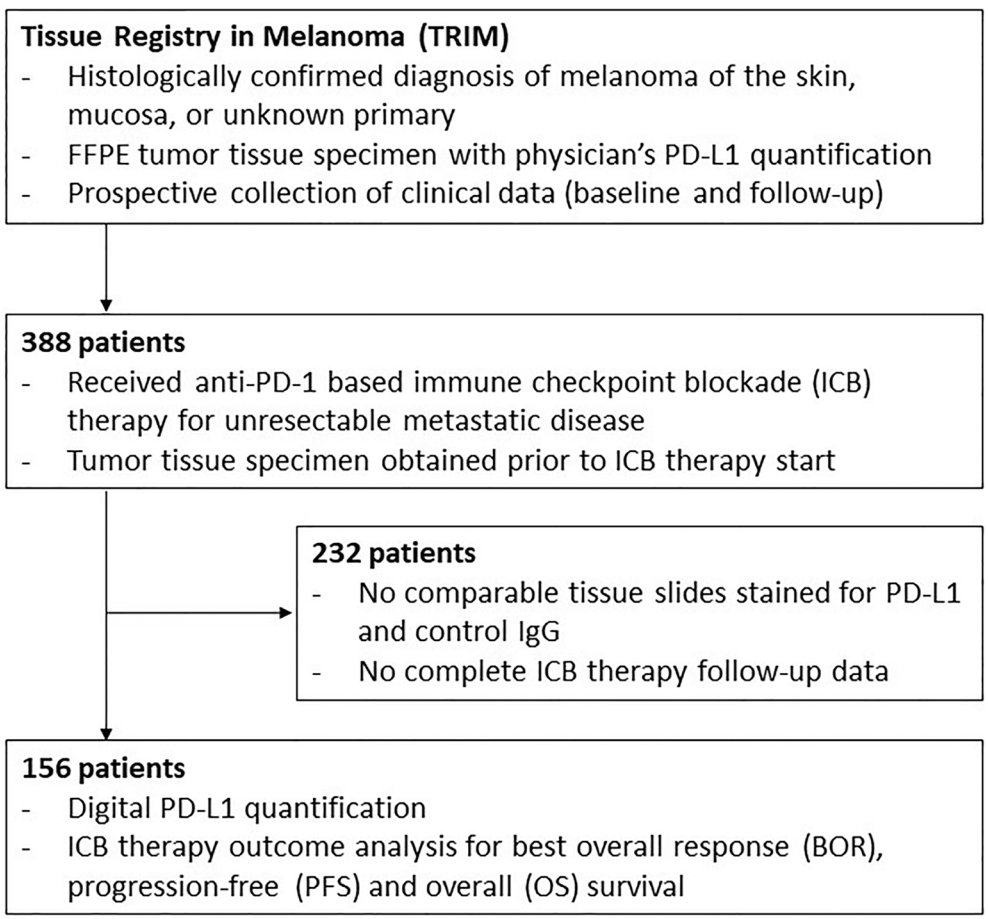


FIGURE 2 | Study flow. Schematic presentation of the study flow. P-values <0.05 are in bold.

expression were obtained from primary tumors in 32/156 (20.5%) and from metastases in 124/156 (79.5%) of cases. 41/156 patients (26.2%) subsequently received treatment with anti-CTLA-4 plus anti-PD-1 ICB, and 115/156 patients (73.8%) received treatment with anti-PD-1 alone. At data cut-off (January 15, 2020) and after a median follow-up time of 26.4 months, patients showed a best objective response rate (BOR) (complete response, CR, plus partial response, PR) of 42.3% to anti-PD-1-based ICB. 74/156 patients (48.1%) died. For detailed clinical patient characteristics see, **Table 1**.

TABLE 1 | Patient characteristics.

	N (%)
Total	156 (100%)
Mean age (range)	63 years (20 – 85 years)
Sex	
male	99 (63.5%)
female	57 (36.5%)
Localization of primary	
skin	140 (89.7%)
mucosa	2 (1.3%)
unknown primary	14 (9%)
Type of melanoma	
acral lentiginous melanoma	11 (7.1%)
lentigo malignant melanoma	2 (1.3%)
melanoma of unknown primary	14 (9.0%)
nodular malignant melanoma	57 (36.5%)
superficial spreading melanoma	26 (16.7%)
unclassifiable malignant melanoma	9 (5.8%)
unknown	37 (23.7%)
BRAF mutation (tumor)	
yes	60 (38.5%)
no	93 (59.6)
unknown	3 (1.9%
AJCC stage and M category	
III	21 (13.5%)
IV M1a	39 (25.0%)
IV M1b	28 (17.9%)
IV M1c	38 (24.4%)
IV M1d	30 (19.2%)
Number of organs involved in metastasis	
≤3	108 (69.2%)
>3	46 (29.5%)
unknown	2 (1.3%)
LDH (serum)	
normal (≤ULN)	104 (66.7%)
elevated (>ULN)	50 (32.1%)
unknown	2 (1.3%)
ECOG performance status	
0	123 (78.8%)
1	28 (17.9%)
>1	4 (2.6%)
unknown	1 (0.6%)
Systemic pre-treatment	
yes	48 (30.8%)
no	108 (69.2%)
PD-1-based ICB therapy	
PD-1 plus CTLA-4	41 (26.2%)
PD-1	115 (73.8%)

Characteristics of the investigated melanoma patient cohort at baseline of PD-1 based immune checkpoint blockade (ICB) therapy. Disease staging was performed according to AJCCv8. LDH, lactate dehydrogenase; ULN, upper limit of normal.

Comparison of PD-L1 Quantification by the Physician and the Digital Algorithm Shows a Concordant Result in Over 60% of Cases

To investigate whether there was comparability between the two methods, we first examined how many patients were scored the same by the physician and by the digital algorithm with respect to PD-L1 positivity. Physician's *versus* digital quantification was PD-L1 positive in 38.5% (n=60/156) *versus* 60.9% of cases (n=95/156), respectively. The PD-L1 quantification of the tumor specimens by the physician and the digital algorithm showed the same result in terms of positivity *versus* negativity in 99 (63.5%) of the analyzed patients, with 49 tumors (31.4%) classified as PD-L1 positive and 50 tumors (32.1%) as PD-L1 negative. 57 tumors (36.5%) were scored differently by the physician *versus* the digital algorithm, with 46 tumors (29.4%) scored as PD-L1 positive by the digital algorithm only and 11 tumors (7.1%) scored as PD-L1 positive by the physician only; **Figure 3A**. The PD-L1 quantification by the physician and the digital algorithm showed a significant correlation (Pearson's correlation; r = 0.39; p <0.001; **Figure 3B**). In summary, 60.3% of patients showed the same assessment regarding PD-L1 positivity by physician and digital algorithm. In the cases that were classified differently by both measurement methods, the digital algorithm showed PD-L1 positive findings more frequently.

Tumor PD-L1 Positivity by Physician's Quantification Predicts Favorable Outcome of Anti-PD-1-Based ICB Therapy

We next investigated the feasibility of physician PD-L1 analysis, traditionally used in the clinic, to predict patient response to therapy and survival. Melanoma patients with PD-L1 positive tumors by physician's quantification (n=60; 38.5%) showed an improved therapy response upon anti-PD-1-based ICB (BOR=54.2%) as compared to patients with PD-L1 negative tumors (n=96; BOR=36.6%; p=0.032). The median PFS after start of anti-PD-1-based ICB in patients with PD-L1 positive tumors by physician's quantification was 10.6 months (95% CI=0–32.6 months); the median OS was not reached. In patients with PD-L1 negative tumors by physician's quantification the median PFS was 5.6 months (95% CI=3.0–8.1 months), and the median OS was 15.6 months (95% CI=6.4–24.8 months). Survival differences between PD-L1 positive and negative tumors by physician's quantification showed borderline significance for PFS (P=0.051), and strong significance for OS (P=0.011); **Figures 4A, B**. A multivariable Cox regression analysis was performed to evaluate the predictive value of tumor PD-L1 expression by physician's quantification for the survival outcome of anti-PD-1-based ICB therapy in metastatic melanoma. Tumor PD-L1 expression by physician quantification was not an independent predictor of PFS (HR= 0.7; 95% CI=0.46–1.06; P=0.094), but of OS (HR=0.54; 95% CI=0.33-0.89; P=0.016); **Supplementary Table 1**. None of the other parameters tested was independently predictive for survival upon anti-PD-1-based ICB therapy. In conclusion, PD-L1

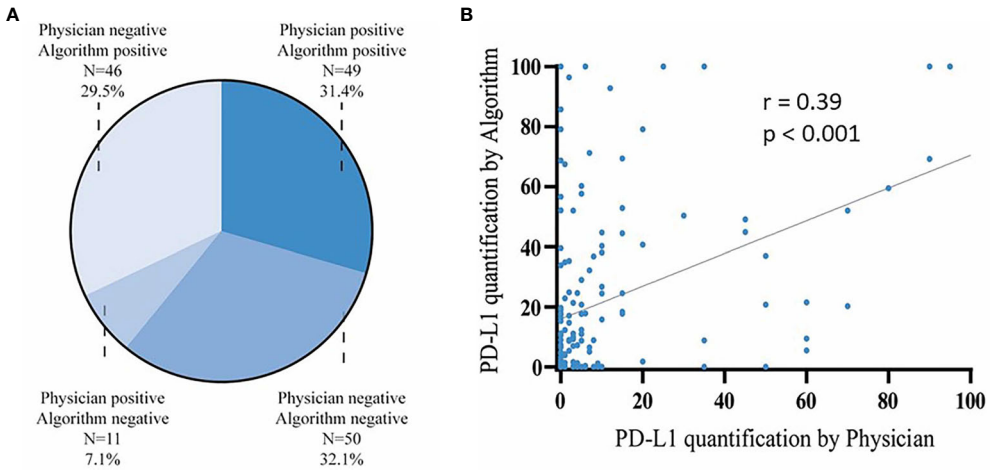


FIGURE 3 | Comparison of PD-L1 calculation by physician and digital algorithm. **(A)** Distribution of PD-L1 quantification in tumor tissue specimen of n=156 melanoma patients by the physician and the digital algorithm. **(B)** Correlation of PD-L1 quantification by the physician (x axis) *versus* the digital algorithm (y axis) in n=156 patients (Pearson's correlation; r = 0.39; p < 0.001).

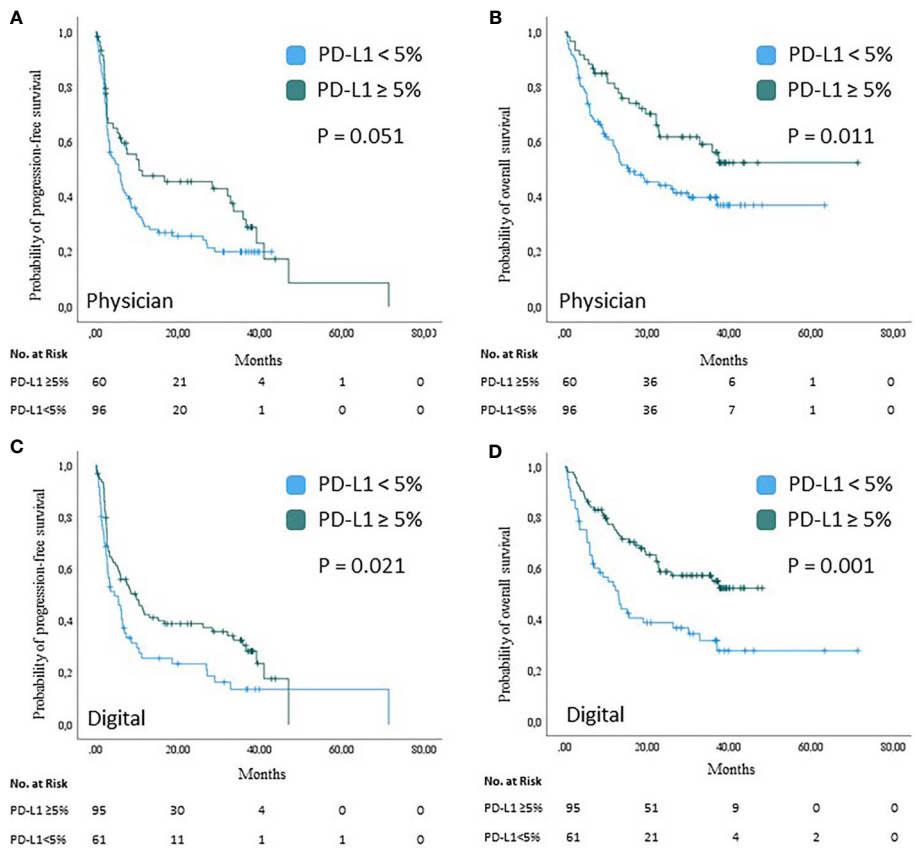


FIGURE 4 | Survival analysis based on PD-L1 expression analysis by physician or digital algorithm. Kaplan-Meier curves showing the probability of progression-free **(A, C)** and overall **(B, D)** survival of n=156 melanoma patients upon treatment with PD-1-based immune checkpoint blockade by tumor PD-L1 expression. Tumor PD-L1 expression was assessed by physician's quantification **(A, B)** and digital quantification **(C, D)**, respectively. Censored observations are indicated by vertical bars; P values were calculated using the log-rank test.

expression analysis conventionally used in the clinic can be used in melanoma by physicians to predict treatment response and patient survival under ICB.

Tumor PD-L1 Positivity by Digital Quantification Predicts Favorable Outcome of Anti-PD-1-Based ICB Therapy

The next step was to investigate whether the newly programmed digital algorithm was also suitable for PD-L1 analysis. Melanoma patients with PD-L1 positive tumors by digital quantification (n=95; 60.9%) showed an improved therapy response upon anti-PD-1 based ICB (BOR=50.5%) as compared to patients with PD-L1 negative tumors (n=61; BOR=32.2%; p=0.026). In patients with PD-L1 positive tumors by digital quantification the median PFS was 9.9 months (95% CI=5.2–14.7 months); the median OS was not reached. In patients with PD-L1 negative tumors by digital quantification the median PFS was 4.6 months (95% CI=1.4–7.8 months), and the median OS was 13.0 months (95% CI=8.6–17.6 months). Survival upon anti-PD-1-based ICB therapy was significantly longer in patients with PD-L1 positive tumors by digital quantification than in patients with PD-L1 negative tumors (PFS, P=0.021; OS, P=0.001); **Figures 4C, D**. A multivariable Cox regression analysis was performed to evaluate the predictive value of tumor PD-L1 expression by digital quantification under consideration of the same prognostic and predictive parameters as mentioned above. Among the parameters tested, the PD-L1 expression by digital quantification proved to be the only independent predictor of survival (PFS, HR=0.57, 95% CI=0.37–0.86, P=0.007; OS, HR=0.44, 95% CI=0.27–0.7, P=0.001); **Supplementary Table 2**. In conclusion, it was shown that the digital algorithm is also suitable to estimate treatment response and patient survival under ICB by PD-L1 expression analysis.

Tumors Showing PD-L1 Positivity by Both Physician's and Digital Quantification Are Associated With a Particularly Favorable Therapy Outcome

Finally, it was investigated whether the combination of both measurement methods can be used to further improve the response to therapy and patient survival. Patients with tumors classified as PD-L1-positive by both methods, physician and digital quantification, showed the highest therapy response to anti-PD1-based ICB (BOR=60.4) compared with patients with tumors assessed as PD-L1-positive by only one method (BOR=37.5%) or with patients with tumors assessed as PD-L1-negative by both methods (BOR=33.4%) (P=0.015) (**Figure 5A**), the median PFS was 11.4 months (95% CI=0-33 months) while the median OS was not reached. Patients with tumors rated PD-L1 positive only by the physician or by the digital algorithm (n=57) had a median PFS of 6.4 months (95% CI=2.5-8.7 months); the median OS was 32.9 months. Patients with tumors classified as PD-L1 negative by both quantification methods (n=50) had a median PFS of 3.6 months (95% CI=0.7-6.5 months) and a median OS of 12.4 months (95% CI=7.1-17.7 months). Thus, tumors classified as PD-L1 positive by both the physician and the digital algorithm are associated with a significant prolongation of the patient's survival upon anti-PD-1-based ICB therapy (PFS, P= 0.016; OS, P=0.001); **Figures 5B, C**. In the multivariable Cox regression analysis using the same cofactors as described above, tumor PD-L1 positivity by both quantification methods independently predicted a favorable PFS (HR=0.53, 95%-CI=0.32–0.86, p=0.011) and OS (HR=0.47, 95%-CI=0.27–0.82, p=0.008) of the respective patients; **Table 2**. Patients whose tumors were tested positive only by the physician or by the digital algorithm showed no relevant differences with regard to PFS and OS as compared to each other. The addition of PD-L1 expression analysis by the digital algorithm to conventional physician analysis has greatly improved the predictive power of PD-L1 analysis in terms of response to therapy and patient survival.

DISCUSSION

Immunohistochemical PD-L1 expression analysis has been shown to be a predictive biomarker for ICB treatment outcomes in numerous tumor entities and, in this regard, is already routinely being considered for treatment decisions in entities such as NSCLC and urogenitary cancers (12). However, in melanoma the role of PD-L1 expression as a predictive biomarker for therapy outcome is currently under debate and has still not entered the clinical routine for treatment decision making. Herein, one major reason is the high inter-observer variability of PD-L1 quantification reported for melanoma, mainly due to melanin pigmentation hampering the evaluation process. To overcome these hurdles, we here investigated the association between pre-treatment tumor PD-L1 expression and ICB therapy outcome using two independent methods of PD-L1 expression quantification, one by trained physicians and the other by a newly proposed digital algorithm. The digital quantification method harbors the advantage to be applicable regardless of the presence of melanin pigmentation. Our results showed a prolonged PFS and OS in melanoma patients whose tumors were classified as PD-L1 positive by both methods of PD-L1 quantification, with the digital quantification not being inferior to the physician quantification.

The positive correlation of pre-treatment tumor PD-L1 expression with PFS and OS observed in this study is consistent with previously published data from clinical trials in metastatic melanoma (2, 25, 26). Interestingly, the combination of PD-L1 quantification methods, the physician's and the digital algorithm method, showed the longest survival for patients with PD-L1 positive tumors with a median PFS of 11.4 months and a median OS not reached, and proved to be independently predictive by multivariable testing. In the existing literature, tumor PD-L1 expression in melanoma is considered to play the role of a prognostic marker but to have little pre-therapeutic predictive value (27). In contrast, our analysis of pre-treatment tumor tissue samples shows that melanoma patients whose tumors were evaluated as PD-L1 positive by both the physicians and the

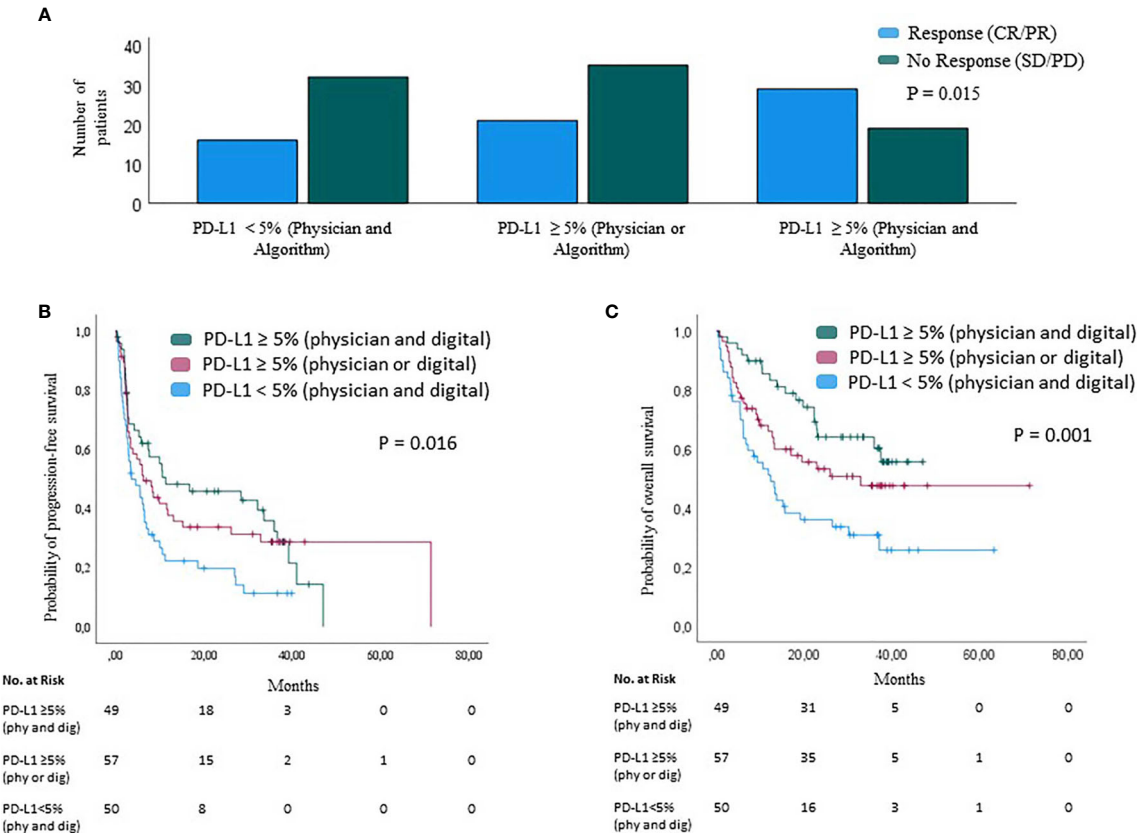


FIGURE 5 | Therapy response and survival analysis based on PD-L1 expression analysis by physician and digital algorithm. Best overall response, BOR **(A)** and survival **(B, C)** of n=156 melanoma patients upon PD-1-based immune checkpoint inhibition by tumor PD-L1 expression. Tumor PD-L1 expression is presented as a combination of physician and digital quantification. **(A)** BOR is highest in patients with tumor PD-L1 positivity by both physician and digital quantification (CR/PR=60.4%; right), compared to patients with tumor PD-L1 positivity by only one of both quantification methods (CR/PR=37.5%; center), and patients whose tumors are classified as PD-L1 negative by both physician and digital quantification (CR/PR=33.4%; left); Chi-square test P = 0.015. **(B, C)** Progression-free **(B)** and overall survival **(C)** by tumor PD-L1 expression combined of physician and digital quantification. P values were calculated using the log-rank test.

digital algorithm had a BOR on ICB of 60.4%, indicating that tissue PD-L1 expression has predictive value.

Currently, targeted therapy with BRAF/MEK inhibition is available for melanoma patients with BRAF mutation as an alternative or an addition to ICB (28–30). In these patients, whose tumors harbor a targetable BRAF mutation, there is a lack of predictive biomarkers that help to choose the optimal individualized therapy. Here, tumor PD-L1 expression quantification could be a helpful tool, assuming that patients showing PD-L1 positivity are more likely to benefit from ICB, and patients with PD-L1-negative tumors may be more likely to benefit from targeted therapy.

Obviously, the use of PD-L1 as a biomarker is difficult, as different cut-offs and a high intratumoral heterogeneity with dynamic changes exist as well as different scoring systems are available. A total of four different scoring systems are established and in clinical use for tumor PD-L1 quantification. For melanoma, the most commonly used scoring system is the Tumor Proportion Score (TPS), which restrictively quantifies only tumor cells that exhibit linear staining of the membrane. Other cancer entities for which the TPS is used include NSCLC and carcinomas of the head and neck. The combined positive score (CPS), which quantifies tumor cells and immune mononuclear cells, is used for urothelial and gastric carcinomas. In urothelial carcinoma, the immune cell score (IC), which quantifies all immune cells stained for PD-L1, is in use. In the melanoma score (MEL score), PDL-1-positive mononuclear immune cells and tumor cells are quantified, similar to the CPS (16, 31, 32). In the present study, the physicians used the restrictive TPS, whereas the digital algorithm used the CPS as classification system that includes PD-L1 expression on associated immune cells. Indeed, these scoring differences explain why the digital quantification showed higher frequencies of PD-L1 positivity compared to the physician's quantification. Interestingly, 63.5% of cases still showed the same result in terms of positivity or negativity.

Since the present algorithm is a pixel-based image analysis algorithm, its application is not limited to PD-L1 analysis and can be readily used for other immunohistochemical staining for quantification in clinical and research settings. In addition,

TABLE 2 | Multivariable cox regression analysis (combined physician's and digital PD-L1 quantification).

Parameters included	PFS		OS	
	Hazard ratio (95% CI)	*p*-value	Hazard ratio (95% CI)	*p*-value
Age (≤65 *versus* >65 years)	0.69 (0.43 – 1.09)	0.11	0.92 (0.56 – 1.51)	0.74
Disease stage (III *versus* IV)	1.58 (0.76 – 3.25)	0.22	1.34 (0.56 – 3.17)	0.50
Localization of primary (skin *versus* other)	1.49 (0.35 – 6.42)	0.59	0.56 (0.08 – 4.22)	0.58
Serum LDH (elevated *versus* normal)	0.83 (0.52 -1.32)	0.44	1.05 (0.64 - 1.71)	0.86
Therapy type (single agent anti-PD-1 *versus* anti-PD-1 plus anti-CTLA-4)	0.70 (0.41 – 1.20)	0.19	0.87 (0.49 – 1.54)	0.64
M category of metastasis (M1a or b *versus* M1c)	0.77 (0.47 – 1.27)	0.30	1.15 (0.64 - 2.05)	0.64
Gender (male versus female)	1.13 (0.73 – 1.75)	0.57	0.90 (0.54 - 1.48)	0.669
BRAF status (mutation versus wildtype)	1.06 (0.67 – 1.66)	0.82	0.92 (0.55 - 1.51)	0.73
Tumor PD-L1 expression by physician's and algorithm's quantification (positive versus negative; cut-off ≥5%)	0.53 (0.32 – 0.86)	**0.011**	0.47 (0.27 – 0.82)	**0.008**

Multivariable Cox regression of the combined PD-L1 analysis by physician and digital algorithm including clinical and molecular parameters determined at the start of anti-PD-1 therapy in n=156 patients.
P-values <0.05 are in bold.

the digital algorithm can also be used for quantification for multiplex immunofluorescence imaging in translational and basic research.

The present study and the digital PD-L1 quantification method also unraveled some limitations. The digital algorithm currently is only a semi-quantitative measuring tool, as the physician still has to select the target tumor areas to be analyzed. In contrast to physician quantification with the currently recommended method TPS, where only tumor cells with PD-L1 membrane staining are counted, the digital algorithm quantifies all cells of the tumor microenvironment and does not distinguish between cytosol staining, nuclear staining or membrane staining similar to CPS. Thus, in the present study, two different investigators (physician *vs.* digital algorithm) were compared which used different scoring systems for quantification (TPS *vs.* CPS). Further modifications, e.g. the addition of artificial intelligence technologies, are required to transform the actual digital algorithm into a measuring instrument that is completely independent from the physician. Another limitation of this study is that we did not analyze melanoma samples from patients who were treated with anti-CTLA-4 monotherapy and therefore cannot conclude to what extent PD-L1 expression plays a role in these patients. However, it must be noted that anti-CTLA-4 monotherapy alone plays almost no role in melanoma therapy any longer. Notably, a large proportion of patients were pre-treated, including BRAF-mutated patients with BRAF inhibitors, which may have influenced the results on treatment efficacy and identification and validation of PD-L1 as a predictive biomarker. In conclusion, our results demonstrate that pre-treatment tumor PD-L1 quantification by a digital algorithm is not inferior to the quantification by physicians as predictors of ICB therapy outcome. Moreover, the combination of both quantification methods significantly improved the predictive value. Accordingly, a digital quantification of tumor PD-L1 expression could facilitate diagnostic procedures, and improve the prediction of treatment outcomes at treatment decision making in patients with metastatic melanoma. Further studies are planned to investigate tumor PD-L1 expression by different methods in melanoma patients treated in the adjuvant setting.

DATA AVAILABILITY STATEMENT

The raw data supporting the conclusions of this article will be made available by the authors, without undue reservation.

ETHICS STATEMENT

The studies involving human participants were reviewed and approved by Ethics committee of the University Duisburg-Essen. The patients/participants provided their written informed consent to participate in this study.

AUTHOR CONTRIBUTIONS

J-MP, CS, DE, and SU did the study design. Digital algorithm was designed by CS and DE. J-MP, RH, PT, JeU, ClP, JoU, AK, ChP, PM, RG, FM, ED, MW, LZ, EL, JB, GL, AR, DS, and SU contributed patient data. J-MP, KG, EH, and SU performed the physician's PD-L1 quantification. All authors contributed to the article and approved the submitted version.

FUNDING

This work was in part supported by Bristol Myers Squibb for the multicenter translational study "Tissue Registry in Melanoma" (TRIM) within the framework of the skin cancer registry ADOREG of the German Dermatologic Cooperative Oncology Group (DeCOG).

ACKNOWLEDGMENTS

We thank the patients who participated in this study, their families, and the staff members at the study sites who cared for them.

SUPPLEMENTARY MATERIAL

The Supplementary Material for this article can be found online at: https://www.frontiersin.org/articles/10.3389/fonc.2021.741993/full#supplementary-material

Supplementary Table 1 | Multivariable Cox regression analysis (physician PD-L1 quantification) . Multivariable Cox regression analysis of tumor PD-L1 expression by physician quantification and covariates at baseline of anti-PD-1 ICB therapy in *n*=156 melanoma patients.

Supplementary Table 2 | Multivariable Cox regression analysis (digital PD-L1 quantification). Multivariable Cox regression analysis of tumor PD-L1 expression by digital quantification and covariates at baseline of anti-PD-1 ICB therapy in n=156 melanoma patients.

REFERENCES

1. Ribas A, Puzanov I, Dummer R, Schadendorf D, Hamid O, Robert C, et al. Pembrolizumab *Versus* Investigator-Choice Chemotherapy for Ipilimumab-Refractory Melanoma (KEYNOTE-002): A Randomised, Controlled, Phase 2 Trial. *Lancet Oncol* (2015) 16:908–18. doi: 10.1016/S1470-2045(15)00083-2
2. Robert C, Long GV, Brady B, Dutriaux C, Maio M, Mortier L, et al. Nivolumab in Previously Untreated Melanoma Without BRAF Mutation. *N Engl J Med* (2015) 372(4):320–30. doi: 10.1056/NEJMoa1412082
3. Schadendorf D, van Akkooi ACJ, Berking C, Griewank KG, Gutzmer R, Hauschild A, et al. Melanoma. *Lancet* (2018) 392(10151):971–84. doi: 10.1016/s0140-6736(18)31559-9
4. Ugurel S, Röhmel J, Ascierto PA, Becker JC, Flaherty KT, Grob JJ, et al. Survival of Patients With Advanced Metastatic Melanoma: The Impact of MAP Kinase Pathway Inhibition and Immune Checkpoint Inhibition - Update 2019. *Eur J Cancer* (2020) 130:126–38. doi: 10.1016/j.ejca.2020.02.021
5. Larkin J, Chiarion-Sileni V, Gonzalez R, Grob JJ, Rutkowski P, Lao CD, et al. Five-Year Survival With Combined Nivolumab and Ipilimumab in Advanced Melanoma. *N Engl J Med* (2019) 381(16):1535–46. doi: 10.1056/NEJMoa1910836
6. Long GV, Stroyakovskiy D, Gogas H, Levchenko E, de Braud F, Larkin J, et al. Dabrafenib and Trametinib *Versus* Dabrafenib and Placebo for Val600 BRAF-Mutant Melanoma: A Multicentre, Double-Blind, Phase 3 Randomised Controlled Trial. *Lancet* (2015) 386(9992):444–51. doi: 10.1016/S0140-6736(15)60898-4
7. Diem S, Kasenda B, Spain L, Martin-Liberal J, Marconcini R, Gore M, et al. Serum Lactate Dehydrogenase as an Early Marker for Outcome in Patients Treated With Anti-PD-1 Therapy in Metastatic Melanoma. *Br J Cancer* (2016) 114(3):256–61. doi: 10.1038/bjc.2015.467
8. Lim SY, Lee JH, Diefenbach RJ, Kefford RF, Rizos H. Liquid Biomarkers in Melanoma: Detection and Discovery. *Mol Cancer* (2018) 17(1):8. doi: 10.1186/s12943-018-0757-5
9. Ugurel S, Schadendorf D, Horny K, Sucker A, Schramm S, Utikal J, et al. Elevated Baseline Serum PD-1 or PD-L1 Predicts Poor Outcome of PD-1 Inhibition Therapy in Metastatic Melanoma. *Ann Oncol* (2020) 31(1):144–52. doi: 10.1016/j.annonc.2019.09.005
10. Weide B, Martens A, Hassel JC, Berking C, Postow MA, Bisschop K, et al. Baseline Biomarkers for Outcome of Melanoma Patients Treated With Pembrolizumab. *Clin Cancer Res an Off J Am Assoc Cancer Res* (2016) 22 (22):5487–96. doi: 10.1158/1078-0432.Ccr-16-0127
11. Tumeh PC, Harview CL, Yearley JH, Shintaku IP, Taylor EJ, Robert L, et al. PD-1 Blockade Induces Responses by Inhibiting Adaptive Immune Resistance. *Nature* (2014) 515(7528):568–71. doi: 10.1038/nature13954
12. Patel SP, Kurzrock R. PD-L1 Expression as a Predictive Biomarker in Cancer Immunotherapy. *Mol Cancer Ther* (2015) 14: (4):847–56. doi: 10.1158/1535-7163.MCT-14-0983
13. Taube JM, Anders RA, Young GD, Xu H, Sharma R, McMiller TL, et al. Colocalization of Inflammatory Response With B7-H1 Expression in Human Melanocytic Lesions Supports an Adaptive Resistance Mechanism of Immune Escape. *Sci Transl Med* (2012) 4(127):127ra37. doi: 10.1126/scitranslmed.3003689
14. Topalian SL, Hodi FS, Brahmer JR, Gettinger SN, Smith DC, McDermott DF, et al. Safety, Activity, and Immune Correlates of Anti-PD-1 Antibody in Cancer. *N Engl J Med* (2012) 366(26):2443–54. doi: 10.1056/NEJMoa1200690
15. Herbst RS, Soria JC, Kowanetz M, Fine GD, Hamid O, Gordon MS, et al. Predictive Correlates of Response to the Anti-PD-L1 Antibody MPDL3280A in Cancer Patients. *Nature* (2014) 515(7528):563–7. doi: 10.1038/nature14011
16. O'Malley DP, Yang Y, Boisot S, Sudarsanam S, Wang J-F, Chizhevsky V, et al. Immunohistochemical Detection of PD-L1 Among Diverse Human Neoplasms in a Reference Laboratory: Observations Based Upon 62,896 Cases. *Mod Pathol* (2019) 32(7):929–42. doi: 10.1038/s41379-019-0210-3
17. Kaunitz GJ, Cottrell TR, Lilo M, Muthappan V, Esandrio J, Berry S, et al. Melanoma Subtypes Demonstrate Distinct PD-L1 Expression Profiles. *Lab Invest* (2017) 97(9):1063–71. doi: 10.1038/labinvest.2017.64
18. Jakobsen MR, Teerapakpinyo C, Shuangshoti S, Keelawat S. Comparison Between Digital Image Analysis and Visual Assessment of Immunohistochemical HER2 Expression in Breast Cancer. *Pathol Res Pract* (2018) 214(12):2087–92. doi: 10.1016/j.prp.2018.10.015
19. Stalhammar G, Robertson S, Wedlund L, Lippert M, Rantalainen M, Bergh J, et al. Digital Image Analysis of Ki67 in Hot Spots is Superior to Both Manual Ki67 and Mitotic Counts in Breast Cancer. *Histopathology* (2018) 72(6):974–89. doi: 10.1111/his.13452
20. Arvaniti E, Fricker KS, Moret M, Rupp N, Hermanns T, Fankhauser C, et al. Automated Gleason Grading of Prostate Cancer Tissue Microarrays via Deep Learning. *Sci Rep* (2018) 8(1):12054. doi: 10.1038/s41598-018-30535-1
21. Koelzer VH, Gisler A, Hanhart JC, Griss J, Wagner SN, Willi N, et al. Digital Image Analysis Improves Precision of PD-L1 Scoring in Cutaneous Melanoma. *Histopathology* (2018) 73(3):397–406. doi: 10.1111/his.13528
22. Therasse P, Arbuck SG, Eisenhauer EA, Wanders J, Kaplan RS, Rubinstein L, et al. New Guidelines to Evaluate the Response to Treatment in Solid Tumors. European Organization for Research and Treatment of Cancer, National Cancer Institute of the United States, National Cancer Institute of Canada. *J Natl Cancer Inst* (2000) 92(3):205–16. doi: 10.1093/jnci/92.3.205
23. Wolchok JD, Kluger H, Callahan MK, Postow MA, Rizvi NA, Lesokhin AM, et al. Nivolumab Plus Ipilimumab in Advanced Melanoma. *N Engl J Med* (2013) 369:122–33. doi: 10.1056/NEJMoa1302369
24. Schindelin J, Arganda-Carreras I, Frise E, Kaynig V, Longair M, Pietzsch T, et al. Fiji: An Open-Source Platform for Biological-Image Analysis. *Nat Methods* (2012) 9(7):676–82. doi: 10.1038/nmeth.2019
25. Larkin J, Chiarion-Sileni V, Gonzalez R, Grob JJ, Cowey CL, Lao CD, et al. Combined Nivolumab and Ipilimumab or Monotherapy in Untreated Melanoma. *N Engl J Med* (2015) 373:23–34. doi: 10.1056/NEJMoa1504030
26. Long GV, Larkin J, Ascierto PA, Hodi FS, Rutkowski P, Sileni V, et al. PD-L1 Expression as a Biomarker for Nivolumab (NIVO) Plus Ipilimumab (IPI) and NIVO Alone in Advanced Melanoma (MEL): A Pooled Analysis. *Ann Oncol* (2016) 27:vi381. doi: 10.1093/annonc/mdw379.07
27. Buder-Bakhaya K, Hassel JC. Biomarkers for Clinical Benefit of Immune Checkpoint Inhibitor Treatment-A Review From the Melanoma Perspective and Beyond. *Front Immunol* (2018) 9:1474. doi: 10.3389/fimmu.2018.01474

28. Eggermont AMM, Blank CU, Mandala M, Long GV, Atkinson V, Dalle S, et al. Adjuvant Pembrolizumab *Versus* Placebo in Resected Stage III Melanoma. *New Engl J Med* (2018) 378(19):1789–801. doi: 10.1056/NEJMoa1802357
29. Long GV, Hauschild A, Santinami M, Atkinson V, Mandalà M, Chiarion-Sileni V, et al. Adjuvant Dabrafenib Plus Trametinib in Stage III BRAF-Mutated Melanoma. *New Engl J Med* (2017) 377(19):1813–23. doi: 10.1056/NEJMoa1708539
30. Weber J, Mandala M, Del Vecchio M, Gogas HJ, Arance AM, Cowey CL, et al. Adjuvant Nivolumab *Versus* Ipilimumab in Resected Stage III or IV Melanoma. *New Engl J Med* (2017) 377(19):1824–35. doi: 10.1056/NEJMoa1709030
31. Daud AI, Wolchok JD, Robert C, Hwu WJ, Weber JS, Ribas A, et al. Programmed Death-Ligand 1 Expression and Response to the Anti-Programmed Death 1 Antibody Pembrolizumab in Melanoma. *J Clin Oncol* (2016) 34(34):4102–9. doi: 10.1200/jco.2016.67.2477
32. Eckstein M, Cimadamore A, Hartmann A, Lopez-Beltran A, Cheng L, Scarpelli M, et al. PD-L1 Assessment in Urothelial Carcinoma: A Practical Approach. *Ann Transl Med* (2019) 7(22):690–. doi: 10.21037/atm.2019.10.24

Conflict of Interest: J-MP served as consultant and/or has received honoraria from Bristol-Myers Squibb, Novartis and received travel support from Bristol-Myers Squibb, Novartis and Therakos. PT declares Invited Speaker´s honoraria from Bristol-Myers Squibb, Novartis, MSD, Pierre-Fabre, CureVac, Roche, Kyowa Kirin, Biofrontera, Advisory Board honoraria from Bristol-Myers Squibb, Novartis, Pierre-Fabre, Merck Serono, Sanofi, Roche, Kyowa Kirin, and Travel support from Bristol-Myers Squibb, and Pierre-Fabre. JoU is on the advisory board or has received honoraria and travel support from Amgen, Bristol Myers Squibb, GSK, LeoPharma, Merck Sharp and Dohme, Novartis, Pierre Fabre, Roche, Sanofi outside the submitted work. ClP received honoraria (speaker honoraria or honoraria as a consultant) and travel support from: Novartis, BMS, Roche, Merck Serono, MSD, Celgene, AbbVie, AMGEN, SUNPHARMA, Allergy Therapeutics and LEO. LZ served as consultant and/or has received honoraria from Roche, Bristol-Myers Squibb, Merck Sharp & Dohme, Novartis, Pierre-Fabre, and Sanofi; Research funding to institution: Novartis; travel support from Merck Sharp & Dohme, Bristol-Myers Squibb, Amgen, Pierre-Fabre, and Novartis, outside the submitted work. EL served as consultant and/or has received honoraria from Amgen, Actelion, Roche, Bris-tol-Myers Squibb, Merck Sharp & Dohme, Novartis, Janssen, Medac, Sanofi, Sunpharma and travel support from Amgen, Merck Sharp & Dohme, Bristol-Myers Squibb, Amgen, Pierre Fabre, Sunpharma and Novartis, outside the submitted work. JB is receiving speaker's bureau honoraria from Amgen, Pfizer, MerckSerono, Recordati and Sanofi, is a paid consultant/advisory board member/DSMB member for 4SC, Almirall, Boehringer Ingelheim, ICON, InProTher, MerckSerono, Pfizer, and Sanofi/Regeneron. His group receives research grants from Merck Serono, HTG, IQVIA, and Alcedis. GL has received travel support from Sun Pharma. AR reported grants from Novartis, Bristol Myers Squibb, and Adtec; personal fees from Merck Sharp & Dohme; and nonfinancial support from Amgen, Roche, Merck Sharp & Dohme, Novartis, Bristol Myers Squibb, and Teva. DS received grants and other support from Bristol-Myers Squibb, personal fees from Bristol-Myers Squibb during the conduct of the study; personal fees from Amgen; personal fees from Boehringer Ingelheim; personal fees from InFlarX; personal fees and other support from Roche; grants, personal fees and other support from Novartis; personal fees from Incyte; personal fees and other support from Regeneron; personal fees from 4SC; personal fees from Sanofi; personal fees from Neracare; personal fees from Pierre-Fabre; personal fees and other support from Merck-EMD; personal fees from Pfizer; personal fees and other support from Philiogen; personal fees from Array, personal fees and other support from MSD Sharp & Dohme, outside the submitted work. SU declares research support from Bristol Myers Squibb and Merck Serono; speakers and advisory board honoraria from Bristol Myers Squibb, Merck Sharp & Dohme, Merck Serono, Novartis and Roche, and travel support from Bristol Myers Squibb, and Merck Sharp & Dohme.

The remaining authors declare that the research was conducted in the absence of any commercial or financial relationships that could be construed as a potential conflict of interest.

The authors declare that this study received funding from Bristol Myers Squibb. The funder had the following involvement with the study: Financing of test material.

Publisher's Note: All claims expressed in this article are solely those of the authors and do not necessarily represent those of their affiliated organizations, or those of the publisher, the editors and the reviewers. Any product that may be evaluated in this article, or claim that may be made by its manufacturer, is not guaranteed or endorsed by the publisher.

Copyright © 2021 Placke, Soun, Bottek, Herbst, Terheyden, Utikal, Pföhler, Ulrich, Kreuter, Pfeiffer, Mohr, Gutzmer, Meier, Dippel, Weichenthal, Zimmer, Livingstone, Becker, Lodde, Sucker, Griewank, Horn, Hadaschik, Roesch, Schadendorf, Engel and Ugurel. This is an open-access article distributed under the terms of the Creative Commons Attribution License (CC BY). The use, distribution or reproduction in other forums is permitted, provided the original author(s) and the copyright owner(s) are credited and that the original publication in this journal is cited, in accordance with accepted academic practice. No use, distribution or reproduction is permitted which does not comply with these terms.

frontiers in Oncology

ORIGINAL RESEARCH
published: 21 October 2021
doi: 10.3389/fonc.2021.765608

Grade 4 Neutropenia Secondary to Immune Checkpoint Inhibition — A Descriptive Observational Retrospective Multicenter Analysis

Anne Zaremba[1], Rafaela Kramer[2,3,4], Viola De Temple[1,5], Stefanie Bertram[6], Martin Salzmann[7], Anja Gesierich[8], Lydia Reinhardt[9,10], Barouyr Baroudjian[11], Michael M. Sachse[12], Gunhild Mechtersheimer[13], Douglas B. Johnson[14], Alison M. Weppler[15], Lavinia Spain[15], Carmen Loquai[16], Milena Dudda[16], Claudia Pföhler[17], Adriana Hepner[18,19], Georgina V. Long[20,21,22], Alexander M. Menzies[20,21,22], Matteo S. Carlino[20,23], Céleste Lebbé[11], Tomohiro Enokida[24], Makoto Tahara[24], Paul J. Bröckelmann[25], Thomas Eigentler[26,27], Katharina C. Kähler[28], Ralf Gutzmer[5], Carola Berking[2,3,4], Selma Ugurel[1], Nadine Stadtler[1], Antje Sucker[1], Jürgen C. Becker[1,27], Elisabeth Livingstone[1], Friedegund Meier[9,10,27], Jessica C. Hassel[7], Dirk Schadendorf[1,27], Maher Hanoun[29], Lucie Heinzerling[2,3,4,30] and Lisa Zimmer[1]*

[1] Department of Dermatology, Venerology and Allergology, University Hospital Essen, Essen, Germany, [2] Department of Dermatology, Universitätsklinikum Erlangen, Friedrich-Alexander-Universität Erlangen-Nürnberg (FAU), Erlangen, Germany, [3] Deutsches Zentrum Immuntherapie (DZI) , Erlangen, Germany, [4] Comprehensive Cancer Center Erlangen-European Metropolitan Area of Nürnberg (CCC ER-EMN), Erlangen, Germany, [5] Department of Dermatology, Mühlenkreiskliniken AöR, Ruhr University Bochum, Minden, Germany, [6] Institute of Pathology, University Hospital Essen, Essen, Germany, [7] Skin Cancer Center, Department of Dermatology and National Center for Tumor Diseases (NCT), University Hospital, Heidelberg, Germany, [8] Department of Dermatology, Venereology and Allergology, University Hospital Würzburg, Würzburg, Germany, [9] Skin Cancer Center at the University Cancer Centre Dresden and National Center for Tumor Diseases, Dresden, Germany, [10] Department of Dermatology, University Hospital Carl Gustav Carus, Technische Universität (TU) Dresden, Dresden, Germany, [11] Université de Paris, Department of Dermatology, AP-HP Hôpital Saint Louis, INSERM U976, Paris, France, [12] Department of Dermatology, Allergology and Phlebology, Bremerhaven Reinkenheide Hospital, Bremerhaven, Germany, [13] Institute of Pathology, University Hospital Heidelberg, Heidelberg, Germany, [14] Vanderbilt University Medical Center, Department of Medicine, Division of Hematology and Oncology, Nashville, TN, United States, [15] Medical Oncology Department, Peter MacCallum Cancer Centre, Melbourne, VIC, Australia, [16] Department of Dermatology, University Medical Center, Mainz, Germany, [17] Department of Dermatology, Saarland University Medical Center, Homburg, Germany, [18] Department of Medical Oncology, Melanoma Institute Australia, Sydney, NSW, Australia, [19] Medical Oncology Service, Instituto do Cancer do Estado de Sao Paulo, Sao Paulo, Brazil, [20] Melanoma Institute Australia, The University of Sydney, Sydney, NSW, Australia, [21] Faculty of Medicine and Health, The University of Sydney, Sydney, NSW, Australia, [22] Royal North Shore and Mater Hospitals, Sydney, NSW, Australia, [23] Westmead and Blacktown Hospitals, Sydney, NSW, Australia, [24] Department of Head and Neck Medical Oncology, National Cancer Center Hospital East, Chiba, Japan, [25] Department I of Internal Medicine, Centre of Integrated Oncology Aachen Bonn Cologne Duesseldorf (CIO ABCD), Faculty of Medicine and University Hospital of Cologne, University of Cologne, Cologne, Germany, [26] Department of Dermatology, University Hospital Tübingen, Germany and Charité – Universitätsmedizin Berlin, Corporate Member of Freie Universität Berlin and Humboldt Universität zu Berlin, Department of Dermatology, Venerology and Allergology, Berlin, Germany, [27] German Cancer Consortium (DKTK), Deutsches Krebsforschungszentrum (DKFZ), Heidelberg, Germany, [28] Department of Dermatology, University Hospital Schleswig Holstein, Kiel, Germany, [29] Department for Hematology and Stem Cell Transplantation, University Hospital Essen, Essen, Germany, [30] Department of Dermatology and Allergy, Ludwig-Maximilians-Universität (LMU), University Hospital, Munich, Germany*

OPEN ACCESS

Edited by:
Gil Bar-Sela, Ha'Emek Medical Center, Israel

Reviewed by:
Tapas Ranjan Behera, Cleveland Clinic, United States
Ilit Turgeman, Rambam Health Care Campus, Israel

***Correspondence:**
Anne Zaremba
anne.zaremba@uk-essen.de

Specialty section:
This article was submitted to Skin Cancer, a section of the journal Frontiers in Oncology

Received: *27 August 2021*
Accepted: *01 October 2021*
Published: *21 October 2021*

Citation:
Zaremba A, Kramer R, De Temple V, Bertram S, Salzmann M, Gesierich A, Reinhardt L, Baroudjian B, Sachse MM, Mechtersheimer G, Johnson DB, Weppler AM, Spain L, Loquai C, Dudda M, Pföhler C, Hepner A, Long GV, Menzies AM, Carlino MS, Lebbé C, Enokida T, Tahara M, Bröckelmann PJ, Eigentler T, Kähler KC, Gutzmer R, Berking C, Ugurel S, Stadtler N, Sucker A, Becker JC, Livingstone E, Meier F, Hassel JC, Schadendorf D, Hanoun M, Heinzerling L and Zimmer L (2021) Grade 4 Neutropenia Secondary to Immune Checkpoint Inhibition — A Descriptive Observational Retrospective Multicenter Analysis. Front. Oncol. 11:765608. doi: 10.3389/fonc.2021.765608

Introduction: Immune checkpoint inhibitors (ICI) are increasingly being used to treat numerous cancer types. Together with improved recognition of toxicities, this has led to more frequent identification of rare immune-related adverse events (irAE), for which specific treatment strategies are needed. Neutropenia is a rare hematological irAE that

has a potential for a high mortality rate because of its associated risk of sepsis. Prompt recognition and timely treatment of this life-threatening irAE are therefore critical to the outcome of patients with immune-related neutropenia.

Methods: This multicenter international retrospective study was conducted at 17 melanoma centers to evaluate the clinical characteristics, diagnostics, treatment, and outcomes of melanoma patients with grade 4 neutropenia (<500 neutrophils/µl blood) treated with ICI between 2014 and 2020. Some of these patients received metamizole in addition to ICI (ICI+/met+). Bone marrow biopsies (BMB) of these patients were compared to BMB from non-ICI treated patients with metamizole-induced grade 4 neutropenia (ICI-/met+).

Results: In total, 10 patients (median age at neutropenia onset: 66 years; seven men) with neutropenia were identified, equating to an incidence of 0.14%. Median onset of neutropenia was 6.4 weeks after starting ICI (range 1.4–49.1 weeks). Six patients showed inflammatory symptoms, including fever (n=3), erysipelas (n=1), pharyngeal abscess (n=1), and mucositis (n=1). Neutropenia was diagnosed in all patients by a differential blood count and additionally performed procedures including BMB (n=5). Nine of 10 patients received granulocyte colony-stimulating factors (G-CSF) to treat their grade 4 neutropenia. Four patients received systemic steroids (including two in combination with G-CSF, and one in combination with G-CSF and additional ciclosporin A). Four patients were treated with one or more antibiotic treatment lines, two with antimycotic treatment, and one with additional antiviral therapy. Five patients received metamizole concomitantly with ICI. One fatal outcome was reported. BMB indicated a numerically lower CD4+ to CD8+ T cells ratio in patients with irNeutropenia than in those with metamizole-induced neutropenia.

Conclusion: Grade 4 neutropenia is a rare but potentially life-threatening side effect of ICI treatment. Most cases were sufficiently managed using G-CSF; however, adequate empiric antibiotic, antiviral, and antimycotic treatments should be administered if neutropenic infections are suspected. Immunosuppression using corticosteroids may be considered after other causes of neutropenia have been excluded.

Keywords: malignant melanoma, immune checkpoint inhibition, adverse events, hematotoxicity, neutropenia

INTRODUCTION

Therapy with immune checkpoint inhibitors (ICI) that target the cytotoxic T-lymphocyte-associated protein-4 (CTLA-4; targeted by ipilimumab) and programmed cell death protein-1 (PD-1; targeted by pembrolizumab and nivolumab), either alone or in combination, achieves durable response rates in a variety of cancer types (1–3). Melanoma, a rare but aggressive skin cancer, is the lead indication for which ICI are approved (4–6). ICI have revolutionized the treatment of melanoma in metastatic settings and more recently in adjuvant and neoadjuvant settings (2, 7–9). As the indications for ICI have expanded, the number of patients treated in this way has risen. This trend is set to continue, because T-cell-targeted immunomodulators are currently used in combination with chemotherapies or as single agents in first- and second-line treatment of around 50 cancer types (10).

Because the use of ICI treatment is increasing, the diagnosis and management of not only common, but also rare, ICI-induced adverse events (AEs) is becoming more important. Adverse events affect 86–96% of patients and result from the loss of self-tolerance, leading to autoimmune-like events that can involve any organ (11). Hematological immune-related adverse events (irAEs) are estimated to affect less than 0.6-1% of ICI-treated patients (12, 13), but they are associated with a relatively high mortality rate of 2-14% (12–15). ICI-induced hematological side effects can affect all blood cell lineages. The most common hematological irAEs comprise anemia, thrombocytopenia, and neutropenia (12–14). In a recent publication, thrombocytopenia and leukopenia were the most common hematological irAEs, each affecting 34% of 50 patients who developed hematological irAEs induced by ICI, followed by neutropenia, which affected 28% of such patients (13).

Neutropenia describes a reduction of neutrophils to fewer than 1500 neutrophils per 1 µl of blood. Common Terminology Criteria for Adverse Events (CTCAE) grade 4 neutropenia, also termed agranulocytosis, involves a further, drug-related reduction of peripheral neutrophils and is defined by a reduction in the total number of neutrophils <500 per 1 µl of blood (16, 17). Sporadic acute grade 4 neutropenia is a very rare condition with an estimated incidence of 2–9 cases per million individuals per year (17). Previous studies have found that between 0% and 23% of cases of drug-induced grade 4 neutropenia are fatal (16). Patients may be completely asymptomatic; however, the classic clinical symptom triad associated with severe neutropenia consists of (i) angina tonsillitis, (ii) fever, and (iii) aphthous stomatitis (16). While neutropenia is a known and well-studied side-effect of intensive chemotherapy, the pathogenesis of conventional drug-induced neutropenia is not completely understood, although involvement of toxic or immunoallergic mechanisms is suspected (17). Apart from chemotherapy, the drugs most commonly associated with neutropenia are thiamazole, clozapine, sulfasalazine, and metamizole (17). Metamizole is a nonsteroidal anti-inflammatory drug (NSAID) with analgesic and antipyretic activity and belongs to the non-opioid analgesics (world health organization [WHO] stage 1). Although routinely used across Europe and Latin America, it has been identified as a disproportionately frequent trigger of grade 4 neutropenia (18). For this reason, it is effectively banned in the United States, Australia and several European countries (e.g. France, the United Kingdom) for pain management (18). Neutropenia has also been described as a fatal side effect of ICI (19). Because ICI-induced grade 4 neutropenia is so rare, only limited evidence exists regarding the incidence, diagnostics, and management of patients with this type of neutropenia. So far, one case series and one meta-analysis (n=34 patients) have studied immune-related neutropenia (irNeutropenia) (19, 20).

In this multicenter retrospective study, we sought to characterize ICI-induced grade 4 neutropenia in patients with advanced melanoma. Our evaluation included clinical signs and symptoms, diagnostic work up, hematopoietic development, treatments, and outcome. In addition, immunohistochemistry (IHC) was performed on bone marrow biopsies (BMB) from patients with ICI-induced grade 4 neutropenia and compared with IHC of BMB from patients with metamizole-induced grade 4 neutropenia, with particular focus on lymphocyte count.

PATIENTS AND METHODS

Patients

We performed a descriptive observational multicenter retrospective study of melanoma patients who developed grade 4 neutropenia after exposure to ICI, which was recorded in a collected query of hematological side effects (13). Patients were screened between January 2014 and July 2020 at 17 tertiary referral centers in Europe, the United States, and Australia. To be included in the study, patients had to meet both of the following eligibility criteria: (1) diagnosis of grade 4 neutropenia according to the CTCAE (version 5.0) and (2) categorized as certainly or probably related to ICI therapy. Recovery was defined as restitution of neutrophil count. Patients were identified from the electronic medical records of the participating centers. To enable calculation of the incidence of grade 4 neutropenia, centers were asked to provide the total number of patients treated with ICI. Centers that could not state the total number of such patients were excluded from the incidence calculation. The following clinicopathological characteristics were collected for all patients: age, sex, melanoma mutational genotype, melanoma stage, systemic treatment, and specific data for neutropenia, i.e., differential blood count, neutrophil count, and BMB results and further diagnostics related to neutropenia. IHC was performed on BMB from patients with grade 4 ICI–metamizole (met)-induced neutropenia (ICI+/met+) and compared with IHC of BMB from non-ICI-treated patients with met-induced grade 4 neutropenia (ICI-/met+). Five non-ICI-treated patients with hematologically diagnosed met-induced grade 4 neutropenia (ICI-/met+) were identified from the electronic medical records of the Department of Hematology and Stem Cell Transplantation of the University Hospital Essen. Because the overall incidence of grade 4 neutropenia is low and prior ICI treatment had to be excluded, non-melanoma patients were selected as the comparison group for grade 4 met-induced neutropenia. Histological evaluation was performed by a local-board certified pathologist. The study was approved by the Ethics Committee of Duisburg-Essen University (19-9075-BO).

Immunohistochemistry

IHC was performed by using the following antibodies:

Antibody	Company	Purchase number	Host	Clonality	Clone	Secondary antibody	Dilution
CD3	CDS	CI597C01	Rabbit	Monoclonal	SP7	OptiView DAB IHC Detection Kit (Roche Diagnostics; IN, USA)	1:200
CD8	Dako	M7103	Mouse	Monoclonal	C8/144B	OptiView DAB IHC Detection Kit	1:150
CD4	Zytomed	503-3352	Rabbit	Monoclonal	SP35	OptiView DAB IHC Detection Kit	1:50
CD20	Roche	5267099001	Mouse	Monoclonal	L26	OptiView DAB IHC Detection Kit	Ready to use

Clusters of differentiation (CD) 20, CD3, CD4, and CD8 were stained using the Ventana Benchmark Ultra platform (Roche Diagnostics). Hematoxylin and eosin staining, Giemsa staining, and naphthol AS-D chloroacetate esterase (ASDCL) were used in accordance with institutional standards. For each sample, the number of positive cells in an area measuring 6.25 mm^2 (10 high-power fields, defined by a field of view of 400× magnification) was counted manually by two blinded independent physicians of the Institute of Dermatology and Dermatohistopathology, University Hospital Essen. The total number of cells in the ICI–met-induced (ICI+/met+) and non-ICI met-induced (ICI-/met+) grade 4 neutropenia BMB samples were compared using the Mann–Whitney U test. One patient

treated with ICI and metamizole (ICI+/met+) and concomitant B-cell chronic lymphocyte leukemia was excluded from CD20+ cell calculation.

RESULTS

Clinical Characteristics of Patients With irNeutropenia (ICI+/met+ and ICI+/met-)

Over a period of 6.5 years between 2014 and 2020, more than 6961 melanoma patients were treated with ICI in 17 cancer centers. Two of these 17 centers were unable to specify the total number of ICI-treated patients. Ten patients (seven men, three women) experienced grade 4 neutropenia (**Table 1**). The incidence was 0.14%, with two centers excluded from the calculation of incidence. Median age at onset of grade 4 irNeutropenia was 66 years (range 28–80). Eight melanoma patients received neutropenia-triggering ICI for advanced disease (ipilimumab plus nivolumab n=7; pembrolizumab n=1), and two patients as adjuvant treatment (pembrolizumab n=1; nivolumab n=1). Five patients had received prior systemic therapy (adjuvant interferon α n=1; PD-1 monotherapy followed by chemotherapy n=1 [stopped 4 months before irNeutropenia]; PD-1 monotherapy within a clinical trial n=1; BRAF and MEK inhibition n=2, **Table 1**). Four patients had hematological comorbidities at the start of ICI therapy, comprising one patient each with the following: B-cell chronic lymphocytic leukemia (B-CLL), monoclonal gammopathy of unknown significance (MGUS), systemic mantle cell lymphoma, and pre-existing non-ir thrombocytopenia and lymphopenia. None of these patients received therapy for the respective hematological comorbidities when starting ICI nor suffered from neutropenia.

Characteristics of Patients With Met-Induced Neutropenia (ICI-/met+)

The ICI-/met+ patients in the comparator cohort were all female (n=5) with a median age of 64 years (range 22–89) at diagnosis of grade 4 neutropenia (**Supplemental Tables 1**, **2**). All patients had BMB for diagnostic purposes.

Clinical Course and Diagnostics of Grade 4 irNeutropenia

The median time from starting ICI to onset of grade 4 neutropenia was 6.4 weeks (range 1.4–49.1). Two patients showed a decrease in cell number in more than one hematological lineage (Pat 3, Pat 6). Six patients received comedication at the time of grade 4 neutropenia, of whom five received metamizole. Additional medications started within 6 weeks before neutropenia onset are shown in **Table 2**. Six of the 10 patients showed inflammatory symptoms including fever (n=3), erysipelas (n=1), pharyngeal abscess formation (n=1), and mucositis (n=1). Two patients presented with unspecific symptoms (loss of appetite n=1; weakness and abdominal pain n=1). Eight patients had additional irAEs. These included colitis/diarrhea (n=2), endocrine AEs (n=2), exanthema (n=2), and hepatitis (n=1). Concurrent AEs occurred before (median 3.9 weeks before irNeutropenia onset n=7, [range 0.4–11.1]) and after (median 2.3 weeks, n=1) irNeutropenia first occurred. All patients developed grade 4 neutropenia with <500 neutrophils per µl of blood. Neutropenia was diagnosed in all patients by a differential blood count (**Table 3**). In individual cases a myelogram (n=1) or autoantibody test and cytogenetic analysis (n=1) was also performed. A BMB was performed in five patients, of whom three (Patients 1, 4, 9) were treated with concomitant metamizole (ICI+/met+; **Table 2** and **Figure 1**). All BMB showed abnormalities in neutrophilic granulopoiesis. No patient showed melanoma infiltration of the bone marrow. Immunohistochemistry of BMB from patients with ICI–met-induced grade 4 neutropenia (ICI+/met+) showed a range of immunohistochemical features (**Figure 1**), including impaired maturation of neutrophilic granulopoiesis (Pat 9) and depletion of granulocytes (Pat 4). The ratio of CD20+ to CD3+ T cells was similar between the ICI+/met+ and ICI-/met+ patients (0.24 vs. 0.23 CD20+ T cells per CD3+ T cell), while the ratio of CD4+ to CD8+ T cells was numerically lower in patients with ICI–met-induced neutropenia (ICI+/met+) than in patients with non-ICI met-induced neutropenia (ICI-/met+) (median 0.68 *vs*. 0.8 CD4+ T cells per CD8+ T cell, **Supplemental Figure 1**).

Management and Outcome of Grade 4 ICI-Induced Neutropenia

The median duration of grade 4 neutropenia among the 10 ICI-treated patients was 9.5 days (range 3–32; **Supplemental Table 1**) and seven patients were hospitalized for treatment. In four patients, neutropenia was complicated by infection. Nine patients showed a maximum neutrophil reduction of >90% from baseline (**Table 3** and **Figure 2**). One patient (Pat 6) had simultaneous thrombocytopenia and worsening of pre-existing anemia, one patient showed a pancytopenia (Pat 3) (**Table 3**). Nine patients received granulocyte (macrophage) colony-stimulating factors (G-CSF) subcutaneously to treat their grade 4 neutropenia. Four patients received systemic steroids (three of whom received concomitant G-CSF). The dosage of systemic steroids varied: One patient received 50 mg prednisolone equivalent three times daily, one patient 20 mg prednisolone once daily, and two patients received bodyweight-adapted 2.5 mg prednisolone per kilogram once daily as initial dose. One patient (Pat 1) received ciclosporin A in addition to systemic steroids. Four patients received one or more antibiotic treatment lines; of these patients, three showed signs of infection including erysipelas, fever, and a pharyngeal abscess (**Table 2**). Two patients received antimycotic treatment, and one an additional antiviral therapy. The duration of neutropenia was longer in all four patients who received corticosteroids (median 11 days) than in the six patients who did not receive corticosteroids (median 8 days). Because of neutropenia, ICI therapy was interrupted in four patients and permanently discontinued in three patients. Most patients (eight of 10) displayed a normalization of the neutrophil count (**Figure 3**). One patient died due to neutropenia (**Figure 3**, Pat 3). Four patients were re-exposed to ICI after resolution of neutropenia. Two continued with the same PD-1 inhibitor, one patient who had initially received

TABLE 1 | Clinical characteristics of patients with irNeutropenia.

	Patient 1	Patient 2	Patient 3	Patient 4	Patient 5	Patient 6	Patient 7	Patient 8	Patient 9	Patient 10
Age at neutropenia onset, years/sex	28.4/F	53.4/M	60.2/M	69.9/M	71.7/M	79.8/M	70.7/F	62.2/M	74.1/M	38.7/F
Checkpoint inhibitor(s) inducing neutropenia and dosage(s)	Ipi (3 mg/kg) + nivo (1 mg/kg)	Pembro (2 mg/kg BW)	Ipi (3 mg/kg) + nivo (1 mg/kg)	Ipi (3 mg/kg) + nivo (1 mg/kg)	Ipi (3 mg/kg) + nivo (1 mg/kg)	Ipi (3 mg/kg) + nivo (1 mg/kg)	Ipi (3 mg/kg) + nivo (1 mg/kg)	Nivo (3 mg/kg BW)	Ipi (3 mg/kg) + nivo (1 mg/kg)	Pembro (200 mg/kg)
Best response to therapy	PD	PR	PD	CR	PD	PR	PD	PD (DD lymphoma)	PD	No PD
Hematological comorbidities	–	–	–	B-CLL	Thrombocytopenia (not immune-related); lymphopenia	MGUS	–	Systemic mantle cell lymphoma	–	–
Melanoma type	Skin	Skin	Mucosal	Skin	Skin	Skin	Mucosal	Skin	Skin	Skin
Mutation status	*BRAF* wt	*NRAS* mut	*BRAF* wt	*BRAF* wt	*BRAF* V600R	*NRAS* mut	*BRAF* wt	*BRAF* K601N	*BRAF* V600E	*BRAF* wt
Adjuvant therapy	Yes (IFN)	–	–	–	–	–	–	Yes (Nivo monotherapy)[#]	–	–
Systemic therapies prior to ICI inducing neutropenia	–	–	PD-1 monotherapy chemotherapy	–	BRAF+MEK inhibitor	–	Nivolumab monotherapy*	–	–	BRAF+MEK inhibitor**
Melanoma stage at start of ICI inducing neutropenia	IV	IV	IV	IV	IV	IV	IV	IIIC	IV	IIIB
LDH elevated at ICI start	Yes	No	No	No	Yes	No	No	No	No	No
Other irAEs	Thyroiditis Hepatitis	Vitiligo Arthritis Nephritis	Pancytopenia	Exanthema Diarrhea	Fatigue Fever	DM type III Hypophysitis Endogenous endophthalmitis Thrombocytopenia Neutropenia	None	Exanthema	Colitis	None
Survival status	Unknown[##]	Dead	Dead***	Alive	Dead	Dead	Alive	Alive	Dead	Alive

BW, bodyweight; CLL, chronic lymphocytic leukemia; CR, complete response; DD, differential diagnosis; DM, diabetes mellitus; F, female; ICI, immune checkpoint inhibitors; IFN, interferon α; ipi, ipilimumab; ir-, immune-related; irAE, immune-related adverse event; LDH, lactate dehydrogenase; M, male; MGUS, monoclonal gammopathy of unknown significance; mut, mutation; nivo, nivolumab; pembro; pembrolizumab; PD, progressive disease; PD-1, programmed death ligand 1; PR, partial response; wt, wildtype.

**within a clinical trial.*

*** not for melanoma, for ganglioglioma.*

****due to neutropenia.*

[#]inducing neutropenia.

[##]alive at last contact, lost to follow-up (returned to home country).

TABLE 2 | Diagnostic methods and treatment of patients with irNeutropenia.

	Patient 1	Patient 2	Patient 3	Patient 4	Patient 5	Patient 6	Patient 7	Patient 8	Patient 9	Patient 10
Time to neutropenia onset after ICI start, weeks	7.3	49.1	6.6	4.6	6.9	18.6	6.1	1.6	2.9	1.4
Additional drugs (started within 6 weeks prior onset of neutropenia)	**Metamizole** Denosumab Dimenhydrinate Propranolol Prednisolone	Clexane Cotrimoxazole Pantoprazole Piperacillin/ tazobactam Methyl-prednisolone Hemodialysis	None	**Metamizole**	None	Hydrocortisone	**Metamizole**	None	**Metamizole**	**Metamizole** Lamotrigine Opipramol Ibuprofen Pantoprazole
Signs and symptoms of neutropenia	Weakness, Erysipelas, Pain	Fever, Weakness	Fever	Mucositis	Fever	Loss of appetite	Pharyngeal abscess	None	None	Weakness, Abdominal pain
Diagnosis of neutropenia	Lab BMB	Lab BMB	Lab Myelogram	Lab BMB	Lab	Lab BMB	Lab ENT examination	Lab	Lab Autoantibodies BMB Cytogenetic analysis	Lab
Systemic steroids	Prednisolone 1 mg/ kg/d (80 mg) IV	Prednisolone 80 mg IV	None	None	Dexamethasone 8 mg IV 3×/ d; Methylprednisolone 1 mg/ kg IV, Methylprednisolone 1 mg/kg p.o.	Prednisolone 20 mg p.o.*	None	None	None	None
Additional treatment	Ciclosporin (175 mg/d) Piperacillin/ tazobactam Vancomycin Ciprofloxacin G-CSF (Filgrastim 30 million IU/day SC) Valaciclovir (1000 mg/d) Fluconazole (100 mg/d)	Amphotericin B G-CSF (Filgrastim 30 million IU/d for 3 days)	G-CSF (Neupogen)	G-CSF	G-CSF (Granocyte SC 1×/d) Piperacillin/tazobactam (4×4.5 g IV) Levofloxacin (500 mg 1×/d)		G-CSF (Neupogen 30 million IU 1× daily for 6 d) Ciprofloxacin (500 mg 1-0-1 for 10 days) Unacid 3 g 1-1-1 (7 d) Amphotericin B	G-CSF	G-CSF Ciprofloxacin	G-CSF
Outcome of neutropenia	Resolved	Resolved	Patient died	Resolved	Resolved	Resolved	Resolved	Resolved	Resolved	Resolved
Re-exposure with irAE-inducing ICI	No	Yes (Ipilimumab)	No	No	No	No	Yes (Nivolumab)	Yes (Nivolumab)	No	Yes (Pembrolizumab)
irAE after re-exposure	–	Arthritis Vitiligo	–	–	–	–	None	Exanthema	–	None

BMB, bone marrow biopsy; ENT, ear-nose-throat; G-CSF, granulocyte colony-stimulating factors; ICI, immune checkpoint inhibition; ipi, ipilimumab; ir-, immune-related; irAE, immune-related adverse event; IV, intravenously; lab, laboratory diagnostics; nivo, nivolumab; SC, subcutaneously; pembro, pembrolizumab.

**started before grade 4 neutropenia.*

TABLE 3 | Blood counts before neutropenia onset and during maximum irNeutropenia.

	Patient 1	Patient 2	Patient 3	Patient 4	Patient 5	Patient 6	Patient 7	Patient 8	Patient 9	Patient 10
Counts before neutropenia onset										
Hb in g/dl	9.7	15.6	11.1	16.1	14.3	7	13.3	12.8	12.5	8.8
Thrombocytes/nl	533	209	427	156	134	280	230	182	127	485
Leukos/nl	10.76	4.7	6.36	7.8	3.69	7	4.89	3.1	5.83	6.6
Neutros/nl	8.64	2.9	4.87	3.74	2.45	3.3	3	2.1	4.26	5
Counts during maximum neutropenia										
Hb in g/dl	9.4	11.5	7.7	12.8	12.7	7.9	11.5	11.8	10.6	8.5
Thrombocytes/nl	366	166	137	329	148	0.3	312	192	175	344
Leukos/nl	0.3	0.98	1.39	2.2	0.92	4.3	0.99	2.36	1.76	1.5
Neutros/nl	Nm**	Nm**	0.02	0.01	0.05	0.3	0.13	0.4	0*	0.06
% Neutrophil decrease from baseline	>99	>99	99.59	99.73	97.96	90.91	95.67	80.95	>99	98.80

hb, hemoglobin; ir-, immune-related; leukos, leukocytes; neutros, neutrocytes; nm, not measurable.

**Segmented-cored.*

***Insufficient cells to detect and count types of leukocytes in differential blood count.*

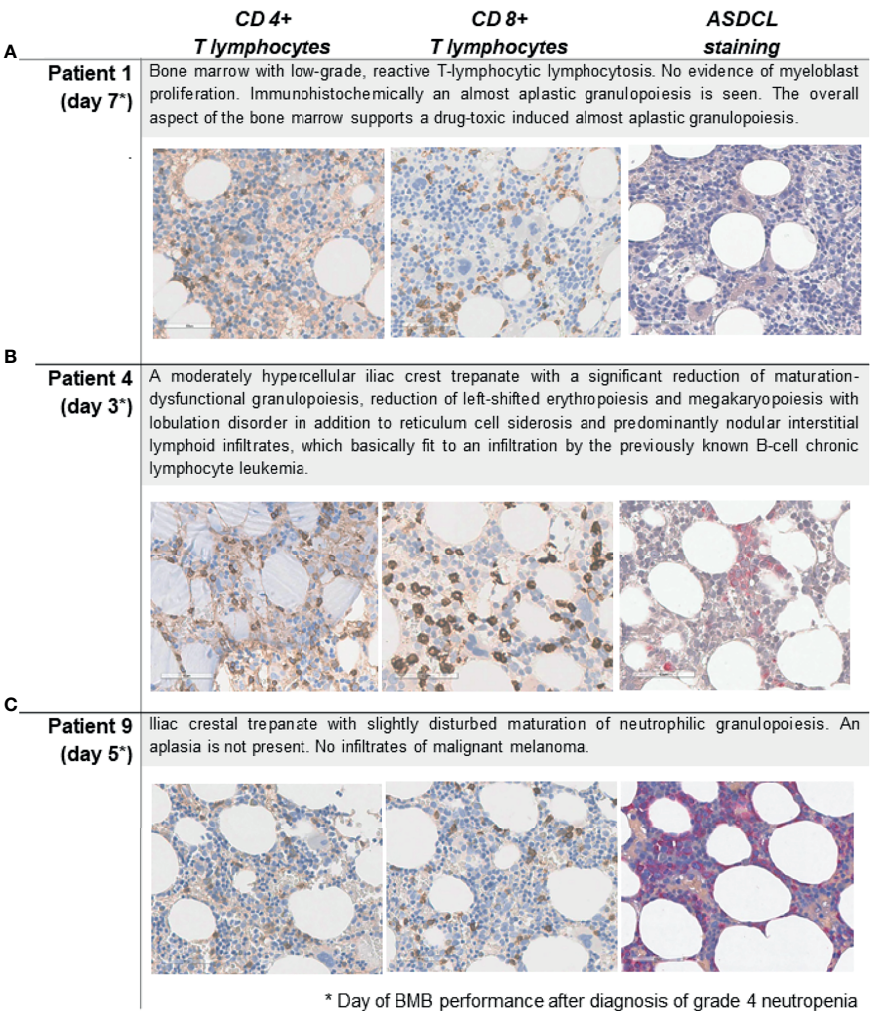


FIGURE 1 | Bone marrow staining for CD4+ T and CD8+ T lymphocytes, and naphthol AS-D chloroacetate esterase (ASDCL) staining for myeloid cells in patients with ICI-induced grade 4 irNeutropenia (n=3). **(A)** Patient 1, **(B)** Patient 4, **(C)** Patient 9. Original magnification 400×. BMB, bone marrow biopsy; CD, cluster of differentiation.

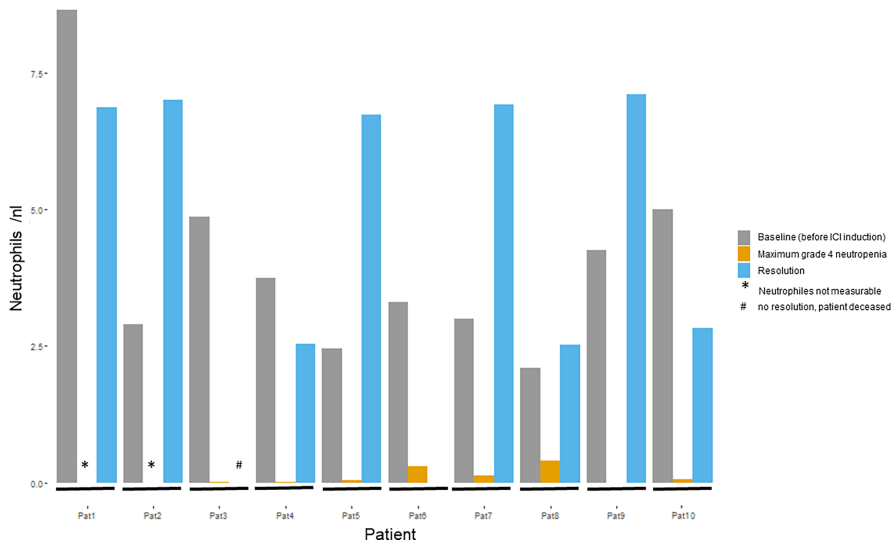


FIGURE 2 | Course of neutrophil granulocytes in patients with grade 4 irNeutropenia (n=10). Figure shows neutrophil values in nl at baseline (before ICI induction), for maximum grade 4 neutropenia, and, if it occurred, after resolution of neutropenia. ICI, immune checkpoint inhibitors; nl, nanoliter.

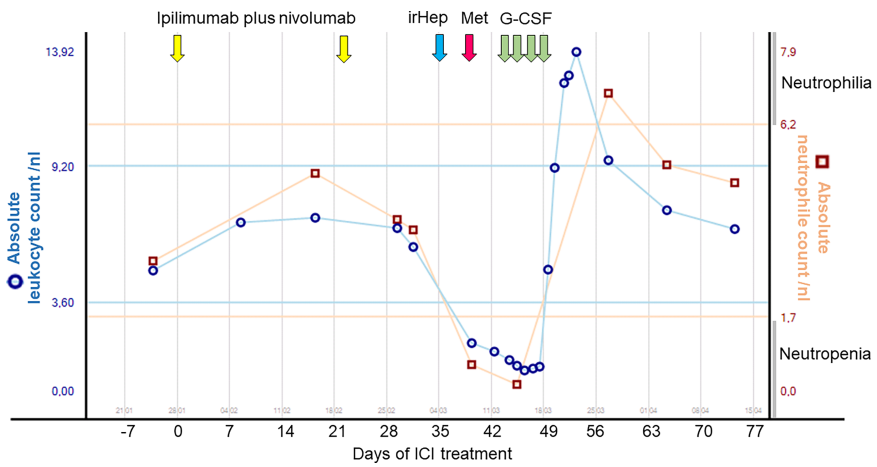


FIGURE 3 | Timeline of patient 7: Neutrophil and leukocyte counts over time following administration of combined ipilimumab–nivolumab and metamizole as well as subsequent treatment interventions. G-CSF, granulocyte colony-stimulating factors; Hep-, hepatitis; ICI, immune checkpoint inhibitor therapy; ir-, immune-related; Met, metamizole; nl, nanoliter.

combined PD-1 and CTLA-4 therapy only continued PD-1 monotherapy, and one patient with initial PD-1 monotherapy received anti-CTLA-4 therapy. None of these patients had a relapse of neutropenia, one of the patients had received metamizole before but not at re-exposure (**Table 2**).

Metamizole-Induced Grade 4 Neutropenia

Patients who received ICI and metamizole (ICI+/met+, n=5) developed neutropenia earlier after starting ICI than patients who did not receive metamizole (ICI+/met-, n=5). Median time to neutropenia onset was 32 days [range 10–51] for ICI+/met+, compared with 48 days [range 11–344] for ICI? A3B2 show $132#?>+/met-. In ICI+/met+ patients, the median time from starting metamizole to onset of neutropenia was 8 days (range 2–43). Patients who received metamizole without ICI (ICI-/met+, n=5) showed a median time to neutropenia onset of 3 days (range 0–1369) after starting metamizole. The duration of grade 4 neutropenia was longer in ICI+/met+ patients (median 11 days, range 4–32 days) than in ICI+/met- patients (median 8 days, range 3–13 days,

Supplemental Table 1). Non-melanoma and non ICI-treated patients with confirmed metamizole-induced grade 4 neutropenia (ICI-/met+) showed a median duration of neutropenia of 13 days (range 6–28 days; **Supplemental Table 1**). All received further systemic medication at neutropenia onset. All ICI-/met + patients developed inflammatory symptoms—some cases of which were severe—and were hospitalized for neutropenia. Regarding diagnostics, all ICI-/met+ patients received a laboratory test and a BMB. All ICI-/met+ patients were treated with G-CSF and broad-spectrum antibiotics. None received systemic steroids. Three patients additionally received antimycotic treatment. Neutropenia resolved in all five patients (**Supplemental Table 2**).

Case Presentation: ICI- or Metamizole-Induced Neutropenia?

CASE 1 (Pat 7): A 70-year-old female patient was diagnosed with mucosal melanoma of the vulva in November 2012. Local excision with a concurrent sentinel lymph node biopsy of the right groin followed by a complete lymph node dissection of the left groin revealed one lymph node metastasis (stage IIIC according to the American Joint Committee on Cancer [AJCC] 2017). Adjuvant radiotherapy of the genital and groin regions was performed. Nine months later, she presented with recurrent metastatic *BRAF*-wildtype melanoma with nodal and pulmonary involvement. She was treated with nivolumab as part of the CheckMate-067 trial and had stable disease for 17 months. After a second local recurrence in August 2018 with only incomplete resection, follow-up treatment with imiquimod was performed. One month later pulmonary metastases reappeared, and ICI with ipilimumab and nivolumab was initiated. After two cycles of ICI, therapy was paused because of grade 2 hepatitis. Initially, systemic steroids were not commenced, and detailed laboratory examinations were performed. Grade 4 neutropenia was diagnosed, and the patient was hospitalized. Detailed medical history revealed that the patient had taken metamizole two days before the onset of neutropenia due to a headache (**Figure 3**). After consultation with the hematological department, systemic treatment of 30 million international units (IU) G-CSF subcutaneously (SC) once daily was initiated. Additionally, 500 mg ciprofloxacin twice daily and amphotericin B was started. One day after admission, the patient complained of a sore throat and was presented to the ear, nose, and throat department. Computerized tomography (CT) of the neck revealed a pharyngeal abscess. The abscess was drained, and antibiotic therapy was escalated to ampicillin and sulbactam. A gradual improvement of the patient's physical fitness and normalization of neutrophils was observed after 5 days. Three months later, CT staging showed pulmonary and mediastinal lymph node progression. Because of a lack of therapy options, the patient was re-exposed to nivolumab monotherapy. It was recommended to avoid metamizole. No recurrence of neutropenia was observed. In this case, the patient's neutropenia could have been triggered by either combined nivolumab–ipilimumab or metamizole, or even by the combination of the three agents.

CASE 2 (Pat 5): A 71-year-old male patient was diagnosed with a $BRAF^{V600R}$-mutated metastatic melanoma stage IV in November 2018. His pre-existing conditions included chronic pancreatitis and non-immune-related thrombocytopenia and lymphopenia, for which he had not received systemic treatment. Systemic therapy for melanoma with combined BRAF–MEK inhibitors was started. He developed progressive disease within 3 months, and therapy was switched to nivolumab plus ipilimumab. After 6.9 weeks of treatment, the patient developed a temperature of 38.0°C. The laboratory work-up revealed grade 4 neutropenia, and the patient was hospitalized. He received systemic steroids (8 mg dexamethasone intravenously [IV] three times daily for two days, followed by 1 mg/kg methylprednisolone IV for three days, and 1 mg/kg methylprednisolone orally onwards according to scheme), G-CSF SC once daily for four days, as well as antibiotic treatment with IV piperacillin/tazobactam (4.5 g four times daily for one week) and levofloxacin (500 mg once). A BMB was not performed. After 3 days of treatment, the patient's neutrophils started to increase, and after 4 days of treatment they normalized. The patient was not re-exposed to ICI and received no further systemic therapy. He died of melanoma 2 months later and 7 months after diagnosis of advanced disease. ICI represents a likely trigger of neutropenia in this case.

DISCUSSION

This international multicenter retrospective analysis reports on one of the largest cohorts of patients with grade 4 neutropenia who were treated with PD-1 inhibitors alone or in combination with ipilimumab. Our findings show that the incidence of grade 4 neutropenia in ICI-treated patients was very low (less than 0.15%), but when it did occur, it was clinically severe and potentially life-threatening. Most patients with grade 4 irNeutropenia presented with clinical symptoms, most often fever and inflammation of the mouth and throat. Half of the patients received metamizole prior to the onset of neutropenia, and this may have contributed or been causal. Therapy with G-CSF was sufficient to achieve neutrophil recovery in 50% of patients; however, one patient (10%) died despite treatment with G-CSF.

Although hematological irAEs are rare, occurring in less than 1% of patients treated with ICI (12, 13), reports of hematological toxicities have increased, possibly because of a more common use of ICI and improved recognition of hematological side effects (21). Neutropenia is one of the most common hematological toxicities, reported in 17% to 26% of patients with hematological irAEs (12–14). Petrelli et al. conducted a meta-analysis that included PD-(L)1-inhibitor-treated patients with several tumor entities. Among 9324 patients from 47 studies, the incidence of grade 3–5 neutropenia was 1.07%, and of febrile neutropenia 0.45% (22). The reported median onset of neutropenia after starting ICI is 10 to 11 weeks, with a median duration (at grade 2 or worse) of 13 to 16.5 days (12, 14, 19). In our study, the onset of high-grade irNeutropenia was earlier (median 6.4 weeks) and the

median duration was shorter (9.5 days). A possible explanation for this difference could be the high percentage of patients treated with combined ICI (70%) and the earlier and more frequent (weekly) laboratory testing of these patients. It is well known that irAEs generally occur earlier in patients receiving the combination regimen than in those receiving nivolumab alone (23). In contrast to the results of Delanoy et al., which showed a recurrence of neutropenia in two-thirds of patients after re-exposure to ICI, and a case described by Boegeholz et al. (12, 19), no recurrence of neutropenia occurred upon re-exposure in our study. This is in line with one case reported by Michot et al. (14). These differing results underscore the uncertain nature of the data and the importance of strategically recording and processing rare side effects (14, 24).

Importantly, four patients (40%) with irNeutropenia in our study had a medical history of previously diagnosed hematological diseases. One (10%) of these patients had B-cell chronic lymphocytic leukemia (CLL), which raises the question whether this could be a risk factor for hematological AEs given the frequent observation of autoimmune-related cytopenias in CLL patients (25). Consistent with our data, the study by Delanoy et al. included three patients (9%) with concomitant B-cell CLL (12). This finding underlines the potential increased risk of hematological immunotoxicity in patients with an underlying mature B lymphoid clone (12). Interestingly, a recent retrospective analysis showed that ICI was efficacious in patients with advanced skin cancer (melanoma and Merkel cell carcinoma) and concomitant hematological malignancies, underlining the potential benefit despite hematological comorbidities (26).

In our study, 50% of patients had concomitant treatment with metamizole for pain therapy. Neutropenia is a rare, well-known side effect of metamizole, and concomitant treatment with metamizole presents a diagnostic challenge in ICI-treated patients. In previous studies (16, 17), the median duration of metamizole treatment before onset of acute neutropenia was short, at only 2 days (16). This is in line with our data, which showed a short median time to neutropenia onset after starting metamizole of 3 days in ICI-/met+ patients, compared with 8 days in patients with additional ICI (ICI+/met+). In contrast, onset of neutropenia after starting ICI was later in ICI+/met- patients (48 days) than in ICI+/met+ patients (32 days). Consistent with these data, the Paul Ehrlich Institute in Germany reported 10 cases of pancytopenia or agranulocytosis after initiation of ICI, with onset of neutropenia after 12 to 274 days (six cases within 12 to 28 days, one case after 85 days, and three cases after 240 to 274 days). Of note, three of 10 had concomitant treatment with metamizole (Bulletin zur Arzneimittelsicherheit, August 4, 2016, Paul Ehrlich Institute and Federal Institute of Drugs and Medical Devices). Taken together, ICI-mediated neutropenia seems more likely to occur later after the start of treatment than metamizole-induced neutropenia. Andersohn et al. reported a median time of 10 days between onset of neutropenia and normalization of neutrophil count for metamizole (16). In our cohort, the median duration of grade 4 neutropenia was 13 days for ICI-/met+ patients, compared with 8 days for ICI+/met- and 11 days for ICI+/met+ patients (**Supplemental Table 1**). Because the median duration of neutropenia only slightly differed between patient groups, a final attribution to the causative drug (ICI or metamizole) was not possible. However, the duration of neutropenia might be prolonged by the application of ICI and metamizole simultaneously, compared with ICI alone.

Bone marrow evaluation is an important diagnostic modality for identifying patients with drug-induced grade 4 neutropenia. Garbe reported an absence of granulopoiesis, a neutrophilic maturation arrest or a hypercellularity with increased myeloid precursors and little maturation in the case of peripheral destruction of neutrophils in patients with non-chemotherapy drug-induced agranulocytosis (17). The presence of promyelocytes or myelocytes in the bone marrow generally indicated a recovery within 7 days (17). Bone marrow biopsies from three patients treated with ICI and concomitant metamizole (ICI+/met+) showed a diverse picture, including depletion of granulocytes and slightly impaired maturation of neutrophilic granulopoiesis (**Figure 1**). This is consistent with previous reports (12, 19, 27) that showed variable findings in BMB of patients with ICI-induced neutropenia, ranging from normocellular marrow to blockade in granulocyte maturation or complete absence of myelopoiesis. The timing of the biopsy after onset of neutropenia could be a reason for these differences. Boegeholz et al. showed small infiltrates of CD8+ predominant lymphocytes and slight lymphocytosis of mostly CD8+ T cells in two patients suffering from neutropenia after ICI (19). We could confirm a slightly lower ratio of CD4+ to CD8+ T cells in ICI–met-induced neutropenia than in met-induced neutropenia, which indicates that CD8+ T cell infiltration could play a role in grade 4 ICI–met neutropenia. The pathogenesis of drug-induced grade 4 neutropenia is not completely understood, although toxic or immunoallergic mechanisms are suspected (17). Toxic mechanisms might rely on polymorphisms of genes that encode enzymes that generate or destroy toxic drug metabolites. Immunoallergic mechanisms are thought to be mediated by drug-dependent or drug-induced antibodies that lead to destruction of the granulocytes in peripheral blood or precursor cells in the bone marrow (17). It has been speculated that irAEs are mediated by autoreactive T cells and antibody-mediated processes (28). Similar to other irAEs, generation of autoreactive T and B cells and a decrease in T regulatory phenotype have been proposed as mechanisms for hematologic toxicities (22).

To date, no uniform treatment recommendations exist for irNeutropenia. Because of its high mortality rate, timely diagnostics and treatment is critical for outcome. Standardized approaches are recommended for management of ir-toxicities (29), but these approaches do not cover neutropenia. Treatment of irAE typically includes downregulation of the immune system with systemic steroids, additional systemic immunosuppressive drugs, and symptomatic therapy depending on the grade of toxicity (11, 23, 30–32). Use of systemic steroids and further immunosuppressants constitutes an additional challenge of neutropenia treatment, because these drugs might act counterproductively during bacterial infections and promote

sepsis. In previous reports, ICI-induced neutropenia was complicated by severe infection and febrile neutropenia in 55% to 68% of patients (12, 14, 19), and three patients died of a bacterial or fungal infection (12, 14, 19, 27). There is a consensus that broad-spectrum antibiotics should be immediately administered in cases of febrile neutropenia. In addition, G-CSF should be used until neutropenia resolves (12, 14, 19, 27). Conflicting recommendations exist regarding the use of systemic steroids (12, 14, 19, 27). The recommendations from two French studies (12, 14) advise that, in the absence of firm evidence of their efficacy, corticosteroids should not be given systematically, because they could accentuate the risk of infection. Based on data from their meta-analysis, Boegeholz et al. concluded that treatment with corticosteroids in combination with G-CSF does not seem to worsen outcomes regarding infection complications, and thus constitutes an acceptable initial treatment approach (19). Consistent with previous data reporting normalization of neutrophil counts in 67% to 82% of patients (12, 14, 19), 90% of the ICI-treated patients in our study showed resolution of grade 4 neutropenia. Almost all our patients (90%) had been treated with G-CSF, three of them in combination with corticosteroids. The therapeutic benefit of steroids remains unclear and should be critically discussed in the context of associated infections on a case-to-case basis. If additional medication can be excluded as a trigger and irNeutropenia is confirmed, corticosteroid treatment can be considered.

Limitations of our study are its retrospective nature, including the possibility of underreporting of side effects by the treating physician. Nonetheless, because of the clinical relevance of this topic and lack of information and treatment recommendations for this rare side effect, we believe it is important to report real-world outcomes of melanoma patients with grade 4 neutropenia who have been treated with ICI, with or without concomitant drugs that can cause neutropenia. Bias might occur as only patients treated at a maximum care hospital were included and real incidences might be higher as not all cases of grade 4 neutropenia are severe. Although we could confirm a slightly lower ratio of CD4+ to CD8+ T cells in patients with ICI–met-induced neutropenia than in those with met-induced neutropenia, the number of patients in the study is small, and findings depend on the time of biopsy. These data should therefore be interpreted with caution.

In conclusion, our retrospective study shows that grade 4 neutropenia is a potential rare side effect of ICI treatment, which can be life-threatening. The vast majority of patients with ICI-induced grade 4 neutropenia presented with inflammatory symptoms and responded to G-CSF treatment, with a normalization of the neutrophil count in 90% of patients. Most patients with inflammatory symptoms were treated with antibiotics and/or antimycotic and antiviral therapies. Early recognition, initiation of therapy and management of inflammatory complications can prevent a fatal outcome. Corticosteroids can be considered in combination with G(M)-CSF for treatment of irNeutropenia after other causes of neutropenia have been excluded. If infections are suspected or inflammatory symptoms arise, broad-spectrum antibiotics should be administered promptly.

DATA AVAILABILITY STATEMENT

The original contributions presented in the study are included in the article/**Supplementary Material**. Further inquiries can be directed to the corresponding authors.

ETHICS STATEMENT

The study including human biological samples and related data was approved by the Ethics Committee of Duisburg-Essen University (19-9075-BO).

AUTHOR CONTRIBUTIONS

AZ and LZ designed the methodology in collaboration with LH, RK, and MH. AZ and LZ wrote the manuscript. AZ and LZ analyzed and interpreted the data. All authors provided data for **Tables 1**–**3**. All authors reviewed the final manuscript.

FUNDING

This work was partly funded by the Deutsche Forschungsgemeinschaft (DFG, German Research Foundation) - SCHA 422/17-1 (KFO 337). The SERIO side effect registry is supported by the Foundation immuno-oncology (Stiftung Immunonkologie), Germany, and the Association for the support of the Cancer Center of the University of Erlangen-Nuremberg (Verein zur Förderung des Tumorzentrums der Universität Erlangen-Nürnberg e.V.), Germany.

ACKNOWLEDGMENTS

The authors are indebted to all patients and their relatives and would like to thank Dorothe Möllmann, Stefanie Richter, and the team from the Institute of Pathology, Essen University Hospital, for laboratory assistance. We acknowledge support by the Open Access Publication Fund of the University of Duisburg-Essen.

SUPPLEMENTARY MATERIAL

The Supplementary Material for this article can be found online at: https://www.frontiersin.org/articles/10.3389/fonc.2021.765608/full#supplementary-material

Supplementary Figure 1 | Mann–Whitney *U* test of patients with irNeutropenia (ICI+/met+, n=3) and patients with met-induced neutropenia (ICI-/met+, n=5). ICI, immune checkpoint inhibitors; ir-, immune-related; met, metamizole

REFERENCES

1. Hodi FS, Chiarion-Sileni V, Gonzalez R, Grob J-J, Rutkowski P, Cowey CL, et al. Nivolumab Plus Ipilimumab or Nivolumab Alone Versus Ipilimumab Alone in Advanced Melanoma (CheckMate 067): 4-Year Outcomes of a Multicentre, Randomised, Phase 3 Trial. *Lancet Oncol* (2018) 19(11):1480–92. doi: 10.1016/S1470-2045(18)30700-9
2. Eggermont AMM, Blank CU, Mandala M, Long GV, Atkinson V, Dalle S, et al. Adjuvant Pembrolizumab Versus Placebo in Resected Stage III Melanoma. *N Engl J Med* (2018) 378(19):1789–801. doi: 10.1056/NEJMoa1802357
3. Wolchok JD, Chiarion-Sileni V, Gonzalez R, Rutkowski P, Grob J-J, Cowey CL, et al. Overall Survival With Combined Nivolumab and Ipilimumab in Advanced Melanoma. *N Engl J Med* (2017) 377(14):1345–56. doi: 10.1056/NEJMoa1709684
4. Robert C, Long GV, Brady B, Dutriaux C, Maio M, Mortier L, et al. Nivolumab in Previously Untreated Melanoma Without BRAF Mutation. *N Engl J Med* (2015) 372(4):320–30. doi: 10.1056/NEJMoa1412082
5. Robert C, Thomas L, Bondarenko I, O'Day S, Weber J, Garbe C, et al. Ipilimumab Plus Dacarbazine for Previously Untreated Metastatic Melanoma. *N Engl J Med* (2011) 364(26):2517–26. doi: 10.1056/NEJMoa1104621
6. Ribas A, Puzanov I, Dummer R, Schadendorf D, Hamid O, Robert C, et al. Pembrolizumab Versus Investigator-Choice Chemotherapy for Ipilimumab-Refractory Melanoma (KEYNOTE-002): A Randomised, Controlled, Phase 2 Trial. *Lancet Oncol* (2015) 16(8):908–18. doi: 10.1016/S1470-2045(15)00083-2
7. Blank CU, Rozeman EA, Fanchi LF, Sikorska K, van de Wiel B, Kvistborg P, et al. Neoadjuvant Versus Adjuvant Ipilimumab Plus Nivolumab in Macroscopic Stage III Melanoma. *Nat Med* (2018) 24(11):1655–61. doi: 10.1038/s41591-018-0198-0
8. Menzies AM, Amaria RN, Rozeman EA, Huang AC, Tetzlaff MT, van de Wiel BA, et al. Pathological Response and Survival With Neoadjuvant Therapy in Melanoma: A Pooled Analysis From the International Neoadjuvant Melanoma Consortium (INMC). *Nat Med* (2021) 27(2):301–9. doi: 10.1038/s41591-020-01188-3
9. Weber J, Mandala M, Del Vecchio M, Gogas HJ, Arance AM, Cowey CL, et al. Adjuvant Nivolumab Versus Ipilimumab in Resected Stage III or IV Melanoma. *N Engl J Med* (2017) 377(19):1824–35. doi: 10.1056/NEJMoa1709030
10. Robert C. A Decade of Immune-Checkpoint Inhibitors in Cancer Therapy. *Nat Commun* (2020) 11(1):3801. doi: 10.1038/s41467-020-17670-y
11. Heinzerling L, de Toni E, Schett G, Hundorfean G, Zimmer L. Checkpoint-Inhibitoren. *Dtsch Arztebl Int* (2019) 116(8):119–26. doi: 10.3238/arztebl.2019.0119
12. Delanoy N, Michot J-M, Comont T, Kramkimel N, Lazarovici J, Dupont R, et al. Haematological Immune-Related Adverse Events Induced by Anti-PD-1 or Anti-PD-L1 Immunotherapy: A Descriptive Observational Study. *Lancet Haematol* (2019) 6(1):e48–57. doi: 10.1016/S2352-3026(18)30175-3
13. Kramer R, Zaremba A, Moreira A, Ugurel S, Johnson DB, Hassel JC, et al. Hematological Immune Related Adverse Events After Treatment With Immune Checkpoint Inhibitors. *Eur J Cancer* (2021) 147:170–81. doi: 10.1016/j.ejca.2021.01.013
14. Michot JM, Lazarovici J, Tieu A, Champiat S, Voisin AL, Ebbo M, et al. Haematological Immune-Related Adverse Events With Immune Checkpoint Inhibitors, How to Manage? *Eur J Cancer* (2019) 122:72–90. doi: 10.1016/j.ejca.2019.07.014
15. Wang DY, Salem J-E, Cohen JV, Chandra S, Menzer C, Ye F, et al. Fatal Toxic Effects Associated With Immune Checkpoint Inhibitors: A Systematic Review and Meta-Analysis. *JAMA Oncol* (2018) 4(12):1721–8. doi: 10.1001/jamaoncol.2018.3923
16. Andersohn F, Konzen C, Garbe E. Systematic Review: Agranulocytosis Induced by Nonchemotherapy Drugs. *Ann Internal Med* (2007) 146 (9):657–65. doi: 10.7326/0003-4819-146-9-200705010-00009
17. Garbe E. Non-Chemotherapy Drug-Induced Agranulocytosis. *Expert Opin Drug Saf* (2007) 6(3):323–35. doi: 10.1517/14740338.6.3.323
18. Kötter T, da Costa BR, Fässler M, Blozik E, Linde K, Jüni P, et al. Metamizole-Associated Adverse Events: A Systematic Review and Meta-Analysis. *PloS One* (2015) 10(4):e0122918. doi: 10.1371/journal.pone.0122918
19. Boegeholz J, Brueggen CS, Pauli C, Dimitriou F, Haralambieva E, Dummer R, et al. Challenges in Diagnosis and Management of Neutropenia Upon Exposure to Immune-Checkpoint Inhibitors: Meta-Analysis of a Rare Immune-Related Adverse Side Effect. *BMC Cancer* (2020) 20(1):300. doi: 10.1186/s12885-020-06763-y
20. Sun Y, Lee SK, Oo TH, Rojas-Hernandez CM. Management of Immune-Mediated Cytopenias in the Era of Cancer Immunotherapy: A Report of 4 Cases. *J Immunother (Hagerstown Md 1997)* (2018) 41(1):32–4. doi: 10.1097/CJI.0000000000000194
21. Davis EJ, Salem JE, Young A, Green JR, Ferrell PB, Ancell KK, et al. Hematologic Complications of Immune Checkpoint Inhibitors. *Oncologist* (2019) 24(5):584–8. doi: 10.1634/theoncologist.2018-0574
22. Petrelli F, Ardito R, Borgonovo K, Lonati V, Cabiddu M, Ghilardi M, et al. Haematological Toxicities With Immunotherapy in Patients With Cancer: A Systematic Review and Meta-Analysis. *Eur J Cancer* (2018) 103:7–16. doi: 10.1016/j.ejca.2018.07.129
23. Hassel JC, Heinzerling L, Aberle J, Bähr O, Eigentler TK, Grimm M-O, et al. Combined Immune Checkpoint Blockade (Anti-PD-1/Anti-CTLA-4): Evaluation and Management of Adverse Drug Reactions. *Cancer Treat Rev* (2017) 57:36–49. doi: 10.1016/j.ctrv.2017.05.003
24. Heinzerling L, Ascierto PA, Dummer R, Gogas H, Grob JJ, Lebbe C, et al. Adverse Events 2.0-Let Us Get SERIOs: New Reporting for Adverse Event Outcomes Needed in the Era of Immunooncology. *Eur J Cancer* (2019) 112:29–31. doi: 10.1016/j.ejca.2019.01.015
25. Vitale C, Salvetti C, Griggio V, Porrazzo M, Schiattone L, Zamprogna G, et al. Preexisting and Treatment-Emergent Autoimmune Cytopenias in Patients With CLL Treated With Targeted Drugs. *Blood* (2021) 137(25):3507–17. doi: 10.1182/blood.2020008201
26. Leiter U, Loquai C, Reinhardt L, Rafei-Shamsabadi D, Gutzmer R, Kaehler K, et al. Immune Checkpoint Inhibition Therapy for Advanced Skin Cancer in Patients With Concomitant Hematological Malignancy: A Retrospective Multicenter DeCOG Study of 84 Patients. *J Immunother Cancer* (2020) 8 (2):1–10. doi: 10.1136/jitc-2020-000897
27. Naqash AR, Appah E, Yang LV, Muzaffar M, Marie MA, McCallen JD, et al. Isolated Neutropenia as a Rare But Serious Adverse Event Secondary to Immune Checkpoint Inhibition. *J Immunother Cancer* (2019) 7(1):169. doi: 10.1186/s40425-019-0648-3
28. Postow MA, Sidlow R, Hellmann MD. Immune-Related Adverse Events Associated With Immune Checkpoint Blockade. *N Engl J Med* (2018) 378 (2):158–68. doi: 10.1056/NEJMra1703481
29. Brahmer JR, Lacchetti C, Schneider BJ, Atkins MB, Brassil KJ, Caterino JM, et al. Management of Immune-Related Adverse Events in Patients Treated With Immune Checkpoint Inhibitor Therapy: American Society of Clinical Oncology Clinical Practice Guideline. *J Clin Oncol* (2018) 36(17):1714–68. doi: 10.1200/JCO.2017.77.6385
30. Zimmer L, Goldinger SM, Hofmann L, Loquai C, Ugurel S, Thomas I, et al. Neurological, Respiratory, Musculoskeletal, Cardiac and Ocular Side-Effects of Anti-PD-1 Therapy. *Eur J Cancer* (2016) 60:210–25. doi: 10.1016/j.ejca.2016.02.024
31. Puzanov I, Diab A, Abdallah K, Bingham CO3rd, Brogdon C, Dadu R, et al. Managing Toxicities Associated With Immune Checkpoint Inhibitors: Consensus Recommendations From the Society for Immunotherapy of Cancer (SITC) Toxicity Management Working Group. *J Immunother Cancer* (2017) 5(1):95. doi: 10.1186/s40425-017-0300-z
32. Haanen J, Carbonnel F, Robert C, Kerr KM, Peters S, Larkin J, et al. Management of Toxicities From Immunotherapy: ESMO Clinical Practice Guidelines for Diagnosis, Treatment and Follow-Up. *Ann Oncol* (2017) 28 (suppl_4):iv119–iv42. doi: 10.1093/annonc/mdx225

Conflict of Interest: AZ received travel support from Novartis, Sanofi Genzyme, and Bristol-Myers Squibb, outside the submitted work. RK has received speaker fees by NG-Akademie GmbH and Hollister Incorporated, outside the submitted work. MS is an honoraria and/or travel grants from Abbvie, Bristol-Myers Squibb, Merck, Merck Sharp & Dohme, Novartis, Pfizer and Sanofi-Aventis. AG: Speaker´s honoraria from Bristol-Myers Squibb, MSD Sharp & Dohme and Roche; intermittent advisory board relationships with Amgen, Bristol-Myers Squibb, Novartis, MSD Sharp & Dohme, Pierre Fabre Pharmaceuticals, Pfizer, Roche and Sanofi Genzyme; travel and congress fee support from Bristol-Myers

Squibb, MSD Sharp & Dohme, Novartis, Pierre Fabre Pharmaceuticals and Roche. Clinical studies: Amgen, Array, Bristol-Myers Squibb, GSK, Novartis, Merck, MSD Sharp & Dohme, Pfizer and Roche. BB received speaker fees for BMS, MSD, Novartis. Travel accomodation: BMS, Pierre Fabre. MS is an honoria for advisory board for Sanofi/Regneron and speaker fees für Novartis Pharma AG. GM has received speaker fees from PharmaMar, outside the submitted work. DJ received advisory board honoraria from BMS, Catalyst, Iovance, Jansen, Merck, Novartis, Oncosec, and Pfizer, and research funding from BMS and Incyte. LS is an honoraria for advisory boards & speaker fees from BMS. CaL received Advisory board: Roche, Novartis, BMS, MSD, SunPharma, Biontech, Kyowa Kirin, Sanofi, Pierre Fabre, Merck; Speakers fee: Roche, Novartis, BMS, MSD, SunPharma, Biontech, Kyowa Kirin, Sanofi, Pierre Fabre, Merck; Travel reimbursement: Roche, Novartis, BMS, MSD, SunPharma, Biontech, Kyowa Kirin, Sanofi, Pierre Fabre, Merck. CP received honoraria (speaker honoraria or honoraria as a consultant) and travel support from: Novartis, BMS, Roche, Merck Serono, MSD, Celgene, AbbVie, Pierre Fabre, SUNPHARMA and LEO. GL is a consultant advisor for Aduro Biotech Inc, Amgen Inc, Array Biopharma inc, Boehringer Ingelheim International GmbH, Bristol-Myers Squibb, Evaxion Biotech A/S, Hexel AG, Highlight Therapeutics S.L., Merck Sharpe & Dohme, Novartis Pharma AG, OncoSec, Pierre Fabre, QBiotics Group Limited, Regeneron Pharmaceuticals Inc, SkylineDX B.V., Specialised Therapeutics Australia Pty Ltd. AM is an honoraria for advisory boards for BMS, MSD, Novartis, Roche, Pierre-Fabre, QBiotics. MC is a consultant advisor for Amgen, BMS, Eisai, Ideaya, MSD, Nektar, Novartis, Oncosec, Pierre-Fabre, Qbiotics, Regeneron, Roche, Merck and Sanofi, and received honoraria from BMS, MSD, and Novartis. CeL received Honoraria: Roche; BMS; Novartis; Amgen; MSD; Pierre Fabre; Pfizer; Incyte; Consulting or Advisory Role: BMS; MSD; Novartis; Amgen; Roche; Merck Serono; Sanofi; Pierre Fabre; Speakers' Bureau: Roche; BMS; Novartis; Amgen; MSD; Research Funding: Roche; BMS; Travel, Accommodations, Expenses: BMS; MSD; Novartis; Sanofi; Pierre Fabre; Other Relationship: Avantis Medical Systems (board). MT received grants and personal fees from MSD, Ono Pharmaceutical, BMS, Bayer, Eisai, Novartis, Pfizer, Rakuten Medical, Merck Biopharma, personal fees from LOXO, Celgene, Amgen, outside the submitted work. PB received research funding from BeiGene, BMS, MSD and Takeda; advisory board honoraria from Takeda; speakers honoraria from BMS and travel support from Celgene, all outside the submitted work. TEi received speaker fees from Novartis, Pierre Fabre, MSD, Sanofi Genzyme, Alirall Hermal and Bristol-Myers Squibb, outside the submitted work. KK has served as consultant or/and has received honoraria from Amgen, Roche, Bristol Myers Squibb, Merck Sharp and Dohme, Pierre Fabre, and Novartis, and received travel support from Amgen, Merck Sharp and Dohme, Bristol Myers Squibb, Amgen, Pierre Fabre, Medac and Novartis. RG: Invited speaker: Roche, BMS, MSD, Novartis, Amgen, Merck Serono, Almirall Hermal, SUN, Sanofi, Pierre-Fabre. Advisory board: BMS, Roche, Novartis, Almirall Hermal, MSD, Amgen, SUN, Sanofi, Pierre-Fabre, 4SC, Bayer, MerckSerono, Pfizer, Immunocore. Research grants: Novartis, Pfizer, Johnson & Johnson, Amgen, Merck-Serono, SUN Pharma, Sanofi. Travel/meeting support: Roche, BMS, SUN, Merck-Serono, Pierre-Fabre, outside the submitted work. CB received advisory board honoraria and/or speaker´s fees from Amgen, BMS, Immunocore, Merck, MSD, Novartis, Pierre Fabre, Regeneron, Roche, and Sanofi-Aventis. SU declares research support from Bristol Myers Squibb and Merck Serono; speakers and advisory board honoraria from Bristol Myers Squibb, Merck Sharp & Dohme, Merck Serono, Novartis and Roche, and travel support from Bristol Myers Squibb, Merck Sharp & Dohme, and Pierre Fabre. JB is receiving speaker's bureau honoraria from Amgen, Pfizer, Recordati and Sanofi, is a paid consultant/advisory board member/DSMB member for Almirall, Boehringer Ingelheim, InProTher, ICON, MerckSerono, Pfizer, 4SC, and Sanofi/Regeneron. His group receives research grants from Bristol-Myers Squibb, Merck Serono, HTG, IQVIA, and Alcedis. EL served as consultant and/or has received honoraria from Bristol-Myers Squibb, Merck Sharp & Dohme, Novartis, Medac, Pierre Fabre, Sanofi, Sunpharma and travel support from Amgen, Merck Sharp & Dohme, Bristol-Myers Squibb, Pierre Fabre, Sunpharma and Novartis, outside the submitted work. FM has received travel support or/and speaker's fees or/and advisor's honoraria by Novartis, Roche, BMS, MSD and Pierre Fabre and research funding from Novartis and Roche. JH received research support from BMS; advisory board honoraria from Pierre Fabre, Sanofi, Sun Pharma and MSD; speakers honoraria from GSK, Amgen, BMS, MSD, Novartis, Roche, Sanofi and Almirall and travel support from Pierre Fabre and 4SC. DS reports personal fees and non-financial support from Roche/Genentech, grants, personal fees, non-financial support and other from BMS, personal fees from Merck Sharp & Dohme, personal fees and non-financial support from Merck Serono, grant, personal fees and non-financial support from Amgen, personal fees from Immunocore, personal fees from Incyte, personal fees from 4SC, personal fees from Pierre Fabre, personal fees and non-financial support from Sanofi/Regeneron, personal fees from Array BioPharma, personal fees from Pfizer, personal fees from Philogen, personal fees from Regeneron, personal fees from Nektar, personal fees from Sandoz, grants, personal fees and non-financial support from Novartis, personal fees and non-financial support from SunPharma, Replimune, Helsinn, OncoSec and InFlaRx outside the submitted work. LH reports Consultancy, speaker fees, travel grants or research funding: BMS, MSD, Merck, Roche, Amgen, Curevac, Novartis, Sanofi, Pierre Fabre. Clinical studies: BMS, MSD, Merck, Roche, Amgen, GSK, Curevac and Novartis. LZ reports being a consultant and/or receiving honoraria from Roche, Bristol-Myers Squibb, Merck Sharp & Dohme, Novartis, Pierre-Fabre, Sunpharma and Sanofi; research funding to institution from Novartis; and travel support from Merck Sharp & Dohme, Bristol-Myers Squibb, Amgen, Pierre-Fabre, Sanofi, Sunpharma and Novartis, outside the submitted work.

The remaining authors declare that the research was conducted in the absence of any commercial or financial relationships that could be construed as a potential conflict of interest.

Publisher's Note: All claims expressed in this article are solely those of the authors and do not necessarily represent those of their affiliated organizations, or those of the publisher, the editors and the reviewers. Any product that may be evaluated in this article, or claim that may be made by its manufacturer, is not guaranteed or endorsed by the publisher.

Copyright © 2021 Zaremba, Kramer, De Temple, Bertram, Salzmann, Gesierich, Reinhardt, Baroudjian, Sachse, Mechtersheimer, Johnson, Weppler, Spain, Loquai, Dudda, Pföhler, Hepner, Long, Menzies, Carlino, Lebbé, Enokida, Tahara, Bröckelmann, Eigentler, Kähler, Gutzmer, Berking, Ugurel, Stadtler, Sucker, Becker, Livingstone, Meier, Hassel, Schadendorf, Hanoun, Heinzerling and Zimmer. This is an open-access article distributed under the terms of the Creative Commons Attribution License (CC BY). The use, distribution or reproduction in other forums is permitted, provided the original author(s) and the copyright owner(s) are credited and that the original publication in this journal is cited, in accordance with accepted academic practice. No use, distribution or reproduction is permitted which does not comply with these terms.

frontiers in Oncology

ORIGINAL RESEARCH
published: 16 November 2021
doi: 10.3389/fonc.2021.737399

Prognosis for Cutaneous Melanoma by Clinical and Pathological Profile: A Population-Based Study

Alessandra Buja[1], Andrea Bardin[1], Giovanni Damiani[2,3,4], Manuel Zorzi[5], Chiara De Toni[1], Riccardo Fusinato[1], Romina Spina[6], Antonella Vecchiato[6], Paolo Del Fiore[6], Simone Mocellin[6,7], Vincenzo Baldo[1], Massimo Rugge[5,8] and Carlo Riccardo Rossi[7]*

[1] Department of Cardiologic, Vascular and Thoracic Sciences, and Public Health, University of Padua, Padua, Italy, [2] Clinical Dermatology, Istituto di Ricovero e Cura a Carattere Scientifico (IRCCS) Istituto Ortopedico Galeazzi, Milan, Italy, [3] Department of Biomedical, Surgical and Dental Sciences, University of Milan, Milan, Italy, [4] PhD Program in Pharmacological Sciences, Department of Pharmaceutical and Pharmacological Sciences, University of Padua, Padua, Italy, [5] Veneto Tumor Registry - Azienda Zero, Padova, Italy, [6] Surgical Oncology Unit, Veneto Institute of Oncology IOV-Istituto di Ricovero e Cura a Carattere Scientifico (IRCCS), Padova, Italy, [7] Department of Surgery, Oncology and Gastroenterology (DISCOG), University of Padua, Padova, Italy, [8] Department of Medicine DIMED, Surgical Pathology & Cytopathology Unit, University of Padova, Padova, Italy

OPEN ACCESS

Edited by:
Elisabeth Livingstone, University Hospital of Essen, Germany

Reviewed by:
Piotr Rutkowski, Maria Sklodowska-Curie National Research Institute of Oncology, Poland
Tapas Ranjan Behera, Cleveland Clinic, United States

***Correspondence:**
Alessandra Buja
alessandra.buja@unipd.it

Specialty section:
This article was submitted to Skin Cancer, a section of the journal Frontiers in Oncology

Received: *06 July 2021*
Accepted: *25 October 2021*
Published: *16 November 2021*

Citation:
Buja A, Bardin A, Damiani G, Zorzi M, De Toni C, Fusinato R, Spina R, Vecchiato A, Del Fiore P, Mocellin S, Baldo V, Rugge M and Rossi CR (2021) Prognosis for Cutaneous Melanoma by Clinical and Pathological Profile: A Population-Based Study. Front. Oncol. 11:737399. doi: 10.3389/fonc.2021.737399

Introduction: Among white people, the incidence of cutaneous malignant melanoma (CMM) has been increasing steadily for several decades. Meanwhile, there has also been a significant improvement in 5-year survival among patients with melanoma. This population-based cohort study investigates the five-year melanoma-specific survival (MSS) for all melanoma cases recorded in 2015 in the Veneto Tumor Registry (North-Est Italian Region), taking both demographic and clinical-pathological variables into consideration.

Methods: The cumulative melanoma-specific survival probabilities were calculated with the Kaplan-Meier method, applying different sociodemographic and clinical-pathological variables. Cox's proportional hazards model was fitted to the data to assess the association between independent variables and MSS, and also overall survival (OS), calculating the hazard ratios (HR) relative to a reference condition, and adjusting for sex, age, site of tumor, histotype, melanoma ulceration, mitotic count, tumor-infiltrating lymphocytes (TIL), and stage at diagnosis.

Results: Compared with stage I melanoma, the risk of death was increased for stage II (HR 3.31, 95% CI: 0.94-11.76, p=0.064), almost ten times higher for stage III (HR 10.51, 95% CI: 3.16-35.02, p<0.001), and more than a hundred times higher for stage IV (HR 117.17, 95% CI: 25.30-542.62, p<0.001). Among the other variables included in the model, the presence of mitoses and histological subtype emerged as independent risk factors for death.

Conclusions: The multivariable analysis disclosed that older age, tumor site, histotype, mitotic count, and tumor stage were independently associated with a higher risk of death. Data on survival by clinical and morphological characteristics could be useful in modelling, planning, and managing the most appropriate treatment and follow-up for patients with CMM.

Keywords: melanoma, clinical characteristics, survival, epidemiology, cancer survival

INTRODUCTION

In recent decades, the incidence of cutaneous malignant melanoma (CMM) in white people has been increasing steadily (1, 2). Meanwhile, a significant improvement in CMM patients' 5-year overall survival has also been reported, and related mostly to the increasing prevalence of cancers detected in their earliest, "thinner" stage" (3, 4). Both the rising incidence of CMM (all stages), and changes in the treatment panorama (also including the advent of targeted therapies) prompt the collection of updated information which might re-orient both prevention efforts and diagnostic/therapeutic strategies.

Based on the natural history of CMM, a well-established set of clinicopathological variables has been significantly correlated with the clinical outcome of melanoma patients. Unfortunately, these data are often inconsistently recorded and/or scattered over different digital archives. This situation interferes with efforts to validate prognostic variables in the "real world" of large-scale population-based studies.

As for the stage-specific survival of CMM patients, most information comes from national cancer registries, and the USA American Surveillance, Epidemiology and End Results program (SEER) in particular (5). To the best of our knowledge, few registry-based studies on the stage-specific survival of CMM patients have been conducted in Italy or elsewhere in Europe in the last two decades (6–10).

The present study investigates the five-year melanoma-specific survival (MSS) for all cases of CMM recorded in 2015 in the resident population of a north-eastern Italian region (Veneto). Both demographic and clinical-pathological variables have been considered to measure their impact on patient survival in this cohort of CMM patients.

MATERIALS AND METHODS

Context

The Italian public national health service (NHS) is financed mainly by general taxation, and is largely managed on a regional basis. NHS policies are grounded on fundamental values of universality, free access, freedom of choice, pluralism in provision, and equity.

In the north-eastern Veneto region of Italy, the Regional Authority has endorsed a number of standardized Diagnostic Therapeutic Protocols (DTPs) for the clinical management of cancer patients. All DPTs have been edited by multidisciplinary task forces including dedicated experts belonging to the Regional Oncology Network (ROV).

This retrospective study on the outcome of CMM patients is based on clinico-pathological information recorded by the Veneto Cancer Registry in 2015 (11).

Study Participants and Data Collection

This retrospective population-based study involves a cohort of 1,279 incident cases of CMM diagnosed in the Veneto region in 2015 (resident population: 4,915,123). For each patient, the following set of clinical-pathological features were considered: a) tumor site (lower limbs, upper limbs, head, hands/feet, trunk); b) CMM histological subtype (lentigo maligna, acral lentiginous, blue nevus, desmoplastic, nodular, superficial spreading, spitzoid); b) growth phase (radial *versus* vertical); c) histologically-proven ulceration (present *versus* absent); d) number of mitoses (categorized as 0-2 or >2) (12); e) tumor-infiltrating lymphocytes, ([TILs] absent *versus* present; f) TNM stage, as established by merging clinical and pathological information available at the time of patient enrolment (13).

Patients were grouped by age in the following brackets: < 40, 40-49, 50-59, 60-69,70-79, 80 years or more.

Statistical Analysis

The number of person-years in the cohort was calculated by taking the date of entry as the time when a tumor was diagnosed, and the date of exit as 31 December 2020 or the time of death or drop-out from follow-up, whichever came first. Patient deaths were considered in the overall survival (OS) analysis regardless of their cause, while only deaths caused by melanoma were considered in the analysis of MSS. The cumulative MSS rates were calculated with the Kaplan-Meier method using different sociodemographic and histopathologic features. Cox's proportional hazards model was fitted to the data to assess the association between both MSS and OS and the previously-detailed independent variables (except for growth type as this variable perfectly predicted the outcome). In the multivariate analysis, we grouped the less common histological categories (acral-lentiginous, blue nevus, desmoplastic, spitzoid) as "Other". A sensitivity analysis was performed, excluding stage IV patients from the multivariate analysis. The assumption of proportionality was accepted for all models. Statistical significance was ascertained using an alpha level of 0.05 and two-sided tests. All data analyses were run using the R statistical package (version 3.6.3; R Studio, Boston, MA).

Ethics

The data analysis was performed on anonymous aggregated data with no chance of individuals being identifiable. Ethical approval for the study was obtained from the Veneto Oncological Institute's Ethics Committee (n. 52/2016).

RESULTS

In 2015, the Veneto Cancer Registry 1,279 incident CMM-patient were registered at. **Table 1** shows patients' demographics (M/F: 1.13; median age: 58 years) and clinical-pathological profiles. Most of the invasive malignancies were diagnosed in the early stage (stage I: 71.8%). The mean follow-up was 1,670 ± 415 days.

Overall, the 5-year OS was 83.8% (95% CI: 81.8, 85.8) and it was higher for females (86.6%; 95% CI: 84.0, 89.4) than for males (81.2%; 95% CI: 78.4, 84.2). Five-year MSS was 92.5% (95% CI: 91.0, 94.0), with no significant survival advantage for females (93.6%; CI: 91.7, 95.6) over males (91.5%; CI: 89.4, 93.7).

TABLE 1 | Baseline characteristics of the study cohort (NOS, not otherwise specified; TILs, tumor infiltrating lymphocytes).

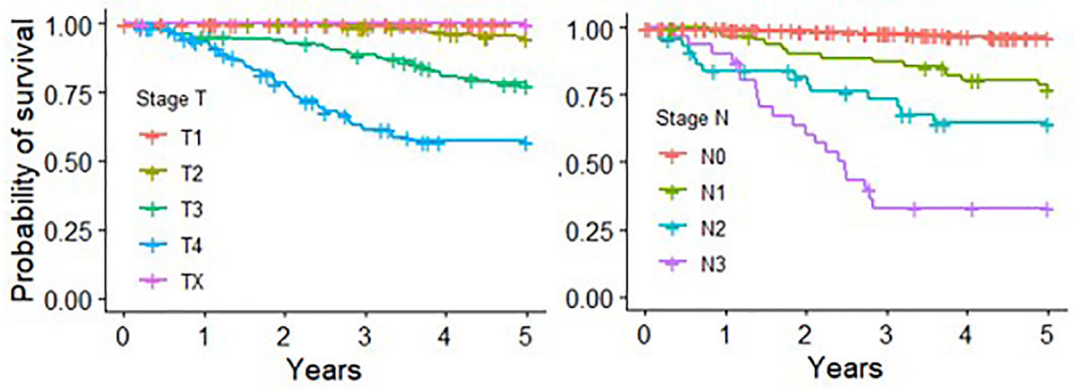
	Number (%)		Number (%)
All patients	1,279 (100)	**Mitotic count**	
Sex		0-2	798 (62.39)
Male	678 (53.0)	>2	252 (19.70)
Female	601 (47.0)	Not known	229 (17.91)
Age (years)		**TILs**	
<40	155 (12.1)	Present	927 (72.5)
40-49	252 (19.7)	Absent	189 (14.8)
50-59	252 (19.7)	Not known	163 (12.7)
60-69	257 (20.1)	**Tumor status (T)**	
70-79	217 (17)	T1	820 (64.1)
80+	146 (11.4)	T2	167 (13.1)
Tumor site		T3	126 (9.8)
Lower limbs	260 (20.33)	T4	98 (7.7)
Upper limbs	195 (15.25)	TX	14 (1.1)
Head	133 (10.40)	Not known	54 (4.2)
Hands/feet	56 (4.38)	**Nodal status (N)**	
Trunk	593 (46.36)	N0	1,119 (87.5)
Not known	42 (3.28)	N1	64 (5)
Histological subtype		N2	45 (3.5)
Superficial spreading melanoma	926 (72.40)	N3	31 (2.4)
Nodular melanoma	159 (12.43)	Not known	20 (1.6)
Lentigo maligna	28 (2.19)	**Metastasis status (M)**	
Acral-lentiginous melanoma	25 (1.95)	M0	1,225 (95.78)
Desmoplastic melanoma	4 (0.31)	M1	26 (2.03)
Blue nevus	1 (0.08)	Not known	28 (2.19)
Spitzoid melanoma	28 (2.19)	**TNM Stage (enrolment)**	
NOS Malignant melanoma	34 (2.66)	I	918 (71.8)
Growth phase		II	161 (12.6)
Horizontal	285 (22.3)	III	117 (9.1)
Vertical	701 (54.8)	IV	26 (2)
Not known	293 (22.9)	Not known	57 (4,5)
Ulceration		**Sentinel lymph node (*)**	
Yes	202 (15.8)	Performed	360 (0.45)
No	1,003 (78.4)	Not performed	86 (80.35)
Not known	74 (5.8)	Not known	2 (19.20)

(*) Only for patients with stage pT1b-pT4b and on stage I-II.

Figure 1 shows Kaplan-Meier MSS curves by TNM clinical-pathological staging at initial diagnosis, which had a strong impact on survival; T, N and M values are also reported. The 5-year MSS was 99.4% (95% CI: 98.9-100.0) for stage I, 82.6% (95% CI: 76.6-89.0) for stage II, 69.3% (95% CI: 61.0-78.7) for stage III, and only 23.0% (95% CI: 10.3-51.4) for stage IV.

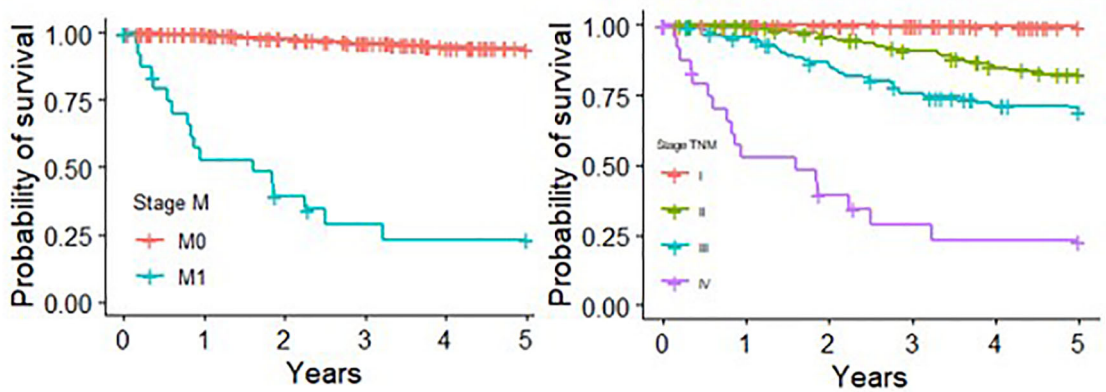
Figures 2, **3** show the Kaplan-Meier MSS curves by each of the pathological variables considered at initial diagnosis (histological subtype, growth phase, mitotic index, ulceration, TILs). The 5-year MSS probability was 99.2% for the category 0-2 mitoses (95% CI: 98.6-99.8), and 76.2% (95% CI: 70.9-82.0) for more than 2 mitoses. Melanoma ulceration significantly affected the probability 5-year MSS (97.6%; 95%CI: 96.7-98.6 without ulceration *versus* 72.5%; 95% CI: 66.2-79.3). As for the tumor's growth phase, survival was better for cases described as RGP (radial growth phase) at diagnosis than for those described as VGP (vertical growth phase): the 5-year MSS probability was 100.0% (95%CI: 100.0-100.0) for the former, and 91.6% (95%CI: 89.6- 93.8) for the latter. TIL status (presence *versus* absence) was associated with a small, but significant impact on 5-year MSS probability(94.4%, 95%CI: 92.9-95.9 *versus* 90.5%, 95%CI: 86.4-94.9, respectively). Finally, the survival analysis by histological subtype at diagnosis showed that nodular melanoma carried the worst 5-year MSS probability, at 70.3% (95%CI: 63.2-78.1). Superficial spreading melanoma had the highest 5-year MSS probability, at 96.9% (95% CI: 95.8-98.1). Intermediate survival probabilities were revealed for lentigo maligna melanoma (92.9%, 95% CI: 83.8-100.0).

Table 2 shows the results of Cox's regression model for MSS, adjusting for sex, age, histological subtype, ulceration, mitoses, site of tumor, stage at diagnosis and TILs. Compared with patients with a melanoma in stage I, the risk of death was increased for stage II (HR=3.31, 95% CI: 0.94-11.76, p=0.064), it was almost ten times higher for stage III (HR=10.51, 95% CI: 3.16-35.02, p<0.001), and it was more than a hundred times higher for stage IV (HR=117.17, 95% CI: 25.30-542.62, p<0.001). Superficial spreading melanoma carried a more than eleven times greater risk of death than lentigo maligna (HR=12.61, 95% CI: 1.42-112.02, p=0.023), and nodular melanoma a fourteen times higher risk (HR=15.04, 95% CI: 1.69-133.30, p=0.015). Sites of tumor involving the lower limbs, upper limbs and trunk had a better prognosis than those involving



Stage T	Sample	Deaths	Survival	95% CI	Log-rank test
T1	820	1	99.9	[99.6, 100.00]	<0.001
T2	167	8	94.9	[91.5, 98.4]	
T3	126	27	77.4	[70.2, 85.3]	
T4	98	35	57.2	[47.3, 69.2]	
TX	14	0	100.0	[100.0, 100.0]	

Stage N	Sample	Deaths	Survival	95% CI	Log-rank test
N0	1119	39	96.4	[95.3, 97.5]	<0.001
N1	64	14	77.0	[67.1, 88.4]	
N2	45	14	64.7	[51.1, 81.8]	
N3	31	20	32.9	[19.6, 55.2]	



Stage M	Sample	Deaths	Survival	95% CI	Log-rank test
M0	1225	68	94.2	[92.9, 95.5]	<0.001
M1	26	17	23.0	[10.3, 51.4]	

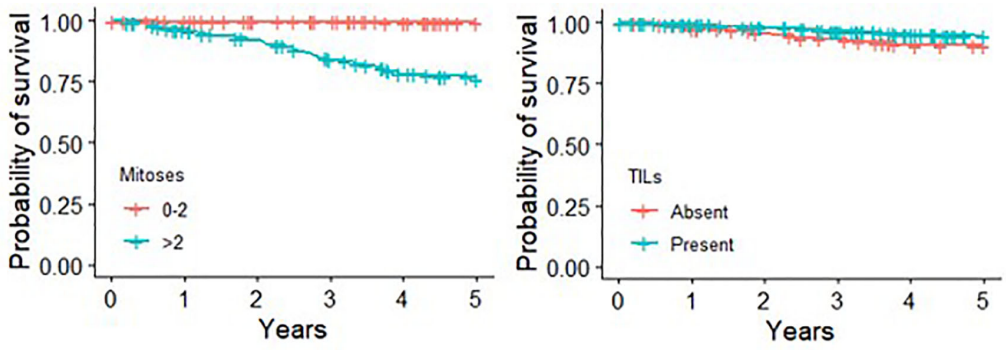
Stage TNM	Sample	Deaths	Survival	95% CI	Log-rank test
I	918	5	99.4	[98.9, 100.0]	<0.001
II	161	25	82.6	[76.6, 89.0]	
III	117	33	69.3	[61.0, 78.7]	
IV	26	17	23.0	[10.3, 51.4]	

FIGURE 1 | Kaplan-Meier curves for melanoma-specific survival by stage (T, N or M, and TNM overall).

the hands and feet, with the difference reaching borderline statistical significance (p=0.058, p=0.083, p=0.066). Among the other variables included the model, the presence of mitoses emerged as an independent risk factor for death (HR=6.85, 95%CI: 2.21-21.28, p<0.001). The sensitivity analysis, excluding stage IV, generated much the same results as the previous model (data not shown). The analysis of overall survival produced similar results too, except that male sex coincided with a significantly worse prognosis (HR=1.75, % CI: 1.18-2.60, p=0.005).

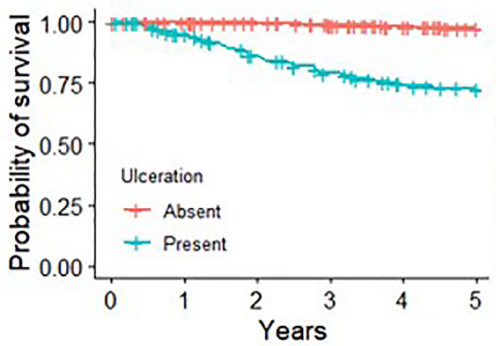
DISCUSSION

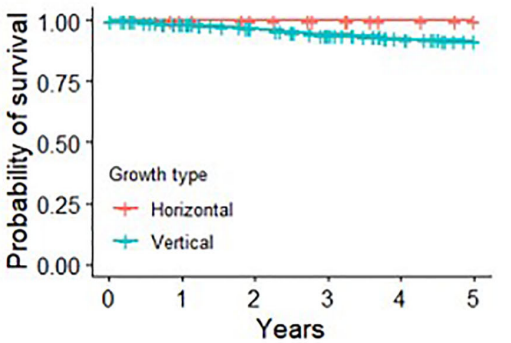
In a population-based cohort of 1,279 incident CMM patients, this study focuses on the prognostic impact of both



Mitoses	Sample	Deaths	Survival	95% CI	Log-rank test
0-2	798	6	99.2	[98.6, 99.8]	<0.001
≥2	252	55	76.2	[70.9, 82.0]	

TILs	Sample	Deaths	Survival	95% CI	Log-rank test
Absent	189	17	90.5	[86.4, 94.9]	0.040
Present	927	50	94.4	[92.9, 95.9]	





Ulceration	Sample	Deaths	Survival	95% CI	Log-rank test
Absent	1003	23	97.6	[96.7, 98.6]	<0.001
Present	202	50	72.5	[66.2, 79.3]	

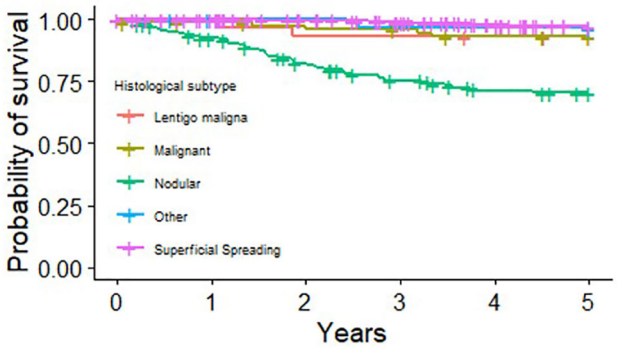
Growth type	Sample	Deaths	Survival	95% CI	Log-rank test
Horizontal	285	0	100.0	[100.0, 100.0]	<0.001
Vertical	701	56	91.6	[89.6, 93.8]	

FIGURE 2 | Kaplan-Meier curves for melanoma-specific survival by presence of ulceration, growth phase, presence of TIL.

demographics and clinical-pathological variables, as recorded in a high-resolution Italian cancer registry.

The results obtained prompt two main types of consideration: one refers to the validation of the CMM-associated prognostic variables in a large cohort of consecutive patients; the other relates to the value of population-based trials for the purpose of updating/improving patient management based on a critical analysis of real-world clinical practice.

As regards the first point, the present results support the prognostic impact of (mostly) well-established clinical-pathological variables (6, 14, 15). In particular, the Kaplan-Meier analysis showed that none of the RGP CMMs resulted in a melanoma-specific death within 5 years after the initial diagnosis (16). The present results also provide evidence to show that extra-nodal metastases from RGP CMMs are extremely rare (less than 3%), while almost all extra-nodal metastatic implants result from "vertically-growing" CMMs (17). Consistently with these findings, both the worst MSS rate and the highest risk of CMM-related death were associated with nodular CMMs. Based on the assumption that any greater risk associated with a nodular histology overlaps with the prognostic impact of a melanoma's thickness and ulceration, the American Joint Committee on



Histological subtype	Sample	Deaths	Survival at 5 years	95% CI	Log-rank test
Lentigo maligna	28	2	92.9	[83.8, 100.0]	<0.001
Nodular melanoma	159	44	70.3	[63.2, 78.1]	
Superficial spreading melanoma	926	27	96.9	[95.8, 98.1]	
Malignant melanoma	74	5	93.0	[87.2, 99.1]	
Other	58	2	96.4	[91.7, 100.0]	

FIGURE 3 | Kaplan-Meier curves for melanoma-specific survival by histological subtype and presence of mitoses.

TABLE 2 | Cox's regression analysis on cutaneous melanoma-specific survival patients, adjusting for sex, age, histological subtype, ulceration, mitotic count, CMM site, stage and TILs, as assessed at the patient's enrolment.

		HR	95% CI	P value
Sex	Female	1.00	–	–
	Male	1.67	0.87 - 3.21	0.120
Age	<40	1.00	–	–
	40-49	1.45	0.17 - 13.55	0.743
	50-59	2.19	0.24 - 20.32	0.489
	60-69	3.28	0.41 - 26.39	0.265
	70-79	7.95	1.02 - 61.91	0.048
	80 or more	3.58	0.43 - 29.79	0.238
CMM site	Hands/feet	1.00	–	–
	Lower limbs	0.34	0.11 - 1.04	0.058
	Upper limbs	0.34	0.10 - 1.15	0.083
	Head	1.83	0.62 - 5.40	0.272
	Hands/feet	1.00	–	–
	Trunk	0.39	0.15 - 1.06	0.066
CMM Histological subtype	Lentigo maligna	1.00	–	–
	Nodular m.	15.04	1.69 - 133.30	0.015
	Superficial spreading m.	12.61	1.42 - 112.02	0.023
	NOS cutaneous m.	6.07	0.46 - 79.67	0.170
	Others	3.26	0.16 - 67.66	0.444
CMM Ulceration	Present	1.00	–	–
	Absent	0.82	0.41 - 1.62	0.562
CMM Mitotic number	0-2	1.00	–	–
	>2	6.85	2.21 - 21.28	<0.001
CMM TILs	Absent	1.00	–	–
	Present	1.70	0.80 - 3.59	0.166
CMM TNM stage	I	1.00	–	–
	II	3.31	0.94 - 11.76	0.064
	III	10.51	3.16 - 35.02	<0.001
	IV	117.17	25.30 - 542.62	<0.001

CMM, cutaneous melanoma; NOS, not otherwise specified; TILs, tumor infiltrating lymphocytes; m, melanoma.
HR, hazard ratio; Assumption of proportionality: p-value 0.577.

Cancer (AJCC)'s staging system does not include the CMM subtype among the "discriminating" prognostic variables (14, 15). A recent analysis of the SEER cohort (18) nonetheless identifies the histological subtype as an independent predictor of survival, even after adjusting for CMM stage, thickness, ulceration, and mitotic index.

Previous studies found that the mitotic rate (more than neoplastic ulceration) is an independent prognostic factors in primary CMMs (irrespective of their thickness) (19–26). The present results associate a number of mitoses with a worse survival, further supporting the inclusion of the mitotic rate in the staging of thin, non-ulcerated CMMs.

A high-resolution cancer registry primarily needs to contain comprehensive, reliable, and accessible clinical information. All these conditions are hard to achieve, and the present study is no exception. In fact, our study suffered from the difficulty of assembling the necessary clinicopathological data, largely because of inconsistencies in the data format and/or their location in different digital repositories. The present study also suffers from a lack of important information on patients' socio-economic profiles and - even more important - data on the molecular biology profile of the malignancies considered (27). In this respect, the present study further supports the crucial importance of promoting standardized/synoptic formats in the recording of clinicopathological variables, as obtained by the main clinical actors involved in patient management (especially oncologists, radiologists, and clinical and surgical pathologists).

Inconsistencies in the recording of diagnostic procedures and the "scattering" of results in different datasets represent major limits to operative efforts to pursue the high-resolution cancer registration potentially capable of providing both clinicians and healthcare policy-makers with reliable information on the clinical management of CMM patients.

DATA AVAILABILITY STATEMENT

The data analyzed in this study is subject to the following licenses/restrictions: The dataset generated as part of the present study is not publicly available, but available from the corresponding author (alessandra.buja@unipd.it) on reasonable request. Requests to access these datasets should be directed to alessandra.buja@unipd.it.

ETHICS STATEMENT

The studies involving human participants were reviewed and approved by Veneto Oncological Institute Ethics Committee (n 695/20.10.2016). Written informed consent for participation was not required for this study in accordance with the national legislation and the institutional requirements.

AUTHOR CONTRIBUTIONS

ABu and GD conceived the presented idea. MZ, RS, AV, PF, and SM collected the data, verified its accuracy, and developed the methods. CT verified the analyses. ABa, ABu, and RF wrote the draft. MR, VB, GD, and ABu. supervised the project and revised the draft. CR found the financial support for the project. All authors read and approved the final manuscript.

FUNDING

CARIPARO - Fondazione Cassa di Risparmio di Padova e Rovigo.

REFERENCES

1. Arnold M, Holterhues C, Hollestein LM, Coebergh JW, Nijsten T, Pukkala E, et al. Trends in Incidence and Predictions of Cutaneous Melanoma Across Europe Up to 2015. *J Eur Acad Dermatol Venereol* (2014) 28(9):1170–8. doi: 10.1111/jdv.12236
2. Jemal A, Saraiya M, Patel P, Cherala SS, Barnholtz-Sloan J, Kim J, et al. Recent Trends in Cutaneous Melanoma Incidence and Death Rates in the United States, 1992-2006. *J Am Acad Dermatol* (2011) 65(5 Suppl 1):S17–25.e1-3. doi: 10.1016/j.jaad.2011.04.032
3. Thomas L, Tranchand P, Berard F, Secchi T, Colin C, Moulin G. Semiological Value of ABCDE Criteria in the Diagnosis of Cutaneous Pigmented Tumors. *Dermatology* (1998) 197(1):11–7. doi: 10.1159/000017969
4. Leiter U, Keim U, Garbe C. Epidemiology of Skin Cancer: Update 2019. *Adv Exp Med Biol* (2020) 1268:123–39. doi: 10.1007/978-3-030-46227-7_6
5. Howlader N, Noone AM, Krapcho M, Miller D, Brest A, Yu M, et al. eds. *SEER Cancer Statistics Review, 1975-2018*. Bethesda, MD: National Cancer Institute (2021). Available at: https://seer.cancer.gov/csr/1975_2018/. based on November 2020 SEER data submission, posted to the SEER web site, April 2021.
6. Svedman FC, Pillas D, Taylor A, Kaur M, Linder R, Hansson J. Stage-Specific Survival and Recurrence in Patients With Cutaneous Malignant Melanoma in Europe - A Systematic Review of the Literature. *Clin Epidemiol* (2016) 8:109–22. doi: 10.2147/CLEP.S99021
7. Mandalà M, Imberti GL, Piazzalunga D, Belfiglio M, Labianca R, Barberis M, et al. Clinical and Histopathological Risk Factors to Predict Sentinel Lymph Node Positivity, Disease-Free and Overall Survival in Clinical Stages I-II AJCC Skin Melanoma: Outcome Analysis From a Single-Institution Prospectively Collected Database. *Eur J Cancer* (2009) 45(14):2537–45. doi: 10.1016/j.ejca.2009.05.034
8. Balzi D, Carli P, Giannotti B, Buiatti E. Skin Melanoma in Italy: A Population-Based Study on Survival and Prognostic Factors. *Eur J Cancer* (1998) 34 (5):699–704. doi: 10.1016/s0959-8049(97)10119-8
9. Cascinelli N, Bombardieri E, Bufalino R, Camerini T, Carbone A, Clemente C, et al. Sentinel and Nonsentinel Node Status in Stage IB and II Melanoma Patients: Two-Step Prognostic Indicators of Survival. *J Clin Oncol* (2006) 24 (27):4464–71. doi: 10.1200/JCO.2006.06.3198
10. Testori A, De Salvo GL, Montesco MC, Trifirò G, Mocellin S, Landi G, et al. Clinical Considerations on Sentinel Node Biopsy in Melanoma From an Italian Multicentric Study on 1,313 Patients (SOLISM-IMI). *Ann Surg Oncol* (2009) 16(7):2018–27. doi: 10.1245/s10434-008-0273-8
11. Guzzinati S, Zorzi M, Rossi CR, Buja A, Italiano I, Fiore AR, et al. High Resolution Registry of Melanoma and Care Pathways Monitoring in the Veneto Region, Italy. In: *ENCR Scientific Meeting*. Copenaghen. Available at: https://www.registrotumoriveneto.it/it/pubblicazioni/convegni/poster/101-2018/234-high-resolution-registry-of-melanoma-and-care-pathways-monitoring-in-the-veneto-region-italy (Accessed Last accessed July 2021).
12. Piñero-Madrona A, Ruiz-Merino G, Cerezuela Fuentes P, Martínez-Barba E, Rodríguez-López JN, Cabezas-Herrera J. Mitotic Rate as an Important

Prognostic Factor in Cutaneous Malignant Melanoma. *Clin Transl Oncol* (2019) 21(10):1348–56. doi: 10.1007/s12094-019-02064-4
13. Edge SB, Compton CC. The American Joint Committee on Cancer: The 7th Edition of the AJCC Cancer Staging Manual and the Future of TNM. *Ann Surg Oncol* (2010) 17(6):1471–4. doi: 10.1245/s10434-010-0985-4
14. Amin MB, Greene FL, Edge SB, Compton CC, Gershenwald JE, Brookland RK, et al. The Eighth Edition AJCC Cancer Staging Manual: Continuing to Build a Bridge From a Population-Based to a More "Personalized" Approach to Cancer Staging. *CA Cancer J Clin* (2017) 67(2):93–9. doi: 10.3322/caac.21388
15. Balch CM, Buzaid AC, Soong SJ, Atkins MB, Cascinelli N, Coit DG, et al. New TNM Melanoma Staging System: Linking Biology and Natural History to Clinical Outcomes. *Semin Surg Oncol* (2003) 21(1):43–52. doi: 10.1002/ssu.10020
16. Betti R, Agape E, Vergani R, Moneghini L, Cerri A. An Observational Study Regarding the Rate of Growth in Vertical and Radial Growth Phase Superficial Spreading Melanomas. *Oncol Lett* (2016) 12(3):2099–102. doi: 10.3892/ol.2016.4813
17. Elder D. Pathology of Melanoma. *Clin Cancer Res* (2006) 12)(7):2308s–11s. doi: 10.1158/1078-0432.CCR-05-2504
18. Lattanzi M, Lee Y, Simpson D, Moran U, Darvishian F, Kim RH, et al. Primary Melanoma Histologic Subtype: Impact on Survival and Response to Therapy. *J Natl Cancer Inst* (2019) 111(2):180–8. doi: 10.1093/jnci/djy086
19. Barnhill RL, Katzen J, Spatz A, Fine J, Berwick M. The Importance of Mitotic Rate as a Prognostic Factor for Localized Cutaneous Melanoma. *J Cutan Pathol* (2005) 32(4):268–73. doi: 10.1111/j.0303-6987.2005.00310.x
20. Vollmer RT. Malignant Melanoma: A Multivariate Analysis of Prognostic Factors. *Pathol Annu* (1989) 24:383.
21. Donizy P, Kaczorowski M, Leskiewicz M, Zietek M, Pieniazek M, Kozyra C, et al. Mitotic Rate Is a More Reliable Unfavorable Prognosticator Than Ulceration for Early Cutaneous Melanoma: A 5-Year Survival Analysis. *Oncol Rep* (2014) 32(6):2735–43. doi: 10.3892/or.2014.3531
22. Evans JL, Vidri RJ, MacGillivray DC, Fitzgerald TL. Tumor Mitotic Rate Is an Independent Predictor of Survival for Nonmetastatic Melanoma. *Surgery* (2018) 164(3):589–93. doi: 10.1016/j.surg.2018.04.016
23. Thompson JF, Soong SJ, Balch CM, Gershenwald JE, Ding S, Coit DG, et al. Prognostic Significance of Mitotic Rate in Localized Primary Cutaneous Melanoma: An Analysis of Patients in the Multi-Institutional American Joint Committee on Cancer Melanoma Staging Database. *J Clin Oncol* (2011) 29(16):2199–205. doi: 10.1200/JCO.2010.31.5812
24. Kashani-Sabet M, Miller JR 3rd, Lo S, Nosrati M, Stretch JR, Shannon KF, et al. Reappraisal of the Prognostic Significance of Mitotic Rate Supports its Reincorporation Into the Melanoma Staging System. *Cancer* (2020) 126 (21):4717–25. doi: 10.1002/cncr.33088
25. Tejera-Vaquerizo A, Pérez-Cabello G, Marínez-Leborans L, Gallego E, Oliver-Martínez V, Martín-Cuevas P, et al. Is Mitotic Rate Still Useful in the Management of Patients With Thin Melanoma? *J Eur Acad Dermatol Venereol* (2017) 31(12):2025–9. doi: 10.1111/jdv.14485
26. Damiani G, Buja A, Grossi E, Rivera M, De Polo A, De Luca G, et al. Use of an Artificial Neural Network to Identify Patient Clusters in a Large Cohort of Patients With Melanoma by Simultaneous Analysis of Costs and Clinical Characteristics. *Acta Derm Venereol* (2020) 100(18):adv00323. doi: 10.2340/00015555-3680
27. Rugge M. Gastric Cancer Risk: Between Genetics and Lifestyle. *Lancet Oncol* (2020) 21(10):1258–60. doi: 10.1016/S1470-2045(20)30432-0

Conflict of Interest: The authors declare that the research was conducted in the absence of any commercial or financial relationships that could be construed as a potential conflict of interest.

Publisher's Note: All claims expressed in this article are solely those of the authors and do not necessarily represent those of their affiliated organizations, or those of the publisher, the editors and the reviewers. Any product that may be evaluated in this article, or claim that may be made by its manufacturer, is not guaranteed or endorsed by the publisher.

Copyright © 2021 Buja, Bardin, Damiani, Zorzi, De Toni, Fusinato, Spina, Vecchiato, Del Fiore, Mocellin, Baldo, Rugge and Rossi. This is an open-access article distributed under the terms of the Creative Commons Attribution License (CC BY). The use, distribution or reproduction in other forums is permitted, provided the original author(s) and the copyright owner(s) are credited and that the original publication in this journal is cited, in accordance with accepted academic practice. No use, distribution or reproduction is permitted which does not comply with these terms.

frontiers in Oncology

ORIGINAL RESEARCH
published: 25 November 2021
doi: 10.3389/fonc.2021.752579

Profile of Basal Cell Carcinoma Mutations and Copy Number Alterations - Focus on Gene-Associated Noncoding Variants

*Paulina Maria Nawrocka[1], Paulina Galka-Marciniak[1], Martyna Olga Urbanek-Trzeciak[1], Ilamathi M-Thirusenthilarasan[1], Natalia Szostak[2], Anna Philips[2], Laura Susok[3], Michael Sand[3,4] and Piotr Kozlowski[1]**

[1] Department of Molecular Genetics, Institute of Bioorganic Chemistry, Polish Academy of Sciences, Poznan, Poland, [2] Laboratory of Bioinformatics, Institute of Bioorganic Chemistry, Polish Academy of Sciences, Poznan, Poland, [3] Department of Dermatology, Venereology and Allergology, St. Josef Hospital, Ruhr-University Bochum, Bochum, Germany, [4] Department of Plastic Surgery, St. Josef Hospital, Catholic Clinics of the Ruhr Peninsula, Essen, Germany Department of Plastic, Reconstructive and Aesthetic Surgery, St. Josef Hospital, Essen, Germany

OPEN ACCESS

Edited by:
Sapna Patel,
University of Texas MD Anderson Cancer Center, United States

Reviewed by:
Scott X Atwood,
University of California, Irvine, United States
Rogelio González Sarmiento,
University of Salamanca, Spain

***Correspondence:**
Piotr Kozlowski
kozlowp@ibch.poznan.pl

Specialty section:
This article was submitted to Skin Cancer, a section of the journal Frontiers in Oncology

Received: 03 August 2021
Accepted: 08 November 2021
Published: 25 November 2021

Citation:
Nawrocka PM, Galka-Marciniak P, Urbanek-Trzeciak MO, M-Thirusenthilarasan I, Szostak N, Philips A, Susok L, Sand M and Kozlowski P (2021) Profile of Basal Cell Carcinoma Mutations and Copy Number Alterations - Focus on Gene-Associated Noncoding Variants. Front. Oncol. 11:752579. doi: 10.3389/fonc.2021.752579

Basal cell carcinoma (BCC) of the skin is the most common cancer in humans, characterized by the highest mutation rate among cancers, and is mostly driven by mutations in genes involved in the hedgehog pathway. To date, almost all BCC genetic studies have focused exclusively on protein-coding sequences; therefore, the impact of noncoding variants on the BCC genome is unrecognized. In this study, with the use of whole-exome sequencing of 27 tumor/normal pairs of BCC samples, we performed an analysis of somatic mutations in both protein-coding sequences and gene-associated noncoding regions, including 5'UTRs, 3'UTRs, and exon-adjacent intron sequences. Separately, in each region, we performed hotspot identification, mutation enrichment analysis, and cancer driver identification with OncodriveFML. Additionally, we performed a whole-genome copy number alteration analysis with GISTIC2. Of the >80,000 identified mutations, ~50% were localized in noncoding regions. The results of the analysis generally corroborated the previous findings regarding genes mutated in coding sequences, including *PTCH1*, *TP53*, and *MYCN*, but more importantly showed that mutations were also clustered in specific noncoding regions, including hotspots. Some of the genes specifically mutated in noncoding regions were identified as highly potent cancer drivers, of which *BAD* had a mutation hotspot in the 3'UTR, *DHODH* had a mutation hotspot in the Kozak sequence in the 5'UTR, and *CHCHD2* frequently showed mutations in the 5'UTR. All of these genes are functionally implicated in cancer-related processes (e.g., apoptosis, mitochondrial metabolism, and *de novo* pyrimidine synthesis) or the pathogenesis of UV radiation-induced cancers. We also found that the identified *BAD* and *CHCHD2* mutations frequently occur in melanoma but not in other cancers *via* The Cancer Genome Atlas analysis. Finally, we identified a frequent deletion of chr9q, encompassing *PTCH1*, and

unreported frequent copy number gain of chr9p, encompassing the genes encoding the immune checkpoint ligands PD-L1 and PD-L2. In conclusion, this study is the first systematic analysis of coding and noncoding mutations in BCC and provides a strong basis for further analyses of the variants in BCC and cancer in general.

Keywords: basal cell carcinoma (BCC), cancer somatic mutations, noncoding mutations, immune checkpoint, copy number alterations, cancer drivers, TERT, DPH3

INTRODUCTION

Basal cell carcinoma (BCC), a type of nonmelanoma skin cancer, is the most common human cancer affecting predominantly elderly people of the Caucasian population (1–3). The lifetime risk of BCC in the Caucasian population is ~30%, and it is higher in men and fair-skinned people. BCC usually occurs sporadically but can also develop as a result of Gorlin syndrome (also known as nevoid basal cell carcinoma syndrome), an autosomal dominant hereditary condition with an incidence of approximately 1:30,000 (4) characterized by the frequent appearance of multiple BCC lesions that develop at a younger age together with skeletal abnormalities, odontogenic keratocysts, and an increased risk of medulloblastoma. Histologically, BCCs are classified into three major subtypes: nodular, which is the most common subtype; superficial; and infiltrative or sclerodermiform. Other subtypes as well as mixed types occur less frequently (5–7). Predominantly, superficial and nodular BCCs are slow-growing, locally invasive, epidermal tumors with a metastasis rate of <0.1% (8, 9), while infiltrative BCCs are characterized by more aggressive, tong-like, subclinical growth patterns mimicking icebergs, as they often grow below clinically healthy-looking skin (10, 11). Although BCC aggressiveness and metastatic potential are overall low, the commonness of BCC and the increasing incidence associated predominantly with aging populations has brought attention to its pathogenesis (2, 3, 12–17). Exposure to ultraviolet (UV) radiation, which can lead to point mutations frequently represented by C>T and CC>TT transitions, is the main causative factor in the pathogenesis of BCC (18). Additional risk factors include ionizing radiation, arsenic ingestion, and immune suppression (19, 20).

BCC is characterized by the highest mutation rate observed among cancers, having over 65 mutations/Mbp (14, 15). The most frequent genetic alterations occurring in BCC are mutations disturbing the hedgehog (SHH/PTCH1/SMO) pathway, predominantly loss-of-function mutations in *PTCH1* but also activating mutations in *SMO*; these genes encode two transmembrane proteins, PTCH1 (also known as Patched1) and SMO (also known as Smoothened), respectively (14, 15). The pathway is activated by the SHH signaling protein (also known as Sonic hedgehog), which binds to the extracellular domain of PTCH1, disabling inhibition of SMO; this in turn activates GLI transcription factors. Germline mutations in *PTCH1* predispose patients to Gorlin syndrome (21).

Previous studies, including whole-exome sequencing (WES) analyses, have also recognized other genes/pathways frequently mutated in BCC, including *TP53, MYCN, PPP6C, PTPN14, STK19*, and *LATS1* (14, 15), as well as genes involved in the RTK-RAS-PI3K and Hippo-YAP pathways (15). However, as an overwhelming majority of BCC genetic studies (as well as those in other cancers) have focused almost exclusively on protein-coding sequences, very little is known about mutations in noncoding regions (noncoding mutations). Noncoding mutations are not studied/reported even if detected, e.g., as a result of WES. On the other hand, it is well known that the noncoding parts of genes, i.e., promoters, introns, or 5' and 3' untranslated regions (5'UTRs and 3'UTRs, respectively), encompass numerous functional elements important for the proper functioning of the genes (22–24). Somatic mutations may disrupt or modify the properties of these elements, acting either as gain- or loss-of-function mutations and thus enhancing/accelerating or switching off the function of some genes. Despite the limited number of studies on noncoding mutations, there are some spectacular examples of noncoding driver mutations, for example, *TERT* promoter mutations, which occur most frequently in melanoma, brain, and bladder cancers but are also reported in BCC (25–27), and mutations in the precursor of miR-142, which frequently occur in non-Hodgkin lymphomas and acute myeloid leukemia [summarized in (28)]. The miRNA biogenesis enzyme DICER has also been shown to bear mutations that could play a role in aberrant miRNA expression in BCC (29–31). It should also be noted that an effort to catalog cancer somatic mutations in the noncoding genome has recently been undertaken (32, 33); however, this pancancer project does not include BCC.

To preliminarily explore the occurrence of noncoding somatic mutations in BCC, we performed WES of over two dozen BCC samples, extending the analysis beyond protein-coding sequences and focusing on gene-associated noncoding regions, i.e., 5'UTRs, 3'UTRs, and exon-adjusted sequences of introns, covered by standard WES approaches. Apart from the fact that our results well-replicate those of previous BCC studies in terms of mutations in protein-coding genes, we showed that a substantial portion of mutations is located in noncoding regions. Many of these mutations frequently recur in particular noncoding regions or in specific hotspot positions. Computational analyses showed that some of the gene mutations in noncoding regions are potential cancer drivers and are functionally related to skin cancers. Additionally, whole-genome copy number alteration (CNA) analysis revealed frequent deletion of chr9q, encompassing *PTCH1*, and unreported frequent amplification of chr9p, including the genes encoding two immune checkpoint ligands PD-L1 and PD-L2.

MATERIALS AND METHODS

Sample Collection and DNA Preparation

A total of 27 pairs of tissue (tumor and normal adjacent healthy skin) were collected from the Department of Plastic Surgery, St. Josef Hospital, Catholic Clinics of the Ruhr Peninsula, Essen, Germany. While excising the BCC tissues with cold steel under local anesthesia, 4-mm punch biopsies were taken from the center of the tumor and from nonlesional epithelial skin (as normal, intraindividual controls). These samples were immediately placed in RNAlater (Qiagen, Hilden, Germany) and stored at −80°C. Tissue homogenization was performed with stainless steel beads of 5 mm (Qiagen) and TissueLyser LT (Qiagen). DNA was extracted with an AllPrep DNA/RNA/miRNA Universal Kit (Qiagen) according to the manufacturer's protocol. All samples were quantified using a NanoDrop One (Thermo Scientific, Waltham, USA) and Qubit fluorometer 3.0 (Invitrogen) (Qubit dsDNA HS Assay (Life Technologies, Carlsbad, USA)), and DNA size and quality were tested using gel electrophoresis.

Exome Sequencing and Data Processing

The library was prepared with 200 ng of high-quality DNA using the SureSelectXT Library Prep Kit (Agilent). A SureSelectXT Human All Exon V6 kit (Agilent) was used for exome capture. Sequencing was performed on an Illumina NovaSeq 6000 (San Diego, USA), generating 2x 100 bp paired-end reads. Library preparation, exome enrichment, and sequencing were performed at CeGaT, Tuebingen, Germany. Demultiplexing of the sequencing reads was performed with Illumina bcl2fastq (2.19). Adapters were trimmed with Skewer (version 0.2.2) (34). The Phred score was given with Illumina standard Phred encoding (offset +33). For each sample, two FASTQ files corresponding to forward and reverse reads were obtained. Next steps were done by us on the Poznan Supercomputing and Networking Center (PSNC) Eagle supercomputer. Paired-end reads were aligned to hg38 using BWA. PCR duplicates were marked and removed with the Picard package. Indel realignments with known sites and base quality score recalibration were performed with GATK version 4.1.2.0. SAM to BAM conversion was done using SAMtools. Somatic single-nucleotide variants were called with MuTect2 (version 4.1.0.0. with the use of the tumor-normal mode). Additionally, to avoid false-positive somatic mutations, we performed filtering for germline variants present in the gnomAD database (version 2.1.1). We also generated and flagged variants with a panel of normals (PoN) comprising variants representing commonly occurring sequencing noise that may mimic low allele-fraction somatic variants. We also added information about the localization of mutations in gene subregions (CDS, 5'UTR, 3'UTR, or introns) by use of an in-house Python script. From the list of somatic mutations, we additionally removed those that did not fulfill the following criteria: (i) at least five alternative allele-supporting reads in a tumor sample; (ii) frequency of alternative allele-supporting reads in a tumor sample of at least 0.05; and (iii) frequency of alternative allele-supporting reads in the tumor sample at least 5× higher than that in the corresponding normal sample.

Validation of Mutations and Sequencing of the *TERT* and *DPH3* Promoters

A panel of 51 mutations detected by WES was validated by Sanger sequencing of the appropriate PCR fragments amplified with primers shown in **Table S1**. The primers used for amplification and sequencing of the *TERT* and *DPH3* promoters are shown in **Table S1**. All fragments were sequenced in two directions with the BigDye v3.1 kit (Applied Biosystems, Foster City, CA, USA), and the sequencing reactions were separated with capillary electrophoresis (POP7 polymer; ABI Prism 3130xl apparatus; Applied Biosystems, Foster City, CA, USA) according to the standard manufacturer's recommendations.

Mutational Signature Analysis

To analyze mutational signatures, we used the web application Mutational Signatures in Cancer [MuSiCa; http://bioinfo.ciberehd.org/GPtoCRC/en/tools.html (35)], allowing the visualization of the somatic mutational profile of each analyzed sample and estimation of the contribution values of the predefined mutational signatures [(36); Catalogue Of Somatic Mutations In Cancer, COSMIC 2020]. Samples BCC14 and BCC21 were excluded from the signature analysis due to an insufficient number of mutations.

Identification of Hotspots, Frequently Mutated Genes, and Cancer Drivers

We defined genomic positions mutated in at least 3 (>10%) samples as hotspots. Mutations occurring in directly adjacent nucleotides were merged into one hotspot.

We defined genes with nonsynonymous mutations in a coding region in at least 5 samples, with mutations in a 5'UTR, in at least 4 samples, with mutations in a 3'UTR in at least 4 samples, and with mutations in introns (up to 40 nt from exon/intron boundaries) in at least 5 samples as frequently mutated. From the analysis, we excluded genes known to be commonly hypermutated with passenger mutations as a result of the increased background mutation rate but not related to cancer, listed in (37). To distinguish synonymous from nonsynonymous mutations, we used the SnpEff - genetic variant annotation and functional effect prediction toolbox (38), available on the Subio platform (Subio, Inc., Kagoshima, Japan, http://www.subio.jp). We also considered splice-site mutations located in introns up to +/-2 nt from exons as coding region mutations.

OncodriveFML (39) was run using the CADD score (hg38, version 1.6). The signature method was set as a complement, the statistical method was set to "amean", and indels were included in the analysis using a max method (max_consecutive was set to 7 as default).

Copy Number Analysis

To identify chromosome arm-level and focal regions that were significantly amplified or deleted, we used GISTIC2 (40) with the following parameters: threshold for copy number amplifications and deletions, 0.2; confidence level to calculate the region containing a driver, 0.9; broad-level analysis; and the arm peel method to reduce noise.

To validate CNAs involving chromosome 9, i.e., chr9p duplications/amplifications (affecting *JAK2*, *PDL1*/*CD274*, and *PDL2*/*CD273*) and chr9q deletions (affecting *PTCH1*), we designed and generated an MLPA assay covering the entire chromosome 9. In total, the assay consisted of 20 probes, including (i) 7 probes distributed over the chr9p (n=5) and chr9q (n=2) arms, 2 probes located in or in close proximity to *JAK2*, *PDL2*, *PDL1*, and *PTCH1* (in total 8 gene-specific probes), and 5 control probes (located on different chromosomes outside of chromosome 9 and regions of known cancer-related genes). The sequences and detailed characteristics of all probes as well as their exact positions are shown in **Table S2**.

The MLPA probes and the probe-set layout were designed according to a previously proposed and well-validated strategy (41, 42). Shortly, each probe was composed of two half-probes of equal size, and the total probe length ranged from 93 to 172 nt. The target sequences for the probes were selected to avoid common SNPs, repeat elements, and sequences of extremely high or low GC content. The MLPA probes were synthesized by IDT (Skokie, IL, USA). The MLPA reactions were run according to the manufacturer's general recommendations (MRC-Holland, Amsterdam, the Netherlands). All reagents except the probe mixes were purchased from MRC-Holland (http://www.mlpa.com). The products of the MLPA reaction were subsequently diluted 20x in HiDi formamide containing GS Liz600, which was used as a DNA sizing standard, and separated *via* capillary electrophoresis (POP7 polymer) in an ABI Prism 3130XL apparatus (Applied Biosystems, Carlsbad, CA, USA). The obtained electropherograms were analyzed using GeneMarker software v2.4.0 (SoftGenetics, State College, PA, USA). For each individual sample, the signal intensity of each probe was divided by the geometric average signal intensity of the control probes to normalize the run-to-run signal variation, and then the normalized signal of each probe in cancer samples was divided by the corresponding signal in the corresponding normal samples and multiplied by 2. The final MLPA result of each sample is presented on a bar-plot, in which the bars show the relative copy number value of the subsequent probes.

TCGA Analysis

To compare the mutations recurring in BCC with mutations in other cancers, we used WES-generated somatic mutation datasets of 10,369 samples representing 33 cancer types generated and deposited in the TCGA repository (http://cancergenome.nih.gov). The full names and abbreviations of all TCGA cancer types are shown in **Table S3**. Somatic mutations were identified against matched normal samples with the use of the standard TCGA pipeline (including the Mutect2, Muse, Varscan, and SomaticSnipper algorithms). We extracted somatic mutation calls (with PASS annotation only) localized in the annotated exons of *BAD*, *DHODH*, *CHCHD2*, *FLG*, and *FLG2* (exon sequences were extended by 2 nt to enable identification of intronic splice-site mutations). The extraction was performed as described in our earlier study (43) with a set of in-house Python scripts available at (https://github.com/martynaut/mirnaome_somatic_mutations).

Mutations Visualization

All mutations were annotated according to HGVS nomenclature (at the transcript and protein levels), and the effects of mutations were defined using the Ensembl Variant Effect Predictor (VEP) tool. For visualization of mutations on gene maps, we used ProteinPaint from St. Jude Children's Research Hospital – PeCan Data Portal (44). The protein domains visualized on gene maps were positioned according to UniProt data (45). The comutation plot showing frequently mutated genes was created with the use of the Python library CoMut (46).

Analysis of RNA Regulatory Motifs

Target predictions were performed with the TargetScan Custom (release 5.2) web tool (47). The secondary RNA structures were predicted using mfold software (48) with default parameters. RNA sequence/structure functional motifs and transcription factor binding sites were analyzed with the RegRNA 2.0 (49) and MotifMap (50) web tools.

Statistics

Specific statistical tests are indicated in the text, and a p-value <0.05 was considered significant. If necessary, p-values were corrected for multiple tests with the Benjamini-Hochberg procedure.

RESULTS

Overall Sequencing and Mutation Occurrence Characterization

We performed WES on 27 paired tumor and corresponding intraindividual control skin DNA samples isolated from 22 nodular and 5 superficial BCC subtypes and corresponding healthy skin tissue. The average coverage of the targeted regions was 183x (185x in normal and 180x in tumor samples), ranging in different samples from 134x to 232x. In total, we identified 84,571 cancer-sample-specific somatic mutations (**Table S4**), of which 42,380 (50.1%) were located in protein-coding (coding) regions, and the remaining 42,191 (49.9%) were located in noncoding regions (**Table 1** and **Figure 1A**). The noncoding regions included (i) 5'UTRs, (ii) ~100 bp fragments of 3'UTRs adjacent to coding sequences (3'UTRs), (iii) exon-adjacent ~100 bp fragments of introns (introns), and (iv) sequences other than those classified above (i-iii), mostly intergenic sequences located upstream and downstream of the first and last gene exons (intergenic regions) (51). The average coverage of the mutated positions was 169x and was slightly higher in coding (195x) than in noncoding regions (142x), whereas the average fraction of reads mapping to alternative alleles was 0.35 (0.33 in coding and 0.40 in noncoding regions). The average mutation rate calculated based on the coding regions was 52.8 mutations/Mbp (ranging from 0.1 to 287.5), which, although slightly lower than that observed before in BCC (15, 52), is still higher than that in any other tested cancer type. Although somewhat counterintuitive, the lower mutation burden in our study than in other BCC studies (15, 52) may result from the much higher sequencing coverage in our study, which gave us much higher statistical power to filter out the fraction of

TABLE 1 | Summary of somatic mutation distribution and mutation types in BCC.

Genomic regions	No. (%) of mutations	Average coverage of mutation positions	Average alternative allele fraction	No. (%) of substitutions	No. (%) of double substitutions	No. (%) of short indels
all mutations	84,571 (100)	169	0.35	79,960 (94.5)	3128 (3.7)	1483 (1.8)
coding	42,380 (50.1)	195	0.33	40,503 (95.6)	1697 (4.0)	180 (0.4)
noncoding	42,191 (49.9)	142	0.37	39,457 (93.5)	1431 (3.4)	1303 (3.1)
introns	32,805 (38.8)	136	0.38	30,655 (93.4)	1076 (3.3)	1074 (3.3)
3'UTR	2,926 (3.5)	154	0.39	2,721 (93.0)	100 (3.4)	105 (3.6)
5'UTR	2,832 (3.3)	163	0.37	2,650 (93.6)	125 (4.4)	57 (2.0)
intergenic region	3,628 (4.3)	167	0.35	3,431 (94.6)	130 (3.6)	67 (1.8)

false-positive mutations. The lower mutation burden in our study may also be explained by the identification in our cohort of two samples with an extremely low mutational burden (<0.2 mutations/Mbp). Most of the identified mutations were single-nucleotide substitutions (79,960 (94.5%), predominantly C>T transitions), followed by double substitutions (3,128 (3.7%), predominantly CC>TT transitions) and short (<4 nt) indels (1.483 (1.8%)) (**Table 1** and **Figure 1B**). The higher frequency of indels in noncoding regions most likely results from the excess of low complexity sequences, which cause polymerase slippage.

To estimate the fraction of false-positive mutations, we resequenced (with Sanger sequencing) 52 mutations representing different types of alterations, including 39 substitutions and 13 indels (**Table S5**). The analysis confirmed 51/52 of the mutations, indicating a very low (2%) fraction of false-positive mutations. The fraction may be even lower, as the only unconfirmed mutation (double substitution CC>TT in *MYCN*) was present in a low fraction of reads (7%), which is generally beyond the sensitivity of Sanger sequencing.

Mutational Signatures

In the next step, we analyzed sample-specific mutational signatures to recognize the mutational processes playing a role in the mutagenesis of the analyzed BCC samples. Shortly, a mutational signature is a frequency pattern for different types of mutations (taking into account direct nucleotide context, -1 and +1 position) characteristic of particular cancer or cancer type. The pattern may reflect a main mutagenic process or a type of DNA repair deficiency that is specific to a given cancer. Originally based on analysis of single nucleotide variants, 30 distinctive mutational signatures were recognized in pancancer (36) but subsequently, the number of specific cancer signatures has been extended taking into account also other types of variants (53). The analysis showed that most of the samples were predominantly associated with signature 7 (average signature contribution (SC) = 0.7) and to a lesser extent with signature 11 (average SC = 0.2) (**Figures 1C, D**). Both signatures consist predominantly of C>T substitutions but differ in the sequence context of the substitutions. Signature 7 is associated with UV irradiation exposure and commonly occurs in melanoma and head and neck cancer. A hallmark of signature 7 is the frequent occurrence of double CC>TT substitutions resulting from UV radiation-induced pyrimidine dimers. Signature 11 was previously found in melanoma and glioblastoma multiforme, often in patients treated with the alkylating agent *temozolomide*, which is also used in BCC therapy. Only one sample (BCC22) showed a stronger association with signature 11 (SC = 0.6) than signature 7 (SC = 0.3). None of the analyzed samples showed an association with signatures 1, 2, 5, and 13, which are frequent in most cancer types. This may indicate that the deamination of 5-methylcytosine (5meC) predominantly induced by AID/APOBEC cytidine deaminases (attributed to the abovementioned signatures) does not play a role in the pathogenesis of BCC.

The comparison of the nodular and superficial BCC samples showed no substantial difference in terms of mutation burden or mutation types, with the exception of the contribution to mutational signature 7, which was higher for the nodular than superficial samples (**Figure 1E**), consistent with the higher UV radiation exposure of nodular BCCs.

Hotspot Mutations

As recurrent mutations may be indicators of the cancer-related function of the mutated genes, we first looked for hotspots defined as genomic positions mutated in at least 3 samples (>10% of the cohort). In total, we identified 43 hotspots, including 23 hotspots in coding and 20 hotspots in noncoding regions (8 in 5'UTRs, 1 in 3'UTRs, and 11 in introns) (**Table S6**). Of the coding hotspots, 16 resulted in missense mutations, and 7 were synonymous substitutions. As the majority of synonymous mutations result from randomly occurring neutral alterations, we did not analyze the synonymous hotspot further. Although it has to be noted that the functionality of individual synonymous mutations cannot be unequivocally ruled out (51, 54, 55). For example, 315 (~2.1%) of the detected in our study synonymous mutations were predicted to be exonic splice-site mutations. Also, synonymous mutations located inside exons may affect different regulatory elements including exonic splicing enhancers and silencers (55). As shown in **Table S6**, some of the hotspots were located in genes annotated in the COSMIC Cancer Gene Census (CGC) database and/or in genes playing a role in cancer or skin function.

Hotspot Mutations in Coding Regions

Of the coding mutations (**Table S6**), the most commonly identified in our study (in 5 samples) was the c.1292C>T (Ser431Phe) substitution, located at chr14:103,131,144 in the Sec6 domain of *TNFAIP2*, which encodes a multifunctional protein playing a role in angiogenesis, inflammation, cell migration and invasion, cytoskeleton remodeling, and cell membrane protrusion formation (56–59). Nonetheless,

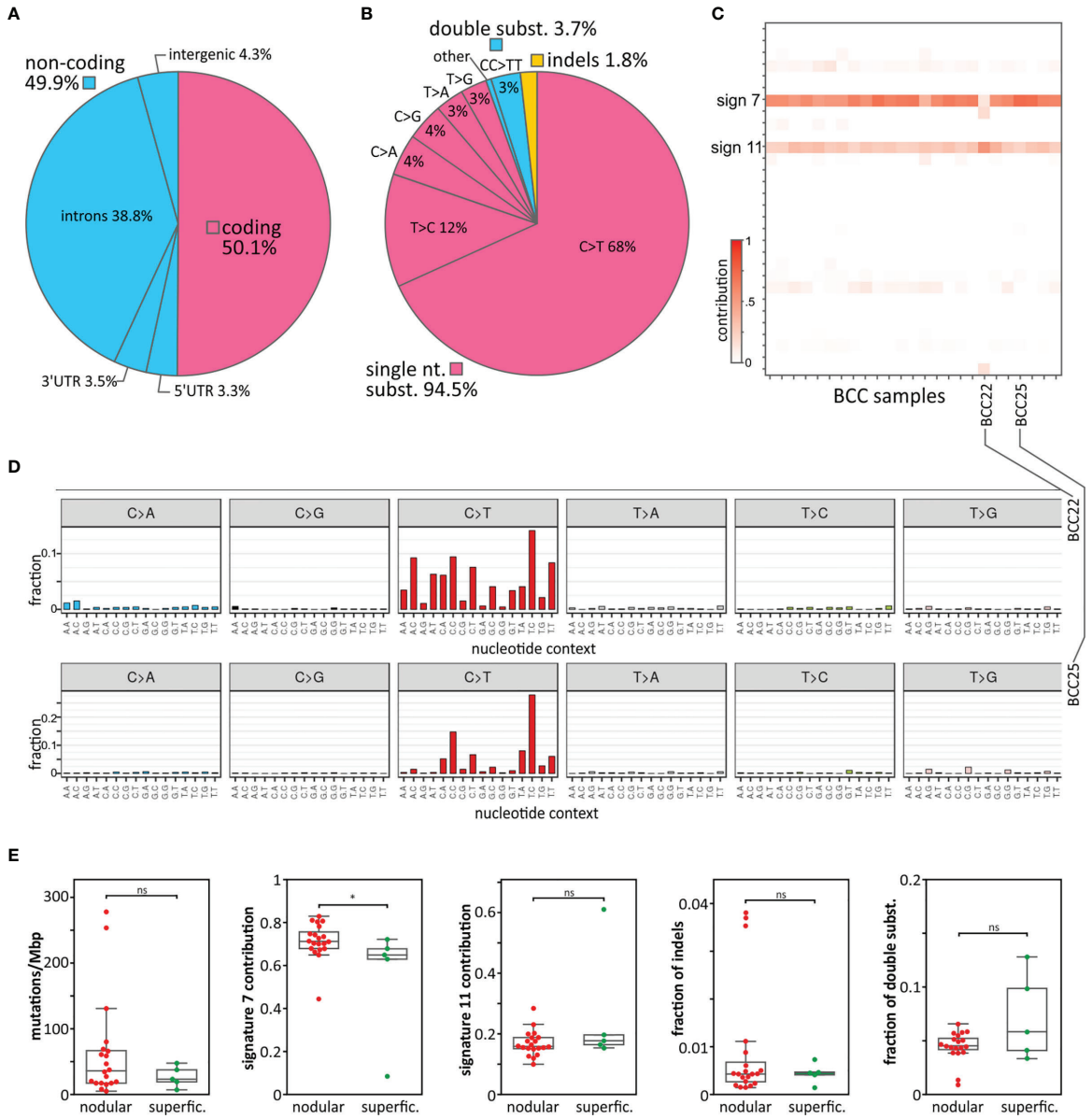


FIGURE 1 | Mutation distribution, mutational signatures, and comparison of superficial and nodular BCC subtypes. **(A)** Frequency of mutations in particular gene/genomic regions. **(B)** Frequency of mutation types. **(C)** Heatmap showing the contribution of the mutational signatures (rows) to the analyzed BCC samples (columns). Higher color intensity indicates a higher contribution (as indicated on the scale bar). **(D)** Representative mutation distribution plots of samples with a high association with signature 7 (sample BCC25) and signature 11 (sample BCC22). **(E)** Comparison of nodular and superficial BCC samples in terms of (from the left) mutational load, signature 7 and signature 11 contributions, frequency of indels, and frequency of double substitutions. *P < 0.05; 'ns' represents that the difference is not statistically significant.

TNFAIP2 is not well-recognized in cancer, and the hotspot or other mutations in the gene have not been reported before. Another coding hotspot, mutated in 3 samples with the c.655C>T (Pro219Ser) substitution, was located at chr7:148,827,237 in *EZH2*; *EZH2* encodes an essential subunit (methyltransferase) of polycomb repressive complex 2 (PRC2), which plays a role in histone methylation and gene silencing (60). *EZH2* is a well-known oncogene associated with a more aggressive form and poorer prognosis of many cancers, including melanoma, squamous cell carcinoma (SCC), and BCC, with demonstrated increased expression in SCC [compared to normal skin and SCC precursor actinic keratosis (AK)] (61) and aggressive BCC (62). Both gain- and loss-of-function mutations in *EZH2* have often been found in myeloid leukemias and lymphomas but are not common in solid tumors. Contrary to the previously detected mutations clustering mostly in the catalytic SET domain (63, 64), the hotspot detected here was located in the N-terminal (NT) part

of the protein, which, among other areas, is responsible for interaction with histones (65). Whether the mutations may affect the interaction warrants further investigation. To the best of our knowledge, this mutation hotspot has not been observed in any cancer, including BCC.

An additional interesting coding hotspot (mutated in 3 samples) was located at chr15:40,382,906-40,382,907. The hotspot was mutated with either the c.71C>T substitution or the c.71_72delinsTT double substitution (note that double substitutions are annotated as deletion/insertion (delins) variants according to HGVS nomenclature), both resulting in the Ser24Phe missense mutation affecting the NT part of the KNSTRN protein [also known as small kinetochore-associated protein (SKAP)], which plays a role in maintaining chromatid cohesion and proper chromatid separation during anaphase (66). *KNSTRN* mutations (predominately the Ser24Phe hotspot mutation) were first detected in 19% of SCCs and 13% of AKs (67). Subsequent analysis of The Cancer Genome Atlas (TCGA) datasets showed that the *KNSTRN* mutations also occur in 5% of melanoma samples but are rare in other cancers. Later, *KNSTRN* mutations were also identified in 2% (15) and 10% (68) of BCCs. These findings together with this study confirm that *KNSTRN* mutations are specific to UV radiation-related skin cancers. Consistent with the role of KNSTRN, it was shown that *KNSTRN* mutations in SCC affect proper chromosome separation and are associated with increased chromosome instability, expressed as a fraction of the genome with copy number alterations (CNAs) (67). Although there was a similar number of tested samples, the association of the KNSTRN mutations with CNAs was not confirmed in BCC, neither in a study by Jaju et al. (68) nor in our study (**Figure S1**). It is worth noting that it was also shown that KNSTRN plays a role in UV radiation-induced apoptosis (69); however, the effect of the mutations on avoidance of apoptosis by BCC cells or any other cancer cells has not yet been tested.

Hotspot Mutations in Noncoding Regions

The most frequently mutated hotspot of all the hotspots detected in the study (mutated in 8 samples) was located at chr11:64,270,066-64,270,067 in the 3'UTR of *BAD* and has never been reported before. The hotspot encompasses 4 different substitutions (c.*142C>A, c.*142C>T, c.*142_*143delinsTT and c.*143C>T; **Table S6** and **Figure 2A**), located 142 or 143 nucleotides (nt) downstream of the stop codon. The protein encoded by the gene is a member of the BCL-2 family, which plays a role in the positive regulation of cell apoptosis. The gene is commonly implicated in many cancers (70, 71); however, to the best of our knowledge, this hotspot has not been reported before in any cancer.

Next, another novel noncoding hotspot mutated in 5 samples located at chr16:72,008,760-72,008,761 in the 5'UTR of *DHODH* was identified. The hotspot encompasses two different substitutions, c.-5G>A and c.-5_-4delinsAA, affecting the Kozak sequence (**Table S6** and **Figure 2B**). *DHODH* is not well studied in cancer, but it has recently been demonstrated that it plays an important role in the carcinogenesis of SCC and other UV radiation-induced skin cancers (72, 73).

Another mutated noncoding hotspot from our study worth mentioning was found in 4 samples with the c.-77C>T substitution and was located at chr7:56,106,490 in the 5'UTR of *CHCHD2*, also known as *MNRR1* (**Table S6** and **Figure 2C**). The analysis of the entire *CHCHD2* 5'UTR showed one more recurrent (in 2 samples) substitution, c.-134G>A, located at chr7:56,106,547, resulting in a total of 6 mutations in the 5'UTR in 6 samples. Interestingly, frequent mutations in the hotspot in the 5'UTR of *CHCHD2* were previously reported in melanoma (74).

Finally, we identified a hotspot located at chr1:153,990,763 in the 5'UTR of *RPS27* (encoding a ribosomal protein component of the 40S subunit) that was mutated in 3 samples with the c.-34C>T substitution. Mutations in the promoter/5'UTR of *RPS27* (including the hotspot mutation) have been identified before in ~10% of melanoma samples (74, 75) but have never been reported in BCC or other skin cancers. Subsequent *in vitro* functional studies showed that the *RPS27* 5'UTR hotspot mutation decreases *RPS27* mRNA levels and that decreased levels of RPS27 are associated with a worse prognosis of melanoma patients and drug (*vemurafenib* and *palbociclib*) sensitivity of melanoma cells (76).

Computational Analysis of the Identified Noncoding Hotspots and Comparison With External Datasets

To further characterize three noncoding hotspot mutations, two not previously reported in *BAD* and *DHODH* and one in *CHCHD2* previously reported in melanoma (74), we analyzed their potential impact with a number of computational tools and investigated their incidence in other cancers using external datasets of a large cohort (>10,000 samples) of TCGA samples, representing 33 different human cancer types (including 469 skin cutaneous melanoma (SKCM) samples but not including BCC or SCC samples). Note that the list and the standard abbreviations of all TCGA cancer types are in **Table S3**.

In total, in the TCGA samples, we identified 28 mutations in the *BAD* 3'UTR (**Figure 2A**). The mutations were found predominantly in SKCM samples (15 mutations in 12 (2.6%) SKCM samples), including 4 mutations in the hotspot (residues c.*142C and c.*143C) identified in BCC, and 6 c.*77C>T mutations, constituting an additional hotspot in the 3'UTR, not occurring in BCC. In other cancers, 3'UTR mutations were very rare (**Figure 2A**). In contrast with the mutation frequency in the 3'UTR, mutations in other parts of the gene, including the coding region (n=26, predominantly missense or synonymous), were rare (not exceeding 1% in any cancer) and randomly distributed between different cancer types (excluding SKCM). The exclusiveness of the SKCM and BCC mutations in the 3'UTR *vs.* other parts of the gene (enrichment compared to other cancer types; Fisher's exact test; $p<0.0001$ and $p=0.0005$, respectively) precludes an accidental occurrence of the mutations, solely as a result of some region- and/or mutagenesis-related mechanisms and argues for the cancer-driven selection of the 3'UTR mutations in BCC and SKCM (and likely also in other UV irradiation-related cancers).

Next, with the use of TargetScan, we identified 3 miRNAs (miR-7515, miR-3202, and miR-6125) whose predicted targets (seed-interacting sequences) were disrupted by hotspot mutations (**Figure 2A**). However, as (i) none of these targets

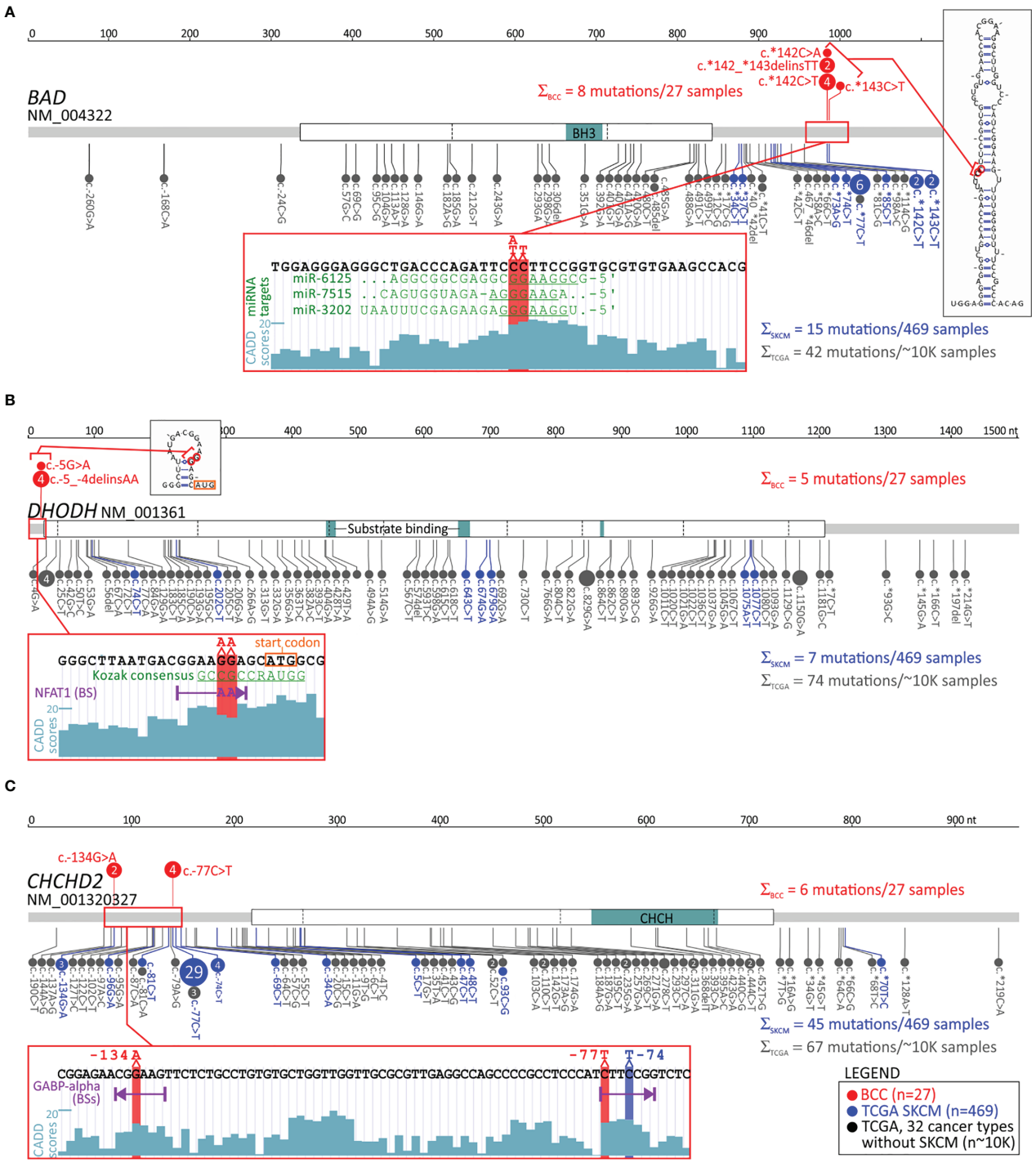


FIGURE 2 | Distribution of mutations in the selected genes with the identified mutation hotspots in noncoding areas. **(A-C)** Maps of the *BAD*, *DHODH*, and *CHCHD2* genes, with the exon structure and protein functional domains indicated. Mutations are visualized in the form of lollipop plots along with the gene maps, and the size of a mutation symbol (circle) is proportional to the number of mutations. Mutations identified in BCC (red) are shown above and mutations identified in SKCM (blue) and other TCGA cancers (gray) are shown below the maps. The inset below each map shows the detailed sequence context of the hotspot mutations, along with CADD score graphs, indicating the functional relevance of particular positions and other sequence characteristics (i.e., (in **A**) predicted miRNA target sites, (in **B**) the Kozak consensus sequence and NFAT1 transcription factor binding sites (BSs) created by the hotspot mutation, and (in **C**) the GABP-alpha transcription factor BSs disrupted by the hotspot mutations). The additional insets in **(A, B)** show computationally predicted RNA secondary structures generated from RNA sequences directly flanking the hotspots. * represents stop codon.

has been validated by any means [miRTarBase (77)], (ii) none of these miRNAs have been confidently validated (*via* miRBase or miRGeneDB), and (iii) none of these miRNAs have been found to have expression levels detectable/confirmed in any of the TCGA cancers, it is very unlikely that any of the identified targets are functional. Additionally, the occurrence of SKCM mutations in different positions across the *BAD* 3'UTR argues against the possibility that the driving force of the mutations is a disruption of a particular miRNA target. Some clue for the functionality of the BCC hotspot may be its location in the 5' arm of the ~40 bp long stable hairpin RNA structure motif (dG=-39.6 Kcal/mol), which is destabilized (by ~2 Kcal/mol) by the hotspot mutations (**Figure 2A**).

The analysis of TCGA data showed no mutation in the BCC hotspot or any other mutation in the *DHODH* 5'UTR in any of the TCGA cancer types, even though different mutations (n=81) were identified in other parts of the gene, including 75 mutations in the coding region (**Figure 2B**). The other mutations, however, were randomly distributed along the gene sequence and between different cancer types, and only two of the coding mutations were deleterious (frameshift) mutations. This result indicates that the *DHODH* 5'UTR hotspot mutations are BCC-specific mutations, and the absence of these mutations in other UV radiation-related cancers makes it unlikely that the frequent occurrence of the mutations in BCC is solely due to a random effect of UV irradiation. The 5'UTR of *DHODH* is very short (21 bp). Although hotspot mutations occurred in the Kozak sequence, which is important for the initiation of translation, neither wild-type nor mutant alleles affected the consensus Kozak sequence nucleotides (at positions -4 and -5); therefore, the ATGpr (78)), and NetStart 1.0 (GedersenAG (79) tools predicted the mutations to have a minor effect on the effectiveness of translation under standard conditions. However, this result does not exclude an effect of the mutations under specific conditions, such as hypoxia, UV exposure, or cancer.

The analysis of RNA secondary structure showed that the hotspot mutations slightly modified (decreased the stability of) a small hairpin motif predicted to be formed by an RNA sequence directly flanking the hotspot (**Figure 2B**). The mutation may also destabilize the potential long-range interaction of the sequence flanking the mutations with the sequence located ~200 nt downstream. Analysis of the 5'UTR sequence (80) showed that the double substitution (GG>AA) at the hotspot creates a consensus binding site for the NFAT1 transcription factor (**Figure 2B**), which is expressed in many tissues, including sun-exposed and non-sun-exposed skin (GTExPortal; GTEx Consortium Science 2020), and implicated in many cancers, including melanoma (81, 82).

In total, in TCGA data, we identified 63 mutations in the *CHCHD2* 5'UTR (**Figure 2C**). The mutations were found predominantly in SKCM samples (40 mutations in 39 (8.5%) samples), including 29 c.-77C>T mutations and 3 c.-134G>A mutations, located in the hotspot positions identified in BCC. Additionally, we identified 4 samples with the c.-74C>T mutation, constituting an additional hotspot in the 5'UTR. Only 5 SKCM mutations were located outside the 5'UTR, 4 in the CDS (2 missense and 2 synonymous), and 1 in the 3'UTR (one mutation) (**Figure 2C**). In other cancers, there were rare 5'UTR mutations, including 4 mutations in HNSC and UCEC, 3 mutations in BRCA, and 12 mutations in other cancers. Three of these mutations coincided with the c.-77 hotspot. The positions of BCC/SKCM hotspot mutations seem to be nonrandom because they were all located in and all disrupted two distinct GABP-alpha transcription factor binding sites [mapped with the use of MotifMap (50)] (**Figure 2C**).

Frequently Mutated Genes

Next, we looked at the overall frequency of mutations in the genes, separately analyzing mutations in coding regions, 5'UTRs, 3'UTRs, and introns (defined in Materials and Methods; listed in **Table S7**). Although they were not considered frequently mutated, in this section, we also report genes with any mutations in a coding region if they were detected in a pathway of a recurrently mutated gene. In the analysis of frequently mutated regions, we focused mostly on genes functionally related to cancer (annotated with CGC and a manual literature search) and genes playing a role in skin function.

Genes Frequently Mutated in Coding Regions

In total, we identified 606 genes frequently mutated in coding regions. The most frequently mutated was *PTCH1*, with a total of 24 mutations in 20 BCC samples, including 5 missense, 4 splice-site, and 15 deleterious (nonsense or frameshift) mutations (**Figure 3A**). Mutation c.3450-1G>A located upstream of exon 21 was one of the splice-site mutations and was also observed in another study (14), which suggests its recurrence in BCC. We tested and confirmed the exon-skipping effect of the mutation with the use of exon-junction PCR and Sanger sequencing analysis (**Figure 3A**). The other genes from the hedgehog pathway recurrently mutated in our cohort were *GLI2*, which was mutated in 5 samples, and *SMO*, which was mutated in 4 samples (**Figure S4** and **Figure 4**). The combined frequency of *SMO* and *GLI2* mutations was much lower in samples with (4/20; 20%) than in those without (4/7; 57%) *PTCH1* mutations, which suggests mutual exclusiveness of these mutations (**Figure 4**). Altogether, 24 (88%) samples had mutations in genes involved in the hedgehog pathway. Other frequently mutated cancer-related genes were *TP53* (7 missense, 8 deleterious, and one splice-site mutation in 13 samples) (**Figure 3B**); *MYCN* (8 missense mutations in 8 samples), *NOTCH1* (8 missense and 2 deleterious mutations in 8 samples), *NOTCH2* (3 missense, 3 deleterious, and 2 splice-site mutations in 7 samples), *NOTCH3* (6 missense mutations in 5 samples; note that the *NOTCH* mutations colocalized with the regions of the loss-of-function mutations identified in other solid tumors, e.g., in SCCs (83), *LATS1* (5 missense and one deleterious mutation in 5 samples), and *ARID1A* (5 missense mutations in 5 samples) (**Figure 4** and **Figure S2**). The mutations in the abovementioned genes are generally consistent with mutations observed before in BCC (14, 15). Additionally, we identified very frequent mutations (18 missense and 1 deleterious) in *PTPRD* (**Figure 3C**), a tumor

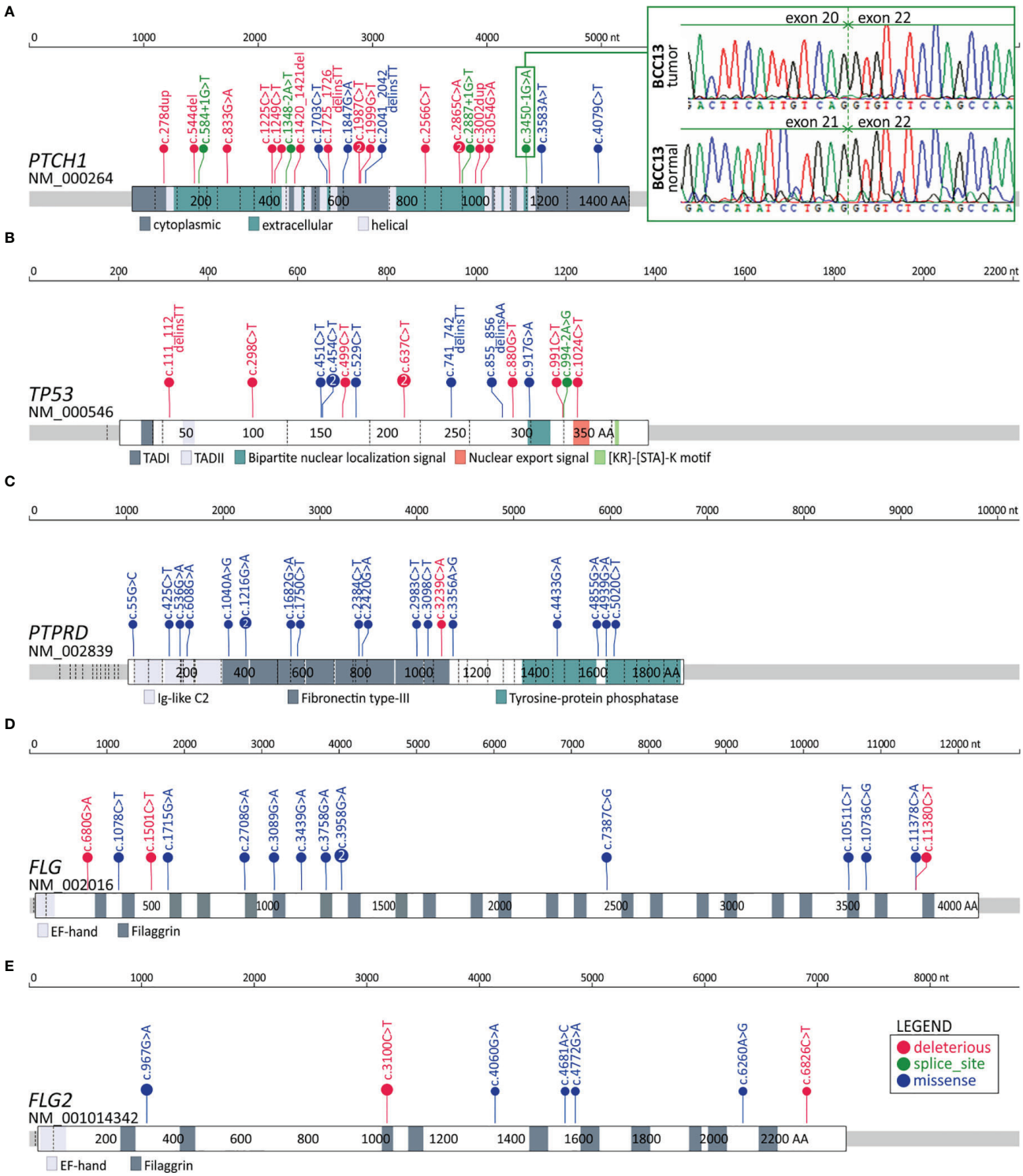


FIGURE 3 | Distribution of the identified mutations in the genes with frequent mutations in the coding sequence. **(A-E)** Maps of the *PTCH1*, *TP53*, *PTPRD*, *FLG*, and *FLG2* genes. Mutations are visualized in the form of lollipop plots along with gene maps; the size of a mutation symbol (circle) is proportional to the number of mutations, and the color indicates the type of mutation (as shown in the legend). Additionally, the inset in **(A)** shows the Sanger sequencing reads depicting the effect of the splice-site mutation c.3450-1G>A on exon 21 skipping.

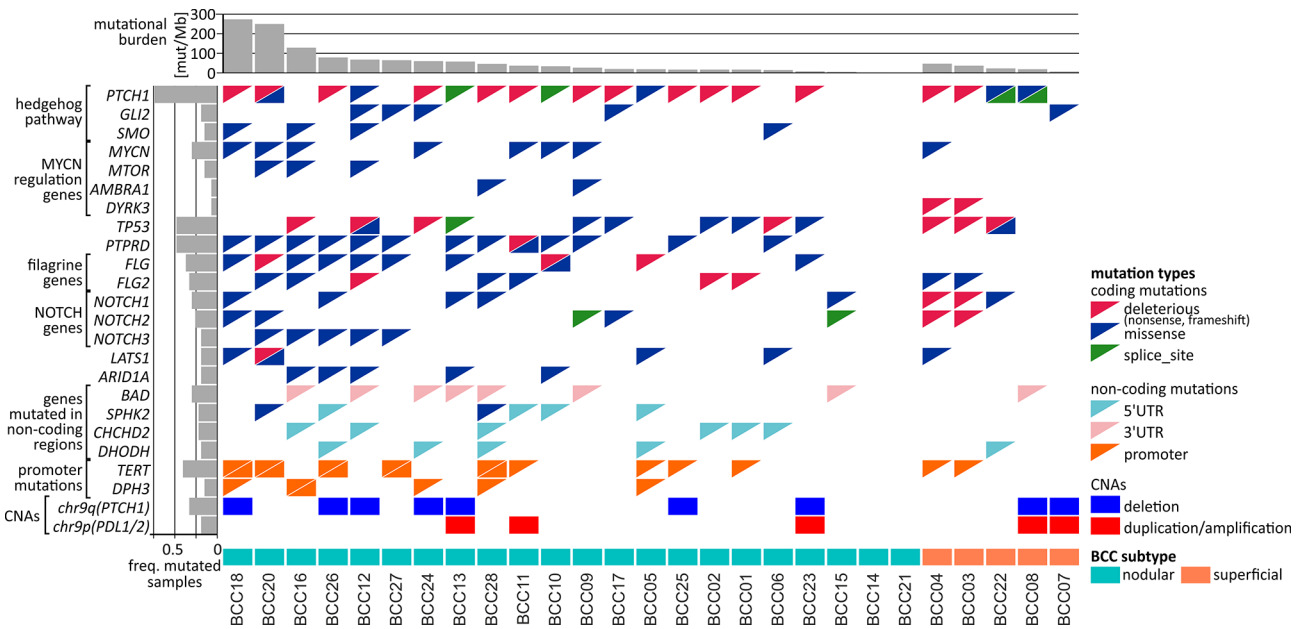


FIGURE 4 | Comutation plot summarizing the somatic alterations in the BCC samples. Columns correspond to the samples, and rows correspond to the selected genes. The color of the mutation presence symbols corresponds to the mutation type, as indicated in the legend on the right. The bar plots above and on the left indicate the mutational burden and the fraction of samples with mutations in particular genes, respectively. The nodular and superficial samples are indicated by color.

suppressor frequently mutated in many cancers, including melanoma and cutaneous SCC (84–88), in 13 samples, but these have never been reported as frequently mutated in BCC.

Interestingly, in addition to mutations in *MYCN*, we also noticed recurrent (although not frequent) mutations in three other genes in the MYC/MTOR regulatory network, i.e., *MTOR*, *DYRK3*, and *AMBRA1* (**Figure 4**), which have not been reported as mutated in BCC. The *MTOR* missense/activating mutations identified in other cancers are considered biomarkers for therapy with mTOR pathway inhibitors (89).

Finally, we found a high frequency of mutations in the *FLG* (15 mutations in 10 samples) and *FLG2* (9 mutations in 9 samples) genes (**Figures 3D, E** and **Figure 4**), encoding profilaggrin and filaggrin-like proteins, precursors of filaggrin. Filaggrin is an important component of the stratum corneum of the epidermis that plays a role in maintaining epithelial homeostasis and barrier functions (90) and is a substrate for trans-urocanic acid (UCA) and pyrrolidone carboxylic acid (PCA), which are suggested to serve as a natural UV radiation barrier (91). Although frequent mutations in the *FLG*/*FLG2* genes have been previously observed in other cancers, the mutations were usually considered random (passenger). Here, however, we observed a relatively high proportion of deleterious nonsense mutations, altogether occurring in 6 samples. Additionally, the analysis of the entire cohort of TCGA samples showed that the frequency of the *FLG*/*FLG2* mutations observed in our study in BCC substantially exceeds the frequencies of the mutations in other cancers, including melanoma (the next most frequently mutated cancer) (**Figure S3**).

Genes Frequently Mutated in Noncoding Regions

Among the 11 genes frequently mutated in the 5'UTR (**Table S7**) there were *DHODH* and *CHCHD2* with the hotspot mutations described above (see subsection Hotspot mutations). Of interest may also be *SPHK2*, with 4 dispersed mutations in 4 samples, whose function as both a proapoptotic gene suppressing cell growth and an oncogene promoting cell proliferation has been proposed (92–96). *SPHK2* also had mutations in its coding region (**Figure 4**).

Among the 11 genes frequently mutated in the 3'UTR (**Table S7**), in addition to BAD described above (see subsection Hotspot mutations), we also identified 8 mutations in the 3'UTR of *SMIM27* (also annotated as lncRNA *TOPORS-AS1*); the overexpression of *SMIM27* was found to be associated with favorable outcomes in breast cancer (97).

Finally, we identified 289 genes (15 annotated in CGC) frequently mutated in introns (**Table S7**). Interestingly, among the genes was *PTCH1*, which, in addition to 4 splice-site mutations (mentioned above), also had other 4 intronic mutations (in total, 8 intronic mutations). Other genes with frequent mutations in introns included *PTPRD* (14 mutations in 9 samples), which also frequently had mutations in the coding region; *NOTCH2* (6 mutations, including 2 splice-site mutations in 6 samples), which also frequently had mutations in the coding region; *ERBB4* (6 mutations in 6 samples), a well-known oncogene playing a role in many cancers [reviewed in (98)]; and *DROSHA* (5 mutations in 5 samples), which encodes a core enzyme (nuclease) of the miRNA processing pathway and has been shown to be upregulated in BCC (99).

Mutations in the *TERT* and *DPH3* Promoters

The only noncoding mutations previously studied in BCC are mutations recurrently occurring in promoters of *TERT* and *DPH3* (27, 100, 101). As these promoters were not covered in our exome sequencing experiment, we performed Sanger sequencing for these regions. As a result, we have detected 16 mutations in 11 (41%) patients in the *TERT* promoter and 6 mutations in 5 (19%) patients in the *DPH3* promoter (**Figure 4**). All *TERT* mutations were detected in previously described positions and well-known hotspots responsible for the recruitment of transcription factors activating expression of *TERT* in cancer, including 2 double substitutions c.-139_-138delinsAA, 9 substitutions c.-146G>A, 2 substitutions c.-101G>A, and 3 other substitutions (c.-150G>A, c.-100G>A, and c.-99G>A). Also, *DPH3* mutations were located in positions described before (27, 102), including 3 double substitutions c.-122_-121delinsTT, and 3 other substitutions (c.-150C>T, c.-122C>T, and c.-121C>T).

Driver Genes in BCC (OncodriveFML Analysis)

To further investigate the mutations/mutated genes, we used OncodriveFML, which allows the prediction of the cancer driver potential of both coding and noncoding regions/genes based on functional mutation (FM) bias (39). As shown in **Figures 5A–C** and **Table S8**, we identified 14 potential cancer driver genes based on mutations in coding regions (CDS-drivers), a disproportionately high number of 36 potential cancer driver genes based on mutations in 5'UTRs (5'UTR-drivers), and 7 potential cancer driver genes based on mutations in 3'UTRs (3'UTR-drivers). No potential cancer driver gene was identified based on the mutations in introns.

In addition to 4 CDS-drivers (*PTCH1*, *TP53*, *TGFB1I1*, and *CARD6*) also identified as frequently mutated, it is worth noting *RORA*, recently shown to play an important role in restraining allergic skin inflammation (103). Other interesting genes were *PRDM9* and *ZNF281*, both of which play a role in DNA repair and have been shown to be responsible for frequent mutations in cancer (104, 105). None of these genes were previously implicated or identified as frequently mutated in BCC.

Among the 5'UTR-drivers, 6 were also identified as frequently mutated: *DHODH*, *CHCHD2*, and *SPHK2* (described above), as well as *POLR2M*, *NPC1*, and *NELL2*. Additionally, it is worth noting *IKBKB* (mutated in 3 samples but not reported before as mutated in BCC) shown to act as a tumor suppressor in nonmelanoma skin cancers and noncancerous skin lesions; it was also shown that deletions of the gene lead to skin inflammation, hair follicle disruption, hyperplasia, and SCC development (106–109).

Among 3'UTR-drivers, two genes (mentioned above), i.e., *BAD* (the most significant 3'UTR-driver) and *SMIM27* were also identified as frequently mutated. Additionally, it is worth mentioning the transcription factor gene *POU3F2* (mutated in 3 samples), that plays a role in the invasiveness and metastasis of melanoma, and is controlled by miR-211 (110, 111) and miR-107 (112). Although the mutations were not located in the predicted miR-107 and miR-211 binding sites, they may affect the structure of the 3'UTR and thus indirectly change accessibility to these or other miRNA targets.

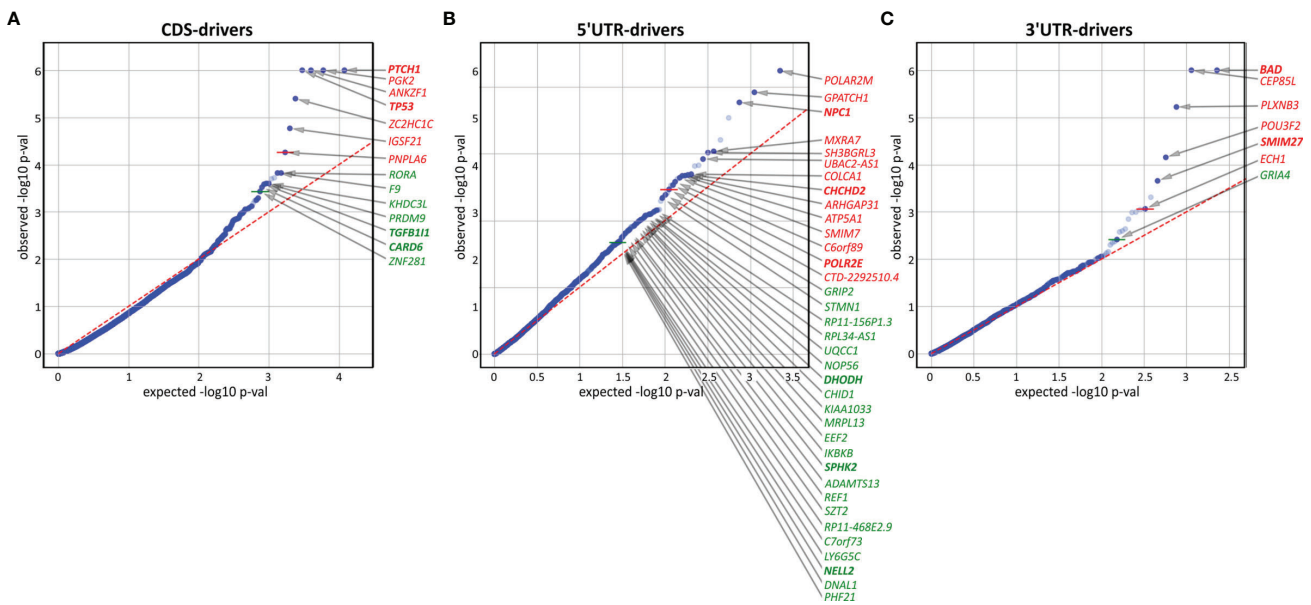


FIGURE 5 | Identification of potential cancer drivers with the use of OncodriveFML. The quantile-quantile (QQ) plots show the distribution of expected (x-axis) and observed (y-axis) p-values corresponding to FM bias calculated (with CADD score) separately for mutations in **(A)** coding regions, **(B)** 5'UTRs, and **(C)** 3'UTRs. The green and red colors indicate genes defined as significant (q<0.025) and highly significant (q<0.01), respectively, according to OncodriveFML recommendation.

Analysis of Copy Number Alterations

As somatic CNAs have not been extensively studied in BCC, in the next step, we performed analysis of both chromosome arm-level and focal CNAs [with GISTIC2 (40)]. At the chromosome arm level, we detected a significant recurring deletion of chr9q (q=1.4x10-6; occurring in 9 samples), involving *PTCH1* (**Figures 4**, **6**), and a significant recurring amplification of chr9p (q=0.05; occurring in 5 samples), involving a region with *CD274* (also known as *PDL1*, encoding PD-L1), *CD273* (also known as *PDL2*, encoding PD-L2), and *JAK2* (**Figures 4**, **6**). Although the loss of chr9q has been frequently observed in BCC (reported as loss-of-heterozygosity of *PTCH1*), gain of chr9p has been reported only in one case of rare metastatic BCC (113). To validate the chromosome 9 CNAs, we developed a multiplex ligation-dependent probe amplification (MLPA) assay with probes covering the entire chromosome 9 but especially focusing on the region containing *PTCH1* (chr9q22.32) and the region harboring *PDL1*, *PDL2*, and *JAK2* (chr9p24.1) (**Figure 6**). The MLPA analysis confirmed CNAs in all tested samples as detected by GISTIC2, and examples are shown in **Figure 6**.

CNA analysis also showed 54 regions of significant focal deletions, including 27 regions containing skin/cancer-related genes, and 56 significant amplifications, including 20 encompassing skin/cancer-related genes (**Figure 6** and **Table S9**). The elements involved in the most significant focal deletions were *CDK11A* (chr1p36.33; q=2.4x10-5; occurring in 6 samples), whose loss induces skin carcinogenesis (114); the *LCE* cluster (chr1q21.3; q=2.4x10-6; occurring in 4 samples), including genes such as *LCE2* and *LCE3*, which play a role in maintaining skin barrier function and whose deletion has been associated with psoriasis (115); and the *HLA-D* cluster (*HLA-DP*, *-DQ*, and *-DR*, chr6p21.32; q=2x10-4; occurring in 3 samples), encoding components of major

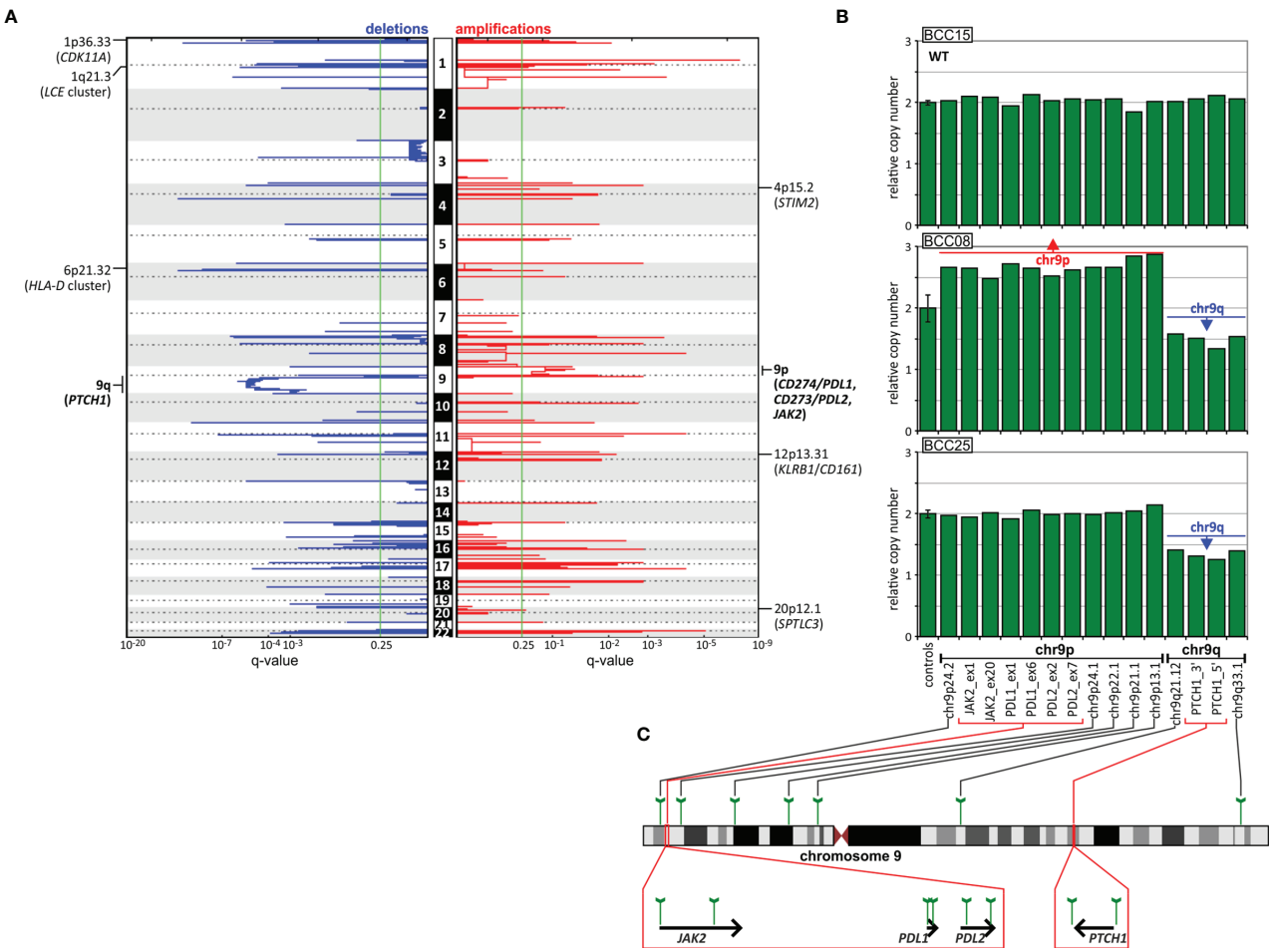


FIGURE 6 | CNA analysis of the BCC samples. **(A)** GISTIC-estimated q-values for deletions (left, blue) and amplifications (right, red) are plotted along with chromosome positions (vertically). The green line indicates the recommended significance threshold, q=0.25. The selected significantly deleted and amplified regions/genes are indicated on the graphs. **(B)** Representative MLPA results (bar plots), showing samples with chromosome 9 CNAs, i.e., chr9q deletion and chr9p amplification, *vs*. a sample (at the top) with the wild-type (WT) copy number genotype. Each bar plot depicts relative copy number values (y-axis) of the probes specific for regions along chromosome 9 and an average (with standard deviation error bar) signal of control probes (x-axis). **(C)** Schematic depictions of the localization of the probes on chromosome 9 and in genes of interest.

histocompatibility complex (MHC) class II molecules, whose increased expression has been associated with increased cancer immunogenicity and better prognosis in BCC, SCC and melanoma (116–122). The skin/cancer-related genes in the most significant focally amplified regions worth mentioning are *STIM2* (chr4p15.2; q=0.16; occurring in 2 samples) (123), *KLRB1/CD161* (chr12p13.31; q=0.007; occurring in 2 samples) (124, 125), and *SPTLC3* (chr20p12.1 q=0.23; occurring in 2 samples) (126).

DISCUSSION

In this study, we detected thousands of mutations in BCC samples, many of which were clustered in specific genes/regions or hotspots located in both coding and noncoding regions. Despite the small size of our dataset, our results are in line with those of previous genomic analyses of coding mutations in BCC (14, 15), which confirms the reliability of our study. We believe that our results may give valuable insights related to general characteristics of mutations such as mutational burden or mutational signatures and in terms of genes identified as recurrently mutated in coding regions.

Moreover, we extended our analysis to noncoding parts of the genes, which altogether were responsible for ~50% of the mutations identified by the standard WES approach. Variants in such areas have usually been ignored in previous BCC genetic studies. Many of the identified noncoding hotspots were located in sequences of genes functionally related to cancer or more specifically to UV radiation-related skin cancers. Some of them were reported before in melanoma or identified by us in melanoma TCGA samples, the cancer type most intensively studied in terms of mutations in noncoding regions (127, 128). Below, we briefly describe the cancer-related role of the three most interesting genes with hotspot mutations in noncoding regions, i.e., *BAD*, *DHODH*, and *CHCHD2*. Interestingly, all these genes have functions related to mitochondrial activity.

Of all the hotspots detected in our study, the most frequently mutated was the hotspot located in the 3'UTR of *BAD*. This hotspot had several different mutations affecting 2 nucleotide positions (142 and 143 nt downstream of the stop codon). Due to these mutations, *BAD* was also classified as being highly mutated in the 3'UTR and as the top most significant potential cancer driver. Consistently, the hotspot and several other positions in the 3'UTR are frequently mutated in melanoma but not in other cancers. BAD belongs to the BCL-2 family, consisting of both proapoptotic and antiapoptotic proteins. It promotes cell death by inducing mitochondrial outer membrane permeabilization (MOMP), allowing the release of cytochrome c, and by antagonizing (dimerizing with) antiapoptotic BCL-2 proteins (129, 130). On the other hand, phosphorylated BAD may also have antiapoptotic properties, e.g., promoting the survival of melanocytes (131, 132). Other functions of BAD include regulation of mitochondrial metabolism (regulation of voltage-dependent anion channels and metabolite passage through the outer mitochondrial membrane) and dynamics (regulation of shape changes) (133–139). Although BAD has not been previously implicated in skin cancers, loss or downregulation of other proapoptotic members of the BCL-2 family, i.e., BAX and PUMA, has been shown to promote the development of BCC, SCC, and cutaneous melanoma (140, 141). Therefore, a similar effect may be induced by mutations causing more efficient downregulation of BAD.

CHCHD2 is a gene with frequent mutations in the 5'UTR, the hotspot mutation c.-77C>T and the recurrent mutation c.-134G>A (77 and 134 upstream of the start codon). Based on the 5'UTR mutations, *CHCHD2* was classified as a high-priority cancer driver. We showed that the *CHCHD2* 5'UTR (predominantly the hotspot position) was also frequently mutated (8%) in the SKCM TCGA samples, which also showed the additional recurrent mutation c.-74C>T. The 5'UTR mutations were also found in whole-genome sequenced Australian melanoma samples (74). The role of the gene has not been intensively studied in cancer, but it was shown that under hypoxic conditions, CHCHD2 is translocated from the mitochondrial intermembrane space to the nucleus, where it binds an oxygen-responsive element in the promoter of *cytochrome oxidase 4I2* (*COX4I2*), encoding a subunit of complex IV of the electron transport chain, and increases its expression. Consequently, *CHCHD2* knockdown downregulates *COX4I2* and decreases cell oxygen consumption (142). It was also shown that CHCHD2 is a negative regulator of mitochondria-mediated apoptosis (143). Liu et al. showed that CHCHD2 interacts with antiapoptotic BCL-XL (from the BCL-2 family), which leads to inhibition of proapoptotic BAX and consequently decreases MOMP and apoptosis. In addition, it was shown that CHCHD2 dysregulates multiple genes that play a role in cell migration and cancer metastasis and that its expression is higher in cell lines derived from more aggressive breast tumors (144). Consistent with the function of CHCHD2 related to mitochondrial metabolism, we found that all BCC/SKCM hotspot/recurrent mutations coincided with and impaired two distinct binding sites of GABP-alpha. As GABP-alpha is known to be a transcription factor involved in the regulation of cellular energy metabolism and cell cycle regulation (145), this finding might hint at a functional role of the mutations in cancer. Of note, germline missense mutations in *CHCHD2* are associated with autosomal dominant Parkinson's disease (146).

DHODH is a gene that showed frequent mutations in the Kozak sequence of the 5'UTR, with hotspot mutations encompassing two different substitutions, c.-5G>A and c.-5_-4delinsAA (4 and 5 nt upstream of the start codon). Based on the identified mutations, *DHODH* was classified as a candidate cancer driver. The analysis of the entire TCGA cohort (~10K samples from 33 cancer types) showed that no other cancer had mutations in the hotspot or the 5'UTR, indicating that the mutations were BCC-specific. Although *DHODH* 5'UTR mutations have never been reported before in any cancer, it was shown very recently that *DHODH* plays a key role in the carcinogenesis of SCC and other UV radiation-induced skin cancers and facilitates the development of precancerous skin lesions (72, 73). Hosseini et al. showed that the DHODH protein level and enzymatic activity are markedly upregulated in irradiated skin and that an increased level of DHODH sensitizes the skin to UV irradiation-induced damage. It was

also shown that DHODH is upregulated in melanoma, in which DHODH inhibition leads to a marked decrease in tumor growth both *in vitro* and in mouse xenograft studies (147). DHODH inactivation inhibits cell proliferation and induces cell cycle arrest at the S phase in BCL-2 (pro-apoptotic) deficient melanoma cells (148). DHODH is embedded in the inner mitochondrial membrane, and its canonical role is in the oxidation of dihydroorotate to orotate, an important step in *de novo* pyrimidine synthesis (which is important in replication and DNA repair). However, a side product of the pathway, ubiquinol (QH2), is a source of electrons in the electron transport chain, and DHODH also plays a role in alternative (glucose-independent) respiration (utilizing amino acids as an energy source) (72, 73, 148), facilitating cancer development in hypoxic conditions. In addition, it was found that in esophageal SCC, elevated DHODH levels promote cell proliferation by stabilizing β-catenin (149). The functional effects of the mutations may result from alteration of the Kozak sequence but also the creation of an NFAT1 transcription factor binding site, which is not present in the wild-type sequence. NFAT1 is a widely distributed isoform of the NFAT family of transcription factors and is expressed in tumor cells and the tumor microenvironment (150). The constitutive activation and overexpression of NFAT1 in many cancer types promote the transcription of genes that are crucial for cancer development and progression, including *COX2*, *MMP7*, *MMP9*, and *MDM2* (151, 152).

It is worth noting that the only noncoding mutations analyzed in BCC before are the mutations in promoters of *TERT* and *DPH3* (27, 100, 101); which are known to be mutated in many cancers, including melanoma (127, 128). Although our WES design generally did not cover promoter regions, with the use of Sanger sequencing, we confirmed high frequency and high recurrence of promoter mutations in *TERT* (41% of patients) and *DPH3* (19%).

Additionally, the whole-genome CNA analysis allowed us to detect two highly significant chromosome-level CNAs. In addition to the expected deletion of chr9q, consistent with the loss of heterozygosity of *PTCH1*, we also detected frequent duplication/amplification of chr9p, encompassing the *PDL1* and *PDL2* genes (which encode the two immune checkpoint proteins PD-L1 and PD-L2, the overexpression of which enables cancer cells to evade the host immune system). Copy number gains of *PDL1* have been observed only in one case of metastatic BCC (113). The patient, who was otherwise resistant to *vismodegib* and *sonidegib*, demonstrated a dramatic response to *nivolumab* (an anti-PD-1 antibody blocking the PD-1/PD-L1 interaction), which strongly suggested that the copy number gain may be a biomarker of sensitivity to anti-PD-1/PD-L1 checkpoint treatments (113). It was also shown in an independent study that some patients (up to ~40%) with advanced BCC (not tested for *PDL1* amplification) respond to *pembrolizumab* (another anti-PD-1 antibody) (113, 153). Therefore, assessment of copy number gains of the *PDL1*/*PDL2* region may help to rationalize such treatment; however, further study with a larger group of samples is required.

Finally, we would like to note the apparent limitations of the study. As it was intended to be a preliminary evaluation of noncoding mutations in BCC, we analyzed only a small number of samples, and as such, we limited the characterization of the identified variants to computational analyses. It has to be also noted that our analysis covered only a small fraction (~1%) of the noncoding genome that cumulatively accounts for ~98% of the genome and contains many different functional elements not covered in our analysis, including promoters, enhancers, and genes of different classes of non-coding RNAs.

In summary, in this study utilizing WES BCC data, we revealed not only mutations in coding regions of previously known BCC-related genes but also frequent mutations in noncoding regions of cancer-related genes, some of which may be strong candidates for new BCC drivers. Although the functional role of the individual identified genes/mutations requires further experimental interrogations, our results provide a strong basis for further analyses of noncoding variants in BCC and other cancer types.

DATA AVAILABILITY STATEMENT

The datasets presented in this study can be found in online repositories. The names of the repository/repositories and accession number(s) can be found below: https://www.ncbi.nlm.nih.gov/, PRJNA747148.

ETHICS STATEMENT

The studies involving human participants were reviewed and approved by bioethics committee of the Ruhr-University of Bochum. The patients/participants provided their written informed consent to participate in this study.

AUTHOR CONTRIBUTIONS

PN extracted the DNA samples, performed almost all experimental and computational analyses, drafted the manuscript (with PK), prepared all figures, tables, and supplementary materials. PG-M participated in the study design, extracted mutations from TCGA, assisted PN in experimental analyses, participated in the manuscript preparation. MU-T prepared the scripts for mutation calling and mutations annotation, assisted PN in computational analyses, participated in the manuscript preparation. IM-T performed the analysis of the NFAT1 TF binding site in the promoter of DHODH, participated in the manuscript preparation. NS participated in CNA analysis with GISTIC2, participated in the manuscript preparation. AP assisted in computational analyses, participated in the manuscript preparation. LS – collected and characterized the BCC samples, participated in the manuscript preparation. MS – participated in conceiving the study, participated in collection and characterization of BCC samples, participated in the manuscript preparation. PK – conceived and supervised the study, drafted the manuscript (with PN), acquired the funding. All authors contributed to the article and approved the submitted version.

FUNDING

This work was supported by research grants from the Polish National Science Centre [2016/22/A/NZ2/00184 and 2020/39/B/NZ5/01970] (to PK).

SUPPLEMENTARY MATERIAL

The Supplementary Material for this article can be found online at: https://www.frontiersin.org/articles/10.3389/fonc.2021.752579/full#supplementary-material

REFERENCES

1. Samarasinghe V, Madan V, Lear JT. Focus on Basal Cell Carcinoma. *J Skin Cancer* (2011) 2011:328615. doi: 10.1155/2011/328615
2. Puig S, Berrocal A. Management of High-Risk and Advanced Basal Cell Carcinoma. *Clin Transl Oncol Off Publ Fed Span Oncol Soc Natl Cancer Inst Mex* (2015) 17:497–503. doi: 10.1007/s12094-014-1272-9
3. Pellegrini C, Maturo MG, Di Nardo L, Ciciarelli V, Gutiérrez García-Rodrigo C, Fargnoli MC. Understanding the Molecular Genetics of Basal Cell Carcinoma. *Int J Mol Sci* (2017) 18(11):2485. doi: 10.3390/ijms18112485
4. Evans DG, Howard E, Giblin C, Clancy T, Spencer H, Huson SM, et al. Birth Incidence and Prevalence of Tumor-Prone Syndromes: Estimates From a UK Family Genetic Register Service. *Am J Med Genet A* (2010) 152A:327–32. doi: 10.1002/ajmg.a.33139
5. Sexton M, Jones DB, Maloney ME. Histologic Pattern Analysis of Basal Cell Carcinoma. Study of a Series of 1039 Consecutive Neoplasms. *J Am Acad Dermatol* (1990) 23:1118–26. doi: 10.1016/0190-9622(90)70344-h
6. Rippey JJ. Why Classify Basal Cell Carcinomas? *Histopathology* (1998) 32:393–8. doi: 10.1046/j.1365-2559.1998.00431.x
7. Raasch BA, Buettner PG, Garbe C. Basal Cell Carcinoma: Histological Classification and Body-Site Distribution. *Br J Dermatol* (2006) 155:401–7. doi: 10.1111/j.1365-2133.2006.07234.x
8. Lo JS, Snow SN, Reizner GT, Mohs FE, Larson PO, Hruza GJ. Metastatic Basal Cell Carcinoma: Report of Twelve Cases With a Review of the Literature. *J Am Acad Dermatol* (1991) 24:715–9. doi: 10.1016/0190-9622(91)70108-e
9. Ting PT, Kasper R, Arlette JP. Metastatic Basal Cell Carcinoma: Report of Two Cases and Literature Review. *J Cutan Med Surg* (2005) 9:10–5. doi: 10.1007/s10227-005-0027-1
10. Crowson AN, Magro CM, Kadin ME, Stranc M. Differential Expression of the Bcl-2 Oncogene in Human Basal Cell Carcinoma. *Hum Pathol* (1996) 27:355–9. doi: 10.1016/s0046-8177(96)90108-2
11. Crowson AN. Basal Cell Carcinoma: Biology, Morphology and Clinical Implications. *Mod Pathol Off J U S Can Acad Pathol Inc* (2006) 19 (Suppl 2): S127–147. doi: 10.1038/modpathol.3800512
12. Epstein EH. Basal Cell Carcinomas: Attack of the Hedgehog. *Nat Rev Cancer* (2008) 8:743–54. doi: 10.1038/nrc2503
13. Iwasaki JK, Srivastava D, Moy RL, Lin HJ, Kouba DJ. The Molecular Genetics Underlying Basal Cell Carcinoma Pathogenesis and Links to Targeted Therapeutics. *J Am Acad Dermatol* (2012) 66:e167–178. doi: 10.1016/j.jaad.2010.06.054
14. Jayaraman SS, Rayhan DJ, Hazany S, Kolodney MS. Mutational Landscape of Basal Cell Carcinomas by Whole-Exome Sequencing. *J Invest Dermatol* (2014) 134:213–20. doi: 10.1038/jid.2013.276
15. Bonilla X, Parmentier L, King B, Bezrukov F, Kaya G, Zoete V, et al. Genomic Analysis Identifies New Drivers and Progression Pathways in Skin Basal Cell Carcinoma. *Nat Genet* (2016) 48:398–406. doi: 10.1038/ng.3525
16. Verkouteren JAC, Ramdas KHR, Wakkee M, Nijsten T. Epidemiology of Basal Cell Carcinoma: Scholarly Review. *Br J Dermatol* (2017) 177:359–72. doi: 10.1111/bjd.15321
17. Peris K, Fargnoli MC, Garbe C, Kaufmann R, Bastholt L, Seguin NB, et al. Diagnosis and Treatment of Basal Cell Carcinoma: European Consensus-Based Interdisciplinary Guidelines. *Eur J Cancer Oxf Engl* (1990) 2019:118:10–34. doi: 10.1016/j.ejca.2019.06.003
18. Gailani MR, Leffell DJ, Ziegler A, Gross EG, Brash DE, Bale AE. Relationship Between Sunlight Exposure and a Key Genetic Alteration in Basal Cell Carcinoma. *J Natl Cancer Inst* (1996) 88:349–54. doi: 10.1093/jnci/88.6.349
19. Maloney ME. Arsenic in Dermatology. *Dermatol Surg Off Publ Am Soc Dermatol Surg Al* (1996) 22:301–4. doi: 10.1111/j.1524-4725.1996.tb00322.x
20. Rubin AI, Chen EH, Ratner D. Basal-Cell Carcinoma. *N Engl J Med* (2005) 353:2262–9. doi: 10.1056/NEJMra044151
21. Palacios-Álvarez I, González-Sarmiento R, Fernández-López E. Gorlin Syndrome. *Actas Dermo Sifiliográficas Engl Ed* (2018) 109:207–17. doi: 10.1016/j.adengl.2018.02.002
22. Diederichs S, Bartsch L, Berkmann JC, Fröse K, Heitmann J, Hoppe C, et al. The Dark Matter of the Cancer Genome: Aberrations in Regulatory Elements, Untranslated Regions, Splice Sites, non-Coding RNA and Synonymous Mutations. *EMBO Mol Med* (2016) 8:442–57. doi: 10.15252/emmm.201506055
23. Leppek K, Das R, Barna M. Functional 5' UTR mRNA Structures in Eukaryotic Translation Regulation and How to Find Them. *Nat Rev Mol Cell Biol* (2018) 19:158–74. doi: 10.1038/nrm.2017.103
24. Lord J, Gallone G, Short PJ, McRae JF, Ironfield H, Wynn EH, et al. Pathogenicity and Selective Constraint on Variation Near Splice Sites. *Genome Res* (2019) 29:159–70. doi: 10.1101/gr.238444.118
25. Horn S, Figl A, Rachakonda PS, Fischer C, Sucker A, Gast A, et al. TERT Promoter Mutations in Familial and Sporadic Melanoma. *Science* (2013) 339:959–61. doi: 10.1126/science.1230062
26. Huang FW, Hodis E, Xu MJ, Kryukov GV, Chin L, Garraway LA. Highly Recurrent TERT Promoter Mutations in Human Melanoma. *Science* (2013) 339:957–9. doi: 10.1126/science.1229259
27. Maturo MG, Rachakonda S, Heidenreich B, Pellegrini C, Srinivas N, Requena C, et al. Coding and Noncoding Somatic Mutations in Candidate Genes in Basal Cell Carcinoma. *Sci Rep* (2020) 10:8005. doi: 10.1038/s41598-020-65057-2
28. Urbanek-Trzeciak MO, Galka-Marciniak P, Nawrocka PM, Kowal E, Szwec S, Giefing M, et al. Pan-Cancer Analysis of Somatic Mutations in miRNA Genes. *EBioMedicine* (2020) 61:103051. doi: 10.1016/j.ebiom.2020.103051
29. Sand M, Skrygan M, Sand D, Georgas D, Hahn SA, Gambichler T, et al. Expression of microRNAs in Basal Cell Carcinoma. *Br J Dermatol* (2012) 167:847–55. doi: 10.1111/j.1365-2133.2012.11022.x
30. Sand M, Hessam S, Amur S, Skrygan M, Bromba M, Stockfleth E, et al. Expression of Oncogenic miR-17-92 and Tumor Suppressive miR-143-145 Clusters in Basal Cell Carcinoma and Cutaneous Squamous Cell Carcinoma. *J Dermatol Sci* (2017) 86:142–8. doi: 10.1016/j.jdermsci.2017.01.012
31. Sand M, Bromba A, Sand D, Gambichler T, Hessam S, Becker JC, et al. Dicer Sequencing, Whole Genome Methylation Profiling, mRNA and smallRNA Sequencing Analysis in Basal Cell Carcinoma. *Cell Physiol Biochem Int J Exp Cell Physiol Biochem Pharmacol* (2019) 53:760–73. doi: 10.33594/000000171
32. Rheinbay E, Nielsen MM, Abascal F, Wala JA, Shapira O, Tiao G, et al. Analyses of non-Coding Somatic Drivers in 2,658 Cancer Whole Genomes. *Nature* (2020) 578:102–11. doi: 10.1038/s41586-020-1965-x
33. Sakthikumar S, Roy A, Haseeb L, Pettersson ME, Sundström E, Marinescu VD, et al. Whole-Genome Sequencing of Glioblastoma Reveals Enrichment of non-Coding Constraint Mutations in Known and Novel Genes. *Genome Biol* (2020) 21:127. doi: 10.1186/s13059-020-02035-x
34. Jiang H, Lei R, Ding S-W, Zhu S. Skewer: A Fast and Accurate Adapter Trimmer for Next-Generation Sequencing Paired-End Reads. *BMC Bioinf* (2014) 15:182. doi: 10.1186/1471-2105-15-182
35. Díaz-Gay M, Vila-Casadesús M, Franch-Expósito S, Hernández-Illán E, Lozano JJ, Castellví-Bel S. Mutational Signatures in Cancer (MuSiCa): A Web Application to Implement Mutational Signatures Analysis in Cancer Samples. *BMC Bioinf* (2018) 19:224. doi: 10.1186/s12859-018-2234-y
36. Alexandrov LB, Nik-Zainal S, Wedge DC, Aparicio SAJR, Behjati S, Biankin AV, et al. Signatures of Mutational Processes in Human Cancer. *Nature* (2013) 500:415–21. doi: 10.1038/nature12477
37. Lawrence MS, Stojanov P, Polak P, Kryukov GV, Cibulskis K, Sivachenko A, et al. Mutational Heterogeneity in Cancer and the Search for New Cancer-Associated Genes. *Nature* (2013) 499:214–8. doi: 10.1038/nature12213

38. Cingolani P, Platts A, Wang LL, Coon M, Nguyen T, Wang L, et al. A Program for Annotating and Predicting the Effects of Single Nucleotide Polymorphisms, SnpEff. *Fly (Austin)* (2012) 6:80–92. doi: 10.4161/fly.19695
39. Mularoni L, Sabarinathan R, Deu-Pons J, Gonzalez-Perez A, López-Bigas N. OncodriveFML: A General Framework to Identify Coding and non-Coding Regions With Cancer Driver Mutations. *Genome Biol* (2016) 17:128. doi: 10.1186/s13059-016-0994-0
40. Mermel CH, Schumacher SE, Hill B, Meyerson ML, Beroukhim R, Getz G. GISTIC2.0 Facilitates Sensitive and Confident Localization of the Targets of Focal Somatic Copy-Number Alteration in Human Cancers. *Genome Biol* (2011) 12:R41. doi: 10.1186/gb-2011-12-4-r41
41. Kozlowski P, Roberts P, Dabora S, Franz D, Bissler J, Northrup H, et al. Identification of 54 Large Deletions/Duplications in TSC1 and TSC2 Using MLPA, and Genotype-Phenotype Correlations. *Hum Genet* (2007) 121:389–400. doi: 10.1007/s00439-006-0308-9
42. Marcinkowska M, Wong K-K, Kwiatkowski DJ, Kozlowski P. Design and Generation of MLPA Probe Sets for Combined Copy Number and Small-Mutation Analysis of Human Genes: EGFR as an Example. *Sci World J* (2010) 10:2003–18. doi: 10.1100/tsw.2010.195
43. Galka-Marciniak P, Urbanek-Trzeciak MO, Nawrocka PM, Kozlowski P. A Pan-Cancer Atlas of Somatic Mutations in miRNA Biogenesis Genes. *Nucleic Acids Res* (2021) 49:601–20. doi: 10.1093/nar/gkaa1223
44. Zhou X, Edmonson MN, Wilkinson MR, Patel A, Wu G, Liu Y, et al. Exploring Genomic Alteration in Pediatric Cancer Using ProteinPaint. *Nat Genet* (2016) 48:4–6. doi: 10.1038/ng.3466
45. UniProt Consortium. UniProt: A Worldwide Hub of Protein Knowledge. *Nucleic Acids Res* (2019) 47:D506–15. doi: 10.1093/nar/gky1049
46. Crowdis J, He MX, Reardon B, Van Allen EM. CoMut: Visualizing Integrated Molecular Information With Comutation Plots. *Bioinformatics* (2020) 36:4348–9. doi: 10.1093/bioinformatics/btaa554
47. Lewis BP, Burge CB, Bartel DP. Conserved Seed Pairing, Often Flanked by Adenosines, Indicates That Thousands of Human Genes are microRNA Targets. *Cell* (2005) 120:15–20. doi: 10.1016/j.cell.2004.12.035
48. Zuker M. Mfold Web Server for Nucleic Acid Folding and Hybridization Prediction. *Nucleic Acids Res* (2003) 31:3406–15. doi: 10.1093/nar/gkg595
49. Huang H-Y, Chien C-H, Jen K-H, Huang H-D. RegRNA: An Integrated Web Server for Identifying Regulatory RNA Motifs and Elements. *Nucleic Acids Res* (2006) 34:W429–434. doi: 10.1093/nar/gkl333
50. Daily K, Patel VR, Rigor P, Xie X, Baldi P. MotifMap: Integrative Genome-Wide Maps of Regulatory Motif Sites for Model Species. *BMC Bioinf* (2011) 12:495. doi: 10.1186/1471-2105-12-495
51. Supek F, Miñana B, Valcárcel J, Gabaldón T, Lehner B. Synonymous Mutations Frequently Act as Driver Mutations in Human Cancers. *Cell* (2014) 156:1324–35. doi: 10.1016/j.cell.2014.01.051
52. Lawrence MS, Stojanov P, Mermel CH, Garraway LA, Golub TR, Meyerson M, et al. Discovery and Saturation Analysis of Cancer Genes Across 21 Tumor Types. *Nature* (2014) 505:495–501. doi: 10.1038/nature12912
53. Alexandrov LB, Kim J, Haradhvala NJ, Huang MN, Tian Ng AW, Wu Y, et al. The Repertoire of Mutational Signatures in Human Cancer. *Nature* (2020) 578:94–101. doi: 10.1038/s41586-020-1943-3
54. Bin Y, Wang X, Zhao L, Wen P, Xia J. An Analysis of Mutational Signatures of Synonymous Mutations Across 15 Cancer Types. *BMC Med Genet* (2019) 20:190. doi: 10.1186/s12881-019-0926-4
55. Sharma Y, Miladi M, Dukare S, Boulay K, Caudron-Herger M, Groß M, et al. A Pan-Cancer Analysis of Synonymous Mutations. *Nat Commun* (2019) 10:2569. doi: 10.1038/s41467-019-10489-2
56. Hase K, Kimura S, Takatsu H, Ohmae M, Kawano S, Kitamura H, et al. M-Sec Promotes Membrane Nanotube Formation by Interacting With Ral and the Exocyst Complex. *Nat Cell Biol* (2009) 11:1427–32. doi: 10.1038/ncb1990
57. Jia L, Zhou Z, Liang H, Wu J, Shi P, Li F, et al. KLF5 Promotes Breast Cancer Proliferation, Migration and Invasion in Part by Upregulating the Transcription of TNFAIP2. *Oncogene* (2016) 35:2040–51. doi: 10.1038/onc.2015.263
58. Xie Y, Wang B. Downregulation of TNFAIP2 Suppresses Proliferation and Metastasis in Esophageal Squamous Cell Carcinoma Through Activation of the Wnt/β-Catenin Signaling Pathway. *Oncol Rep* (2017) 37:2920–8. doi: 10.3892/or.2017.5557
59. Jia L, Shi Y, Wen Y, Li W, Feng J, Chen C. The Roles of TNFAIP2 in Cancers and Infectious Diseases. *J Cell Mol Med* (2018) 22:5188–95. doi: 10.1111/jcmm.13822
60. Kodach LL, Jacobs RJ, Heijmans J, van Noesel CJM, Langers AMJ, Verspaget HW, et al. The Role of EZH2 and DNA Methylation in the Silencing of the Tumour Suppressor RUNX3 in Colorectal Cancer. *Carcinogenesis* (2010) 31:1567–75. doi: 10.1093/carcin/bgq147
61. Xie Q, Wang H, Heilman ER, Walsh MG, Haseeb MA, Gupta R. Increased Expression of Enhancer of Zeste Homolog 2 (EZH2) Differentiates Squamous Cell Carcinoma From Normal Skin and Actinic Keratosis. *Eur J Dermatol EJD* (2014) 24:41–5. doi: 10.1684/ejd.2013.2219
62. Rao RC, Chan MP, Andrews CA, Kahana A. EZH2, Proliferation Rate, and Aggressive Tumor Subtypes in Cutaneous Basal Cell Carcinoma. *JAMA Oncol* (2016) 2:962–3. doi: 10.1001/jamaoncol.2016.0021
63. Bödör C, Grossmann V, Popov N, Okosun J, O'Riain C, Tan K, et al. EZH2 Mutations are Frequent and Represent an Early Event in Follicular Lymphoma. *Blood* (2013) 122:3165–8. doi: 10.1182/blood-2013-04-496893
64. Donaldson-Collier MC, Sungalee S, Zufferey M, Tavernari D, Katanayeva N, Battistello E, et al. EZH2 Oncogenic Mutations Drive Epigenetic, Transcriptional, and Structural Changes Within Chromatin Domains. *Nat Genet* (2019) 51:517–28. doi: 10.1038/s41588-018-0338-y
65. Weaver TM, Liu J, Connelly KE, Coble C, Varzavand K, Dykhuizen EC, et al. The EZH2 SANT1 Domain is a Histone Reader Providing Sensitivity to the Modification State of the H4 Tail. *Sci Rep* (2019) 9:987. doi: 10.1038/s41598-018-37699-w
66. Fang L, Seki A, Fang G. SKAP Associates With Kinetochores and Promotes the Metaphase-to-Anaphase Transition. *Cell Cycle* (2009) 8:2819–27. doi: 10.4161/cc.8.17.9514
67. Lee CS, Bhaduri A, Mah A, Johnson WL, Ungewickell A, Aros CJ, et al. Recurrent Point Mutations in the Kinetochore Gene KNSTRN in Cutaneous Squamous Cell Carcinoma. *Nat Genet* (2014) 46:1060–2. doi: 10.1038/ng.3091
68. Jaju PD, Nguyen CB, Mah AM, Atwood SX, Li J, Zia A, et al. Mutations in the Kinetochore Gene KNSTRN in Basal Cell Carcinoma. *J Invest Dermatol* (2015) 135:3197–200. doi: 10.1038/jid.2015.339
69. Lu S, Wang R, Cai C, Liang J, Xu L, Miao S, et al. Small Kinetochore Associated Protein (SKAP) Promotes UV-Induced Cell Apoptosis Through Negatively Regulating pre-mRNA Processing Factor 19 (Prp19). *PloS One* (2014) 9:e92712. doi: 10.1371/journal.pone.0092712
70. Marchion DC, Cottrill HM, Xiong Y, Chen N, Bicaku E, Fulp WJ, et al. BAD Phosphorylation Determines Ovarian Cancer Chemosensitivity and Patient Survival. *Clin Cancer Res* (2011) 17:6356–66. doi: 10.1158/1078-0432.CCR-11-0735
71. Stickles XB, Marchion DC, Bicaku E, Al Sawah E, Abbasi F, Xiong Y, et al. BAD-Mediated Apoptotic Pathway is Associated With Human Cancer Development. *Int J Mol Med* (2015) 35:1081–7. doi: 10.3892/ijmm.2015.2091
72. Hosseini M, Dousset L, Mahfouf W, Serrano-Sanchez M, Redonnet-Vernhet I, Mesli S, et al. Energy Metabolism Rewiring Precedes UVB-Induced Primary Skin Tumor Formation. *Cell Rep* (2018) 23:3621–34. doi: 10.1016/j.celrep.2018.05.060
73. Hosseini M, Dousset L, Michon P, Mahfouf W, Muzotte E, Bergeron V, et al. UVB-Induced DHODH Upregulation, Which is Driven by STAT3, is a Promising Target for Chemoprevention and Combination Therapy of Photocarcinogenesis. *Oncogenesis* (2019) 8:52. doi: 10.1038/s41389-019-0161-z
74. Hayward NK, Wilmott JS, Waddell N, Johansson PA, Field MA, Nones K, et al. Whole-Genome Landscapes of Major Melanoma Subtypes. *Nature* (2017) 545:175–80. doi: 10.1038/nature22071
75. Dutton-Regester K, Gartner JJ, Emmanuel R, Qutob N, Davies MA, Gershenwald JE, et al. A Highly Recurrent RPS27 5'UTR Mutation in Melanoma. *Oncotarget* (2014) 5:2912–7. doi: 10.18632/oncotarget.2048
76. Floristán A, Morales L, Hanniford D, Martinez C, Castellano-Sanz E, Dolgalev I, et al. Functional Analysis of RPS27 Mutations and Expression in Melanoma. *Pigment Cell Melanoma Res* (2020) 33:466–79. doi: 10.1111/pcmr.12841
77. Huang H-Y, Lin Y-C-D, Li J, Huang K-Y, Shrestha S, Hong H-C, et al. Mirtarbase 2020: Updates to the Experimentally Validated microRNA-

Target Interaction Database. *Nucleic Acids Res* (2020) 48:D148–54. doi: 10.1093/nar/gkz896
78. Salamov AA, Nishikawa T, Swindells MB. Assessing Protein Coding Region Integrity in cDNA Sequencing Projects. *Bioinforma Oxf Engl* (1998) 14:384–90. doi: 10.1093/bioinformatics/14.5.384
79. Peitsch MC. Large Scale Protein Modelling and Model Repository. *Proc Int Conf Intell Syst Mol Biol* (1997) 5:234–6.
80. Chang T-H, Huang H-Y, Hsu JB-K, Weng S-L, Horng J-T, Huang H-D. An Enhanced Computational Platform for Investigating the Roles of Regulatory RNA and for Identifying Functional RNA Motifs. *BMC Bioinf* (2013) 14:S4. doi: 10.1186/1471-2105-14-S2-S4
81. Shoshan E, Braeuer RR, Kamiya T, Mobley AK, Huang L, Vasquez ME, et al. NFAT1 Directly Regulates IL8 and MMP3 to Promote Melanoma Tumor Growth and Metastasis. *Cancer Res* (2016) 76:3145–55. doi: 10.1158/0008-5472.CAN-15-2511
82. Shen Y, Song Z, Lu X, Ma Z, Lu C, Zhang B, et al. Fas Signaling-Mediated T H 9 Cell Differentiation Favors Bowel Inflammation and Antitumor Functions. *Nat Commun* (2019) 10:2924. doi: 10.1038/s41467-019-10889-4
83. Wang NJ, Sanborn Z, Arnett KL, Bayston LJ, Liao W, Proby CM, et al. Loss-Of-Function Mutations in Notch Receptors in Cutaneous and Lung Squamous Cell Carcinoma. *Proc Natl Acad Sci* (2011) 108:17761–6. doi: 10.1073/pnas.1114669108
84. Purdie KJ, Lambert SR, Teh M-T, Chaplin T, Molloy G, Raghavan M, et al. Allelic Imbalances and Microdeletions Affecting the PTPRD Gene in Cutaneous Squamous Cell Carcinomas Detected Using Single Nucleotide Polymorphism Microarray Analysis. *Genes Chromosomes Cancer* (2007) 46:661–9. doi: 10.1002/gcc.20447
85. Veeriah S, Brennan C, Meng S, Singh B, Fagin JA, Solit DB, et al. The Tyrosine Phosphatase PTPRD is a Tumor Suppressor That is Frequently Inactivated and Mutated in Glioblastoma and Other Human Cancers. *Proc Natl Acad Sci* (2009) 106:9435–40. doi: 10.1073/pnas.0900571106
86. Walia V, Prickett TD, Kim J-S, Gartner JJ, Lin JC, Zhou M, et al. Mutational and Functional Analysis of the Tumor-Suppressor PTPRD in Human Melanoma. *Hum Mutat* (2014) 35:1301–10. doi: 10.1002/humu.22630
87. Peyser ND, Du Y, Li H, Lui V, Xiao X, Chan TA, et al. Loss-Of-Function PTPRD Mutations Lead to Increased STAT3 Activation and Sensitivity to STAT3 Inhibition in Head and Neck Cancer. *PloS One* (2015) 10:e0135750. doi: 10.1371/journal.pone.0135750
88. Szaumkessel M, Wojciechowska S, Janiszewska J, Zemke N, Byzia E, Kiwerska K, et al. Recurrent Epigenetic Silencing of the PTPRD Tumor Suppressor in Laryngeal Squamous Cell Carcinoma. *Tumor Biol* (2017) 39:1010428317691427. doi: 10.1177/1010428317691427
89. Adib E, Klonowska K, Giannikou K, Do KT, Pruitt-Thompson S, Bhushan K, et al. Phase II Clinical Trial of Everolimus in a Pan-Cancer Cohort of Patients With mTOR Pathway Alterations. *Clin Cancer Res* (2021) 27 (14):3845–53. doi: 10.1158/1078-0432.CCR-20-4548
90. Wu Z, Hansmann B, Meyer-Hoffert U, Gläser R, Schröder J-M. Molecular Identification and Expression Analysis of Filaggrin-2, a Member of the S100 Fused-Type Protein Family. *PloS One* (2009) 4(4):e5227. doi: 10.1371/journal.pone.0005227
91. Leman G, Moosbrugger-Martinz V, Blunder S, Pavel P, Dubrac S. 3d-Organotypic Cultures to Unravel Molecular and Cellular Abnormalities in Atopic Dermatitis and Ichthyosis Vulgaris. *Cells* (2019) 8(5):489. doi: 10.3390/cells8050489
92. Liu H, Toman RE, Goparaju SK, Maceyka M, Nava VE, Sankala H, et al. Sphingosine Kinase Type 2 is a Putative BH3-Only Protein That Induces Apoptosis. *J Biol Chem* (2003) 278:40330–6. doi: 10.1074/jbc.M304455200
93. Igarashi N, Okada T, Hayashi S, Fujita T, Jahangeer S, Nakamura S. Sphingosine Kinase 2 is a Nuclear Protein and Inhibits DNA Synthesis. *J Biol Chem* (2003) 278:46832–9. doi: 10.1074/jbc.M306577200
94. Maceyka M, Sankala H, Hait NC, Le Stunff H, Liu H, Toman R, et al. SphK1 and SphK2, Sphingosine Kinase Isoenzymes With Opposing Functions in Sphingolipid Metabolism. *J Biol Chem* (2005) 280:37118–29. doi: 10.1074/jbc.M502207200
95. Van Brocklyn JR, Jackson CA, Pearl DK, Kotur MS, Snyder PJ, Prior TW. Sphingosine Kinase-1 Expression Correlates With Poor Survival of Patients With Glioblastoma Multiforme: Roles of Sphingosine Kinase Isoforms in Growth of Glioblastoma Cell Lines. *J Neuropathol Exp Neurol* (2005) 64:695–705. doi: 10.1097/01.jnen.0000175329.59092.2c
96. Gao P, Smith CD. Ablation of Sphingosine Kinase-2 Inhibits Tumor Cell Proliferation and Migration. *Mol Cancer Res MCR* (2011) 9:1509–19. doi: 10.1158/1541-7786.MCR-11-0336
97. Su X, Malouf GG, Chen Y, Zhang J, Yao H, Valero V, et al. Comprehensive Analysis of Long non-Coding RNAs in Human Breast Cancer Clinical Subtypes. *Oncotarget* (2014) 5:9864–76. doi: 10.18632/oncotarget.2454
98. Segers VFM, Dugaucquier L, Feyen E, Shakeri H, De Keulenaer GW. The Role of ErbB4 in Cancer. *Cell Oncol Dordr* (2020) 43:335–52. doi: 10.1007/s13402-020-00499-4
99. Sand M, Gambichler T, Skrygan M, Sand D, Scola N, Altmeyer P, et al. Expression Levels of the microRNA Processing Enzymes Drosha and Dicer in Epithelial Skin Cancer. *Cancer Invest* (2010) 28:649–53. doi: 10.3109/07357901003630918
100. Griewank KG, Murali R, Schilling B, Schimming T, Möller I, Moll I, et al. TERT Promoter Mutations are Frequent in Cutaneous Basal Cell Carcinoma and Squamous Cell Carcinoma. *PloS One* (2013) 8:e80354. doi: 10.1371/journal.pone.0080354
101. Scott GA, Laughlin TS, Rothberg PG. Mutations of the TERT Promoter are Common in Basal Cell Carcinoma and Squamous Cell Carcinoma. *Mod Pathol Off J U S Can Acad Pathol Inc* (2014) 27:516–23. doi: 10.1038/modpathol.2013.167
102. Di Nardo L, Pellegrini C, Di Stefani A, Ricci F, Fossati B, Del Regno L, et al. Molecular Alterations in Basal Cell Carcinoma Subtypes. *Sci Rep* (2021) 11:13206. doi: 10.1038/s41598-021-92592-3
103. Malhotra N, Leyva-Castillo JM, Jadhav U, Barreiro O, Kam C, O'Neill NK, et al. Rorα-Expressing T Regulatory Cells Restrain Allergic Skin Inflammation. *Sci Immunol* (2018) 3(21):eaa06923. doi: 10.1126/sciimmunol.aao6923
104. Houle AA, Gibling H, Lamaze FC, Edgington HA, Soave D, Fave M-J, et al. Aberrant PRDM9 Expression Impacts the Pan-Cancer Genomic Landscape. *Genome Res* (2018) 28:1611–20. doi: 10.1101/gr.231696.117
105. Nicolai S, Mahen R, Raschellà G, Marini A, Pieraccioli M, Malewicz M, et al. ZNF281 is Recruited on DNA Breaks to Facilitate DNA Repair by non-Homologous End Joining. *Oncogene* (2020) 39:754–66. doi: 10.1038/s41388-019-1028-7
106. Pasparakis M, Courtois G, Hafner M, Schmidt-Supprian M, Nenci A, Toksoy A, et al. TNF-Mediated Inflammatory Skin Disease in Mice With Epidermis-Specific Deletion of IKK2. *Nature* (2002) 417:861–6. doi: 10.1038/nature00820
107. Stratis A, Pasparakis M, Markur D, Knaup R, Pofahl R, Metzger D, et al. Localized Inflammatory Skin Disease Following Inducible Ablation of I Kappa B Kinase 2 in Murine Epidermis. *J Invest Dermatol* (2006) 126:614–20. doi: 10.1038/sj.jid.5700092
108. Cornish GH, Tung SL, Marshall D, Ley S, Seddon BP. Tissue Specific Deletion of Inhibitor of Kappa B Kinase 2 With OX40-Cre Reveals the Unanticipated Expression From the OX40 Locus in Skin Epidermis. *PloS One* (2012) 7(2):e32193. doi: 10.1371/journal.pone.0032193
109. Kirkley KS, Walton KD, Duncan C, Tjalkens RB. Spontaneous Development of Cutaneous Squamous Cell Carcinoma in Mice With Cell-Specific Deletion of Inhibitor of κb Kinase 2. *Comp Med* (2017) 67:407–15.
110. Boyle GM, Woods SL, Bonazzi VF, Stark MS, Hacker E, Aoude LG, et al. Melanoma Cell Invasiveness is Regulated by miR-211 Suppression of the BRN2 Transcription Factor. *Pigment Cell Melanoma Res* (2011) 24:525–37. doi: 10.1111/j.1755-148X.2011.00849.x
111. Simmons JL, Pierce CJ, Al-Ejeh F, Boyle GM. MITF and BRN2 Contribute to Metastatic Growth After Dissemination of Melanoma. *Sci Rep* (2017) 7:10909. doi: 10.1038/s41598-017-11366-y
112. Zhao G, Wei Z, Guo Y. MicroRNA-107 is a Novel Tumor Suppressor Targeting POU3F2 in Melanoma. *Biol Res* (2020) 53:11. doi: 10.1186/s40659-020-00278-3
113. Ikeda S, Goodman AM, Cohen PR, Jensen TJ, Ellison CK, Frampton G, et al. Metastatic Basal Cell Carcinoma With Amplification of PD-L1: Exceptional Response to Anti-PD1 Therapy. *NPJ Genomic Med* (2016) 1:1–5. doi: 10.1038/npjgenmed.2016.37
114. Chandramouli A, Shi J, Feng Y, Holubec H, M.Shanas R, Bhattacharyya AK, et al. Haploinsufficiency of the Cdc2l Gene Contributes to Skin Cancer

Development in Mice. *Carcinogenesis* (2007) 28:2028–35. doi: 10.1093/carcin/bgm066
115. de Cid R, Riveira-Munoz E, Zeeuwen PLJM, Robarge J, Liao W, Dannhauser EN, et al. Deletion of the Late Cornified Envelope LCE3B and LCE3C Genes as a Susceptibility Factor for Psoriasis. *Nat Genet* (2009) 41:211–5. doi: 10.1038/ng.313
116. Myskowski PL, Pollack MS, Schorr E, Dupont B, Safai B. Human Leukocyte Antigen Associations in Basal Cell Carcinoma. *J Am Acad Dermatol* (1985) 12:997–1000. doi: 10.1016/s0190-9622(85)70127-2
117. Hua LA, Kagen CN, Carpenter RJ, Goltz RW. HLA and Beta 2-Microglobulin Expression in Basal and Squamous Cell Carcinomas of the Skin. *Int J Dermatol* (1985) 24:660–3. doi: 10.1111/j.1365-4362.1985.tb05719.x
118. Markey AC, Churchill LJ, MacDonald DM. Altered Expression of Major Histocompatibility Complex (MHC) Antigens by Epidermal Tumours. *J Cutan Pathol* (1990) 17:65–71. doi: 10.1111/j.1600-0560.1990.tb00058.x
119. Streilein JW. Immunogenetic Factors in Skin Cancer. *N Engl J Med* (1991) 325:884–7. doi: 10.1056/NEJM199109193251210
120. García-Plata D, Mozos E, Carrasco L, Solana R. HLA Molecule Expression in Cutaneous Squamous Cell Carcinomas: An Immunopathological Study and Clinical-Immunohistopathological Correlations. *Histol Histopathol* (1993) 8:219–26.
121. Johnson DB, Estrada MV, Salgado R, Sanchez V, Doxie DB, Opalenik SR, et al. Melanoma-Specific MHC-II Expression Represents a Tumour-Autonomous Phenotype and Predicts Response to Anti-PD-1/PD-L1 Therapy. *Nat Commun* (2016) 7:10582. doi: 10.1038/ncomms10582
122. Chen Y-Y, Chang W-A, Lin E-S, Chen Y-J, Kuo P-L. Expressions of HLA Class II Genes in Cutaneous Melanoma Were Associated With Clinical Outcome: Bioinformatics Approaches and Systematic Analysis of Public Microarray and RNA-Seq Datasets. *Diagnostics* (2019) 9(2):59. doi: 10.3390/diagnostics9020059
123. Stanisz H, Saul S, Müller CSL, Kappl R, Niemeyer BA, Vogt T, et al. Inverse Regulation of Melanoma Growth and Migration by Orai1/STIM2-Dependent Calcium Entry. *Pigment Cell Melanoma Res* (2014) 27:442–53. doi: 10.1111/pcmr.12222
124. Isvoranu G, Surcel M, Huică R-I, Munteanu AN, Pîrvu IR, Ciotaru D, et al. Natural Killer Cell Monitoring in Cutaneous Melanoma - New Dynamic Biomarker. *Oncol Lett* (2019) 17:4197–206. doi: 10.3892/ol.2019.10069
125. Sanchez-Canteli M, Hermida-Prado F, Sordo-Bahamonde C, Montoro-Jiménez I, Pozo-Agundo E, Allonca E, et al. Lectin-Like Transcript 1 (LLT1) Checkpoint: A Novel Independent Prognostic Factor in HPV-Negative Oropharyngeal Squamous Cell Carcinoma. *Biomedicines* (2020) 8 (12):535. doi: 10.3390/biomedicines8120535
126. Lone MA, Hülsmeier AJ, Saied EM, Karsai G, Arenz C, von Eckardstein A, et al. Subunit Composition of the Mammalian Serine-Palmitoyltransferase Defines the Spectrum of Straight and Methyl-Branched Long-Chain Bases. *Proc Natl Acad Sci* (2020) 117:15591–8. doi: 10.1073/pnas.2002391117
127. Thomas NE, Edmiston SN, Tsai YS, Parker JS, Googe PB, Busam KJ, et al. Utility of TERT Promoter Mutations for Cutaneous Primary Melanoma Diagnosis. *Am J Dermatopathol* (2019) 41:264–72. doi: 10.1097/DAD.0000000000001259
128. Shaughnessy M, Njauw C-N, Artomov M, Tsao H. Classifying Melanoma by TERT Promoter Mutational Status. *J Invest Dermatol* (2020) 140:390–394.e1. doi: 10.1016/j.jid.2019.06.149
129. Yang E, Zha J, Jockel J, Boise LH, Thompson CB, Korsmeyer SJ. Bad, a Heterodimeric Partner for Bcl-xL and Bcl-2, Displaces Bax and Promotes Cell Death. *Cell* (1995) 80:285–91. doi: 10.1016/0092-8674(95)90411-5
130. Datta SR, Dudek H, Tao X, Masters S, Fu H, Gotoh Y, et al. Akt Phosphorylation of BAD Couples Survival Signals to the Cell-Intrinsic Death Machinery. *Cell* (1997) 91:231–41. doi: 10.1016/s0092-8674(00)80405-5
131. Sastry KSR, Al-Muftah MA, Li P, Al-Kowari MK, Wang E, Ismail Chouchane A, et al. Targeting Proapoptotic Protein BAD Inhibits Survival and Self-Renewal of Cancer Stem Cells. *Cell Death Differ* (2014) 21:1936–49. doi: 10.1038/cdd.2014.140
132. Sastry KS, Ibrahim WN, Chouchane AI. Multiple Signaling Pathways Converge on Proapoptotic Protein BAD to Promote Survival of Melanocytes. *FASEB J* (2020) 34:14602–14. doi: 10.1096/fj.202001260RR
133. Vander Heiden MG, Li XX, Gottleib E, Hill RB, Thompson CB, Colombini M. Bcl-xL Promotes the Open Configuration of the Voltage-Dependent Anion Channel and Metabolite Passage Through the Outer Mitochondrial Membrane. *J Biol Chem* (2001) 276:19414–9. doi: 10.1074/jbc.M101590200
134. Danial NN, Gramm CF, Scorrano L, Zhang C-Y, Krauss S, Ranger AM, et al. BAD and Glucokinase Reside in a Mitochondrial Complex That Integrates Glycolysis and Apoptosis. *Nature* (2003) 424:952–6. doi: 10.1038/nature01825
135. Seo SY, Chen Y, Ivanovska I, Ranger AM, Hong SJ, Dawson VL, et al. BAD Is a Pro-Survival Factor Prior to Activation of Its Pro-Apoptotic Function*. *J Biol Chem* (2004) 279:42240–9. doi: 10.1074/jbc.M406775200
136. Danial NN, Walensky LD, Zhang C-Y, Choi CS, Fisher JK, Molina AJA, et al. Dual Role of Proapoptotic BAD in Insulin Secretion and Beta Cell Survival. *Nat Med* (2008) 14:144–53. doi: 10.1038/nm1717
137. Roy SS, Madesh M, Davies E, Antonsson B, Danial N, Hajnóczky G. Bad Targets the Permeability Transition Pore Independent of Bax or Bak to Switch Between Ca2+-Dependent Cell Survival and Death. *Mol Cell* (2009) 33:377–88. doi: 10.1016/j.molcel.2009.01.018
138. Berman SB, Chen Y, Qi B, McCaffery JM, Rucker EB, Goebbels S, et al. Bcl-X L Increases Mitochondrial Fission, Fusion, and Biomass in Neurons. *J Cell Biol* (2009) 184:707–19. doi: 10.1083/jcb.200809060
139. Aouacheria A, Baghdiguian S, Lamb HM, Huska JD, Pineda FJ, Hardwick JM. Connecting Mitochondrial Dynamics and Life-or-Death Events *via* Bcl-2 Family Proteins. *Neurochem Int* (2017) 109:141–61. doi: 10.1016/j.neuint.2017.04.009
140. Tomková H, Fujimoto W, Arata J. Expression of the Bcl-2 Homologue Bax in Normal Human Skin, Psoriasis Vulgaris and non-Melanoma Skin Cancers. *Eur J Dermatol EJD* (1998) 8:256–60.
141. Karst AM, Dai DL, Martinka M, Li G. PUMA Expression is Significantly Reduced in Human Cutaneous Melanomas. *Oncogene* (2005) 24:1111–6. doi: 10.1038/sj.onc.1208374
142. Aras S, Bai M, Lee I, Springett R, Hüttemann M, Grossman LI. MNRR1 (Formerly CHCHD2) is a Bi-Organellar Regulator of Mitochondrial Metabolism. *Mitochondrion* (2015) 20:43–51. doi: 10.1016/j.mito.2014.10.003
143. Liu Y, Clegg HV, Leslie PL, Di J, Tollini LA, He Y, et al. CHCHD2 Inhibits Apoptosis by Interacting With Bcl-X L to Regulate Bax Activation. *Cell Death Differ* (2015) 22:1035–46. doi: 10.1038/cdd.2014.194
144. Aras S. Mitochondrial Autoimmunity and MNRR1 in Breast Carcinogenesis. *BMC Cancer* (2019) 19:411. doi: 10.1186/s12885-019-5575-7
145. Rosmarin AG, Resendes KK, Yang Z, McMillan JN, Fleming SL. GA-Binding Protein Transcription Factor: A Review of GABP as an Integrator of Intracellular Signaling and Protein-Protein Interactions. *Blood Cells Mol Dis* (2004) 32:143–54. doi: 10.1016/j.bcmd.2003.09.005
146. Funayama M, Ohe K, Amo T, Furuya N, Yamaguchi J, Saiki S, et al. CHCHD2 Mutations in Autosomal Dominant Late-Onset Parkinson's Disease: A Genome-Wide Linkage and Sequencing Study. *Lancet Neurol* (2015) 14:274–82. doi: 10.1016/S1474-4422(14)70266-2
147. White RM, Cech J, Ratanasirintrawoot S, Lin CY, Rahl PB, Burke CJ, et al. DHODH Modulates Transcriptional Elongation in the Neural Crest and Melanoma. *Nature* (2011) 471:518–22. doi: 10.1038/nature09882
148. Garcia-Bermudez J, Baudrier L, La K, Zhu XG, Fidelin J, Sviderskiy VO, et al. Aspartate is a Limiting Metabolite for Cancer Cell Proliferation Under Hypoxia and in Tumors. *Nat Cell Biol* (2018) 20:775–81. doi: 10.1038/s41556-018-0118-z
149. Qian Y, Liang X, Kong P, Cheng Y, Cui H, Yan T, et al. Elevated DHODH Expression Promotes Cell Proliferation *via* Stabilizing β-Catenin in Esophageal Squamous Cell Carcinoma. *Cell Death Dis* (2020) 11:1–13. doi: 10.1038/s41419-020-03044-1
150. Qin J-J, Nag S, Wang W, Zhou J, Zhang W-D, Wang H, et al. NFAT as Cancer Target: Mission Possible? *Biochim Biophys Acta* (2014) 1846:297–311. doi: 10.1016/j.bbcan.2014.07.009
151. Mancini M, Toker A. NFAT Proteins: Emerging Roles in Cancer Progression. *Nat Rev Cancer* (2009) 9:810–20. doi: 10.1038/nrc2735
152. Zhang X, Zhang Z, Cheng J, Li M, Wang W, Xu W, et al. Transcription Factor NFAT1 Activates the Mdm2 Oncogene Independent of P53. *J Biol Chem* (2012) 287:30468–76. doi: 10.1074/jbc.M112.373738

153. Chang ALS, Tran DC, Cannon JGD, Li S, Jeng M, Patel R, et al. Pembrolizumab for Advanced Basal Cell Carcinoma: An Investigator-Initiated, Proof-of-Concept Study. *J Am Acad Dermatol* (2019) 80:564–6. doi: 10.1016/j.jaad.2018.08.017

Conflict of Interest: The authors declare that the research was conducted in the absence of any commercial or financial relationships that could be construed as a potential conflict of interest.

Publisher's Note: All claims expressed in this article are solely those of the authors and do not necessarily represent those of their affiliated organizations, or those of the publisher, the editors and the reviewers. Any product that may be evaluated in this article, or claim that may be made by its manufacturer, is not guaranteed or endorsed by the publisher.

Copyright © 2021 Nawrocka, Galka-Marciniak, Urbanek-Trzeciak, M-Thirusenthilarasan, Szostak, Philips, Susok, Sand and Kozlowski. This is an open-access article distributed under the terms of the Creative Commons Attribution License (CC BY). The use, distribution or reproduction in other forums is permitted, provided the original author(s) and the copyright owner(s) are credited and that the original publication in this journal is cited, in accordance with accepted academic practice. No use, distribution or reproduction is permitted which does not comply with these terms.

frontiers in Oncology

SYSTEMATIC REVIEW
published: 07 December 2021
doi: 10.3389/fonc.2021.772165

Predictive Performance of Serum S100B *Versus* LDH in Melanoma Patients: A Systematic Review and Meta-Analysis

*Eszter Anna Janka[1], Tünde Várvölgyi[1], Zoltán Sipos[2], Alexandra Soós[2], Péter Hegyi[2], Szabolcs Kiss[2,3], Fanni Dembrovszky[2], Dezső Csupor[2,4], Patrik Kéringer[2], Dániel Pécsi[2], Margit Solymár[2] and Gabriella Emri[1]**

[1] Department of Dermatology, Faculty of Medicine, University of Debrecen, Debrecen, Hungary, [2] Institute for Translational Medicine, Medical School, University of Pécs, Pécs, Hungary, [3] Doctoral School of Clinical Medicine, University of Szeged, Szeged, Hungary, [4] Department of Pharmacognosy, Faculty of Pharmacy, University of Szeged, Szeged, Hungary

OPEN ACCESS

Edited by:
Kalijn Bol,
Radboud University Nijmegen Medical Centre, Netherlands

Reviewed by:
Luca Falzone,
Istituto Nazionale Tumori Fondazione G. Pascale (IRCCS), Italy
Andrzej T Slominski,
University of Alabama at Birmingham, United States

***Correspondence:**
Gabriella Emri
gemri@med.unideb.hu

Specialty section:
This article was submitted to Skin Cancer, a section of the journal Frontiers in Oncology

Received: *07 September 2021*
Accepted: *11 November 2021*
Published: *07 December 2021*

Citation:
Janka EA, Várvölgyi T, Sipos Z, Soós A, Hegyi P, Kiss S, Dembrovszky F, Csupor D, Kéringer P, Pécsi D, Solymár M and Emri G (2021) Predictive Performance of Serum S100B Versus LDH in Melanoma Patients: A Systematic Review and Meta-Analysis. Front. Oncol. 11:772165. doi: 10.3389/fonc.2021.772165

Background: Currently, no consensus on the use of blood tests for monitoring disease recurrence in patients with resected melanoma exists. The only meta-analysis conducted in 2008 found that elevated serum S100B levels were associated with significantly worse survival in melanoma patients. Serum LDH is an established prognostic factor in patients with advanced melanoma.

Objective: To compare the discriminative and prognostic ability of serum S100B with that of serum LDH in patients with melanoma.

Methods: This systematic review and meta-analysis were reported in accordance with the PRISMA Statement. The study protocol was registered in the International Prospective Register of Systematic Reviews (PROSPERO; CRD42019137138).

Results: A quantitative analysis of data from 6 eligible studies included 1,033 patients with cutaneous melanoma. The discriminative ability of serum S100B at identifying disease relapse [pooled Area Under the ROC (AUROC) 78.64 (95% CI 70.28; 87.01)] was significantly greater than the discriminative ability of serum LDH [AUROC 64.41 (95% CI 56.05; 7278)] (p=0.013). Ten eligible studies with 1,987 patients were included in the risk of death analysis. The prognostic performance of serum S100B [pooled estimate of adjusted hazard ratio (HR) 1.78 (95% CI 1.38; 2.29)] was independent but not superior to that of serum LDH [HR 1.60 (95% CI 1.36; 2.29)].

Limitations: A relatively small number of articles were eligible and there was considerable heterogeneity across the included studies.

Conclusions: Serum biomarkers may provide relevant information on melanoma patient status and should be further researched. Serum S100B is a valid marker for diagnosis of melanoma recurrence.

Systematic Review Registration: The study protocol was registered in the International Prospective Register of Systematic Reviews (PROSPERO; CRD42019137138).

Keywords: melanoma, S100B, LDH, ROC, COX, meta-analysis

INTRODUCTION

The prevalence of melanoma is increasing worldwide among fair-skinned populations (1). Age-standardized world incidence rates are 0.33-35.8 per 100,000 according to the GLOBOCAN 2020 statistics (2). Melanoma is a cancer arising from the malignant transformation of pigment producing melanocytes. Ultraviolet radiation is an important risk factor for development of melanoma (3). However, the road from sun exposure to cutaneous melanoma is complex and diverse (3). Ultraviolet light is absorbed by nucleic acids, proteins or other endogenous chromophores, triggering biological processes in skin cells (3, 4). The degree of ultraviolet radiation induced stress and the protection against this stress are influenced both intracellular and intercellular molecular interactions (3). The interaction of variable environmental exposure and different genetic susceptibility and other host factors lead to the formation of melanomas with different biological behaviour and clinical characteristics (3, 5). In addition, melanoma derived proopiomelanocortin peptides, glucocorticoids, neurotransmitters, hormones, and intermediates of melanogenesis can affect the local and systemic immune responses, leading to tumor progression and therapy resistance (5). The synthesis of melanin is a tightly regulated multistep biochemical process (5). Melanogenesis can affect melanoma behaviour and disease outcome through regulation of cellular metabolism, and protecting melanoma cells against radiotherapy (6).

Melanoma is a tumor with a high risk of metastasis, and although disease relapse occurs most frequently in the first 3 years after resection of primary tumor, metastasis can occur any time and at any site (7). Thus, easily accessed (e.g., blood) cancer biomarkers for the early detection of disease relapse are urgently needed. The biomarkers should also provide prognostic information related to tumor biology and mirror tumor burden when traditional radiological criteria are not applicable to assess clinical benefit from therapy (8–10). Such biomarkers could improve patient outcomes. Furthermore, therapeutic response to immune checkpoint inhibitors or selective tyrosine kinase inhibitors is heterogeneous due to the complex interactions between the host and tumor (11–13). It is of great interest to identify biomarkers predicting clinical benefit from a particular therapy. Valid prognostic biomarkers associated with a specific aspect of tumor progression and metastasis are good candidates for such predictive models (11–14).

Serum lactate dehydrogenase (LDH) was the first prognostic blood biomarker to be included in the American Joint Committee on Cancer (AJCC) staging system for patients with metastatic melanoma3. In two meta-analyses performed by Petrelli et al. in 2015 and 2019, the prognostic effects of elevated serum LDH proved to be significant in melanoma (15, 16). Serum LDH correlates with tumor volume and necrosis and is not specific to tumor type (15). In addition, an elevation in serum LDH levels may correlate with tissue damage independent of malignancy. The tumor marker, S100B, is more specific to melanoma (9, 17, 18). Serum levels of S100B reflect tumor volume in metastatic disease; however, serum S100B levels can also be elevated in many other diseases, such as cardiovascular diseases, liver cirrhosis, migraine, chronic kidney disease, previous stroke, vitiligo, breast cancer, and SARS-CoV-2 infection (19–21). The only meta-analysis focused on serum S100B and melanoma showed that elevated serum S100B levels are associated with significantly worse survival in patients with melanoma (22).

Serum tumor markers usually have both prognostic and diagnostic predictive value to varying degrees (9, 10). From a diagnostic perspective, serum S100B levels are monitored in many cancer centers to detect disease relapse, while serum LDH is monitored less frequently in melanoma patients. A strong statistical correlation between S100B expression in melanoma tumor tissue samples and tumor stage has been found, and S100B protein is a possible target of therapeutic intervention (23–25). However, the estimates of sensitivity and specificity of serum S100B are highly variable (32-94% and 76-97%, respectively (26). Currently, no consensus on the use of blood tests for monitoring disease recurrence in patients with resected melanoma exists (27–30).

Although many serologic protein and non-protein markers that could aid early diagnosis of melanoma relapse as well as indicate patients' prognosis have been reported, often primary studies are of variable quality and the findings are inconsistent (11, 23). Systematic reviews and meta-analyses are considered the reliable form to summarize the evidence about the prognostic and diagnostic value of particular factors (31). Meta-analysis to demonstrate whether serum S100B is a valid marker for the diagnosis of melanoma recurrence has not yet been published (23).

The objective of this study was to compare the prognostic and diagnostic abilities of serum S100B and serum LDH in patients with melanoma. Studies using Receiver Operating Characteristic (ROC) curves and Cox multivariate proportional-hazards models were included. The advantage of ROC is that the Area Under the ROC (AUROC) can be used to compare the accuracy of different diagnostic tests (32). The Cox regression model allows to detect and adjust for imbalance in prognostic variables; thus, it can be used to estimate more precisely a marker-dependent prognosis (33).

METHODS

This systematic review and meta-analysis were reported in accordance with the Preferred Reporting Items for Systematic

Reviews and Meta-Analyses (PRISMA) Statement (31, 34, 35) (**Supplementary Table 1**: PRISMA-DTA Checklist). The study protocol was registered in the International Prospective Register of Systematic Reviews (PROSPERO; CRD42019137138).

Deviation from the Registered Protocol

No subgroup analysis was planned. However, one eligible primary diagnostic effect study included patients with uveal melanoma, all other patients had cutaneous melanoma. Because the pathogenesis of uveal is different from cutaneous melanoma, the quantitative analysis was performed with the studies in which cutaneous melanoma patients were included. In addition, a diagnostic effect meta-analysis, which also included the study with uveal melanoma patients, was performed.

Eligibility Criteria

Review questions were formulated using the PICOTS system according to the CHecklist for critical Appraisal and data extraction for systematic Reviews of prediction Modelling Studies (CHARMS) adapted to reviews of diagnostic effect studies and prognostic factor studies (31). The questions were formulated to determine whether elevated serum S100B is a more reliable marker than elevated serum LDH for predicting disease relapse in patients with different stages of melanoma and to determine whether elevated serum S100B is a more reliable marker than elevated serum LDH for predicting the risk of death and survival rates in metastatic melanoma. Articles providing information on S100B and LDH measurements at relapse confirmed by imaging and/or histopathological examination or overall risk of death and survival rates 1 and 2 years after S100B and LDH measurements were included. Studies assigning weights to the selected predictors (S100B and LDH) using Receiver Operating Characteristic (ROC) curves and Cox multivariate proportional-hazards models were included. The set of adjustment factors differed across primary prognostic studies. According to our pre-specifications, the studies included in the analysis used a minimum set of these factors: LDH and S100B plus at least one additional established prognostic marker, e.g., site of metastases or the presence of cerebral metastasis. If the patients enrolled in the study received therapy, we chose the results of the Cox model that was also adjusted for treatment. The findings should be useful for dermatologists and oncologists in the care of patients with melanoma.

Search Strategy and Study Selection

MEDLINE, Embase, and the Cochrane Central Register of Controlled Trials were systematically searched from inception until January 15, 2021. The search included only English-language studies. Only the predictive factors in question and the targeted disease were used as keywords and terms for searching, including *S100B* or *S100* or *S-100B* or *S-100* and *lactate dehydrogenase* or *LDH* and *melanoma* in MEDLINE (*via* PubMed) and *melanoma* and *S100B* and *lactate dehydrogenase* in Embase and the Cochrane Central Register of Controlled Trials.

Data Extraction

We followed the recommendations of CHARMS for data extraction (31). The items needed for the meta-analysis, assessment of applicability, and risk of bias were collected in Excel tables in a standard manner. First author and design of the study, the country where the study was conducted, and the year of publication, size of population (with and without metastasis, if applicable), inclusion and exclusion criteria for patient enrollment, demography (age, sex), information about the method and cut point of S100B and LDH measurement and reference test, the baseline prognostic factors used in Cox models, and outcome data of interest were extracted. Search, study selection, and data extraction were done by EAJ and GE, independently, and a consensus was reached through discussion.

Assessment of Applicability and Risk of Bias (ROB)

Two authors (EAJ, GE) independently assessed study quality, and consensus was facilitated by flow diagrams for primary studies. To assess ROB and concerns regarding the applicability of diagnostic accuracy studies, the Quality Assessment of Diagnostic Accuracy Studies (QUADAS-2) tool was used (36). ROB of prognostic factor studies was assessed according to the Quality In Prognosis Studies (QUIPS) tool (37).

Statistical Analysis

Heterogeneity across studies was assessed using the I^2 statistics, where $I^2 = 100\% \times (Q - df)/Q$ and represents the magnitude of the heterogeneity (moderate: 30–60%; substantial: 50–90%; considerable: 75–100%) (38). Pooled estimates (AUROC with 95% confidence intervals, sensitivity, specificity, adjusted HR with 95% confidence intervals, survival rates (1-year, 2-year) with 95% confidence intervals) were calculated using a DerSimonian-Laird random-effect model (39). Funnel plots and Egger's tests were applied to access the presence of publication bias. Statistical analyses were performed with Stata 16.1 data analysis and statistical software (Stata Corp LLC, College Station, TX, USA) and R package, version 4.0.3. (R Foundation for Statistical Computing).

RESULTS

Study Selection and Characteristics of Included Studies

The literature search yielded 478 records (**Figure 1**). After the removal of non-English-language studies and duplicates, 389 articles remained. Based on titles or abstracts, 92 articles were selected for full-text screening. Thirteen full-texts were not available and 62 did not meet eligibility criteria. Finally, 7 primary diagnostic effect studies (6 cutaneous melanoma, 1 uveal melanoma) (40–46) and 10 primary prognostic factor studies (47–56) were selected for the qualitative and quantitative synthesis. Characteristics of the included studies are summarized in **Tables 1**–**3** and **Figure 2**.

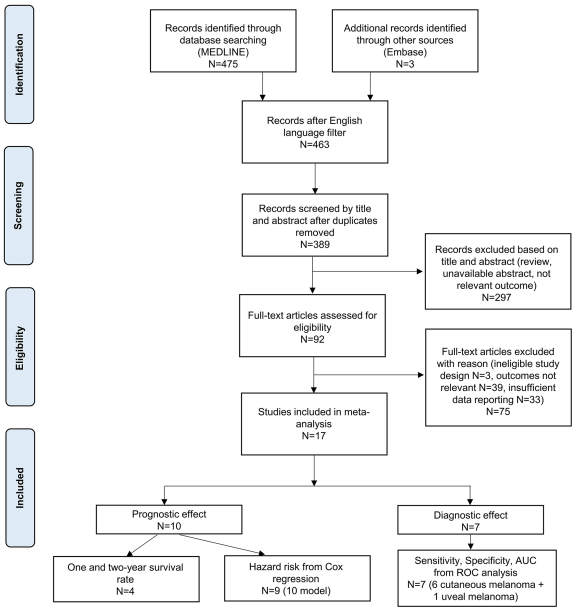


FIGURE 1 | PRISMA flowchart. AUC, area under curve; ROC, Receiver Operating Characteristic.

Quality of the Included Studies

The qualitative evaluation demonstrated that many studies were performed with bias; the greatest risk of bias was found in the study reference standards. Imaging techniques with different sensitivities and specificities as a reference standard for detection of disease relapse varied depending on the stage in the diagnostic accuracy studies. Because not all domains could be rated as having low ROB, the overall judgment was avoided. Publication bias was unlikely according to the Funnel plot for AUROC (**Supplementary Figures 1**, **2**). The Funnel plot and Egger's test did not verify publication bias for Cox hazard ratios (p=0.245 for S100B; p=0.344 for LDH) (**Supplementary Figure 3**).

Diagnostic Effect Meta-Analysis

Six eligible studies with 1,033 patients with cutaneous melanoma were included in the meta-analysis. The quantitative evaluation showed that discriminative ability of S100B to correctly identify patients with or without melanoma relapse [AUROC 78.64 (70.28; 87.01)] was significantly (p=0.013) greater than the discriminative ability of LDH [AUROC 64.41 (56.05; 72.78)] (**Figure 3**). In addition, sensitivity and specificity were analyzed in these studies using predefined cut-off points (**Table 1**) for the dichotomized continuous values of serum S100B and LDH. The pooled sensitivity of S100B [61.35% (95% CI 48.90; 73.80)] was significantly higher (p=0.017) than the pooled sensitivity of LDH [33.93% (95% CI 17.21; 50.65)] (**Supplementary Figure 4**). The pooled specificity of S100B [87.30% (95% CI 81.10; 93.49)] was similar (p=0.557) to the pooled specificity of LDH [90.70% (95% CI 84.89; 96.51] (**Supplementary Figure 5**). The ROC optimized cut-off point for serum S100B was higher than the cutoff predefined by the manufacturer and was associated with higher specificity, but lower sensitivity (40, 43).

A quantitative analysis of data from 7 eligible studies included 1,167 participants (n=1,033 cutaneous melanoma, n=134 uveal melanoma). The discriminative ability of serum S100B to correctly identify patients with or without disease relapse [AUROC 79.75 (95% CI 72.28; 87.21)] did not differ significantly (p=0.061) from the discriminative ability of serum LDH [AUROC 68.18 (95% CI 57.65; 78.69)] (**Supplementary Figure 6**). The pooled sensitivity of serum S100B [61.37% (95% CI 50.21; 72.54)] was significantly higher (p=0.024) than the sensitivity of LDH [37.47% (95% CI 21.20; 53.73)] (**Supplementary Figure 7**). The pooled specificity of S100B [89.22% (95% CI 84.00; 94.43)] was similar (p=0.643) to the pooled specificity of LDH [91.25% (95% CI 86.40; 96.10)] (**Supplementary Figure 8**).

Prognostic Effect Meta-Analysis

Ten eligible studies with 1,987 participants were included (**Table 2**) in the adjusted hazard ratios analysis using the Cox multivariate proportional-hazards models of overall survival (**Figure 4**). There were no significant differences between the hazard ratios associated with elevated serum S100B levels [1.78 (1.38; 2.29)] and the hazard ratios of elevated LDH levels [1.60 (1.36; 1.88)] (p=0.389). Both elevated serum S100B levels and elevated LDH levels predicted a higher risk of death in patients with metastatic melanoma.

Four eligible studies with 1,940 participants were included in the analysis of one-, and two-year survival rates (**Table 3**). The pooled one-year survival rate of patients with normal serum

TABLE 1 | Characteristics of included diagnostic effect studies in the meta-analysis.

						AUC (ROC analysis), Sensitivity, Specificity						
First author (Year of publication)	**Country**	**Design of the study**	**Settings**	**Population**	**Female %**	**S100B cutoff (μg/L)**	**S100B methods**	**LDH cutoff (IU/L)**	**LDH methods**	**Total number of patients**	**No. of patients with regional or distant metastasis**	**No. of patients without regional or distant metastasis**
Henry et al., 2012 (40)	France	prospective	single center	Stage I-IV melanoma (unknown SLN status, stage I-II at inclusion 44%)	41.3	0.15	LIAISON® Sangtec® 100	ULN (240)	automated colourimetric assay	121	43	78
Díaz-Lagares et al., 2011 (41)	Spain	retrospective	single center	Stage I-IV melanoma	54	0.1	Elecsys® S100	ULN (292)	automated colourimetric assay	176	110	66
Garbe et al., 2003 (42)	Germany	prospective	single center	Stage II-III melanoma (unknown SLN status, stage II at inclusion 56%)	56.8	0.12	LIA-mat® Sangtec® 100	ULN (240)	automated colourimetric assay	296	41	255
Garnier et al., 2007 (43)	France	prospective	single center	Stage I-IV melanoma (stage I-II at inclusion 34%)	46.5	0.12	LIA-mat® Sangtec® 100	ULN (439)	automated colourimetric assay	170	113	57
Mohammed et al., 2001 (44)	United Kingdom	prospective	single center	Stage I-IV melanoma (stage I-II at inclusion 12%)	50.6	0.15	LIA-mat® Sangtec® 100	ULN (500)	automated colourimetric assay	164	85	79
Maier et al., 2012 (45)	Germany	retrospective	single center	Stage I-IV melanoma	43.4	0.11	Elecsys® S100	ULN (250)	automated colourimetric assay	106	24	82
Missotten et al., 2007 (46)	The Netherlands	retrospective	single center	Nonmetastatic and metastatic uveal melanoma	N.R.	0.16	LIAISON® Sangtec® 100	ULN (450)	automated colourimetric assay	134	30	104

SLN, sentinel lymph node; ULN, upper limit normal; N.R., not reported.
Cutoff levels for serum S100B were selected as the 95th percentile of the control group defined by the manufacturer (40, 43, 44) or a previous report (45), or determined by including healthy individuals in the study (41, 42, 46). ROC optimized cutoffs were reported in only a few studies (40, 43). Colorimetric assays were used in all selected studies for determining serum LDH. The cutoff was usually the upper limit of the normal (ULN) level as defined by the local laboratory.

S100B levels was significantly higher [55.92% (39.91%; 71.92%)] than the one-year survival rate of patients with elevated serum S100B levels [28.08% (10.83%; 45.34%)] (p=0.033) (**Supplementary Figure 9**). A similar trend was observed for the two-year survival rate [normal serum S100B: 32.51% (24.36%; 40.67%); elevated serum S100B: 14.68% (5.77%; 23.58%)], but the difference was not significant (p=0.082) (**Supplementary Figure 10**). The one-year survival rate was higher for patients with normal serum LDH levels [46.16% (29.25%; 63.06%)] than the one-year survival rate for patients with elevated serum LDH levels [25.94 (8.15%; 43.72%)], but the difference was not significant (p=0.152) (**Supplementary Figure 11**). The results for the two-year survival rate were similar [normal LDH levels: 26.94% (17.96%; 35.93%); elevated LDH levels: 13.39% (5.04%; 21.74)] (p=0.207) (**Supplementary Figure 12**). We found no significant differences between the prognostic performance of serum S100B and serum LDH for predicting one-year (p=0.886) (**Supplementary Figure 13**) or two-year (p=0.921) survival rates (**Supplementary Figure 14**).

DISCUSSION

Intracellular S100 proteins are Ca2+- and Zn2+-sensors involved in several protein interactions regulating a wide variety of cellular processes, including transcription, protein phosphorylation, motility, energy metabolism, which may affect tumor growth (57–59). In addition, extracellular S100B is a damage-associated molecular pattern protein, which may promote tumor progression by contributing to cancer-associated inflammation or by activating signaling pathways in melanoma cells *via* receptors for advanced glycation end products (57–59). The main source of elevated serum S100B levels in melanoma is the passive release from damaged/necrotic cells; however, the same tumor burden

TABLE 2 | Characteristics of included prognostic effect (Cox regression) studies in the meta-analysis.

Hazard risk (Cox regression)										
First author (Year of publication)	**Country**	**Design of the study**	**Settings**	**Population**	**Female %**	**S100B cutoff (µg/L)**	**S100B methods**	**LDH cutoff (IU/L)**	**LDH methods**	**Total number of patients**
Weide et al., 2012 (47)	Germany	prospective	multicenter	Resectable and nonresectable stage IV	43.6	0.15; 0.10	Sangtec® 100 ELISA, Elecsys® S100	ULN	automated colourimetric assay	586
Weide et al., 2013 (48)	Germany	prospective	multicenter	Nonresectable stage IV with first-line systemic therapy	41.5	0.15; 0.10	Sangtec® 100 ELISA, Elecsys® S100	ULN	automated colourimetric assay	372
Wagner cohort 1, 2018 (51)	Germany	retrospective	single center	Nonresectable stage III/ stage IV with anti-PD1 therapy	42.1	0.3	N.R.	1.5xULN	automated colourimetric assay	152
Wagner cohort 2, 2018 (51)	Germany	retrospective	single center	Nonresectable stage III/ stage IV with anti-PD1 + anti-CTLA4 therapy	41.9	0.3	N.R.	1.5xULN	automated colourimetric assay	86
Amaral, Kiecker et. al., 2020 (50)	Germany	retrospective	multicenter	Nonresectable stage IV (brain met) with combined immunotherapy	36.8	0.11	Elecsys® S100	250	automated colourimetric assay	265/322
Amaral, Schulze et. al., 2020 (52)	Germany	prospective	single center	Nonresectable stage IV with combined immunotherapy	39	0.15	LIA-mat® Sangtec® 100	ULN	automated colourimetric assay	55/59
Damuzzo et al., 2016 (53)	Italy	prospective	single center	Nonresectable stage IV with anti-CTLA-4 therapy	34.1	0.16	LIAISON® Sangtec® 100	450	automated colourimetric assay	44
Eigentler et al., 2011 (54)	Germany	retrospective	multicenter	Nonresectable stage IV (brain metastasis)	44	ULN	N.R.	ULN	automated colourimetric assay	270/464
Wevers et al., 2013 (55)	The Netherlands	prospective	single center	Resectable stage III	47.1	0.15, 0.20	Nichols Advantage, Sangtec® 100 ELISA	250	automated colourimetric assay	75
Schmidt et al., 2005 (56)	Denmark	retrospective	single center	Nonresectable stage IV treated with IL2-based immunotherapy	44	0.15	LIAISON® Sangtec® 100	500	automated colourimetric assay	82

SLN, sentinel lymph node; ULN, upper limit normal; N.R., not reported.

may or may not cause an elevation of S100B serum levels (57). In tumor cells dependent on glycolysis, lactate production increases substantially due to the increased expression and activity of LDH, which converts pyruvate to lactate. Lactate, which is exported by tumor cells, may promote angiogenesis, metastasis, therapy resistance, and immunosuppression (60). In malignant cells at the more oxygenated tumor periphery, lactate is utilized as an energetic source; lactate must be converted to pyruvate *via* LDH for this purpose (60, 61). Elevated serum LDH in patients with advanced melanoma is primarily due to release from glycolytic tumor cells (LDH3 and 4) (61).

In our meta-analysis, the pooled AUROC for correctly identifying disease relapse proved to be significantly higher for serum S100B than for serum LDH, indicating that serum S100B is a more suitable marker for tumor recurrence during follow-up of patients with cutaneous melanoma. Of note, S100B is the only serum biomarker supported by sufficient data that is routinely available in most hospitals. The serum S100B concentration was shown to be significantly higher in patients of stage III or IV than in those of stages I and II, and significantly higher in patients of stage IV than stage III (62). Serum S100B, however, seemed incapable of predicting sentinel lymph node status (63). Importantly, Abraha et al. found that diagnostic accuracy for detecting advanced disease may be higher by combining an elevated serum S100B and a Breslow tumor thickness of >4mm (62). Elevated levels of serum S100B occur in a number of conditions (19); thus, these findings support that monitoring S100B is recommended primarily in cases of melanoma with a high risk of relapse. Nevertheless, when a pre-specified cutoff (the upper limit of normal or ROC optimized) was used, serum S100B and LDH proved to be similarly and highly specific and moderately sensitive; however, the sensitivity of serum S100B was significantly higher compared to serum LDH. This result suggests that monitoring serum S100B might indicate the need for an imaging examination to detect disease relapse earlier than serum LDH. Further studies, both in clinical trials and in real-world populations, are needed to clarify how the measurement method, cut point, reference test, and patient population affect the accuracy of serum S100B for the detection of disease recurrence. These studies could also explore the sources of the considerable heterogeneity observed in our meta-analysis (31). Nevertheless, melanoma is heterogeneous in terms of biological behavior, due to the heterogeneity of the genome and proteome; the identification of a single biomarker that can be used widely is

TABLE 3 | Characteristics of included prognostic effect (Survival rate) studies in the meta-analysis.

					Survival rate (one- and two-year)					
First author (Year of publication)	**Country**	**Design of the study**	**Settings**	**Population**	**Female %**	**S100B cutoff (μg/L)**	**S100B methods**	**LDH cutoff (IU/L)**	**LDH methods**	**Total number of patients**
Weide et al., 2012 (47)	Germany	prospective	multicenter	Resectable and nonresectable stage IV	43.6	0.15; 0.10	Sangtec® 100 ELISA, Elecsys® S100	ULN	automated colourimetric assay	855
Weide et al., 2013 (48)	Germany	prospective	multicenter	Nonresectable stage IV with first-line systemic therapy	41.5	0.15; 0.10	Sangtec® 100 ELISA, Elecsys® S100	ULN	automated colourimetric assay	499
Weide et al., 2016 (49)	Germany	prospective	multicenter	Nonresectable stage IV	41.3	0.10	Elecsys® S100	250	automated colourimetric assay	206
Amaral, Kiecker et. al., 2020 (50)	Germany	retrospective	multicenter	Nonresectable stage IV (brain metastasis) with combined immunotherapy	36.8	0.11	Elecsys® S100	250	automated colourimetric assay	380

SLN, sentinel lymph node; ULN, upper limit normal; N.R., not reported.

difficult (3). Further studies are needed to identify additional biomarkers that could be used in combination with serum S100B to increase the chances of early detection of disease relapse (45).

A number of circulating biomarkers are being investigated that may help us in follow-up. Compared to tissue tumor biopsy, peripheral blood sample (liquid biopsy) is more readily available and less heterogeneous (13). Many serologic markers such as enzymes [e.g., matrix metalloproteinase-9 (MMP-9)], secreted proteins (e.g., melanoma inhibiting activity), metabolites of the melanin synthesis pathway (e.g., 5-S-cysteinyl-dopa), circulating nucleic acids (e.g., tyrosinase mRNA, circulating-free DNA BRAFV600E mutation), and peripheral blood immune markers (e.g., soluble PD-L1) have been shown to correlate with tumor progression, survival or response to treatment in patients with melanoma (9–14, 23, 30, 64, 65). Properly designed, conducted, analyzed and reported prediction model studies will determine how to use these markers with the greatest clinical benefit (11, 31, 66, 67).

In a subgroup of patients with metastatic melanoma, the levels of serum S100B were not elevated and many studies and reviews have been published on the prognostic effect of serum S100B (17, 18, 29, 68–70). Because of the strong discriminative

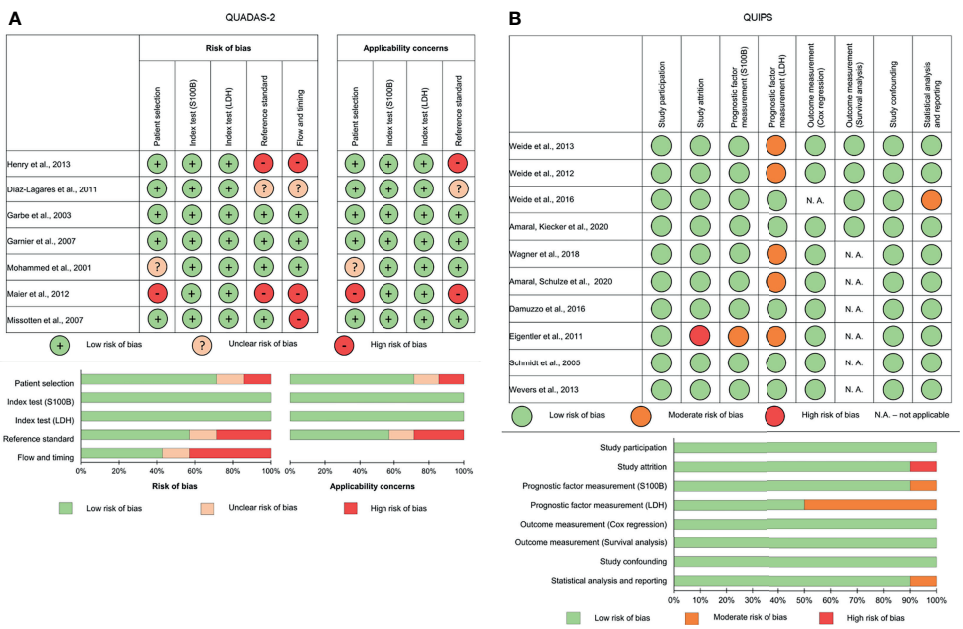


FIGURE 2 | Results of quality assessment according to the Quality Assessment of Diagnostic Accuracy Studies (QUADAS-2) **(A)** and Quality In Prognosis Studies (QUIPS) **(B)** tools.

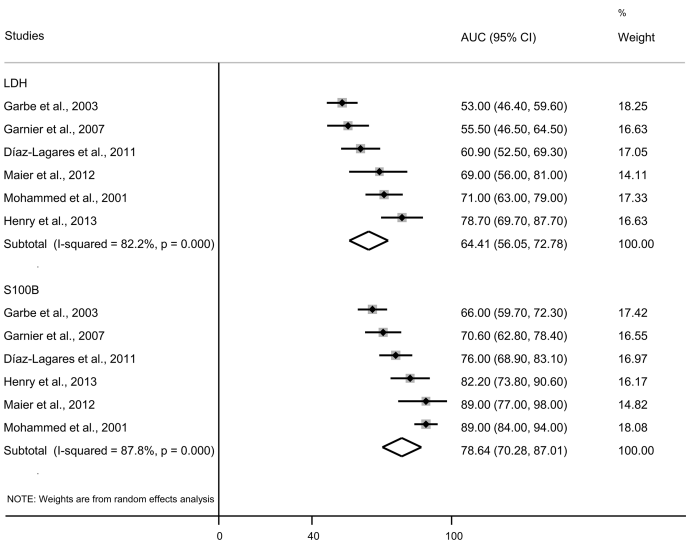


FIGURE 3 | Forest plot presenting AUC with 95% CI from ROC curve for S100B and LDH. AUC, area under the curve; CI, confidence intervals; LDH, lactate dehydrogenase.

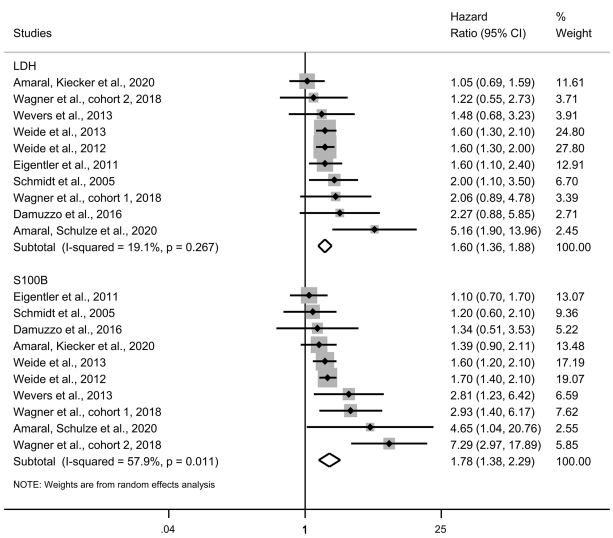


FIGURE 4 | Forest plot presenting adjusted hazard ratios with 95% CI from Cox multivariate proportional-hazards models of overall survival. CI, confidence intervals; LDH, lactate dehydrogenase.

ability of serum S100B in identifying metastatic disease, the inclusion of studies on patients with all stages of melanoma was considered to be inappropriate for prognostic effect analysis; thus, only studies in which metastatic patients were included were selected. Surprisingly, very few eligible studies were identified because of the scarcity of multivariate analyses, patient selection bias, and significant reporting bias on outcomes in prognostic studies in the field. The Cox regression models that were included in the analysis used established prognostic markers as adjustment factors, e.g., site of metastases, the presence of brain metastasis, treatment. According to our results, the summary adjusted hazard ratio for S100B was similar to that for LDH, i.e. serum S100B has a similar prognostic value as serum LDH in patients with metastatic melanoma. Importantly, in accordance with the different biology coupled with elevated levels of serum LDH and S100B, the studies included in the meta-analysis indicated that the prognostic ability of the two markers was independent. Reviewing the literature, we found only one meta-analysis that examined the association between serum S100B levels and

melanoma prognosis. In this meta-analysis, elevated serum S100B levels were associated with significantly poorer survival in melanoma patients (22). MMP-9 plays an important role in melanoma invasiveness. In one study, elevated serum MMP-9 levels and the circulating-free DNA BRAFV600E mutation were found to be associated with poor progression-free survival and overall survival. MMP-9 may be a promising indicator of the response to BRAF inhibitors in combination with the detection of the BRAFV600E mutation (12). The programmed cell death protein 1/programmed cell death ligand 1 (PD-1/PD-L1) axis plays an important role in circumventing immune surveillance. There is a need for a biomarker that would predict the efficacy of PD-1/PD-L1 inhibitors in patients with metastatic melanoma. Yue C et al. found that a decrease in circulating PD-L1 + tumor cell count was associated with a strong antitumor response. Also, patients with high levels of PD-L1 + circulating tumor cells at baseline are generally susceptible to anti-PD-L1 therapy (71). Since serum S100B and LDH monitoring also appear to be prognostically useful in melanoma patients during BRAF-inhibitor or immune checkpoint inhibitor treatment (69, 70, 72, 73), the combination of these markers could be further evaluated in predictive models identifying subgroups with differential treatment effects. The novelty of this meta-analysis was the comparative approach, the analysis of multiple outcomes, and the inclusion of logistic regression models. Furthermore, the results were derived from the analysis of data from patient populations with more than 1,000 participants for each of the studied outcomes.

LIMITATIONS

A high risk of bias regarding statistical analysis and reporting domain was detected in many predictive studies screened for analysis, but the bias was lower in the selected studies due to the applied inclusion criteria. This, in turn, led to only a few articles being eligible for data extraction, which is a limitation of this meta-analysis. In addition, there was considerable heterogeneity across the included studies. The immunoassays used for measuring serum S100B and the cutoff for determining normal *versus* elevated S100B levels were not completely uniform across studies. The adjustment factors in the prognostic studies were also not uniform. A limitation of this review is that a majority of eligible prognostic studies came from Germany (German Central Malignant Melanoma Registry), although the data were collected from different periods and/or from an intentionally chosen different setting. Our attempt to contact the first author to obtain information on the extent of potential overlap between populations of prognostic factor studies performed by the same research group was unsuccessful.

CONCLUSIONS

The applicability of serum S100B and serum LDH for predicting the progression of melanoma was studied in this review from both diagnostic and prognostic viewpoints. We found that the discriminative ability of serum S100B at identifying disease relapse was greater than that of serum LDH. Since a relapse of melanoma is associated with elevated serum S100B levels in only a subset of patients, serum S100B should be considered in combination with additional serum biomarkers in a multivariable diagnostic prediction model. Furthermore, serum S100B had a similar and independent prognostic strength in metastatic melanoma compared with serum LDH, suggesting that the implementation of both markers in a multivariable prognostic prediction model development would be advantageous. To increase the degree of confidence in the prognostic and diagnostic abilities of various biomarkers, primary predictor studies conducted and reported in accordance with the corresponding quality assessment tools are important.

DATA AVAILABILITY STATEMENT

The original contributions presented in the study are included in the article/**Supplementary Material**. Further inquiries can be directed to the corresponding author.

AUTHOR CONTRIBUTIONS

Concept and design: EJ, PH, ZS, and GE. Review questions were formulated by EJ and GE, guided by PH and DP. The applicability of the selected studies to the review question was determined by two authors (EJ and GE), independently, then a consensus was reached through discussion. Search, study selection, and data extraction: EJ and GE. Risk of bias assessment: EJ and GE. Statistical analysis: ZS and AS. Drafting of the manuscript: EJ, TV, and GE. Critical revision of the manuscript: all authors. All authors contributed to the article and approved the submitted version.

FUNDING

This work was supported by the ÚNKP-20-4 New National Excellence Program of the Ministry for Innovation and Technology from the source of the National Research, Development and Innovation Fund. Furthermore, the project was supported by the European Union and the European Regional Development Fund GINOP-2.3.2-15-2016-00005 and Hungarian Scientific Research Fund NKFIH K120206.

SUPPLEMENTARY MATERIAL

The Supplementary Material for this article can be found online at: https://www.frontiersin.org/articles/10.3389/fonc.2021.772165/full#supplementary-material

REFERENCES

1. Schadendorf D, van Akkooi ACJ, Berking C, Griewank KG, Gutzmer R, Hauschild A, et al. Melanoma. *Lancet (London England)* (2018) 392 (10151):971–84. doi: 10.1016/S0140-6736(18)31559-9
2. IARC. *International Agency for Research on Cancer, 2020. Lyon* (2020). Available at: http://www.iarc.fr/ (Accessed Last 14 May 2021).
3. Emri G, Paragh G, Tosaki A, Janka E, Kollar S, Hegedus C, et al. Ultraviolet Radiation-Mediated Development of Cutaneous Melanoma: An Update. *J Photochem Photobiol B* (2018) 185:169–75. doi: 10.1016/j.jphotobiol.2018.06.005
4. Slominski AT, Zmijewski MA, Plonka PM, Szaflarski JP, Paus R. How UV Light Touches the Brain and Endocrine System Through Skin, and Why. *Endocrinology* (2018) 159(5):1992–2007. doi: 10.1210/en.2017-03230
5. Slominski AT, Carlson JA. Melanoma Resistance: A Bright Future for Academicians and a Challenge for Patient Advocates. *Mayo Clin Proc* (2014) 89(4):429–33. doi: 10.1016/j.mayocp.2014.02.009
6. Slominski RM, Zmijewski MA, Slominski AT. The Role of Melanin Pigment in Melanoma. *Exp Dermatol* (2015) 24(4):258–9. doi: 10.1111/exd.12618
7. Gershenwald JE, Scolyer RA, Hess KR, Sondak VK, Long GV, Ross MI, et al. Melanoma Staging: Evidence-Based Changes in the American Joint Committee on Cancer Eighth Edition Cancer Staging Manual. *CA Cancer J Clin* (2017) 67(6):472–92. doi: 10.3322/caac.21409
8. Aide N, Hicks RJ, Le Tourneau C, Lheureux S, Fanti S, Lopci E. FDG PET/CT for Assessing Tumour Response to Immunotherapy : Report on the EANM Symposium on Immune Modulation and Recent Review of the Literature. *Eur J Nucl Med Mol Imaging* (2019) 46(1):238–50. doi: 10.1007/s00259-018-4171-4
9. Vereecken P, Cornelis F, Van Baren N, Vandersleyen V, Baurain JF. A Synopsis of Serum Biomarkers in Cutaneous Melanoma Patients. *Dermatol Res Pract* (2012) 2012:260643. doi: 10.1155/2012/260643
10. Wakamatsu K, Fukushima S, Minagawa A, Omodaka T, Hida T, Hatta N, et al. Significance of 5-S-Cysteinyldopa as a Marker for Melanoma. *Int J Mol Sci* (2020) 21(2):432. doi: 10.3390/ijms21020432
11. Kitano S, Nakayama T, Yamashita M. Biomarkers for Immune Checkpoint Inhibitors in Melanoma. *Front Oncol* (2018) 8:270. doi: 10.3389/fonc.2018.00270
12. Salemi R, Falzone L, Madonna G, Polesel J, Cina D, Mallardo D, et al. MMP-9 as a Candidate Marker of Response to BRAF Inhibitors in Melanoma Patients With BRAF(V600E) Mutation Detected in Circulating-Free DNA. *Front Pharmacol* (2018) 9:856. doi: 10.3389/fphar.2018.00856
13. Yi M, Jiao D, Xu H, Liu Q, Zhao W, Han X, et al. Biomarkers for Predicting Efficacy of PD-1/PD-L1 Inhibitors. *Mol Cancer* (2018) 17(1):129. doi: 10.1186/s12943-018-0864-3
14. Zhou J, Mahoney KM, Giobbie-Hurder A, Zhao F, Lee S, Liao X, et al. Soluble PD-L1 as a Biomarker in Malignant Melanoma Treated With Checkpoint Blockade. *Cancer Immunol Res* (2017) 5(6):480–92. doi: 10.1158/2326-6066.CIR-16-0329
15. Petrelli F, Cabiddu M, Coinu A, Borgonovo K, Ghilardi M, Lonati V, et al. Prognostic Role of Lactate Dehydrogenase in Solid Tumors: A Systematic Review and Meta-Analysis of 76 Studies. *Acta Oncol* (2015) 54(7):961–70. doi: 10.3109/0284186X.2015.1043026
16. Petrelli F, Ardito R, Merelli B, Lonati V, Cabiddu M, Seghezzi S, et al. Prognostic and Predictive Role of Elevated Lactate Dehydrogenase in Patients With Melanoma Treated With Immunotherapy and BRAF Inhibitors: A Systematic Review and Meta-Analysis. *Melanoma Res* (2019) 29(1):1–12. doi: 10.1097/CMR.0000000000000520
17. Kruijff S, Hoekstra HJ. The Current Status of S-100B as a Biomarker in Melanoma. *Eur J Surg Oncol* (2012) 38(4):281–5. doi: 10.1016/j.ejso.2011.12.005
18. Harpio R, Einarsson R. S100 Proteins as Cancer Biomarkers With Focus on S100B in Malignant Melanoma. *Clin Biochem* (2004) 37(7):512–8. doi: 10.1016/j.clinbiochem.2004.05.012
19. Heizmann CW. S100 Proteins: Diagnostic and Prognostic Biomarkers in Laboratory Medicine. *Biochim Biophys Acta Mol Cell Res* (2019) 1866 (7):1197–206. doi: 10.1016/j.bbamcr.2018.10.015
20. Gebhardt C, Lichtenberger R, Utikal J. Biomarker Value and Pitfalls of Serum S100B in the Follow-Up of High-Risk Melanoma Patients. *J Dtsch Dermatol Ges* (2016) 14(2):158–64. doi: 10.1111/ddg.12727
21. Aceti A, Margarucci LM, Scaramucci E, Orsini M, Salerno G, Di Sante G, et al. Serum S100B Protein as a Marker of Severity in Covid-19 Patients. *Sci Rep* (2020) 10(1):18665. doi: 10.1038/s41598-020-75618-0
22. Mocellin S, Zavagno G, Nitti D. The Prognostic Value of Serum S100B in Patients With Cutaneous Melanoma: A Meta-Analysis. *Int J Cancer* (2008) 123(10):2370–6. doi: 10.1002/ijc.23794
23. Tandler N, Mosch B, Pietzsch J. Protein and Non-Protein Biomarkers in Melanoma: A Critical Update. *Amino Acids* (2012) 43(6):2203–30. doi: 10.1007/s00726-012-1409-5
24. Leclerc E, Heizmann CW, Vetter SW. RAGE and S100 Protein Transcription Levels Are Highly Variable in Human Melanoma Tumors and Cells. *Gen Physiol Biophys* (2009) 28 Spec No Focus:F65–75.
25. Wu KJ, Ho SH, Wu C, Wang HD, Ma DL, Leung CH. Simultaneous Blocking of the Pan-RAF and S100B Pathways as a Synergistic Therapeutic Strategy Against Malignant Melanoma. *J Cell Mol Med* (2021) 25(4):1972–81. doi: 10.1111/jcmm.15994
26. Ertekin SS, Podlipnik S, Ribero S, Molina R, Rios J, Carrera C, et al. Monthly Changes in Serum Levels of S100B Protein as a Predictor of Metastasis Development in High-Risk Melanoma Patients. *J Eur Acad Dermatol Venereology JEADV* (2020) 34(7):1482–8. doi: 10.1111/jdv.16212
27. Dummer R, Hauschild A, Lindenblatt N, Pentheroudakis G, Keilholz U, Committee EG. Cutaneous Melanoma: ESMO Clinical Practice Guidelines for Diagnosis, Treatment and Follow-Up. *Ann Oncol* (2015) 26 Suppl 5:v126–32. doi: 10.1093/annonc/mdv297
28. Coit DG, Thompson JA, Albertini MR, Barker C, Carson WE, Contreras C, et al. Cutaneous Melanoma, Version 2.2019, NCCN Clinical Practice Guidelines in Oncology. *J Natl Compr Canc Netw* (2019) 17(4):367–402. doi: 10.6004/jnccn.2019.0018
29. Beyeler M, Waldispuhl S, Strobel K, Joller-Jemelka HI, Burg G, Dummer R. Detection of Melanoma Relapse: First Comparative Analysis on Imaging Techniques *Versus* S100 Protein. *Dermatol (Basel Switzerland)* (2006) 213 (3):187–91. doi: 10.1159/000095034
30. Revythis A, Shah S, Kutka M, Moschetta M, Ozturk MA, Pappas-Gogos G, et al. Unraveling the Wide Spectrum of Melanoma Biomarkers. *Diagnostics (Basel)* (2021) 11(8):1341. doi: 10.3390/diagnostics11081341
31. Riley RD, Moons KGM, Snell KIE, Ensor J, Hooft L, Altman DG, et al. A Guide to Systematic Review and Meta-Analysis of Prognostic Factor Studies. *BMJ (Clinical Res ed)* (2019) 364:k4597. doi: 10.1136/bmj.k4597
32. Jones CM, Athanasiou T. Summary Receiver Operating Characteristic Curve Analysis Techniques in the Evaluation of Diagnostic Tests. *Ann Thorac Surg* (2005) 79(1):16–20. doi: 10.1016/j.athoracsur.2004.09.040
33. Christensen E. Multivariate Survival Analysis Using Cox's Regression Model. *Hepatology* (1987) 7(6):1346–58. doi: 10.1002/hep.1840070628
34. Moher D, Liberati A, Tetzlaff J, Altman DG, Group P. Preferred Reporting Items for Systematic Reviews and Meta-Analyses: The PRISMA Statement. *PloS Med* (2009) 6(7):e1000097. doi: 10.1371/journal.pmed.1000097
35. Salameh JP, Bossuyt PM, McGrath TA, Thombs BD, Hyde CJ, Macaskill P, et al. Preferred Reporting Items for Systematic Review and Meta-Analysis of Diagnostic Test Accuracy Studies (PRISMA-DTA): Explanation, Elaboration, and Checklist. *BMJ (Clinical Res ed)* (2020) 370:m2632. doi: 10.1136/bmj.m2632
36. Whiting PF, Rutjes AW, Westwood ME, Mallett S, Deeks JJ, Reitsma JB, et al. QUADAS-2: A Revised Tool for the Quality Assessment of Diagnostic Accuracy Studies. *Ann Internal Med* (2011) 155(8):529–36. doi: 10.7326/0003-4819-155-8-201110180-00009
37. Hayden JA, van der Windt DA, Cartwright JL, Cote P, Bombardier C. Assessing Bias in Studies of Prognostic Factors. *Ann Internal Med* (2013) 158(4):280–6. doi: 10.7326/0003-4819-158-4-201302190-00009
38. Higgins JPT GSe. *Cochrane Handbook for Systematic Reviews of Interventions Version 5.1.0 [Updated March 2011]. The Cochrane Collaboration* (2011). Available at: http://handbook.cochrane.org.
39. DerSimonian R, Laird N. Meta-Analysis in Clinical Trials. *Control Clin Trials* (1986) 7(3):177–88. doi: 10.1016/0197-2456(86)90046-2
40. Henry L, Fabre C, Guiraud I, Bastide S, Fabbro-Peray P, Martinez J, et al. Clinical Use of P-Proteasome in Discriminating Metastatic Melanoma Patients: Comparative Study With LDH, MIA and S100B Protein. *Int J Cancer* (2013) 133(1):142–8. doi: 10.1002/ijc.27991
41. Diaz-Lagares A, Alegre E, Arroyo A, Gonzalez-Cao M, Zudaire ME, Viteri S, et al. Evaluation of Multiple Serum Markers in Advanced Melanoma. *Tumour Biol* (2011) 32(6):1155–61. doi: 10.1007/s13277-011-0218-x

42. Garbe C, Leiter U, Ellwanger U, Blaheta HJ, Meier F, Rassner G, et al. Diagnostic Value and Prognostic Significance of Protein S-100beta, Melanoma-Inhibitory Activity, and Tyrosinase/MART-1 Reverse Transcription-Polymerase Chain Reaction in the Follow-Up of High-Risk Melanoma Patients. *Cancer* (2003) 97(7):1737–45. doi: 10.1002/cncr.11250
43. Garnier JP, Letellier S, Cassinat B, Lebbe C, Kerob D, Baccard M, et al. Clinical Value of Combined Determination of Plasma L-DOPA/tyrosine Ratio, S100B, MIA and LDH in Melanoma. *Eur J Cancer (Oxford Engl 1990)* (2007) 43 (4):816–21. doi: 10.1016/j.ejca.2006.11.022
44. Mohammed MQ, Abraha HD, Sherwood RA, MacRae K, Retsas S. Serum S100beta Protein as a Marker of Disease Activity in Patients With Malignant Melanoma. *Med Oncol (Northwood London England)* (2001) 18(2):109–20. doi: 10.1385/mo:18:2:109
45. Maier T, Laubender RP, Sturm RA, Klingenstein A, Korting HC, Ruzicka T, et al. Osteopontin Expression in Plasma of Melanoma Patients and in Melanocytic Tumours. *J Eur Acad Dermatol Venereology JEADV* (2012) 26 (9):1084–91. doi: 10.1111/j.1468-3083.2011.04210.x
46. Missotten GS, Korse CM, van Dehn C, Linders TC, Keunen JE, Jager MJ, et al. S-100B Protein and Melanoma Inhibitory Activity Protein in Uveal Melanoma Screening. A Comparison With Liver Function Tests. *Tumour Biol* (2007) 28(2):63–9. doi: 10.1159/000099151
47. Weide B, Elsasser M, Buttner P, Pflugfelder A, Leiter U, Eigentler TK, et al. Serum Markers Lactate Dehydrogenase and S100B Predict Independently Disease Outcome in Melanoma Patients With Distant Metastasis. *Br J Cancer* (2012) 107(3):422–8. doi: 10.1038/bjc.2012.306
48. Weide B, Richter S, Buttner P, Leiter U, Forschner A, Bauer J, et al. Serum S100B, Lactate Dehydrogenase and Brain Metastasis Are Prognostic Factors in Patients With Distant Melanoma Metastasis and Systemic Therapy. *PloS One* (2013) 8(11):e81624. doi: 10.1371/journal.pone.0081624
49. Weide B, Schafer T, Martens A, Kuzkina A, Uder L, Noor S, et al. High GDF-15 Serum Levels Independently Correlate With Poorer Overall Survival of Patients With Tumor-Free Stage III and Unresectable Stage IV Melanoma. *J Invest Dermatol* (2016) 136(12):2444–52. doi: 10.1016/j.jid.2016.07.016
50. Amaral T, Kiecker F, Schaefer S, Stege H, Kaehler K, Terheyden P, et al. Combined Immunotherapy With Nivolumab and Ipilimumab With and Without Local Therapy in Patients With Melanoma Brain Metastasis: A DeCOG* Study in 380 Patients. *J Immunother Cancer* (2020) 8(1):e000333. doi: 10.1136/jitc-2019-000333
51. Wagner NB, Forschner A, Leiter U, Garbe C, Eigentler TK. S100B and LDH as Early Prognostic Markers for Response and Overall Survival in Melanoma Patients Treated With Anti-PD-1 or Combined Anti-PD-1 Plus Anti-CTLA-4 Antibodies. *Br J Cancer* (2018) 119(3):339–46. doi: 10.1038/s41416-018-0167-x
52. Amaral T, Schulze M, Sinnberg T, Nieser M, Martus P, Battke F, et al. Are Pathogenic Germline Variants in Metastatic Melanoma Associated With Resistance to Combined Immunotherapy? *Cancers* (2020) 12(5):1101. doi: 10.3390/cancers12051101
53. Damuzzo V, Solito S, Pinton L, Carrozzo E, Valpione S, Pigozzo J, et al. Clinical Implication of Tumor-Associated and Immunological Parameters in Melanoma Patients Treated With Ipilimumab. *Oncoimmunology* (2016) 5 (12):e1249559. doi: 10.1080/2162402x.2016.1249559
54. Eigentler TK, Figl A, Krex D, Mohr P, Mauch C, Rass K, et al. Number of Metastases, Serum Lactate Dehydrogenase Level, and Type of Treatment Are Prognostic Factors in Patients With Brain Metastases of Malignant Melanoma. *Cancer* (2011) 117(8):1697–703. doi: 10.1002/cncr.25631
55. Wevers KP, Kruijff S, Speijers MJ, Bastiaannet E, Muller Kobold AC. Hoekstra HJ. S-100B: A Stronger Prognostic Biomarker Than LDH in Stage IIIB-C Melanoma. *Ann Surg Oncol* (2013) 20(8):2772–9. doi: 10.1245/s10434-013-2949-y
56. Schmidt H, Sorensen BS, Fode K, Nexo E, von der Maase H. Tyrosinase Messenger RNA in Peripheral Blood Is Related to Poor Survival in Patients With Metastatic Melanoma Following Interleukin-2-Based Immunotherapy. *Melanoma Res* (2005) 15(5):409–16. doi: 10.1097/00008390-200510000-00009
57. Sorci G, Riuzzi F, Arcuri C, Tubaro C, Bianchi R, Giambanco I, et al. S100B Protein in Tissue Development, Repair and Regeneration. *World J Biol Chem* (2013) 4(1):1–12. doi: 10.4331/wjbc.v4.i1.1
58. Olaoba OT, Kadasah S, Vetter SW, Leclerc E. RAGE Signaling in Melanoma Tumors. *Int J Mol Sci* (2020) 21(23):8989. doi: 10.3390/ijms21238989
59. Leclerc E, Heizmann CW. The Importance of Ca2+/Zn2+ Signaling S100 Proteins and RAGE in Translational Medicine. *Front Biosci (Schol Ed)* (2011) 3:1232–62. doi: 10.2741/223
60. Perez-Tomas R, Perez-Guillen I. Lactate in the Tumor Microenvironment: An Essential Molecule in Cancer Progression and Treatment. *Cancers* (2020) 12(11):3244. doi: 10.3390/cancers12113244
61. Ho J, de Moura MB, Lin Y, Vincent G, Thorne S, Duncan LM, et al. Importance of Glycolysis and Oxidative Phosphorylation in Advanced Melanoma. *Mol Cancer* (2012) 11:76. doi: 10.1186/1476-4598-11-76
62. Abraha HD, Fuller LC, Du Vivier AW, Higgins EM, Sherwood RA. Serum S-100 Protein: A Potentially Useful Prognostic Marker in Cutaneous Melanoma. *Br J Dermatol* (1997) 137(3):381–5. doi: 10.1111/j.1365-2133.1997.tb03742.x
63. Egberts F, Momkvist A, Egberts JH, Kaehler KC, Hauschild A. Serum S100B and LDH Are Not Useful in Predicting the Sentinel Node Status in Melanoma Patients. *Anticancer Res* (2010) 30(5):1799–805.
64. Stark MS, Klein K, Weide B, Haydu LE, Pflugfelder A, Tang YH, et al. The Prognostic and Predictive Value of Melanoma-Related MicroRNAs Using Tissue and Serum: A MicroRNA Expression Analysis. *EBioMedicine* (2015) 2 (7):671–80. doi: 10.1016/j.ebiom.2015.05.011
65. Slostad JA, Liu MC, Allred JB, Erickson LA, Rumilla KM, Block MS, et al. BRAF V600 Mutation Detection in Plasma Cell-Free DNA: NCCTG N0879 (Alliance). *Mayo Clin Proc Innov Qual Outcomes* (2021) 5(6):1012–20. doi: 10.1016/j.mayocpiqo.2021.05.003
66. Moons KGM, Wolff RF, Riley RD, Whiting PF, Westwood M, Collins GS, et al. PROBAST: A Tool to Assess Risk of Bias and Applicability of Prediction Model Studies: Explanation and Elaboration. *Ann Internal Med* (2019) 170(1): W1–33. doi: 10.7326/M18-1377
67. Kluger HM, Hoyt K, Bacchiocchi A, Mayer T, Kirsch J, Kluger Y, et al. Plasma Markers for Identifying Patients With Metastatic Melanoma. *Clin Cancer Res* (2011) 17(8):2417–25. doi: 10.1158/1078-0432.CCR-10-2402
68. Frauchiger AL, Dummer R, Mangana J. Serum S100B Levels in Melanoma. *Methods Mol Biol* (2019) 1929:691–700. doi: 10.1007/978-1-4939-9030-6_43
69. Felix J, Cassinat B, Porcher R, Schlageter MH, Maubec E, Pages C, et al. Relevance of Serum Biomarkers Associated With Melanoma During Follow-Up of Anti-CTLA-4 Immunotherapy. *Int Immunopharmacol* (2016) 40:466–73. doi: 10.1016/j.intimp.2016.09.030
70. Sanmamed MF, Fernandez-Landazuri S, Rodriguez C, Lozano MD, Echeveste JI, Perez Gracia JL, et al. Relevance of MIA and S100 Serum Tumor Markers to Monitor BRAF Inhibitor Therapy in Metastatic Melanoma Patients. *Clin Chim Acta* (2014) 429:168–74. doi: 10.1016/j.cca.2013.11.034
71. Yue C, Jiang Y, Li P, Wang Y, Xue J, Li N, et al. Dynamic Change of PD-L1 Expression on Circulating Tumor Cells in Advanced Solid Tumor Patients Undergoing PD-1 Blockade Therapy. *Oncoimmunology* (2018) 7(7):e1438111. doi: 10.1080/2162402x.2018.1438111
72. Abusaif S, Jradi Z, Held L, Pflugfelder A, Weide B, Meier F, et al. S100B and Lactate Dehydrogenase as Response and Progression Markers During Treatment With Vemurafenib in Patients With Advanced Melanoma. *Melanoma Res* (2013) 23(5):396–401. doi: 10.1097/CMR.0b013e3283650741
73. Gassenmaier M, Lenders MM, Forschner A, Leiter U, Weide B, Garbe C, et al. Serum S100B and LDH at Baseline and During Therapy Predict the Outcome of Metastatic Melanoma Patients Treated With BRAF Inhibitors. *Target Oncol* (2021) 16(2):197–205. doi: 10.1007/s11523-021-00792-8

Conflict of Interest: The authors declare that the research was conducted in the absence of any commercial or financial relationships that could be construed as a potential conflict of interest.

Publisher's Note: All claims expressed in this article are solely those of the authors and do not necessarily represent those of their affiliated organizations, or those of the publisher, the editors and the reviewers. Any product that may be evaluated in this article, or claim that may be made by its manufacturer, is not guaranteed or endorsed by the publisher.

Copyright © 2021 Janka, Várvölgyi, Sipos, Soós, Hegyi, Kiss, Dembrovszky, Csupor, Kéringer, Pécsi, Solymár and Emri. This is an open-access article distributed under the terms of the Creative Commons Attribution License (CC BY). The use, distribution or reproduction in other forums is permitted, provided the original author(s) and the copyright owner(s) are credited and that the original publication in this journal is cited, in accordance with accepted academic practice. No use, distribution or reproduction is permitted which does not comply with these terms.

frontiers in Oncology

CASE REPORT
published: 09 December 2021
doi: 10.3389/fonc.2021.749834

Immune Checkpoint Inhibitor Induced Pericarditis and Encephalitis in a Patient Treated With Ipilimumab and Nivolumab for Metastatic Melanoma: A Case Report and Review of the Literature

Jorja Braden[1]* *and Jenny H. Lee*[1,2]

[1] Department of Medical Oncology, Chris O'Brien Lifehouse, Sydney, NSW, Australia, [2] Department of Biomedical Sciences, Macquarie University, Sydney, NSW, Australia

Immune checkpoint inhibitors (ICIs) have dramatically improved outcomes in melanoma. Common ICI toxicities have become familiar to clinicians; however, rare delayed toxicities remain challenging given the paucity of data with such presentations. We present the unique case of a 61-year-old with metastatic melanoma with two rare, delayed ICI-induced toxicities. After resection of a large symptomatic parietal metastases, this patient received two doses of combination ipilimumab and nivolumab. Five weeks following his second dose, he developed ICI-induced pericarditis with associated pericardial effusion and early signs of tamponade. Corticosteroids were not administered due to a concurrent cerebral abscess. Administration of colchicine, ibuprofen, judicious monitoring, and cessation of immunotherapy led to the complete resolution of the effusion over several weeks. Seven months following his last dose of immunotherapy, the patient developed ICI-associated grade four autoimmune encephalitis, presenting as status epilepticus. High-dose steroid initiation led to rapid clinical improvement. The patient remains in near-complete response on imaging with no recurrence of pericardial effusion and partial resolution of neurological symptoms. ICI-induced pericardial disease and encephalitis carry substantial mortality rates and prompt diagnosis and management is critical. Clinicians must therefore remain vigilant for these rare toxicities regardless of duration of drug exposure or time since cessation of therapy.

Keywords: immunotherapy, melanoma, immune-related adverse effects, pericarditis, encephalitis, delayed immune reaction

OPEN ACCESS

Edited by:
Vladimir Spiegelman, Penn State Milton S. Hershey Medical Center, United States

Reviewed by:
Carlo Gabriele Tocchetti, University of Naples Federico II, Italy
Andrea Camerini, Azienda Usl Toscana nord ovest, Italy

***Correspondence:**
Jorja Braden
jorja.braden@melanoma.org.au

Specialty section:
This article was submitted to Skin Cancer, a section of the journal Frontiers in Oncology

Received: *30 July 2021*
Accepted: *16 November 2021*
Published: *09 December 2021*

Citation:
Braden J and Lee JH (2021) Immune Checkpoint Inhibitor Induced Pericarditis and Encephalitis in a Patient Treated With Ipilimumab and Nivolumab for Metastatic Melanoma: A Case Report and Review of the Literature. Front. Oncol. 11:749834. doi: 10.3389/fonc.2021.749834

INTRODUCTION

The combination of immune checkpoint inhibitors (ICIs) ipilimumab and nivolumab have drastically improved outcomes for advanced melanoma patients with 5-year survival rates of 52% (1). This comes at the cost of increased rates of ICI-induced toxicities. The combination is associated with higher rates of a broad range of ICI-induced toxicities when compared to

single-agent checkpoint inhibition, contributing to higher morbidity and mortality in these patients (1, 2). Severe ICI-induced pericarditis and encephalitis are exceedingly rare clinical entities accounting for far less than 1% of ICI toxicities and delayed events increase the rarity of such cases. With a paucity of data and a range of presentations, diagnosis and management remain a significant challenge. We report the case of a patient with two sequential rare ICI-associated toxicities of grade 3 pericarditis and grade 4 encephalitis presenting 1.5 months and 7.5 months after brief exposure to ipilimumab and nivolumab treatment for metastatic melanoma.

CASE PRESENTATION

A 61-year-old male was diagnosed with *de novo* metastatic melanoma in January 2020 after presenting with sudden onset left upper limb dyspraxia and confusion. Comorbidities included hemochromatosis and a distant history of meningococcal meningitis. Magnetic resonance imaging (MRI) brain demonstrated a large right parietal lesion. Computed tomography (CT) and positron emission tomography (PET) scan revealed left upper and lower lobe lung lesions, solitary liver lesion, and base of skull lesion. Histopathology confirmed BRAF/NRAS wild-type metastatic melanoma. He proceeded with resection of the right parietal lobe metastases in February followed by ipilimumab (3 mg/kg)/nivolumab (1 mg/kg) commencing in March (**Figure 1**).

MRI brain on the April 3 demonstrated intracranial recurrence with PET/CT confirming stable extracranial disease. A redo craniotomy was performed on April 8, complicated by the development of cerebral abscess and ventriculitis requiring burr hole and drainage. Cultures confirmed corynebacterium acnes and he commenced intravenous (IV) Cephalothin for a total of 12 weeks. Six weeks following his last dose of immunotherapy and while on IV antibiotics for his cerebral abscess, the patient developed severe peripheral edema, dyspnea, and tachycardia. Electrocardiograph (ECG) demonstrated sinus tachycardia, left axis deviation, and right bundle branch block. Transthoracic echocardiogram (TTE) revealed a new circumferential pericardial effusion with early signs of tamponade. Serial troponins remained normal, and cardiac MRI showed no evidence of myocarditis. A diagnosis of ICI-induced pericarditis with associated pericardial effusion was made. The patient was commenced on aggressive diuresis, colchicine 500 mcg daily and ibuprofen 500 mg three times daily. The active decision to withhold high-dose corticosteroids was made given the patient's concomitant cerebral abscess. He was monitored with weekly echocardiograms by the treating cardiologist with gradual resolution of the pericardial effusion over 4 weeks. Immunotherapy was discontinued. In June 2020, the patient had a further recurrence of brain metastases. A third resection followed by stereotactic radiosurgery to the cavity were completed at that time.

Seven months following cessation of immunotherapy, the patient presented with sudden onset aphasia, left lower limb myoclonic jerks, and confusion. Further history revealed that the patient had developed subtle behavioral changes in the weeks prior. CT brain and angiogram showed no evidence of acute cerebrovascular event, infection, or intracranial disease progression. Laboratory results showed a normal CRP (0.7 m/L) and mild hyponatremia (129 mmol/L). An MRI brain revealed T2/FLAIR hyperintensity in the right mesotemporal lobe with differentials including encephalitis or postictal changes (**Figure 2**). Electroencephalogram (EEG) demonstrated lateralizing periodic discharges from the right temporal region. Empirical acyclovir was commenced following a lumbar puncture that demonstrated a mild elevation of protein 0.62 g/L, normal white cell count, negative bacterial/fungal cultures, and negative viral PCR panel. Despite up titration of antiepileptics, the patient continued to deteriorate with increasing confusion, fluctuating level of consciousness, persistent dysphasia, and development of visual hallucinations. Autoimmune encephalitis and antineuronal antibody panels were normal. ICI-induced encephalitis was considered the most likely diagnosis and methylprednisolone 500 mg IV/day was initiated, continued for 3 days, and followed by 2 days of 250 mg IV/day. There was a rapid and remarkable improvement in symptoms following steroid administration. A repeat EEG showed resolution of lateralizing periodic discharges from the right temporal region. He was discharged on 80 mg oral prednisone, which was slowly weaned over 2 months.

The patient has continued on surveillance since cessation of immunotherapy in April 2020. His most recent imaging in

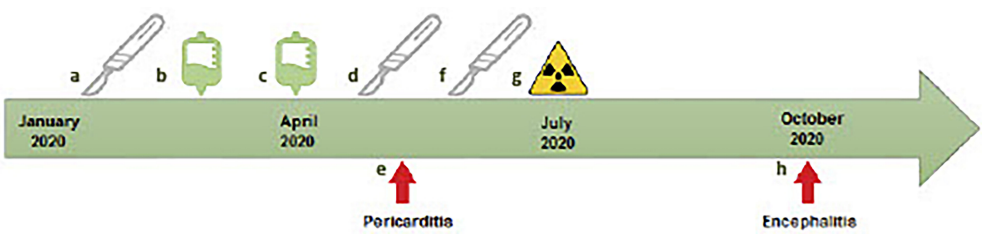


FIGURE 1 | Timeline of case report of patient with rare delayed immune-related toxicities. **(A)** February 14, 2020, first brain metastasis resection. **(B)** March 2020, first cycle ipilimumab/nivolumab. **(C)** April 4, second cycle ipilimumab/nivolumab. **(D)** April 8, second brain metastasis resection. **(E)** May 12, presentation with immune-related pericarditis. **(F)** June 24, third brain metastasis resection. **(G)** July 14, stereotactic radiosurgery of resection cavity. **(H)** Presentation with auto-immune encephalitis.



FIGURE 2 | Serial MRI brain showing development of encephalitis and serial PET/CT demonstrating the patient's durable response to immunotherapy. **(A)** MRI brain with gadolinium Sept 2, 2020—no abnormalities in medial temporal region. **(B)** MRI brain October 29, 2020 shows new T2/FLAIR hyperintensity in the right medial temporal lobes. **(C)** PET/CT March 2020. **(D)** PET CT March 2021.

March 2021 demonstrated an ongoing near-complete response of his metastatic melanoma. His pericarditis has not recurred with significant but partial neurological recovery from his grade 4 encephalitis.

DISCUSSION

Immune-related adverse events (irAEs) remain a major challenge, contributing to morbidity and mortality for melanoma patients. Immune-related cardiac toxicity and neurologic toxicities account for a high proportion of fatal immune-related toxicities (2). For the majority of patients, these irAEs occur early; however, a minority of patients will develop irAEs late in treatment or following treatment cessation (2, 3). The definition of a delayed autoimmune adverse event (DIRE) is varied in literature. The majority of clinical trials define delayed safety adverse events as greater than 90 days after discontinuation of immunotherapy and thus this timeframe has been used in several recent reviews to define DIREs (3). A review by Couey et al. (3) included a collation of 194 trials and 367 case reports and only identified 25 DIREs, 2 pericarditis, and no encephalitis cases, highlighting the exceptional rarity of these cases.

Immune-related pericardial disease is rare and variably reported in the literature. The incidence of pericardial disease reported in a recent pharmacovigilance study was reported at 0.36% with combination anti-PD1 and anti-CTLA4 (4). Immune-related pericardial disease has a wide variation in both onset and presentation and in some instances may well be under-reported due to the variability in severity. Such variation may lead to delayed diagnosis and treatment. This is a significant concern due to the relatively high mortality rates associated with immune-related cardiac toxicity. ICI-induced pericarditis has a fatality rate of 13% (5). Further to this, pericardial disease may be associated with myocarditis, which carries a significantly higher mortality rate reported as high as 65.6% in combination immunotherapy (4). Taking into account variability in the literature, pericardial disease is most often seen early during treatment with the majority of patients developing cardiac toxicities within the first month of commencement of immunotherapy (4, 6). Patients with symptomatic pericardial disease often present with chest pain, signs and symptoms of right heart failure, or tamponade (7). Essential investigations include ECG, cardiac biomarkers, and echocardiogram. Cardiac MRI is a critical investigation to assess for myocarditis and should be completed where possible given the mortality rates associated with myocarditis (4, 5). Performance of pericardiocentesis is highly varied among institutions' literature (5, 7) and should of course be balanced against the risks of this invasive procedure. Analysis of pericardial fluid can provide key diagnostic information. ICI-associated pericardial effusions commonly demonstrate a lymphocyte-rich infiltrate and the absence of malignant cells (5). As with most severe irAEs, high-dose corticosteroids are recommended; however, guidelines are based on limited case series. Cautiously selected patients may be suitable for management without high-dose corticosteroids *via* utilization of anti-inflammatories commonly employed for non-ICI-induced pericarditis, such as colchicine and ibuprofen. Such an approach is resource intensive as it requires close monitoring with serial TTEs and close cardiologist follow-up. On review of available literature, we identified two cases of ICI-induced pericarditis managed successfully without use of high-dose steroids. One case (5) was managed with therapeutic pericardiocentesis resulting in resolution of the effusion. The second case was successfully treated with colchicine and ibuprofen alone (8). This case highlights an approach that may be considered for patients with ICI-induced pericarditis where high dose steroids are contraindicated.

ICI-induced encephalitis is another extremely rare irAE with rates of 0.92% reported with combination immunotherapy (9, 10). ICI-induced encephalitis is reported to occur early during treatment with a median onset of 61 days reported in a large pharmacovigilance study by Johnson et al. (10). ICI-induced encephalitis typically presents with symptoms including altered mentation, speech disturbance, and altered level of consciousness (11). Diagnostic workup should be prioritized to exclude infectious etiologies. Diagnosis is often challenging given common overlapping toxicities. In this case, such overlapping toxicities included three cerebral metastasectomies, stereotactic radiotherapy, and a recent cerebral abscess. Key investigations for ICI-induced encephalitis include but are not limited to CT and MRI brain, EEG, LP with viral PCR and culture, autoimmune and paraneoplastic panels, serum inflammatory markers, and electrolytes (11). MRI changes typical of autoimmune encephalitis can include T2/FLAIR changes of the limbic system (11). CSF may show elevated white blood cell

count and/or elevated protein levels. Prompt initiation of corticosteroids is crucial to decrease morbidity and mortality (12) in patients who develop ICI encephalitis with a mortality rate approaching 20% (2, 12).

Our case presented with ICI-induced encephalitis 7.5 months after cessation of immunotherapy. On review of the literature, we could identify only one other case of delayed ICI-induced encephalitis (13). Both cases were in patients who received treatment for prior brain metastases, responded rapidly to high-dose corticosteroids with partial neurological recovery in the short term. No medium- to long-term follow-up to assess ongoing neurological recovery was available for these cases.

CONCLUSION

Combination immunotherapy has a wide range of potentially fatal immune-related toxicities with both ICI-induced pericarditis and ICI-induced encephalitis contributing to a high proportion of these fatalities (2). This case highlights the challenges clinicians face with life-threatening toxicity emerging many months after treatment cessation. As ipilimumab and nivolumab become more frequently employed and with an increasing population of long-term survivors, this case emphasizes the importance of constant vigilance for such toxicities. Ongoing collaboration and research are needed to produce robust guidelines to support clinicians in managing these rare presentations.

DATA AVAILABILITY STATEMENT

The original contributions presented in the study are included in the article/supplementary material. Further inquiries can be directed to the corresponding author.

ETHICS STATEMENT

Ethical review and approval was not required for the study on human participants in accordance with the local legislation and institutional requirements. The patients/participants provided their written informed consent to participate in this study. Written informed consent was obtained from the individual(s) for the publication of any potentially identifiable images or data included in this article.

AUTHOR CONTRIBUTIONS

All authors listed have made a substantial, direct, and intellectual contribution to the work and approved it for publication.

REFERENCES

1. Larkin J, Chiarion-Sileni V, Gonzalez R, Grob JJ, Rutkowski P, Lao CD, et al. Five-Year Survival With Combined Nivolumab and Ipilimumab in Advanced Melanoma. *N Engl J Med* (2019) 381(16):1535–46. doi: 10.1056/NEJMoa1910836
2. Wang DY, Salem JE, Cohen JV, Chandra S, Menzer C, Ye F, et al. Fatal Toxic Effects Associated With Immune Checkpoint Inhibitors: A Systematic Review and Meta-Analysis. *JAMA Oncol* (2018) 4(12):1721–8. doi: 10.1001/jamaoncol.2018.3923
3. Couey MA, Bell RB, Patel AA, Romba MC, Crittenden MR, Curti BD, et al. Delayed Immune-Related Events (DIRE) After Discontinuation of Immunotherapy: Diagnostic Hazard of Autoimmunity at a Distance. *J Immunother Cancer* (2019) 7(1):165. doi: 10.1186/s40425-019-0645-6
4. Salem JE, Manouchehri A, Moey M, Lebrun-Vignes B, Bastarache L, Pariente A, et al. Cardiovascular Toxicities Associated With Immune Checkpoint Inhibitors: An Observational, Retrospective, Pharmacovigilance Study. *Lancet Oncol* (2018) 19(12):1579–89. doi: 10.1016/S1470-2045(18)30608-9
5. Chen D-Y, Huang W-K, Wu C-C, Chang V, Chen J-S, Chuang C-K, et al. Cardiovascular Toxicity of Immune Checkpoint Inhibitors in Cancer Patients: A Review When Cardiology Meets Immuno-Oncology. *J Formosan Med Assoc* (2020) 119(10):1461–75. doi: 10.1016/j.jfma.2019.07.025
6. Canale ML, Camerini A, Casolo G, Lilli A, Bisceglia I, Parrini I, et al. Incidence of Pericardial Effusion in Patients With Advanced Non-Small Cell Lung Cancer Receiving Immunotherapy. *Adv Ther* (2020) 37(7):3178–84. doi: 10.1007/s12325-020-01386-y
7. Palaskas N, Morgan J, Daigle T, Banchs J, Durand JB, Hong D, et al. Targeted Cancer Therapies With Pericardial Effusions Requiring Pericardiocentesis Focusing on Immune Checkpoint Inhibitors. *Am J Cardiol* (2019) 123(8):1351–7. doi: 10.1016/j.amjcard.2019.01.013
8. Chahine J, Collier P, Maroo A, Tang WHW, Klein Allan L. Myocardial and Pericardial Toxicity Associated With Immune Checkpoint Inhibitors in Cancer Patients. *JACC: Case Rep* (2020) 2(2):191–9. doi: 10.1016/j.jaccas.2019.11.080
9. Larkin J, Chmielowski B, Lao CD, Hodi FS, Sharfman W, Weber J, et al. Neurologic Serious Adverse Events Associated With Nivolumab Plus Ipilimumab or Nivolumab Alone in Advanced Melanoma, Including a Case Series of Encephalitis. *Oncologist* (2017) 22(6):709–18. doi: 10.1634/theoncologist.2016-0487
10. Johnson DB, Manouchehri A, Haugh AM, Quach HT, Balko JM, Lebrun-Vignes B, et al. Neurologic Toxicity Associated With Immune Checkpoint Inhibitors: A Pharmacovigilance Study. *J Immunother Cancer* (2019) 7(1):134. doi: 10.1186/s40425-019-0617-x
11. Spain L, Walls G, Julve M, O'Meara K, Schmid T, Kalaitzaki E, et al. Neurotoxicity From Immune-Checkpoint Inhibition in the Treatment of Melanoma: A Single Centre Experience and Review of the Literature. *Ann Oncol* (2017) 28(2):377–85. doi: 10.1093/annonc/mdw558
12. Gkoufa A, Gogas H, Diamantopoulos PT, Ziogas DC, Psichogiou M. Encephalitis in a Patient With Melanoma Treated With Immune Checkpoint Inhibitors: Case Presentation and Review of the Literature. *J Immunother* (2020) 43(7):224–9. doi: 10.1097/CJI.0000000000000326
13. Shah N, Jacob J, Househ Z, Shiner E, Baird L, Soudy H, et al. Unchecked Immunity: A Unique Case of Sequential Immune-Related Adverse Events With Pembrolizumab. *J ImmunoTher Cancer* (2019) 7(1):247. doi: 10.1186/s40425-019-0727-5

Conflict of Interest: JL is on the advisory board for Sanofi and has received honorarium from MSD, BMS, Novartis and travel support from BioRad.

The remaining author declares that the research was conducted in the absence of any commercial or financial relationships that could be construed as a potential conflict of interest.

Publisher's Note: All claims expressed in this article are solely those of the authors and do not necessarily represent those of their affiliated organizations, or those of the publisher, the editors and the reviewers. Any product that may be evaluated in this article, or claim that may be made by its manufacturer, is not guaranteed or endorsed by the publisher.

Copyright © 2021 Braden and Lee. This is an open-access article distributed under the terms of the Creative Commons Attribution License (CC BY). The use, distribution or reproduction in other forums is permitted, provided the original author(s) and the copyright owner(s) are credited and that the original publication in this journal is cited, in accordance with accepted academic practice. No use, distribution or reproduction is permitted which does not comply with these terms.

frontiers in Oncology

ORIGINAL RESEARCH
published: 24 December 2021
doi: 10.3389/fonc.2021.763895

Vitamin D Enhances Anticancer Properties of Cediranib, a VEGFR Inhibitor, by Modulation of VEGFR2 Expression in Melanoma Cells

Anna Piotrowska[1], *Fernando Pereira Beserra*[2], *Justyna Marta Wierzbicka*[1], *Joanna Irena Nowak*[1] *and Michał Aleksander Żmijewski*[1]*

[1] Department of Histology, Faculty of Medicine, Medical University of Gdańsk, Gdańsk, Poland, [2] Institute of Biosciences, São Paulo State University, São Paulo, Brazil

OPEN ACCESS

Edited by:
Sapna Patel,
University of Texas MD Anderson Cancer Center, United States

Reviewed by:
Gagan Chhabra,
University of Wisconsin-Madison, United States
William B. Grant,
Sunlight Nutrition and Health Research Center, United States
Andrzej T. Slominski,
University of Alabama at Birmingham, United States

***Correspondence:**
Michał Aleksander Żmijewski
mzmijewski@gumed.edu.pl

Specialty section:
This article was submitted to Skin Cancer, a section of the journal Frontiers in Oncology

Received: 24 August 2021
Accepted: 01 December 2021
Published: 24 December 2021

Citation:
Piotrowska A, Beserra FP, Wierzbicka JM, Nowak JI and Żmijewski MA (2021) Vitamin D Enhances Anticancer Properties of Cediranib, a VEGFR Inhibitor, by Modulation of VEGFR2 Expression in Melanoma Cells. Front. Oncol. 11:763895. doi: 10.3389/fonc.2021.763895

Regardless of the recent groundbreaking introduction of personalized therapy, melanoma continues to be one of the most lethal skin malignancies. Still, a substantial proportion of patients either fail to respond to the therapy or will relapse over time, representing a challenging clinical problem. Recently, we have shown that vitamin D enhances the effectiveness of classical chemotherapeutics in the human malignant melanoma A375 cell line. In search for new combination strategies and adjuvant settings to improve melanoma patient outcomes in the current study, the effects of cediranib (AZD2171), an oral tyrosine kinase inhibitor of VEGFR1-3, PDGFR, and c-KIT, used in combination either with $1,25(OH)_2D_3$ or with low-calcemic analog calcipotriol were tested on four human malignant melanoma cell lines (A375, MNT-1, RPMI-7951, and SK-MEL-28). Melanoma cells were pretreated with vitamin D and subsequently exposed to cediranib. We observed a marked decrease in melanoma cell proliferation (A375 and SK-MEL-28), G2/M cell cycle arrest, and a significant decrease in melanoma cell mobility in experimental conditions used (A375). Surprisingly, concurrently with a very desirable decrease in melanoma cell proliferation and mobility, we noticed the upregulation of VEGFR2 at both protein and mRNA levels. No effect of vitamin D was observed in MNT-1 and RPMI-7951 melanoma cells. It seems that vitamin D derivatives enhance cediranib efficacy by modulation of VEGFR2 expression in melanoma cells expressing VEGFR2. In conclusion, our experiments demonstrated that vitamin D derivatives hold promise as novel adjuvant candidates to conquer melanoma, especially in patients suffering from vitamin D deficiency. However, further extensive research is indispensable to reliably assess their potential benefits for melanoma patients.

Keywords: melanoma, vitamin D, calcipotriol, cediranib, anti-angiogenic therapy, VEGFR, VEGFR inhibitors

INTRODUCTION

Melanoma, although representing a minor fraction of all skin malignancies, remains the most lethal form (1, 2). Before the modern era, patients with advanced melanoma could expect a 5-year survival rate of 10% (3). Beginning in 2011, novel therapies, including immunotherapy with immune checkpoint inhibitors CTLA-4 or PD-1, as well as targeted therapy with BRAF and MEK inhibitors, have become a key breakthrough in the clinical landscape of melanoma treatment (4). Unprecedented in cancer

medicine, from 2013 to 2016, overall melanoma mortality decreased by 17.9% (5). Nevertheless, regardless of the groundbreaking treatment options, most patients invariably relapse from BRAF/MEK signaling inhibition within a year from treatment commencement (6). About 50% of patients treated with immune checkpoints inhibitors do not respond due to primary resistance and a great proportion of responders experience tumor relapse within 2 years (7, 8). Current 5-year survival rate for metastatic melanoma is therefore 27% (9). What is more, the incidence of melanoma is constantly rising worldwide, and currently, melanoma is expected to be the fifth most common cancer in both males and females, as estimated by the American Cancer Society (9). Therefore, it seems to be highly reasonable to focus on new combination strategies and adjuvant settings to improve melanoma patient outcomes (4).

Vitamin D is a secosteroid endogenously produced in the skin from its precursor, 7-dehydrocholesterol, using the energy of UVB irradiation (10, 11). It should be emphasized that vitamin D3 is biologically inert and requires two subsequent hydroxylations to gain its hormonal functions. First, hydroxylation at C-25 takes place in the liver, and second, at C-1α in kidneys, giving the most active form $1,25(OH)_2D_3$, calcitriol (11, 12). The extrarenal expression of vitamin D hydroxylases was proven in many different sites, such as lymph nodes, placenta, breast, and colon (13); however, it should be underlined that the skin is the only organ equipped with the whole pathway of vitamin D synthesis and activation (14, 15). Apart from a historically known role in regulation of calcium homeostasis, vitamin D has widely appreciated anticancer properties, including antiproliferative, antiangiogenic, and pro-differentiative effects in various types of cancer (10). Therefore, vitamin D is considered for cancer prevention, as the recent VITAL study (16–18) and some former studies (19, 20) suggest that vitamin D supplementation has beneficial effects in reducing risks of cancer. A very recent study has shown that among patients with newly resected stage II melanoma who received adjuvant vitamin D3 (100,000 IU every 50 days), individuals with low Breslow score (<3 mm) had a double increase in 25OHD levels from baseline after 4 months, whereas patients with Breslow score ≥3 mm had a significantly lower increase over time. After 12 months, subjects with low 25OHD levels and Breslow score ≥3 mm had shorter disease-free survival ($p = 0.02$) compared to those with Breslow score <3 mm and/or high levels of 25OHD (21). At baseline, 80% of these melanoma patients were vitamin D insufficient (21). This observation underlines the role of vitamin D supplementation status of patients in melanoma prognosis. Indeed, the National Institute for Health and Care Excellence guidelines clearly recommend that assessment of vitamin D levels and relevant advice should be an inherent aspect of the management of patients with melanoma at the secondary care level (22). Currently, the role of vitamin D supplementation on cutaneous malignant melanoma outcome is assessed in the ViDMe trial (23). Additionally, an inverse correlation has also been documented between the expression of the vitamin D receptor (VDR) and a crucial vitamin D activating enzyme (CYP27B1) with melanoma progression and disease outcome (24–26). Furthermore, as revealed by analysis of transcriptome of melanoma patients, VDR expression was independently protective for melanoma-related death in both primary and metastatic disease (27). What is more, it was shown that active forms of vitamin D improve efficacy of several anticancer drugs, such as cisplatin (28, 29), dacarbazine (30), doxorubicin (31), and proton therapy (32). It is also suggested that vitamin D immune-modulating ability could offer indications for a novel vitamin D application in melanoma patients receiving immunotherapy (33).

Currently, the upper normal limit of 25(OH)D in blood serum, used in clinic as a biomarker of vitamin D status (34), is defined at 100 ng/ml (35). A recent study suggests that extended intakes of 20,000 IU/day to 60,000 IU/day, associated with 25OHD blood levels ranging as high as 384 mg/dl, were found to be safe without any evidence of toxicity (36). However, considering patient safety, the major disadvantage of vitamin D and its natural active metabolite—$1,25(OH)_2D_3$—is that prolonged supplementation with high doses (>50,000 IU per day for several months), which could be beneficial in the cancer therapy, may also lead, although not necessarily, to hypercalcemia (12, 37). In our constant work to select most potent but low calcemic vitamin D analogs, we have investigated the series of CYP11A1 metabolites of vitamin D (30, 38, 39), which are products of a recently discovered novel pathway of vitamin D metabolism and activation (40–43), modified vitamin D_2 analogs (44), and vitamin D analogs with the shortened side chain (15, 45) as to their efficacy against melanoma cell lines. Simultaneously, we have also explored whether vitamin D and its non- or low-calcemic analogs will enhance the effectiveness of classical chemotherapeutics, cisplatin and dacarbazine, in the human malignant melanoma A375 cell line (30). We showed that both calcitriol and calcipotriol exhibited modulatory effects on the melanoma cells treated with dacarbazine, decreasing the half maximal inhibitory concentration (IC50, calcitriol only) for the drug, stimulating G1/G0 arrest, and causing a marked decrease in the mitochondrial transmembrane potential (30). In the current study, we have focused our attention on the antiangiogenic compound, cediranib, and its combination with calcitriol and low-calcemic vitamin D analog, calcipotriol, shown to be as potent as $1,25(OH)_2D_3$ in human malignant melanoma cells (30).

MATERIALS AND METHODS

Chemicals

$1,25(OH)_2D_3$ was purchased in Sigma-Aldrich (Merck KGaA, Darmstadt, Germany). Calcipotriol was a gift from the Pharmaceutical Research Institute (Warsaw, Poland). Cediranib (AZD2171) was purchased from Selleck Chemicals (Houston, TX, USA).

Cell Culture

Human melanoma A375 cell line (CRL–1619), RPMI-7951 (HTB-66), MNT-1, and SK-MEL-28 were from the American Type Culture Collection (Manassas, VA, USA). The A375 cell line is derived from a skin melanoma of a 54-year-old female. It should be underlined that these cells carry two mutant genes, B-RAF and

CDKN2, both associated with melanoma of sun-damaged skin (46). Since UV radiation is considered the most important environmental risk factor for cutaneous melanoma (47) and it is estimated that 60%–70% of cutaneous malignant melanomas are thought to be caused by ultraviolet (UV) radiation exposure (48), we therefore consider A375 melanoma cells as a particularly good model for our study. A375 cells were cultured in Dulbecco's modified Eagle's medium (DMEM, Sigma–Aldrich; Merck KGaA) supplemented with 10% fetal bovine serum (FBS) (Biological Industries, Israel) and 1% penicillin/streptomycin (Sigma–Aldrich; Merck KGaA) in an incubator with 5% CO_2 at 37˚C. RPMI-7951 cells were cultured in Minimum Essential Medium Eagle, with Earle's salts and non-essential amino acids (MEM, Sigma–Aldrich; Merck KGaA), supplemented with 10% FBS (Biological Industries, Israel), 1% penicillin/streptomycin (Sigma–Aldrich; Merck KGaA), 1 mM sodium pyruvate, and 2 mM L-glutamine (Sigma–Aldrich; Merck KGaA, both). MNT-1 cells were cultured in MEM (Sigma–Aldrich; Merck KGaA) Alpha Modification, supplemented with 20% FBS (Biological Industries, Israel), 1% penicillin/streptomycin, 10 mM HEPES, 2 mM L-glutamine, 1 mM sodium pyruvate, non-essential amino acids (Sigma–Aldrich; Merck KGaA, all listed before), and 10% AIM-V™ Medium (Thermofisher Scientific, Waltham, USA). SK-MEL-28 cells were cultured in MEM (Sigma–Aldrich; Merck KGaA) Alpha Modification, supplemented with 10% FBS (Biological Industries, Israel), 1% penicillin/streptomycin (Sigma–Aldrich; Merck KGaA), and 2 mM L-glutamine (Sigma–Aldrich; Merck KGaA). Appropriate medium supplemented with 5 times lower concentration of charcoal–stripped FBS was used for all procedures where the effects of vitamin D derivatives were examined (2% for A375, RPMI-7951, and SK-MEL-28 cell lines and 4% for MNT-1 cells).

Proliferation Assay

The sulforhodamine B (SRB) assay was performed according to the procedure previously described (49). Briefly, the human melanoma A375 cells were seeded in 96–well plates (3,000 cells per well), cultured overnight, and then treated simultaneously with serial dilutions of cediranib (0.01–1,000 nM) and vitamin D analogs (calcitriol or calcipotriol) at 100 nM concentration, being tested for an additional 72 h. Cells were fixed with 10% trichloroacetic acid for 1 h at 4˚C. Following washing (5× with distilled water), the staining solution composed of 0.4% SRB (Sigma–Aldrich; Merck KGaA) in acetic acid was added to each well for 15 min, followed by washing with 1% acetic acid. The SRB dye was solubilized using a solution of 10 mM buffered Tris Base (pH 10.5) and the absorbance was measured at 570 nm using an Epoch™ microplate spectrophotometer (BioTek Instruments, Inc., Winooski, VT, USA).

Cell Cycle Analysis

The cell cycle status was analyzed based on quantification of DNA content using flow cytometry. Melanoma cells were treated for 24 h with vitamin D compounds (calcitriol or calcipotriol) at 100 nM concentration, followed by 72 h incubation with cediranib at 500 or 1,000 nM concentration. Trypsinized human malignant melanoma cells together with cells from culture medium were fixed in 70% ethanol for 24–48 h at 4°C, then treated with ribonuclease to remove any contaminating RNA, and the DNA was stained with propidium iodide (PI; Sigma–Aldrich; Merck KGaA) for 30 min at 37°C. The fluorescence of the PI–stained cells was measured by flow cytometry (FACSCalibur™; Becton, Dickinson and Company, Franklin, Lakes, NJ, USA). The results were analyzed using the CellQuest™ Pro Software version 6.0 (Becton, Dickinson and Company) and expressed as a percentage of cells with DNA content corresponding to apoptotic/necrotic cells (subG1 fraction) or cells in G1, S, and G2/M phases of the cycle. **Supplementary Figure 1** presents row cytometrical data.

Wound Closure Rate

A375 melanoma cells were seeded on an 8-well chamber slide (3×10^5 cells per well) and were cultured overnight. Melanoma cells were pretreated with vitamin D compounds (calcitriol or calcipotriol) at 100 nM concentration. After 24 h, a mechanical wound was created by physical scraping using a pipette tip in a confluent cell monolayer. Cediranib at 500 or 1,000 nM concentration was diluted in a fresh medium and added to the cells for 72 h and cell migration process was observed. The experiment was carried out as a live imaging with Olympus cellVivo IX83 and cell free area was calculated as a percentage closure relative to original size [(wound area in μm^2)*100/(original wound area in μm^2)] with the Olympus cellSens software with use of TruAI technology.

VEGFR2 Extracellular Expression

A375 melanoma cells were treated for 24 h with vitamin D compounds (calcitriol or calcipotriol) at 100 nM concentration, followed by 24 h incubation with cediranib at 500 or 1,000 nM concentration. Trypsinized human malignant melanoma cells at 1×10^6 density were harvested by centrifugation and rinsed two times in 3 ml of incubation buffer (0.5% bovine serum albumin in PBS). Following 10 min blocking in the incubation buffer, cells were stained for 30 min at room temperature with primary antibody anti-VEGFR2 (Cell Signaling, cat. no. 2479, rabbit monoclonal, 1:200) dissolved in the incubation buffer. Following rinsing 2× in incubation buffer, cells were incubated for 30 min with the secondary antibody (goat anti-rabbit IgG ThermoFisher Scientific A11008, 1:500) diluted in the incubation buffer. Cells were rinsed 2× with incubation buffer, dissolved in 0.5 ml of PBS and analyzed cytometrically on FACSCalibur™ (Becton, Dickinson and Company, Franklin, Lakes, NJ, USA) using the CellQuest™ Pro Software version 6.0 (Becton, Dickinson and Company). The results were expressed as a fluorescence geometric mean.

Immunoblotting

After preincubation either with $1,25(OH)_2D_3$ or with calcipotriol at 100 nM concentration for 24 h, A375, SK-MEL-28, RPMI-7951 or MNT-1 melanoma cells were treated for an additional 24 h with cediranib at 500 or 1,000 nM concentration. Subsequently, cells were scraped and lysed in the presence of ice-cold RIPA buffer (Sigma–Aldrich; Merck KGaA) supplemented with protease inhibitor cocktail. Protein concentrations were determined by the Bradford assay. An equal amount of protein from each sample (40 μg) was loaded per lane, and proteins were resolved by SDS-PAGE (4%–20% Mini-PROTEAN® TGX Stain-Free™ Protein Gels, Bio-Rad Laboratories, Hercules, CA, USA) and then transferred onto an Immun-Blot™ PVDF membrane (Bio-Rad Laboratories, Hercules,

CA, USA). The membranes were incubated with primary antibodies: anti-VDR (mouse monoclonal, 1:1,000; Santa Cruz sc-13133), anti-VEGFR1 (rabbit polyclonal, 1:1,000; Cell Signaling Technology 2893), anti-VEGFR2 (rabbit monoclonal, 1:1,000; Cell Signaling Technology 2479), anti-PDGFR alpha (rabbit monoclonal, 1:1,000; Cell Signaling Technology 3174), anti-PDGFR beta (rabbit monoclonal, 1:1,000; Cell Signaling Technology 3169), or HRP-conjugated anti-β-actin antibody (mouse monoclonal, 1:10,000; Santa Cruz Biotechnology, sc-47778) overnight at 4°C. After three washes in TBST, secondary goat anti-rabbit antibodies conjugated to horseradish peroxidase (1:10,000; Santa Cruz Biotechnology, sc-2004) or secondary bovine anti-mouse antibodies conjugated to horseradish peroxidase (1:20,000; Santa Cruz Biotechnology, sc-2371) were added, and following incubation for 1 h at room temperature, blots were developed with Western Lightning® Ultra chemiluminescent substrate (PerkinElmer, Inc. Waltham, MA, USA) according to the manufacturer's protocol. Changes in protein level were assessed by densitometric scanning of the bands and corrected for β-actin loading control.

Immunocytochemistry

A375 melanoma cells were seeded in 8-well chambers. Cells were preincubated for 24 h with vitamin D derivatives at 100 nM concentration and subsequently incubated for an additional 24 h with cediranib at 500 or 1,000 nM concentration. Following fixing with 4% paraformaldehyde (PFA) for 10 min at room temperature (RT), cells were permeabilized in 0.2% Triton X-100 solution in PBS for 10 min. Blocking was performed with 1% BSA in PBS for 30 min at RT. Following washing 3 × 5 min in PBS, primary antibodies were applied to the cells (VEGFR2 rabbit monoclonal, 1:200; Cell Signaling Technology 2479; EEA1 mouse monoclonal, 1:250, BD Biosciences 610457) and incubated at 4°C overnight. Following rinsing 3 × 5 min in PBS, slides were incubated with an appropriate secondary antibody (A11008 goat anti-rabbit IgG Alexa Fluor 488, 1:500; A11008 donkey anti-mouse IgG Alexa Fluor 594, 1:500, Life Technologies) for 1 h at RT. Following rinsing, cultures were counterstained with DAPI (Sigma–Aldrich; Merck KGaA). Images were collected with Olympus cellVivo IX83 and analyzed with Olympus cellSens software.

RT-PCR

After preincubation either with $1,25(OH)_2D_3$ or with calcipotriol at 100 nM concentration for 24 h, A375 melanoma cells were treated for an additional 24 h with cediranib at 500 or 1,000 nM concentration. Subsequently, total RNA was extracted by using the ExtractME®Total RNA Kit (Blirt, Poland, EM09.1-250), according to the manufacturer's instructions. The concentration and purity of isolated RNA were measured by an EpochMicroplate Spectrophotometer (BioTek, USA). Extracted RNA was reverse transcribed and cDNA synthesized using RevertAid™ First Strand cDNA Synthesis Kit (Thermo Fisher Scientific Inc., USA). Real-Time PCR was performed using a StepOnePlus™ Real-Time PCR System (LifeTechnologies-Applied Biosystems, Grand Island, NY, USA) with RealTime AMPLIFYME SYBR™ Green No-ROX Mix (Blirt, Poland, AM01). All primers were purchased from Sigma-Aldrich (Merck KGaA). The expression of the genes was normalized by comparative -ΔΔCt method, using RPL37A as a housekeeping gene, followed by calibration (fold change) to normalized expression data of samples from control (ratio = 1). To ensure specificity of the PCR amplification, dynamic melting curve analysis was performed for all reactions. Primer sequences are summarized in **Table 1**.

Statistical Analyses

Statistical analysis was performed using GraphPad Prism v 7.05 (GraphPad Software, San Diego, CA, USA) or Microsoft Excel. Data were subjected to Student's *t*-test (for two groups), one-way or two-way analysis of variance and appropriate post-hoc test (the ANOVA Tukey's or Sidak's multiple comparison test). Data are expressed as mean of 3 to 5 independent experiments ± S.D ($n = 2–6$ in each). Differences are shown as significant at $^{*}p < 0.05$,$^{**}p < 0.01$, $^{***}p < 0.001$, or $^{****}p < 0.0001$ as indicated.

RESULTS

Vitamin D Analogs Significantly Decrease Viability of A375 and SK-MEL-28 Melanoma Cells Treated With Cediranib

As established by SRB proliferation assay, cediranib alone inhibited A375 melanoma cell proliferation maximally about 6% at 1,000 nM concentration during 72 h of incubation (**Figures 1A,**

TABLE 1 | Primer sequences.

Gene	Forward primer 3'–5'	Reverse primer 5'–3'
RPL37A	TTCTGATGGCGGACTTTACC	CACTTGCTCTTTCTGTGGCA
VEGFR1	TCCAAGAAGTGACACCGAGA	TTGTGGGCTAGGAAACAAGG
VEGFR2	GACTTGGCCTCGGTCATTTA	ACACGACTCCATGTTGGTCA
PDGRFa	TGGATTGAACCCTGCTGATG	ATCAGCCTGCTT CATGTCCAT
PDGFRb	CACAATGACTCCCGTGGACTG	CATCATTAGGGAGGAAGCCCA
VEGFA	AAGGAGGAGGGCAGAATCAT	GCAGTAGCTGCGCTGATAGA
VEGFC	TGAACACCAGCACGAGCTAC	GCCTTGAGAGAGAGGCACTG
VEGFD	TGGAACAGAAGACCACTCTCATCT	GCAACGATCTTCGTCAAACATC
VDR	CCAGTTCGTGTGAATGATGG	GTCGTCCATGGTGAAGGA
CYP27B1	TGTTTGCATTTGCTCAGA	CCGGGAGAGCTCATACAG
CYP2R1	AGAGACCCAGAAGTGTTCCAT	GTCTTTCAGCACAGATGAGGTA
CYP3A4	AAGGCACCACCCACCTATGATACT	TACTTTGGGTCACGGTGAAGAGCA
CYP24A1	GCAGCCTAGTGCAGATTT	ATTCACCCAGAACTGTTG

B). However, simultaneous treatment with cediranib and 1,25 $(OH)_2D_3$ or calcipotriol, at 100 nM concentration, resulted in a profound decrease in the proliferation of melanoma cells. The effect of vitamin D derivatives varied as to the level of maximal inhibition of melanoma cell proliferation, which ranged from approximately 30% for cediranib and 1,25$(OH)_2D_3$ (**Figure 1A**) to 43% for cediranib and calcipotriol (**Figure 1B**), $p < 0.0001$ both. Similar effects were observed in SK-MEL-28 melanoma cells. Cediranib alone inhibited proliferation of the cells maximally about 12% at 1,000 nM under experimental conditions used (**Figures 1C, D**). Simultaneous treatment with cediranib and 1,25$(OH)_2D_3$ or calcipotriol, at 100 nM concentration, resulted in further decrease in the proliferation of melanoma cells. The effect of vitamin D derivatives varied as to the level of maximal inhibition of melanoma cell proliferation, which ranged from approximately 26% for cediranib and 1,25$(OH)_2D_3$ (**Figure 1C**) to 22% for cediranib and calcipotriol (**Figure 1D**), $p < .05$ both. On the other hand, treatment of MNT-1 and RPMI-7951 melanoma cells with cediranib in the presence of 1,25$(OH)_2D_3$ (**Figures 1E–H**) or calcipotriol did not show additive effect of co-treatment. Cediranib alone inhibited proliferation of these melanoma cells maximally about 11% or 18%, respectively, at 1,000 nM concentration during 72 h of incubation.

Vitamin D Derivatives Trigger G2/M Cell Cycle Arrest in A375 Malignant Melanoma Cells Treated With Cediranib

Since the most profound effect of vitamin D analogs to the inhibition of melanoma cell proliferation treated with cediranib was observed in A375 cells, this line was used as a model for further detailed analysis. In agreement with our previous studies (15, 44), treatment of A375 melanoma cells with vitamin D resulted in G0/G1 (G0/G1—stationary/growth phase) cell cycle arrest (**Figures 2A, B**). G0/G1 arrest was observed also in

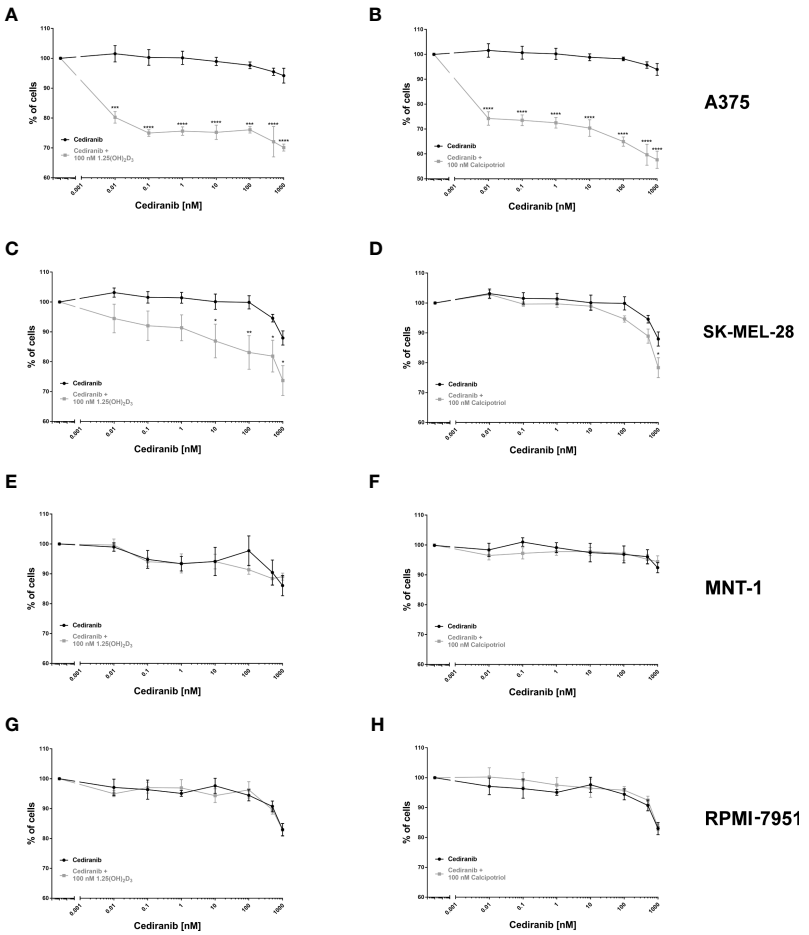


FIGURE 1 | The effect of cediranib or its combination with vitamin D analogs [left column—1,25$(OH)_2D_3$; right column—calcipotriol] on the proliferation of human malignant melanoma A375, MNT-1, RPMI-7951, and SK-MEL-28 cells [**(A, B)**—A375; **(C, D)**—SK-MEL-28; **(E, F)**—MNT-1 and **(G, H)**—RPMI-7951 cell lines]. The cells were treated with serial dilutions (0.01–1,000 nM) of cediranib alone or in combination either with 1,25$(OH)_2D_3$ or with calcipotriol for 72 h. The same cediranib data are plotted in each graph from the same melanoma cell line, except for MNT-1 cells. Data are shown as mean from three or four independent experiments (n = 4–6 in each) ± SEM. Statistical significance between plots (between relevant concentrations of cediranib alone or with vitamin D) was estimated using two–way ANOVA and presented as $^*p < 0.05$; $^{**}p < 0.01$, $^{***}p < 0.001$, or $^{****}p < 0.0001$.

melanoma cells treated with cediranib, $p < 0.0001$ (**Figure 2**). Additionally, we noticed an increase in the number of SubG1 cells, indicating induction of apoptosis by cediranib in melanoma cells, $p < 0.0001$ (**Figure 2**). To investigate the mechanism of proliferation inhibition of melanoma A375 cells by the combination of vitamin D analogs with cediranib, melanoma cells were pretreated either with $1,25(OH)_2D_3$ (**Figure 2A**) or with calcipotriol (**Figure 2B**) at 100 nM concentration for 24 h and then incubated with cediranib at 500 or 1,000 nM for an additional 72 h. Preincubation of melanoma cells with $1,25(OH)_2D_3$ (**Figure 2A**) prior to cediranib treatment for 72 h resulted in an increase in the percentage of cells in the G2/M phase (preparation for mitosis/mitosis) in comparison to cells without pretreatment, $p < 0.001$ for cediranib at 500 nM concentration and $p < 0.05$ for cediranib at 1,000 nM concentration (**Figure 2A**), which was accompanied by a proportional decrease in the number of SubG1 cells (SubG1—apoptotic/necrotic cells). Similar results were observed for calcipotriol (**Figure 2B**); however, we noticed an increase in the percentage of cells not only in the G2/M phase, but also in the S phase, in comparison to cells without pretreatment.

Pretreatment With Vitamin D Derivatives Significantly Decreases Mobility of A375 Melanoma Cells Treated With Cediranib

Cellular motility and migration are well-established hallmarks of malignant tumors spreading their metastases (50). We recorded therefore migration of A375 melanoma cells and wound closure live with Olympus cellVivo IX83 every 30 min for 72 h and cell free area was calculated as a percentage of closure relative to its original size. The wound closure curves (**Figure 3**) revealed that non-treated malignant melanoma A375 cells approached up to 38% closure and migrate faster than cells from any treatment groups ($p < 0.0001$ for any treatment group vs. control, not marked in **Figure 3**). In agreement with our previous study (15), we observed that $1,25(OH)_2D_3$ efficiently inhibited melanoma cell migration ($p < 0.0001$ vs. control, not marked in **Figure 3**) during 72 h, leaving approximately 70% of the wound original size. Interestingly, calcipotriol was even more efficient than $1,25(OH)_2D_3$, leaving as much as 81.5% of the wound original size. Curiously, cediranib at both tested concentrations, 500 and 1,000 nM, inhibited melanoma cell migration to a similar extent, leaving approximately 74%–75% of the wound original size. It should be emphasized, however, that vitamin D pretreatment profoundly diminished cellular mobility in melanoma cells treated with cediranib. The most efficient reduction of melanoma cells mobility was observed in cells 24 h pretreated with $1,25(OH)_2D_3$ and incubated subsequently for 72 h with cebiranib at 500 nM, in which the wound area was reduced by only 15% [$p < 0.0001$ for melanoma cells $1,25(OH)_2D_3$ pretreated and incubated with cediranib at 500 nM concentration vs. 500 nM cediranib alone; **Figure 3**], giving a further significant 10% reduction in cellular mobility as compared to monotreatment with cediranib. Substantial 8% reduction in cellular mobility was observed also in melanoma cells pretreated with calcipotriol compared to monotreatment with cediranib.

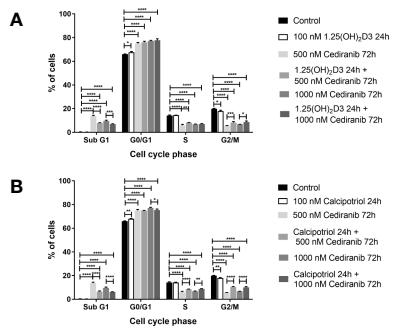


FIGURE 2 | The effect of 24-h preincubation with $1,25(OH)_2D_3$ **(A)** or calcipotriol **(B)** at 100 nM concentration on the distribution of human malignant melanoma A375 cells treated for 72 h with cediranib throughout the phases of the cell cycle (SubG1—apoptotic/necrotic cells, G1—growth, S—DNA synthesis, G2/M—preparation for mitosis/mitosis). Cells were harvested, stained with propidium iodide, and analyzed by flow cytometry. The data are presented as the mean ± standard deviation ($n = 3$). The same control and cediranib data are plotted in each graph. Statistical significance was estimated using two–way ANOVA followed by Tukey's multiple comparison test and presented as $^*p < 0.05$; $^{**}p < 0.01$; $^{***}p < 0.001$, $^{****}p < 0.0001$. The results are representative of four experiments.

Vitamin D Derivatives Increase the Extracellular Expression of VEGFR2 in A375 Malignant Melanoma Cells Treated With Cediranib

Since cediranib is a small-molecule inhibitor of several tyrosine kinases, including VEGFR1 and VEGFR2, of which the latter seems to play a predominant role (51), we investigated therefore whether vitamin D preincubation will affect the extracellular expression of VEGFR2 in A375 melanoma cells exposed to cediranib. We noticed that cediranib alone did not influence the extracellular expression of VEGFR2 in A375 melanoma cells during 24-h incubation (**Figure 4**). However, the extracellular expression of VEGFR2 increased significantly in melanoma cells pretreated either with $1,25(OH)_2D_3$ (**Figure 4A**) or with calcipotriol (**Figure 4B**) for 24 h as compared to monotreatment with cediranib or to control cells.

Vitamin D Derivatives Upregulate VEGFR2 Protein Level in Malignant Melanoma Cells Treated With Cediranib

Next, we checked whether the preincubation of A375 melanoma cells with vitamin D derivatives affected the protein level of VEGFR1, VEGFR2, PDGFRa, PDGFRb, or VDR after subsequent treatment with cediranib (**Figure 5**). No significant effect was observed as to the VEGFR1 or PDGFRb protein level neither by $1,25(OH)_2D_3$, nor by cediranib under the experimental conditions used (**Figures 5A, E**, respectively). We also noticed that the expression of VEGFR2 at the protein level was not changed by cediranib alone (**Figure 5B**). However, we

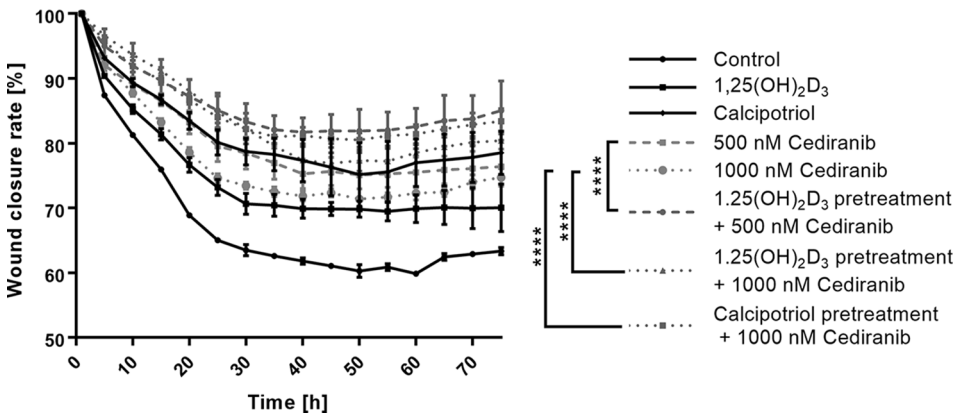


FIGURE 3 | The effect of 24-h preincubation with vitamin D analogs at 100 nM concentration on the rate of a wound closure in A375 human malignant melanoma cells treated for 72 h with cediranib either at 500 or at 1,000 nM concentration. The cell-free area of each wound was measured at the different time points, every 30 min for 72 h as a live imaging in Olympus cell Vivo IX 83, and results were calculated in % as a wound closure rate with the Olympus cell Vivo IX 83 software. Statistical values were calculated with one-way analysis of variance and Tukey's post-hoc test and presented as $^{****}p < 0.0001$.

observed a significant increase in VEGFR2 protein level in melanoma cells pretreated with vitamin D (although in case of calcipotriol, only with cediranib at 500 nM concentration). Both vitamin D derivatives increased the VDR protein level (**Figure 5C**). Cediranib alone increased the protein level of PDGFRa ($p < 0.05$), while preincubation with $1,25(OH)_2D_3$ reversed that effect for cediranib at 1,000 nM concentration, $p < 0.01$ (**Figure 5D**).

Since we observed the upregulation of VEGFR2, at both protein level and its extracellular expression, under experimental conditions, concurrently with a very desirable decrease in A375 melanoma cell proliferation and mobility, we hypothesized whether the presence of VEGFR2 protein or its level could potentially influence the extent to which $1,25(OH)_2D_3$ may enhance the cytotoxic effect of cediranib in MNT-1, RPMI-7951, and SK-MEL-28 melanoma cells. We checked, therefore, whether the preincubation of aforementioned melanoma cell lines with $1,25(OH)_2D_3$ affected the protein level of VEGFR2, PDGFRa, or VDR, after subsequent treatment with cediranib (**Figure 6**). No significant effect was observed as to the VDR protein level neither by $1,25(OH)_2D_3$, nor by cediranib under the experimental conditions used in MNT-1 melanoma cells (**Figure 6**). However, we observed a significant increase in VDR protein level in RPMI-7951 and SK-MEL-28 melanoma cells treated with $1,25(OH)_2D_3$ (**Figures 6C, I**). No significant effect was observed as to the PDGFRa protein level neither by $1,25(OH)_2D_3$, nor by cediranib under the experimental conditions used in RPMI-7951 and SK-MEL-28 melanoma cells (**Figures 6B, H**); what is more, we did not detect any PDGFRa protein product in MNT-1 melanoma cells (**Figure 6E**). Interestingly, we did not detect any VEGFR2 protein product neither in MNT-1, nor in RPMI-7951 melanoma cells (**Figures 6D, G**). However, we observed a significant increase in VEGFR2 protein level in SK-MEL-28 melanoma cells treated with cediranib alone or cediranib with $1,25(OH)_2D_3$ (**Figure 6A**), which underlines the key role of VEGFR2 in an interaction between vitamin D and cediranib.

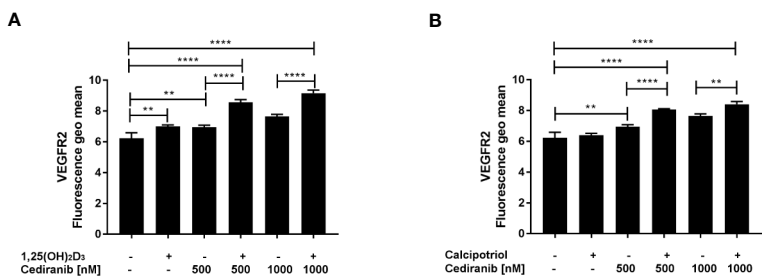


FIGURE 4 | The effect of 24-h preincubation with 1,25(OH)2D3 **(A)** or calcipotriol **(B)** at 100 nM concentration on the extracellular expression of the VEGFR2 in A375 melanoma cells treated subsequently for 24 h with cediranib at 500 or 1,000 nM concentration. Cells were stained with appropriate antibody (see *Materials and Methods* section) and analyzed cytometrically. The data are presented as the mean ± standard deviation ($n = 3$). The same control and cediranib data are plotted in each graph. Statistical significance was estimated using one–way ANOVA followed by Tukey's multiple comparison test and presented as $^{**}p < 0.01$ or $^{****}p < 0.0001$. The results are representative of three experiments.

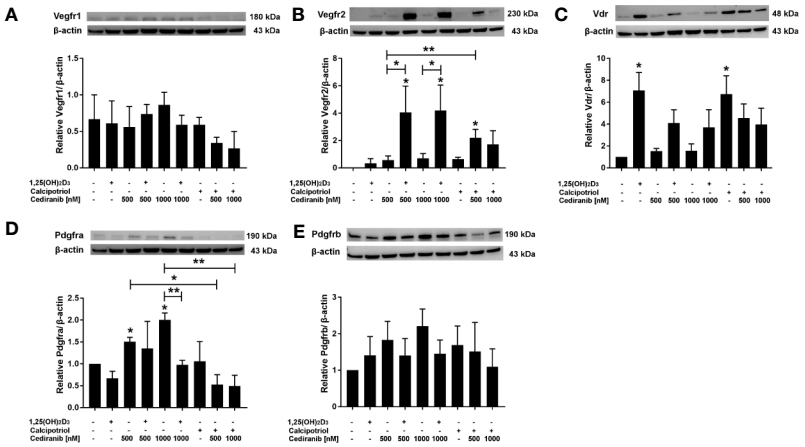


FIGURE 5 | The effect of 24-h preincubation with vitamin D analogs at 100 nM concentration on VEGFR1 **(A)**, VEGFR2 **(B)**, VDR **(C)**, PDGFRa **(D)**, and PDGFRb **(E)** protein level in A375 melanoma cells treated subsequently for 24 h with cediranib at 500 or 1,000 nM concentration. Protein levels were measured by Western blotting, with β-actin used as a control. Data are shown as mean from three independent experiments ± SEM. $^{*}p < 0.05$ and $^{**}p < 0.01$ vs. untreated control or between the two groups indicated by the bracket.

To further explore the mechanism underlying the observed increase of VEGFR2 protein level by vitamin D in A375 melanoma cells treated with cediranib, we checked whether this protein is sequestered in early endosomes for potential recycling or degradation, as suggested recently (52). We did not observe, however, any co-localization of VEGFR2 and EEA1, which is a marker of early endosomes (**Figure 7**).

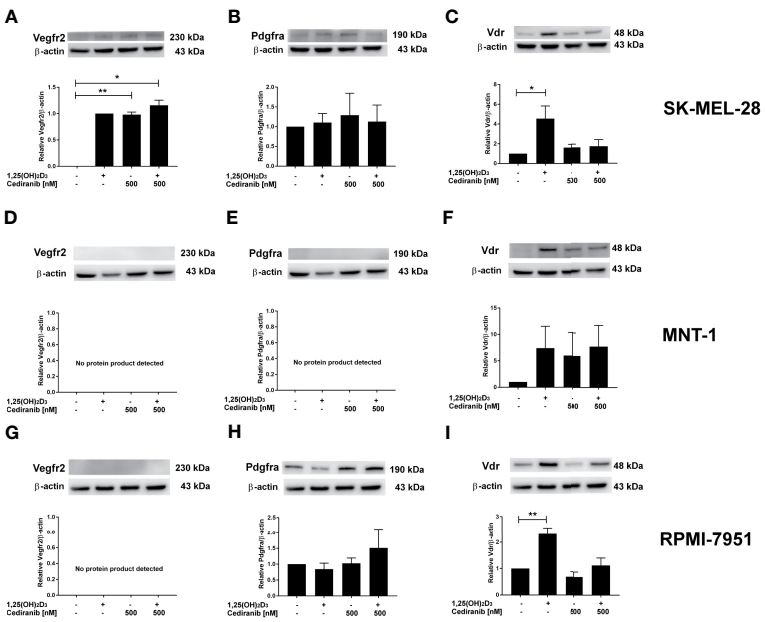


FIGURE 6 | The effect of 24-h preincubation with $1,25(OH)_2D_3$ at 100 nM concentration on VDR **(C, F, I)**, PDGFRa **(B, E, H)**, and VEGFR2 **(A, D, G)** protein level in SK-MEL-28 **(A–C)**, MNT-1 **(D–F)**, and RPMI-7951 **(G–I)** melanoma cells treated subsequently for 24 h with cediranib at 500 nM concentration. Protein levels were measured by Western blotting, with β-actin used as a control. Data are shown as mean from three independent experiments ± SEM. Statistical significance was estimated using one-way ANOVA followed by Tukey's multiple comparison test and presented as $^{*}p < 0.05$ and $^{**}p < 0.01$ vs. untreated control or between the two groups indicated by the bracket.

Vitamin D Derivatives Modulate Expression of VEGFR2, VEGFA, PDGFRa, and PDGFRb at the mRNA Level in A375 Malignant Melanoma Cells Treated With Cediranib

In order to verify the aforementioned changes in protein level, the impact of $1,25(OH)_2D_3$ on the expression of selected VEGF-associated genes was tested in melanoma cells treated with cediranib (**Figure 8**). Although cediranib alone did not influence mRNA level for VEGFR1 (**Figure 8A**), we observed an increase in mRNA level in melanoma cells treated with the combination of $1,25(OH)_2D_3$ and cediranib at both tested concentrations ($p < 0.05$ vs. control). No significant effect of cediranib alone was observed on the mRNA level of VEGFR2; however, consistent with immunoblotting described above, we observed a marked increase in VEGFR2 mRNA level in melanoma cells pretreated with $1,25(OH)_2D_3$ ($p < 0.01$, **Figure 8B**). Both $1,25(OH)_2D_3$ and cediranib resulted in an increase in mRNA level for VEGFR3 ($p < 0.05$, **Figure 8C**), with an increasing trend in melanoma cells pretreated with vitamin D subsequently exposed to cediranib, yet without statistical significance in the latter. Interestingly, cediranib alone at 500 nM concentration decreased the mRNA level for VEGF-A ($p < 0.01$, **Figure 8D**), while pretreatment of A375 melanoma cells with $1,25(OH)_2D_3$ resulted in an increase in the relevant mRNA in melanoma cells incubated subsequently with cediranib at 1,000 nM concentration ($p < 0.05$). No significant effect was observed in the expression of VEGF-C under the experimental conditions used (**Figure 8E**). mRNA level for VEGF-D was elevated by both $1,25(OH)_2D_3$ and cediranib ($p < 0.05$, **Figure 8F**), and it was elevated also in melanoma cells pretreated with vitamin D. Finally, we observed an increase in mRNA level for PDGFRa and PDGFRb in melanoma cells treated with cediranib at 1,000 nM concentration ($p < 0.05$, **Figures 8G, H**, respectively); the effect was further exacerbated by vitamin D pretreatment ($p < 0.05$ for PDGFRa and $p < 0.01$ for PDGFRb vs. monotreatment).

Then, we also analyzed the expression of several vitamin D-related genes in the experimental conditions used. We observed that VDR mRNA level was elevated in A375 melanoma cells pretreated with vitamin D and subsequently incubated with cediranib at 1,000 nM concentration ($p < 0.05$, **Figure 9A**). No significant effect was observed in the expression of CYP27B1 under the experimental conditions used (**Figure 9B**). Cediranib treatment resulted, however, in an increase in mRNA level for CYP3A4 and CYP2R1 in melanoma cells pretreated with $1,25(OH)_2D_3$ ($p < 0.05$ vs. control and vs. monotreatment, **Figures 9C, D**, respectively). Lastly, consistent with our previous results (30) and literature data (53), we observed a marked increase in mRNA level for CYP24A1 ($p < 0.01$, **Figure 9E**) in melanoma cells treated with $1,25(OH)_2D_3$. Interestingly, the effect was invariably observed in cells treated subsequently with cediranib. In fact, the mRNA level of CYP24A1 was the highest in melanoma cells treated with cediranib following vitamin D pretreatment ($p < 0.01$ vs. monotreatment).

DISCUSSION

Advanced metastatic melanoma is widely known as one of the most aggressive skin malignancies. Regardless of improvements in the recent decade, a remarkable proportion of patients still fail to respond to the therapy or will relapse over time (4). Increased

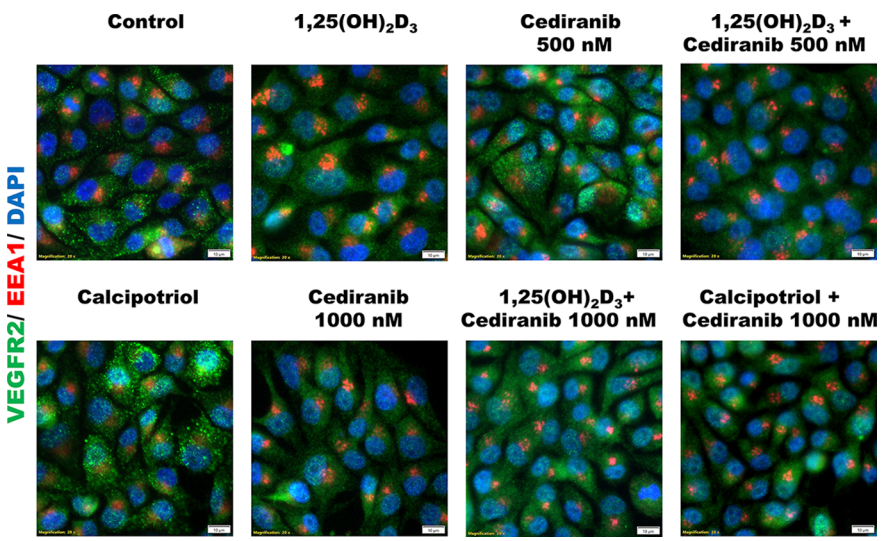


FIGURE 7 | Immunofluorescent detection of VEGFR2 (green) or EEA1 (red) in A375 melanoma cells. Melanoma cells were preincubated with vitamin D derivatives for 24 h and subsequently treated with cediranib at 500 or 1,000 nM concentration for another 24 h. Nuclei were counterstained with DAPI (shown in blue). Magnification 200×.

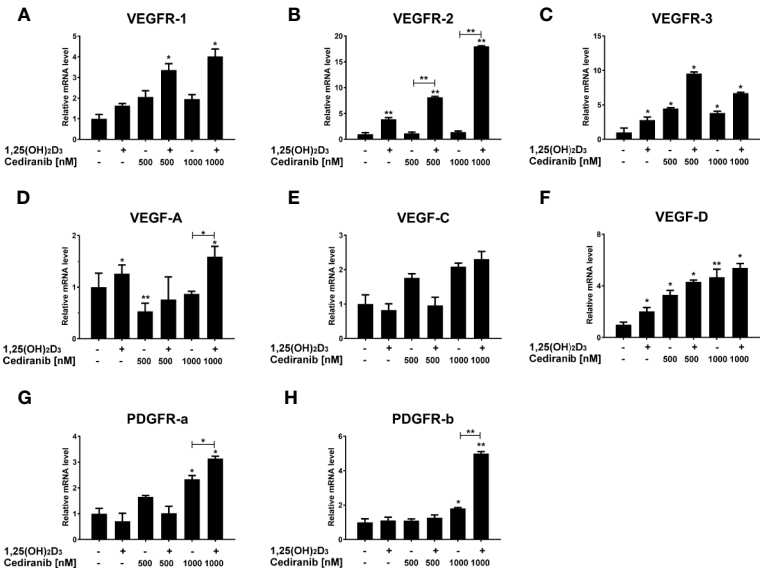


FIGURE 8 | The effect of 24-h preincubation with $1,25(OH)_2D_3$ at 100 nM concentration on VEGFR1 **(A)**, VEGFR2 **(B)**, VEGFR3 **(C)**, VEGFA **(D)**, VEGFC **(E)**, VEGFD **(F)**, PDGFRa **(G)**, and PDGFRb **(H)** gene expression in A375 melanoma cells treated subsequently for 24 h with cediranib at 500 or 1,000 nM concentration. mRNA levels were measured by qPCR. The results are representative of three experiments carried out in duplicate. *$p < 0.05$ and **$p < 0.01$ vs. untreated control or between the two groups indicated by the bracket.

effort in search for the neoadjuvant and adjuvant settings may therefore help to improve long-term outcomes for melanoma-suffering patients. In that field, vitamin D seems to be a promising and reasonable remedy, acting as both a chemopreventive and therapeutic agent (47). Firstly, it is well documented that vitamin D protects against DNA damage (54, 55) and therefore against UV-induced carcinogenesis (56–58), since UV is considered as the major environmental risk factor for melanoma development (47). Secondly, vitamin D deficiency is a well-established cancer risk factor (59), while vitamin D supplementation was shown to reduce the incidence of advanced and fatal cancer (18). What is more, vitamin D deficiency is associated with higher Breslow thickness and mortality in melanoma patients (60). Furthermore, an increase in 25-hydroxyvitamin D_3 level in vitamin D-deficient melanoma patients already undergoing treatment improved their outcomes in comparison to individuals who remained vitamin D deficient (61). Finally, an inverse correlation between vitamin D receptor, VDR, and 1α-hydroxylase (CYP27B1), the enzyme responsible for the synthesis of the biologically active form of vitamin D, was documented with melanoma progression and disease outcome (25, 26).

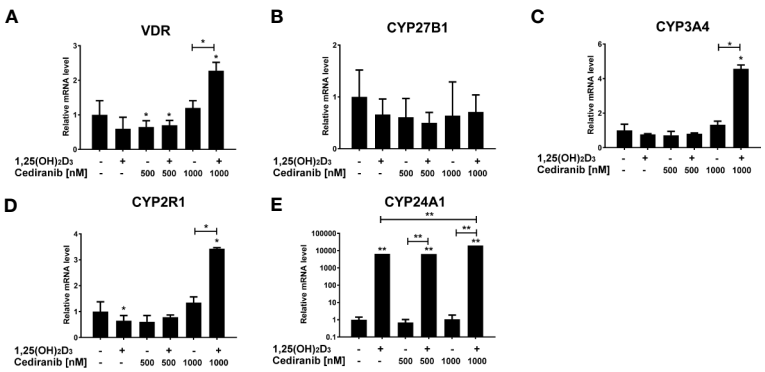


FIGURE 9 | The effect of 24-h preincubation with $1,25(OH)_2D_3$ at 100 nM concentration on VDR **(A)**, CYP27B1 **(B)**, CYP3A4 **(C)**, CYP2R1 **(D)**, and CYP24A1 **(E)** gene expression in A375 melanoma cells treated subsequently for 24 h with cediranib at 500 or 1,000 nM concentration. mRNA levels were measured by qPCR. The results are representative of three experiments carried out in duplicate. *$p < 0.05$ and **$p < 0.01$ vs. untreated control or between the two groups indicated by the bracket.

Our previous study revealed that two vitamin D analogs, calcitriol and low calcemic calcipotriol, exhibited modulatory effects on the A375 melanoma cells treated with dacarbazine, decreasing the half maximal inhibitory concentration (IC50, calcitriol only) for the drug, stimulating G1/G0 arrest, and causing a marked decrease in the mitochondrial transmembrane potential under given experimental conditions (30). Since the process of angiogenesis is crucial for growth, progression, and metastasis of the majority of solid tumors, including melanomas (62, 63), in the current study, the effects of cediranib, an oral tyrosine kinase inhibitor (TKI) of VEGFR1-3, PDGFR, and c-KIT (64), used in combination either with $1,25(OH)_2D_3$ or with low-calcemic analog calcipotriol, were tested in the same A375 human malignant melanoma cell line, carrying the $BRAF^{V600E}$ mutation, very common in melanoma patients (65), which was shown to be pro-angiogenic in several human tumors (66). Selected experiments were also carried out in MNT-1, RPMI-7951, and SK-MEL-28 melanoma cell lines. Cediranib as a single agent is associated predominantly with hypertension, diarrhea, dysphonia, and proteinuria, as shown in a phase I study (67). The most frequent non-hematologic adverse events observed in patients with metastatic or recurrent malignant melanoma treated with cediranib in a phase II study were hypertension (78%), fatigue (69%), diarrhea (69%), and anorexia and nausea (each 57%) (68). It should be emphasized that melanomas express high levels of VEGF, VEGFR1, VEGFR2, and VEGFR3, which is further associated with poor prognosis (69, 70). Quite unexpectedly, it was shown that adjuvant treatment with bevacizumab, an anti-VEGF monoclonal antibody, after resection of high-risk melanoma significantly improves disease-free interval, rather than overall survival (66). In fact, bevacizumab as a monotherapy does not offer any significant survival benefit over traditional therapies (71, 72). Therefore, antiangiogenic therapies in melanoma are rather supportive to other forms of treatment. However, various configurations of combination therapies with antiangiogenic bevacizumab against melanoma are currently being investigated in clinical trials (73). Very interestingly, as documented recently by Atzori (74), VEGFR1 inhibition might potentiate the effects of vemurafenib-based therapies for melanoma treatment and, what is more, counteract resistance development to this BRAF inhibitor, since the latter was associated with higher expression of VEGF receptors. Although cediranib alone was not sufficiently effective as a first-line therapy in untreated patients with metastatic or recurrent malignant melanoma, as shown in a phase II study (68), of the 17 patients evaluable for response, 2 patients had stable disease >/= 6 months, and the disease was stable in 8 patients and progressive in 9 patients, with no objective responses seen. Still, the authors concluded that the potential of cediranib may be enhanced in combination with other agents (68). Furthermore, it was shown recently on patient-derived organoid models of endometrial cancer that cediranib but not bevacizumab synergizes with chemotherapy, decreasing cell viability when combined with paclitaxel as compared to treatment with paclitaxel alone (75). Currently, there is an ongoing phase I clinical trial, NCT01364051, for patients with clinically unresectable solid tumors, including stage IV cutaneous melanoma and malignant melanoma, and for whom there is no standard therapy, in which patients are receiving cediranib with selumetinib, an oral MEK 1/2 inhibitor. In our experiments, vitamin D derivatives were used at 100 nM concentration, corresponding to the optimal serum $25(OH)D_3$ level (75–125 nM) (76), which is used in clinic as a biomarker of vitamin D status. We have shown that supplementation with vitamin D improves the effectiveness of anti-angiogenic compound, cediranib, against A375 and SK-MEL-28 human melanoma cells, as we observed a marked decrease in melanoma cell proliferation (in both lines), G2/M cell cycle arrest, and a significant decrease in melanoma cell mobility (tested only in A375 melanoma cells). A similar observation was recently described in Hec50 cells, an endometrial adenocarcinoma, in which the combination of paclitaxel and cediranib produced a profound increase in the accumulation of cells in mitosis as assessed by the percentage of cells in G2/M by flow cytometry compared to paclitaxel alone (75). On the other hand, we did not observe any influence of vitamin D on proliferation of MNT-1 and RPMI-7951 melanoma cells treated with cediranib. The study of Atzori (74) suggested that VEGFR1 upregulation might contribute to melanoma progression and spreading. Overexpressed VEGFR2 in gastric cancer cells increased cellular proliferation and invasion *in vitro* as well as tumor formation in xenograft models (77). The pro-metastatic role of VEGFR2 was also postulated in osteosarcoma (78). Surprisingly, we observed the upregulation of VEGFR2 in experimental conditions used concurrently with a very desirable decrease in melanoma cell proliferation and mobility. Interestingly, it seems that vitamin D derivatives enhance cediranib efficacy by modulation of VEGFR2 expression in melanoma cells, as we observed a significant increase in VEGFR2 level at both protein and mRNA levels, along with the extracellular VEGFR2 expression, in vitamin D-pretreated A375 melanoma cells incubated further with cediranib. Thus, the extent to which vitamin D exacerbates cytotoxicity of cediranib against melanoma cells seems to depend firstly on the presence of VEGFR2 in these cells and secondly on its level. The most profound increase in cediranib cytotoxicity by supplementation with vitamin D was observed in A375 melanoma cells, in which we noticed the upregulation of VEGFR2, at both the protein and mRNA level, as well as its extracellular expression, in experimental conditions used, concurrently with a very desirable decrease in melanoma cell proliferation and mobility. The VEGFR2 protein level was several times higher in vitamin D-pretreated cells compared to monotreatment with cediranib. Similarly, in SK-MEL-28 cells, simultaneous treatment with cediranib and $1,25(OH)_2D_3$ or calcipotriol, at 100 nM concentration, resulted in a further decrease in the proliferation of these melanoma cells, which was accompanied by an increase in the protein level of VEGFR2 compared to control cells in experimental conditions used, although there was no difference in the VEGFR2 protein level compared to monotreatment with cediranib. On the other hand, in MNT-1

and RPMI-7951 melanoma cells, in which we did not observe any enhancement of cediranib cytotoxicity by supplementation with vitamin D, we did not detect any VEGFR2 protein in the experimental conditions used. It should be noted that VEGFR2 is considered a predominant receptor triggering VEGF signaling in cells (73, 79). Out of the three primary VEGF receptors, VEGFR2 is considered the dominant effector and the most relevant in the metastatic melanoma microenvironment, although the study of Molhoek and coworkers showed that a relatively low percentage of melanoma cells express VEGFR2 (80). However, yet another study underlines that it is VEGFR2 that might be a new prognostic marker in malignant melanoma (81).

Possibly, the astonishing upregulation of VEGFR2 observed in A375 and SK-MEL-28 melanoma cells in our experimental conditions may be considered as an adaptive strategy activated by vitamin D, in which increased availability of VEGFR2 on the melanoma cell surface potentiates the response to its inhibitor, cediranib, or elevated expression of the receptor is a response to inhibition of the downstream signaling from the receptor.

We also observed an increase in VDR mRNA level as well as CYP3A4 and CYP2R1 in A375 cells, the enzymes responsible for 25-hydroxylation of vitamin D en route to its final activation, in melanoma cells treated with cediranib at 1,000 nM concentration, which were $1,25(OH)_2D_3$ pretreated, underlining an intensified vitamin D activation in these conditions ($p < 0.05$, **Figure 9**). Thus, it is possible that cediranib actually improves the sensitivity of cells to vitamin D.

In conclusion, although recent innovative immunotherapies and targeted therapies have vastly ameliorated the management of metastatic melanoma, in light of impending resistance development, more effective strategies for treatment of melanoma patients are still urgently needed. We demonstrated that vitamin D derivatives hold promise as novel adjuvant candidates to conquer melanoma, which may be considered for clinical applications, especially in vitamin D-deficient melanoma patients, as they are widely available, non-toxic, and relatively inexpensive. However, further extensive and complex studies are needed to assess their potential expected benefits for melanoma patients.

DATA AVAILABILITY STATEMENT

The datasets used and/or analyzed during the current study are available from the corresponding author on reasonable request.

AUTHOR CONTRIBUTIONS

AP and MAŻ conceived, designed, and supervised the study. AP, FBP, JIN, and JMW performed the experiments. AP and MAŻ analyzed the data. AP and MAŻ wrote the manuscript. All authors contributed to the article and approved the submitted version.

FUNDING

This study was supported by grant no. MN 01–0250/08/280 from the Medical University of Gdansk (Gdansk, Poland) to AP. The authors would like also to thank São Paulo Research Foundation (FAPESP) for the grant support: 2017/17600-1.

SUPPLEMENTARY MATERIAL

The Supplementary Material for this article can be found online at: https://www.frontiersin.org/articles/10.3389/fonc.2021.763895/full#supplementary-material

Supplementary Figure 1 | The effect of 24 hours preincubation with vitamin D analogs at 100 nM concentration on the distribution of human malignant melanoma A375 cells treated for 72 hours with cediranib throughout phases of the cell cycle (M1: SubG1—apoptotic/necrotic cells, M2: G1—growth, M3: S—DNA synthesis, M4: G2/M—preparation for mitosis/mitosis). Cells were harvested, stained with propidium iodide and analyzed by Flow Cytometry. Presented panels show representative data plots for relevant treatments.

Supplementary Figure 2 | The effect of 24 hours preincubation with vitamin D analogs at 100 nM concentration on the extracellular expression of the VEGFR2 in A375 melanoma cells treated subsequently for 24 hours with cediranib at 500 or 1000 nM concentration. Cells were stained with appropriate antibody (see Materials and methods section) and analyzed cytometrically. Presented panels show representative data plots for relevant treatments.

REFERENCES

1. Thomas D, Bello DM. Adjuvant Immunotherapy for Melanoma. *J Surg Oncol* (2021) 123(3):789–97. doi: 10.1002/jso.26329
2. Eddy K, Shah R, Chen S. Decoding Melanoma Development and Progression: Identification of Therapeutic Vulnerabilities. *Front Oncol* (2020) 10:626129. doi: 10.3389/fonc.2020.626129
3. Patton EE, Mueller KL, Adams DJ, Anandasabapathy N, Aplin AE, Bertolotto C, et al. Melanoma Models for the Next Generation of Therapies. *Cancer Cell* (2021) 39(5):610–31. doi: 10.1016/j.ccell.2021.01.011
4. Ascierto PA, Puzanov I, Agarwala SS, Blank C, Carvajal RD, Demaria S, et al. Perspectives in Melanoma: Meeting Report From the "Melanoma Bridge" (December 5th-7th, 2019, Naples, Italy). *J Transl Med* (2020) 18(1):346. doi: 10.1186/s12967-020-02482-x
5. Berk-Krauss J, Stein JA, Weber J, Polsky D, Geller AC. New Systematic Therapies and Trends in Cutaneous Melanoma Deaths Among US Whites, 1986-2016. *Am J Public Health* (2020) 110(5):731–3. doi: 10.2105/AJPH.2020.305567
6. Trotta AP, Gelles JD, Serasinghe MN, Loi P, Arbiser JL, Chipuk JE. Disruption of Mitochondrial Electron Transport Chain Function Potentiates the Pro-Apoptotic Effects of MAPK Inhibition. *J Biol Chem* (2017) 292(28):11727–39. doi: 10.1074/jbc.M117.786442
7. Trojaniello C, Vitale MG, Scarpato L, Esposito A, Ascierto PA. Melanoma Immunotherapy: Strategies to Overcome Pharmacological Resistance. *Expert Rev Anticancer Ther* (2020) 20(4):289–304. doi: 10.1080/14737140.2020.1745634
8. Imbert C, Montfort A, Fraisse M, Marcheteau E, Gilhodes J, Martin E, et al. Resistance of Melanoma to Immune Checkpoint Inhibitors Is Overcome by Targeting the Sphingosine Kinase-1. *Nat Commun* (2020) 11(1):437. doi: 10.1038/s41467-019-14218-7
9. Siegel RL, Miller KD, Fuchs HE, Jemal A. Cancer Statistics, 2021. *CA Cancer J Clin* (2021) 71(1):7–33. doi: 10.3322/caac.21654
10. Chen J, Tang Z, Slominski AT, Li W, Żmijewski MA, Liu Y. Vitamin D and its Analogs as Anticancer and Anti-Inflammatory Agents. *Eur J Med Chem* (2020) 207:112738. doi: 10.1016/j.ejmech.2020.112738
11. Slominski AT, Brozyna AA, Zmijewski MA, Jozwicki W, Jetten AM, Mason RS, et al. Vitamin D Signaling and Melanoma: Role of Vitamin D and its Receptors in Melanoma Progression and Management. *Lab Invest* (2017) 97(6):706–24. doi: 10.1038/labinvest.2017.3

12. Jeon SM, Shin EA. Exploring Vitamin D Metabolism and Function in Cancer. *Exp Mol Med* (2018) 50(4):1–14. doi: 10.1038/s12276-018-0038-9
13. Chang SW, Lee HC. Vitamin D and Health - The Missing Vitamin in Humans. *Pediatr Neonatol* (2019) 60(3):237–44. doi: 10.1016/j.pedneo.2019.04.007
14. Wierzbicka J, Piotrowska A, Zmijewski MA. The Renaissance of Vitamin D. *Acta Biochim Pol* (2014) 61:679–86. doi: 10.18388/abp.2014_1830
15. Piotrowska A, Wierzbicka J, Kwiatkowska K, Chodyński M, Kutner A, Żmijewski MA. Antiproliferative Activity of Side-Chain Truncated Vitamin D Analogs (PRI-1203 and PRI-1204) Against Human Malignant Melanoma Cell Lines. *Eur J Pharmacol* (2020) 881:173170. doi: 10.1016/j.ejphar.2020.173170
16. Manson JE, Cook NR, Lee IM, Christen W, Bassuk SS, Mora S, et al. Vitamin D Supplements and Prevention of Cancer and Cardiovascular Disease. *N Engl J Med* (2019) 380(1):33–44. doi: 10.1056/NEJMoa1809944
17. Grant WB, Boucher BJ. Why Secondary Analyses in Vitamin D Clinical Trials Are Important and How to Improve Vitamin D Clinical Trial Outcome Analyses-A Comment on "Extra-Skeletal Effects of Vitamin D, Nutrients 2019, 11, 1460". *Nutrients* 11(9):2182. doi: 10.3390/nu11092182
18. Chandler PD, Chen WY, Ajala ON, Hazra A, Cook N, Bubes V, et al. Effect of Vitamin D3 Supplements on Development of Advanced Cancer: A Secondary Analysis of the VITAL Randomized Clinical Trial. *JAMA Netw Open* (2020) 3 (11):e2025850. doi: 10.1001/jamanetworkopen.2020.25850
19. Lappe JM, Travers-Gustafson D, Davies KM, Recker RR, Heaney RP. Vitamin D and Calcium Supplementation Reduces Cancer Risk: Results of a Randomized Trial. *Am J Clin Nutr* (2007) 85(6):1586–91. doi: 10.1093/ajcn/85.6.1586
20. Holick MF. Cancer, Sunlight and Vitamin D. *J Clin Transl Endocrinol* (2014) 1 (4):179–86. doi: 10.1016/j.jcte.2014.10.001
21. Johansson H, Spadola G, Tosti G, Mandalà M, Minisini AM, Queirolo P, et al. Vitamin D Supplementation and Disease-Free Survival in Stage II Melanoma: A Randomized Placebo Controlled Trial. *Nutrients* (2021) 13(6):1931. doi: 10.3390/nu13061931
22. Gupta M, Maamoun W, Maher M, Jaffe W. Ensuring Universal Assessment and Management of Vitamin D Status in Melanoma Patients at Secondary Care Level: A Service Improvement Project. *Br J Hosp Med (Lond)* (2020) 81 (10):1–5. doi: 10.12968/hmed.2020.0128
23. De Smedt J, Van Kelst S, Boecxstaens V, Stas M, Bogaerts K, Vanderschueren D, et al. Vitamin D Supplementation in Cutaneous Malignant Melanoma Outcome (ViDMe): A Randomized Controlled Trial. *BMC Cancer* (2017) 17 (1):562. doi: 10.1186/s12885-017-3538-4
24. Brozyna AA, Jozwicki W, Janjetovic Z, Slominski AT. Expression of Vitamin D Receptor Decreases During Progression of Pigmented Skin Lesions. *Hum Pathol* (2011) 42(5):618–31. doi: 10.1016/j.humpath.2010.09.014
25. Brozyna AA, Jozwicki W, Janjetovic Z, Slominski AT. Expression of the Vitamin D-Activating Enzyme 1alpha-Hydroxylase (CYP27B1) Decreases During Melanoma Progression. *Hum Pathol* (2013) 44(3):374–87. doi: 10.1016/j.humpath.2012.03.031
26. Brozyna AA, Jozwicki W, Slominski AT. Decreased VDR Expression in Cutaneous Melanomas as Marker of Tumor Progression: New Data and Analyses. *Anticancer Res* (2014) 34(6):2735–43.
27. Muralidhar S, Filia A, Nsengimana J, Poźniak J, O'Shea SJ, Diaz JM, et al. Vitamin D-VDR Signaling Inhibits Wnt/β-Catenin-Mediated Melanoma Progression and Promotes Antitumor Immunity. *Cancer Res* (2019) 79 (23):5986–98. doi: 10.1158/0008-5472.CAN-18-3927
28. Ma Y, Yu WD, Trump DL, Johnson CS. 1,25D3 Enhances Antitumor Activity of Gemcitabine and Cisplatin in Human Bladder Cancer Models. *Cancer* (2010) 116(13):3294–303. doi: 10.1002/cncr.25059
29. Huang Z, Zhang Y, Li H, Zhou Y, Zhang Q, Chen R, et al. Vitamin D Promotes the Cisplatin Sensitivity of Oral Squamous Cell Carcinoma by Inhibiting LCN2-Modulated NF-κb Pathway Activation Through RPS3. *Cell Death Dis* (2019) 10(12):936. doi: 10.1038/s41419-019-2177-x
30. Piotrowska A, Wierzbicka J, Rybarczyk A, Tuckey RC, Slominski AT, Zmijewski MA. Vitamin D and its Low Calcemic Analogs Modulate the Anticancer Properties of Cisplatin and Dacarbazine in the Human Melanoma A375 Cell Line. *Int J Oncol* (2019) 54(4):1481–95. doi: 10.3892/ijo.2019.4725
31. Wietrzyk J, Nevozhay D, Filip B, Milczarek M, Kutner A. The Antitumor Effect of Lowered Doses of Cytostatics Combined With New Analogs of Vitamin D in Mice. *Anticancer Res* (2007) 27(5a):3387–98.
32. Podgorska E, Drzal A, Matuszak Z, Swakon J, Slominski A, Elas M, et al. Calcitriol and Calcidiol Can Sensitize Melanoma Cells to Low(-)LET Proton Beam Irradiation. *Int J Mol Sci* (2018) 19(8):2236. doi: 10.3390/ijms19082236
33. Stucci LS, D'Oronzo S, Tucci M, Macerollo A, Ribero S, Spagnolo F, et al. Vitamin D in Melanoma: Controversies and Potential Role in Combination With Immune Check-Point Inhibitors. *Cancer Treat Rev* (2018) 69:21–8. doi: 10.1016/j.ctrv.2018.05.016
34. Araki T, Holick MF, Alfonso BD, Charlap E, Romero CM, Rizk D, et al. Vitamin D Intoxication With Severe Hypercalcemia Due to Manufacturing and Labeling Errors of Two Dietary Supplements Made in the United States. *J Clin Endocrinol Metab* (2011) 96(12):3603–8. doi: 10.1210/jc.2011-1443
35. Holick MF, Binkley NC, Bischoff-Ferrari HA, Gordon CM, Hanley DA, Heaney RP, et al. Evaluation, Treatment, and Prevention of Vitamin D Deficiency: An Endocrine Society Clinical Practice Guideline. *J Clin Endocrinol Metab* (2011) 96(7):1911–30. doi: 10.1210/jc.2011-0385
36. McCullough PJ, Lehrer DS, Amend J. Daily Oral Dosing of Vitamin D3 Using 5000 TO 50,000 International Units a Day in Long-Term Hospitalized Patients: Insights From a Seven Year Experience. *J Steroid Biochem Mol Biol* (2019) 189:228–39. doi: 10.1016/j.jsbmb.2018.12.010
37. Koul PA, Ahmad SH, Ahmad F, Jan RA, Shah SU, Khan UH. Vitamin D Toxicity in Adults: A Case Series From an Area With Endemic Hypovitaminosis D. *Oman Med J* (2011) 26(3):201–4. doi: 10.5001/omj.2011.49
38. Slominski AT, Janjetovic Z, Kim TK, Wright AC, Grese LN, Riney SJ, et al. Novel Vitamin D Hydroxyderivatives Inhibit Melanoma Growth and Show Differential Effects on Normal Melanocytes. *Anticancer Res* (2012) 32 (9):3733–42.
39. Slominski AT, Brożyna AA, Skobowiat C, Zmijewski MA, Kim TK, Janjetovic Z, et al. On the Role of Classical and Novel Forms of Vitamin D in Melanoma Progression and Management. *J Steroid Biochem Mol Biol* (2018) 177:159–70. doi: 10.1016/j.jsbmb.2017.06.013
40. Slominski AT, Kim TK, Shehabi HZ, Semak I, Tang EK, Nguyen MN, et al. *In Vivo* Evidence for a Novel Pathway of Vitamin D(3) Metabolism Initiated by P450scc and Modified by CYP27B1. *FASEB J* (2012) 26(9):3901–15. doi: 10.1096/fj.12-208975
41. Slominski AT, Kim TK, Shehabi HZ, Tang EK, Benson HA, Semak I, et al. *In Vivo* Production of Novel Vitamin D2 Hydroxy-Derivatives by Human Placentas, Epidermal Keratinocytes, Caco-2 Colon Cells and the Adrenal Gland. *Mol Cell Endocrinol* (2014) 383(1-2):181–92. doi: 10.1016/j.mce.2013.12.012
42. Slominski AT, Li W, Kim TK, Semak I, Wang J, Zjawiony JK, et al. Novel Activities of CYP11A1 and Their Potential Physiological Significance. *J Steroid Biochem Mol Biol* (2015) 151:25–37. doi: 10.1016/j.jsbmb.2014.11.010
43. Slominski AT, Kim TK, Li W, Postlethwaite A, Tieu EW, Tang EK, et al. Detection of Novel CYP11A1-Derived Secosteroids in the Human Epidermis and Serum and Pig Adrenal Gland. *Sci Rep* (2015) 5:14875. doi: 10.1038/srep14875
44. Piotrowska A, Wierzbicka J, Nadkarni S, Brown G, Kutner A, Zmijewski MA. Antiproliferative Activity of Double Point Modified Analogs of 1,25-Dihydroxyvitamin D(2) Against Human Malignant Melanoma Cell Lines. *Int J Mol Sci* (2016) 17(1):76. doi: 10.3390/ijms17010076
45. Zmijewski MA, Li W, Chen J, Kim TK, Zjawiony JK, Sweatman TW, et al. Synthesis and Photochemical Transformation of 3beta,21-Dihydroxypregna-5,7-Dien-20-One to Novel Secosteroids That Show Anti-Melanoma Activity. *Steroids* (2011) 76(1-2):193–203. doi: 10.1016/j.steroids.2010.10.009
46. Avram S, Coricovac DE, Pavel IZ, Pinzaru I, Ghiulai R, Baderca F, et al. Standardization of A375 Human Melanoma Models on Chicken Embryo Chorioallantoic Membrane and Balb/c Nude Mice. *Oncol Rep* (2017) 38 (1):89–99. doi: 10.3892/or.2017.5658
47. Brozyna AA, Hoffman RM, Slominski AT. Relevance of Vitamin D in Melanoma Development, Progression and Therapy. *Anticancer Res* (2020) 40(1):473–89. doi: 10.21873/anticanres.13976
48. Sample A, He YY. Mechanisms and Prevention of UV-Induced Melanoma. *Photodermatol Photoimmunol Photomed* (2018) 34(1):13–24. doi: 10.1111/phpp.12329
49. Piotrowska A, Wierzbicka J, Slebioda T, Wozniak M, Tuckey RC, Slominski AT, et al. Vitamin D Derivatives Enhance Cytotoxic Effects of H2O2 or

Cisplatin on Human Keratinocytes. *Steroids* (2016) 110:49–61. doi: 10.1016/j.steroids.2016.04.002
50. Wang X, Lan H, Li J, Su Y, Xu L. Muc1 Promotes Migration and Lung Metastasis of Melanoma Cells. *Am J Cancer Res* (2015) 5(9):2590–604.
51. Matulonis UA, Berlin S, Ivy P, Tyburski K, Krasner C, Zarwan C, et al. Cediranib, an Oral Inhibitor of Vascular Endothelial Growth Factor Receptor Kinases, is an Active Drug in Recurrent Epithelial Ovarian, Fallopian Tube, and Peritoneal Cancer. *J Clin Oncol* (2009) 27(33):5601–6. doi: 10.1200/JCO.2009.23.2777
52. Kaur G, Lakkaraju A. Early Endosome Morphology in Health and Disease. *Adv Exp Med Biol* (2018) 1074:335–43. doi: 10.1007/978-3-319-75402-4_41
53. Reichrath J, Rech M, Moeini M, Meese E, Tilgen W, Seifert M. *In Vitro* Comparison of the Vitamin D Endocrine System in 1,25(OH)2D3-Responsive and -Resistant Melanoma Cells. *Cancer Biol Ther* (2007) 6(1):48–55. doi: 10.4161/cbt.6.1.3493
54. Slominski AT, Janjetovic Z, Kim TK, Wasilewski P, Rosas S, Hanna S, et al. Novel non-Calcemic Secosteroids That are Produced by Human Epidermal Keratinocytes Protect Against Solar Radiation. *J Steroid Biochem Mol Biol* (2015) 148:52–63. doi: 10.1016/j.jsbmb.2015.01.014
55. Gordon-Thomson C, Gupta R, Tongkao-on W, Ryan A, Halliday GM, Mason RS. 1alpha,25 Dihydroxyvitamin D3 Enhances Cellular Defences Against UV-Induced Oxidative and Other Forms of DNA Damage in Skin. *Photochem Photobiol Sci* (2012) 11(12):1837–47. doi: 10.1039/c2pp25202c
56. Jiang YJ, Teichert AE, Fong F, Oda Y, Bikle DD. 1alpha,25(OH)2-Dihydroxyvitamin D3/VDR Protects the Skin From UVB-Induced Tumor Formation by Interacting With the Beta-Catenin Pathway. *J Steroid Biochem Mol Biol* (2013) 136:229–32. doi: 10.1016/j.jsbmb.2012.09.024
57. Bikle DD, Jiang Y, Nguyen T, Oda Y, Tu CL. Disruption of Vitamin D and Calcium Signaling in Keratinocytes Predisposes to Skin Cancer. *Front Physiol* (2016) 7:296. doi: 10.3389/fphys.2016.00296
58. Holick MF. Sunlight, Ultraviolet Radiation, Vitamin D and Skin Cancer: How Much Sunlight do We Need? *Adv Exp Med Biol* (2014) 810:1–16. doi: 10.1007/978-1-4939-0437-2_1
59. Yin L, Ordonez-Mena JM, Chen T, Schottker B, Arndt V, Brenner H. Circulating 25-Hydroxyvitamin D Serum Concentration and Total Cancer Incidence and Mortality: A Systematic Review and Meta-Analysis. *Prev Med* (2013) 57(6):753–64. doi: 10.1016/j.ypmed.2013.08.026
60. Tsai TY, Kuo CY, Huang YC. The Association Between Serum Vitamin D Level and Risk and Prognosis of Melanoma: A Systematic Review and Meta-Analysis. *J Eur Acad Dermatol Venereol* (2020) 34(8):1722–9. doi: 10.1111/jdv.16189
61. Timerman D, McEnery-Stonelake M, Joyce CJ, Nambudiri VE, Hodi FS, Claus EB, et al. Vitamin D Deficiency is Associated With a Worse Prognosis in Metastatic Melanoma. *Oncotarget* (2017) 8(4):6873–82. doi: 10.18632/oncotarget.14316
62. Delgado-Hernández R, Hernández-Balmaseda I, Rodeiro-Guerra I, Cesar Rodriguez Gonzalez J, De Wever O, Logie E, et al. Anti-Angiogenic Effects of Mangiferin and Mechanism of Action in Metastatic Melanoma. *Melanoma Res* (2020) 30(1):39–51. doi: 10.1097/CMR.0000000000000647
63. Simonsen TG, Gaustad JV, Rofstad EK. Bevacizumab Treatment of Meningeal Melanoma Metastases. *J Transl Med* (2020) 18(1):13. doi: 10.1186/s12967-020-02212-3
64. Tsao AS, Moon J, Wistuba II, Vogelzang NJ, Kalemkerian GP, Redman MW, et al. Phase I Trial of Cediranib in Combination With Cisplatin and Pemetrexed in Chemonaive Patients With Unresectable Malignant Pleural Mesothelioma (SWOG S0905). *J Thorac Oncol* (2017) 12(8):1299–308. doi: 10.1016/j.jtho.2017.05.021
65. Chacon AC, Melucci AD, Qin SS, Prieto PA. Thinking Small: Small Molecules as Potential Synergistic Adjuncts to Checkpoint Inhibition in Melanoma. *Int J Mol Sci* (2021) 22(6):3228. doi: 10.3390/ijms22063228
66. Corrie PG, Marshall A, Nathan PD, Lorigan P, Gore M, Tahir S, et al. Adjuvant Bevacizumab for Melanoma Patients at High Risk of Recurrence: Survival Analysis of the AVAST-M Trial. *Ann Oncol* (2018) 29(8):1843–52. doi: 10.1093/annonc/mdy229
67. Drevs J, Siegert P, Medinger M, Mross K, Strecker R, Zirrgiebel U, et al. Phase I Clinical Study of AZD2171, an Oral Vascular Endothelial Growth Factor Signaling Inhibitor, in Patients With Advanced Solid Tumors. *J Clin Oncol* (2007) 25(21):3045–54. doi: 10.1200/JCO.2006.07.2066
68. McWhirter E, Quirt I, Gajewski T, Pond G, Wang L, Hui J, et al. A Phase II Study of Cediranib, an Oral VEGF Inhibitor, in Previously Untreated Patients With Metastatic or Recurrent Malignant Melanoma. *Invest New Drugs* (2016) 34(2):231–5. doi: 10.1007/s10637-016-0324-0
69. Domingues B, Lopes JM, Soares P, Populo H. Melanoma Treatment in Review. *Immunotargets Ther* (2018) 7:35–49. doi: 10.2147/ITT.S134842
70. Mehnert JM, McCarthy MM, Jilaveanu L, Flaherty KT, Aziz S, Camp RL, et al. Quantitative Expression of VEGF, VEGF-R1, VEGF-R2, and VEGF-R3 in Melanoma Tissue Microarrays. *Hum Pathol* (2010) 41(3):375–84. doi: 10.1016/j.humpath.2009.08.016
71. Jour G, Ivan D, Aung PP. Angiogenesis in Melanoma: An Update With a Focus on Current Targeted Therapies. *J Clin Pathol* (2016) 69(6):472–83. doi: 10.1136/jclinpath-2015-203482
72. D'Aguanno S, Mallone F, Marenco M, Del Bufalo D, Moramarco A. Hypoxia-Dependent Drivers of Melanoma Progression. *J Exp Clin Cancer Res* (2021) 40(1):159. doi: 10.1186/s13046-021-01926-6
73. Bogusławska-Duch J, Ducher M, Małecki M. Resistance of Melanoma Cells to Anticancer Treatment: A Role of Vascular Endothelial Growth Factor. *Postepy Dermatol Alergol* (2020) 37(1):11–8. doi: 10.5114/ada.2020.93378
74. Atzori MG, Ceci C, Ruffini F, Trapani M, Barbaccia ML, Tentori L, et al. Role of VEGFR-1 in Melanoma Acquired Resistance to the BRAF Inhibitor Vemurafenib. *J Cell Mol Med* (2020) 24(1):465–75. doi: 10.1111/jcmm.14755
75. Bi J, Dixit G, Zhang Y, Devor EJ, Losh HA, Newtson AM, et al. Advantages of Tyrosine Kinase Anti-Angiogenic Cediranib Over Bevacizumab: Cell Cycle Abrogation and Synergy With Chemotherapy. *Pharm (Basel)* (2021) 14(7):682. doi: 10.3390/ph14070682
76. Pludowski P, Holick MF, Grant WB, Konstantynowicz J, Mascarenhas MR, Haq A, et al. Vitamin D Supplementation Guidelines. *J Steroid Biochem Mol Biol* (2018) 175:125–35. doi: 10.1016/j.jsbmb.2017.01.021
77. Lian L, Li XL, Xu MD, Li XM, Wu MY, Zhang Y, et al. VEGFR2 Promotes Tumorigenesis and Metastasis in a Pro-Angiogenic-Independent Way in Gastric Cancer. *BMC Cancer* (2019) 19(1):183. doi: 10.1186/s12885-019-5322-0
78. Zheng B, Zhou C, Qu G, Ren C, Yan P, Guo W, et al. VEGFR2 Promotes Metastasis and PD-L2 Expression of Human Osteosarcoma Cells by Activating the STAT3 and RhoA-ROCK-LIMK2 Pathways. *Front Oncol* (2020) 10:543562. doi: 10.3389/fonc.2020.543562
79. Pisacane AM, Risio M. VEGF and VEGFR-2 Immunohistochemistry in Human Melanocytic Naevi and Cutaneous Melanomas. *Melanoma Res* (2005) 15(1):39–43. doi: 10.1097/00008390-200502000-00007
80. Molhoek KR, Erdag G, Rasamny JK, Murphy C, Deacon D, Patterson JW, et al. VEGFR-2 Expression in Human Melanoma: Revised Assessment. *Int J Cancer* (2011) 129(12):2807–15. doi: 10.1002/ijc.25963
81. Seyed Jafari SM, Wiedmer C, Cazzaniga S, Frangež Ž, Shafighi M, Beltraminelli H, et al. Correlation of Vascular Endothelial Growth Factor Subtypes and Their Receptors With Melanoma Progression: A Next-Generation Tissue Microarray (ngTMA) Automated Analysis. *PloS One* (2018) 13(11):e0207019. doi: 10.1371/journal.pone.0207019

Conflict of Interest: The authors declare that the research was conducted in the absence of any commercial or financial relationships that could be construed as a potential conflict of interest.

Publisher's Note: All claims expressed in this article are solely those of the authors and do not necessarily represent those of their affiliated organizations, or those of the publisher, the editors and the reviewers. Any product that may be evaluated in this article, or claim that may be made by its manufacturer, is not guaranteed or endorsed by the publisher.

Copyright © 2021 Piotrowska, Beserra, Wierzbicka, Nowak and Żmijewski. This is an open-access article distributed under the terms of the Creative Commons Attribution License (CC BY). The use, distribution or reproduction in other forums is permitted, provided the original author(s) and the copyright owner(s) are credited and that the original publication in this journal is cited, in accordance with accepted academic practice. No use, distribution or reproduction is permitted which does not comply with these terms.

frontiers in Oncology

SYSTEMATIC REVIEW
published: 27 January 2022
doi: 10.3389/fonc.2022.817510

Predictive Values of Pathological and Clinical Risk Factors for Positivity of Sentinel Lymph Node Biopsy in Thin Melanoma: A Systematic Review and Meta-Analysis

Hanzi Huang[†], *Ziyao Fu*[†], *Jiang Ji*, *Jiuzuo Huang*[*] *and Xiao Long*[*]

Department of Plastic Surgery, Peking Union Medical College Hospital (PUMCH), Chinese Academy of Medical Sciences and Peking Union Medical College, Beijing, China

OPEN ACCESS

Edited by:
Sapna Patel,
University of Texas MD Anderson Cancer Center, United States

Reviewed by:
Andrzej T. Slominski,
University of Alabama at Birmingham, United States
Simone Ribero,
University of Turin, Italy

***Correspondence:**
Jiuzuo Huang
hjz1983@126.com
Xiao Long
pumclongxiao@126.com

[†]*These authors have contributed equally to this work and share first authorship*

Specialty section:
This article was submitted to Skin Cancer, a section of the journal Frontiers in Oncology

Received: *18 November 2021*
Accepted: *10 January 2022*
Published: *27 January 2022*

Citation:
Huang H, Fu Z, Ji J, Huang J and Long X (2022) Predictive Values of Pathological and Clinical Risk Factors for Positivity of Sentinel Lymph Node Biopsy in Thin Melanoma: A Systematic Review and Meta-Analysis. Front. Oncol. 12:817510. doi: 10.3389/fonc.2022.817510

Background: The indications for sentinel lymph node biopsy (SLNB) for thin melanoma are still unclear. This meta-analysis aims to determine the positive rate of SLNB in thin melanoma and to summarize the predictive value of different high-risk features for positive results of SLNB.

Methods: Four databases were searched for literature on SLNB performed in patients with thin melanoma published between January 2000 and December 2020. The overall positive rate and positive rate of each high-risk feature were calculated and obtained with 95% confidence intervals (CIs). Both unadjusted odds ratios (ORs) and adjusted ORs (AORs) of high-risk features were analyzed. Pooled effects were estimated using random-effects model meta-analyses.

Results: Sixty-six studies reporting 38,844 patients with thin melanoma who underwent SLNB met the inclusion criteria. The pooled positive rate of SLNB was 5.1% [95% confidence interval (CI) 4.9%-5.3%]. Features significantly predicted a positive result of SLNB were thickness≥0.8 mm [AOR 1.94 (95%CI 1.28-2.95); positive rate 7.0% (95%CI 6.0-8.0%)]; ulceration [AOR 3.09 (95%CI 1.75-5.44); positive rate 4.2% (95%CI 1.8-7.2%)]; mitosis rate >0/mm2 [AOR 1.63 (95%CI 1.13-2.36); positive rate 7.7% (95%CI 6.3-9.1%)]; microsatellites [OR 3.8 (95%CI 1.38-10.47); positive rate 16.6% (95%CI 2.4-36.6%)]; and vertical growth phase [OR 2.76 (95%CI 1.72-4.43); positive rate 8.1% (95%CI 6.3-10.1%)].

Conclusions: The overall positive rate of SLNB in thin melanoma was 5.1%. The strongest predictor for SLN positivity identified was microsatellites on unadjusted analysis and ulceration on adjusted analysis. Breslow thickness ≥0.8 mm and mitosis rate >0/mm^2 both predict SLN positivity in adjusted analysis and increase the positive rate to 7.0% and 7.7%. We suggest patients with thin melanoma with the above high-risk features should be considered for giving an SLNB.

Keywords: thin melanoma, sentinel lymph node biopsy, positive rate, ulceration, microsatellites, Breslow thickness, mitosis rate

INTRODUCTION

The incidence of melanoma has been increasing rapidly over the past few decades, with 100,350 new cases diagnosed in America in 2020, most of which are thin melanoma (T1, ≤1.0 mm) (1). Although thin melanomas have a relatively good prognosis with a 10-year survival rate of more than 95%, the absolute number of deaths is notable because of the volume of the disease (2).

To identify melanoma with a poor prognosis and provide more precise treatment, sentinel lymph node biopsy (SLNB) was proposed by surgeons. SLNB is generally considered appropriate for melanoma of T2 or thicker, but the indications for sentinel lymph node biopsy for thin melanoma are still controversial. The positive rate of SLNB for thin melanoma reported by previous studies is approximately 5% (3–5). In addition, SLNB carries a false negative rate of 12.5% (6) and several unwanted complications, including infection (2.9%), seroma (5.1%), hematoma (0.5%), lymphoedema (1.3%), and nerve injury (0.3%) (7).

It is critical to recognize thin melanoma with high-risk pathologic features and to reduce unnecessary invasive manipulation. The mainstream view is that SLNB should be performed in thin melanomas only if high-risk features are indicating SLNB positivity and worse prognosis, such as Breslow thickness >0.75 mm, ulceration, Clark level IV/V, and/or high mitotic rate (4, 8). The American Joint Committee on Cancer (AJCC) 8th edition of the guidelines for melanoma published in 2018 is currently in wide clinical use. T1 melanoma was reclassified into T1a (<0.8 mm) and T1b (0.8-1.0 mm, or any ulceration ≤1 mm) (9). According to the National Comprehensive Cancer Network (NCCN) guidelines of cutaneous melanoma, SLNB is recommended for T1b melanoma or T1a lesions with mitosis rate ≥2/mm^2, lymphovascular invasion, or other combination of risk factors (10). In the European consensus-based interdisciplinary guideline for melanoma, however, SLNB is recommended only for melanoma ≥0.8 mm with ulceration, mitosis rate ≥1/mm^2, microsatellites, or other risk factors (11).

The purpose of this meta-analysis was to determine the positive rate of SLNB in thin melanoma and to summarize the predictive value of different clinical and high-risk pathological features for positive results of SLNB.

METHODS

This meta-analysis followed and adhered to the Preferred Reporting Items for Systematic Reviews and Meta-Analyses guidelines.

Search Strategy

We searched literature published between January 2000 and December 2020 from the PubMed, Embase, Web of Science, and Cochrane Library databases. English articles with "melanoma", or "melanomas", and "sentinel lymph node biopsy", or "SLNB", or "SNB" were screened. Through reviewing the titles and abstracts of the retrieved literature, we selected potentially eligible studies preliminarily and further reviewed the full texts to determine whether they met the inclusion criteria. Two authors (HHZ & FZY) reviewed all literature obtained and examined whether each of them met the inclusion criteria.

To reduce potential bias due to the small sample size, we set the included criteria, which require a sample size for each study to be larger than 50. The inclusion criteria were as follows: including patients with a pathologic diagnosis of thin melanoma (Breslow thickness ≤1.0 mm) in the study; performing SLNB for >50 patients with thin melanoma, and reporting an SLN positivity rate. Reference lists of included articles and related literature were manually searched to complete the deficiency of computer search.

When multiple studies reported overlapping or duplicate patient sources, only the most recent and comprehensive study was included. Studies that did not report negative sentinel lymph nodes (SLNs) or included a single isolated high-risk pathologic feature were excluded. Case reports, literature reviews, commentaries, editorials, letters, and conference abstracts were also excluded.

Data Extraction and Quality Assessment

The following data were extracted from studies: 1) study information, including first author and publication year; 2) patient characteristics, including the number of SLNBs performed in patients with thin melanoma, clinical feature (primary tumor location), high-risk pathologic features [Breslow thickness, mitosis rate, Clark Level, ulceration, regression, microsatellites, vertical growth phase, tumor-infiltrating lymphocytes (TIL) and lymphovascular invasion (LVI)]; 3) outcomes, including the number of positive SLNs found in patients with thin melanoma and number of patients with thin melanoma reporting both positive SLN and high-risk features; 4) adjusted odds ratio (OR) for each high-risk pathologic feature if available.

Two authors (HHZ & FZY) used the Newcastle Ottawa Scale (NOS) to assess the risk of bias in the included studies. The NOS evaluates literature quality in three aspects: selection, comparability, and outcomes. The maximum score was 9, and a score greater than 6 is considered to indicate a low risk of bias.

Statistical Analysis

The primary outcome was the positive rate of SLNB in thin melanoma (Breslow thickness ≤ 1.0 mm), and the pooled effect was calculated and obtained with 95% confidence intervals (CIs). Forest plots were constructed to visually represent the results. The secondary outcomes were the predictive value of high-risk pathologic and clinical features for positive results of SLNB. Unadjusted ORs and adjusted ORs were pooled and analyzed using a random-effects model. Additionally, pooled positive rates of SLNB in patients with each pathologic feature were calculated. Heterogeneity among studies was calculated by the I^2 measure of inconsistency, and an I^2>50% indicated significant heterogeneity. The presence of publication bias was investigated visually using a funnel plot. Meta-analysis was performed by Stata/MP software (version 16.0 for Windows, StataCorp LLC, College Station, TX77845, USA).

RESULTS

Characteristics of Included Studies

The process of study selection is described in **Figure 1**. A total of 6424 articles were obtained through retrieval, and 66 of them met the inclusion criteria. All of the included studies were retrospective, reporting 38,844 patients with thin melanoma who underwent SLNB (**Table 1**) (8, 12–76). The number of included patients in each study ranged from 51 to 9186, with a median of 205. A total of 2117 (5.45%) positive SLN cases were found among all patients. Thirty-eight of the 66 included studies reported at least one high-risk pathologic feature that may be associated with SLN positivity. A median NOS score of 7 (range from 6 to 8) indicated that the risk of bias of the included studies was small. No study was excluded based on the NOS quality assessment. No significant publication bias among the included studies was found by funnel plot (**Figure 2**).

Outcomes

For the primary outcome, a pooled positive rate of SLNB was estimated by applying the random effect model, calculated as 5.1% (95% CI, 4.5% to 5.6%, **Figure 3**). Significant heterogeneity between studies was detected (I^2 = 73.6%, p<0.001). The unadjusted ORs and pooled positive rate of each high-risk pathologic and clinical feature for SLN positivity is shown in **Table 2**. Breslow thickness ≥0.8 mm, presence of ulceration, mitosis rate >0/mm^2, Clark level IV/V, and vertical growth phase showed a significant association with SLN positivity in unadjusted analysis. All of the above pathologic features showed a pooled positive rate higher than 5.1% except for the presence of ulceration. Notably, we found the presence of microsatellites to be most strongly associated with SLN positivity, with an unadjusted OR of 3.8 (95% CI, 1.38 to 10.47) and a pooled positive rate of 16.6% (95% CI, 2.4% to 36.6%).

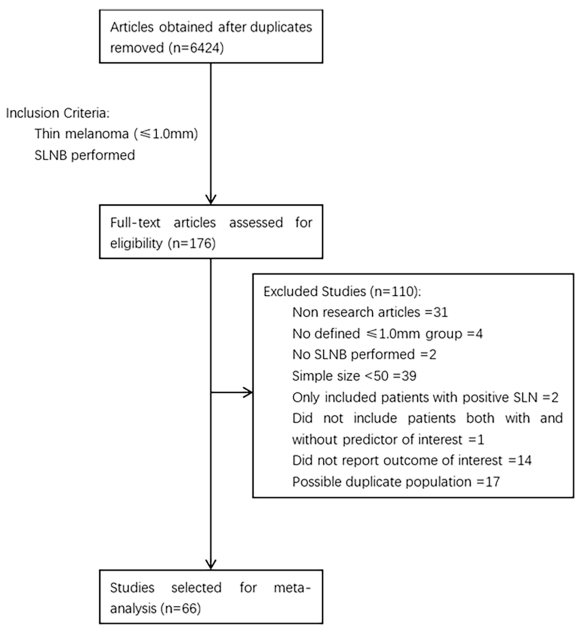


FIGURE 1 | Process study selection.

The adjusted ORs of pathologic features are shown in **Table 3**. There were only 11 studies that had adjusted OR data that could be analyzed. Pathologic features that were available for adjusted analysis were limited as the presence of ulceration, Breslow thickness ≥0.8 mm, mitosis rate >0/mm^2, Clark level IV/V, and the presence of regression. Breslow thickness ≥0.8 mm, presence of ulceration, mitosis rate >0/mm^2 showed a significant association with SLN positivity in the adjusted analysis, while Clark level IV/V did not show a significant correlation with SLN positivity. Among these, the presence of ulceration was the strongest predictor of positive SLNB results in the adjusted analysis, with an adjusted OR of 2.75 (95%CI, 1.65 to 4.60).

The associations between SLN positivity and the primary tumor location, the absence or presence of regression, LVI, or TIL were found with insufficient evidence.

DISCUSSION

It is critical to identify thin melanoma with a worse prognosis so that patients can be able to receive precise therapies. Researchers around the world have been interested in investigating an effective prediction for the prognosis of thin melanoma. Several pieces of research have been published in the past few years. This study is the most recent and most comprehensive meta-analysis to date. Compared with the previous meta-analysis, this study included 19 newly published research articles since 2015, reporting 26,308 patients in total who had a diagnosis of thin melanoma and underwent SLNB.

The pooled estimated positive rate of SLNB in thin melanoma in this study was 5.1%, with a 95% CI of 4.5% to 5.6%. This result is similar to those found in preexisting meta-analyses, which reported pooled positive rates of 5.6%, 4.5%, and 5.1% (3–5), but we got narrower confidence intervals. A 5% risk threshold is often used for surgeons suggesting to perform SLNB for a patient (37, 77). Generally, SLNB is offered to patients with primary melanoma with Breslow thickness ≥0.8 mm with additional risk factors. But different risk factors are recommended in different guidelines (10, 11). Therefore we analyzed the predictive value of multiple pathological and clinical features for the positive SLN.

In this study, we not only updated the predictive value of pathologic features explored in the previous meta-analysis but also paid attention to primary tumor location, which was reported to be correlated with a positive SLN (34). We yielded some different results. Ulceration, Clark level, and Breslow thickness were commonly recorded features in patients, reporting in 37.9%, 36.4%, and 34.8% of included studies, respectively. In the unadjusted analysis in our study, we recognized the same significant predictors as the previous meta-analysis and the primary tumor location was not significantly related to SLN positivity. And in the adjusted analysis in our study, however, the presence of ulceration was

TABLE 1 | Characteristic of the 66 included studies.

Study	Year	Total No. of thin melanoma patients undergoing SLNB	Total No. of thin melanoma patients with positive SLN (%)	High-risk features reported	Risk of bias Score (NOS) (Max=9)
Theile et al. (12)	2020	240	14 (5.8%)	Thickness, ulceration	6
Skochdopole et al. (13)	2020	4332	229 (5.3%)	Thickness	6
Kocsis et al. (14)	2020	78	9 (11.5%)	Ulceration, regression	7
Hu et al. (15)	2020	238	19 (8.0%)	Nil	7
Antonialli et al. (16)	2020	399	27 (6.8%)	Nil	7
Tejera-Vaquerizo et al. (17)	2019	1083	73 (6.7%)	Nil	8
Santos et al. (18)	2019	137	10 (7.3%)	Thickness, ulceration, MR, TIL, regression, CL, microsatellites	8
Piazzalunga et al. (19)	2019	1272	76 (6.0%)	Thickness, ulceration, MR, CL	7
Conic et al. (8)	2019	9186	457 (5.0%)	thickness, ulceration, MR, regression, CL	8
Verver et al. (20)	2018	1607	115 (7.2%)	Nil	7
Stiegel et al. (21)	2018	326	25 (7.7%)	Nil	8
Nguyen et al. (22)	2018	142	7 (4.9%)	Nil	6
Isaksson et al. (23)	2018	1038	49 (4.7%)	Thickness, ulceration, MR	6
Herbert et al. (24)	2018	1129	49 (4.3%)	thickness	7
Tejera-Vaquerizo et al. (25)	2017	203	14 (6.9%)	MR, regression, microsatellites	7
Joyce et al. (26)	2017	65	1 (1.5%)	Thickness, ulceration	8
Wat et al. (27)	2016	171	15 (8.8%)	MR	7
Rubinstein et al. (28)	2016	252	6 (2.4%)	Nil	8
Hieken et al. (29)	2015	4410	283 (6.4%)	Nil	7
Voit et al. (30)	2014	288	15 (5.2%)	Nil	7
Mitteldorf et al. (31)	2014	207	38 (18.4%)	Thickness, ulceration, MR, regression, CL	7.5
Bartlett et al. (32)	2014	781	29 (3.7%)	Thickness, ulceration, MR, TIL, regression, CL, LVI, microsatellites	6.5
Balch et al. (33)	2014	1213	73 (6.0%)	Nil	6
Venna et al. (34)	2013	484	34 (7.0%)	Thickness, ulceration, MR, TIL, CL, LVI	6
van den Broek et al. (35)	2013	61	0 (0.0%)	Nil	6
Mozzillo et al. (36)	2013	492	24 (4.9%)	Ulceration, MR	8
Han et al. (37)	2013	1250	65 (5.2%)	Thickness, ulceration, MR, TIL, regression, CL, LVI, VGP	7.5
Cooper et al. (38)	2013	189	3 (1.6%)	Ulceration, MR, CL	7
Chu et al. (39)	2013	106	3 (2.8%)	Ulceration, MR, CL	8
Ponti et al. (40)	2012	286	3 (1.0%)	Nil	6
Murali et al. (41)	2012	432	29 (6.7%)	Thickness, ulceration, MR, CL, LVI, microsatellites	7
Koshenkov et al. (42)	2012	72	6 (8.3%)	Ulceration, CL	6
Hinz et al. (43)	2012	121	5 (4.1%)	Thickness, ulceration, CL	8
Han et al. (44)	2012	271	22 (8.1%)	Thickness, ulceration, MR, TIL, regression, CL, VGP	7
Elsaesser et al. (45)	2012	212	2 (0.9%)	Nil	7
Yonick et al. (46)	2011	147	16 (10.9%)	Nil	6
Lowe et al. (47)	2011	260	9 (3.5%)	Nil	7

(Continued)

TABLE 1 | Continued

Study	Year	Total No. of thin melanoma patients undergoing SLNB	Total No. of thin melanoma patients with positive SLN (%)	High-risk features reported	Risk of bias Score (NOS) (Max=9)
Vermeeren et al. (48)	2010	78	5 (6.4%)	Thickness, ulceration, CL	7
Socrier et al. (49)	2010	68	9 (13.2%)	Regression	6.5
Santillan et al. (50)	2010	72	5 (6.9%)	Nil	7
Mitra et al. (51)	2010	320	24 (7.5%)	Nil	6
Kunte et al. (52)	2010	147	11 (7.5%)	Thickness	7
Ellis et al. (53)	2010	105	2 (1.9%)	Nil	7
Testori et al. (54)	2009	358	4 (1.1%)	Nil	7
Wright et al. (55)	2008	631	31 (4.9%)	Thickness, ulceration, CL	6.5
Roulin et al. (56)	2008	51	3 (5.9%)	CL	7
Kaur et al. (57)	2008	62	2 (3.2%)	Regression	7.5
Starz and Balda (58)	2007	87	10 (11.5%)	Nil	6.5
Koskivuo et al. (59)	2007	141	5 (3.5%)	Nil	7
Vaquerano et al. (60)	2006	91	6 (6.6%)	Nil	7
Ranieri et al. (61)	2006	184	12 (6.5%)	Thickness, ulceration, regression, CL, VGP	7
Nowecki et al. (62)	2006	260	17 (6.5%)	Nil	7
Karakousis et al. (63)	2006	882	38 (4.3%)	Thickness, ulceration, MR, regression, CL, VGP	8
Hershko et al. (64)	2006	64	5 (7.8%)	CL	7
Cascinelli et al. (65)	2006	145	6 (4.1%)	Nil	7
Rex et al. (66)	2005	73	3 (4.1%)	Nil	7
Puleo et al. (67)	2005	409	20 (4.9%)	CL	7
Kesmodel et al. (68)	2005	181	9 (5.0%)	Thickness, ulceration, MR, CL	7
Stitzenberg et al. (69)	2004	146	6 (4.1%)	Ulceration, regression, CL	6
Borgognoni et al. (70)	2004	114	2 (1.8%)	Nil	7
Rousseau et al. (71)	2003	388	4 (1.0%)	Nil	6
Oliveira Filho et al. (72)	2003	77	6 (7.8%)	Ulceration, regression, CL, VGP	7
Jacobs et al. (73)	2003	63	2 (3.2%)	CL	6
Bleicher et al. (74)	2003	272	8 (2.9%)	Thickness	6
Agnese et al. (75)	2003	91	1 (1.1%)	Nil	7
Statius Muller et al. (76)	2001	104	7 (6.7%)	Thickness	7

SLNB, sentinel lymph node biopsy; CL, Clark level; MR, mitotic rate; TIL, tumor-infiltrating lymphocytes; VGP, vertical growth phase; LVI, lymphovascular invasion; PTL, primary tumor location.

the most predictive factor for SLN positivity, while Clark level IV/V did not show a significant correlation with SLN positivity.

A limitation of the previous meta-analysis is the relatively small sample size of included studies. Only one study provided the data on the pathologic features of patients with a sample size larger than 1,000 for analysis. Several large-scale studies were published after 2015 which supplemented the insufficiency of the previous meta-analysis in the adjusted odds ratios analyses. In our study, 6 pieces of literature with a sample size larger than 1,000 were included. The largest one is the study of Conic, et al. published in 2019 with a sample size of 9,186, and it provided data on pathologic features that are available for both unadjusted and adjusted OR analyzing. Thus, we could obtain more accurate predictive values of pathologic and clinical features for SLN positivity. And the 95% CIs of unadjusted ORs for all features analyzed in our study were narrower than those reported in the previous meta-analysis.

The presence of microsatellites was recognized to have a 3.8-fold higher risk and positive rate of 16.6% for SLN positivity in our study, which means it is the strongest predictor among the

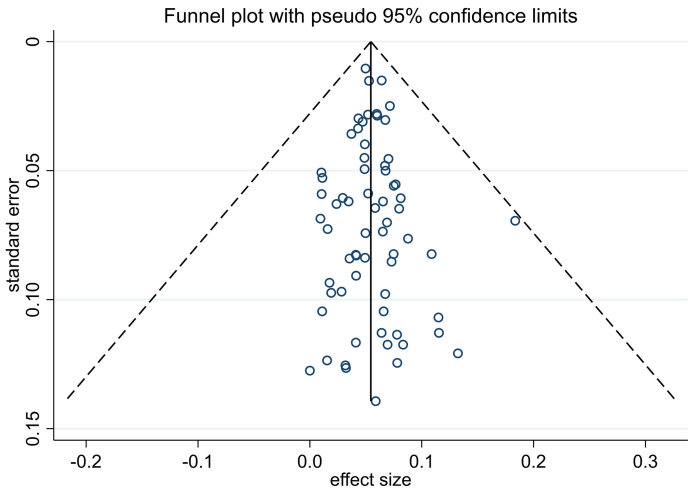


FIGURE 2 | Funnel plot of included studies.

pathologic features we analyzed. Microsatellites are a rarely present pathologic feature associated with poor prognosis and are more likely found in thicker melanoma (78). Four studies in our meta-analysis including 1411 patients with thin melanoma reported data on microsatellites (18, 25, 32, 41). Two of them demonstrated a remarkable increase in SLN positive rate when microsatellites were present, but none of the four studies found it statistically significant because of the infrequence of events.

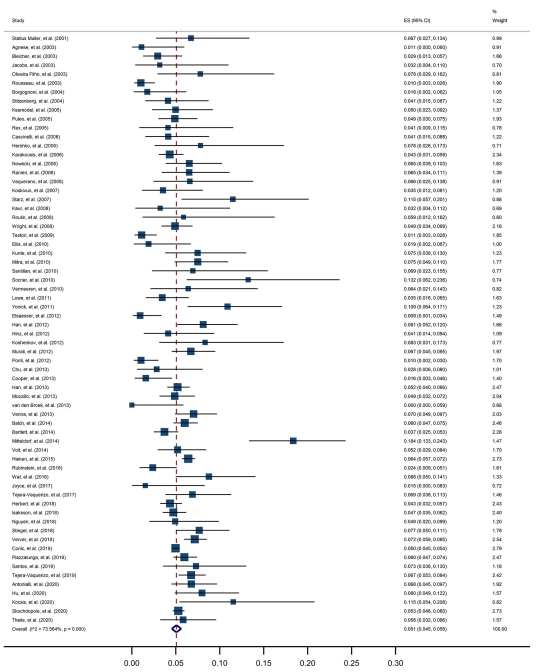


FIGURE 3 | Meta-analysis of sentinel lymph node biopsy positivity in thin melanoma.

Adjusted analysis for microsatellites was not available because relevant researches were too few. And it is the same reason why the adjusted analysis was not done for the vertical growth phase. Regression in primary melanoma has been reported as a protective factor that relates to lower SLN positivity (79) and lower risk of death (80). A host immunologic response to the tumor is considered to play a role in the presence of regression. However, regression did not show significance relativity of SLN positivity in unadjusted analysis nor adjusted analysis in this study.

The pooled positive rate of SLNB in thin melanoma in this study was 5.1%. When patients were confirmed with melanomas of Breslow thickness ≥0.8 mm or mitosis rate >0/mm^2, the pooled positive rate of SLNB would rise to 7.0% and 7.7%, respectively. Therefore, we suggest that surgeons should consider giving SLNB to such patients. And when a combination of high-risk features is found, the patient should be informed of the even higher rate of SLN positivity.

Our study has some limitations. All studies performed SLNB only in patients with thin melanoma when there was any high-risk feature; therefore, the overall positive rate of SLNB was undoubtedly higher than the true incidence of SLN positivity in all thin melanomas. Significant heterogeneity among the included studies (I^2 = 73.6%, p<0.001) was found using a weight estimated random-effects model in the meta-analysis. This probably resulted from several included studies with a higher proportion of positive SLNs. The reporting of identical pathologic features, such as mitosis rate, differed in some of the included studies by defining different cutoff values. This may lead to bias in analyzing its odds ratio. Since this meta-analysis was based on the study level, this variation could also increase the heterogeneity. A patient-level meta-analysis may help to avoid this variation and assess adjusted ORs for more pathologic features. For pathologic features such as microsatellites and the vertical growth phase, more research is needed to clarify their predictive value with larger data sets. Besides the risk factors

TABLE 2 | Predictive value of high-risk pathologic and clinical features for sentinel lymph node biopsy positivity.

Predictor	No. of studies	No. of thin melanoma patients undergoing SLNB	No. of thin melanoma patients with positive SLN	No. of patients with positive SLN and predictor	Unadusted Odds Ratio (95%CI)	Pooled Positive Rate (95%CI) (%)
Breslow thickness <0.8mm	23	23426	1228	469	–	2.9 (2.1–3.7)
Breslow thickness ≥0.8mm	23	23426	1228	759	1.61 (1.42–1.82)	7.0 (6.0–8.0)
Ulceration	25	17768	1108	115	1.60 (1.30–1.97)	4.2 (1.8–7.2)
Regression	14	11065	585	119	0.89 (0.72–1.11)	5.2 (2.9–8.1)
Clark Level IV/V	24	15198	803	421	1.68 (1.45–1.95)	6.6 (5.7–7.6)
Mitosis Rate >0/mm^2	18	15002	801	584	2.22 (1.88–2.63)	7.7 (6.3–9.1)
Tumor-infiltrating Lymphocytes	5	1613	91	51	0.69 (0.43–1.10)	4.3 (2.5–6.5)
Lymphovascular Invasion	4	1973	119	6	2.39 (1.00–5.75)	12.9 (0–37.4)
Microsatellites	4	1411	77	5	3.80 (1.38–10.47)	16.6 (2.4–36.6)
Vertical Growth Phase	5	1821	112	91	2.76 (1.72–4.43)	8.1 (6.3–10.1)
Primary Tumor Location (trunk vs others)	20	17345	1025	432	1.10 (0.96–1.26)	6.2 (4.5–8.2)
Primary Tumor Location (extremities vs others)	20	17345	1025	457	0.98 (0.86–1.12)	6.4 (4.4–8.7)

TABLE 3 | Pooled adjusted odds ratio of high-risk pathologic features.

Predictor	No. of studies	No. of thin melanoma patients undergoing SLNB	Adjusted Odds Ratio	95%CI
Ulceration	8	14003	2.75	1.65–4.60
Breslow thickness ≥0.8mm	10	19381	1.94	1.28–2.95
Mitosis Rate >0/mm^2	8	12101	1.63	1.13–2.36
Clark Level IV/V	9	11924	1.24	0.84–1.84
Regression	7	9881	1.20	0.89–1.63

analyzed in this study, there are other factors that affect the prognosis of melanoma. Melanin pigmentation plays a role in regulating melanocyte and neighboring cells' behavior (81). It protects melanocytes from UVR but at times accelerates the progression of melanoma and makes melanocytes resistant to different types of therapy (82–84). And as a result, melanin pigmentation shortens overall survival and disease-free survival in metastatic melanoma (82). However, no study has reported the relationship between melanin pigmentation and a positive sentinel lymph node. We look forward to future researches.

CONCLUSION

The overall positive rate of SLNB in thin melanoma in this study was 5.1%. The strongest predictor for SLN positivity identified was the presence of microsatellites on unadjusted analysis and the presence of ulceration on adjusted analysis. Breslow thickness ≥0.8 mm and mitosis rate >0/mm^2 both predict SLN positivity in adjusted analysis and increase the positive rate to 7.0% and 7.7%. We suggest patients with thin melanoma with the above high-risk features should be considered for giving an SLNB.

DATA AVAILABILITY STATEMENT

The original contributions presented in the study are included in the article/supplementary material. Further inquiries can be directed to the corresponding authors.

AUTHOR CONTRIBUTIONS

JH and XL contributed to conception and design of the study. ZF and HH performed articles review and quality assessments. HH performed the data analyses and wrote the first draft of manuscript. JJ, ZF, and HH wrote sections of the manuscript. JJ, JH, and XL helped perform the analysis with constructive discussions. All authors contributed to manuscript revision, read, and approved the submitted version.

REFERENCES

1. Siegel RL, Miller KD, Jemal A. Cancer Statistics 2020. *CA Cancer J Clin* (2020) 70(1):7–30. doi: 10.3322/caac.21590
2. Landow SM, Gjelsvik A, Weinstock MA. Mortality Burden and Prognosis of Thin Melanomas Overall and by Subcategory of Thickness, SEER Registry Data 1992-2013. *J Am Acad Dermatol* (2017) 76(2):258–63. doi: 10.1016/j.jaad.2016.10.018
3. Warycha MA, Zakrzewski J, Ni QH, Shapiro RL, Berman RS, Pavlick AC, et al. Meta-Analysis of Sentinel Lymph Node Positivity in Thin Melanoma (<= 1 Mm). *Cancer* (2009) 115(4):869–79. doi: 10.1002/cncr.24044

4. Cordeiro E, Gervais MK, Shah PS, Look Hong NJ, Wright FC. Sentinel Lymph Node Biopsy in Thin Cutaneous Melanoma: A Systematic Review and Meta-Analysis. *Ann Surg Oncol* (2016) 23(13):4178–88. doi: 10.1245/s10434-016-5137-z
5. Appleton SE, Fadel Z, Williams JS, Bezuhly M. Vertical Growth Phase as a Prognostic Factor for Sentinel Lymph Node Positivity in Thin Melanomas: A Systematic Review and Meta-Analysis. *Plast Reconstr Surg* (2018) 141 (6):1529–40. doi: 10.1097/prs.0000000000004395
6. Valsecchi ME, Silbermins D, de Rosa N, Wong SL, Lyman GH. Lymphatic Mapping and Sentinel Lymph Node Biopsy in Patients With Melanoma: A Meta-Analysis. *J Clin Oncol* (2011) 29(11):1479–87. doi: 10.1200/jco.2010.33.1884
7. Moody JA, Ali RF, Carbone AC, Singh S, Hardwicke JT. Complications of Sentinel Lymph Node Biopsy for Melanoma - A Systematic Review of the Literature. *Eur J Surg Oncol* (2017) 43(2):270–7. doi: 10.1016/j.ejso.2016.06.407
8. Conic RRZ, Ko J, Damiani G, Funchain P, Knackstedt T, Vij A, et al. Predictors of Sentinel Lymph Node Positivity in Thin Melanoma Using the National Cancer Database. *J Am Acad Dermatol* (2019) 80(2):441–7. doi: 10.1016/j.jaad.2018.08.051
9. Gershenwald JE, Scolyer RA. Melanoma Staging: American Joint Committee on Cancer (AJCC) 8th Edition and Beyond. *Ann Surg Oncol* (2018) 25 (8):2105–10. doi: 10.1245/s10434-018-6513-7
10. Coit DG, Thompson JA, Albertini MR, Barker C, Carson WE, Contreras C, et al. Cutaneous Melanoma, Version 2.2019, NCCN Clinical Practice Guidelines in Oncology. *J Natl Compr Canc Netw* (2019) 17(4):367–402. doi: 10.6004/jnccn.2019.0018
11. Garbe C, Amaral T, Peris K, Hauschild A, Arenberger P, Bastholt L, et al. European Consensus-Based Interdisciplinary Guideline for Melanoma. Part 2: Treatment - Update 2019. *Eur J Cancer* (2020) 126:159–77. doi: 10.1016/j.ejca.2019.11.015
12. Theile H, Moore J, Dunn N, Cossio D, Forristal CE, Green AC, et al. Regional Nodal Metastasis and 5-Year Survival in Patients With Thin Melanoma in Queensland: A Population-Based Study. *ANZ J Surg* (2020) 90(4):503–7. doi: 10.1111/ans.15804
13. Skochdopole AJ, Kutlu OC, Engelhardt KE, Lancaster WP, Abbott AM, Camp ER. High Mitotic Rate Predicts Sentinel Lymph Node Involvement in Thin Melanomas. *J Surg Res* (2020) 256:198–205. doi: 10.1016/j.jss.2020.06.045
14. Kocsis A, Karsko L, Kurgyis Z, Besenyi Z, Pavics L, Dosa-Racz E, et al. Is it Necessary to Perform Sentinel Lymph Node Biopsy in Thin Melanoma? A Retrospective Single Center Analysis. *Pathol Oncol Res* (2020) 26(3):1861–8. doi: 10.1007/s12253-019-00769-z
15. Hu Y, Briggs A, Gennarelli RL, Bartlett EK, Ariyan CE, Coit DG, et al. Sentinel Lymph Node Biopsy for T1b Melanoma: Balancing Prognostic Value and Cost. *Ann Surg Oncol* (2020) 27(13):5248–56. doi: 10.1245/s10434-020-08558-8
16. Antonialli AZ, Bertolli E, de Macedo MP, Pinto CAL, Calsavara VF, Neto JPD. How Does the Mitotic Index Impact Patients With T1 Melanoma? Comparison Between the 7th and 8th Edition of the American Joint Committee on Cancer Melanoma Staging System. *Bras Dermatol* (2020) 95 (6):691–5. doi: 10.1016/j.abd.2020.03.020
17. Tejera-Vaquerizo A, Ribero S, Puig S, Boada A, Paradela S, Moreno-Ramírez D, et al. Survival Analysis and Sentinel Lymph Node Status in Thin Cutaneous Melanoma: A Multicenter Observational Study. *Cancer Med* (2019) 8 (9):4235–44. doi: 10.1002/cam4.2358
18. Santos FMD, Silva FCD, Pedron J, Furian RD, Fortes C, Bonamigo RR. Association Between Tumor-Infiltrating Lymphocytes and Sentinel Lymph Node Positivity in Thin Melanoma. *Bras Dermatol* (2019) 94(1):47–51. doi: 10.1590/abd1806-4841.20197414
19. Piazzalunga D, Ceresoli M, Allievi N, Ribero S, Quaglino P, Di Lorenzo S, et al. Can Sentinel Node Biopsy be Safely Omitted in Thin Melanoma? Risk Factor Analysis of 1272 Multicenter Prospective Cases. *Eur J Surg Oncol* (2019) 45 (5):820–4. doi: 10.1016/j.ejso.2018.11.022
20. Verver D, Louwman WJ, Koljenović S, Verhoef C, Grünhagen DJ, van Akkooi ACJ. Improved Stratification of Pt1 Melanoma According to the 8th American Joint Committee on Cancer Staging Edition Criteria: A Dutch Population-Based Study. *Eur J Cancer* (2018) 92:100–7. doi: 10.1016/j.ejca.2017.10.031
21. Stiegel E, Xiong D, Ya J, Funchain P, Isakov R, Gastman B, et al. Prognostic Value of Sentinel Lymph Node Biopsy According to Breslow Thickness for Cutaneous Melanoma. *J Am Acad Dermatol* (2018) 78(5):942–8. doi: 10.1016/j.jaad.2018.01.030
22. Nguyen B, Karia PS, Hills VM, Besaw RJ, Schmults CD. Impact of National Comprehensive Cancer Network Guidelines on Case Selection and Outcomes for Sentine Lymph Node Biopsy in Thin Melanoma. *Dermatol Surg* (2018) 44 (4):493–501. doi: 10.1097/DSS.0000000000001369
23. Isaksson K, Nielsen K, Mikiver R, Nieweg OE, Scolyer RA, Thompson JF, et al. Sentinel Lymph Node Biopsy in Patients With Thin Melanomas: Frequency and Predictors of Metastasis Based on Analysis of Two Large International Cohorts. *J Surg Oncol* (2018) 118(4):599–605. doi: 10.1002/jso.25208
24. Herbert G, Karakousis GC, Bartlett EK, Zaheer S, Graham D, Czerniecki BJ, et al. Transected Thin Melanoma: Implications for Sentinel Lymph Node Staging. *J Surg Oncol* (2018) 117(4):567–71. doi: 10.1002/jso.24930
25. Tejera-Vaquerizo A, Pérez-Cabello G, Marínez-Leborans L, Gallego E, Oliver-Martínez V, Martín-Cuevas P, et al. Is Mitotic Rate Still Useful in the Management of Patients With Thin Melanoma? *J Eur Acad Dermatol Venereol* (2017) 31(12):2025–9. doi: 10.1111/jdv.14485
26. Joyce KM, McInerney NM, Piggott RP, Martin F, Jones DM, Hussey AJ, et al. Analysis of Sentinel Node Positivity in Primary Cutaneous Melanoma: An 8-Year Single Institution Experience. *Ir J Med Sci* (2017) 186(4):847–53. doi: 10.1007/s11845-017-1559-2
27. Wat H, Senthilselvan A, Salopek TG. A Retrospective, Multicenter Analysis of the Predictive Value of Mitotic Rate for Sentinel Lymph Node (SLN) Positivity in Thin Melanomas. *J Am Acad Dermatol* (2016) 74(1):94–101. doi: 10.1016/j.jaad.2015.09.014
28. Rubinstein JC, Han G, Jackson L, Bulloch K, Ariyan S, Narayan D, et al. Regression in Thin Melanoma Is Associated With Nodal Recurrence After a Negative Sentinel Node Biopsy. *Cancer Med* (2016) 5(10):2832–40. doi: 10.1002/cam4.922
29. Hieken TJ, Grotz TE, Comfere NI, Inselman JW, Habermann EB. The Effect of the AJCC 7th Edition Change in T1 Melanoma Substaging on National Utilization and Outcomes of Sentinel Lymph Node Biopsy for Thin Melanoma. *Melanoma Res* (2015) 25(2):157–63. doi: 10.1097/cmr.0000000000000143
30. Voit CA, Gooskens SLM, Siegel P, Schaefer G, Schoengen A, Röwert J, et al. Ultrasound-Guided Fine Needle Aspiration Cytology as an Addendum to Sentinel Lymph Node Biopsy can Perfect the Staging Strategy in Melanoma Patients. *Eur J Cancer* (2014) 50(13):2280–8. doi: 10.1016/j.ejca.2014.05.027
31. Mitteldorf C, Bertsch HP, Jung K, Thoms KM, Schön MP, Tronnier M, et al. Sentinel Node Biopsy Improves Prognostic Stratification in Patients With Thin (Pt1) Melanomas and an Additional Risk Factor. *Ann Surg Oncol* (2014) 21(7):2252–8. doi: 10.1245/s10434-014-3641-6
32. Bartlett EK, Gimotty PA, Sinnamon AJ, Wachtel H, Roses RE, Schuchter L, et al. Clark Level Risk Stratifies Patients With Mitogenic Thin Melanomas for Sentinel Lymph Node Biopsy. *Ann Surg Oncol* (2014) 21(2):643–9. doi: 10.1245/s10434-013-3313-y
33. Balch CM, Thompson JF, Gershenwald JE, Soong SJ, Ding S, McMasters KM, et al. Age as a Predictor of Sentinel Node Metastasis Among Patients With Localized Melanoma: An Inverse Correlation of Melanoma Mortality and Incidence of Sentinel Node Metastasis Among Young and Old Patients. *Ann Surg Oncol* (2014) 21(4):1075–81. doi: 10.1245/s10434-013-3464-x
34. Venna SS, Thummala S, Nosrati M, Leong SP, Miller JR3rd, Sagebiel RW, et al. Analysis of Sentinel Lymph Node Positivity in Patients With Thin Primary Melanoma. *J Am Acad Dermatol* (2013) 68(4):560–7. doi: 10.1016/j.jaad.2012.08.045
35. van den Broek FJ, Sloots PC, de Waard JWD, Roumen RM. Sentinel Lymph Node Biopsy for Cutaneous Melanoma: Results of 10 Years' Experience in Two Regional Training Hospitals in the Netherlands. *Int J Clin Oncol* (2013) 18(3):428–34. doi: 10.1007/s10147-012-0399-3
36. Mozzillo N, Pennacchioli E, Gandini S, Caracò C, Crispo A, Botti G, et al. Sentinel Node Biopsy in Thin and Thick Melanoma. *Ann Surg Oncol* (2013) 20(8):2780–6. doi: 10.1245/s10434-012-2826-0
37. Han DL, Zager JS, Shyr Y, Chen HD, Berry LD, Iyengar S, et al. Clinicopathologic Predictors of Sentinel Lymph Node Metastasis in Thin Melanoma. *J Clin Oncol* (2013) 31(35):4387–93. doi: 10.1200/JCO.2013.50.1114

38. Cooper C, Wayne JD, Damstetter EM, Martini M, Gordon J, Guitart J, et al. A 10-Year, Single-Institution Analysis of Clinicopathologic Features and Sentinel Lymph Node Biopsy in Thin Melanomas. *J Am Acad Dermatol* (2013) 69(5):693–9. doi: 10.1016/j.jaad.2013.07.016
39. Chu VH, Tetzlaff MT, Torres-Cabala CA, Prieto VG, Bassett R, Gershenwald JE, et al. Impact of the 2009 (7th Edition) AJCC Melanoma Staging System in the Classification of Thin Cutaneous Melanomas. *BioMed Res Int* (2013) 2013:898719. doi: 10.1155/2013/898719
40. Ponti G, Pollio A, Cesinaro AM, Pellacani G, Magnoni C, Seidenari S. Value and Prognostic Significance of Mitotic Rate in a Retrospective Series of Pt1 Cutaneous Malignant Melanoma Patients. *Cancer Epidemiol* (2012) 36 (3):303–5. doi: 10.1016/j.canep.2011.11.003
41. Murali R, Haydu LE, Quinn MJ, Saw RPM, Shannon K, Spillane AJ, et al. Sentinel Lymph Node Biopsy in Patients With Thin Primary Cutaneous Melanoma. *Ann Surg* (2012) 255(1):128–33. doi: 10.1097/SLA.0b013e3182306c72
42. Koshenkov VP, Shulkin D, Bustami R, Chevinsky AH, Whitman ED. Role of Sentinel Lymphadenectomy in Thin Cutaneous Melanomas With Positive Deep Margins on Initial Biopsy. *J Surg Oncol* (2012) 106(4):363–8. doi: 10.1002/jso.23093
43. Hinz T, Ahmadzadehfar H, Wierzbicki A, Höller T, Wenzel J, Biersack HJ, et al. Prognostic Value of Sentinel Lymph Node Biopsy in 121 Low-Risk Melanomas (Tumour Thickness <1.00 Mm) on the Basis of a Long-Term Follow-Up. *Eur J Nucl Med Mol Imaging* (2012) 39(4):581–8. doi: 10.1007/s00259-011-2009-4
44. Han D, Yu DH, Zhao XH, Marzban SS, Messina JL, Gonzalez RJ, et al. Sentinel Node Biopsy Is Indicated for Thin Melanomas >= 0.76 Mm. *Ann Surg Oncol* (2012) 19(11):3335–42. doi: 10.1245/s10434-012-2469-1
45. Elsaesser O, Leiter U, Buettner PG, Eigentler TK, Meier F, Weide B, et al. Prognosis of Sentinel Node Staged Patients With Primary Cutaneous Melanoma. *PLoS One* (2012) 7(1):e29791. doi: 10.1371/journal.pone.0029791
46. Yonick DV, Ballo RM, Kahn E, Dahiya M, Yao K, Godellas C, et al. Predictors of Positive Sentinel Lymph Node in Thin Melanoma. *Am J Surg* (2011) 201 (3):324–327; discussion 327-328. doi: 10.1016/j.amjsurg.2010.09.011
47. Lowe M, Hill N, Page A, Chen S, Delman KA. The Impact of Shave Biopsy on the Management of Patients With Thin Melanomas. *Am Surg* (2011) 77 (8):1050–3. doi: 10.1177/000313481107700826
48. Vermeeren L, van der Ent F, Sastrowijoto P, Hulsewé K. Sentinel Lymph Node Biopsy in Patients With Thin Melanoma: Occurrence of Nodal Metastases and its Prognostic Value. *Eur J Dermatol* (2010) 20(1):30–4. doi: 10.1684/ejd.2010.0837
49. Socrier Y, Lauwers-Cances V, Lamant L, Garrido I, Lauwers F, Lopez R, et al. Histological Regression in Primary Melanoma: Not a Predictor of Sentinel Lymph Node Metastasis in a Cohort of 397 Patients. *Br J Dermatol* (2010) 162 (4):830–4. doi: 10.1111/j.1365-2133.2009.09606.x
50. Santillan AA, Messina JL, Marzban SS, Crespo G, Sondak VK, Zager JS. Pathology Review of Thin Melanoma and Melanoma in Situ in a Multidisciplinary Melanoma Clinic: Impact on Treatment Decisions. *J Clin Oncol* (2010) 28(3):481–6. doi: 10.1200/jco.2009.24.7734
51. Mitra A, Conway C, Walker C, Cook M, Powell B, Lobo S, et al. Melanoma Sentinel Node Biopsy and Prediction Models for Relapse and Overall Survival. *Br J Cancer* (2010) 103(8):1229–36. doi: 10.1038/sj.bjc.6605849
52. Kunte C, Geimer T, Baumert J, Konz B, Volkenandt M, Flaig M, et al. Prognostic Factors Associated With Sentinel Lymph Node Positivity and Effect of Sentinel Status on Survival: An Analysis of 1049 Patients With Cutaneous Melanoma. *Melanoma Res* (2010) 20(4):330–7. doi: 10.1097/CMR.0b013e32833ba9ff
53. Ellis MC, Weerasinghe R, Corless CL, Vetto JT. Sentinel Lymph Node Staging of Cutaneous Melanoma: Predictors and Outcomes. *Am J Surg* (2010) 199 (5):663–8. doi: 10.1016/j.amjsurg.2010.01.019
54. Testori A, De Salvo GL, Montesco MC, Trifirò G, Mocellin S, Landi G, et al. Clinical Considerations on Sentinel Node Biopsy in Melanoma From an Italian Multicentric Study on 1,313 Patients (SOLISM-IMI). *Ann Surg Oncol* (2009) 16(7):2018–27. doi: 10.1245/s10434-008-0273-8
55. Wright BE, Scheri RP, Ye X, Faries MD, Turner RR, Essner R, et al. Importance of Sentinel Lymph Node Biopsy in Patients With Thin Melanoma. *Arch Surg* (2008) 143(9):892–9. doi: 10.1001/archsurg.143.9.892
56. Roulin D, Matter M, Bady P, Liénard D, Gugerli O, Boubaker A, et al. Prognostic Value of Sentinel Node Biopsy in 327 Prospective Melanoma Patients From a Single Institution. *Eur J Surg Oncol* (2008) 34(6):673–9. doi: 10.1016/j.ejso.2007.07.197
57. Kaur C, Thomas RJ, Desai N, Green MA, Lovell D, Powell BWEM, et al. The Correlation of Regression in Primary Melanoma With Sentinel Lymph Node Status. *J Clin Pathol* (2008) 61(3):297–300. doi: 10.1136/jcp.2007.049411
58. Starz H, Balda BR. Benefit of Sentinel Lymphadenectomy for Patients With Nonulcerated Cutaneous Melanomas in the Breslow Range Between 0.76 and 1 Mm: A Follow-Up Study of 148 Patients. *Int J Cancer* (2007) 121(3):689–93. doi: 10.1002/ijc.22707
59. Koskivuo I, Talve L, Vihinen P, Mäki M, Vahlberg T, Suominen E. Sentinel Lymph Node Biopsy in Cutaneous Melanoma: A Case-Control Study. *Ann Surg Oncol* (2007) 14(12):3566–74. doi: 10.1245/s10434-007-9606-2
60. Vaquerano J, Kraybill WG, Driscoll DL, Cheney R, Kane JM3rd. American Joint Committee on Cancer Clinical Stage as a Selection Criterion for Sentinel Lymph Node Biopsy in Thin Melanoma. *Ann Surg Oncol* (2006) 13(2):198–204. doi: 10.1245/aso.2006.03.092
61. Ranieri JM, Wagner JD, Wenck S, Johnson CS, Coleman JJ3rd. The Prognostic Importance of Sentinel Lymph Node Biopsy in Thin Melanoma. *Ann Surg Oncol* (2006) 13(7):927–32. doi: 10.1245/aso.2006.04.023
62. Nowecki ZI, Rutkowski P, Nasierowska-Guttmejer A, Ruka W. Survival Analysis and Clinicopathological Factors Associated With False-Negative Sentinel Lymph Node Biopsy Findings in Patients With Cutaneous Melanoma. *Ann Surg Oncol* (2006) 13(12):1655–63. doi: 10.1245/s10434-006-9066-0
63. Karakousis GC, Gimotty PA, Botbyl JD, Kesmodel SB, Elder DE, Elenitsas R, et al. Predictors of Regional Nodal Disease in Patients With Thin Melanomas. *Ann Surg Oncol* (2006) 13(4):533–41. doi: 10.1245/aso.2006.05.011
64. Hershko DD, Robb BW, Lowy AM, Ahmad SA, Ramadas GH, Soldano DA, et al. Sentinel Lymph Node Biopsy in Thin Melanoma Patients. *J Surg Oncol* (2006) 93(4):279–85. doi: 10.1002/jso.20415
65. Cascinelli N, Bombardieri E, Bufalino R, Camerini T, Carbone A, Clemente C, et al. Sentinel and Nonsentinel Node Status in Stage IB and II Melanoma Patients: Two-Step Prognostic Indicators of Survival. *J Clin Oncol* (2006) 24 (27):4464–71. doi: 10.1200/jco.2006.06.3198
66. Rex J, Paradelo C, Mangas C, Hilari JM, Fernandez-Figueras MT, Fraile M, et al. Single-Institution Experience in the Management of Patients With Clinical Stage I and II Cutaneous Melanoma: Results of Sentinel Lymph Node Biopsy in 240 Cases. *Dermatol Surg* (2005) 31(11):1385–93. doi: 10.1097/00042728-200511000-00002
67. Puleo CA, Messina JL, Riker AI, Glass LF, Nelson C, Cruse CW, et al. Sentinel Node Biopsy for Thin Melanomas: Which Patients Should be Considered? *Cancer Control* (2005) 12(4):230–5. doi: 10.1177/107327480501200404
68. Kesmodel SB, Karakousis GC, Botbyl JD, Canter RJ, Lewis RT, Wahl PM, et al. Mitotic Rate as a Predictor of Sentinel Lymph Node Positivity in Patients With Thin Melanomas. *Ann Surg Oncol* (2005) 12(6):449–58. doi: 10.1245/aso.2005.04.027
69. Stitzenberg KB, Groben PA, Stern SL, Thomas NE, Hensing TA, Sansbury LB, et al. Indications for Lymphatic Mapping and Sentinel Lymphadenectomy in Patients With Thin Melanoma (Breslow Thickness < or =1.0 Mm). *Ann Surg Oncol* (2004) 11(10):900–6. doi: 10.1245/aso.2004.10.002
70. Borgognoni L, Urso C, Vaggelli L, Brandani P, Gerlini G, Reali UM. Sentinel Node Biopsy Procedures With an Analysis of Recurrence Patterns and Prognosis in Melanoma Patients: Technical Advantages Using Computer-Assisted Gamma Probe With Adjustable Collimation. *Melanoma Res* (2004) 14(4):311–9. doi: 10.1097/01.cmr.0000133968.28172.6e
71. Rousseau DLJr., Ross MI, Johnson MM, Prieto VG, Lee JE, Mansfield PF, et al. Revised American Joint Committee on Cancer Staging Criteria Accurately Predict Sentinel Lymph Node Positivity in Clinically Node-Negative Melanoma Patients. *Ann Surg Oncol* (2003) 10(5):569–74. doi: 10.1245/aso.2003.09.016
72. Oliveira Filho RS, Ferreira LM, Biasi LJ, Enokihara MMSS, Paiva GR, Wagner J. Vertical Growth Phase and Positive Sentinel Node in Thin Melanoma. *Braz J Med Biol Res* (2003) 36(3):347–50. doi: 10.1590/S0100-879X2003000300009
73. Jacobs IA, Chang CK, DasGupta TK, Salti GI. Role of Sentinel Lymph Node Biopsy in Patients With Thin (<1 Mm) Primary Melanoma. *Ann Surg Oncol* (2003) 10(5):558–61. doi: 10.1245/aso.2003.10.025

74. Bleicher RJ, Essner R, Foshag LJ, Wanek LA, Morton DL. Role of Sentinel Lymphadenectomy in Thin Invasive Cutaneous Melanomas. *J Clin Oncol* (2003) 21(7):1326–31. doi: 10.1200/jco.2003.06.123
75. Agnese DM, Abdessalam SF, Burak WEJr., Magro CM, Pozderac RV, Walker MJ. Cost-Effectiveness of Sentinel Lymph Node Biopsy in Thin Melanomas. *Surgery* (2003) 134(4):542–547; discussion 547-548. doi: 10.1016/s0039-6060(03)00275-7
76. Statius Muller MG, Van Leeuwen PAM, Van Diest PJ, Vuylsteke R.J.C.L.M., Pijpers R, Meijer S. No Indication for Performing Sentinel Node Biopsy in Melanoma Patients With a Breslow Thickness of Less Than 0.9 Mm. *Melanoma Res* (2001) 11(3):303–7. doi: 10.1097/00008390-200106000-00013
77. Wrightson WR, Wong SL, Edwards MJ, Chao C, Reintgen DS, Ross MI, et al. Complications Associated With Sentinel Lymph Node Biopsy for Melanoma. *Ann Surg Oncol* (2003) 10(6):676–80. doi: 10.1245/aso.2003.10.001
78. Bartlett EK, Gupta M, Datta J, Gimotty PA, Guerry D, Xu XW, et al. Prognosis of Patients With Melanoma and Microsatellitosis Undergoing Sentinel Lymph Node Biopsy. *Ann Surg Oncol* (2014) 21(3):1016–23. doi: 10.1245/s10434-013-3388-5
79. Ribero S, Gualano MR, Osella-Abate S, Scaioli G, Bert F, Sanlorenzo M, et al. Association of Histologic Regression in Primary Melanoma With Sentinel Lymph Node Status: A Systematic Review and Meta-Analysis. *JAMA Dermatol* (2015) 151(12):1301–7. doi: 10.1001/jamadermatol.2015.2235
80. Gualano MR, Osella-Abate S, Scaioli G, Marra E, Bert F, Faure E, et al. Prognostic Role of Histological Regression in Primary Cutaneous Melanoma: A Systematic Review and Meta-Analysis. *Br J Dermatol* (2018) 178(2):357–62. doi: 10.1111/bjd.15552
81. Slominski A, Kim TK, Brożyna AA, Janjetovic Z, Brooks DL, Schwab LP, et al. The Role of Melanogenesis in Regulation of Melanoma Behavior: Melanogenesis Leads to Stimulation of HIF-1α Expression and HIF-Dependent Attendant Pathways. *Arch Biochem Biophys* (2014) 563:79–93. doi: 10.1016/j.abb.2014.06.030
82. Brożyna AA, Jozwicki W, Carlson JA, Slominski AT. Melanogenesis Affects Overall and Disease-Free Survival in Patients With Stage III and IV Melanoma. *Hum Pathol* (2013) 44(10):2071–4. doi: 10.1016/j.humpath.2013.02.022
83. Slominski RM, Zmijewski MA, Slominski AT. The Role of Melanin Pigment in Melanoma. *Exp Dermatol* (2015) 24(4):258–9. doi: 10.1111/exd.12618
84. Brozyna AA, Jozwicki W, Roszkowski K, Filipiak J, Slominski AT. Melanin Content in Melanoma Metastases Affects the Outcome of Radiotherapy. *Oncotarget* (2016) 7(14):17844–53. doi: 10.18632/oncotarget.7528

Conflict of Interest: The authors declare that the research was conducted in the absence of any commercial or financial relationships that could be construed as a potential conflict of interest.

Publisher's Note: All claims expressed in this article are solely those of the authors and do not necessarily represent those of their affiliated organizations, or those of the publisher, the editors and the reviewers. Any product that may be evaluated in this article, or claim that may be made by its manufacturer, is not guaranteed or endorsed by the publisher.

Copyright © 2022 Huang, Fu, Ji, Huang and Long. This is an open-access article distributed under the terms of the Creative Commons Attribution License (CC BY). The use, distribution or reproduction in other forums is permitted, provided the original author(s) and the copyright owner(s) are credited and that the original publication in this journal is cited, in accordance with accepted academic practice. No use, distribution or reproduction is permitted which does not comply with these terms.

frontiers in Oncology

ORIGINAL RESEARCH
published: 08 March 2022
doi: 10.3389/fonc.2022.836859

Immune Checkpoint Inhibitor-Induced Hypophysitis and Patterns of Loss of Pituitary Function

Shlomit Jessel[1‡], Sarah A. Weiss[1†‡], Matthew Austin[1], Amit Mahajan[2], Katrina Etts[1], Lin Zhang[1], Lilach Aizenbud[1], Ana Luisa Perdigoto[3], Michael Hurwitz[1], Mario Sznol[1], Kevan C. Herold[3] and Harriet M. Kluger[1]*

[1] Department of Medicine (Medical Oncology), Yale University School of Medicine, New Haven, CT, United States,
[2] Department of Radiology and Biomedical Imaging, Yale University School of Medicine, New Haven, CT, United States,
[3] Department of Medicine (Endocrinology), Yale University School of Medicine, New Haven, CT, United States

Background: Immune checkpoint inhibitors (ICI) are clinically active across multiple tumor types but the associated immune-related adverse events (irAEs) lead to treatment delays or discontinuation and negatively impact quality-of-life. Hypophysitis is often a permanent irAE that may affect multiple pituitary hormonal axes. Here we comprehensively characterize our institution's clinical experience with ICI-induced hypophysitis and the associated patterns of pituitary function loss.

Methods: Patients with solid tumors, mostly melanoma and renal cell carcinoma (RCC), treated with ICI at Yale Cancer Center were prospectively enrolled from October 2016-May 2021. Demographics and clinical data were obtained from the medical record including type and timing of irAEs. Patients were included in this cohort if hypophysitis was diagnosed by pre-specified biochemical and clinical parameters.

Results: The overall incidence of hypophysitis was 69/490 (14%) in patients with melanoma (n=58, 84%), RCC (n=10,14%), and merkel cell carcinoma (n=1, 1%) who received ipilimumab plus nivolumab (77%; 53/69), anti-PD-(L)1 (17%; 12/69), or ipilimumab monotherapy (6%; 4/69). Of the 69 patients analyzed, median time to hypophysitis on combination ICI versus anti-PD-1 was 2.8 vs. 4.1 months. The incidence of hypophysitis in patients with melanoma was 25% (46/187) with ipilimumab plus nivolumab and 5% (7/129) with anti-PD-(L)1 compared to 9% (7/77) and 8% (3/37), respectively, in patients with RCC. Patients who developed hypophysitis on combination ICI had a higher rate of headache (p=0.05) and co-occurring irAEs (p=0.01) compared anti-PD-(L1)1 monotherapy. At a median follow-up of 2.2 years, 77% of patients were alive. Objective response rates to ICI in melanoma patients were higher than previously reported for unselected populations. Central hypothyroidism and hypogonadism were the most common pituitary axes affected after the adrenal axis. In select cases, there was evidence of spontaneous rebound in free testosterone levels after an initial decline.

OPEN ACCESS

Edited by:
Sapna Patel, University of Texas MD Anderson Cancer Center, United States

Reviewed by:
Simone Scagnoli, Sapienza University of Rome, Italy
Amin Nassar, Brigham and Women's Hospital and Harvard Medical School, United States

***Correspondence:**
Sarah A. Weiss
saweiss@cinj.rutgers.edu

†Present address:
Sarah A. Weiss, Rutgers Cancer Institute of New Jersey, New Brunswick, NJ, United States

‡These authors have contributed equally to this work

Specialty section:
This article was submitted to Skin Cancer, a section of the journal Frontiers in Oncology

Received: 16 December 2021
Accepted: 11 February 2022
Published: 08 March 2022

Citation:
Jessel S, Weiss SA, Austin M, Mahajan A, Etts K, Zhang L, Aizenbud L, Perdigoto AL, Hurwitz M, Sznol M, Herold KC and Kluger HM (2022) Immune Checkpoint Inhibitor-Induced Hypophysitis and Patterns of Loss of Pituitary Function. Front. Oncol. 12:836859. doi: 10.3389/fonc.2022.836859

Conclusions: We demonstrate a higher rate of ICI-induced hypophysitis than previously reported, which may be reflective of real-world practice due to increased awareness as experience with ICI has grown. In select cases, there was evidence of rebound in free testosterone and/or gonadotropins but not in adrenal axis hormones.

Keywords: hypophysitis, immune checkpoint inhibitors (ICI), immune-related adverse events, melanoma, endocrinopathy

INTRODUCTION

Monoclonal antibodies against PD-(L)1 and CTLA-4 have revolutionized cancer treatment and are FDA-approved for numerous oncologic indications for both unresectable disease and as adjuvant therapy for resected disease. Although immune checkpoint inhibitors (ICI) are clinically active in a proportion of patients across multiple tumor types, not all patients respond. A second major limitation of ICI is the unpredictable development of immune mediated adverse events (irAEs) which can negatively impact quality of life and often lead to treatment delays or discontinuation. The vast majority of irAEs can be managed with immunosuppressants, most commonly corticosteroids, however rare fatalities secondary to refractory irAEs have been reported (1). This is particularly challenging in the adjuvant setting, when many patients are already surgically cured. Prompt recognition and management of irAEs have improved as clinical experience with ICI has grown. However, organ-specific characterization of these irAEs including the pathogenesis, molecular and immunologic determinants, patient susceptibility, and association with anti-tumor immunity is less understood, and no predictive biomarkers are available.

Skin, gastrointestinal, and hepatic irAEs are generally the most common, but virtually any organ can be impacted by ICI either during the course of treatment or occasionally months to years after treatment has been stopped (2, 3). The majority of irAEs are reversible once promptly diagnosed and managed however a small percentage, most commonly endocrinopathies, are long-lasting or irreversible and can require long-standing replacement therapy. Several studies have suggested a link between immune-mediated endocrinopathies and survival including thyroid disease (4–6), but these findings are not necessarily generalizable and may depend on the ICI regimen, tumor type, and the affected organ (7). After thyroid dysfunction, hypophysitis is the second most common immune-mediated endocrinopathy. The diagnosis is made based upon a combination of pituitary and effector hormone laboratory abnormalities, clinical symptoms, and radiographic findings of pituitary inflammation. In clinical trials of patients with advanced melanoma, the incidence of immune-mediated hypophysitis has differed based on the ICI regimen. The incidence of hypophysitis has ranged from 1-18% in patients treated with ipilimumab (8–13), 0.5-1.5% for PD-1 inhibitors (2, 12, 14), and up to 13% for combination therapy with ipilimumab plus nivolumab (10, 15, 16). Of note, not all of these studies mandated measurement of pituitary hormones, and the real-world incidence of hypophysitis might in fact be higher. For example, a case series of patients with melanoma treated with ICI report hypophysitis in an estimated 10% on combination therapy and 5% on anti-PD-1 (17). However, most case series report on anti-PD-1 alone rather than ipilimumab plus nivolumab and others lack a denominator to be able to reliably calculate the true incidence of hypophysitis (18, 19). Inflammation that affects adrenocorticotropic hormone (ACTH) producing cells causing central adrenal insufficiency is most common, but disruptions to other hormonal pathways can occur, for example resulting in central hypothyroidism and hypogonadotropic hypogonadism (17). The purpose of this study is to comprehensively characterize the clinical experience of ICI-induced hypophysitis and patterns of pituitary function loss from a single institution.

METHODS

Patients treated with ICI in Yale Cancer Center's Melanoma and Renal Cell Carcinoma (RCC) Programs were prospectively enrolled on protocol #0608001773, approved by the Yale University Institutional Review Board. The objectives of this protocol are to characterize irAEs and identify biomarkers and mechanisms of immunologic responses that contribute to irAEs in cancer patients treated with ICI. Key criteria for inclusion were adults with melanoma, renal cell carcinoma, and merkel cell carcinoma treated with ICI which are the tumor types seen in our practice. Written informed consent was obtained from all subjects. Demographic, clinical, radiographic, and pathologic data including tumor type, ICI regimen, response to treatment, and survival status were recorded for each subject and were available by review of the electronic medical record. The date, duration, and type of each irAE that developed during the course of ICI treatment, including hypophysitis, was documented for each patient. Serial blood draws for research were performed, when possible, pre-treatment at cycles 1 through 4 and every 3 months thereafter and/or at the time of ICI-induced toxicity and while on steroids. Blood samples were processed and stored in our dedicated biorepository.

Patients were included in this analysis if they had evidence of hypophysitis defined by: 1) suggestive clinical symptoms such as fatigue, headache, nausea or vomiting; and 2) biochemical parameters consistent with pituitary hormone deficiency which included low cortisol and abnormalities in the following hormones, as clinically indicated: ACTH, thyroid stimulating hormone (TSH), free T4, luteinizing hormone (LH), follicle stimulating hormone (FSH), and testosterone in males.

Central hypothyroidism was defined as low or low-normal free T4 and low or inappropriately normal TSH. Central

hypogonadism in men was defined as low testosterone and low or inappropriately normal LH. Free testosterone levels were measured by ELISA (ALPCO, #11-FTSHU-E01, Salem, NH, USA) on available serum from male patients who developed hypophysitis including at baseline, time of hypophysitis diagnosis, and post-hypophysitis, when available. Expected normal free testosterone values from this assay are 5.7-30.7 pg/mL for males between the ages of 40 to 59 years old and 5.9-27 pg/mL for males ≥ 60 years old. The lower limit of detection for the test is 0.018 pg/mL. LH was measured on the same samples by ELISA (ALPCO, #11-LUTHU-E01, Salem, NH, USA). The normal LH range for males is 1.5-9.3 IU/L. The lower limit of detection for this assay is 0.2 IU/L.

Brain MRIs that were performed within 1 month of development of hypophysitis were retrospectively re-reviewed by an independent radiologist (A.M.) for pituitary enlargement. Statistical methods were descriptive. All patients were analyzed from start of treatment until the data cut-off of July 19, 2021. For comparison of clinical features between the patients treated with ipilimumab plus nivolumab versus anti-PD-1 alone, t-tests were used to compare means between the groups and the Chi Square test was used for categorical variables. Best overall response (BOR) was defined as the best response [complete response (CR), partial response (PR), stable disease (SD), or progressive disease (PD)] documented on at least two consecutive imaging studies from the start of the ICI regimen on which the patient developed hypophysitis.

RESULTS

Patient Characteristics and Incidence of Hypophysitis

Between October 2016 and May 2021, 490 patients receiving ICI were enrolled on the protocol with the majority having melanoma (n=320), renal cell carcinoma (n=115), or merkel cell carcinoma (n=12). Several other cancer types were also included: biliary tract carcinoma (n=2), basal cell carcinoma (n=3), breast (n=7), lung (n=14), colon (n=3), gastroesophageal (n=4), pancreatic (n=2), prostate (n=3), rectal (n=1), and cutaneous squamous cell carcinoma (n=4). Sixty-nine out of 490 patients on ICI (14%) developed hypophysitis. Our analysis focuses on these 69 patients with hypophysitis. The tumor types represented in this cohort were reflective of the patients who were treated in the Yale Melanoma and RCC Programs and included melanoma (n=58, 84%), RCC (n=10,14%), and merkel cell carcinoma (n=1, 1%). By ICI regimen, hypophysitis developed in 19% (53/277) of patients who received ipilimumab plus nivolumab and in 6% (12/212) of patients who received anti-PD-1. The sample size of patients who received ipilimumab only was too small to calculate the hypophysitis incidence. For patients who received ipilimumab plus nivolumab, there was a higher incidence of hypophysitis in those with melanoma (25%; 46/187) versus RCC (9%; 7/77) (p=0.004). Of note, patients with melanoma generally received ipilimumab at 3 mg/kg instead of 1 mg/kg, the standard of care for RCC. Incidence of hypophysitis on anti-PD-1 monotherapy was 5% (7/129) in patients with melanoma and 8% (3/37) in patients with RCC. Ten percent (1/10) of patients with Merkel cell carcinoma treated with anti-PD-1 developed hypophysitis. Demographics and clinical characteristics of these patients are outlined in **Table 1**. The majority of patients were male (68%). Median age at the time of development of immune-mediated hypophysitis was 64 years.

Timing and Type of Therapy

The majority of patients were treatment-naive (71%), and 17 out of 20 with prior therapies had received prior ICI. At the time hypophysitis developed, patients were receiving ipilimumab plus nivolumab (77%; 53/69), anti-PD-(L)1 monotherapy (12%; 8/69), anti-PD-(L)1 with the addition of an investigational agent (6%; 4/69), or ipilimumab monotherapy (6%; 4/69) (**Table 1**). Median time to hypophysitis diagnosis from the start of the ICI regimen was 95 days (range 23-523) and after 4 cycles of therapy (range 1-18). Median time to hypophysitis differed by ICI regimen, occurring earlier for patients who received ipilimumab plus nivolumab (2.8 months) compared to anti-PD-1 monotherapy (4.1 months) (p=0.0006) (**Table 1**). There were several cases of delayed development of hypophysitis (**Supplementary Figure 1**). Eight patients (12%) developed hypophysitis 6-12 months after starting their ICI regimen with 6 out of 8 having received ipilimumab plus nivolumab. Three patients (4%) developed hypophysitis after 1 year. Two had received anti-PD-(L)1 and 1 received ipilimumab. The longest time to development of hypophysitis was 523 days in a patient with RCC treated with atezolizumab plus bevacizumab.

Clinical Presentation

All patients were symptomatic at the time hypophysitis was diagnosed. The most common presentations were fatigue (86%),

TABLE 1 | Baseline clinical characteristics.

Characteristic	N=69	%
Gender		
Male	47	68%
Female	22	32%
Age at time of hypopituitarism		
Median	64	–
Range	32-83	–
Tumor type		
Melanoma	58	84%
Renal cell carcinoma	10	14%
Merkel cell carcinoma	1	1%
Systemic Therapy Regimen at time of Hypophysitis		
Ipilimumab and Nivolumab	53	77%
Anti-PD-(L)1	8	12%
Ipilimumab	4	6%
Anti-PD-(L)1 + Investigational Drug	4	6%
Prior Systemic Therapy		
Yes	21	30%
No	48	70%
Prior ICI		
Yes	17	25%
No	52	75%

headache (43%), nausea and/or vomiting (39%), hypotension (7%), and/or visual changes (4%) (**Table 2**). Patients who received ipilimumab plus nivolumab were more likely to experience a headache at time of hypophysitis diagnosis compared to those treated with anti-PD-(L)1 monotherapy (47% vs. 17%, p=0.05), but there were no significant differences in frequency of nausea and/or vomiting, hypotension, or fatigue between the groups.

Co-occurring irAEs, defined as irAEs other than hypophysitis that developed within a 3-month window from the time of hypophysitis diagnosis, developed in 46% (32/69) of patients (**Table 3**) but development of irAEs at any timepoint during ICI therapy were more common in patients who received ipilimumab plus nivolumab compared to anti-PD-1 alone (83% vs. 50%, p=0.01) (**Table 2**). The most common additional irAEs were colitis (35%), rash (25%), and hepatitis (25%). Other endocrinopathies that developed were thyroid dysfunction, which is discussed separately below, and ICI-induced diabetes in three patients (4%). Three additional patients who had pre-existing type II diabetes at baseline experienced worsening of their diabetes while on ICI and became insulin-dependent. All six of these patients were treated with ipilimumab plus nivolumab. At any point in the treatment course, 75% of patients developed at least 1 additional irAE, excluding central hypothyroidism secondary to hypophysitis (**Table 3**). Half of patients who received anti-PD-(L)1 therapy had hypophysitis as their only irAE compared to only 17% of patients on ipilimumab plus nivolumab (p=0.01).

TABLE 3 | Clinical presentation of hypophysitis and association with other irAEs.

Clinical Presentation		
Fatigue	59	86%
Headache	30	43%
Nausea/Vomiting	27	39%
Hypotension	5	7%
Visual Changes	3	4%
Co-occurring irAEs within 3 months		
Yes	32	46%
No	37	54%
Other irAEs by organ system*		
Colitis	24	35%
Rash (poorly documented)	17	25%
Hepatitis	17	25%
Primary Hypothyroidism	11	16%
Arthritis	6	9%
Isolated thyroiditis	6	9%
Pneumonitis	6	9%
Pancreatitis	4	6%
Nephritis	4	6%
Sicca	4	6%
Ocular Toxicity	4	6%
Diabetes	3	4%
Neurotoxicity	2	3%
Myositis	2	3%
Number of co-occurring organ-specific irAEs		
0 (hypophysitis only)	17	25%
1	21	30%
2	16	23%
3	8	12%
4	5	7%
5	1	1%
8	1	1%

**Cases of hypothyroidism secondary to hypophysitis are not included.*

Clinical Outcomes

Median follow-up time, defined as from the date of hypophysitis diagnosis to death or last follow-up, was 2.2 years. Sixty-seven patients received treatment for advanced disease while only two were on adjuvant anti-PD-1. For the 46 patients with unresectable melanoma who received ipilimumab plus nivolumab, BOR was CR (n=18; 39%), PR (n=15; 33%), SD (n=3; 7%), and PD (n=10; 22%). In the 7 melanoma patients who received anti-PD-1, BOR was CR (n=4; 57%), PR (n=1; 14%), and PD (n=2; 29%). In the 10 patients with RCC, BOR was PR

TABLE 2 | Time to hypophysitis diagnosis, presenting symptoms, and co-occurring irAEs.

Characteristic	**Ipi+Nivo n=53 (%)**	**Anti-PD-(L)1 n=12 (%)**	**Ipi n=4 (%)**	**p-value***
Timing				
Median ICI cycles until hypophysitis	4	6.5	4.5	**<0.0001**
(range)	(1-9)	(2-13)	(3-7)	
Median days on ICI until hypophysitis	84	124	132	**0.0006**
(range)	(23-259)	(44-523)	(91-399)	
Presenting symptom(s)				
Fatigue	46 (87)	10 (83)	3 (75)	0.75
Headache	25 (47)	2 (17)	3 (75)	**0.05**
Nausea/vomiting	19 (36)	6 (50)	2 (50)	0.36
Hypotension	3 (6)	2 (17)	0 (0)	0.20
Other irAE(s)¥				
Any	44 (83)	6 (50)	2 (50)	**0.01**
Co-occurring thyroid dysfunction				
Primary Hypothyroidism	9 (17)	1 (8)	1 (25)	0.76
Transient hyperthyroidism without subsequent hypothyroidism	6 (11)	0 (0)	0 (0)	NA
Central Hypothyroidism	19 (36)	2 (17)	3 (75)	0.2

**p-values comparing ipi+nivo to anti-PD-1.*

¥Excludes cases of hypothyroidism secondary to hypophysitis; at any point on ICI therapy.

Bold denotes statistically significant.

(n=4; 40%), SD (n=4; 40%), and PD (n=2; 20%). The one patient with Merkel cell carcinoma had progressive disease. At the data cut-off, 77% of patients were alive and 23% were deceased.

Biochemical Analyses

Figure 1A demonstrates the proportion of patients with central hypothyroidism or hypogonadism, stratified by ICI regimen. Ipilimumab was not included in the Figure due to the low number of patients (n=4) on ipilimumab monotherapy in our cohort. By definition, serum cortisol was low in all 69 patients. ACTH was measured in 51% (35/69) of patients and was universally low. The low cortisol was associated with hyponatremia in 25% (17/69) of cases. There was only 1 case of hyperkalemia and while the initial ACTH was high in this case likely due to pituitary inflammation, the ACTH value subsequently became low and along with a low cortisol measurement, was reflective of a central process. The remainder of the hormones and/or their effectors were measured as clinically indicated.

TSH/Free T4

At the time of hypophysitis diagnosis, TSH was measured in 100% (69/69) of patients and free T4 was measured in 80% (55/69). Twenty-three (33%) patients were euthyroid and 5 patients (7%) had pre-existing hypothyroidism and were already on replacement therapy prior to the diagnosis of hypophysitis. Thyroid dysfunction was identified in 41/69 patients as: central hypothyroidism (35%; 24/69), primary hypothyroidism (16%; 11/69), and isolated hyperthyroidism without subsequent

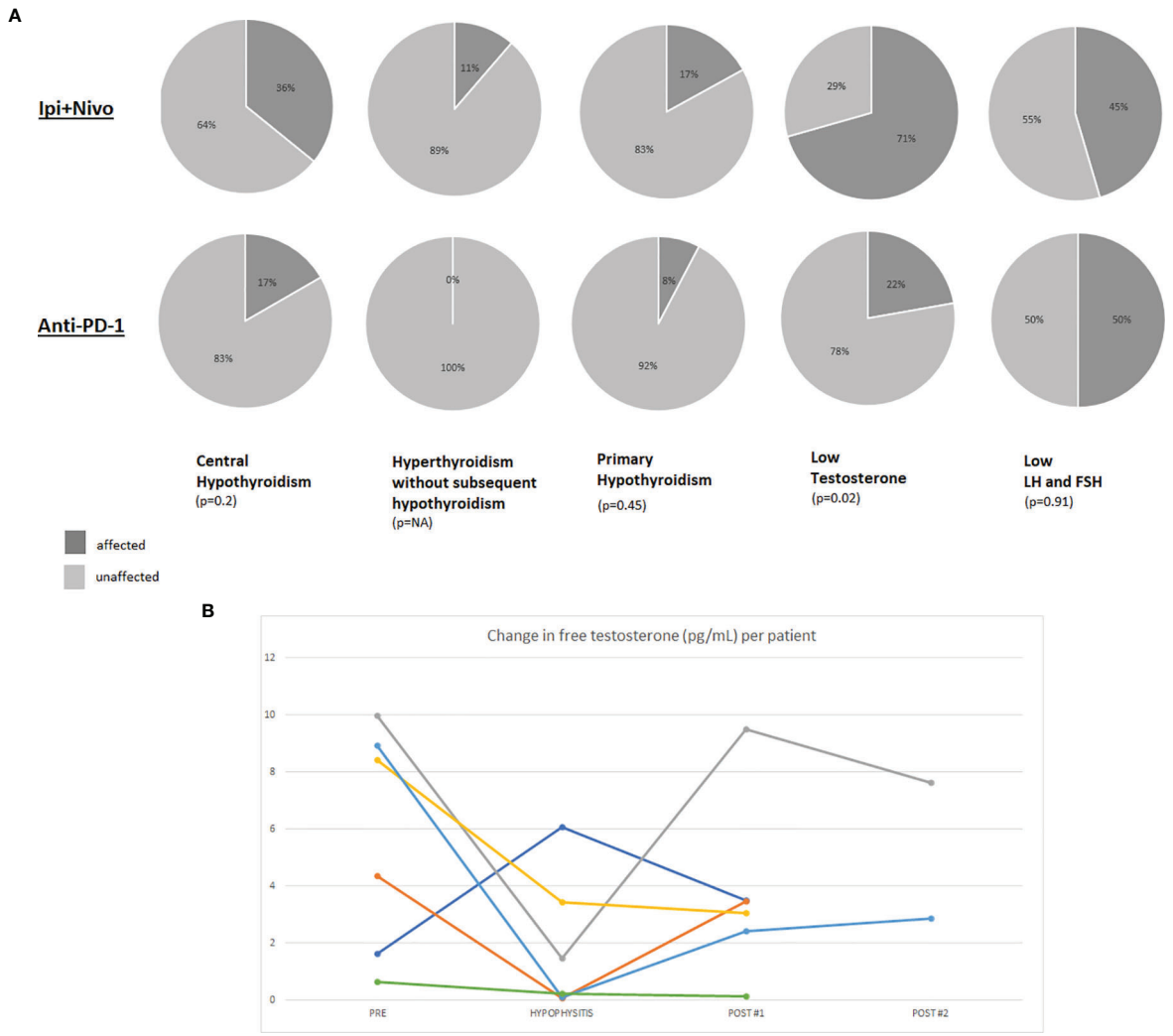


FIGURE 1 | **(A)** Pie charts representing the percentage of hypophysitis patients who were affected by hormonal axis deficiencies. The denominator for each pie chart represents the number of patients who were evaluated with diagnostic laboratory tests for the particular axis since not certain hormones and their effectors were not routinely tested in all patients. Results are presented for patients who developed hypophysitis on ipilimumab plus nivolumab or anti-PD-(L)1. **(B)** Line graph demonstrating changes in free testosterone (pg/mL) per patient relative to the time of hypophysitis diagnosis. A standardized assay for free testosterone was performed on male patients with stored blood samples collected on our protocol.

hypothyroidism (9%; 6/69). Central hypothyroidism, primary hypothyroidism, and isolated thyroiditis all occurred at higher rates in patients on ipilimumab plus nivolumab compared to anti-PD-1 monotherapy.

Testosterone

Total and/or free serum testosterone was measured in 20 of the 47 male patients (43%) as clinically indicated and was below the normal range in the majority (15/20; 70%). However these levels were not all obtained at the time of hypophysitis diagnosis. As part of our protocol, patients had blood available for analysis from several time points including pre-toxicity, time of hypophysitis diagnosis, and post-hypophysitis. Free testosterone, FSH and LH were tested at these timepoints from available serum (**Supplementary Table 1**). Out of 47 male patients with hypophysitis, twenty had research bloods available for analysis: 7 from pre- and post-hypophysitis diagnosis, 6 from pre, time of hypophysitis, and post; 6 at time of hypophysitis and post-hypophysitis. Two patients were excluded from the analysis for lack of interpretable timepoints (one patient had blood from before and at diagnosis of hypophysitis and the other only had samples from after diagnosis). Overall, samples were available to calculate change in free testosterone levels from prior to and after development of hypophysitis (n=7), prior to and at diagnosis of hypophysitis (n=5), and at and after the diagnosis of hypophysitis (n=10). Free testosterone decreased in 5 out of 7 patients from baseline to the time of hypophysitis diagnosis. In the 6 patients for which free testosterone measurements from all three timepoints were available, there were varying degrees of recovery of testosterone production after diagnosis of hypophysitis (**Figure 1B** and **Supplementary Figure 2**). Three of the six patients had a rebound in their free testosterone after developing hypophysitis. The rebound levels were obtained at 201, 371, and 394 days (mean: 268 days) post-hypophysitis. Since the timing of the samples was variable and distant from the diagnosis of hypophysitis, we are unable to report whether the free testosterone recovery occurred even sooner. LH decreased at time of hypophysitis in 2 of the 6 cases. All 6 patients had received ipilimumab plus nivolumab.

Brain MRI Findings

Forty-nine patients (71%) had an MRI of the brain performed within 1 month (range -28 to +30 days; median -1 day) of developing hypophysitis, either due to neurologic symptoms or as a routine follow-up scan while on ICI (**Table 4**). Of the 49 patients with available brain imaging, 23 (47%) had radiographic evidence of pituitary enlargement that further supported the diagnosis of hypophysitis. Of the 23 patients with pituitary enlargement, 16 (70%) presented with headache. The majority of these patients (n=20; 87%) received ipilimumab plus nivolumab. Conversely, while not all patients with pituitary enlargement on imaging presented with headache, not all patients with a headache had evidence of pituitary enlargement. Of the 30 patients who presented with headache, 26 had MRI brain imaging available for review and 16 (62%) had radiographic evidence of pituitary enlargement. In patients treated with ipilimumab plus nivolumab, 20/41 (49%) available brain MRIs demonstrated evidence of pituitary enlargement versus only 1/5 (20%) in patients treated with anti-PD-(L)1 monotherapy (p=0.22).

DISCUSSION

Here we report on our single institution experience with hypophysitis in patients treated with ICI, the majority of whom had melanoma. The incidence of hypophysitis in our cohort overall was 19% in patients treated with ipilimumab plus nivolumab and 6% for anti-PD-1, and highest for patients with melanoma treated with ipilimumab plus nivolumab (25%). Although these rates are higher than the incidence reported in ICI clinical trials for patients with melanoma (8, 10–12, 15, 20), they may be more reflective of real-world practice and an increased awareness and recognition of this irAE. Although the incidence of hypophysitis in melanoma patients treated with ipilimumab plus nivolumab may be even higher than expected, our series is one of the largest to report this.

Patients who developed hypophysitis from ipilimumab plus nivolumab compared to anti-PD-1 monotherapy tended to present earlier, usually within the first 3-4 months of ICI initiation, with higher rates of headache and co-occurring irAEs. Although most cases of hypophysitis arose early, three patients developed hypophysitis over 1 year after starting ICI. Case reports of late-onset hypophysitis presenting months after discontinuation of ICI have previously been reported (21, 22). Our data reinforce the importance of ongoing monitoring for irAE development beyond the ICI treatment period.

TABLE 4 | MRI brain imaging available within 1 month of clinical hypophysitis diagnosis.

	ALL n=49 (%)	Ipi+nivo n=41 (%)	Anti-PD-(L)1 n=5 (%)	Ipi n=3 (%)
Pituitary enlargement	23 (47)	20 (49)	1 (20)	2 (67)
With headache	16 (70)	14 (70)	0 (0)	2 (100)
Without headache	7 (30)	6 (30)	1 (100)	0 (0)
Timing of pituitary enlargement on imaging in relation to clinical hypophysitis diagnosis				
Pre-diagnosis	11 (48)	9 (45)	1 (100)	1 (50)
Day-of diagnosis	8 (35)	8 (40)	0 (0)	0 (0)
Post-diagnosis	4 (17)	3 (15)	0 (0)	1 (50)
Normal sized pituitary	26 (53)	21 (51)	4 (80)	1 (33)
With headache	9 (35)	8 (38)	0 (0)	1 (100)

Regarding the presenting symptoms of hypophysitis, headache occurred more commonly in the combination ICI group compared to anti-PD-1 monotherapy (47% vs. 17%), often with pituitary enlargement on MRI, but not always, and rarely in patients on anti-PD-1 monotherapy, in support of prior studies (18). While MRI brain may be useful as a contributory data point for the evaluation of ICI-induced hypophysitis, the absence of pituitary enlargement is not diagnostic, and headache may still be an attributable symptom of hypophysitis in the absence of pituitary enlargement on MRI. Most of the MRIs performed on patients in this series were done for surveillance for brain metastasis, and the variable timing of brain imaging in relation to the clinical hypophysitis diagnosis in this cohort revealed that pituitary enlargement on MRI may occur before a biochemical diagnosis of hypophysitis is made. Incidental finding of pituitary enlargement on MRI brain in a patient receiving or previously on ICI should prompt a clinical and laboratory assessment for active or impending hypophysitis.

Almost half of patients experienced at least one co-occurring irAE and 75% developed another irAE at some point during their ICI treatment course, reinforcing that the diagnosis of hypophysitis should prompt an assessment for co-occurring irAEs and an awareness for future irAEs that may develop. For example, six patients developed insulin-dependent diabetes, whether presenting as new, acute-onset (n=3) or with worsening hyperglycemia in a background of pre-existing diabetes (n=3). ICI-induced diabetes is a rare but often permanent endocrinopathy requiring life-long insulin therapy. Other cases of ICI-induced diabetes and hypophysitis have been reported (23), including in 5% of patients with ICI-induced hypophysitis in the World Health Organization's pharmacovigilance database (24) and reflective of our data here.

There are conflicting data on whether the development of irAEs is associated with improved clinical outcomes. In our cohort, after a median follow-up of 2.2 years, objective response rate (CR + PR) was 74% ((18 + 16)/46) for the melanoma patients who developed hypophysitis on ipilimumab plus nivolumab and 71% ((4 + 1)/7) for anti-PD-1, both of which are higher than that reported in the literature (25). At the time of data cut-off, the majority of patients remain alive. Although our study does not include a matched comparator arm of patients who did not develop hypophysitis, melanoma patients treated with ipilimumab plus nivolumab who developed hypophysitis as a whole had improved clinical outcomes. This conclusion is supported by a prior study of patients with ipilimumab-induced hypophysitis who had improved overall survival compared to patients without hypophysitis (26). Furthermore, a small study has also suggested that the development of pituitary-related irAEs in patients with melanoma treated with ICI is associated with prolonged overall survival compared to those who did not develop hypophysitis (27). The RCC cohort sample size is too small to draw similar conclusions from, but BOR of PR occurred in 40% (n=4) patients, 3 of whom received ipilimumab plus nivolumab and one who received atezolizumab plus bevacizumab.

While our protocol allows for enrollment of all patients treated with ICI whether in the neoadjuvant, adjuvant, or metastatic setting, only 2 of the 69 patients in this cohort who developed hypophysitis were on adjuvant therapy. Although this raises the question of whether the incidence of hypophysitis is less in the adjuvant setting compared to the metastatic setting, the denominator of patients on adjuvant therapy in our database was not available at this time. Of note, all adjuvant patients were treated with anti-PD-1 monotherapy. In CheckMate 238, the incidence of hypophysitis was 1.5% with adjuvant nivolumab and 10.6% with adjuvant ipilimumab in patients with resected stage IIB-IV melanoma (12). At the 4-year follow-up, late emergent TRAEs (voluntarily reported > 100 days after the last dose of ICI) were uncommon and hypophysitis was identified in <1% of patients in either adjuvant arm (28). Despite the low rate of hypophysitis in the adjuvant setting and with PD-1 inhibitors overall, ICI-induced endocrinopathies that develop are typically permanent and require life-long replacement therapy. This can affect quality-of-life and should be a consideration in the risk-benefit analysis when offering patients adjuvant ICI, particularly in patients with earlier stage IIB-IIIA disease or in those patients who have a BRAF V600 mutation and may be eligible for adjuvant targeted therapy instead, which does not pose a risk for permanent endocrinopathies.

Our study was not designed to determine whether the incidence of ICI-induced hypophysitis differs by tumor type since the majority of patients enrolled on our protocol had melanoma. We cannot draw broad conclusions regarding the small numbers of patients with hypophysitis who had RCC or merkel cell carcinoma. In a large meta-analysis studying ICI-induced endocrinopathies in patients with solid tumors, 85 out of 6472 patients developed hypophysitis, and among these 76 had melanoma (15). Interestingly, hypophysitis has not been reported in phase III trials of ipilimumab plus nivolumab for treatment-naïve clear cell RCC or for stage IV or recurrent non-small cell lung cancer. However, this may have been mostly impacted by the fact that only treatment-related AEs that occurred in >15% of patients were reported (29, 30) and this would likely exclude hypophysitis. The higher incidence in melanoma patients on ipilimumab plus nivolumab compared to RCC patients might reflect the difference in standard practice dosing, as the approved regimen for melanoma involves a higher dose of ipilimumab. It is also possible that there are specific antigens and epitopes uniquely expressed only in melanoma that are shared with otherwise normal pituitary tissue, resulting in cross reactivity from peripheral circulating T-cells.

Finally, there are limited data describing the impact of ICI on other hormonal axes during the development of hypophysitis. We demonstrate that central hypothyroidism occurs in roughly one-third of patients who develop hypophysitis on combination ICI and in almost 20% on anti-PD-1 monotherapy. Furthermore, low testosterone was identified in the majority of male patients with hypophysitis in whom it was checked. While age may be a contributing factor, hypogonadism may be an underrecognized and under-tested occurrence in association with hypophysitis. Testing is therefore warranted in men who develop hypophysitis especially if they report ongoing non-specific symptoms such as fatigue, depressed mood and/or libido, or more overtly, hot

flashes. Interestingly, a small proportion of patients had an initial drop in free testosterone at the time of hypophysitis diagnosis with spontaneous rebound or recovery of free testosterone in the months after developing hypophysitis. There was no recovery of the adrenal axis, consistent with prior reports (31), as all patients who developed hypophysitis in this cohort remain on some level of steroid replacement although some doses were able to be lowered with time. Regarding the thyroid hormones, once central hypothyroidism developed, patients were kept on levothyroxine and attempts were not made to wean patients off this medication. Conversely, the gonadal axis appears to be capable of a certain degree of recovery in this cohort. There are limited data on recovery patterns, however in one published cohort, 63% (12/19) of patients who developed central hypogonadism in association with hypophysitis had spontaneous recovery at a median of 17 weeks (32). Another study of ipilimumab-induced hypophysitis reported resolution of central hypothyroidism and hypogonadism in 64% and 45% of studied cases, respectively (31).

While the mechanisms of ICI-induced endocrinopathies including hypophysitis and the precipitating factors are not fully elucidated, CTLA-4 polymorphisms have been associated with autoimmune endocrinopathies (33). The incidence of hypophysitis and radiographic evidence of pituitary enlargement is higher with ipilimumab-containing regimens, supported by the finding that CTLA-4 is expressed in the pituitary (34), and by murine studies demonstrating the development of anti-pituitary antibodies in mice treated with anti-CTLA-4 (35). Patients treated with ipilimumab who developed hypophysitis also had evidence of anti-pituitary antibodies targeting various cell types including thyrotrophs, corticotrophs, and gonadotrophs, but this differed by individual patient. It is still unclear if PD-1 or PD-L1 is expressed in the pituitary (33, 35).

We acknowledge several limitations to this analysis, including the single institution nature of the study and the non-uniformity of diagnoses and categories of ICI therapy. While cortisol is frequently checked in our clinical practice upon suspicion of hypophysitis, we did not prospectively measure cortisol levels on all patients, including those who are asymptomatic, so we do not know the true incidence of hypophysitis. Additionally, measurement of other pituitary axis hormones was variable. When checked, the blood was drawn at variable time points in relation to the timing of hypophysitis and the decision to check was often impacted by other clinical symptomatology and whether the patient was evaluated by an endocrinologist or not.

In conclusion, irAEs can cause significant impact to a patient's quality of life and may necessitate treatment delays or discontinuation. Hypophysitis is typically an irreversible irAE that can be managed with maintenance steroid replacement, however in rare cases it can be life-threatening. Moreover, it can impact quality of life and fertility, and can pose a challenge with use of further therapies such as cytokine therapies. Studies to better understand how to predict development of irAEs, including hypophysitis, and which patients are most susceptible, are underway.

DATA AVAILABILITY STATEMENT

Availability of the dataset can be discussed on a case-by-case basis with the corresponding author. Requests to access the datasets should be directed to saweiss@cinj.rutgers.edu.

ETHICS STATEMENT

The studies involving human participants were reviewed and approved by Yale University Institutional Review Board. The patients/participants provided their written informed consent to participate in this study.

AUTHOR CONTRIBUTIONS

SJ, SW, and HK contributed to conception and design of the study. SJ, MA, SW, KE, LZ, and LA contributed to and organized the database. Patients were recruited and cared for in the clinical practices of SW, HK, MS, MH, and KH where the clinical data was collected. SJ performed the testosterone and gonadotropin assays. AM reviewed available MRIs of the brain and assisted with interpretation of imaging data. KH and AP provided feedback on the specifics of presenting the endocrinopathies. SW wrote the first draft of the manuscript. All authors contributed to manuscript revision, read, and approved the submitted version.

FUNDING

This study received funding from P30DK116577 (KH), R01 CA227473 (KH, HK), K12CA215110 (SW, AP, HK), and the Yale SPORE in Skin Cancer P50 CA121974 (HK). The funders were not involved in the study design, collection, analysis, interpretation of data, the writing of this article or the decision to submit it for publication.

SUPPLEMENTARY MATERIAL

The Supplementary Material for this article can be found online at: https://www.frontiersin.org/articles/10.3389/fonc.2022.836859/full#supplementary-material

Supplementary Figure 1 | Cumulative incidence of ICI-induced hypophysitis in patients with melanoma over time in months.

Supplementary Figure 2 | Serial free testosterone values drawn from male patients on immune checkpoint inhibitors pre-hypophysitis (baseline), at the time hypophysitis was diagnosed, and post-hypophysitis (POST #1 and POST #2).

REFERENCES

1. Wang DY, Salem JE, Cohen JV, Chandra S, Menzer C, Ye F, et al. Fatal Toxic Effects Associated With Immune Checkpoint Inhibitors: A Systematic Review and Meta-Analysis. *JAMA Oncol* (2018) 4(12):1721–8. doi: 10.1001/jamaoncol.2018.3923
2. Wolchok JD, Chiarion-Sileni V, Gonzalez R, Rutkowski P, Grob JJ, Cowey CL, et al. Overall Survival With Combined Nivolumab and Ipilimumab in Advanced Melanoma. *N Engl J Med* (2017) 377(14):1345–56. doi: 10.1056/NEJMoa1709684
3. Couey MA, Bell RB, Patel AA, Romba MC, Crittenden MR, Curti BD, et al. Delayed Immune-Related Events (DIRE) After Discontinuation of Immunotherapy: Diagnostic Hazard of Autoimmunity at a Distance. *J Immunother Cancer* (2019) 7(1):165. doi: 10.1186/s40425-019-0645-6
4. Muir CA, Clifton-Bligh RJ, Long GV, Scolyer RA, Lo SN, Carlino MS, et al. Thyroid Immune-Related Adverse Events Following Immune Checkpoint Inhibitor Treatment. *J Clin Endocrinol Metab* (2021) 106(9):e3704–e13. doi: 10.1210/clinem/dgab263
5. Kotwal A, Kottschade L, Ryder M. PD-L1 Inhibitor-Induced Thyroiditis Is Associated With Better Overall Survival in Cancer Patients. *Thyroid* (2020) 30 (2):177–84. doi: 10.1089/thy.2019.0250
6. Osorio JC, Ni A, Chaft JE, Pollina R, Kasler MK, Stephens D, et al. Antibody-Mediated Thyroid Dysfunction During T-Cell Checkpoint Blockade in Patients With non-Small-Cell Lung Cancer. *Ann Oncol* (2017) 28(3):583–9. doi: 10.1093/annonc/mdw640
7. Xing P, Zhang F, Wang G, Xu Y, Li C, Wang S, et al. Incidence Rates of Immune-Related Adverse Events and Their Correlation With Response in Advanced Solid Tumours Treated With NIVO or NIVO+IPI: A Systematic Review and Meta-Analysis. *J Immunother Cancer* (2019) 7(1):341. doi: 10.1186/s40425-019-0779-6
8. Hodi FS, O'Day SJ, McDermott DF, Weber RW, Sosman JA, Haanen JB, et al. Improved Survival With Ipilimumab in Patients With Metastatic Melanoma. *N Engl J Med* (2010) 363(8):711–23. doi: 10.1056/NEJMoa1003466
9. Robert C, Schachter J, Long GV, Arance A, Grob JJ, Mortier L, et al. Pembrolizumab Versus Ipilimumab in Advanced Melanoma. *N Engl J Med* (2015) 372(26):2521–32. doi: 10.1056/NEJMoa1503093
10. Larkin J, Chiarion-Sileni V, Gonzalez R, Grob JJ, Cowey CL, Lao CD, et al. Combined Nivolumab and Ipilimumab or Monotherapy in Untreated Melanoma. *N Engl J Med* (2015) 373(1):23–34. doi: 10.1056/NEJMoa1504030
11. Eggermont AM, Chiarion-Sileni V, Grob JJ, Dummer R, Wolchok JD, Schmidt H, et al. Adjuvant Ipilimumab Versus Placebo After Complete Resection of High-Risk Stage III Melanoma (EORTC 18071): A Randomised, Double-Blind, Phase 3 Trial. *Lancet Oncol* (2015) 16(5):522–30. doi: 10.1016/s1470-2045(15)70122-1
12. Weber J, Mandala M, Del Vecchio M, Gogas HJ, Arance AM, Cowey CL, et al. Adjuvant Nivolumab Versus Ipilimumab in Resected Stage III or IV Melanoma. *N Engl J Med* (2017) 377(19):1824–35. doi: 10.1056/NEJMoa1709030
13. Byun DJ, Wolchok JD, Rosenberg LM, Girotra M. Cancer Immunotherapy - Immune Checkpoint Blockade and Associated Endocrinopathies. *Nat Rev Endocrinol* (2017) 13(4):195–207. doi: 10.1038/nrendo.2016.205
14. Robert C, Long GV, Brady B, Dutriaux C, Maio M, Mortier L, et al. Nivolumab in Previously Untreated Melanoma Without BRAF Mutation. *N Engl J Med* (2015) 372(4):320–30. doi: 10.1056/NEJMoa1412082
15. Barroso-Sousa R, Barry WT, Garrido-Castro AC, Hodi FS, Min L, Krop IE, et al. Incidence of Endocrine Dysfunction Following the Use of Different Immune Checkpoint Inhibitor Regimens: A Systematic Review and Meta-Analysis. *JAMA Oncol* (2018) 4(2):173–82. doi: 10.1001/jamaoncol.2017.3064
16. Shoushtari AN, Friedman CF, Navid-Azarbaijani P, Postow MA, Callahan MK, Momtaz P, et al. Measuring Toxic Effects and Time to Treatment Failure for Nivolumab Plus Ipilimumab in Melanoma. *JAMA Oncol* (2018) 4(1):98–101. doi: 10.1001/jamaoncol.2017.2391
17. Kassi E, Angelousi A, Asonitis N, Diamantopoulos P, Anastasopoulou A, Papaxoinis G, et al. Endocrine-Related Adverse Events Associated With Immune-Checkpoint Inhibitors in Patients With Melanoma. *Cancer Med* (2019) 8(15):6585–94. doi: 10.1002/cam4.2533
18. Faje A, Reynolds K, Zubiri L, Lawrence D, Cohen JV, Sullivan RJ, et al. Hypophysitis Secondary to Nivolumab and Pembrolizumab is a Clinical Entity Distinct From Ipilimumab-Associated Hypophysitis. *Eur J Endocrinol* (2019) 181(3):211–9. doi: 10.1530/eje-19-0238
19. Garon-Czmil J, Petitpain N, Rouby F, Sassier M, Babai S, Yéléhé-Okouma M, et al. Immune Check Point Inhibitors-Induced Hypophysitis: A Retrospective Analysis of the French Pharmacovigilance Database. *Sci Rep* (2019) 9 (1):19419. doi: 10.1038/s41598-019-56026-5
20. Robert C, Ribas A, Schachter J, Arance A, Grob JJ, Mortier L, et al. Pembrolizumab Versus Ipilimumab in Advanced Melanoma (KEYNOTE-006): *Post-Hoc* 5-Year Results From an Open-Label, Multicentre, Randomised, Controlled, Phase 3 Study. *Lancet Oncol* (2019) 20(9):1239–51. doi: 10.1016/s1470-2045(19)30388-2
21. Antoniou S, Bazazo G, Röckl L, Papadakis M, Berg C. Late-Onset Hypophysitis After Discontinuation of Nivolumab Treatment for Advanced Skin Melanoma: A Case Report. *BMC Endocr Disord* (2021) 21(1):191. doi: 10.1186/s12902-021-00854-y
22. Otsubo K, Nakatomi K, Furukawa R, Ashida K, Yoneshima Y, Nakanishi Y, et al. Two Cases of Late-Onset Secondary Adrenal Insufficiency After Discontinuation of Nivolumab. *Ann Oncol* (2017) 28(12):3106–7. doi: 10.1093/annonc/mdx497
23. Boswell L, Casals G, Blanco J, Jiménez A, Aya F, de Hollanda A, et al. Onset of Fulminant Type 1 Diabetes Mellitus Following Hypophysitis After Discontinuation of Combined Immunotherapy. A Case Report. *J Diabetes Investig* (2021) 12(12):2263–66. doi: 10.1111/jdi.13604
24. Guerrero E, Johnson DB, Bachelot A, Lebrun-Vignes B, Moslehi JJ, Salem JE. Immune Checkpoint Inhibitor-Associated Hypophysitis-World Health Organisation VigiBase Report Analysis. *Eur J Cancer* (2019) 113:10–3. doi: 10.1016/j.ejca.2019.03.002
25. Postow MA, Chesney J, Pavlick AC, Robert C, Grossmann K, McDermott D, et al. Nivolumab and Ipilimumab Versus Ipilimumab in Untreated Melanoma. *N Engl J Med* (2015) 372(21):2006–17. doi: 10.1056/NEJMoa1414428
26. Faje AT, Lawrence D, Flaherty K, Freedman C, Fadden R, Rubin K, et al. High-Dose Glucocorticoids for the Treatment of Ipilimumab-Induced Hypophysitis is Associated With Reduced Survival in Patients With Melanoma. *Cancer* (2018) 124(18):3706–14. doi: 10.1002/cncr.31629
27. Kobayashi T, Iwama S, Yasuda Y, Okada N, Okuji T, Ito M, et al. Pituitary Dysfunction Induced by Immune Checkpoint Inhibitors Is Associated With Better Overall Survival in Both Malignant Melanoma and Non-Small Cell Lung Carcinoma: A Prospective Study. *J Immunother Cancer* (2020) 8(2): e000779. doi: 10.1136/jitc-2020-000779
28. Ascierto PA, Del Vecchio M, Mandalá M, Gogas H, Arance AM, Dalle S, et al. Adjuvant Nivolumab Versus Ipilimumab in Resected Stage IIIB-C and Stage IV Melanoma (CheckMate 238): 4-Year Results From a Multicentre, Double-Blind, Randomised, Controlled, Phase 3 Trial. *Lancet Oncol* (2020) 21 (11):1465–77. doi: 10.1016/s1470-2045(20)30494-0
29. Motzer RJ, Tannir NM, McDermott DF, Aren Frontera O, Melichar B, Choueiri TK, et al. Nivolumab Plus Ipilimumab Versus Sunitinib in Advanced Renal-Cell Carcinoma. *N Engl J Med* (2018) 378(14):1277–90. doi: 10.1056/NEJMoa1712126
30. Hellmann MD, Paz-Ares L, Bernabe Caro R, Zurawski B, Kim SW, Carcereny Costa E, et al. Nivolumab Plus Ipilimumab in Advanced Non-Small-Cell Lung Cancer. *N Engl J Med* (2019) 381(21):2020–31. doi: 10.1056/NEJMoa1910231
31. Min L, Hodi FS, Giobbie-Hurder A, Ott PA, Luke JJ, Donahue H, et al. Systemic High-Dose Corticosteroid Treatment Does Not Improve the Outcome of Ipilimumab-Related Hypophysitis: A Retrospective Cohort Study. *Clin Cancer Res* (2015) 21(4):749–55. doi: 10.1158/1078-0432.Ccr-14-2353
32. Nguyen H, Shah K, Waguespack SG, Hu MI, Habra MA, Cabanillas ME, et al. Immune Checkpoint Inhibitor Related Hypophysitis: Diagnostic Criteria and Recovery Patterns. *Endocr Relat Cancer* (2021) 28(7):419–31. doi: 10.1530/erc-20-0513
33. Chang LS, Barroso-Sousa R, Tolaney SM, Hodi FS, Kaiser UB, Min L. Endocrine Toxicity of Cancer Immunotherapy Targeting Immune Checkpoints. *Endocr Rev* (2019) 40(1):17–65. doi: 10.1210/er.2018-00006
34. Caturegli P, Di Dalmazi G, Lombardi M, Grosso F, Larman HB, Larman T, et al. Hypophysitis Secondary to Cytotoxic T-Lymphocyte-Associated Protein 4 Blockade: Insights Into Pathogenesis From an Autopsy Series. *Am J Pathol* (2016) 186(12):3225–35. doi: 10.1016/j.ajpath.2016.08.020

35. Iwama S, De Remigis A, Callahan MK, Slovin SF, Wolchok JD, Caturegli P. Pituitary Expression of CTLA-4 Mediates Hypophysitis Secondary to Administration of CTLA-4 Blocking Antibody. *Sci Transl Med* (2014) 6 (230):230ra45. doi: 10.1126/scitranslmed.3008002

Conflict of Interest: Author MH has consulted for Bristol Myers Squibb, CRISPR Therapeutics, Exelixis, and Nektar Therapeutics; received research funds from Achilles Therapeutics, Apexigen, Arrowhead, Arvinas, Astellas, AstraZeneca, Bayer, Bristol Myer Squibb, CRISPR Therapeutics, Corvus, Eli Lilly, Endocyte, Genentech, Genmab, GSK, Innocrin, Iovance, KSQ, Merck, Nektar Therapeutics, Novartis, Pfizer, Progenics, Sanofi Aventis, Seattle Genetics, Tmunity, Torque, and Unum; and has another relationship with Gamida Cell and Arvinas. Author HK has consulted for: Nektar, Iovance, Immunocore, Celldex, Array Biopharma, Merck, Elevate Bio, Instil Bio, Bristol-Myers Squibb, Clinigen, Shionogi, Chemocentryx, Calithera, and Signatero. Author MS has consulted for Adaptimmune, Pfizer, Kadmon, Pierre-Fabre, Biond, Nextcure, Incyte, Alligator, Bristol-Myers, Ocellaris, Simcha, Rootpath, Numab, Evolveimmune, Biontech, Immunocore, Glaxo Smith Kline, Adagene, Asher, Kanaph, iTEOS, Genocea, Trillium, Sapience, Targovax, Molecular Partners, Ontario Institute for Cancer Research, Jazz Pharmaceuticals, Gilead, Innate pharma, Tessa, Stcube, Oncosec, Regeneron, Astra Zeneca, Agenus, Idera, Apexigen, Verastem, Rubius, Genentech-Roche, Boston Pharmaceuticals, Servier, Dragonfly, Boehringer Ingelheim, Nektar, Pieris, Abbvie, Zelluna, and Seattle Genetics. Author MS has stock in: Johnson and Johnson, Glaxo-Smith Kline. Author MS has stock options in: Adaptive Biotechnologies, Amphivena, Intensity, Actym, Evolveimmune, Nextcure, Repertoire, Oncohost, Rootpath, Asher. Author SW has consulted for Array Biopharma and Magellan Rx. Institutional research funds have been granted by Bristol-Myers Squibb and Apexigen (HK, SW) and Merck (HK).

The remaining authors declare that the research was conducted in the absence of any commercial or financial relationships that could be construed as a potential conflict of interest.

Publisher's Note: All claims expressed in this article are solely those of the authors and do not necessarily represent those of their affiliated organizations, or those of the publisher, the editors and the reviewers. Any product that may be evaluated in this article, or claim that may be made by its manufacturer, is not guaranteed or endorsed by the publisher.

Copyright © 2022 Jessel, Weiss, Austin, Mahajan, Etts, Zhang, Aizenbud, Perdigoto, Hurwitz, Sznol, Herold and Kluger. This is an open-access article distributed under the terms of the Creative Commons Attribution License (CC BY). The use, distribution or reproduction in other forums is permitted, provided the original author(s) and the copyright owner(s) are credited and that the original publication in this journal is cited, in accordance with accepted academic practice. No use, distribution or reproduction is permitted which does not comply with these terms.

frontiers in Oncology

REVIEW
published: 10 March 2022
doi: 10.3389/fonc.2022.837059

Non-Melanoma Skin Cancers and Other Cutaneous Manifestations in Bone Marrow Failure Syndromes and Rare DNA Repair Disorders

Jennie Vagher†, *Amanda Gammon*†, *Wendy Kohlmann and Joanne Jeter**

Family Cancer Assessment Clinic, Huntsman Cancer Institute, University of Utah, Salt Lake City, UT, United States

Although most non-melanoma skin cancers are felt to be sporadic in origin, these tumors do play a role in several cancer predisposition syndromes. The manifestations of skin cancers in these hereditary populations can include diagnosis at extremely early ages and/or multiple primary cancers, as well as tumors at less common sites. Awareness of baseline skin cancer risks for these individuals is important, particularly in the setting of treatments that may compromise the immune system and further increase risk of cutaneous malignancies. Additionally, diagnosis of these disorders and management of non-cutaneous manifestations of these diseases have profound implications for both the patient and their family. This review highlights the current literature on the diagnosis, features, and non-melanoma skin cancer risks associated with lesser-known cancer predisposition syndromes, including bone marrow failure disorders, genomic instability disorders, and base excision repair disorders.

Keywords: non-melanoma skin cancer, cancer predisposition syndromes, bone marrow failure syndromes, skin cancer genetics, genomic instability disorders

OPEN ACCESS

Edited by:
Sapna Patel,
University of Texas MD Anderson Cancer Center, United States

Reviewed by:
Vijay Menon,
Yale University, United States
Maria Helena Ornellas,
Universidade Estadual do Rio de Janeiro, Brazil

****Correspondence:***
Joanne Jeter
Joanne.Jeter@hci.utah.edu

†These authors have contributed equally to this work and share first authorship

Specialty section:
This article was submitted to Skin Cancer, a section of the journal Frontiers in Oncology

Received: *16 December 2021*
Accepted: *17 February 2022*
Published: *10 March 2022*

Citation:
Vagher J, Gammon A, Kohlmann W and Jeter J (2022) Non-Melanoma Skin Cancers and Other Cutaneous Manifestations in Bone Marrow Failure Syndromes and Rare DNA Repair Disorders. Front. Oncol. 12:837059. doi: 10.3389/fonc.2022.837059

INTRODUCTION

Non-melanoma skin cancers are very common, but their hereditary risk factors receive little attention. In the general population, incidence of basal cell and squamous cell cancers varies significantly depending on geographic location, which is tied to levels of ultraviolet (UV) radiation exposure and population demographics. A systematic review of non-melanoma skin cancer incidence reported basal cell carcinoma incidence of 76.21/100,000 person-years and squamous cell carcinoma incidence of 22.65/100,000 person-years in England (1). By contrast, the reported incidences from Australia were markedly higher (884/100,000 for basal cell carcinoma & 387/100,000 person-years for squamous cell carcinoma). Data from both countries also showed marked regional differences (1) However, due to the high incidence rate and the low potential for metastatic disease, comprehensive data on non-melanoma skin cancer is often not recorded in cancer statistic databases such as the Surveillance, Epidemiology, and End Results Program (SEER) or GLOBOCAN (2, 3). This practice makes estimating its true worldwide incidence difficult (1, 2). While UV radiation exposure remains the primary risk factor for cutaneous non-melanoma skin cancer, this review highlights multiple genetic conditions that elevate the risk of skin cancer.

Of note, our review does not cover Nevoid Basal Cell Carcinoma syndrome (NBCCS) (also known as Gorlin syndrome or basal cell nevus syndrome (BCNS)). NBCCS is associated with a high lifetime risk for basal cell carcinoma (~90% of individuals with NBCCS) as well as an elevated risk for medulloblastoma. Multiple comprehensive reviews have been published on NBCCS, including Bresler 2016, as well as updates to management guidelines (4, 5). This review will synthesize the current literature on non-melanoma skin cancer risk in the following cancer predisposition syndromes: Telomere Biology Disorders, Fanconi anemia, Xeroderma pigmentosum, Bloom syndrome, Werner syndrome, Rothmund-Thompson syndrome, and Ferguson-Smith syndrome. This review will provide an overview of syndromic manifestations, incidence of skin cancers, and treatment/surveillance implications with the purpose of increasing provider awareness and correct diagnosis.

BONE MARROW FAILURE SYNDROMES

Telomere biology disorders and Fanconi Anemia are the most common bone marrow failure syndromes. Their causes lie in telomere maintenance and DNA repair, significantly disrupting the body's ability to protect itself from cancer development. Affected individuals have characteristic dermatologic features and experience elevated risks for young onset non-melanoma skin cancers, in addition to other risks for solid tumors and hematologic malignancy.

TELOMERE BIOLOGY DISORDERS

The telomere biology disorders (TBDs) constitute a spectrum of clinical disorders arising from short telomeres. Professor Ferdinand Zinsser is widely credited with the first publication on dyskeratosis congenita (DC), a subtype of the TBDs, in 1910 (6, 7). Classic DC is associated with the triad of oral leukoplakia, nail dystrophy, and reticulated skin pigmentation. However, since discovery of the *DKC1* gene in 1999, 13 more genes have been identified that cause short telomeres, leading the designation of TBDs as a reflection of the fundamental biology that unites these disorders (8, 9). In general, TBDs predispose individuals to develop bone marrow failure, acute myeloid leukemia/myelodysplastic syndrome (AML/MDS), interstitial lung disease, liver cirrhosis, and/or features of premature aging (i.e. early greying of the hair). Cutaneous manifestations associated with TBDs include both phenotypic manifestations, such as hyperkeratosis and/or reticulated skin pigmentation, as well as an increased risk to develop cutaneous carcinomas. Due to the changing landscape of TBDs, underdiagnosis of TBDs remains a challenge and the overall incidence is unknown. It is estimated that the classic subtype of TBDs, DC, has an incidence of 1 in 1,000,000, though DC accounts for less than 5% of all TBDs (10). The most common cause of mortality is bone marrow failure, followed by pulmonary complications and cancer (10).

Mechanism

Telomeres consist of double stranded TTAGGG nucleotide repeats at the ends of eukaryotic chromosomes, which protect these chromosomal ends from normally occurring DNA damage signaling and repair activities created by DNA breaks (11). Telomere length varies considerably within different populations, and telomere shortening is a normal consequence of aging (11). With every cell division, telomere lengths decrease. Eventually a critical threshold is reached, triggering cellular senescence, and some cells may then undergo apoptosis (10, 11).

The telomerase complex, including telomere reverse transcriptase (TERT) and its RNA component (TERC), is responsible for adding nucleotide repeats to telomeric ends (12). The shelterin subunits and complex, including protection of telomeres 1 (POT1), are involved in creating and stabilizing the T-loop structure, preventing DNA damage response, recruiting telomerase, and regulating telomere elongation (10). The CST (CTC1-STN1-TEN1) complex and other proteins play a role in telomere maintenance. Other reviews have been published on the mechanisms of telomeres (11).

Genes/Inheritance

Pathogenic germline variants (PGV) in 14 genes have been described as the cause for the TBDs, including *TERT*. Variants in these genes can be inherited in x-linked recessive, autosomal dominant, and autosomal recessive patterns; however, it is also possible for an individual to have a TBD due to a *de novo* PGV. There is considerable genetic heterogeneity, and most of the genes associated with TBDs have associations with multiple TBD subtypes and inheritance patterns. For example, DKC1 is associated with x-linked recessive disease, but PGV in this gene can be seen in individuals with classic DC features as well as those who present in infancy with Hoyeraal-Hreidarsson syndrome (HH). PGV in genes such as *RTEL1*, *TINF2*, and *ACD* are associated with autosomal dominant (heterozygous) risks for pulmonary fibrosis or bone marrow failure as well as autosomal recessive (homozygous or compound heterozygous) risks for HH. Variants in *NAF1, TERT, TERC, PARN*, and *RTEL1* have been associated with clinical presentations of pulmonary fibrosis, liver disease, or bone marrow failure in middle or later age (8). In individuals who have autosomal dominant disease, genetic anticipation affecting disease severity in successive generations has been reported (13, 14).

Means of Diagnosis

The diagnosis of TBDs is complex. Though genetic testing can aid in making the diagnosis of a TBD, it is not the gold standard. Individuals needing diagnostic testing are recommended to undergo flow cytometry with fluorescent *in situ* hybridization (flow FISH) in leukocyte subsets (15). Flow FISH is the only

clinical validated test proven for TBD diagnosis (16). Total lymphocyte telomeres measured to be less than the 1st centile for age are 97% sensitive and 91% specific with a positive predictive value of 85% for the diagnosis of a TBD (15). Accelerated telomere shortening is induced by exposure to intensive chemotherapies, which can affect the results of telomere length measurement testing (17). More studies are needed to determine the effect of different treatments on telomere attrition.

Genetic testing, once very short telomeres are identified, complements clinical evaluations and telomere length measurement testing. Genetic testing can also be useful to help determine inheritance patterns, to identify genotype-phenotype correlations, and to offer to family members seeking knowledge of disease status. Approximately 20-30% of individuals diagnosed with classic DC do not have an identifiable PGV, which means a substantial number of patients who have a diagnosable TBD *via* telomere length measurement testing do not have a PGV and a diagnosis may be missed if relying on genetic testing alone (18).

Population/Epidemiology

The overall incidence of TBDs cannot be accurately estimated. DC has an incidence of 1 in 1,000,000, though DC accounts for less than 5% of all TBDs (10). It is estimated that 41% of familial mixed hematologic and interstitial lung disease and 3% of familial hematologic disorders are due to TBDs (19). As with most genetic predispositions, it is likely that TBDs are underdiagnosed, which contributes to the difficulty in calculating incidence.

Clinical Characteristics: Cutaneous

TBDs are associated with the classic mucocutaneous triad of nail hypoplasia, reticulated skin pigmentation, and oral leukoplakia. Though this triad is diagnostic, it may be absent or progressive in individuals, leading to underdiagnosis. In a publication of 60 individuals with DC, 37% had the complete clinical triad, while 10% lacked all triad features (8, 20). Other cutaneous findings have been reported such as adermatoglyphia (loss of fingerprints), palmoplantar hyperkeratosis, hyperhidrosis, premature graying, scalp/eyelash hair loss, epiphora, and lash irritation (20, 21). Individuals who are carriers of *DKC1* PGVs may have some features of the mucocutaneous triad, but largely remain asymptomatic.

Clinical Characteristics: Non-Cutaneous

Bone marrow failure (aplastic anemia) may be the first presenting feature of TBDs, and the risk is highest for individuals who have classic DC (about 80-90% lifetime risk) (22). Risks to develop AML and MDS are most significant over age 50. In a recent publication, approximately 18 of 180 patients with a TBD were diagnosed with AML or MDS (23). Other hematologic conditions have been described, such as macrocytosis, isolated cytopenias, paroxysmal nocturnal hemoglobinuria and essential thrombocythemia (24).

Incidence of Skin Cancer

Cutaneous squamous cell carcinomas (cSCCs) have been reported in 1.5% of individuals with TBDs and are diagnosed at young ages. There is a significantly increased risk to develop mucosal SCCs, especially in the buccal mucosa, nasopharynx, esophagus, rectum, vagina, and cervix (25). For the purpose of this review, we will focus on cSCCs; other publications have reported on risks for mucosal SCCs in the TBD population (10, 18). A summary of publications reporting on non-melanoma skin cancer in chronological order will be included below.

Data from the United Kingdom Dyskeratosis Congenita Registry (DCR) in 2000 reported 148 patients with TBDs and eight solid tumors amongst the patients. There was a single patient reported with cutaneous carcinoma unspecified at age 20 years. It is unclear if the patient with cutaneous carcinoma in this series was male or female and whether this was a pre-transplant diagnosis (22).

A literature review and quantitative analysis from the National Cancer Institute's Inherited Bone Marrow Failure Syndrome (NCI IBMFS) was published in 2009. The literature review (1910-2008) reported 60 solid tumors in 51 patients. This included eight patients with cSCCs, diagnosed at a median age of 21 with a range of diagnosis between age 4 and 43. A male predominance was reported (7 males and 1 female). All of these skin carcinomas were reported prior to hematopoietic stem cell transplant (HSCT). The quantitative analysis (2002-2008) included 50 patients. Of these patients, there was a single case of cutaneous carcinoma and this patient was diagnosed with BCC one year after HSCT at age 29 (26, 27).

Another literature review in 2010 included 560 cases of TBDs in the literature. Of these patients, six total cSCCs were reported, with five being reported in male patients. The median age of diagnosis was 18, and the range was age four to 34 (28).

Data from NCI IBMFS in 2018 included 197 TBD patients from 108 families. This analysis (2002-2016) reported 14 SCC and six BCC in nine patients. Of these nine patients, 5 of these patients reported two or more skin cancers (2 patients with two each, 2 with three each, and one with five). An additional skin cancer (age and subtype unknown) was reported in a TBD patient during the development of the manuscript, bringing the total skin cancers in this cohort to 10. The age of skin cancer diagnoses ranged from 14 to 54 with a median age of 35 at diagnosis (18).

Other registry TBD cohorts exist, though some registries have intentionally excluded cutaneous cancer diagnoses and it is unclear if cutaneous cancers were intentionally excluded in others due to limitations in methodology (23, 29).

Surveillance and Management Considerations: Cutaneous

Thorough skin examinations with a dermatologist are recommended at least annually, though starting age for screening is not specified (21, 30). Often SCC arises from leukoplakic plaques, and dermatology exams are recommended to focus on mucosal and genital areas. Surveillance for head and neck SCC is recommended to start at age 16 (31). According to

data presented, age of cSCCs ranged from age four to age 54 with median ages of 18, 21, and 35 from the NCI IBMFS and literature review data sets (18, 26–28). The data is limited regarding the number of cSCCs reported in those under age 18, so there are gaps in our understanding of whether skin exams would be beneficial in adolescence. In other cancer predisposition syndromes, the youngest known age of a diagnosis provides a guide of when to start surveillance, so for TBDs, age four would be the youngest diagnosis and thus an appropriate age to start skin exams (28).

Prevention strategies are also recommended, including limiting sun exposure, using sunscreen regularly, using facial moisturizer with sunscreen every day, wearing hats and sun protective clothing, avoiding tanning beds, awareness of reflected sun off of snow and water, and performing regular self-skin exams (10, 21). To the authors' knowledge, no discussion of best treatment for non-melanoma skin cancers has been proposed.

Surveillance and Management Considerations: Non-Cutaneous

Published guidelines for the management of TBDs suggest baseline surveillance and annual surveillance depending on clinical presentation. In addition to dermatologic screening as discussed above, individuals are recommended to undergo evaluation for risks relating to hematology, pulmonology, immunology, otolaryngology, and gastroenterology, among other specialty providers. Bone marrow failure is typically treated with bone marrow transplant. Recommendations can be complex given the needs of this patient population, so referral to a center that has expertise in the management of bone marrow failure syndromes is recommended (21).

FANCONI ANEMIA

Fanconi anemia (FA) is a heterogeneous syndrome associated with DNA repair defects. FA is associated with risks for bone marrow failure, acute myeloid leukemia/myelodysplastic syndrome, congenital abnormalities, endocrine anomalies, and/or solid cancers. Dr. Guido Fanconi's characterization of three brothers in a family in 1927 lead to the naming of FA, though it was not for another 40 years that the mechanism of spontaneous chromosomal breakage was identified as the etiology of FA (32, 33). The cutaneous manifestations associated with FA include both phenotypic manifestations, such as café au lait macules, as well as an increased risk to develop cutaneous carcinomas. The most common solid tumor in individuals with FA are head and neck squamous cell carcinomas (HNSCC), but Wilms tumor and medulloblastoma are also seen. FA is primarily an autosomal recessive condition. FA affects 1 in 100,000 births in the USA, and there are well known founder effects causing higher incidences amongst populations outside of the USA. The main causes of death are cancer, bleeding, infection, and complications from hematopoietic stem cell transplant (HSCT) (34). Survival has improved in high resource countries due to a reduction in mortality by bleeding or infection complications, leading to a need for increased awareness of skin cancer risks in this population (35).

Mechanism

The FA pathway assists in DNA repair, DNA replication, and other cellular processes. A principal function of this pathway is to remove a critical barrier, interstrand crosslink lesions (ICL), which interfere with DNA replication and genetic transcription and must be repaired or bypassed for cells to survive (36). Both nucleotide excision repair and homologous recombination pathways are required to make major repairs to ICLs (37). Each human cell has to repair approximately 10 interstrand crosslinks per day, and between 20-40 lesions can lead to cell death (38, 39). Interstrand crosslinks are generated both exogenously and endogenously, and when unrepaired, they lead to DNA breakage and chromosomal rearrangements, which lead to the development of cancer (39, 40). The FA pathway is the only known mechanism of repair for interstrand crosslink lesions (41). There is also increasing evidence that subsets of FA proteins contribute to other pathways (37, 41).

Specifically relating to non-melanoma skin cancers, a recent publication has highlighted alternative mechanisms to explain an increased risk for skin cancers suggesting that individuals with FA have inherent subclinical dermatologic vulnerabilities causing the significant risk to develop SCC (42). The authors hypothesize that inherited structural defects of the FA epidermis (and potentially mucosa) cause vulnerabilities to mechanical and/or environmental stress, thus further compounding the existing genome instability to promote SCC (42). The FA pathway is essential in the developing epidermis for sustained keratinocyte adhesion and appropriate restraint of proliferation (42).

Means of Diagnosis

Cells from patients with Fanconi Anemia are extremely sensitive to ICL-generating agents, such as mitomycin C (MMC) or diepoxybutane (DEB). Thus, the gold standard test for the diagnosis of FA is a chromosome breakage analysis (CBA) performed on a blood sample. Genetic testing can aid in the diagnosis of FA, but is typically only performed after a CBA. CBA may not be definitive due to mosaicism in peripheral blood, hypomorphic variants, and other chromosomal instability disorders that mimic FA (43). Interpretation of a CBA should made with a genetics provider familiar with BMF syndromes and testing, especially if there is a high level of concern for underlying FA.

Genes/Inheritance

There are over 20 genes that have been implicated in the etiology of FA (42). All pathogenic variants in these genes are associated with autosomal recessive disease with the exception of *FANCB* (x-linked) and *FANCR* (autosomal dominant). The majority of FA is associated with pathogenic variants in the *FANCA* gene (44). Importantly, most individuals who are carriers for FA do not have any associated risks with being carriers; rather, determining carrier status is most important for family

planning. A portion of individuals who are carriers for FA will have an increased risk to develop adult-onset cancers, such as breast or ovarian cancers. Pathogenic variants in *BRCA2/FANCD1, PALB2/FANCN, BRIP1/FANCJ*, and *RAD51C/FANCO* have known adult-onset cancer risks, and there are recommendations for carriers to have increased cancer surveillance, consider chemoprevention, or undergo preventative surgeries (45).

Population/Epidemiology

FA affects 1 in 100,000 births in the USA, with a carrier frequency of approximately 1 in 181 (range 1:156-1:209) in the USA (46). There are known founder effects in genetically isolated populations, causing a birth incidence in Afrikaners of 1 in 22,000 (1:88) and in Israel of 1 in 45,000 (1:93) (46, 47). The Spanish Gypsy population has the highest carrier frequency for FA with a founder *FANCA* variant (1:64-1:70) while a significant portion (1%) of Bantu speaking Black individuals in Southern Africa have a founder *FANCG* variant (48, 49).

Clinical Characteristics: Cutaneous

Pigmentary changes of the skin have been reported by case series as the most common (up to 68%) cutaneous skin feature in FA. These pigmentary changes include cafe-au-lait macules (CALMs), flexural hyperpigmentation, and hypopigmented macules (32, 50). In a recent review of cutaneous features in FA, at least one cutaneous feature was present in 97% of participants with the most common being CALMs. Both a combination of diffuse hyperpigmented and hypopigmented macules and a combination of CALMs with hypopigmented macules are cutaneous features that may help to differentiate FA from other genetic syndromes with similar presentations (50).

Clinical Characteristics: Non-Cutaneous

Cytopenia and bone marrow failure are the most common presenting features in FA. Most individuals with FA will develop a cytopenia progressing to bone marrow failure. Thrombocytopenia with red blood cell macrocytosis and elevated fetal hemoglobin often lead to the diagnosis of FA (51). Individuals with FA present with bone marrow failure at various times in life, and the literature suggests 75% present within the first decade of life (28, 52, 53). Adults with FA do not typically present with bone marrow failure, but rather due to a diagnosis of cancer or severe toxicity after chemotherapy for treatment of a malignancy (52–54). There are risks to develop AML and MDS, both in childhood and adulthood (55, 56).

Incidence of Skin Cancer

Cutaneous squamous cell carcinomas (cSCCs) have been reported in individuals with FA, though the exact risk to develop cSCCs in FA is unknown. There is a significantly increased risk to develop mucosal SCCs, especially in the buccal mucosa, nasopharynx, esophagus, rectum, vagina, and cervix (25). For the purpose of this review, we will focus on cSCCs (and other non-melanoma skin cancers), as other publications have reported on risks for mucosal SCCs in the FA population (57, 58). A summary of publications reporting on non-melanoma skin cancers in chronological order will be included below.

The International Fanconi Anemia Registry (IFAR) in 2003 reported on 754 individuals with FA. This included three individuals who reported cSCCs. Median and age range of diagnoses were not available (53).

Data from the National Cancer Institute's Inherited Bone Marrow Failure Syndrome (NCI IBMFS) in 2010 included 66 patients with FA. In this analysis (2002-2008), two diagnoses of cSCCs at age 33 and 38 and one diagnosis of BCC at age 31 were reported (27).

In 2016, the Italian Fanconi Anemia Registry reported 180 individuals with FA. Of these patients, 20 developed solid tumors. This included one individual with a diagnosis of unspecified skin cancer. Age of diagnosis was not available. This patient was reported to have multiple tumors, including a genital tract, breast, and head/neck tumor (34).

Data from the NCI IBMFS in 2018 included 163 individuals with FA. In this analysis (2002-2016), 23 SCC and 12 BCC were diagnosed amongst 11 patients. The median age of diagnosis was 33 years old, and the range of diagnosis was from age 26 to 41. Eight patients reported at least two skin cancers (six patients with two, one with three, and one with 17 separate skin cancers). An additional unspecified skin cancer (age unknown) was reported in an FA patient during the development of the manuscript, bringing the total skin cancers in this cohort to 36 (18).

A recent study from a German Bone Marrow Failure Registry in 2021 reported 421 individuals with FA. Of these patients, 33 patients developed cancer. This included one individual with a skin carcinoma NOS at age 15 prior to the development of AML at age 16. Notably in this cohort, cancer risks into adulthood (over age 17) were not ascertained, which limits cancers reported and the true estimate of cutaneous carcinomas may be underrepresented due to the age cutoff (59).

Data from a Cincinnati-based FA cohort in 2021 included 105 individuals with FA. Of these patients, nine patients reported a history of cutaneous SCC or BCC. There was no median age of diagnosis nor any range of diagnoses reported, though all of these patients were adults when they were included in the publication (between ages 24 to 51). There was one case of melanoma in this publication. Age of diagnosis was not included, but the site of the lesion was on the breast. Three of the patients included were post-transplant, including a patient who reported 50+ cSCCs (42).

Other FA cohort publications exist, but do not include any cases of non-melanoma skin cancers (28, 29, 60). An interesting note is that melanoma is rarely reported in individuals with FA. A hypothesis has been proposed that the FA pathway may be protective against melanoma tumorigenesis in patients with FA (61).

Surveillance and Management Considerations: Cutaneous

Total body skin examinations are recommended annually starting at the age of 18. Despite the recommendation to start surveillance in young adulthood, preventative behaviors for sun

protection and avoidance should be implemented at an early age. These include limiting sun exposure, using sunscreen regularly, wearing hats and sun protective clothing, avoiding tanning beds, and performing regular self-skin exams (51).

In the general population, therapies such as topical chemotherapy agents (5-Fluorouracil) and other drugs that stimulate an immune response to target precancerous lesions or cancers may be utilized to treat non-melanoma or melanoma skin cancers. The tolerability and efficacy of these agents in FA have not been well-studied. In this population, the best curative option to treat non-melanoma skin cancers and melanoma remains surgical removal (51).

Surveillance and Management Considerations: Non-Cutaneous

Guidelines for the management of FA are published through the Fanconi Anemia Research Foundation (34). Guidelines suggest baseline surveillance and annual surveillance depending on clinical presentation. In addition to the dermatologic screening detailed above, individuals are recommended to undergo evaluation for risks relating to hematology, immunology, otolaryngology, and gastroenterology, among other specialty providers. Cancer or aplastic anemia treatment may require dose reduction depending on chemotherapy utilized as well as avoidance of use of radiation therapy. Bone marrow failure often requires hematopoietic stem cell transplant. Recommendations can be complex given the needs of this patient population, so referral to a center that has expertise in the management of bone marrow failure syndromes is recommended.

GENOMIC INSTABILITY SYNDROMES

The following three syndromes, Bloom, Werner, and Rothmund-Thomson, share multiple features. Their causes lie primarily in the genes which encode for the RecQ family of helicases. Lack of these helicase proteins results in genomic instability, causing disruption in multiple body processes, including aging, growth, immunity, cell resistance to UV radiation, and DNA repair. Affected individuals have characteristic dermatologic features and experience elevated risks for young onset non-melanoma skin cancers, sometimes with unusual histologies or locations.

BLOOM SYNDROME

In 1954, dermatologist Dr. David Bloom first reported on three individuals with similar features suggesting a syndrome: growth deficiency, unique erythematous lesions on the face over the cheeks and nose (butterfly rash), and significant sun sensitivity leading to additional skin lesions on the lips, eyes, and other sun exposed areas (62). This syndrome now bears Dr. Bloom's name and is also associated with immunodeficiency, increased cancer risks, lung disease, diabetes, and fertility concerns (premature menopause/male infertility). Much of the available research on Bloom syndrome comes from the Bloom Syndrome Registry, which was started in 1960 at Weill Cornell Medicine (Cornell University) (http://www.med.cornell.edubsr/).

Mechanism

Bloom syndrome results from a lack of functional BLM protein. BLM is a DNA helicase responsible for restricting sister chromatid exchanges (SCE). BLM is in a family of RecQ helicases that includes WRN and RECQL4, responsible for Werner syndrome and Rothmund-Thompson syndrome, respectively. Absence of functional BLM leads to significantly increased rates of SCE during DNA replication, which leads to elevated genomic instability. Injecting a line of Bloom syndrome cells with cDNA containing working copies of BLM results in normal rates of SCE (63). BLM's helicase activity is also directly involved with the double stranded DNA break repair process through interaction with DNA2, RPA, and the Mre11-Rad50-Nbs1 (MRN) complex (64).

Genes/Inheritance

Bloom syndrome is an autosomal recessive condition caused by biallelic pathogenic variants in the *BLM* gene, also called *RECQL3*. Most *BLM* pathogenic variants result in protein truncation (63). In an evaluation of the 64 different *BLM* pathogenic mutations reported by individuals in the Bloom Syndrome registry, 54 were variants leading to protein truncation and 10 were missense variants (65). Backers et al. recently described an individual with clinical Bloom syndrome who had a deep intronic variant in *BLM* (c.3020-258A>G, intron 15) along with a nonsense variant in exon 18 (called c.3379C>T, p.Gln1127Ter) on the opposite allele (66).

Means of Diagnosis

The very high level of SCE seen in Bloom syndrome cells is pathognomonic for the condition. SCE analysis was used for many years to confirm a diagnosis of Bloom syndrome (67). Today molecular genetic testing of *BLM* to assess for biallelic mutations is the initial test when Bloom syndrome is suspected clinically.

Population/Epidemiology

Bloom syndrome is very rare, with less than 300 affected individuals reported in the Bloom syndrome registry. A higher incidence of Bloom syndrome is seen in the Ashkenazi Jewish population due to the presence of a common founder variant (called c.2207_2212delinsTAGATTC). Studies estimate between 1 in 37 to 1 in 100 individuals of Ashkenazi Jewish decent are heterozygous carriers of this pathogenic variant in *BLM* (68, 69). A less common founder variant in the Ashkenazi Jewish population is c.2407dupT.

Clinical Characteristics: Cutaneous

The red "butterfly" rash (erythema and telangiectasias) seen on the cheeks, nose, eyelids, and ears of individuals with Bloom syndrome typically develops within the first year of life (67, 70, 71). This rash is correlated with the onset of sun exposure for the affected child. The rash can also affect the arms and hands and can worsen with continued sun exposure (67, 71). Individuals with Bloom syndrome

also have elevated rates of café-au-lait macule development and areas of hypopigmentation (67, 70, 71). Cheilitis and poikiloderma can also be present (67, 71).

Clinical Characteristics: Non-Cutaneous

Patients with Bloom syndrome typically show growth deficiency prenatally and into adulthood (70). Attainment of developmental milestones and cognitive factors are not typically impacted by Bloom syndrome (70). Individuals can experience immunodeficiency. While infections can be frequent, they are not often severe (72). Impaired fertility can be seen in both women and men with Bloom syndrome. Most men reported with Bloom syndrome are infertile and many women experience early menopause (67, 71, 73). Risks for endocrine dysfunction, particularly diabetes and hypothyroidism, are also elevated (67).

A range of non-cutaneous malignancies have been reported in Bloom syndrome. Leukemia and lymphoma are the most common, followed by colon and breast cancers (67). Using data from the 277 individuals enrolled in the Bloom syndrome registry at that time, Cuniff et al. reported that 33.4% developed cancer by age 25 and 80.9% developed cancer by age 40 (67).

Incidence of Skin Cancer

Within the Bloom syndrome registry data, basal cell carcinoma is the most frequently reported cutaneous cancer (13 reported basal cell carcinomas among 277 registry patients) (67). Mean age at basal cell carcinoma diagnosis was 28 (range 18-38) (67). Only 4 squamous cell carcinomas were reported (age range 35-36), as well as 4 undefined skin cancers (67). No melanoma diagnoses are known among patients enrolled in the Bloom syndrome registry (67).

Surveillance and Management Considerations: Cutaneous

Individuals with Bloom syndrome are recommended to limit sun exposure and utilize sun protective behaviors (including frequent application of SPF 30 sunscreen and use of protective clothing). Annual dermatology exams are also recommended, although no specific starting age is specified (67).

Surveillance and Management Considerations: Non-Cutaneous

Comprehensive management recommendations for individuals with Bloom syndrome based on data from the Bloom Syndrome Registry can be found in Cuniff et al. (67). In terms of cancer surveillance, individuals with Bloom syndrome are recommended to undergo annual colonoscopy, with FIT stool testing every 6 months, starting at age 10-12 (31, 67). While a moderately increased risk for colon cancer has been described in heterozygous carriers of a single pathogenic *BLM* variant, data has remained mixed on this association and no changes to colorectal cancer screening are currently recommended (74, 75). Annual breast MRI is recommended to begin at age 18 for individuals at elevated breast cancer risk (31, 67). Due to concerns about ionizing radiation conferring an increased risk for secondary malignancy, screening imaging should utilize MRI or ultrasound whenever possible (67). Individuals with Bloom syndrome should be alert for signs of leukemia and lymphoma, including increasing pallor, fatigue, enlarging lymph nodes, abnormal bleeding or weight loss, and petechiae (67). Screening for lymphoma *via* whole body MRI every 1-2 years is recommended to begin at age 12-13 (67). For Wilms tumor, abdominal ultrasound every 3 months until age 8 is recommended, along with awareness of symptoms (abdominal mass, blood in the urine) (67).

Treatment of malignancies in patients with Bloom syndrome is complicated by increased sensitivity to radiotherapy and chemotherapy, leading to elevated adverse reactions and secondary malignancies (67, 76). Reduction in chemotherapy dosage (suggested 50% or lower) has been recommended (67). Use of radiation therapy should be avoided whenever possible (67).

Immunodeficiency screening is recommended for anyone with Bloom syndrome who experiences recurrent infection or is being treated with immunosuppressive drugs (67). Growth hormone treatment can also be considered to potentially impact growth deficiency (67).

WERNER SYNDROME

Dr. Otto Werner first detailed this syndrome in 1904 (77, 78). The primary clinical presentation of Werner syndrome is of premature aging. The first sign of Werner syndrome can be slowed growth starting around puberty, although many affected individuals are not diagnosed until their late 30s-40s (79). Additional symptoms of Werner syndrome, including bilateral cataracts, thinning of the skin, and hair graying, generally present in a person's 20s. Median life expectancy for individuals with Werner syndrome is age 54, with cancer and atherosclerosis driving mortality (77, 79, 80). The International Werner Syndrome Registry at the University of Washington (https://dlmp.uw.edu/research-center/werner/registry) and the Japanese Werner Consortium at Chiba University are the leading sources of research on Werner syndrome.

Mechanism

Werner syndrome results from the myriad effects of increased genomic instability due to lack of function of the WRN protein. WRN has both helicase and exonuclease functions (79, 81). It is involved with multiple factors in the base excision repair and double strand break DNA repair pathways (82). WRN is also believed to assist with telomere maintenance and to interact with intricate DNA formations during transcription and replication (79, 83, 84). Laarmann et al. showed that functional WRN is necessary for full endothelial cell motility; they propose that lack of WRN function may lead to the increased atherosclerosis risks in Werner syndrome in multiple ways, due to detrimental impacts on blood vessel repair and inflammation (82).

Genes/Inheritance

Werner syndrome is an autosomal recessive condition caused by biallelic pathogenic variants in *WRN* (81). As of 2017, a total of 83 different pathogenic variants in *WRN* have been described, per data from the International Werner Syndrome Registry and Japanese Werner Consortium, plus published literature (79). A complete list of these variants is available at http://www.pathology.washington.edu/research/werner/database/. The most frequent WRN pathogenic variant in the Japanese population is c.3139-1G>C, which has been reported to account for 70.7% of WRN pathogenic variants in the Japanese Werner Consortium (79). Two additional WRN variants are relatively common in Japan, c.1105C>T and c.3446delA (79). Most pathogenic variants in *WRN* lead to protein truncation, although a few missense variants have also been reported that disrupt protein function (79).

Means of Diagnosis

Werner syndrome can be clinically diagnosed using a set of criteria proposed by the International Registry of Werner Syndrome (84). The cardinal signs are defined as: 1) bilateral cataracts, 2) premature graying/thinning of the scalp hair, 3) specific dermatological features (tight and atrophic skin, skin ulceration, hyperkeratosis, subcutaneous atrophy (regional), altered pigmentation, and "bird-like" facies), and 4) short stature. Additional signs of Werner syndrome include: diabetes, flat feet, osteoporosis, osteosclerosis of distal phalanges of fingers/toes, soft issue calcification, vocal changes, premature atherosclerosis or heart attack, and hypogonadism (84). To have a definite diagnosis of Werner syndrome, individuals need to have all four cardinal signs, plus two additional signs. A probable diagnosis of Werner syndrome occurs in patients with bilateral ocular cataracts, premature graying/thinning of the scalp hair, and the dermatological features outlined above plus two additional signs (84). Identification of biallelic pathogenic *WRN* variants can help further distinguish a diagnosis of Werner syndrome from other syndromes which can cause features of premature aging.

Population/Epidemiology

While individuals with Werner syndrome have been identified worldwide, the majority of reported cases of Werner syndrome (approximately 60%-80%) have been identified in Japan (Takeomoto & Yokote 2020). In Japan, approximately 3 in 100,000 individuals have Werner syndrome (2005 Shibuya).

Clinical Characteristics: Cutaneous

Development of skin ulcers is a primary source of morbidity for individuals with Werner syndrome. Approximately 40% of individuals with Werner syndrome develop skin ulceration (85). They most commonly develop at pressure points on the leg, ankle, soles of the feet, and elbows (86).

Skin thinning, tightness, and dryness are common signs of premature dermatological aging in Werner syndrome (85). Patients can be prone to developing calluses, which if not treated, can progress to skin ulcers (85). Poikiloderma has also been reported in patients with Werner syndrome (85).

Clinical Characteristics: Non-Cutaneous

Individuals with Werner syndrome develop multiple features of aging significantly earlier than the general population, including early hair graying, type II diabetes, cataracts, and arteriosclerosis (77). Of note, an increased risk for dementia or age-related cognitive impairment has not been reported in Werner syndrome (84). It is estimated that 55% of individuals with Werner syndrome develop type II diabetes, with a mean age of onset in the late 30s (87). Osteoporosis has been documented in approximately 41% of patients with Werner syndrome (88).

The most common non-cutaneous cancers associated with Werner syndrome include thyroid cancer (particularly follicular type), soft-tissue sarcomas, leukemia/pre-leukemia/lymphoma, and osteosarcoma (77, 80). The estimated median age for cancer diagnosis for patients with Werner syndrome living in Japan is 44.5 years (80). An elevated incidence of meningioma development (both benign and malignant) has also been reported in Werner syndrome (80). A systemic review of cancer incidence reported in Werner syndrome found that 22% of individuals developed multiple primary malignancies (80).

Incidence of Skin Cancer

Non-melanoma skin cancer (basal and squamous cell) has been reported in individuals with Werner syndrome. In the systemic review noted above, non-melanoma skin cancer accounted for 4.8% of all reported malignancies in patients with Werner syndrome (12 cases among 189 patients) (80). An earlier review of malignancies reported in Werner syndrome between 1939 – August 1995 identified 10 cutaneous non-melanoma cancers out of a total 186 reported neoplasms (89).

Individuals with Werner syndrome have an elevated risk for melanoma, particularly uncommon forms of melanoma. Shibuya et al., reported on a 44 year-old woman with Werner syndrome who developed three primary malignant melanomas (one labial, two on sole of the left foot) (77). They identified 26 other reported individuals in the literature with Werner syndrome and melanoma, including two other patients with multiple primary melanomas (77). Of note, 15 of the reported malignant melanomas were acral while 10 occurred intranasal (77). Lauper found a standardized incidence ratio (SIR) for melanoma in patients with Werner syndrome of 53.5 compared to the general Osakan population (80).

Surveillance and Management Considerations: Cutaneous

Treatment and management of skin ulcers is a key concern for patients with Werner syndrome. Topical medications and dressings are primarily recommended for treatment of skin ulcers (86). Surgical intervention with skin grafts can be considered for ulcers that are resistant to healing (86). Annual dermatology exam is recommended for patients starting at the time of diagnosis with Werner syndrome to assess for calluses, ulcers, and malignancies (90). Special care should be taken

during the dermatology exam to carefully examine any area suspicious for an ulcer or callus as cutaneous malignancies have been reported in the same areas as well (86). Concerns regarding adverse effects from chemotherapy for malignancies (cutaneous and non-cutaneous), including elevated immunosuppression and potential for secondary malignancies, have been raised for patients with Werner syndrome, although few examples of adverse effects of treatment have been reported to date (77, 80).

Surveillance and Management Considerations: Non-Cutaneous

A comprehensive update to management recommendations for Werner syndrome was recently published in the journal Geriatrics and Gerontology International (91). Bringing together Werner syndrome experts, the authors created consensus recommendations for the treatment and management of primary Werner syndrome features, including dyslipidemia and fatty liver, sarcopenia, diabetes, osteoporosis, infection, skin ulcers, and tendon calcifications.

ROTHMUND THOMSON SYNDROME

Rothmund-Thomson syndrome (RTS) was first described in 1868 by ophthalmologist Auguste Rothmund (92). It is characterized by dermatological features (rash progressing to poikiloderma), bilateral juvenile cataracts, short stature, dystrophic hair/nails, elevated risk for cancer (particularly osteosarcoma), and increased risk for infertility. Cognition is typically unaffected. Malignancy is a significant cause of mortality in RTS, but lifespan can be otherwise normal (93). Rothmund-Thomson has been classified into two types, with Type II being the most common. Patients with Type I RTS do not appear to have the same elevated cancer risks or skeletal anomalies seen in many individuals with Type II, but do develop bilateral cataracts (which is not generally seen with RTS II) (94, 95).

Mechanism

Rothmund-Thomson syndrome results from loss of functional RECQL4 or ANAPC1. RECQL4 is a DNA helicase in the same family as WRN and BLM (96). REQL4 appears to be involved in double stranded DNA repair through stabilization of the Mre11-Rad50-Nbs1 complex; absence of functional RECQL led to premature degradation of the MRN complex *in vitro* (97). APC1 is a ubiquitin ligase and the protein coded for by *ANAPC1*. APC1 is key to appropriate movement of cells through the cell cycle, in particular the transition from metaphase to anaphase, as well as regulation of DNA replication (94, 98).

Genes/Inheritance

Rothmund-Thomson syndrome (RTS) is an autosomal recessive condition most often caused by pathogenic variants in *RECQL4*. Recently, pathogenic variants in *ANAPC1* have been associated with autosomal recessive RTS Type I (94). Pathogenic variants in *RECQL4* are associated with RTS Type II.

Means of Diagnosis

The pattern of poikiloderma development in early childhood is highly characteristic of Rothmund-Thomson syndrome and distinct from the butterfly rash that develops in Bloom syndrome. Genetic testing of REQL4 and ANAPC1 can also assist in confirming a diagnosis of RTS. Approximately 30% of individuals affected with RTS will not have identifiable pathogenic variants in *REQL4* or *ANAPC1* (93).

Population/Epidemiology

Rothmund-Thomson is a very rare hereditary condition, with fewer than 500 cases reported in the literature (93, 95). Carrier frequency is currently unclear.

Clinical Characteristics: Cutaneous

The typical initial presenting symptom of Rothmund-Thomson syndrome is a facial rash (most often presenting between ages 3-6 months, although can start later up to age 2) (99). This rash can spread to the buttocks and later develops into poikiloderma. Poikiloderma describes a collection of cutaneous features include skin atrophy, telangiectasias, and areas of hyper/hypo pigmentation.

Clinical Characteristics: Non-Cutaneous

Osteosarcoma risk is particularly elevated in young individuals with RTS, with the median age of diagnosis being 10 (31). Among a cohort of 41 patients with RTS described by Wang et al., 32% developed an osteosarcoma (99). Skeletal anomalies including altered or missing thumbs, ulnar defects, or patellar hypoplasia (93). Osteopenia requiring endocrine management can occur, as well as infertility (99).

Incidence of Skin Cancer

Both basal cell and squamous cell carcinoma have been reported in individuals with RTS. Due to the rarity of RTS, lifetime risk for non-melanoma skin cancers in the RTS population is unclear, but believed to be elevated over the general population with a trend toward younger age at onset (100–102). Stinco et al. reported a history of multiple cutaneous malignancies in a man with RTS and reviewed published reports of cutaneous malignancies in RTS (102). In total, they identified reports of 61 patients with RTS in the literature who developed at least one malignancy. Among these 61 patients, 11 developed squamous cell carcinoma (including 3 patients with SCC of the tongue), 3 developed basal cell carcinoma (including one woman who developed 11 basal cell carcinomas between the ages of 46-63), two had Bowen's disease, and one had a verrucous carcinoma (102).

The following reports were included in the review by Stinco et al. Piquero-Casals et al. reported on three siblings with RTS Type II with cutaneous squamous cell carcinoma (100). One sibling was diagnosed with a verrucous carcinoma of the foot at age 38 and a squamous cell carcinoma (SCC) of the hand at age 48 (100). Another sibling was diagnosed with squamous cell

carcinoma at the base of the thumb at age 41. The third affected sibling was diagnosed with an SCC after biopsy of an ulcer on his left heel at age 35. All three SCCs were HPV negative (100).

Surveillance and Management Considerations: Cutaneous

Annual dermatology exams are recommended for individuals with RTS to screen for skin cancers and provide treatment for skin concerns (no starting age for the exams is specified) (31). Treatment of telangiectasias for cosmetic concerns can be completed using pulsed dye laser treatment. Reported treatment of skin cancers in affected patients was largely through excision (with skin grafts when necessary) (102).

Surveillance and Management Considerations: Non-Cutaneous

A baseline skeletal survey is recommended for patients with RTS before age 5 to look for skeletal anomalies (31). Annual ophthalmology exams are also recommended to screen for cataract development, although an age to start is not specified (31).

XERODERMA PIGMENTOSUM

Xeroderma Pigmentosum (XP) was first described in 1874 by Moriz Kaposi in the dermatology textbook he wrote with Ferdinand von Hebra. XP is characterized by extreme photosensitivity. Average lifespan is reduced in individuals with XP, with the median age at death being between 29-37, depending on the presence or absence of neurological involvement (103). Skin cancer is the most common cause of mortality, followed by neurological impairment and non-cutaneous malignancies (104).

Mechanism

XP is most often caused by problems in the nucleotide excision repair pathway, which is responsible for repairing damage to skin cells from UV exposure (105). Eight different complementation groups were initially defined for XP and are now linked to individual genes (with the exception of *ERCC1*) (103).

Genes/Inheritance

XP is an autosomal recessive condition. To date, biallelic pathogenic variants in nine genes have been associated with XP: *DDB2*, *ERCC1*, *ERCC2*, *ERCC3*, *ERCC4*, *ERCC5*, *POLH*, *XPA*, and *XPC*.

Means of Diagnosis

XP is typically clinically diagnosed based on dermatologic features, with genetic testing used to confirm a diagnosis and provide additional phenotype/genotype information.

Population/Epidemiology

A number of founder pathogenic variants have been identified worldwide, including IVS3-1G>C in *XPA* in Japan (carrier frequency of 1 in 100) (106, 107). In part due to the existence of multiple founder pathogenic variants across numerous countries and differences in consanguinity rates among populations, prevalence of XP differs among countries. Likewise, the proportion of XP attributable to different genes varies from country to country (**Table 1** summarizes data from the US) (104). In the US and Europe, approximately 1 in 1,000,000 individuals have XP. In Japan, approximately 1 in 22,000 people are affected with XP (107). Increased prevalence has also been reported in North Africa and the Middle East.

Clinical Characteristics: Cutaneous

XP causes extreme UV light sensitivity. Approximately 60% of affected individuals will develop blistering sunburns with UV light exposure, while 40% have the ability to tan rather than burn (104). There is evidence for a genotype/phenotype correlation with the tendency to burn/blister in the sun. Patients considered to have XP complementation group C (associated with pathogenic variants in XPC), report higher levels of tanning rather than burning on sun exposure, while patients with XP complementation groups A or D (associated with *XPA* or *ERCC2* respectively) reported more frequently burning easily in the sun (104). It has been noted that XP patients who tend to tan rather than burn are often diagnosed with younger onset skin cancers, which may be due to less frequent sun protective behaviors (104). Nearly all individuals with XP develop small pigmented, freckle-like macules on the skin in areas of UV exposure (face, back of neck, back of hands, upper chest) in early childhood (106). Skin erythema and development of actinic keratoses are common in areas of UV exposure.

Clinical Characteristics: Non-Cutaneous

It is estimated that 25%-30% of individuals with XP have neurological symptoms, including worsening cognitive impairment, absent or reduced deep tendon reflexes, sensorineural hearing loss, and acquired microcephaly (106). In patients with neurological complications from XP, hearing loss can start in childhood and complete loss may be apparent around age 15 (106). Difficulties with walking can also start in the pre-teen years and progress to needing ambulatory assistance (such as wheelchair use) by approximately age 15 (106). Joint contractures and difficulties with feeding and respiration can present in mid-late teenage years as well. Neurodegeneration can be seen on CT and MRI with evidence of brain atrophy in multiple areas (106).

Incidence of Skin Cancer

Individuals with XP have high risks for young onset non-melanoma and melanoma skin cancers. For patients under the age of 20, XP results in an approximate 10,000-fold increase in non-melanoma skin cancer risk and a 2,000-fold increase in melanoma risk (104). In reviewing the records of all 106 patients with XP admitted to the NIH between 1971-2009, 64 (60%) had been diagnosed with non-melanoma skin cancer (104). Age at non-melanoma skin cancer diagnosis ranged from 1-32 years, with a median age of 9. Of the 38 patients with a melanoma diagnosis, 33 (87%) of them also had a history of non-melanoma

TABLE 1 | Characteristics of Cancer Predisposition Syndromes Associated with Non-Melanoma Skin Cancers.

Disorder (Incidence of disorder)	Mode of diagnosis	Genes associated	Inheritance pattern	Percent of syndrome associated with PV in gene
Fanconi Anemia (108)	Chromosome breakage analysis *via* Mitomycin C chromosome breakage study (MMC) and diepoxybutane (DEB) assay	*FANCA*	AR	60%
		FANCB	XL	2%
		FANCC	AR	12%
		BRCA2 (FANCD1)	AR	2%
		FANCD2	AR	2%
		FANCE	AR	2%
		FANCF	AR	2%
		FANCG	AR	10%
		FANCI	AR	<2%
		BRIP1 (FANCJ)	AR	<2%
		FANCL	AR	Rare
		FANCM	AR	Rare
		PALB2 (FANCN)	AR	Rare
		RAD51C (FANCO)	AR	Rare
		SLX4 (FANCP)	AR	Rare
		ERCC4 (FANCQ)	AR	Rare
		RAD51 (FANCR)	AD	Rare
		BRCA1 (FANCS)	AR	Rare
		UBE2T (FANCT)	AR	Rare
		XRCC2 (FANCU)	AR	Rare
		REV7 (FANCV)	AR	Rare
Telomere biology disorders (109)	Telomere length measurement *via* flow FISH	*DKC1*	XLR	20-25%
		TINF2	AD, AR	12-20%
		TERC	AD, AR	5-10%
		TERT	AD, AR	1-7%
		NOP10	AD, AR	<1%
		NHP2	AD, AR	<1%
		CTC1	AR	1-3%
		RTEL1	AD, AR	2-8%
		Unknown		20-30%
Bloom syndrome (110)	Clinical features ("butterfly rash"), genetic testing	*BLM*	AR	100%
Werner Syndrome (90)	Clinical diagnostic criteria, genetic testing	*WRN*	AR	Near 100%
Rothmund-Thomson (93)	Clinical features (poikiloderma pattern), genetic testing	*ANAPC1*	AR	10%
		RECQL4	AR	60%
Ferguson-Smith syndrome	Clinical features of numerous MSSE, genetic testing	*TGFBR1*	AD	Not available
Xeroderma Pigmentosum (104)	Severe photosensitivity, genetic testing	*DDB2*	AR	3% (US)
		ERCC1	AR	Rare (US)
		ERCC2	AR	28% (US)
		ERCC3	AR	1% (US)
		ERCC4	AR	0% (US)
		ERCC5	AR	3% (US)
		POLH	AR	7% (US)
		XPA	AR	9% (US)
		XPC	AR	43% (US)

AD, autosomal dominant; AR, autosomal recessive; MSSE, multiple self-healing squamous epithelioma; PV, pathogenic variant; XL, X-linked; XLR, X-linked recessive.

skin cancer (104) Age at first melanoma diagnosis ranged from 2-47 years, with the median age at 22 years (104). Many individuals had a history of numerous skin cancer diagnoses (104). One specific patient had a history of 284 basal cell carcinomas, 12 squamous cell carcinomas, and 24 melanomas (all verified with pathology records) (104). Mucocutaneous oral cancers are also seen more frequently in individuals with XP, due to UV exposure in this area. Squamous cell carcinoma of the tongue tip was reported by Wade and Plotnick in two patients with XP (111). Saleh and Elansary reported the presence of an oral angiokeratoma on the tongue of a 20 year-old male patient with XP (112).

Surveillance and Management Considerations: Cutaneous

The most imperative management recommendation for individuals with XP is to avoid UV exposure (31). Use of

sunscreen and protective clothing (including long sleeves, long pants, hats, scarves, gloves, visors, and sunglasses) while outside during the day is imperative (31, 106). UV exposure within the home should be reduced through using low UV emission lightbulbs (such as LED) and applying UV protection to windows (31). Dermatology exams are recommended every 3 months, beginning at age of diagnosis (31).

Treatment of skin cancers is ideally completed with surgical excision (106). Radiation treatment of malignancies should be avoided (31).

Surveillance and Management Considerations: Non-Cutaneous

Ophthalmology exams are recommended every 3-6 months to monitor for ocular complications (106). Frequent auditory and neurological evaluations are recommended (31, 106). The needs of patients with neurological symptoms for supportive interventions/aides should be monitored. Hearing and mobility aides, as well as later intensive assistance with feeding and respiration, can be necessary (106)

FERGUSON-SMITH SYNDROME

Among the syndromes discussed in this review, Ferguson-Smith syndrome is unique. It appears to only predispose to cutaneous findings, which typically resolve on their own, but can be significantly disfiguring. J Ferguson-Smith reported the first documented case in a 23 year-old male in 1934 at a meeting of the North British Dermatological Society (113). This condition is very rare, with just over 100 cases reported worldwide. The primary cutaneous manifestation of Ferguson-Smith syndrome is the development of multiple self-healing squamous epitheliomas (MSSE).

Mechanism

Ferguson-Smith syndrome results from the loss of TGFBR1. The product of *TGFBR1* acts as a tumor suppressor and shows loss of heterozygosity in MSSE cells (114, 115).

Genes/Inheritance

Ferguson-Smith is an autosomal dominant condition resulting from pathogenic variants in *TGFBR1.* Pathogenic variants in *TGFBR1* are also associated with a separate condition, Loeys-Dietz syndrome. Loeys-Dietz syndrome is a connective tissue disorder causing an increased risk for aortic aneurysm. Affected individuals characteristically have bifid uvula, hypertelorism, and arterial tortuosity (116). Loss of function pathogenic variants causing a dominant negative effect are proposed to cause Loeys-Dietz syndrome while Ferguson-Smith syndrome appears to result from pathogenic variants causing haploinsufficiency (116, 117). Reported pathogenic variants in *TGFBR1* resulting in Ferguson-Smith syndrome are truncating or missense variants (114).

Means of Diagnosis

No formal clinical diagnostic criteria for Ferguson-Smith syndrome have been published. Diagnosis is made based on dermatological examination and identification of multiple MSSE (biopsy proven). Genetic testing of *TGFBR1* can assist in further confirming a diagnosis.

Population/Epidemiology

The first reported case of Ferguson-Smith syndrome and most subsequent families have been identified in Scotland (113, 118).

Clinical Characteristics: Cutaneous

The primary cutaneous manifestation of Ferguson-Smith syndrome is the development of multiple self-healing squamous epitheliomas (MSSE). These lesions typically present on the face and extremities (arms, legs) (113). MSSE appear very

TABLE 2 | Malignant and Non-Malignant Cutaneous Findings in Cancer Predisposition Syndromes.

Syndrome	Non-malignant cutaneous features	Non-melanoma skin cancer associations	Melanoma associations
Telomere Biology Disorders	Reticulated skin pigmentation, dermatoglyphia, palmoplantar hyperkeratosis, hyperhidrosis, premature graying, scalp/eyelash hair loss, epiphora, and lash irritation	Squamous cell carcinoma (SCC) and basal cell carcinoma (BCC)	None reported
Fanconi Anemia	Café au lait macules, hypopigmented macules and patches, skinfold freckle-like macules	SCC and BCC	Only one reported patient with melanoma
Bloom Syndrome	Erythematous rash over nose, cheeks, eyelids, lips "butterfly rash"	BCC (most common), some SCC reported	None reported
Werner Syndrome	Prematurely aging skin (thinning, tight)	SCC and BCC	Significantly elevated risk
Rothmund-Thomson Syndrome	Poikilodermas, sensitivity to UV radiation	SCC and BCC	
Xeroderma Pigmentosum	Extreme UV radiation sensitivity, blistering sunburns	Significantly elevated risk for BCC and SCC	Significantly elevated risk
Ferguson-Smith Syndrome	Multiple self-healing squamous epitheliomas (MSSE)	MSSE can appear similar to SCC	None reported

UV, ultraviolet.

TABLE 3 | Resources for Selected Cancer Predisposition Syndromes.

Disorder	Support group or resource name	Support group	Research/ Registry	Educational resource	Financial support available	URL
Fanconi Anemia	Fanconi Anemia Research Fund	X	X	X	X	https://www.fanconi.org/
	Genereviews			X		https://www.ncbi.nlm.nih.gov/books/NBK1401/
Telomere Biology Disorders	Team Telomere	X	X	X	X	https://teamtelomere.org/
	Genereviews			X		https://www.ncbi.nlm.nih.gov/books/NBK22301/
Bloom Syndrome	Bloom Syndrome Registry (Weil Cornell)		X	X		http://www.med.cornell.edu/bsr/
	Bloom Syndrome Association (NH)	X	X	X	X	https://www.bloomsyndromeassociation.org/
Werner Syndrome	International Werner Syndrome Registry (Univ of WA)		X	X		https://dlmp.uw.edu/research-center/werner/registry
	Japanese Werner Syndrome Consortium		X			Not currently available online
Rothmund-Thomson	RTS Foundation		X	X		https://www.rtsplace.org
Xeroderma Pigmentosum	Xeroderma Pigmentosum Society (NY)	X		X		https://www.xps.org/
	XP Support Group (UK)	X		X	X	https://xpsupportgroup.org.uk/

similar to invasive squamous cell carcinomas, yet heal spontaneously over time (119). Development of MSSEs typically starts in an affected individual's late teens/20s.

Clinical Characteristics: Non-Cutaneous

Individuals with Ferguson-Smith syndrome are not known to have an increased risk for other health concerns unrelated to MSSE.

Surveillance and Management Considerations: Cutaneous

Surgical removal of MSSE from regions of the skin at elevated risk for squamous cell cancer development is recommended. However, due to the usually benign nature of MSSE, extensive surgery is to be avoided if possible.

CONCLUSION

The diagnosis of non-melanoma skin cancers in individuals at early ages and/or with other syndromic features presents an opportunity to identify cancer predisposition syndromes. Though non-melanoma skin cancers may not be the most prominent feature of many of the syndromes reviewed in this article, there is a need for dermatology and oncology providers to be aware of these conditions nonetheless. The cutaneous malignancies and other cutaneous features associated with these syndromes is summarized in **Table 2**, and additional online resources for these syndromes are given in **Table 3**. Cutaneous malignancies for people with these conditions tend to be treated surgically, as for cutaneous non-melanoma skin cancers in the general population. However, appropriate testing and accurate diagnosis for these cancer predisposition syndromes are critical for management of associated health risks for these patients and their family members.

AUTHOR CONTRIBUTIONS

JV, AG, WK, and JJ contributed to conception and design of the manuscript. AG and JV wrote the first draft of the manuscript. All authors contributed to manuscript revision, read, and approved the submitted version.

FUNDING

This publication utilized the Genetic Counseling Shared Resource at Huntsman Cancer Institute at the University of Utah and was supported by the National Cancer Institute of the National Institutes of Health under Award Number P30CA042014.

REFERENCES

1. Lomas A, Leonardi-Bee J, Bath-Hextall F. A Systematic Review of Worldwide Incidence of Nonmelanoma Skin Cancer. *Br J Dermatol* (2012) 166(5):1069–80. doi: 10.1111/j.1365-2133.2012.10830.x
2. Sung H, Ferlay J, Siegel RL, Laversanne M, Soerjomataram I, Jemal A, et al. Global Cancer Statistics 2020: GLOBOCAN Estimates of Incidence and Mortality Worldwide for 36 Cancers in 185 Countries. *CA Cancer J Clin* (2021) 71(3):209–49. doi: 10.3322/caac.21660
3. Peris K, Fargnoli MC, Garbe C, Kaufmann R, Bastholt L, Seguin NB, et al. Diagnosis and Treatment of Basal Cell Carcinoma: European Consensus-Based Interdisciplinary Guidelines. *Eur J Cancer* (2019) 118:10–34. doi: 10.1016/j.ejca.2019.06.003
4. Bresler SC, Padwa BL, Granter SR. Nevoid Basal Cell Carcinoma Syndrome (Gorlin Syndrome). *Head Neck Pathol* (2016) 10(2):119–24. doi: 10.1007/s12105-016-0706-9
5. Foulkes WD, Kamihara J, Evans DGR, Brugieres L, Bourdeaut F, Molenaar JJ, et al. Cancer Surveillance in Gorlin Syndrome and Rhabdoid Tumor

Predisposition Syndrome. *Clin Cancer Res* (2017) 23(12):e62–7. doi: 10.1158/1078-0432.CCR-17-0595
6. Walne AJ, Dokal I. Dyskeratosis Congenita: A Historical Perspective. *Mech Ageing Dev* (2008) 129(1-2):48–59. doi: 10.1016/j.mad.2007.10.006
7. Zinnsser F. Atrophia Cutis Reticularis Cum Pigmentatione, Dystrophia Unguium Et Leukoplakia Oris. *Ikonogr Dermatol (Hyoto)* (1906) 5:219–23.
8. Savage SA. Beginning at the Ends: Telomeres and Human Disease. *F1000Research* (2018) 7:1–16. doi: 10.12688/f1000research.14068.1
9. Knight S, Heiss N, Vulliamy T, Greschner S, Stavrides G, Pai G, et al. X-Linked Dyskeratosis Congenita Is Predominantly Caused by Missense Mutations in the DKC1 Gene. *Am J Hum Genet* (1999) 65(1):50–8. doi: 10.1086/302446
10. Niewisch MR, Savage SA. An Update on the Biology and Management of Dyskeratosis Congenita and Related Telomere Biology Disorders. *Expert Rev Hematol* (2019) 12(12):1037–52. doi: 10.1080/17474086.2019.1662720
11. Bertuch AA. The Molecular Genetics of the Telomere Biology Disorders. *RNA Biol* (2016) 13(8):696–706. doi: 10.1080/15476286.2015.1094596
12. Schmidt JC, Cech TR. Human Telomerase: Biogenesis, Trafficking, Recruitment, and Activation. *Genes Dev* (2015) 29(11):1095–105. doi: 10.1101/gad.263863.115
13. Vulliamy T, Marrone A, Szydlo R, Walne A, Mason PJ, Dokal I, et al. Disease Anticipation Is Associated With Progressive Telomere Shortening in Families With Dyskeratosis Congenita Due to Mutations in TERC. *Nat Genet* (2004) 36(5):447–9. doi: 10.1038/ng1346
14. Dokal I, Vulliamy T, Mason P, Bessler M. Clinical Utility Gene Card for: Dyskeratosis Congenita–Update 2015. *Eur J Hum Genet* (2015) 23(4):558–8. doi: 10.1038/ejhg.2014.170
15. Alter BP, Rosenberg PS, Giri N, Baerlocher GM, Lansdorp PM, Savage SA, et al. Telomere Length Is Associated With Disease Severity and Declines With Age in Dyskeratosis Congenita. *Haematologica* (2012) 97(3):353. doi: 10.3324/haematol.2011.055269
16. Alter BP, Baerlocher GM, Savage SA, Chanock SJ, Weksler BB, Willner JP, et al. Very Short Telomere Length by Flow Fluorescence *In Situ* Hybridization Identifies Patients With Dyskeratosis Congenita. *Blood J Am Soc Hematol* (2007) 110(5):1439–47. doi: 10.1182/blood-2007-02-075598
17. Wang J, Lu X, Sakk V, Klein CA, Rudolph KL. Senescence and Apoptosis Block Hematopoietic Activation of Quiescent Hematopoietic Stem Cells With Short Telomeres. *Blood J Am Soc Hematol* (2014) 124(22):3237–40. doi: 10.1182/blood-2014-04-568055
18. Alter BP, Giri N, Savage SA, Rosenberg PS. Cancer in the National Cancer Institute Inherited Bone Marrow Failure Syndrome Cohort After Fifteen Years of Follow-Up. *Haematologica* (2018) 103(1):30. doi: 10.3324/haematol.2017.178111
19. Feurstein S, Adegunsoye A, Mojsilovic D, Vij R, West DePersia AH, Rajagopal PS, et al. Telomere Biology Disorder Prevalence and Phenotypes in Adults With Familial Hematologic and/or Pulmonary Presentations. *Blood Adv* (2020) 4(19):4873–86. doi: 10.1182/bloodadvances.2020001721
20. Ward SC, Savage SA, Giri N, Alter BP, Rosenberg PS, Pichard DC, et al. Beyond the Triad: Inheritance, Mucocutaneous Phenotype, and Mortality in a Cohort of Patients With Dyskeratosis Congenita. *J Am Acad Dermatol* (2018) 78(4):804–6. doi: 10.1016/j.jaad.2017.10.017
21. Savage S, Cook E. *Dyskeratosis Congenita and Telomere Biology Disorders: Diagnosis and Management Guidelines*. New York, NY: Dyskeratosis Congenita Outreach Inc (2015).
22. Dokal I. Dyskeratosis Congenita in All Its Forms. *Br J Haematol* (2000) 110 (4):768–79. doi: 10.1046/j.1365-2141.2000.02109.x
23. Schratz KE, Haley L, Danoff SK, Blackford AL, DeZern AE, Gocke CD, et al. Cancer Spectrum and Outcomes in the Mendelian Short Telomere Syndromes. *Blood* (2020) 135(22):1946–56. doi: 10.1182/blood.2019003264
24. Kam ML, Nguyen TT, Ngeow JY. Telomere Biology Disorders. *NPJ Genomic Med* (2021) 6(1):1–13. doi: 10.1038/s41525-021-00198-5
25. Nikolaou V, Stratigos AJ, Tsao H. Hereditary Nonmelanoma Skin Cancer. *Semin Cutaneous Med Surg* (2012) 31(4):204–10. NIH Public Access. doi: 10.1016/j.sder.2012.08.005
26. Alter BP, Giri N, Savage SA, Rosenberg PS. Cancer in Dyskeratosis Congenita. *Blood J Am Soc Hematol* (2009) 113(26):6549–57. doi: 10.1182/blood-2008-12-192880
27. Alter BP, Giri N, Savage SA, Peters JA, Loud JT, Leathwood L, et al. Malignancies and Survival Patterns in the National Cancer Institute Inherited Bone Marrow Failure Syndromes Cohort Study. *Br J Haematol* (2010) 150(2):179–88. doi: 10.1111/j.1365-2141.2010.08212.x
28. Shimamura A, Alter BP. Pathophysiology and Management of Inherited Bone Marrow Failure Syndromes. *Blood Rev* (2010) 24(3):101–22. doi: 10.1016/j.blre.2010.03.002
29. Tamary H, Nishri D, Yacobovich J, Zilber R, Dgany O, Krasnov T, et al. Frequency and Natural History of Inherited Bone Marrow Failure Syndromes: The Israeli Inherited Bone Marrow Failure Registry. *haematologica* (2010) 95(8):1300. doi: 10.3324/haematol.2009.018119
30. Savage SA, Dokal I, Armanios M, Aubert G, Cowen EW, Domingo DL, et al. Dyskeratosis Congenita: The First NIH Clinical Research Workshop. *Pediatr Blood Cancer* (2009) 53(3):520–23.
31. Walsh MF, Chang VY, Kohlmann WK, Scott HS, Cunniff C, Bourdeaut F, et al. Recommendations for Childhood Cancer Screening and Surveillance in DNA Repair Disorders. *Clin Cancer Res* (2017) 23(11):e23–31. doi: 10.1158/1078-0432.CCR-17-0465
32. Wang LL, Levy ML. Rothmund–Thomson Syndrome, Bloom Syndrome, Dyskeratosis Congenita, Fanconi Anaemia and Poikiloderma With Neutropenia. *Harper's Textbook Pediatr Dermatol* (2019) p:1786–801. doi: 10.1002/9781119142812.ch140
33. Lobitz S, Velleuer E. Guido Fanconi (1892–1979): A Jack of All Trades. *Nat Rev Cancer* (2006) 6(11):893–8. doi: 10.1038/nrc2009
34. Risitano AM, Marotta S, Calzone R, Grimaldi F, Zatterale A. Twenty Years of the Italian Fanconi Anemia Registry: Where We Stand and What Remains to Be Learned. *Hematologica* (2016) 101(3):319. doi: 10.3324/haematol.2015.133520
35. Bhandari J, Thada PK, Puckett Y. Fanconi Anemia. In: *StatPearls*. Treasure Island (FL): StatPearls Publishing (2022) Available from: https://www.ncbi.nlm.nih.gov/books/NBK559133/.
36. Rodríguez A, D'Andrea A. *Fanconi Anemia Pathway*. *Curr Biol* (2017) 27 (18):R986–8. doi: 10.1016/j.cub.2017.07.043
37. Ceccaldi R, Sarangi P, D'Andrea AD. The Fanconi Anaemia Pathway: New Players and New Functions. *Nat Rev Mol Cell Biol* (2016) 17(6):337–49. doi: 10.1038/nrm.2016.48
38. Grillari J, Katinger H, Voglauer R. Contributions of DNA Interstrand Cross-Links to Aging of Cells and Organisms. *Nucleic Acids Res* (2007) 35 (22):7566–76. doi: 10.1093/nar/gkm1065
39. Clauson C, Schärer OD, Niedernhofer L. Advances in Understanding the Complex Mechanisms of DNA Interstrand Cross-Link Repair. *Cold Spring Harbor Perspect Biol* (2013) 5(10):a012732. doi: 10.1101/cshperspect.a012732
40. Lopez-Martinez D, Liang C-C, Cohn MA. Cellular Response to DNA Interstrand Crosslinks: The Fanconi Anemia Pathway. *Cell Mol Life Sci* (2016) 73(16):3097–114. doi: 10.1007/s00018-016-2218-x
41. Sumpter RJr., Levine B. Emerging Functions of the Fanconi Anemia Pathway at a Glance. *J Cell Sci* (2017) 130(16):2657–62. doi: 10.1242/jcs.204909
42. Ruiz-Torres S, Brusadelli MG, Witte DP, Wikenheiser-Brokamp KA, Sauter S, Nelson AS, et al. Inherited DNA Repair Defects Disrupt the Structure and Function of Human Skin. *Cell Stem Cell* (2021) 28(3):424–435.e6. doi: 10.1016/j.stem.2020.10.012
43. Nicoletti E, Rao G, Bueren JA, Río P, Navarro S, Surrallés J, et al. Mosaicism in Fanconi Anemia: Concise Review and Evaluation of Published Cases With Focus on Clinical Course of Blood Count Normalization. *Ann Hematol* (2020) 99(5):913–24. doi: 10.1007/s00277-020-03954-2
44. Nalepa G, Clapp DW. Fanconi Anaemia and Cancer: An Intricate Relationship. *Nat Rev Cancer* (2018) 18(3):168–85. doi: 10.1038/nrc.2017.116
45. Daly MB, Pal T, Berry MP, Buys SS, Dickson P, Domchek SM, et al. Genetic/Familial High-Risk Assessment: Breast, Ovarian, and Pancreatic, Version 2.2021, NCCN Clinical Practice Guidelines in Oncology. *J Natl Compr Canc Netw* (2021) 19(1):77–102. doi: 10.6004/jnccn.2021.0001
46. Rosenberg PS, Tamary H, Alter BP. How High Are Carrier Frequencies of Rare Recessive Syndromes? Contemporary Estimates for Fanconi Anemia in the United States and Israel. *Am J Med Genet Part A* (2011) 155(8):1877–83. doi: 10.1002/ajmg.a.34087

47. Rosendorff J, Bernstein R, Macdougall L, Jenkins T, Opitz JM, Reynolds JF. Fanconi Anemia: Another Disease of Unusually High Prevalence in the Afrikaans Population of South Africa. *Am J Med Genet* (1987) 27(4):793–7. doi: 10.1002/ajmg.1320270408
48. Callén E, Casado JA, Tischkowitz MD, Bueren JA, Creus A, Marcos R, et al. A Common Founder Mutation in FANCA Underlies the World's Highest Prevalence of Fanconi Anemia in Gypsy Families From Spain. *Blood* (2005) 105(5):1946–9. doi: 10.1182/blood-2004-07-2588
49. Morgan NV, Essop F, Demuth I, de Ravel T, Jansen S, Tischkowitz M, et al. A Common Fanconi Anemia Mutation in Black Populations of Sub-Saharan Africa. *Blood* (2005) 105(9):3542–4. doi: 10.1182/blood-2004-10-3968
50. Ruggiero JL, Dodds M, Freese R, Polcari IC, Maguiness S, Hook KP, et al. Cutaneous Findings in Fanconi Anemia. *J Am Acad Dermatol* (2021) 85 (5):1253–8. doi: 10.1016/j.jaad.2020.08.047
51. *Fanconi Anemia Clinical Care Guidelines* (2020). Available at: https://www.fanconi.org/images/uploads/other/Fanconi_Anemia_Clinical_Care_Guidelines_5thEdition_web.pdf.
52. Alter BP, Greene MH, Velazquez I, Rosenberg PS. Cancer in Fanconi Anemia. *Blood J Am Soc Hematol* (2003) 101(5):2072–2. doi: 10.1182/blood-2002-11-3597
53. Kutler DI, Singh B, Satagopan J, Batish SD, Berwick M, Giampietro PF, et al. A 20-Year Perspective on the International Fanconi Anemia Registry (IFAR). *Blood J Am Soc Hematol* (2003) 101(4):1249–56. doi: 10.1182/blood-2002-07-2170
54. Huck K, Hanenberg H, Gudowius S, Fenk R, Kalb R, Neveling K, et al. Delayed Diagnosis and Complications of Fanconi Anaemia at Advanced Age–a Paradigm. *Br J Haematol* (2006) 133(2):188–97. doi: 10.1111/j.1365-2141.2006.05998.x
55. Alter BP. Fanconi Anemia and the Development of Leukemia. *Best Pract Res Clin Haematol* (2014) 27(3-4):214–21. doi: 10.1016/j.beha.2014.10.002
56. Mitchell R, Wagner JE, Hirsch B, DeFor TE, Zierhut H, MacMillan ML. Haematopoietic Cell Transplantation for Acute Leukaemia and Advanced Myelodysplastic Syndrome in F Anconi Anaemia. *Br J Haematol* (2014) 164 (3):384–95. doi: 10.1111/bjh.12634
57. Kutler DI, Auerbach AD, Satagopan J, Giampietro PF, Batish SD, Huvos AG, et al. High Incidence of Head and Neck Squamous Cell Carcinoma in Patients With Fanconi Anemia. *Arch Otolaryngol Head Neck Surg* (2003) 129(1):106–12. doi: 10.1001/archotol.129.1.106
58. Van Zeeburg HJ, Snijders PJ, Wu T, Gluckman E, Soulier J, Surralles J, et al. Clinical and Molecular Characteristics of Squamous Cell Carcinomas From Fanconi Anemia Patients. *JNCI: J Natl Cancer Institute* (2008) 100 (22):1649–53. doi: 10.1093/jnci/djn366
59. Dutzmann CM, Spix C, Popp I, Kaiser M, Erdmann F, Erlacher M, et al. Cancer in Children With Fanconi Anemia and Ataxia-Telangiectasia—A Nationwide Register-Based Cohort Study in Germany. *J Clin Oncol* (2021) JCO. 21.01495. doi: 10.1200/JCO.21.01495
60. Rosenberg PS, Alter BP, Ebell W. Cancer Risks in Fanconi Anemia: Findings From the German Fanconi Anemia Registry. *Haematologica* (2008) 93 (4):511–7. doi: 10.3324/haematol.12234
61. García-de-Teresa B, Rodríguez A, Frias S. Causes and Consequences of Chromosomal Instability in Fanconi Anemia. *Alterations at Cell Organism Level Preprints* (2020). doi: 10.20944/preprints202011.0563.v1
62. Bloom D. Congenital Telangiectatic Erythema Resembling Lupus Erythematosus in Dwarfs; Probably a Syndrome Entity. *AMA Am J Dis Child* (1954) 88(6):754–8. doi: 10.1001/archpedi.1954.02050100756008
63. Ellis NA, Proytcheva M, Sanz MM, Ye TZ, German J. Transfection of BLM Into Cultured Bloom Syndrome Cells Reduces the Sister-Chromatid Exchange Rate Toward Normal. *Am J Hum Genet* (1999) 65(5):1368–74. doi: 10.1086/302616
64. Nimonkar AV, Genschel J, Kinoshita E, Polaczek P, Campbell JL, Wyman C, et al. BLM-DNA2-RPA-MRN and EXO1-BLM-RPA-MRN Constitute Two DNA End Resection Machineries for Human DNA Break Repair. *Genes Dev* (2011) 25(4):350–62. doi: 10.1101/gad.2003811
65. German J, Sanz MM, Ciocci S, Ye TZ, Ellis NA. Syndrome-Causing Mutations of the BLM Gene in Persons in the Bloom's Syndrome Registry. *Hum Mutat* (2007) 28(8):743–53. doi: 10.1002/humu.20501
66. Backers L, Parton B, De Bruyne M, Tavernier SJ, Van Den Bogaert K, Lambrecht BN, et al. Missing Heritability in Bloom Syndrome: First Report of a Deep Intronic Variant Leading to Pseudo-Exon Activation in the BLM Gene. *Clin Genet* (2021) 99(2):292–7. doi: 10.1111/cge.13859
67. Cunniff C, Djavid AR, Carrubba S, Cohen B, Ellis NA, Levy CF, et al. Health Supervision for People With Bloom Syndrome. *Am J Med Genet A* (2018) 176(9):1872–81. doi: 10.1002/ajmg.a.40374
68. Li L, Eng C, Desnick RJ, German J, Ellis NA. Carrier Frequency of the Bloom Syndrome Blmash Mutation in the Ashkenazi Jewish Population. *Mol Genet Metab* (1998) 64(4):286–90. doi: 10.1006/mgme.1998.2733
69. Shahrabani-Gargir L, Shomrat R, Yaron Y, Orr-Urtreger A, Groden J, Legum C. High Frequency of a Common Bloom Syndrome Ashkenazi Mutation Among Jews of Polish Origin. *Genet Test* (1998) 2(4):293–6. doi: 10.1089/gte.1998.2.293
70. German J. Bloom's Syndrome. I. Genetical and Clinical Observations in the First Twenty-Seven Patients. *Am J Hum Genet* (1969) 21(2):196–227.
71. Masmoudi A, Marrakchi S, Kamoun H, Chaaben H, Ben Salah G, Ben Salah R, et al. Clinical and Laboratory Findings in 8 Patients With Bloom's Syndrome. *J Dermatol Case Rep* (2012) 6(1):29–33. doi: 10.3315/jdcr.2012.1086
72. Schoenaker MHD, Henriet SS, Zonderland J, van Deuren M, Pan-Hammarstrom Q, Posthumus-van Sluijs SJ, et al. Immunodeficiency in Bloom's Syndrome. *J Clin Immunol* (2018) 38(1):35–44. doi: 10.1007/s10875-017-0454-y
73. Chisholm CA, Bray MJ, Karns LB. Successful Pregnancy in a Woman With Bloom Syndrome. *Am J Med Genet* (2001) 102(2):136–8. doi: 10.1002/ajmg.1437
74. de Voer RM, Hahn MM, Mensenkamp AR, Hoischen A, Gilissen C, Henkes A, et al. Deleterious Germline BLM Mutations and the Risk for Early-Onset Colorectal Cancer. *Sci Rep* (2015) 5:14060. doi: 10.1038/srep14060
75. Weiss JM, Gupta S, Burke CA, Axell L, Chen LM, Chung DC, et al. NCCN Guidelines(R) Insights: Genetic/Familial High-Risk Assessment: Colorectal, Version 1.2021. *J Natl Compr Canc Netw* (2021) 19(10):1122–32. doi: 10.1164/jnccn.2021.0048
76. Thomas ER, Shanley S, Walker L, Eeles R. Surveillance and Treatment of Malignancy in Bloom Syndrome. *Clin Oncol (R Coll Radiol)* (2008) 20(5):375–9. doi: 10.1016/j.clon.2008.01.007
77. Shibuya H, Kato A, Kai N, Fujiwara S, Goto M. A Case of Werner Syndrome With Three Primary Lesions of Malignant Melanoma. *J Dermatol* (2005) 32 (9):737–44. doi: 10.1111/j.1346-8138.2005.tb00835.x
78. Werner O. On Cataract in Conjunction With Scleroderma. *Adv Exp Med Biol* (1985) 190:1–14. doi: 10.1007/978-1-4684-7853-2_1
79. Yokote K, Chanprasert S, Lee L, Eirich K, Takemoto M, Watanabe A, et al. WRN Mutation Update: Mutation Spectrum, Patient Registries, and Translational Prospects. *Hum Mutat* (2017) 38(1):7–15. doi: 10.1002/humu.23128
80. Lauper JM, Krause A, Vaughan TL, Monnat RJ Jr. Spectrum and Risk of Neoplasia in Werner Syndrome: A Systematic Review. *PloS One* (2013) 8(4): e59709. doi: 10.1371/journal.pone.0059709
81. Yu CE, Oshima J, Wijsman EM, Nakura J, Miki T, Piussan C, et al. Mutations in the Consensus Helicase Domains of the Werner Syndrome Gene. Werner's Syndrome Collaborative Group. *Am J Hum Genet* (1997) 60 (2):330–41.
82. Laarmann K, Kress JM, Kaina B, Fritz G. Werner Syndrome (WRN) DNA Helicase and Base Excision Repair (BER) Factors Maintain Endothelial Homeostasis. *DNA Repair (Amst)* (2019) 73:17–27. doi: 10.1016/j.dnarep.2018.10.005
83. Lee JW, Harrigan J, Opresko PL, Bohr VA. Pathways and Functions of the Werner Syndrome Protein. *Mech Ageing Dev* (2005) 126(1):79–86. doi: 10.1016/j.mad.2004.09.011
84. Oshima J, Sidorova JM, Monnat RJJr. Werner Syndrome: Clinical Features, Pathogenesis and Potential Therapeutic Interventions. *Ageing Res Rev* (2017) 33:105–14. doi: 10.1016/j.arr.2016.03.002
85. Kubota Y, Takemoto M, Taniguchi T, Motegi SI, Taniguchi A, Nakagami H, et al. Management Guideline for Werner Syndrome 2020. 6. Skin Ulcers Associated With Werner Syndrome: Prevention and Non-Surgical and Surgical Treatment. *Geriatr Gerontol Int* (2021) 21(2):153–9. doi: 10.1111/ggi.14096
86. Motegi SI, Takemoto M, Taniguchi T, Kubota Y, Taniguchi A, Nakagami H, et al. Management Guideline for Werner Syndrome 2020. 7. Skin Ulcer Associated With Werner Syndrome: Dermatological Treatment. *Geriatr Gerontol Int* (2021) 21(2):160–2. doi: 10.1111/ggi.14077

87. Takemoto M, Kubota Y, Taniguchi T, Motegi SI, Taniguchi A, Nakagami H, et al. Management Guideline for Werner Syndrome 2020. 3. Diabetes Associated With Werner Syndrome. *Geriatr Gerontol Int* (2021) 21 (2):142–5. doi: 10.1111/ggi.14083
88. Mori S, Takemoto M, Kubota Y, Taniguchi T, Motegi SI, Taniguchi A, et al. Management Guideline for Werner Syndrome 2020. 4. Osteoporosis Associated With Werner Syndrome. *Geriatr Gerontol Int* (2021) 21 (2):146–9. doi: 10.1111/ggi.14078
89. Goto M, Miller RW, Ishikawa Y, Sugano H. Excess of Rare Cancers in Werner Syndrome (Adult Progeria). *Cancer Epidemiol Biomarkers Prev* (1996) 5(4):239–46.
90. Oshima J, Martin GM, Hisama FM. Werner Syndrome. In: MP Adam, et al, editors. *GeneReviews((R))*. Seattle (WA): University of Washington, Seattle (1993). Available from: https://www.ncbi.nlm.nih.gov/books/NBK1514/
91. Takemoto M, Yokote K. Preface to Management Guideline for Werner Syndrome 2020. *Geriatr Gerontol Int* (2021) 21(2):131–2. doi: 10.1111/ggi.14074
92. Rothmund A. Ueber Cataracten in Verbindung Mit Einer Eigenth¸Mlichen Hautdegeneration. *Archiv f¸r Ophthalmologie* (2007) 14:159–82. doi: 10.1007/BF02720945
93. Wang LL, Plon SE. Rothmund-Thomson Syndrome. In: MP Adam, et al, editors. *GeneReviews((R))*. Seattle (WA): University of Washington, Seattle (1993) Available from: https://www.ncbi.nlm.nih.gov/books/NBK1237/.
94. Ajeawung NF, Nguyen TTM, Lu L, Kucharski TJ, Rousseau J, Molidperee S, et al. Mutations in ANAPC1, Encoding a Scaffold Subunit of the Anaphase-Promoting Complex, Cause Rothmund-Thomson Syndrome Type 1. *Am J Hum Genet* (2019) 105(3):625–30. doi: 10.1016/j.ajhg.2019.06.011
95. Colombo EA, Locatelli A, Cubells Sanchez L, Romeo S, Elcioglu NH, Maystadt I, et al. Rothmund-Thomson Syndrome: Insights From New Patients on the Genetic Variability Underpinning Clinical Presentation and Cancer Outcome. *Int J Mol Sci* (2018) 19(4):1103. doi: 10.3390/ijms19041103
96. Shamanna RA, Singh DK, Lu H, Mirey G, Keijzers G, Salles B, et al. RECQ Helicase RECQL4 Participates in non-Homologous End Joining and Interacts With the Ku Complex. *Carcinogenesis* (2014) 35(11):2415–24. doi: 10.1093/carcin/bgu137
97. Kim H, Choi H, Im JS, Park SY, Shin G, Yoo JH, et al. Stable Maintenance of the Mre11-Rad50-Nbs1 Complex is Sufficient to Restore the DNA Double-Strand Break Response in Cells Lacking RecQL4 Helicase Activity. *J Biol Chem* (2021) 297(4):101148. doi: 10.1016/j.jbc.2021.101148
98. Eguren M, Manchado E, Malumbres M. Non-Mitotic Functions of the Anaphase-Promoting Complex. *Semin Cell Dev Biol* (2011) 22(6):572–8. doi: 10.1016/j.semcdb.2011.03.010
99. Wang LL, Levy ML, Lewis RA, Chintagumpala MM, Lev D, Rogers M, et al. Clinical Manifestations in a Cohort of 41 Rothmund-Thomson Syndrome Patients. *Am J Med Genet* (2001) 102(1):11–7. doi: 10.1002/1096-8628(20010722)102:1<11::AID-AJMG1413>3.0.CO;2-A
100. Piquero-Casals J, Okubo AY, Nico MM. Rothmund-Thomson Syndrome in Three Siblings and Development of Cutaneous Squamous Cell Carcinoma. *Pediatr Dermatol* (2002) 19(4):312–6. doi: 10.1046/j.1525-1470.2002.00089.x
101. Marin-Bertolin S, Amorrortu-Velayos J, Aliaga Boniche A. Squamous Cell Carcinoma of the Tongue in a Patient With Rothmund-Thomson Syndrome. *Br J Plast Surg* (1998) 51(8):646–8. doi: 10.1054/bjps.1998.0050
102. Stinco G, Governatori G, Mattighello P, Patrone P. Multiple Cutaneous Neoplasms in a Patient With Rothmund-Thomson Syndrome: Case Report and Published Work Review. *J Dermatol* (2008) 35(3):154–61. doi: 10.1111/j.1346-8138.2008.00436.x
103. Kraemer KH, DiGiovanna JJ. Xeroderma Pigmentosum. In: MP Adam, et al, editors. *GeneReviews((R))*. Seattle (WA): University of Washington, Seattle (1993). Available from: https://www.ncbi.nlm.nih.gov/books/NBK1397/
104. Bradford PT, Goldstein AM, Tamura D, Khan SG, Ueda T, Boyle J, et al. Cancer and Neurologic Degeneration in Xeroderma Pigmentosum: Long Term Follow-Up Characterises the Role of DNA Repair. *J Med Genet* (2011) 48(3):168–76. doi: 10.1038/218652a0
105. Cleaver JE. Defective Repair Replication of DNA in Xeroderma Pigmentosum. *Nature* (1968) 218(5142):652–6. doi: 10.1038/218652a0
106. Moriwaki S, Kanda F, Hayashi M, Yamashita D, Sakai Y, Nishigori C, et al. Xeroderma Pigmentosum Clinical Practice Guidelines. *J Dermatol* (2017) 44 (10):1087–96. doi: 10.1111/1346-8138.13907
107. Hirai Y, Kodama Y, Moriwaki S, Noda A, Cullings HM, Macphee DG, et al. Heterozygous Individuals Bearing a Founder Mutation in the XPA DNA Repair Gene Comprise Nearly 1% of the Japanese Population. *Mutat Res* (2006) 601(1-2):171–8. doi: 10.1016/j.mrfmmm.2006.06.01
108. Mehta PA, Ebens C. Fanconi Anemia. In: MP Adam, et al, editors. *GeneReviews((R))*. Seattle (WA): University of Washington, Seattle (1993). Available from: https://www.ncbi.nlm.nih.gov/books/NBK1401/
109. Savage SA. Dyskeratosis Congenita. In: MP Adam, et al, editors. *GeneReviews(®)*. Seattle (WA: University of Washington, Seattle Copyright © 1993-2021, University of Washington, Seattle. GeneReviews is a registered trademark of the University of Washington, Seattle. All rights reserved (1993).
110. Cunniff C, Bassetti JA, Ellis NA. Bloom's Syndrome: Clinical Spectrum, Molecular Pathogenesis, and Cancer Predisposition. *Mol Syndromol* (2017) 8 (1):4–23. doi: 10.1159/000452082
111. Wade MH, Plotnick H. Xeroderma Pigmentosum and Squamous Cell Carcinoma of the Tongue. Identification of Two Black Patients as Members of Complementation Group C. *J Am Acad Dermatol* (1985) 12 (3):515–21. doi: 10.1016/S0190-9622(85)70072-2
112. Saleh W, Elansary M. First Report of Oral Angiokeratoma in a Xeroderma Pigmentosum. *Int J Surg Case Rep* (2021) 88:106513. doi: 10.1016/j.ijscr.2021.106513
113. Smith JF. A CASE OF MULTIPLE PRIMARY SQUAMOUS CELLED CARCINOMATA OF THE SKIN IN A YOUNG MAN, WITH SPONTANEOUS HEALING *. *Br J Dermatol* (1934) 46:267–72. doi: 10.1111/j.1365-2133.1934.tb09778.x
114. Goudie DR, D'Alessandro M, Merriman B, Lee H, Szeverenyi I, Avery S, et al. Multiple Self-Healing Squamous Epithelioma Is Caused by a Disease-Specific Spectrum of Mutations in TGFBR1. *Nat Genet* (2011) 43(4):365–9. doi: 10.1038/ng.780
115. Bose S, Morgan LJ, Booth DR, Goudie DR, Ferguson-Smith MA, Richards FM. The Elusive Multiple Self-Healing Squamous Epithelioma (MSSE) Gene: Further Mapping, Analysis of Candidates, and Loss of Heterozygosity. *Oncogene* (2006) 25(5):806–12. doi: 10.1038/sj.onc.1209092
116. Fujiwara T, Takeda N, Hara H, Morita H, Kishihara J, Inuzuka R, et al. Distinct Variants Affecting Differential Splicing of TGFBR1 Exon 5 Cause Either Loeys-Dietz Syndrome or Multiple Self-Healing Squamous Epithelioma. *Eur J Hum Genet* (2018) 26(8):1151–8. doi: 10.1038/s41431-018-0127-1
117. Goudie D. Multiple Self-Healing Squamous Epithelioma (MSSE): A Digenic Trait Associated With Loss of Function Mutations in TGFBR1 and Variants at a Second Linked Locus on the Long Arm of Chromosome 9. *Genes (Basel)* (2020) 11(12):1–12. doi: 10.3390/genes11121410
118. Bale SJ. The "Sins" of the Fathers: Self-Healing Squamous Epithelioma in Scotland. *J Cutan Med Surg* (1999) 3(4):207–10. doi: 10.1177/120347549900300411
119. Ferguson-Smith MA, Wallace DC, James ZH, Renwick JH. Multiple Self-Healing Squamous Epithelioma. *Birth Defects Orig Artic Ser* (1971) 7(8):157–63.

Author Disclaimer: The content is solely the responsibility of the authors and does not necessarily represent the official views of the NIH.

Conflict of Interest: The authors declare that the research was conducted in the absence of any commercial or financial relationships that could be construed as a potential conflict of interest.

Publisher's Note: All claims expressed in this article are solely those of the authors and do not necessarily represent those of their affiliated organizations, or those of the publisher, the editors and the reviewers. Any product that may be evaluated in this article, or claim that may be made by its manufacturer, is not guaranteed or endorsed by the publisher.

Copyright © 2022 Vagher, Gammon, Kohlmann and Jeter. This is an open-access article distributed under the terms of the Creative Commons Attribution License (CC BY). The use, distribution or reproduction in other forums is permitted, provided the original author(s) and the copyright owner(s) are credited and that the original publication in this journal is cited, in accordance with accepted academic practice. No use, distribution or reproduction is permitted which does not comply with these terms.

frontiers in Oncology

MINI REVIEW
published: 16 March 2022
doi: 10.3389/fonc.2022.837057

Considerations for Germline Testing in Melanoma: Updates in Behavioral Change and Pancreatic Surveillance for Carriers of *CDKN2A* Pathogenic Variants

Kristen Pauley[1†], *Ambreen Khan*[1†], *Wendy Kohlmann*[1] *and Joanne Jeter*[2*]

[1] *Family Cancer Assessment Clinic, Huntsman Cancer Institute, Salt Lake City, UT, United States,* [2] *Department of Internal Medicine, Huntsman Cancer Institute, Salt Lake City, UT, United States*

OPEN ACCESS

Edited by:
Joshua Arbesman, Cleveland Clinic, United States

Reviewed by:
Lorenza Pastorino, University of Genoa, Italy
Pauline Funchain, Cleveland Clinic, United States

***Correspondence:**
Joanne Jeter
Joanne.Jeter@hci.utah.edu

[†]*These authors have contributed equally to this work and share first authorship*

Specialty section:
This article was submitted to Skin Cancer, a section of the journal Frontiers in Oncology

Received: *16 December 2021*
Accepted: *23 February 2022*
Published: *16 March 2022*

Citation:
Pauley K, Khan A, Kohlmann W and Jeter J (2022) Considerations for Germline Testing in Melanoma: Updates in Behavioral Change and Pancreatic Surveillance for Carriers of CDKN2A Pathogenic Variants. Front. Oncol. 12:837057. doi: 10.3389/fonc.2022.837057

The largest proportion of hereditary melanoma cases are due to pathogenic variants (PVs) in the *CDKN2A/p16* gene, which account for 20%-40% of familial melanomas and confer up to a 30%-70% lifetime risk for melanoma in individuals with these variants. In addition, PVs in the *CDKN2A* gene also increase risk for pancreatic cancer (~5–24% lifetime risk). Individuals with PVs in the *CDKN2A* gene also tend to have an earlier onset of cancer. Despite these known risks, uptake of germline testing has been limited in the past, largely due to perceptions of limited benefit for patients. Prevention recommendations have been developed for individuals with *CDKN2A* PVs as well the providers who care for them. On the patient level, behavioral modifications regarding melanoma prevention such as wearing sunscreen, limiting prolonged sun exposure and practicing general sun safety can help reduce risks. Germline testing can provide motivation for some individuals to adhere to these lifestyle changes. On the provider level, pancreatic cancer surveillance for individuals with *CDKN2A* PVs has been increasingly endorsed by expert consensus, although the efficacy of these surveillance methods remains under study. This review summarizes the updated surveillance guidelines for individuals with *CDKN2A* PVs and explores the impact of genetic counseling and testing in influencing behavioral changes in these individuals.

Keywords: CDKN2A, melanoma, pancreatic cancer, surveillance, behavior change, hereditary cancer syndromes

BACKGROUND

Most melanomas are sporadic; however, between 7-15% of melanomas occur in those with a family history of the cancer (1, 2). Many factors are involved in increasing an individual's risk for melanoma, most of which influence a family as a whole. While sun exposure experiences, skin pigmentation, and geographic location have been well-characterized as risk factors (3–8), more recently, genetics have been a topic of interest in the melanoma world. Germline pathogenic variants (PVs) in a number of genes predispose to melanoma (9–12), but the largest proportion of

familial melanoma cases (20%-40%) are due to PVs in the gene *CDKN2A (cyclin-dependent kinase inhibitor 2A)* (2, 12).

CDKN2A functions as a tumor suppressor gene, and somatic *CDKN2A* PVs are commonly found in both sporadic and hereditary melanomas (1). This gene is located on chromosome 9p21.3 and has two main transcripts (isoforms 1 and 4). Isoform 1 encodes the protein p16 (INK4a), while isoform 4 encodes the protein p14 (ARF). Germline PVs in the *CDKN2A* gene more commonly affect protein p16 than p14 and typically affect function of the G1/S checkpoint in the cell cycle by inhibiting cyclin-dependent kinases CDK4 and CDK6. This inhibition allows for uncontrolled cellular proliferation, which has many downstream carcinogenic affects (13). For simplicity, we will be using *CDKN2A* to refer to the PVs that occur in the p16 isoform as these are more common and better described than PVs in the p14 isoform.

FAMILIAL ATYPICAL MULTIPLE MOLE MELANOMA SYNDROME

Germline PVs in the *CDKN2A* gene are consistent with the condition called familial atypical multiple mole melanoma syndrome (FAMMM) (13). FAMMM is an autosomal dominant condition characterized by a large number of melanocytic nevi (often >50), up to 65-fold increased risk for cutaneous melanoma, and a 13-47-fold increased risk for pancreatic cancer (13–15). This translates to a 30%-70% lifetime risk for melanoma and a 5%-24% lifetime risk for pancreatic cancer (16, 17). In addition, other cancers have been observed in carriers, although actionable guidelines for increased surveillance for these cancers are not available at this time (18, 19).The penetrance rate for melanoma in individuals with *CDKN2A* PVs is estimated at 58-92% by age 80 (13, 20, 21). This variance in penetration may be related to location and associated sun exposure, although studies are conflicting on this point (22, 23). Variants in *MC1R*, often but not always associated with a red hair phenotype, can act as a modifier gene for *CDKN2A* mutation carriers, as well as their known effect as an independent low-penetrance susceptibility gene for melanoma (24). Histopathologic characteristics and somatic mutations of melanomas in individuals with *CDKN2A* PVs are similar to those with sporadic melanoma (13, 14, 25–28). Of note, several *CDKN2A* patients have been reported with melanomas with coexisting *BRAF* and *NRAS* mutations, which is uncommon in sporadic melanomas (28). Higher melanoma mortality rates have been described in *CDKN2A* families than in wild-type melanoma families (10); however other studies have found no difference in survival rates between *CDKN2A* carriers and non-carriers (29). (see **Table 1**)

Clinical characteristics of FAMMM include a large number of atypical melanocytic nevi; however, multiple nevi, while characteristic, are not diagnostic of FAMMM (1, 32). Multiple and/or dysplastic nevi are not restricted to inherited syndromes and are considered a strong risk factor for both sporadic melanoma and melanoma in *CDKN2A* carriers (33–36). Atypical nevi may transform into malignant melanoma, but melanomas in FAMMM patients often also develop on normal skin (13, 33, 37, 38).

Melanoma diagnosis in FAMMM cohorts typically occurs over a decade earlier than that in sporadic melanoma cases. Sporadic melanoma is typically diagnosed between the ages of 53-61, whereas individuals with a *CDKN2A* PV are often diagnosed between ages 30-45 (1, 39–41). The youngest reported cases of melanoma in FAMMM families have been seen at age 13 (42, 43). Additionally, individuals with *CDKN2A* PVs have an increased probability of multiple primary melanomas: one study reported a 23% incidence of second melanoma primary diagnosed within 5 years of the first, representing a 10-fold increase over that of melanoma patients without *CDKN2A* PVs (39). In a genotype-phenotype correlation study, multiple primary melanomas were the most predictive

TABLE 1 | Summary of data on age of onset, penetrance and lifetime risks of FAMMM-associated cancer.

Cancer	Age of onset	Penetrance	Lifetime risks
Melanoma	30-45 years	58%-92% by age 80	30%-70% absolute risk, depending on other risk factors (family history, geographic location, others) (16, 17)
Pancreatic	58 years	Not well established One Dutch study quotes 17% penetrance by 75 years (30)	5%-24% absolute risk (16, 17) Relative risk = 43.8 95% CI = 13.8 – 139 (31)
Astrocytoma/Brain	Not well established	n/a	Relative risk = 1.9, 95% CI = 0.2 to 7.1, P = 0.58 (19)
Wilms tumor	Not well established	n/a	Relative risk = 40.4, 95% CI = 3.4 to 352.7, P = 0.005 (19)
Colon/GI	Not well established	n/a	Relative risk= 1.9 95% CI = 0.9 to 3.4, P = 0.10 (19)
Respiratory/lung	Not well established	n/a	Relative risk = 15.6 95% CI = 5.4 to 46 (31) Relative risk = 1.4, CI = 0.6 to 3.0, P = 0.44 (19)
Upper digestive	Not well established	n/a	Relative risk = 17.1 95% CI = 6.3 to 46.5 (31)

n/a, Not available.

factor for presence of a CDKN2A mutation (44). Given the earlier presentation of melanoma in this population and potential for multiple primary lesions, increased and intensive surveillance for cutaneous melanomas is routinely recommended with screening starting at a young age (13, 45).

MELANOMA SURVEILLANCE

Many groups have provided recommendations for high-risk families with *CDKN2A* PVs, which include increased frequency of clinical skin examinations beginning in childhood (12, 46, 47). Suggested surveillance include clinical skin examinations yearly or biannually starting from age 10 with monthly self-examination of the skin beginning in childhood (47). When identified, suspicious moles should be biopsied and removed (47). Lifestyle modifications have been recommended for individuals with *CDKN2A* PVs that include limiting exposure to the sun and to ultraviolet radiation. Protective clothing should be worn when exposure is unavoidable (47). (see **Table 2**)

Full body skin examinations should include the scalp, oral mucosa, and genitals, as significant variability has been reported regarding location of melanomas (41). A healthcare provider should examine nevi for features of melanoma every 6 to 12 months. The patient should look for abnormalities in growth, shape or coloring through self-examinations of the skin. The ABCDE features (Asymmetry, Border irregularity, Color variegation, Diameter >6mm, Evolution) of melanoma should be screened for in these patients (13, 48).

BEHAVIORAL CHANGES IN *CDKN2A* CARRIERS

Predictive genetic testing has been shown to increase the uptake of cancer screening and prevention (51–53). In the past, concerns were raised about offering predictive DNA analysis for families suspicious of harboring a *CDKN2A* PV outside of defined research protocols. The concern was that the likelihood of finding a PV was low and the efficacy of melanoma prevention was lacking (54). In general meta-analysis of the benefits of predictive genetic testing for disease prevention in cohorts of multiple complex hereditary conditions showed mixed results (52, 55). In studies of *CDNK2A* carriers specifically, positive outcomes were reported one year post-counseling, including fewer reported sunburns and lower daily ultraviolet radiation dose compared to baseline analysis (53). Another study found that two years following genetic counseling, unaffected *CDKN2A* carriers reported improvements in following the recommendation to undergo annual total body skin examinations and increased thoroughness in their monthly skin self-examinations (51). Genetic counseling is recommended by the NCCN for familial melanoma following the "rule of three," including three family members with melanoma/pancreatic cancer/astrocytoma on the same side of the family or an individual with three malignant melanomas or associated tumors (49).

Genetic testing to identify hereditary cancer risks has the potential for preventative surveillance and medical management options if a genetic predisposition is identified in an individual. While some hereditary cancer syndromes have surveillance guidelines that require routine medical follow-ups and options for additional imaging or surgery to reduce risks, hereditary predisposition to melanoma can be complicated by its multifactorial nature. The greater onus of prevention may fall on the individual. Behavioral modifications such as wearing sunscreen, limiting prolonged sun exposure and practicing general sun safety can allow some individuals to feel a greater sense of control in their medical management, but can also create limitations for other individuals who may not feel adequately prepared to make such behavioral modifications (56, 57).

Given the risk for melanoma is impacted by environmental factors such as UV exposure, a deeper understanding of the behavioral changes among individuals with a *CDKN2A* PV is important in tailoring medical management and targeting surveillance efforts. Several studies have indicated that identification of carrier status with a *CDKN2A* pathogenic

TABLE 2 | Summary of surveillance recommendations for *CDKN2A* carriers.

Cancer	Initiation	Methods	Interval	Additional information
Melanoma	10 years	Self-examination	Monthly	Look for abnormalities in growth, shape, or coloring
		Clinical skin examination including: - Nevi - Scalp - Oral mucosa - Genitals (47)	Yearly or biannually	ABCDE Features: - Asymmetry - Border irregularity - Color variegation - Diameter >6mm - Evolution (48)
Pancreatic	40 years or 10 years earlier than earliest age of diagnosis in family	EUS and/or MRCP (49, 50)	Yearly if no abnormalities found	Should be performed at experienced high-volume centers (49)
		Fasting blood glucose and/or HbA1c (50)	Routine	
Astrocytoma/Brain, Wilms, Colon, Upper GI, Respiratory Tract	No consensus	No consensus	No consensus	

variant can have cognitive and behavioral impacts beyond family history-based risk assessment alone (53, 58, 59). For example, one study showed that two years after undergoing genetic testing, *CDKN2A* carriers without a personal history of melanoma were found to have a 30% increase in adherence to total body skin examination (TBSEs) (p=0.032, one tailed) (60). This adherence was comparable to family members with melanoma who tested positive for the PV (p= 0.635).

While receiving a test result indicating a *CDKN2A* PV has been showing to have dramatic effects on behavior, not all patients undergoing testing will receive this result. Testing negative for a familial *CDKN2A* has not been found to have negative effects such as promoting increased UV exposure. At-risk relatives from melanoma-prone families without a known genetic etiology and for whom genetic testing was not available, also have been shown to benefit from genetic counseling about melanoma risk. Following genetic counseling they also exhibited significantly decreased UV exposure, though not as quickly or to the extent as *CDKN2A* carriers (53).

CDKN2A testing and test reporting in these studies was conducted in the setting of pre- and post-test genetic counseling. Pairing genetic testing with appropriate genetic counseling will maximize the benefit of this information for patients. Studies have shown that relatives at risk for *CDKN2A* PVs exhibit high levels of interest in genetic testing, similar to levels of interest in families with other hereditary cancer syndromes.

PREDICTIVE GENETIC TESTING FOR MINORS

Offering genetic testing to children is recommended only for conditions in which early intervention is available and the potential benefit of testing at that age outweighs the potential psychological harms (13). While the melanoma risk associated with *CDKN2A* PVs typically present in adulthood, screening recommendations initiate at age 10. Additionally, childhood is a time of significant UV exposure, and testing earlier in life may present an opportunity to minimize exposures that would contribute to melanoma risk later in life.

Genetic testing and counseling for *CDKN2A* has been shown to improve photoprotective behaviors among children (ages 10-15y), decrease sunburns by over 50% (p>.05), and increase adherence to sun-protective behaviors (55.6% vs. 88.9%, p = 0.04) one year after genetic counseling and testing (61). The decrease in sunburns and adherence to sun protection was reported equally by both carriers and non-carriers (p > 0.05) highlighting the importance of pre-test genetic counseling in improving awareness regarding sun-protective behaviors (61). There was no perceived increase noted in anxiety or depression among minors who underwent genetic testing for *CDKN2A*. Counseling and testing of children may heighten parents' awareness of the need for sun protection in childhood.

It should be acknowledged that there are many barriers to sustainable and life-long behavioral changes and these can be challenging for individuals and families. According to Wu et al., peer influence can be an important factor impacting engagement in sun protective behaviors among children (56). Family modeling and communication, such as parents modeling preventative behaviors, can allow for improved engagement in sun protective behaviors among children. Interventions targeting education for broader populations regarding sun protection and dispelling of myths related to UV exposure/sun safety, such as the perception of reduced UVR exposure in winter, may be beneficial in addressing gaps in education and awareness among the general population.

PANCREATIC CANCER SURVEILLANCE

Pancreatic ductal adenocarcinoma (PDAC) is seen in association with FAMMM as the second most frequent cancer diagnosis in these kindreds (14, 15). Pancreatic cancer is often diagnosed at later stages, which is associated with poorer prognoses (62, 63). Less than ¼ of patients are candidates for potentially curative surgical resection at the time of diagnosis (64), therefore early detection is extremely important in improving survival outcomes (50).

While effective screening and prevention measures for melanoma exist, the efficacy of pancreatic cancer surveillance has not been as well established (65). It is also unknown how individuals with a *CDKN2A* PV may make behavioral changes regarding their pancreatic cancer risk, given there is greater individual control over melanoma prevention than pancreatic cancer prevention, at least at this time. In one study disclosing the return of research results, 85.7% (n = 12) of *CDKN2A* carriers indicated that they planned to have their pancreas checked in the next six months. However, not all carriers who intended to be screened for pancreatic cancer did so within six months. Those with positive *CDKN2A* results were more likely to communicate these results to their healthcare teams than non-carriers (66).

PDAC SURVEILLANCE GUIDELINES

Pancreatic cancer screening guidelines have evolved over the years. Most recently, the International Cancer of the Pancreas Screening (CAPS) Consortium and the National Comprehensive Cancer Network (NCCN) have established consensus guidelines for surveillance of high-risk individuals (49, 50). Current CAPS and NCCN recommendations support pancreatic cancer screening for individuals with *CDKN2A* PVs, regardless of their family history.

For CDKN2A PV carriers, these guidelines recommend initiation of surveillance 10 years earlier than the earliest age of pancreatic cancer diagnosis in the family, or at age 40, whichever is earlier. The NCCN guidelines recommend that individuals considered to be at high risk for pancreatic cancer pursue these screenings at experienced high-volume centers after having in-depth discussions about the benefits and limitations of these screenings with their healthcare providers (49).

Surveillance methods include annual imaging with endoscopic ultrasound (EUS) and/or MRI/Magnetic resonance cholangiopancreatography (MRCP) per both CAPS and NCCN recommendations. CAPS guidelines recommend routine testing for late onset diabetes with fasting blood glucose and/or HbA1c, adding that high-risk individuals with new-onset diabetes should prompt additional screening (50). One year interval surveillance was recommended for those without abnormalities on imaging (49, 50). However, the CAPS Consortium did not reach a consensus on how to alternate the two screening modalities (50).

The Dutch Familial Pancreatic Cancer surveillance study performed a prospective study aimed at determining the long-term yield of PDAC surveillance in high-risk individuals between the years 2006-2019 (63). PDACs found through surveillance in the high-risk group were more likely to be resectable than sporadic PDACs diagnosed on the basis of development of symptoms. Of the 96 participants with CDKN2A PVs in this study, 7 were found to have PDAC through surveillance. EUS was found to be a superior imaging tool at detecting PDAC lesions with a solid component when compared to MRI/MRCP, while MRI/MRCP was found to be more sensitive at identifying small (sub-cm) cystic lesions. The diagnostic yield of PDAC was beneficial in high-risk patients, including those with *CDKN2A* PVs, but timely identification of disease in these patients still remains challenging. Individuals included in the study were highly adherent to scheduled procedures, which suggests that those with PDAC susceptibility PVs are ideally suited for increased surveillance (63).

Other studies have shown that PDAC surveillance of *CDKN2A* PV carriers is beneficial in detecting PDACs at a more resectable stage (66). Prospective screening data from three European centers were collected. Of those individuals who participated in surveillance programs diagnosed with PDAC, the resection rate was found to be 75% with a 5-year survival rate of 24% (compared historically to 13-21.2% with a 5-year survival rate of 4-7% for sporadic PDAC) (62, 66).

A second study following patients enrolled in the Cancer of the Pancreas Screening cohort also found strong evidence supporting the use of pancreatic surveillance in high-risk individuals (62, 67). This study found the majority of PDACs detected during screening to be resectable (90%) with a significantly increased 3-year survival outcome (85%). These two studies highlight the potential benefit of PDAC surveillance in high-risk cohorts and were used to justify the update to the CAPS guidelines (50).

CONCLUSIONS

Historically germline genetic testing for cancer susceptibility was encouraged for genes with established clinical utility (68, 69). For many years, *CDKN2A* genetic testing has been felt to limit uptake on this basis. In recent years, developments in the behavioral science literature as well as the pancreatic surveillance literature have altered the risk-benefit ratio in *CDKN2A* testing. Behavioral literature has demonstrated increased sun-protective behaviors and surveillance, not just for individuals who were positive for *CDKN2A* PVs but also for those who underwent genetic evaluation for this condition. Additionally, pancreatic surveillance has been effective in identifying asymptomatic pancreatic cancers in this population and may be effective in down staging this disease. For this reason, expert consensus has recommended pancreatic cancer surveillance for all individuals with *CDKN2A* PVs (49, 50). Based on data emerging in these two areas, re-evaluation of the clinical utility of germline *CDKN2A* testing is appropriate.

AUTHOR CONTRIBUTIONS

AK, KP, WK, and JJ contributed to conception and design of the manuscript. AK and KP wrote the first draft of the manuscript. All authors contributed to manuscript revision, read, and approved the submitted version.

ACKNOWLEDGMENTS

The authors extend gratitude to Katy Nottingham, for editorial assistance. This publication utilized the Genetic Counseling Shared Resource at Huntsman Cancer Institute at the University of Utah and was supported by the National Cancer Institute of the National Institutes of Health under Award Number P30CA042014.

REFERENCES

1. Toussi A, Mans N, Welborn J, Kiuru M. Germline Mutations Predisposing to Melanoma. *J Cutaneous Pathol* (2020) 47(7):606–16. doi: 10.1111/cup.13689
2. Soura E, Eliades PJ, Shannon K, Stratigos AJ, Tsao H. Hereditary Melanoma: Update on Syndromes and Management: Genetics of Familial Atypical Multiple Mole Melanoma Syndrome. *J Am Acad Dermatol* (2016) 74 (3):395–407quiz 8–10. doi: 10.1016/j.jaad.2015.08.038
3. Arnold M, de Vries E, Whiteman DC, Jemal A, Bray F, Parkin DM, et al. Global Burden of Cutaneous Melanoma Attributable to Ultraviolet Radiation in 2012. *Int J Cancer* (2018) 143(6):1305–14. doi: 10.1002/ijc.31527
4. Eide MJ, Weinstock MA. Association of UV Index, Latitude, and Melanoma Incidence in Nonwhite Populations–US Surveillance, Epidemiology, and End Results (SEER) Program, 1992 to 2001. *Arch Dermatol* (2005) 141(4):477–81. doi: 10.1001/archderm.141.4.477
5. Elwood JM, Jopson J. Melanoma and Sun Exposure: An Overview of Published Studies. *Int J Cancer* (1997) 73(2):198–203. doi: 10.1002/(SICI)1097-0215(19971009)73:2<198::AID-IJC6>3.0.CO;2-R
6. Oliveria SA, Saraiya M, Geller AC, Heneghan MK, Jorgensen C. Sun Exposure and Risk of Melanoma. *Arch Dis Child* (2006) 91(2):131–8. doi: 10.1136/adc.2005.086918
7. Qureshi AA, Laden F, Colditz GA, Hunter DJ. Geographic Variation and Risk of Skin Cancer in US Women. Differences Between Melanoma, Squamous Cell Carcinoma, and Basal Cell Carcinoma. *Arch Intern Med* (2008) 168 (5):501–7. doi: 10.1001/archinte.168.5.501
8. Scherer D, Kumar R. Genetics of Pigmentation in Skin Cancer–A Review. *Mutat Res* (2010) 705(2):141–53. doi: 10.1016/j.mrrev.2010.06.002
9. Aoude LG, Heitzer E, Johansson P, Gartside M, Wadt K, Pritchard AL, et al. POLE Mutations in Families Predisposed to Cutaneous Melanoma. *Fam Cancer* (2015) 14(4):621–8. doi: 10.1007/s10689-015-9826-8

10. Pissa M, Helkkula T, Appelqvist F, Silander G, Borg ÅVerifytat, Pettersson J, et al. CDKN2A Genetic Testing in Melanoma-Prone Families in Sweden in the Years 2015–2020: Implications for Novel National Recommendations. *Acta Oncol* (2021) 60(7):888–96. doi: 10.1080/0284186X.2021.1914346
11. Robles-Espinoza CD, Harland M, Ramsay AJ, Aoude LG, Quesada V, Ding Z, et al. POT1 Loss-of-Function Variants Predispose to Familial Melanoma. *Nat Genet* (2014) 46(5):478–81. doi: 10.1038/ng.2947
12. Rossi M, Pellegrini C, Cardelli L, Ciciarelli V, Di Nardo L, Fargnoli MC. Familial Melanoma: Diagnostic and Management Implications. *Dermatol Pract Concept* (2019) 9(1):10–6. doi: 10.5826/dpc.0901a03
13. Eckerle Mize D, Bishop M, Resse E, Sluzevich J. Familial Atypical Multiple Mole Melanoma Syndrome. In: DL Riegert-Johnson, LA Boardman, T Hefferon, M Roberts, editors. *Cancer Syndromes*. Bethesda (MD: National Center for Biotechnology Information (US) Copyright © 2009-, Douglas L Riegert-Johnson (2009).
14. Goldstein AM, Fraser MC, Struewing JP, Hussussian CJ, Ranade K, Zametkin DP, et al. Increased Risk of Pancreatic Cancer in Melanoma-Prone Kindreds With P16 INK4 Mutations. *N Engl J Med* (1995) 333(15):970–5. doi: 10.1056/NEJM199510123331504
15. Habbe N, Langer P, Sina-Frey M, Bartsch D. Familial Pancreatic Cancer Syndromes. *Endocrinol Metab Clinics North Am* (2006) 35:417–30, xi. doi: 10.1016/j.ecl.2006.02.016
16. Hruban RH, Canto MI, Goggins M, Schulick R, Klein AP. Update on Familial Pancreatic Cancer. *Adv Surg* (2010) 44:293–311. doi: 10.1016/j.yasu.2010.05.011
17. Canto MI, Harinck F, Hruban RH, Offerhaus GJ, Poley JW, Kamel I, et al. International Cancer of the Pancreas Screening (CAPS) Consortium Summit on the Management of Patients With Increased Risk for Familial Pancreatic Cancer. *Gut* (2013) 62(3):339–47. doi: 10.1136/gutjnl-2012-303108
18. Middlebrooks CD, Stacey ML, Li Q, Snyder C, Shaw TG, Richardson-Nelson T, et al. Analysis of the *CDKN2A* Gene in FAMMM Syndrome Families Reveals Early Age of Onset for Additional Syndromic Cancers. *Cancer Res* (2019) 79(11):2992–3000. doi: 10.1158/0008-5472.CAN-18-1580
19. Mukherjee B, Delancey JO, Raskin L, Everett J, Jeter J, Begg CB, et al. Risk of Non-Melanoma Cancers in First-Degree Relatives of CDKN2A Mutation Carriers. *J Natl Cancer Inst* (2012) 104(12):953–6. doi: 10.1093/jnci/djs221
20. Parker JF, Florell SR, Alexander A, DiSario JA, Shami PJ, Leachman SA. Pancreatic Carcinoma Surveillance in Patients With Familial Melanoma. *Arch Dermatol* (2003) 139(8):1019–25. doi: 10.1001/archderm.139.8.1019
21. Rulyak SJ, Lowenfels AB, Maisonneuve P, Brentnall TA. Risk Factors for the Development of Pancreatic Cancer in Familial Pancreatic Cancer Kindreds. *Gastroenterology* (2003) 124(5):1292–9. doi: 10.1016/S0016-5085(03)00272-5
22. Bishop DT, Demenais F, Goldstein AM, Bergman W, Bishop JN, Bressac-de Paillerets B, et al. Geographical Variation in the Penetrance of CDKN2A Mutations for Melanoma. *J Natl Cancer Inst* (2002) 94(12):894–903. doi: 10.1093/jnci/94.12.894
23. Cust AE, Harland M, Makalic E, Schmidt D, Dowty JG, Aitken JF, et al. Melanoma Risk for CDKN2A Mutation Carriers Who Are Relatives of Population-Based Case Carriers in Australia and the UK. *J Med Genet* (2011) 48(4):266–72. doi: 10.1136/jmg.2010.086538
24. Santillan AA, Cherpelis BS, Glass LF, Sondak VK. Management of Familial Melanoma and Nonmelanoma Skin Cancer Syndromes. *Surg Oncol Clin N Am* (2009) 18(1):73–98, viii. doi: 10.1016/j.soc.2008.08.003
25. Ford D, Bliss JM, Swerdlow AJ, Armstrong BK, Franceschi S, Green A, et al. Risk of Cutaneous Melanoma Associated With a Family History of the Disease. *Int J Cancer* (1995) 62(4):377–81. doi: 10.1002/ijc.2910620403
26. Eskandarpour M, Hashemi J, Kanter L, Ringborg U, Platz A, Hansson J. Frequency of UV-Inducible NRAS Mutations in Melanomas of Patients With Germline CDKN2A Mutations. *JNCI: J Natl Cancer Institute* (2003) 95(11):790–8. doi: 10.1093/jnci/95.11.790
27. Zebary A, Omholt K, van Doorn R, Ghiorzo P, Harbst K, Hertzman Johansson C, et al. Somatic BRAF and NRAS Mutations in Familial Melanomas With Known Germline CDKN2A Status: A Genomel Study. *J Invest Dermatol* (2014) 134(1):287–90. doi: 10.1038/jid.2013.270
28. Jovanovic B, Egyhazi S, Eskandarpour M, Ghiorzo P, Palmer JM, Bianchi Scarrà G, et al. Coexisting NRAS and BRAF Mutations in Primary Familial Melanomas With Specific CDKN2A Germline Alterations. *J Invest Dermatol* (2010) 130(2):618–20. doi: 10.1038/jid.2009.287
29. Dalmasso B, Pastorino L, Ciccarese G, Andreotti V, Grillo F, Mastracci L, et al. CDKN2A Germline Mutations are Not Associated With Poor Survival in an Italian Cohort of Melanoma Patients. *J Am Acad Dermatol* (2019) 80(5):1263–71. doi: 10.1016/j.jaad.2018.07.060
30. Vasen H, Ibrahim I, Ponce CG, Slater EP, Matthäi E, Carrato A, et al. Benefit of Surveillance for Pancreatic Cancer in High-Risk Individuals: Outcome of Long-Term Prospective Follow-Up Studies From Three European Expert Centers. *J Clin Oncol* (2016) 34(17):2010–9. doi: 10.1200/JCO.2015.64.0730
31. Helgadottir H, Höiom V, Jönsson G, Tuominen R, JIngvar C, Borg A, et al. High Risk of Tobacco-Related Cancers in CDKN2A Mutation-Positive Melanoma Families. *J Med Genet* (2014) 51(8):545–52. doi: 10.1136/jmedgenet-2014-102320
32. Bishop JA, Wachsmuth RC, Harland M, Bataille V, Pinney E, Mac KP, et al. Genotype/Phenotype and Penetrance Studies in Melanoma Families With Germline CDKN2A Mutations. *J Invest Dermatol* (2000) 114(1):28–33. doi: 10.1046/j.1523-1747.2000.00823.x
33. Carey WPJr., Thompson CJ, Synnestvedt M, Dt G, Halpern A, Schultz D, et al. Dysplastic Nevi as a Melanoma Risk Factor in Patients With Familial Melanoma. *Cancer* (1994) 74(12):3118–25. doi: 10.1002/1097-0142(19941215)74:12<3118::AID-CNCR2820741210>3.0.CO;2-7
34. Swerdlow AJ, English J, MacKie RM, O'Doherty CJ, Hunter JA, Clark J, et al. Benign Melanocytic Naevi as a Risk Factor for Malignant Melanoma. *(Clin Res Ed)* (1986) 292(6535):1555–9. doi: 10.1136/bmj.292.6535.1555
35. Halpern AC, Guerry Dt, Elder DE, Clark WHJr., Synnestvedt M, Norman S, et al. Dysplastic Nevi as Risk Markers of Sporadic (Nonfamilial) Melanoma. *A Case-Control Study Arch Dermatol* (1991) 127(7):995–9. doi: 10.1001/archderm.127.7.995
36. Bataille V, Bishop JA, Sasieni P, Swerdlow AJ, Pinney E, Griffiths K, et al. Risk of Cutaneous Melanoma in Relation to the Numbers, Types and Sites of Naevi: A Case-Control Study. *Br J Cancer* (1996) 73(12):1605–11. doi: 10.1038/bjc.1996.302
37. Czajkowski R, Placek W, Drewa G, Czajkowska A, Uchańska G. FAMMM Syndrome: Pathogenesis and Management. *Dermatol Surg* (2004) 30(2 Pt 2):291–6. doi: 10.1111/j.1524-4725.2004.30088.x
38. Kelly JW, Yeatman JM, Regalia C, Mason G, Henham AP. A High Incidence of Melanoma Found in Patients With Multiple Dysplastic Naevi by Photographic Surveillance. *Med J Aust* (1997) 167(4):191–4. doi: 10.5694/j.1326-5377.1997.tb138843.x
39. van der Rhee JI, Krijnen P, Gruis NA, de Snoo FA, Vasen HFA, Putter H, et al. Clinical and Histologic Characteristics of Malignant Melanoma in Families With a Germline Mutation in CDKN2A. *J Am Acad Dermatol* (2011) 65(2):281–8. doi: 10.1016/j.jaad.2010.06.044
40. Goldstein AM, Chan M, Harland M, Gillanders EM, Hayward NK, Avril MF, et al. High-Risk Melanoma Susceptibility Genes and Pancreatic Cancer, Neural System Tumors, and Uveal Melanoma Across Genomel. *Cancer Res* (2006) 66(20):9818–28. doi: 10.1158/0008-5472.CAN-06-0494
41. Måsbäck A, Olsson H, Westerdahl J, Sandberg T, Borg A, Jonsson N, et al. Clinical and Histopathological Features of Malignant Melanoma in Germline CDKN2A Mutation Families. *Melanoma Res* (2002) 12(6):549–57. doi: 10.1097/00008390-200212000-00004
42. Lynch HT, Brand RE, Hogg D, Deters CA, Fusaro RM, Lynch JF, et al. Phenotypic Variation in Eight Extended CDKN2A Germline Mutation Familial Atypical Multiple Mole Melanoma-Pancreatic Carcinoma-Prone Families: The Familial Atypical Mole Melanoma-Pancreatic Carcinoma Syndrome. *Cancer* (2002) 94(1):84–96. doi: 10.1002/cncr.10159
43. Gironi LC, Colombo E, Farinelli P, Giorgione R, Bozzola C, Ogliara P, et al. Germline CDKN2A Mutations in Childhood Melanoma: A Case of Melanoma-Pancreatic Cancer Syndrome. *Int J Dermatol* (2015) 54(12):e553–5. doi: 10.1111/ijd.12933
44. Pedace L, De Simone P, Castori M, et al. Clinical Features Predicting Identification of CDKN2A Mutations in Italian Patients With Familial Cutaneous Melanoma. *Cancer Epidemiol* (2011) 35(6):e116–20. doi: 10.1016/j.canep.2011.07.007
45. Goldstein AM, Struewing JP, Chidambaram A, Fraser MC, Tucker MA. Genotype-Phenotype Relationships in U.S. Melanoma-Prone Families With CDKN2A and CDK4 Mutations. *J Natl Cancer Inst* (2000) 92(12):1006–10. doi: 10.1093/jnci/92.12.1006

46. Niendorf KB, Tsao H. Cutaneous Melanoma: Family Screening and Genetic Testing. *Dermatol Ther* (2006) 19(1):1–8. doi: 10.1111/j.1529-8019.2005.00050.x
47. *CDKN2A Mutations: Cancer Risk and Management Recommendations 2020* (2020). UT Southwestern Harold C: Simmons Comprehensive Cancer Center. Available at: https://s3-us-west-2.amazonaws.com/utsw-patientcare-web-production/documents/Familial_Atypical_Mole_Melanoma_CDKN2A.pdf (Accessed November 30, 2021).
48. Abbasi NR, Shaw HM, Rigel DS, Friedman RJ, McCarthy WH, Osman I, et al. Early Diagnosis of Cutaneous Melanoma: Revisiting the ABCD Criteria. *Jama* (2004) 292(22):2771–6. doi: 10.1001/jama.292.22.2771
49. National Comprehensive Cancer Network. *Genetic/Familial High-Risk Assessment: Breast, Ovarian and Pancreatic (Version 1.2022)* . Available at: https://www.nccn.org/guidelines/guidelines-detail?category=2&id=1503 (Accessed December 10, 2021).
50. Goggins M, Overbeek KA, Brand R, Syngal S, Del Chiaro M, Bartsch DK, et al. Management of Patients With Increased Risk for Familial Pancreatic Cancer: Updated Recommendations From the International Cancer of the Pancreas Screening (CAPS) Consortium. *Gut* (2020) 69(1):7–17. doi: 10.1136/gutjnl-2019-319352corr1
51. Aspinwall LG, Taber JM, Kohlmann W, Leaf SL, Leachman SA. Unaffected Family Members Report Improvements in Daily Routine Sun Protection 2 Years Following Melanoma Genetic Testing. *Genet Med* (2014) 16(11):846–53. doi: 10.1038/gim.2014.37
52. Hollands GJ, French DP, Griffin SJ, Prevost AT, Sutton S, King S, et al. The Impact of Communicating Genetic Risks of Disease on Risk-Reducing Health Behaviour: Systematic Review With Meta-Analysis. *BMJ* (2016) 352:i1102. doi: 10.1136/bmj.i1102
53. Stump TK, Aspinwall LG, Drummond DM, Taber JM, Kohlmann W, Champine M, et al. CDKN2A Testing and Genetic Counseling Promote Reductions in Objectively Measured Sun Exposure One Year Later. *Genet Med* (2020) 22(1):26–34. doi: 10.1038/s41436-019-0608-9
54. Kefford RF, Mann GJ. Is There a Role for Genetic Testing in Patients With Melanoma? *Curr Opin Oncol* (2003) 15(2):157–61. doi: 10.1097/00001622-200303000-00007
55. Frieser MJ, Wilson S, Vrieze S. Behavioral Impact of Return of Genetic Test Results for Complex Disease: Systematic Review and Meta-Analysis. *Health Psychol* (2018) 37(12):1134–44. doi: 10.1037/hea0000683
56. Wu YP, Parsons BG, Mooney R, Aspinwall LG, Cloyes K, Hay JL, et al. Barriers and Facilitators to Melanoma Prevention and Control Behaviors Among at-Risk Children. *J Community Health* (2018) 43(5):993–1001. doi: 10.1007/s10900-018-0516-y
57. Tripp MK, Peterson SK, Prokhorov AV, Shete SS, Lee JE, Gershenwald JE, et al. Correlates of Sun Protection and Sunburn in Children of Melanoma Survivors. *Am J Prev Med* (2016) 51(3):e77–85. doi: 10.1016/j.amepre.2016.02.032
58. Aspinwall LG, Stump TK, Taber JM, Drummond DM, Kohlmann W, Champine M, et al. Genetic Test Reporting of CDKN2A Provides Informational and Motivational Benefits for Managing Melanoma Risk. *Transl Behav Med* (2018) 8(1):29–43. doi: 10.1093/tbm/ibx011
59. Aspinwall LG, Leaf SL, Kohlmann W, Dola ER, Leachman SA. Patterns of Photoprotection Following CDKN2A/P16 Genetic Test Reporting and Counseling. *J Am Acad Dermatol* (2009) 60(5):745–57. doi: 10.1016/j.jaad.2008.12.034
60. Aspinwall LG, Taber JM, Leaf SL, Kohlmann W, Leachman SA. Melanoma Genetic Counseling and Test Reporting Improve Screening Adherence Among Unaffected Carriers 2 Years Later. *Cancer Epidemiol Biomarkers Prev* (2013) 22(10):1687–97. doi: 10.1158/1055-9965.EPI-13-0422
61. Stump TK, Aspinwall LG, Kohlmann W, Champine M, Hauglid J, Wu YP, et al. Genetic Test Reporting and Counseling for Melanoma Risk in Minors May Improve Sun Protection Without Inducing Distress. *J Genet Couns* (2018) 27(4):955–67. doi: 10.1007/s10897-017-0185-5
62. Huang L, Jansen L, Balavarca Y, Molina-Montes E, Babaei M, van der Geest L, et al. Resection of Pancreatic Cancer in Europe and USA: An International Large-Scale Study Highlighting Large Variations. *Gut* (2019) 68(1):130–9. doi: 10.1136/gutjnl-2017-314828
63. Overbeek KA, Levink IJM, Koopmann BDM, Harinck F, Konings ICAW, Ausems MGEM, et al. Long-Term Yield of Pancreatic Cancer Surveillance in High-Risk Individuals. *Gut* (2021):gutjnl-2020-323611. doi: 10.1136/gutjnl-2020-323611
64. Gudjonsson B. Pancreatic Cancer: 80 Years of Surgery—Percentage and Repetitions. *HPB Surg* (2016) 2016:6839687. doi: 10.1155/2016/6839687
65. Poruk KE, Firpo MA, Adler DG, Mulvihill SJ. Screening for Pancreatic Cancer: Why, How, and Who? *Ann Surg* (2013) 257(1):17–26. doi: 10.1097/SLA.0b013e31825ffbfb
66. Leof ER, Zhu X, Rabe KG, McCormick JB, Petersen GM, Radecki Breitkopf C. Pancreatic Cancer and Melanoma Related Perceptions and Behaviors Following Disclosure of CDKN2A Variant Status as a Research Result. *Genet Med* (2019) 21(11):2468–77. doi: 10.1038/s41436-019-0517-y
67. Robson ME, Bradbury AR, Arun B, Domchek SM, Ford JM, Hampel HL, et al. American Society of Clinical Oncology Policy Statement Update: Genetic and Genomic Testing for Cancer Susceptibility. *J Clin Oncol* (2015) 33(31):3660–7. doi: 10.1200/JCO.2015.63.0996
68. ACMG Board of Directors. Clinical Utility of Genetic and Genomic Services: A Position Statement of the American College of Medical Genetics and Genomics. *Genet Med* (2015) 17:505–7. doi: 10.1038/gim.2015.41
69. Canto MI, Almario JA, Schulick RD, Yeo CJ, Klein A, Blackford A, et al. Risk of Neoplastic Progression in Individuals at High Risk for Pancreatic Cancer Undergoing Long-Term Surveillance. *Gastroenterology* (2018) 155(3):740–51.e2. doi: 10.1053/j.gastro.2018.05.035

Author Disclaimer: The content is solely the responsibility of the authors and does not necessarily represent the official views of the NIH.

Conflict of Interest: The authors declare that the research was conducted in the absence of any commercial or financial relationships that could be construed as a potential conflict of interest.

Publisher's Note: All claims expressed in this article are solely those of the authors and do not necessarily represent those of their affiliated organizations, or those of the publisher, the editors and the reviewers. Any product that may be evaluated in this article, or claim that may be made by its manufacturer, is not guaranteed or endorsed by the publisher.

Copyright © 2022 Pauley, Khan, Kohlmann and Jeter. This is an open-access article distributed under the terms of the Creative Commons Attribution License (CC BY). The use, distribution or reproduction in other forums is permitted, provided the original author(s) and the copyright owner(s) are credited and that the original publication in this journal is cited, in accordance with accepted academic practice. No use, distribution or reproduction is permitted which does not comply with these terms.

frontiers in Oncology

ORIGINAL RESEARCH
published: 18 March 2022
doi: 10.3389/fonc.2022.853076

Second Primary Malignancies in Patients With Melanoma Subtypes: Analysis of 120,299 Patients From the SEER Database (2000-2016)

Asad Loya[1], *Dan S. Gombos*[2,3,4] *and Sapna P. Patel*[5*]

[1] School of Medicine, Baylor College of Medicine, Houston, TX, United States, [2] Section of Ophthalmology, Department of Head and Neck Surgery, The University of Texas MD Anderson Cancer Center, Houston, TX, United States, [3] Department of Pediatrics, Division of Cancer Medicine, Baylor College of Medicine, Houston, TX, United States, [4] Department of Ophthalmology & Visual Sciences, The University of Texas Medical Branch at Galveston, Galveston, TX, United States, [5] Department of Melanoma Medical Oncology, The University of Texas MD Anderson Cancer Center, Houston, TX, United States

OPEN ACCESS

Edited by:
James L. Fisher,
The Ohio State University,
United States

Reviewed by:
Paolo Del Fiore,
Istituto Oncologico Veneto (IRCCS),
Italy
Amarinder Singh Thind,
University of Wollongong, Australia

***Correspondence:**
Sapna P. Patel
sppatel@mdanderson.org

Specialty section:
This article was submitted to Skin Cancer, a section of the journal Frontiers in Oncology

Received: 12 January 2022
Accepted: 21 February 2022
Published: 18 March 2022

Citation:
Loya A, Gombos DS and Patel SP (2022) Second Primary Malignancies in Patients With Melanoma Subtypes: Analysis of 120,299 Patients From the SEER Database (2000-2016). Front. Oncol. 12:853076. doi: 10.3389/fonc.2022.853076

Purpose: Evaluate incidence of second primary malignancies (SPM) after non-acral cutaneous melanoma (NACM), acral lentiginous melanoma (ALM), mucosal melanoma (MM), and uveal melanoma (UM).

Patients and Methods: First primary NACM, ALM, MM, and UM cases diagnosed 2000-2016 were extracted from SEER. Seer*Stat was used to calculate excess absolute risks (EAR) and standardized incidence ratios (SIR) of SPMs relative to a matched cohort from the general population. P-value of 0.05 determined significance.

Results: Inclusion criteria was met by 109,385 patients with NACM, 2166 with ALM, 2498 with MM, and 6250 with UM. Increased incidence of malignancies occurred after NACM (SIR 1.51; 95%CI, 1.49-1.54), ALM (SIR 1.59; 95%CI, 1.40-1.81), MM (SIR 2.14; 95%CI, 1.85-2.45), and UM (SIR 1.24; 95%CI, 1.14-1.34) relative to the general population. Cutaneous melanoma occurred more frequently after NACM (SIR 9.54; 95%CI, 9.27-9.83), ALM (SIR 12.19; 95%CI, 9.70-15.14), MM (SIR 10.05; 95%CI, 7.18-13.68), and UM (SIR 2.91; 95%CI, 2.27-3.66). Patients with initial NACM (SIR 2.44; 95%CI, 1.64-3.51) and UM (SIR 44.34; 95%CI, 29.91-63.29) demonstrated increased incidence of eye and orbit melanoma. Renal malignancies occurred more frequently after NACM (SIR 1.24; 95%CI, 1.11-1.38), MM (SIR 3.54; 95%CI, 1.62-6.72) and UM (SIR 1.68; 95%CI, 1.09-2.48). Increased incidence of thyroid malignancies was observed after NACM (SIR 1.83; 95%CI, 1.61-2.06), ALM (SIR 3.74; 95%CI, 1.71-7.11), MM (SIR 4.40; 95%CI, 1.77-9.06), and UM (SIR 3.79; 95%CI, 2.52-5.47). Increased incidence of lymphoma was observed after NACM (SIR 1.20; 95%CI, 1.09-1.31) and ALM (SIR 2.06; 95%CI, 1.13-3.46).

Conclusion: Patients with NACM, ALM, MM, and UM have increased incidence of SPMs compared to that expected from the general population. Each of these melanoma subtypes had increased occurrence of cutaneous melanoma and thyroid cancer; some, but not all, had increased occurrence of renal malignancies, eye and orbit melanoma, and lymphoma.

Keywords: second primary malignancies, melanoma, melanoma subtypes, uveal melanoma, non-acral cutaneous melanoma, acral lentiginous melanoma, mucosal melanoma, standardized incidence ratios

BACKGROUND

Malignant melanoma, a serious and devastating disease, originates from melanocytes within the non-glabrous skin (non-acral cutaneous melanoma), palm and sole glabrous skin (acral lentiginous melanoma), mucosal membranes (mucosal melanoma), and the uvea (uveal melanoma) (1–3). Non-acral cutaneous melanoma (NACM) represents the most common subtype of melanoma, accounting for close to 90% of diagnoses; acral lentiginous melanoma (ALM), mucosal melanoma (MM), and uveal melanoma (UM) largely comprise the remainder of cases (4–6). Despite a shared cell origin, these subtypes differ greatly by genetic composition (1, 7), treatment response (8), and clinical outcomes (4, 6).

NACM generally portends a better prognosis than ALM, MM or UM, with 5-year survival rates of 91.3%, 80.3%, 34.0%, and 78.4% respectively (4, 6). If complete remission is attained, patient care becomes increasingly focused on surveillance for recurrences and management of cancer sequalae; second primary malignancies (SPMs) embody one such sequela. Although incidence of SPMs has been investigated for patients with cutaneous melanoma (CM; encompasses NACM and ALM) (9–11) and UM (12, 13), limited literature exists on SPMs specific to MM (14) and ALM (15). Prior study of SPMs associated with mucosal melanoma (14) are limited solely to those arising from the sinonasal cavity and prior study of SPMs associated with ALM (15) focuses on an exclusively Korean population; both lack site-specific SPM risk investigation. With gaps in current literature, consensus cancer guidelines provided by organizations such as National Comprehensive Cancer Network (NCCN) (16–18), Cancer Care Ontario (CCO) (19), Canadian Medical Association (CMA), and European Society for Medical Oncology (ESMO) (20) provide either no or very limited discussion on SPM risk and follow-up after these malignancies.

In order to address this literature gap, we conducted a retrospective analysis of the SEER database to evaluate if patients with NACM, ALM, MM, and UM demonstrate increased incidence for SPMs compared to the general population in the contemporary era (2000-2016). We performed additional analysis to identify specific sites and latency periods with elevated risk for secondary malignancies. We conduct, to the best of our knowledge, the first investigation of site-specific SPM risk after MM and ALM. National Cancer Institute's (NCI) Surveillance, Epidemiology, and End Results (SEER) registries (21), a national population-based cancer database, has been used and validated for such analyses in the past (9–12, 22).

PATIENTS AND METHODS

Data Source

Cases of melanoma were extracted from the SEER database, which is comprised of up to 21 cancer registries that geographically account for approximately 36.7% of the US population (21). The specific dataset used for this study, "Incidence - SEER 18 Regs excluding AK Research Data, Nov 2018 Sub (2000-2016)", contained data from 18 registries with cases diagnosed between 2000 and 2016. The SEER program tracks incidence of new tumors and documents demographic, treatment, tumor, and survival data; however, it does not include behavioral risk factors (e.g. smoking, physical inactivity) and comorbid diseases. Institutional review board approval was not required for this study, as it utilized only deidentified data with permission from NCI.

Data Collection

Patients diagnosed with NACM, ALM, MM, and UM between 2000-2016 were included in the study; cases that were not first primary malignancies, were diagnosed by death certificate, were diagnosed by autopsy record, or were of unknown age were excluded from analysis.

Cases of NACM were identified using International Classification of Diseases for Oncology third edition (ICD-O-3) morphological codes 8721/3-8743/3; 8745/3-8790/3 (malignant melanoma excluding malignant melanoma, NOS & acral lentiginous melanoma) and topographical codes C44.0-44.9 (skin). ALM was identified using morphological code 8744/3 (acral lentiginous melanoma) and topographical codes C44.6-C44.7 (skin of upper limb, shoulder, lower limb, and hip). MM cases were identified using morphological codes 8720/3-8790/3 (melanoma) and topographical codes C00.0–C06.9 (lip, tongue, gum, palate, mouth); C09.0–C14.8 (tonsil, oropharynx, nasopharynx, pyriform sinus, hypopharynx); C15.0–C16.9 (esophagus, stomach); C19.9–C21.8 (rectosigmoid junction, rectum, anus/anal canal); C30.0 (nasal cavity); C31.0–C31.9 (accessory sinuses); C51.0–C51.9 (vulva); C52.9–C53.9 (vagina, cervix uteri); C60.0–C63.9 (male genital organs); C64.9–C68.9 (urinary tract). Lastly, UM was identified using morphological codes 8720-8790 (melanoma) and topographical codes C69.2 (retina); C69.3 (choroid); C69.4 (ciliary body, iris). "Retinal" melanomas (0.9%; 56/6250) were included as they most likely represent misclassification of uveal melanoma, a phenomenon described in previous studies (12, 23). ICD-O-3 codes used to identify NACM (6), ALM (6), MM (4), and UM (23) were

consistent with prior studies investigating these malignancies. Patient demographics collected included age at diagnosis, race, and sex. Tumor data included laterality, histology, and site of origin.

Statistical Analysis

Demographic and tumor data was tabulated. The multiple primary standardized incidence ratio (MP-SIR) algorithm of the Seer*stat program (version 8.3.6.1) was used to obtain standardized incidence ratios (SIR) and excess absolute risk (EAR) for second primary malignancies in patients with NACM, ALM, MM, and UM compared to a reference group representative of the general population, with similar sex, race (white/unknown, black, other) age-group (5-year interval), and calendar year of diagnosis (5-year interval). The algorithm was then further used to identify specific latency periods in which there was increased incidence of SPMs relative to the reference population. The authors (AL, SP, DSG) examined the site-specific analysis to identify trends across melanoma subtypes.

Analysis was limited to second malignancies only (early exit at next malignancy) to isolate relationship of subsequent malignancies with the first primary. Only malignant neoplasms diagnosed greater than two months after the melanoma diagnosis were considered to be second primaries, in order to distinguish them from concurrent malignancies discovered during screening. The reference population linked to the SEER database is comprised of Census Bureau data, through partnership with the National Center for Health Statistics (https://seer.cancer.gov/popdata/). An alpha level of significance of 0.05 was used for the study, and EAR was calculated per 10,000 individuals. IBM Statistical Product and Service Solutions (SPSS) version 26 and Microsoft Excel version 16.38 were used to conduct descriptive analysis and generate charts.

RESULTS

Baseline Characteristics

Inclusion criteria was met by 109,385 patients with NACM, 2166 patients with ALM, 2498 patients with MM, and 6250 patients with UM for a total of 120,299 patients. The median (+/- SD) follow-up period for patients with NACM was 5.6 (+/- 4.7) years, with ALM was 4.3 (+/- 4.5) years, with MM was 1.7 (+/- 3.6) years, and with UM was 4.8 (+/- 4.4) years. During this period 11.4% (12472/109,385) of NACM patients, 10.8% (235/2166) of ALM patients, 8.1% (203/2498) of MM patients, and 9.4% (586/6250) of UM patients developed SPMs.

Most patients with initial NACM (56.1%; 61,385/109,385) and UM (52.4%; 3274/6250) were male, whereas most patients with initial ALM (55.4%; 1201/2166) and MM (71.8%; 1793/2498) were female. Majority of patients with NACM (94.5%;103,390/109,385), ALM (81.7%; 1770/2166), MM (84.9%; 2120/2498) and UM (96.2%; 6012/6250) were white. Almost all diagnoses of initial NACM (99.9%; 109,285/109,385), ALM (100%; 2166/2166), and MM (99.8%; 2493/2498) were microscopically confirmed whereas only 53.8% (3365/6250) of UM cases were microscopically confirmed. Additional patient characteristics are displayed in **Table 1**.

SPM Incidence

Relative to the general population, an increased incidence of new malignancies was observed in patients with initial NACM (SIR 1.51; 95% CI, 1.49 to 1.54; EAR 64.46), ALM (SIR 1.59; 95% CI, 1.40 to 1.81; EAR 79.56), MM (SIR 2.14; 95% CI, 1.85 to 2.45; EAR 153.59), and UM (SIR 1.24; 95% CI, 1.14 to 1.34; EAR 33.04). Notably, increased incidence of secondary CM, eye and orbit melanoma, kidney cancer, thyroid cancer, and lymphoma were observed across some melanoma subtypes (**Table 2** and **Figure 1**).

CM occurred more frequently in patients with initial NACM (SIR 9.54; 95% CI, 9.27 to 9.83; EAR 60.72), ALM (SIR 12.19; 95% CI, 9.70 to 15.14; EAR 68.41), MM (SIR 10.05; 95% CI, 7.18 to 13.68; EAR 51.23), and UM (SIR 2.91; 95% CI, 2.27 to 3.66; EAR 13.75) than expected from the general population. On the other hand, only patients with initial NACM (SIR 2.44; 95% CI, 1.64 to 3.51; EAR 0.26) and UM (SIR 44.34; 95% CI, 29.91 to 63.29; EAR 8.54) demonstrated increased incidence of eye and orbit melanoma, whereas patients with ALM (SIR 0.00; 95% CI, 0.00 to 20.09; EAR -0.17) and MM (SIR 0.00; 95% CI, 0.00 to 29.94; EAR -0.18) demonstrated no significant difference from the reference population. Renal malignancies were noted to occur more frequently in patients with NACM (SIR 1.24; 95% CI, 1.11 to 1.38; EAR 0.96), MM (SIR 3.54; 95% CI, 1.62 to 6.72; EAR 9.19) and UM (SIR 1.68; 95% CI, 1.09 to 2.48; EAR 2.95), but not ALM (SIR 1.61; 95% CI, 0.65 to 3.32; EAR 2.41). Increased incidence of thyroid malignancies was observed in patients with initial NACM (SIR 1.83; 95% CI, 1.61 to 2.06; EAR 1.79), ALM (SIR 3.74; 95% CI, 1.71 to 7.11; EAR 5.99), MM (SIR 4.40; 95% CI, 1.77 to 9.06; EAR 7.69), and UM (SIR 3.79; 95% CI, 2.52 to 5.47; EAR 6.00). Lastly, increased incidence of lymphoma was observed in patients with initial NACM (SIR 1.20; 95% CI, 1.09 to 1.31; EAR 1.17) and ALM (SIR 2.06; 95% CI, 1.13 to 3.46; EAR 6.55) but not MM (SIR 1.55; 95% CI, 0.62 to 3.20; EAR 3.55) or UM (SIR 0.90; 95% CI, 0.55 to 1.39; EAR -0.63).

SPM Latency Analysis

Patients with NACM demonstrated elevated incidence of overall SPMs during the first year (2-11 months) following diagnosis (SIR 2.12; 95% CI 2.03 to 2.21), 1-5 years following diagnosis (SIR 1.57; 95% CI 1.53 to 1.61), 5-10 years following diagnosis (SIR 1.30; 95% CI 1.25 to 1.34), and greater than 10 years following diagnosis (SIR 1.21; 95% CI 1.15 to 1.28). Similarly, patients with MM had increased incidence of overall SPMs during the first year (2-11 months) following diagnosis (SIR 2.38; 95% CI 1.81 to 3.08), 1-5 years following diagnosis (SIR 2.12; 95% CI 1.72 to 2.58), 5-10 years following diagnosis (SIR 1.81; 95% CI 1.24 to 2.56), and greater than 10 years following diagnosis (SIR 2.24; 95% CI 1.23 to 3.76). In contrast, those with ALM only had increased incidence of overall SPMs the first year following diagnosis (SIR 1.98; 95% CI 1.45 to 2.66) and 1-5 years following diagnosis (SIR 1.72; 95% CI 1.43 to 2.06). Those with UM demonstrated elevated incidence of overall SPMs during the first year following diagnosis (SIR 1.53;

TABLE 1 | Demographic, tumor, and treatment characteristics of patients with first primary melanoma.

		Non-Acral Cutaneous Melanoma				Acral Lentiginous Melanoma				Mucosal Melanoma				Uveal Melanoma			
		Overall Cohort (n=109,385)		SPM Cohort (n=12472)		Overall Cohort (n=2166)		SPM Cohort (n=235)		Overall Cohort (n=2498)		SPM Cohort (n=203)		Overall Cohort (n=6250)		SPM Cohort (n=586)	
		Count	N %	Count	N %	Count	N %	Count	N %	Count	N %	Count	N %	Count	N %	Count	N %
Age-groups	0-49 years	32956	30.1%	1941	15.6%	480	22.2%	21	8.9%	342	13.7%	21	10.3%	1333	21.3%	52	8.9%
	50-64 years	35988	32.9%	4238	34.0%	670	30.9%	70	29.8%	698	27.9%	61	30.0%	2353	37.6%	234	39.9%
	65+ years	40441	37.0%	6293	50.5%	1016	46.9%	144	61.3%	1458	58.4%	121	59.6%	2564	41.0%	300	51.2%
Sex	Female	48000	43.9%	4194	33.6%	1201	55.4%	110	46.8%	1793	71.8%	148	72.9%	2976	47.6%	247	42.2%
	Male	61385	56.1%	8278	66.4%	965	44.6%	125	53.2%	705	28.2%	55	27.1%	3274	52.4%	339	57.8%
Race	White	103390	94.5%	12307	98.7%	1770	81.7%	193	82.1%	2120	84.9%	179	88.2%	6012	96.2%	574	98.0%
	Black	323	0.3%	43	0.3%	185	8.5%	19	8.1%	139	5.6%	8	3.9%	54	0.9%	3	0.5%
	Asian/Pacific Islander	611	0.6%	46	0.4%	170	7.8%	22	9.4%	208	8.3%	16	7.9%	74	1.2%	5	0.9%
	American Indian/Alaska Native	210	0.2%	14	0.1%	12	0.6%	0	0.0%	17	0.7%	0	0.0%	16	0.3%	3	0.5%
	Unknown	4851	4.4%	62	0.5%	29	1.3%	1	0.4%	14	0.6%	0	0.0%	94	1.5%	1	0.2%
Diagnostic Confirmation	Microscopic	109285	99.9%	12469	100.0%	2166	100.0%	235	100.0%	2493	99.8%	201	99.0%	3365	53.8%	310	52.9%
	Not microscopic	15	0.0%	3	0.0%	0	0.0%	0	0.0%	4	0.2%	2	1.0%	2800	44.8%	270	46.1%
	Unknown	85	0.1%	0	0.0%	0	0.0%	0	0.0%	1	0.0%	0	0.0%	85	1.4%	6	1.0%
Summary stage	Carcinoma *In situ*	0	0.0%	0	0.0%	0	0.0%	0	0.0%	0	0.0%	0	0.0%	0	0.0%	0	0.0%
	Localized	95812	87.6%	11050	88.6%	1471	67.9%	163	69.4%	676	27.1%	83	40.9%	0	0.0%	0	0.0%
	Regional	10209	9.3%	1147	9.2%	582	26.9%	63	26.8%	337	13.5%	22	10.8%	0	0.0%	0	0.0%
	Distant	1607	1.5%	99	0.8%	85	3.9%	6	2.6%	241	9.6%	10	4.9%	0	0.0%	0	0.0%
	Unknown/unstaged	1757	1.6%	176	1.4%	28	1.3%	3	1.3%	1244	49.8%	88	43.3%	6250	100.0%	586	100.0%

SPM, second primary malignancy.

TABLE 2 | Notable second primary malignancies by specific site following first primary melanoma.

	NACM (n=109,385)		ALM (n=2166)		MM (n=2498)		UM (n=6250)	
	O/E (95%CI)	EAR[a]	O/E (95%CI)	EAR[a]	O/E (95%CI)	EAR[a]	O/E (95%CI)	EAR[a]
All Sites	1.51* (1.49-1.54)	64	1.59* (1.4-1.81)	80	2.14* (1.85-2.45)	154	1.24* (1.14-1.34)	33
Melanoma of the Skin	9.54* (9.27-9.83)	61	12.19* (9.7-15.14)	68	10.05* (7.18-13.68)	51	2.91* (2.27-3.66)	14
Kidney	1.24* (1.11-1.38)	1	1.61 (0.65-3.32)	2	3.54* (1.62-6.72)	9	1.68* (1.09-2.48)	3
Eye and Orbit - Melanoma	2.44* (1.64-3.51)	0	0 (0-20.09)	0	0 (0-29.94)	0	44.34* (29.91-63.29)	9
Thyroid	1.83* (1.61-2.06)	2	3.74* (1.71-7.11)	6	4.40* (1.77-9.06)	8	3.79* (2.52-5.47)	6
Lymphoma	1.20* (1.09-1.31)	1	2.06* (1.13-3.46)	7	1.55 (0.62-3.2)	4	0.9 (0.55-1.39)	-1

ALM, acral lentiginous melanomal, confidence interval; E, expected; EAR, excess absolute risk; MM, mucosal melanoma; NACM, non-acral cutaneous melanoma; O, observed, SIR, standardized incidence ratio; UM, uveal melanoma.

**P < 0.05.*

[a]*Excess absolute risk is per 10,000.*

95% CI 1.24 to 1.86; EAR 69.12), 1-5 years following diagnosis (SIR 1.21; 95% CI 1.07 to 1.37; EAR 28.62), and 5-10 years following diagnosis (SIR 1.20; 95% CI 1.02 to 1.39; EAR 27.78). High-risk latency periods further differed by SPM types (**Table 3** and **Supplementary Material**).

DISCUSSION

Using a national cancer database, we analyzed 120,299 patients with various melanoma subtypes and found an elevated incidence of SPMs relative to the general population. Notably, all four melanoma subtypes (NACM, ALM, MM, UM) demonstrated increased risk of secondary CM and thyroid cancer, and some but not all melanoma subtypes demonstrated increased risk for secondary renal malignancies (NACM, MM, UM), eye and orbit melanoma (NACM, UM), and lymphoma (NACM, ALM).

A biologic rationale exists for the findings in our study. CM and thyroid cancers commonly harbor oncogenic mutations of the mitogen-activated protein kinase (MAPK) pathway (24–29). Renal cancers share immunogenicity and *BAP1* aberrations with CM and UM (30–35). Lymphomas and melanomas are associated with decreased immune surveillance (36–43).

Although historic and smaller retrospective analyses of the SEER database have examined SPMs following CM (9, 10) and UM (12), herein we provide, to the best of our knowledge, the first investigation of site-specific SPM risk after MM and ALM. Moreover, through analysis of UM in a larger and more contemporary cohort, we highlight increased incidence of secondary thyroid malignancies, a finding undetected in prior investigation (12). Bradford, et al. (9) and Spanogle, et al. (10) investigated incidence of SPMs following CM in various subsets of the SEER database and both found increased incidence of secondary CM, eye and orbit melanoma, thyroid cancer, renal cancer, and lymphoma. Similarly, Vakharia, et al. (11) in their investigation of secondary malignancies excluding CM demonstrated increased risk for these sites. Their findings (9–11) were consistent with our findings of SPMs following NACM. Laíns, et al. (12) investigated risk of second primary malignancies following UM and found increased incidence for secondary CM, eye and orbit melanoma, and renal cancer but not a significant increase in thyroid cancer. However, the study (12) showed a strong trend of increased thyroid cancer (SIR 2.06, 95% CI 0.99 to 3.78) in a cohort of 3976 patients, which with increased power may have captured a significant result similar to our study.

Despite a growing body of literature on SPMs, national consensus guidelines such as NCCN (16–18) (US), Canada CCO (19) (Canada), CMA (Canada) and ESMO (20) (Europe) sparsely address secondary malignancies in their follow-up recommendations. Canadian (19) and European (20) guidelines discuss only an increased risk for secondary cutaneous malignancies after initial CM and the importance of long-term dermatological surveillance; these guidelines lack SPM follow-up recommendations specific to ALM, MM, and UM. American consensus guidelines provide slightly more insight on non-cutaneous SPMs following CM by discussing the role of genetic testing in determining SPM risk and by providing guidance on when to consider such testing (16). However, American guidelines do not remark on the increased incidence of lymphoma or thyroid cancer (16). Moreover, these guidelines state that CM is not associated with an increased risk for UM (17).

Indeed, developing follow-up recommendations poses a challenge as cost, clinical benefit, and burden of increased health-care visits must all be balanced. Nonetheless, increased awareness of the associations studied herein are paramount to guiding appropriate clinician judgement when caring for melanoma patients; discussion of up-to-date evidence in national guidelines can improve patient care and long-term health outcomes. With a more appropriate index of suspicion, lesions (e.g. renal cyst, thyroid nodule) and atypical findings discovered during diagnostic or surveillance imaging that may otherwise have been dismissed as benign may instead be deemed to warrant additional follow-up. Furthermore, symptoms concerning for an associated SPM (e.g. visual flashers and floaters) can be interpreted more appropriately and potentially lead to earlier diagnosis. The high-risk latency periods identified by this study may provide additional clinical insight when deciding further management for patients presenting with these signs or symptoms.

The authors propose that cost effective screening such as total body skin exams be recommended for patients with all subtypes (NACM, ALM, MM, UM) of melanoma; prior studies (44, 45) support the economic efficiency of targeted screening strategies

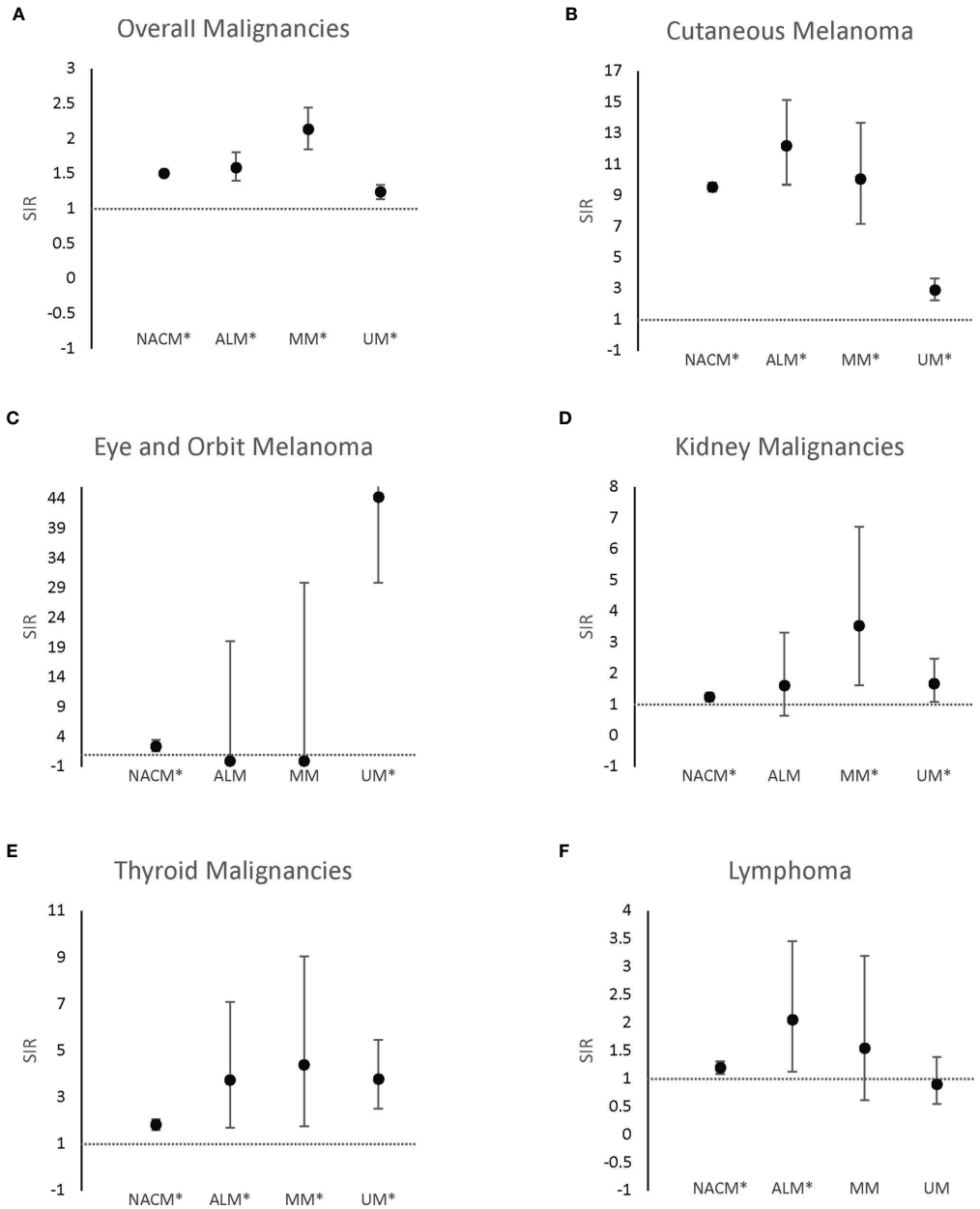


FIGURE 1 | Standardized incidence ratios of secondary malignancies grouped by category. Standardized incidence ratios of overall secondary malignancies **(A)**, secondary cutaneous melanoma **(B)**, secondary eye and orbit melanoma **(C)**, secondary kidney malignancies **(D)**, secondary thyroid malignancies **(E)**, and secondary lymphoma **(F)** following first primary melanomas. ALM, acral lentiginous melanoma; MM, mucosal melanoma, NACM, non-acral cutaneous melanoma; UM, uveal melanoma. *p<0.05.

in high-risk groups. The authors suggest that patients with NACM should receive routine complete eye exams (including dilated fundus exam) at least as often as recommend for asymptomatic adults without risk factors for ocular disease by American Academy of Ophthalmology (AAO) guidelines (46): every 5 to 10 years when less than 40 years of age, every 2 to 4 years when between 40 and 54 years of age, every 1 to 3 years when between 55 and 64 years of age, and every 1 to 2 years when 65 or more years of age. Surveillance for SPM in patients undergoing screening measures versus those who do not undergo these screening exams may further elucidate the role and feasibility of monitoring for the development of cancer in these patients. Moreover, it would be prudent to identify high-risk groups and factors through prediction models for subsequent melanoma, such as those described by Cust et al. (47), to help guide effective recommendations.

TABLE 3 | Risk of second primary malignancy distributed by time from diagnosis of first primary malignancy.

		2-11 months SIR (95%CI)	12-59 months SIR (95%CI)	60-119 months SIR (95%CI)	120+ months SIR (95%CI)
Non-Acral Cutaneous Melanoma	All Sites	2.12* (2.03-2.21)	1.57* (1.53-1.61)	1.30* (1.25-1.34)	1.21* (1.15-1.28)
	Melanoma of the Skin	16.94* (15.9-18.04)	10.45* (10.01-10.9)	7.03* (6.6-7.47)	5.68* (5.11-6.29)
	Kidney	2.04* (1.59-2.59)	1.16 (0.97-1.37)	0.94 (0.74-1.18)	1.41* (1.04-1.86)
	Eye and Orbit - Melanoma	0.67 (0.02-3.72)	3.26* (1.9-5.23)	2.50* (1.14-4.75)	1.29 (0.16-4.65)
	Thyroid	4.71* (3.72-5.87)	1.82* (1.49-2.19)	1.15 (0.86-1.5)	1 (0.61-1.54)
	Lymphoma	2.22* (1.83-2.68)	1.12 (0.97-1.29)	0.9 (0.74-1.09)	1.14 (0.86-1.47)
Acral Lentiginous Melanoma	All Sites	1.98* (1.45-2.66)	1.72* (1.43-2.06)	1.29 (0.96-1.7)	1.21 (0.73-1.9)
	Melanoma of the Skin	14.45* (7.9-24.24)	14.95* (10.94-19.94)	8.49* (4.85-13.79)	7.56* (2.77-16.45)
	Thyroid	5.96 (0.72-21.55)	5.47* (2.01-11.9)	1.43 (0.04-7.96)	0 (0-13.6)
	Lymphoma	5.88* (2.16-12.8)	1.88 (0.69-4.09)	1.09 (0.13-3.92)	0 (0-5.02)
Mucosal Melanoma	All Sites	2.38* (1.81-3.08)	2.12* (1.72-2.58)	1.81* (1.24-2.56)	2.24* (1.23-3.76)
	Melanoma of the Skin	10.37* (4.97-19.08)	13.01* (8.42-19.2)	3.76 (0.77-10.98)	6.73 (0.82-24.32)
	Kidney	7.79* (2.53-18.17)	1.6 (0.19-5.77)	2.11 (0.05-11.73)	5.76 (0.15-32.09)
	Thyroid	10.98* (2.99-28.12)	3.94 (0.81-11.52)	0 (0-11.1)	0 (0-27.61)
Uveal Melanoma	All Sites	1.53* (1.24-1.86)	1.21* (1.07-1.37)	1.20* (1.02-1.39)	1.12 (0.85-1.44)
	Melanoma of the Skin	4.41* (2.41-7.39)	2.68* (1.81-3.82)	2.58* (1.55-4.03)	2.97* (1.36-5.63)
	Kidney	4.58* (2.09-8.69)	1.31 (0.6-2.5)	1.15 (0.37-2.68)	1.18 (0.14-4.27)
	Eye and Orbit - Melanoma	32.63* (6.73-95.36)	44.80* (24.49-75.16)	66.25* (35.27-113.28)	0 (0-48.57)
	Thyroid	11.20* (5.59-20.04)	3.80* (2.02-6.49)	0.46 (0.01-2.56)	3.68 (0.76-10.77)

CI, confidence interval; SIR, standardized incidence ratio.
**P < 0.05.*

Limitations in the Study Design

An important limitation of the SEER database and our study is the possibility of miscoding a recurrence as a second primary malignancy when pathologic evaluation is unavailable and tumor location is identical. This most directly impacts the calculation of secondary eye and orbit melanoma after initial UM (6.67% cases without microscopic confirmation), as UM is largely diagnosed clinically through examination and imaging rather than pathologically (48); indeed, this finding is more likely representative of recurrences rather than true SPMs. Another important limitation is the inability of Seer.Stat's MP-SIR algorithm to analyze site-specific secondary malignancy incidence beyond those preset in the software. As a result, we were unable to provide analysis on incidence of NACM and ALM as secondary malignancies, and instead had them grouped as secondary CM. Other limitations include other possible miscoding and inability to account for variables not included within the database. Additionally, patients that moved to a geographical area not covered by SEER could be lost to follow-up leading to underreporting. Despite these limitations, however, the national database has been validated for SPM analyses (9–12, 22).

CONCLUSIONS

We found patients with NACM, ALM, MM, and UM to have increased incidence of SPMs compared to that expected from the general population. Each of these melanoma subtypes had increased occurrence of secondary CM and thyroid cancer; some, but not all, had increased occurrence of secondary renal malignancies, eye and orbit melanoma, and lymphoma. These patients may benefit from cost-effective screening methods such as full body skin exams. Patients with NACM should, at a minimum, receive age-appropriate comprehensive eye screening per national guidelines. Increased awareness of these associations is prudent to guiding clinical follow-up and additional studies are necessary to identify best-practice screening guidelines.

DATA AVAILABILITY STATEMENT

The original contributions presented in the study are included in the article/**Supplementary Material**. Further inquiries can be directed to the corresponding author.

AUTHOR CONTRIBUTIONS

Conception: SP. Study design: AL, DG, and SP. Statistical analysis: AL. Data interpretation: AL, DG, and SP. Manuscript preparation: AL, DG, and SP. All authors contributed to the article and approved the submitted version.

SUPPLEMENTARY MATERIAL

The Supplementary Material for this article can be found online at: https://www.frontiersin.org/articles/10.3389/fonc.2022.853076/full#supplementary-material

REFERENCES

1. Bastian BC. The Molecular Pathology of Melanoma: An Integrated Taxonomy of Melanocytic Neoplasia. *Annu Rev Pathol Mech Dis* (2014) 9 (1):239–71. doi: 10.1146/annurev-pathol-012513-104658
2. Jovanovic P, Mihajlovic M, Djordjevic-Jocic J, Vlajkovic S, Cekic S, Stefanovic V. Ocular Melanoma: An Overview of the Current Status. *Int J Clin Exp Pathol* (2013) 6(7):1230–44.
3. Mihajlovic M, Vlajkovic S, Jovanovic P, Stefanovic V. Primary Mucosal Melanomas: A Comprehensive Review. *Int J Clin Exp Pathol* (2012) 5 (8):739–53.
4. Bishop KD, Olszewski AJ. Epidemiology and Survival Outcomes of Ocular and Mucosal Melanomas: A Population-Based Analysis. *Int J Cancer* (2014) 134(12):2961–71. doi: 10.1002/ijc.28625
5. McLaughlin CC, Wu XC, Jemal A, Martin HJ, Roche LM, Chen VW. Incidence of Noncutaneous Melanomas in the U.S. *Cancer* (2005) 103 (5):1000–7. doi: 10.1002/cncr.20866
6. Bradford PT, Goldstein AM, McMaster ML, Tucker MA. Acral Lentiginous Melanoma: Incidence and Survival Patterns in the United States, 1986-2005. *Arch Dermatol* (2009) 145(4):427–34. doi: 10.1001/archdermatol.2008.609
7. Curtin JA, Busam K, Pinkel D, Bastian BC. Somatic Activation of KIT in Distinct Subtypes of Melanoma. *J Clin Oncol* (2006) 24(26):4340–6. doi: 10.1200/JCO.2006.06.2984
8. Shoushtari AN, Munhoz RR, Kuk D, Ott PA, Johnson DB, Tsai KK, et al. The Efficacy of Anti-PD-1 Agents in Acral and Mucosal Melanoma. *Cancer* (2016) 122(21):3354–62. doi: 10.1002/cncr.30259
9. Bradford PT, Freedman DM, Goldstein AM, Tucker MA. Increased Risk of Second Primary Cancers After a Diagnosis of Melanoma. *Arch Dermatol* (2010) 146(3):265–72. doi: 10.1001/archdermatol.2010.2
10. Spanogle JP, Clarke CA, Aroner S, Swetter SM. Risk of Second Primary Malignancies Following Cutaneous Melanoma Diagnosis: A Population-Based Study. *J Am Acad Dermatol* (2010) 62(5):757–67. doi: 10.1016/j.jaad.2009.07.039
11. Vakharia PP, Kelm RC, Orrell KA, Patel KR, Singam V, Ali Y, et al. Risks for Noncutaneous Second Primary Malignancy in Cutaneous Malignant Melanoma Survivors: An Analysis of Data From the Surveillance, Epidemiology, and End Results (SEER) Program. *Int J Dermatol* (2020) 59 (4):463–8. doi: 10.1111/ijd.14781
12. Laíns I, Bartosch C, Mondim V, Healy B, Kim IK, Husain D, et al. Second Primary Neoplasms in Patients With Uveal Melanoma: A SEER Database Analysis. *Am J Ophthalmol* (2016) 165:54–64. doi: 10.1016/j.ajo.2016.02.022
13. Diener-West M, Reynolds SM, Agugliaro DJ, Caldwell R, Cumming K, Earle JD, et al. Second Primary Cancers After Enrollment in the COMS Trials for Treatment of Choroidal Melanoma: COMS Report No. 25. *Arch Ophthalmol* (2005) 123(5):601–4. doi: 10.1001/archopht.123.5.601
14. Ganti A, Plitt MA, Kuan EC, Kuhar HN, Batra PS, Tajudeen BA. Risk of Second Primary Malignancy in Patients With Sinonasal Tumors: A Population-Based Cohort Study. *Int Forum Allergy Rhinol* (2018) 8(6):756–62. doi: 10.1002/ALR.22092
15. Bae SH, Seon HJ, Choi YD, Shim HJ, Lee JB, Yun SJ. Other Primary Systemic Cancers in Patients With Melanoma: Analysis of Balanced Acral and Nonacral Melanomas. *J Am Acad Dermatol* (2016) 74(2):333–40. doi: 10.1016/J.JAAD.2015.09.047
16. NCCN Clinical Practice Guidelines in Oncology. *Cutaneous Melanoma (Version 3.2020)* Plymouth Meeting, PA: National Comprehensive Cancer Network (2020).
17. NCCN Clinical Practice Guidelines in Oncology. *Uveal Melanoma (Version 1.2020)* Plymouth Meeting, PA: National Comprehensive Cancer Network (2020).
18. NCCN Clinical Practice Guidelines in Oncology. *Head and Neck Cancers (Version 2.2020)* Plymouth Meeting, PA: National Comprehensive Cancer Network (2020).
19. Rajagopal S, Souter LH, Baetz T, McWhirter E, Knight G, Rosen CF, et al. *Follow-Up of Patients With Cutaneous Melanoma Who Were Treated With Curative Intent*. Toronto (ON): Cancer Care Ontario (2015).
20. Michielin O, Van Akkooi ACJ, Ascierto PA, Dummer R, Keilholz UCommittee G. Cutaneous Melanoma: ESMO Clinical Practice Guidelines for Diagnosis, Treatment and Follow-Up †. (2019) 30(12):1884–901. doi: 10.1093/annonc/mdz411
21. *Surveillance, Epidemiology, and End Results (SEER) Program*. Available at: www.seer.cancer.gov.
22. Vasudevan V, Cheung MC, Yang R, Zhuge Y, Fischer AC, Koniaris LG, et al. Pediatric Solid Tumors and Second Malignancies: Characteristics and Survival Outcomes. *J Surg Res* (2010) 160(2):184–9. doi: 10.1016/j.jss.2009.05.030
23. Aronow ME, Topham AK, Singh AD. Uveal Melanoma: 5-Year Update on Incidence, Treatment, and Survival (SEER 1973-2013). *Ocul Oncol Pathol* (2018) 4(3):145–51. doi: 10.1159/000480640
24. Davies H, Bignell GR, Cox C, Stephens P, Edkins S, Clegg S, et al. Mutations of the BRAF Gene in Human Cancer. *Nat 2002 4176892* (2002) 417(6892):949–54. doi: 10.1038/nature00766
25. Flaherty KT, McArthur G. BRAF, a Target in Melanoma. *Cancer* (2010) 116 (21):4902–13. doi: 10.1002/CNCR.25261
26. Xing M. Molecular Pathogenesis and Mechanisms of Thyroid Cancer. *Nat Rev Cancer 2013 133* (2013) 13(3):184–99. doi: 10.1038/nrc3431
27. Pozdeyev N, Lund G, McDermott MT. Molecular Pathogenesis of Thyroid Cancer and Oncogenes in Thyroid Cancer. *Thyroid Cancer* (2016) 2016:17–30. doi: 10.1007/978-1-4939-3314-3_3
28. Xing M. BRAF Mutation in Thyroid Cancer. *Endocr Relat Cancer* (2005) 12 (2):245–62. doi: 10.1677/ERC.1.0978
29. Kim SJ, Lee J, Soh EY. The Clinical Significance of the BRAF Mutation in Patients With Papillary Thyroid Cancer. *J Endocr Surg* (2017) 17(4):175–83. doi: 10.16956/JES.2017.17.4.175
30. Foretová L, Navrátilová M, Svoboda M, Házová J, Vašíčková P, Šťahlová EH, et al. BAP1 Syndrome - Predisposition to Malignant Mesothelioma, Skin and Uveal Melanoma, Renal and Other Cancers. *Klin Onkol* (2019) 32 (Supplementum2):2S118–22. doi: 10.14735/AMKO2019S118
31. Shao YF, Debenedictis M, Yeaney G, Singh AD. Germ Line BAP1 Mutation in Patients With Uveal Melanoma and Renal Cell Carcinoma. *Ocul Oncol Pathol* (2021) 7(5):340–5. doi: 10.1159/000516695
32. Walpole S, Pritchard AL, Cebulla CM, Pilarski R, Stautberg M, Davidorf FH, et al. Comprehensive Study of the Clinical Phenotype of Germline BAP1 Variant-Carrying Families Worldwide. *JNCI J Natl Cancer Inst* (2018) 110 (12):1328–41. doi: 10.1093/JNCI/DJY171
33. Bertolotto C, Lesueur F, Giuliano S, Strub T, de Lichy M, Bille K, et al. A SUMOylation-Defective MITF Germline Mutation Predisposes to Melanoma and Renal Carcinoma. *Nature* (2011) 480(7375):94–8. doi: 10.1038/nature10539
34. Laitman Y, Newberg J, Molho RB, Jin DX, Friedman E. The Spectrum of Tumors Harboring BAP1 Gene Alterations. *Cancer Genet* (2021) 256-257:31–5. doi: 10.1016/J.CANCERGEN.2021.03.007
35. Louie BH, Kurzrock R. BAP1: Not Just a BRCA1-Associated Protein. *Cancer Treat Rev* (2020) 90. doi: 10.1016/J.CTRV.2020.102091
36. Lund I, Hernandez-Ilizaliturri FJ, Torka P. Frequency and Timing of Other Primary Cancers in Patients With Chronic Lymphocytic Leukemia (CLL): A 17-Year Longitudinal Study. *Leuk Lymphoma* (2022) 13:1–10. doi: 10.1080/10428194.2021.2012662
37. Jhunjhunwala S, Hammer C, Delamarre L. Antigen Presentation in Cancer: Insights Into Tumour Immunogenicity and Immune Evasion. *Nat Rev Cancer* (2021) 21(5):298–312. doi: 10.1038/S41568-021-00339-Z
38. Vinay DS, Ryan EP, Pawelec G, Talib WH, Stagg J, Elkord E, et al. Immune Evasion in Cancer: Mechanistic Basis and Therapeutic Strategies. *Semin Cancer Biol* (2015) 35(Suppl):S185–98. doi: 10.1016/J.SEMCANCER.2015.03.004
39. Eddy K, Chen S. Overcoming Immune Evasion in Melanoma. *Int J Mol Sci* (2020) 21(23):1–48. doi: 10.3390/IJMS21238984
40. Sharma P, Hu-Lieskovan S, Wargo JA, Ribas A. Primary, Adaptive, and Acquired Resistance to Cancer Immunotherapy. *Cell* (2017) 168(4):707–23. doi: 10.1016/J.CELL.2017.01.017
41. Liu WR, Shipp MA. Signaling Pathways and Immune Evasion Mechanisms in Classical Hodgkin Lymphoma. *Blood* (2017) 130(21):2265–70. doi: 10.1182/BLOOD-2017-06-781989
42. Upadhyay R, Hammerich L, Peng P, Brown B, Merad M, Brody JD. Lymphoma: Immune Evasion Strategies. *Cancers (Basel)* (2015) 7(2):736–62. doi: 10.3390/CANCERS7020736
43. Menter T, Tzankov A. Mechanisms of Immune Evasion and Immune Modulation by Lymphoma Cells. *Front Oncol* (2018) 8:54. doi: 10.3389/FONC.2018.00054

44. Matsumoto M, Secrest A, Anderson A, Saul MI, Ho J, Kirkwood JM, et al. Estimating the Cost of Skin Cancer Detection by Dermatology Providers in a Large Health Care System. *J Am Acad Dermatol* (2018) 78(4):701–9.e1. doi: 10.1016/j.jaad.2017.11.033
45. Freedberg KA, Geller AC, Miller DR, Lew RA, Koh HK. Screening for Malignant Melanoma: A Cost-Effectiveness Analysis. *J Am Acad Dermatol* (1999) 41(5 I):738–45. doi: 10.1016/S0190-9622(99)70010-1
46. Feder RS, Olsen TW, Prum BE Jr, Summers CG, Olson RJ, Williams RD, et al. Comprehensive Adult Medical Eye Evaluation. *Ophthalmology* (2016) 123(1): P209–36. doi: 10.1016/j.ophtha.2015.10.047
47. Cust AE, Badcock C, Smith J, Thomas NE, Haydu LE, Armstrong BK, et al. A Risk Prediction Model for Development of Subsequent Primary Melanoma in a Population-Based Cohort. *Br J Dermatol* (2020) 182(5):1148. doi: 10.1111/BJD.18524
48. Chattopadhyay C, Kim DW, Gombos DS, Oba J, Qin Y, Williams MD, et al. Uveal Melanoma: From Diagnosis to Treatment and the Science in Between. *Cancer* (2016) 122(15):2299–312. doi: 10.1002/cncr.29727

Conflict of Interest: The authors declare that the research was conducted in the absence of any commercial or financial relationships that could be construed as a potential conflict of interest.

Publisher's Note: All claims expressed in this article are solely those of the authors and do not necessarily represent those of their affiliated organizations, or those of the publisher, the editors and the reviewers. Any product that may be evaluated in this article, or claim that may be made by its manufacturer, is not guaranteed or endorsed by the publisher.

Copyright © 2022 Loya, Gombos and Patel. This is an open-access article distributed under the terms of the Creative Commons Attribution License (CC BY). The use, distribution or reproduction in other forums is permitted, provided the original author(s) and the copyright owner(s) are credited and that the original publication in this journal is cited, in accordance with accepted academic practice. No use, distribution or reproduction is permitted which does not comply with these terms.

frontiers in Oncology

CASE REPORT
published: 31 March 2022
doi: 10.3389/fonc.2022.836845

Case Report: Delayed Onset Multi-Organ Toxicities in a Melanoma Patient Achieving Complete Response to BRAF/MEK Inhibition

Hannah M. Knochelmann[1,2], Michael Brandon Ware[2], Aditya Rali[3], Susanne Linderman[3,4], Jessica G. Shantha[3], David H. Lawson[5], Melinda Yushak[5], Robert Swerlick[6], Chrystal M. Paulos[2], Steven Yeh[3,7] and Ragini Kudchadkar[5*]*

[1] Department of Microbiology & Immunology, Medical University of South Carolina, Charleston, SC, United States, [2] Department of Surgery: Oncology, Winship Cancer Institute, Emory University, Atlanta, GA, United States, [3] Emory Eye Center, Department of Ophthalmology, Emory University School of Medicine, Atlanta, GA, United States, [4] Emory Vaccine Center, Emory University School of Medicine, Atlanta, GA, United States, [5] Department of Hematology and Medical Oncology, Winship Cancer Institute of Emory University, Atlanta, GA, United States, [6] Department of Dermatology, Emory University School of Medicine, Atlanta, GA, United States, [7] Truhlsen Eye Institute, Department of Ophthalmology, University of Nebraska Medical Center, Omaha, NE, United States

OPEN ACCESS

Edited by:
Sapna Patel,
University of Texas MD Anderson Cancer Center, United States

Reviewed by:
Yong-Chen Lu,
University of Arkansas for Medical Sciences, United States
Rohan Garje,
The University of Iowa, United States

***Correspondence:**
Ragini Kudchadkar
rkudcha@emory.edu
Hannah M. Knochelmann
knochelm@musc.edu

Specialty section:
This article was submitted to Skin Cancer, a section of the journal Frontiers in Oncology

Received: 16 December 2021
Accepted: 21 February 2022
Published: 31 March 2022

Citation:
Knochelmann HM, Ware MB, Rali A, Linderman S, Shantha JG, Lawson DH, Yushak M, Swerlick R, Paulos CM, Yeh S and Kudchadkar R (2022) Case Report: Delayed Onset Multi-Organ Toxicities in a Melanoma Patient Achieving Complete Response to BRAF/MEK Inhibition. Front. Oncol. 12:836845. doi: 10.3389/fonc.2022.836845

Autoimmune toxicities, while common following treatment with cancer immunotherapies, are not well-characterized in patients treated with BRAF/MEK inhibitors. Emerging data suggest that autoimmune effects may be linked with superior responses to both treatment modalities; however, there is little evidence describing mechanisms of immune-related toxicity for patients on BRAF/MEK inhibitors. Here we describe the experience of a 59-year-old HLA-A2, A29, B27-positive male with recurrent/metastatic melanoma. After progression on checkpoint inhibitor therapy, he was treated with dabrafenib/trametinib followed by encorafenib/binimetinib, which were well-tolerated and resulted in a complete response. Eighteen months into BRAF/MEK inhibitor therapy, and three months after initially finding a complete response, he developed a series of sudden-onset, severe toxicities: namely, bilateral panuveitis, cytopenias, joint pain, skin rash, hypercalcemia, and interstitial nephritis, which led to BRAF/MEKi cessation. Immunological analyses revealed induction of a peripheral type-17 cytokine signature characterized by high IL-23, IL-6, IL-10, IL-17A/F, IL-1β, and IL-21 among other cytokines in plasma corresponding with the height of symptoms. These findings highlight a novel instance of delayed autoimmune-like reaction to BRAF/MEK inhibition and identify a possible role for Th/Tc17 activation in their pathogenesis thus warranting future clinical and immunological characterization.

Keywords: BRAF/MEKi, melanoma, autoimmune toxicity, uveitis, Th17/Tc17

INTRODUCTION

Immunotherapies and targeted therapies have changed the face of melanoma management for patients over the past decade. While both classes of therapies have prolonged survival in patients with metastatic disease, immune-related toxicities can occur and necessitate careful management. Mechanisms underlying toxicities of checkpoint inhibitors are most likely directly related to the

specific drug activity through immune activation. For BRAF inhibitors (BRAFi), immune-pattern toxicities are less understood, but could reflect either off-target antigen-specific immune responses or generalized inflammatory processes. Additionally, each therapy has a distinct timeline in which most toxicities manifest. In patients treated with CTLA-4 therapy, maculopapular or eczematous rashes often emerge within 3–6 weeks of starting treatment, while PD-1 blockade can induce manifestations like psoriatic plaques, vitiligo or blistering from 4 to 10 months after therapy initiation (1). BRAF/MEKi combinations can also instigate skin reactions on the face/neck, trunk, and extremities which often appear within two weeks of starting therapy (1). While cutaneous neoplasms were frequent side effects of BRAFi monotherapy, the combination BRAF/MEKi reduced their incidence (2), and newer BRAFi like encorafinib have different tolerability profiles compared to their earlier generation counterparts as reviewed previously (3). For both types of therapy, there is an emerging association between autoimmune-like adverse events, including, uveitis, vitiligo, erythema nodosum, keratitis sicca, and progression-free survival (PFS) in patients (4, 5). Whether the timing, number, or localization of the toxicities is related to eventual outcome is poorly understood.

Severe adverse events appear to be rare in large populations receiving BRAF/MEK inhibitors despite evidence of a tail of the survival curve indicating long-term responsiveness (6). A phase III trial evaluating adjuvant dabrafenib/trametinib for patients with stage III melanoma demonstrated that 52% of patients receiving the combination therapy were alive after 5 years without relapse relative to 36% receiving placebo (7). From these 435 patients, uveitis was documented in only 2 patients, acute renal failure in 2 patients, and severe generalized rash in only 1 patient. In contrast, mild rashes were reported in 25% of patients on combination therapy. Additionally, in a cohort of 78 patients treated with BRAFi or BRAFi/MEKi, 10 experienced a combination of events, namely, vitiligo, uveitis, erythema nodosum, and keratitis sicca (4). Events promoting the incidence of these reactions in studied populations are not well understood but could be related to direct toxicity of the drug especially when observed early after treatment initiation, or perhaps immune reactivity or cross-reactivity against tumor and self. These data further indicate that the incidence of multi-organ toxicity is relatively rare in this treatment population.

Here, we report a case of a melanoma patient with a history of progression on checkpoint immunotherapy, who subsequently was an exceptional responder to adjuvant BRAF/MEKi and experienced uncharacteristically delayed and severe multi-organ toxicities. Immunologic analyses throughout the treatment course revealed peripheral cytokine release that corresponded with toxicities over time. Our findings correlate the systemic, acute clinical autoimmune responses with heightened release of type-17 cytokines during the manifestation and resolution of autoimmune toxicities. This report provides insight into clinical disease responses and immune-related adverse events, implicating a novel response/toxicity profile corresponding with Th17/Tc17 activation.

MELANOMA COURSE

The course of melanoma management is described here and represented over a timeline in **Figure 1A**. A 59-year-old Caucasian man with a history of stage IIIB melanoma was evaluated in the clinic after the acute onset of eye redness, rash, and joint pain. He had been diagnosed with stage IIIB melanoma four years prior after a biopsy of a pigmented lesion showed a 0.85 mm melanoma on the left scalp, which subsequently underwent wide local excision with negative margins. Seventeen months later, the patient presented with a palpable cervical lymph node which was biopsied and showed metastatic disease, and thus underwent left neck dissection. His disease, at this time, was positive for the BRAF V600K mutation. The patient was enrolled on the Checkmate 915 study (CA209-915) where he received one dose of the combination of ipilimumab/nivolumab immunotherapy in the adjuvant setting. One month after the initial dose, a recurrent subcutaneous nodule was noted in the neck and therefore he was taken off the study due to progression of the disease. The recurrent nodule was resected, and the patient was initiated on adjuvant nivolumab.

Following two cycles of adjuvant nivolumab, the patient reported headaches and pain at the occiput. A physical exam revealed recurrent, unresectable disease with multiple new subcutaneous metastases, and a computed tomography further identified progression in the cervical lymph nodes (**Figure 1B**). A biopsy of the subcutaneous metastasis was obtained and analyzed for immune infiltration, which found sparse $CD8^+$ and $CD45^+$ cells, with any positive cells residing primarily at the periphery of the nodule.

Due to disease progression on PD-1 therapy, he started targeted therapy using dabrafenib/trametinib. After approximately a year, the patient was switched to encorafenib/binimetinib for reasons related to comfort and quality of life (avoiding food effects), not specifically due to intolerability. The patient responded well to targeted therapy and had complete resolution of hypermetabolic disease as determined by PET imaging (**Figure 1B**).

However, three months after first observing his complete response to encorafenib/binimetinib, and 1.5 years into treatment on BRAF/MEK inhibitors generally, the patient presented to the clinic with bilateral wrist swelling, a widespread skin rash, and eye redness. A biopsy of the skin revealed non-necrotizing granulomatous inflammation in the superficial dermis with a mixture of epithelioid histiocytes and lymphocytes throughout, which was considered not diagnostically-specific. There were no infectious organisms or exogenous materials identified within the skin lesions. Bilateral eye redness prompted an ophthalmology consult, leading to a diagnosis of panuveitis detailed below. In the setting of these systemic symptoms, encorafenib/binimetinib was held. Soon after, a dose reduction and reintroduction of BRAF/MEKi was attempted; however, the patient then developed an acute kidney injury (creatinine up to 2.19 from 1.3 baseline) that required inpatient hospitalization. Urinalysis revealed granular casts with unclear cellular components; therefore, the differential included

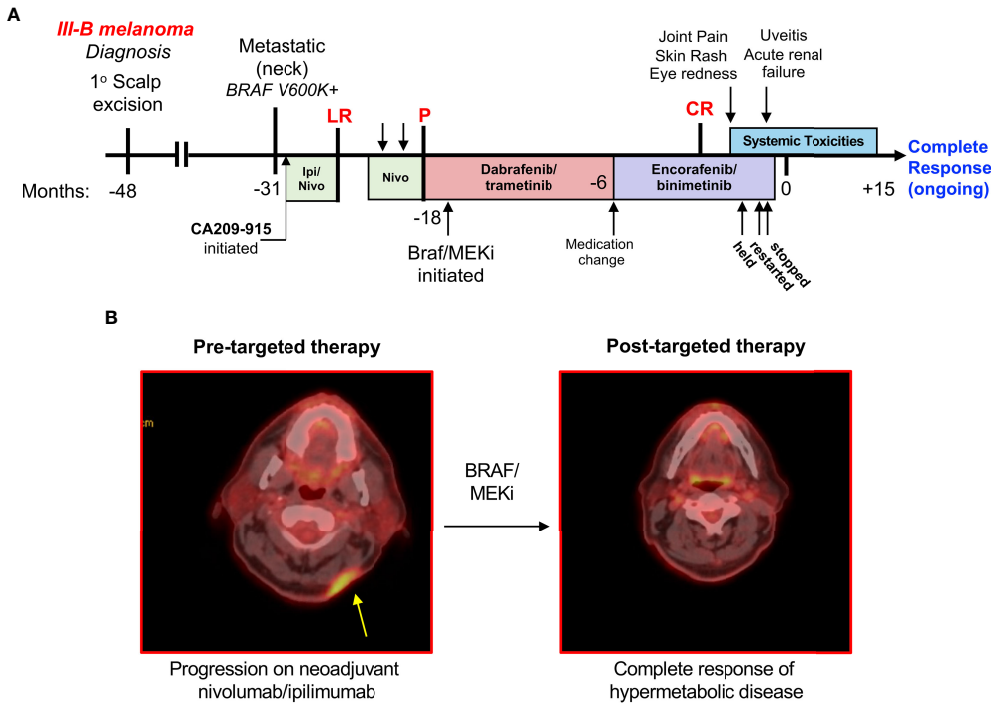


FIGURE 1 | Timeline of therapy and toxicity in a patient who experienced a complete response to BRAF/MEKi. **(A)** A patient whose BRAF V600K+ metastatic melanoma was unresponsive to combination ipilimumab/nivolumab and nivolumab monotherapy eventually responded well to BRAF/MEKi. This patient was treated with dabrafenib/trametinib for a year, followed by 6 months of encorafenib/binimetinib. After this time, the patient experienced significant multi-organ toxicities. LR, local recurrence; P, progression; CR, complete response. **(B)** (*left*) Positron emission tomography depicting recurrence within scar after multiple resections of in-transit metastasis and adjuvant nivolumab-ipilimumab. (*right*) Complete response of all hypermetabolic disease after treatment with BRAF-MEK inhibitors which developed approximately 3 months prior to the onset of toxicities described.

either autoimmune nephritis or drug-induced direct tubular toxicity. Renal function improved with IV fluids over the course of two days, therefore a biopsy of the kidney was not obtained. However, in the setting of lymphocytic inflammation in the dermis in addition to panuveitis, the diagnosis of autoimmune nephritis appeared more likely.

Due to these toxicities, the patient was taken off BRAF/MEK inhibitors. His skin rash was resolved with topical corticosteroids, and his nephritis overall improved significantly with oral steroids. He remains in a complete response off therapy for 18 months at the time of this publication.

UVEITIS DIAGNOSIS AND TREATMENT

Ophthalmic History

The patient was referred for ophthalmology evaluation for bilateral eye redness and blurred vision beginning 5 days after restarting dose-reduced encorafenib/binimetinib (previously held due to toxicities as described above). The patient also described intermittent ocular pain and photophobia. His presenting visual acuity was deemed 20/20 in both eyes. Slit lamp exam showed bilateral conjunctival injection. In the right eye, trace anterior chamber cells were seen with a few keratic precipitates. In the left eye, rare anterior chamber cell and keratic precipitates were observed. The anterior vitreous showed trace cells in the right and rare cells in the left eye. Funduscopic exam revealed a cup-to-disc ratio of 0.3 without optic nerve edema in both eyes. In the right eye, bilateral hypopigmented spots were identified along the inferior arcade, in addition to yellow hypopigmented spots outside the superior/inferior vascular arcades with little at the posterior pole (**Figure 2**). In the left eye, hypopigmented lesions were identified inferior to the arcade (**Figure 2**).

Fluorescein angiography (FA) and choroidal indocyanine green (ICG) angiography were obtained to evaluate the retinal and choroidal vasculature. Areas of hypofluorescence were identified inferonasal to the optic nerve in the right eye. Late frames showed hyperfluorescence of optic nerves bilaterally, possibly indicating breakdown of the inner blood-retinal barrier. ICG angiography, strikingly, revealed diffuse choroidal involvement which was not readily appreciable on prior exam (**Figure 2**). Multiple patches of hypocyanescence within the posterior pole and mid-peripheral retina were identified in the right eye, indicating a greater level of inflammation than was clinically appreciated. The left eye similarly showed multiple oval

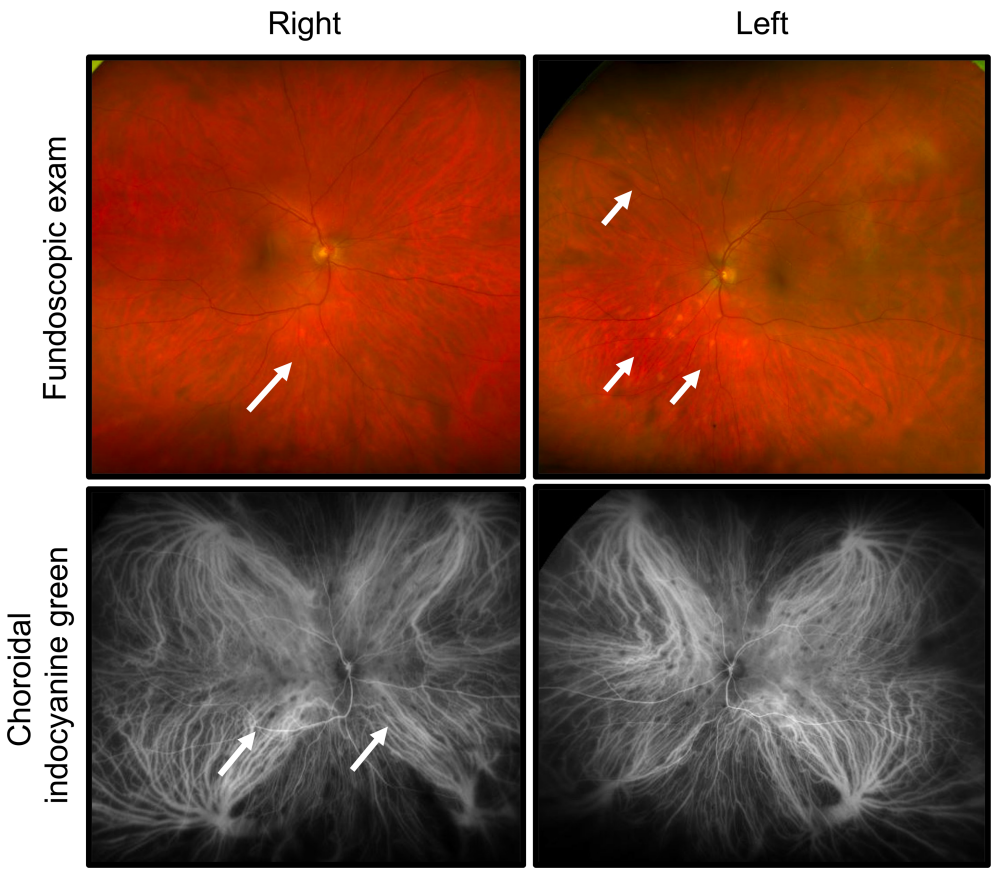


FIGURE 2 | Development of bilateral panuveitis during treatment with encorafinib/binimetanib. Fundoscopic exam revealed hypopigmented lesions bilaterally. In the right eye, hypopigmented lesions were identified along the inferior arcade and yellow hypopigmentation was seen superior/inferior arcades. In the left eye, hypopigmented spots were appreciated along the inferior arcade. Choroidal indocyanine green angiography identified diffuse choroidal involvement with patchy areas of hypocyanescence.

patches of hypocyanescence within the posterior pole and nasal mid periphery.

Optical coherence tomography (OCT) showed cells in the posterior hyaloid face of the vitreous but no evidence of cystoid macular edema was found in either eye, although more cells were present in the right than in the left eye.

These findings were most consistent with bilateral panuveitis, identified as slightly worse involvement in the right over left eye, with evidence of active, anterior segment inflammation. To treat the anterior uveitis the patient received prednisolone acetate (1%) 4× daily tapering over 1 month given the ophthalmic symptoms and low-grade inflammation. While visual acuity was excellent for the patient, his anterior uveitis was likely contributing to his photophobia, which improved with topical corticosteroid.

Follow Up

The patient returned for ophthalmology follow up approximately 1 month later. The reported symptoms improved, although complaints of mild residual blurred vision remained. A slit lamp exam showed resolution of the conjunctival injection bilaterally. There were few keratic precipitates in the right over the left eye and the presence of anterior chamber cells had resolved in both eyes. Funduscopic exam remained stable.

At four-month follow up, the patient's visual acuity remained stable at 20/20 with no evidence of recurrent anterior uveitis. Funduscopic exam of both eyes remained unchanged. ICG angiography revealed fewer lesions in the right eye, which also appeared less prominent than on a previous exam. A significant reduction in density of areas of hypocyanescence was also appreciated. ICG in the left eye also showed significant reduction in the density of the lesions.

IMMUNE CYTOKINE PROFILE AND T CELL REACTIVITY

During the patient's hospitalization with acute kidney injury there was evidence of pancytopenias showing low total WBC

count and ANC (**Figure 3A**). A sharp change in calcium and chloride were evident, though the calcium was not high enough to be considered the driver of renal injury (**Figure 3A**). Given the inflammatory clinical picture, we performed multiple analyses to investigate the specifics of immune activation in this patient. The patient was found to be HLA-A2, HLA-A29, and HLA-B27 positive. We next conducted a thorough analysis of peripheral plasma cytokines to identify immune signatures associated with systemic toxicities. The time when the patient was admitted is designated as time "0" in **Figure 3**. Relative to healthy donor

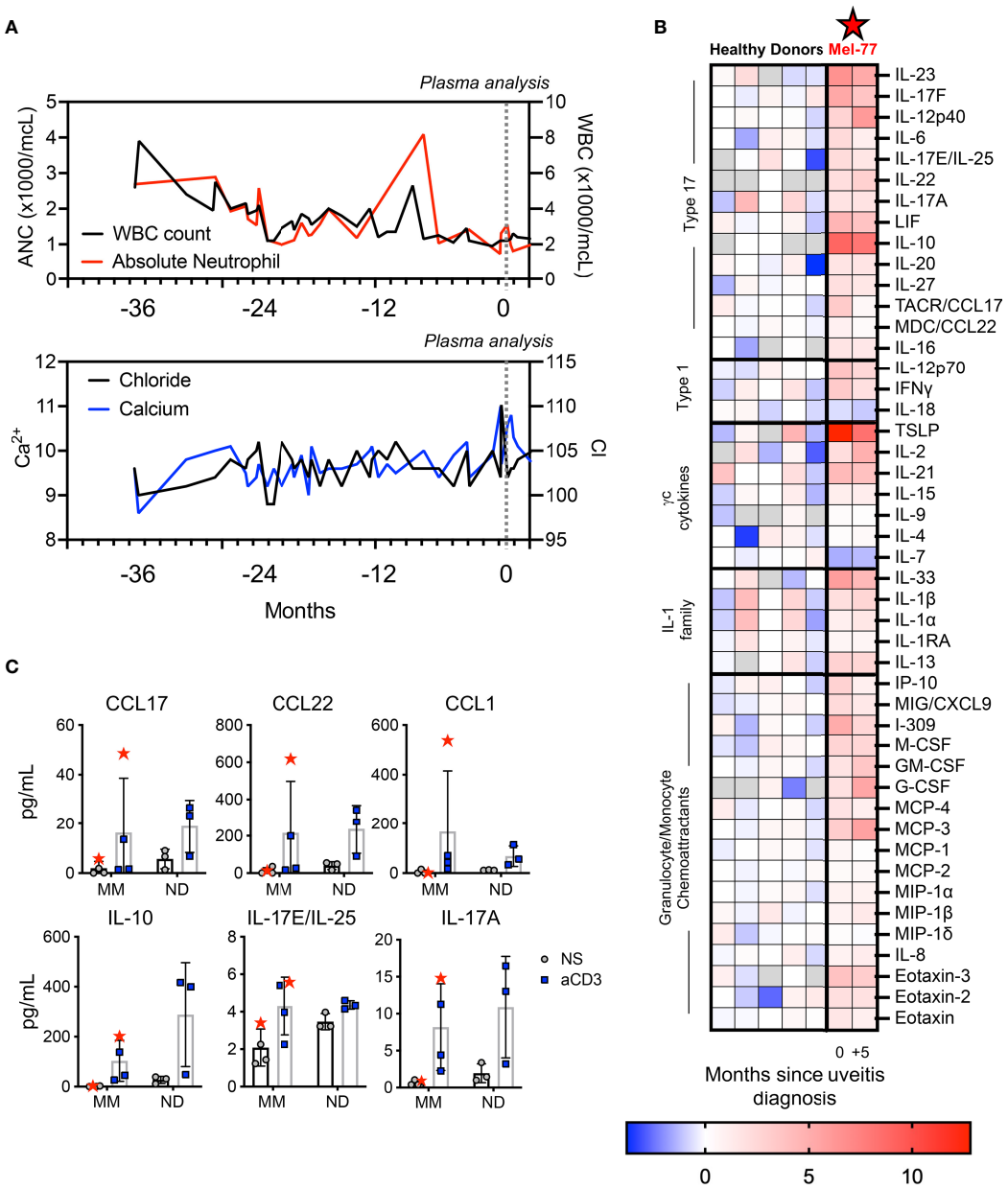


FIGURE 3 | Pronounced peripheral inflammation coincided with toxicities in the patient. **(A)** Lab values over three years of melanoma treatment, with T0 representing the time of inpatient care for renal failure. **(B)** Heat map displays ± log2 fold change of the plasma cytokines of the patient relative to the median value for five healthy donor plasma samples. The five healthy donors are also displayed on the left. The two time points for the patient, 0 and +5, are indicated to correspond with **(A)** and indicate 5-month follow-up. Gray boxes indicate the value was below the limit of detection for the assay. **(C)** PBMCs were stimulated overnight with 1 ug/ml plate bound αCD3 agonist. Samples from three other pre-treatment metastatic melanoma patients (MM) and three healthy donors (ND) are shown as controls. The patient studied here is indicated as Mel-77 (red star).

controls, the patient's plasma broadly showed higher levels of multiple cytokines and chemokines reflecting Tc/Th17-type profiles. Specifically, cytokines that were most upregulated included TSLP, IL-23, the IL-17 family, IL-10, IL-6, IL-21, IL-1β, and the chemokines, CCL17 and CCL1 (I-309) (**Figure 3B**). Some cytokines were comparable to normal donors, such as IL-15, IL-4, IL-9, and IL1RA (**Figure 3B**). This inflammatory picture coincided with the symptoms experienced by the patient, who recovered from the most severe toxicities soon after analysis. At five-month follow-up, while the peripheral symptoms had abated some but were still present, the peripheral plasma profile looked similar to T0, although the absolute concentrations of many cytokines were overall diminished (**Figure 3B**).

To further understand whether immune hyperactivity could be related to the autoimmune manifestations in our patient (Mel-77) compared to other melanoma patients, we performed T-cell functional assays to assess specific immune responses of interest. Specifically, we activated PBMCs with αCD3 agonist from T0 for our patient, relative to PBMCs from other healthy donors and other individuals with metastatic melanoma (MM) whose blood was collected prior to initiating any therapy (**Figure 3C**). We found that with forced T-cell activation *via* αCD3 agonist, the PBMCs of the patient released IL-17 and IL-10 at levels not uncharacteristically high relative to healthy donors but was often on the high end of melanoma patients (**Figure 3C**). In contrast, chemokines released from PBMCs with T-cell activation, namely, CCL17, CCL22, and CCL1 were vastly different for our patient relative to both other melanoma patients and healthy donor samples (**Figure 3C**). These functional assays suggested that while the intrinsic ability of the T cells of our patient to release cytokines in the *ex vivo* setting did not appear different from other cancer patients or healthy donors, these immune cells appeared to be activated and hyperfunctional within the patient. These findings reveal a new aspect of T-cell activation in a melanoma patient who responded well to BRAF/MEKi, with implications related to tumor regression and/or autoimmune toxicity.

DISCUSSION

In patients receiving immunotherapy, immune related adverse events can result from multiple mechanisms, including cross-reactivity of activated T cells against self-antigens, autoantibody production, disinhibition of normally tolerant T cells against self-tissue, or widespread cytokine release causing tissue inflammation (8). For example, uveitis and vitiligo have been reported in melanoma patients infused with TIL (tumor-infiltrating lymphocyte) therapy (9), CTLA-4 blockade with gp100 vaccine (10), and also single agent CTLA-4 blockade (11). Interestingly, adverse events like vitiligo are frequently associated with improved responses to therapy (12). In BRAF/MEK inhibition, while the incidence of grade 3–4 adverse events is about 40–50% of patients, severe autoimmune toxicities are relatively rare (13). However, few patients experience toxicities with putative immune mechanisms like vitiligo, uveitis, erythema nodosum, and keratitis sicca. In these patients, the overall mPFS on BRAF/MEKi was found to be substantially higher (48 months over 6 months) for patients with at least one of those adverse events relative to those experiencing no immune adverse events (4).

While it seems logical that the mechanisms leading to uveitis or vitiligo induction would be similar between checkpoint blockade and BRAF/MEKi, the impact of BRAF/MEK targeted therapy on the immune system is less clear. Several reports describe that BRAK/MEKi impacts myeloid cells, dampening suppressor cells which licenses more potent immunity. For example, BRAFi suppress myeloid-derived suppressor cells (MDSCs) in melanoma patients (14), and MDSCs have been found to repopulate tumors that become resistant to BRAFi which hinders the immune response (15). BRAFi can also improve immunogenicity (16) and sensitize tumors to granzyme-dependent lysis by $CD8^+$ T cells (17). These agents dampen T cell activation, particularly *in vitro*, yet bolster effective antitumor activity within *in vivo* models (18, 19). Further, MEKi can shift T-cell metabolic fitness towards longer-lived phenotypes that avoid exhaustion and persist in the tumor microenvironment (20). The impact of BRAF/MEKi on T helper immunity remains undescribed, although one report distinguishes that Th17-signatures in melanoma metastases are more strongly associated with BRAF mutations relative to a Th1 immune profile (21).

The patient presented here demonstrated an exceptional response to BRAF/MEKi and continues to be a complete responder at most recent follow up. Toxicities with immune involvement, such as uveitis, granulomatous skin rash, arthralgia, and interstitial nephritis, were observed after nearly 18 months on treatment. Further, these toxicities responded well or resolved completely with systemic and topical corticosteroids. To our knowledge, there have been no reports of patients experiencing delayed onset autoimmune toxicities after treatment with BRAF/MEKi for longer than a year. Collectively, this case highlights unique, potentially immune-based toxicities of BRAF/MEK inhibitors in an individual with an exceptional response to treatment.

We observed a clear activation of type-17 cytokine signatures in the periphery of this patient, both at the time of initial renal impairment and persisting at the 5-month follow up. IL-17, classically produced by $CD4^+$ Th17 cells and can be produced $CD8^+$ Tc17 cells, is functionally important for immunity to extracellular pathogens, and promotes neutrophil recruitment. However, self-reactive Th17 cells have been implicated in autoimmune diseases like psoriasis, multiple sclerosis, and inflammatory bowel disease among others (22). While the patient recovered from renal injury, some evidence of sustained skin and ocular involvement remained despite withdrawal of therapy. In parallel with his symptoms, high levels of IL-17 and related cytokines were sustained but dampened after 5 months. IL-1β was also upregulated in this patient relative to healthy donors: it has been reported that dabrafenib can stimulate dendritic cells to release IL-1β (23),

which is known to promote inflammatory Th17 polarization and could be a driver of the peripheral IL-17 induction (24). Despite these data, there are limited reports on Th17 activation in patients treated with BRAF/MEKi and none that relate this cell type to toxicity. Indeed, in a patient with colorectal cancer, IL-17 blockade was given to ameliorate toxicity induced by PD-1 therapy; unfortunately, this intervention eventually led to tumor recurrence (25).

While peripheral activation of type-17 signatures was observed, the specificities of the induced Th17/Tc17 cells remains unclear. The tumor-promoting versus tumor-eradicating ability of Th17 cells remains controversial (22); though evidence exists that depending on their phenotype, Th17 cells may fuel tumor growth, or they may promote robust tumor clearance (26–28). It is possible that common melanoma antigens like MART-1, NY-ESO, or gp100 could be the target of these Th17/Tc17 cells, or perhaps other antigens released in response to tumor destruction could have promoted their development. Alternatively, these cells could be bystander or self-reactive cells with no true role in tumor eradication. Investigation of TCR clonality paired with T cell activation phenotypes in response to targeted therapy would contribute to understanding the T cell dynamics related to tumor response and autoimmune toxicities. Self-reactive B cells may also play a role, where class switching could be influenced by the observed inflammatory markers. Future studies will investigate Th17/Tc17 cells in melanoma patients to discern their changes in clonality and response to targeted therapies.

The presence of three HLA alleles (HLA-A2, HLA-A29, and HLA-B27) with established linkage to various autoimmune ocular manifestations was intriguing. Reflecting on the uveitis symptoms of the patient after BRAF/MEKi therapy, we recognized that HLA-A2 has known linkage to Vogt–Koyanagi–Harada syndrome and HLA-A29 is strongly associated with birdshot chorioretinopathy (29). Additionally, HLA-B27 is linked with anterior uveitis (30). HLA-B27 is also associated with ankylosing spondylitis, which is naturally driven by IL-17 and is responsive to IL-17 blockade (31). Whether the IL-17 response seen during this toxicity manifestation of the patient is related to his immunogenetics, or whether IL-17 production was related to tumor-specific, or off-tumor immune activation is an important area of future follow up. Given these HLA subtypes, which have been associated with ocular and systemic immune manifestations, it is possible that the patient could have had an increased risk of uveitis and other immune-related adverse events at baseline.

In summary, we report here a complete response of the patient to BRAF/MEKi that was associated with delayed onset autoimmune-like manifestations emerging over 18 months after therapy initiation. Given the pronounced peripheral type-17 cytokines at the height of the toxicities of the patient, questions regarding whether blockade of cytokines like IL-6, IL-17, IL-23, or IL-1 would ameliorate toxicity and whether immunity would be impaired are relevant. These findings are informative for oncologists and patients alike that severe reactions could emerge with late onset, and thus careful follow-up is important. Furthermore, future studies to understand the mechanistic pathways related to toxicity and response to targeted therapies are necessary.

METHODS

Ethics and Approval

This study was approved prior to initiation under the Institutional Review Board at Emory University (IRB00046593). All patient information was deidentified prior to transfer to the research laboratory. Peripheral blood from other metastatic melanoma patients for use in mechanistic studies were collected at the Medical University of South Carolina with oversight and approval from the Institutional Review Board of the institution.

Patient Samples

Peripheral blood was collected in EDTA-coated tubes and brought to the research lab in a deidentified manner. Peripheral blood mononuclear cells (PBMC) were isolated using a Ficoll gradient and used directly for functional analysis.

Cytokine Multiplex

Plasma was isolated after centrifuging peripheral blood at 1,000*g*, 4°C for 10 min, and was stored at −80°C until analysis. Analysis was performed using a 71-plex Human Discovery assay cytokine panel by the Eve Technologies Corporation (Alberta, Canada).

Immune Functional Assays

PBMCs from normal donors and melanoma patients were activated with 1 mg/ml plate bound CD3 agonist (OKT3, Biolegend). After 24 hours, supernatant was collected and stored at −20°C. Supernatants were analyzed undiluted for concentrations of cytokines and chemokines (Eve Technologies).

DATA AVAILABILITY STATEMENT

The raw data supporting the conclusions of this article will be made available by the authors, without undue reservation.

ETHICS STATEMENT

The studies involving human participants were reviewed and approved by the IRB at Emory University, IRB00046593. The patients/participants provided their written informed consent to participate in this study. Written informed consent was obtained from the individual(s) for the publication of any potentially identifiable images or data included in this article.

AUTHOR CONTRIBUTIONS

HK, DL, CP, SY, and RK conceptualized the manuscript and designed experiments. HK, CP, SY, and RK wrote and edited the

manuscript. HK performed experiments. MBW, AR, and SL provided experimental support. JS, MY, and RS, provided guidance and critically edited the manuscript. All authors listed have made a substantial, direct, and intellectual contribution to the work and approved it for publication.

FUNDING

This work was supported by the NCI F30 243307 and the NIH GM008716 to HK, the NCI grants R01 CA175061 and R01 CA208514 to CP, and the V Foundation Translational Award to CP and RK.

ACKNOWLEDGMENTS

We are thankful for the subject of this work who graciously volunteered his time and effort to support scientific learning through sharing his experience. We are grateful for all individuals who support research studies in the hopes of understanding and improving clinical outcomes.

REFERENCES

1. Russo I, Zorzetto L, Chiarion Sileni V, Alaibac M. Cutaneous Side Effects of Targeted Therapy and Immunotherapy for Advanced Melanoma. *Scientifica (Cairo)* (2018) 2018:5036213–13. doi: 10.1155/2018/5036213
2. Flaherty KT, Infante JR, Daud A, Gonzalez R, Kefford RF, Sosman J, et al. Combined BRAF and MEK Inhibition in Melanoma With BRAF V600 Mutations. *New Engl J Med* (2012) 367(18):1694–703. doi: 10.1056/NEJMoa1210093
3. Koelblinger P, Thuerigen O, Dummer R. Development of Encorafenib for BRAF-Mutated Advanced Melanoma. *Curr Opin Oncol* (2018) 30(2):125–33. doi: 10.1097/CCO.0000000000000426
4. Ben-Betzalel G, Baruch EN, Boursi B, Steinberg-Silman Y, Asher N, Shapira-Frommer R, et al. Possible Immune Adverse Events as Predictors of Durable Response to BRAF Inhibitors in Patients With BRAF V600–Mutant Metastatic Melanoma. *Eur J Cancer* (2018) 101:229–35. doi: 10.1016/j.ejca.2018.06.030
5. Topalian SL, Hodi FS, Brahmer JR, Gettinger SN, Smith DC, McDermott DF, et al. Five-Year Survival and Correlates Among Patients With Advanced Melanoma, Renal Cell Carcinoma, or Non–Small Cell Lung Cancer Treated With Nivolumab. *JAMA Oncology* (2019) 5:1411–20.
6. Michielin O, Atkins MB, Koon HB, Dummer R, Ascierto PA. Evolving Impact of Long-Term Survival Results on Metastatic Melanoma Treatment. *J Immunother Cancer* (2020) 8(2):e000948. doi: 10.1136/jitc-2020-000948
7. Dummer R, Hauschild A, Santinami M, Atkinson V, Mandalà M, Kirkwood JM, et al. Five-Year Analysis of Adjuvant Dabrafenib Plus Trametinib in Stage III Melanoma. *N Engl J Med* (2020) 383(12):1139–48. doi: 10.1056/NEJMoa2005493
8. Sullivan RJ, Weber JS. Immune-Related Toxicities of Checkpoint Inhibitors: Mechanisms and Mitigation Strategies. *Nat Rev Drug Discov* (2021). doi: 10.1038/s41573-021-00259-5
9. Yeh S, Karne NK, Kerkar SP, Heller CK, Palmer DC, Johnson LA, et al. Ocular and Systemic Autoimmunity After Successful Tumor-Infiltrating Lymphocyte Immunotherapy for Recurrent, Metastatic Melanoma. *Ophthalmology* (2009) 116(5):981–89.e1. doi: 10.1016/j.ophtha.2008.12.004
10. Robinson MR, Chan CC, Yang JC, Rubin BI, Gracia GJ, Sen HN, et al. Cytotoxic T Lymphocyte-Associated Antigen 4 Blockade in Patients With Metastatic Melanoma: A New Cause of Uveitis. *J Immunother* (2004) 27 (6):478–9. doi: 10.1097/00002371-200411000-00008
11. Crosson JN, Laird PW, Debiec M, Bergstrom CS, Lawson DH, Yeh S. Vogt-Koyanagi-Harada-Like Syndrome After CTLA-4 Inhibition With Ipilimumab for Metastatic Melanoma. *J Immunother* (2015) 38(2):80–4. doi: 10.1097/cji.0000000000000066
12. Nakamura Y, Tanaka R, Asami Y, Teramoto Y, Imamura T, Sato S, et al. Correlation Between Vitiligo Occurrence and Clinical Benefit in Advanced Melanoma Patients Treated With Nivolumab: A Multi-Institutional Retrospective Study. *J Dermatol* (2017) 44(2):117–22. doi: 10.1111/1346-8138.13520
13. Heinzerling L, Eigentler TK, Fluck M, Hassel JC, Heller-Schenck D, Leipe J, et al. Tolerability of BRAF/MEK Inhibitor Combinations: Adverse Event Evaluation and Management. *ESMO Open* (2019) 4(3):e000491–e91. doi: 10.1136/esmoopen-2019-000491
14. Schilling B, Paschen A. Immunological Consequences of Selective BRAF Inhibitors in Malignant Melanoma: Neutralization of Myeloid-Derived Suppressor Cells. *Oncoimmunology* (2013) 2(8):e25218–e18. doi: 10.4161/onci.25218
15. Steinberg SM, Shabaneh TB, Zhang P, Martyanov V, Li Z, Malik BT, et al. Myeloid Cells That Impair Immunotherapy Are Restored in Melanomas with Acquired Resistance to BRAF Inhibitors. *Cancer Res* (2017) 77(7):1599-610. doi: 10.1158/0008-5472.Can-16-1755
16. Donia M, Fagone P, Nicoletti F, Andersen RS, Høgdall E, Straten PT, et al. BRAF Inhibition Improves Tumor Recognition by the Immune System: Potential Implications for Combinatorial Therapies Against Melanoma Involving Adoptive T-Cell Transfer. *Oncoimmunol* (2012) 1(9):1476–83. doi: 10.4161/onci.21940
17. Atay C, Kwak T, Lavilla-Alonso S, Donthireddy L, Richards A, Moberg V, et al. BRAF Targeting Sensitizes Resistant Melanoma to Cytotoxic T Cells. *Clin Cancer Res* (2019) 25(9):2783. doi: 10.1158/1078-0432.CCR-18-2725
18. Liu L, Mayes PA, Eastman S, Shi H, Yadavilli S, Zhang T, et al. The BRAF and MEK Inhibitors Dabrafenib and Trametinib: Effects on Immune Function and in Combination With Immunomodulatory Antibodies Targeting PD-1, PD-L1, and CTLA-4. *Clin Cancer Res* (2015) 21(7):1639. doi: 10.1158/1078-0432.CCR-14-2339
19. Hu-Lieskovan S, Mok S, Homet Moreno B, Tsoi J, Robert L, Goedert L, et al. Improved Antitumor Activity of Immunotherapy With BRAF and MEK Inhibitors in BRAF(V600E) Melanoma. *Sci Trans Med* (2015) 7 (279):279ra41–79ra41. doi: 10.1126/scitranslmed.aaa4691
20. Verma V, Jafarzadeh N, Boi S, Kundu S, Jiang Z, Fan Y, et al. MEK Inhibition Reprograms CD8+ T Lymphocytes Into Memory Stem Cells With Potent Antitumor Effects. *Nat Immunol* (2021) 22(1):53–66. doi: 10.1038/s41590-020-00818-9
21. Tomei S, Bedognetti D, De Giorgi V, Sommariva M, Civini S, Reinboth J, et al. The Immune-Related Role of BRAF in Melanoma. *Mol Oncol* (2015) 9(1):93–104. doi: 10.1016/j.molonc.2014.07.014
22. Knochelmann HM, Dwyer CJ, Bailey SR, Amaya SM, Elston DM, Mazza-McCrann JM, et al. When Worlds Collide: Th17 and Treg Cells in Cancer and Autoimmunity. *Cell Mol Immunol* (2018) 15(5):458–69. doi: 10.1038/s41423-018-0004-4
23. Hajek E, Krebs F, Bent R, Haas K, Bast A, Steinmetz I, et al. BRAF Inhibitors Stimulate Inflammasome Activation and Interleukin 1 Beta Production in Dendritic Cells. *Oncotarget* (2018) 9(47):28294–308. doi: 10.18632/oncotarget.25511
24. Chung Y, Chang SH, Martinez GJ, Yang XO, Nurieva R, Kang HS, et al. Critical Regulation of Early Th17 Cell Differentiation by Interleukin-1 Signaling. *Immunity* (2009) 30(4):576–87. doi: 10.1016/j.immuni.2009.02.007
25. Esfahani K, Miller W. Reversal of Autoimmune Toxicity and Loss of Tumor Response by Interleukin-17 Blockade. *N Engl J Med* (2017) 376:1989–91. doi: 10.1056/NEJMc1703047

26. Muranski P, Boni A, Antony P, Cassard L, Irvine K, Kaiser AD, et al. Tumor-Specific Th17-Polarized Cells Eradicate Large Established Melanoma. *Blood* (2008) 112(2):362–72. doi: 10.1182/blood-2007-11-120998
27. Knochelmann HM, Dwyer CJ, Smith AS, Bowers JS, Wyatt MM, Nelson MH, et al. IL6 Fuels Durable Memory for Th17 Cell–Mediated Responses to Tumors. *Cancer Res* (2020) 80(18):3920–32. doi: 10.1158/0008-5472.Can-19-3685
28. Kryczek I, Zhao E, Liu Y, Wang Y, Vatan L, Szeliga W, et al. Human TH17 Cells are Long-Lived Effector Memory Cells. *Sci Transl Med* (2011) 3 (104):104ra00. doi: 10.1126/scitranslmed.3002949
29. Zucchiatti I, Miserocchi E, Sacconi R, Bandello F, Modorati G. Hla-A29-Positive Uveitis: Birdshot Chorioretinopathy, What Else? *Case Rep Ophthalmol* (2013) 4(3):287–93. doi: 10.1159/000357276
30. McCannel CA, Holland GN, Helm CJ, Cornell PJ, Winston JV, Rimmer TG. Causes of Uveitis in the General Practice of Ophthalmology. UCLA Community-Based Uveitis Study Group. *Am J Ophthalmol* (1996) 121 (1):35–46. doi: 10.1016/s0002-9394(14)70532-x
31. Sieper J, Poddubnyy D. Axial Spondyloarthritis. *Lancet* (2017) 390 (10089):73–84. doi: 10.1016/s0140-6736(16)31591-4

Conflict of Interest: The authors declare that the research was conducted in the absence of any commercial or financial relationships that could be construed as a potential conflict of interest.

Publisher's Note: All claims expressed in this article are solely those of the authors and do not necessarily represent those of their affiliated organizations, or those of the publisher, the editors and the reviewers. Any product that may be evaluated in this article, or claim that may be made by its manufacturer, is not guaranteed or endorsed by the publisher.

Copyright © 2022 Knochelmann, Ware, Rali, Linderman, Shantha, Lawson, Yushak, Swerlick, Paulos, Yeh and Kudchadkar. This is an open-access article distributed under the terms of the Creative Commons Attribution License (CC BY). The use, distribution or reproduction in other forums is permitted, provided the original author(s) and the copyright owner(s) are credited and that the original publication in this journal is cited, in accordance with accepted academic practice. No use, distribution or reproduction is permitted which does not comply with these terms.

frontiers | Frontiers in Oncology

ORIGINAL RESEARCH
published: 11 April 2022
doi: 10.3389/fonc.2022.835929

Cancer Progression Gene Expression Profiling Identifies the Urokinase Plasminogen Activator Receptor as a Biomarker of Metastasis in Cutaneous Squamous Cell Carcinoma

Elahe Minaei[1,2], *Simon A. Mueller*[3,4], *Bruce Ashford*[1,3,5,6], *Amarinder Singh Thind*[1,6], *Jenny Mitchell*[5], *Jay R. Perry*[1,2], *Benjamin Genenger*[1,2], *Jonathan R. Clark*[3,7,8], *Ruta Gupta*[3,8,9] *and Marie Ranson*[1,2*]

[1] Illawarra Health and Medical Research Institute (IHMRI), Wollongong, NSW, Australia, [2] School of Chemistry and Molecular Bioscience, University of Wollongong, Wollongong, NSW, Australia, [3] Department of Head and Neck Surgery, Sydney Head and Neck Cancer Institute, Chris O'Brien Lifehouse, Sydney, NSW, Australia, [4] Department for Otorhinolaryngology, Head and Neck Surgery, Zurich University Hospital University of Zurich, Zurich, Switzerland, [5] Illawarra and Shoalhaven Local Health District (ISLHD), Wollongong, NSW, Australia, [6] School of Medicine, University of Wollongong, Wollongong, NSW, Australia, [7] Royal Prince Alfred Institute of Academic Surgery, Sydney Local Health District, Sydney, NSW, Australia, [8] Central Clinical School, Faculty of Medicine and Health, The University of Sydney, Sydney, NSW, Australia, [9] NSW Health Pathology, Department of Tissue Pathology and Diagnostic Oncology, Royal Prince Alfred Hospital, Sydney, NSW, Australia

OPEN ACCESS

Edited by:
Xunwei Wu,
Shandong University, China

Reviewed by:
Mingxing Lei,
Chongqing University, China
Jinfeng Wu,
Fudan University, China

***Correspondence:**
Marie Ranson
mranson@uow.edu.au

Specialty section:
This article was submitted to Skin Cancer, a section of the journal Frontiers in Oncology

Received: *15 December 2021*
Accepted: *03 March 2022*
Published: *11 April 2022*

Citation:
Minaei E, Mueller SA, Ashford B, Thind AS, Mitchell J, Perry JR, Genenger B, Clark JR, Gupta R and Ranson M (2022) Cancer Progression Gene Expression Profiling Identifies the Urokinase Plasminogen Activator Receptor as a Biomarker of Metastasis in Cutaneous Squamous Cell Carcinoma. Front. Oncol. 12:835929. doi: 10.3389/fonc.2022.835929

Cutaneous squamous cell carcinoma (cSCC) of the head and neck region is the second most prevalent skin cancer, with metastases to regional lymph nodes occurring in 2%–5% of cases. To further our understanding of the molecular events characterizing cSCC invasion and metastasis, we conducted targeted cancer progression gene expression and pathway analysis in non-metastasizing (PRI-) and metastasizing primary (PRI+) cSCC tumors of the head and neck region, cognate lymph node metastases (MET), and matched sun-exposed skin (SES). The highest differentially expressed genes in metastatic (MET and PRI+) versus non-metastatic tumors (PRI-) and SES included *PLAU*, *PLAUR*, *MMP1*, *MMP10*, *MMP13*, *ITGA5*, *VEGFA*, and various inflammatory cytokine genes. Pathway enrichment analyses implicated these genes in cellular pathways and functions promoting matrix remodeling, cell survival and migration, and epithelial to mesenchymal transition, which were all significantly activated in metastatic compared to non-metastatic tumors (PRI-) and SES. We validated the overexpression of urokinase plasminogen activator receptor (uPAR, encoded by *PLAUR*) in an extended patient cohort by demonstrating higher uPAR staining intensity in metastasizing tumors. As pathway analyses identified epidermal growth factor (EGF) as a potential upstream regulator of

PLAUR, the effect of EGF on uPAR expression levels and cell motility was functionally validated in human metastatic cSCC cells. In conclusion, we propose that uPAR is an important driver of metastasis in cSCC and represents a potential therapeutic target in this disease.

Keywords: cutaneous squamous cell carcinoma (cSSC), urokinase plasminogen activator receptor (uPAR), urokinase plasminogen activator (uPA), metastasis, matrix metalloproteinase (MMP), extracellular matrix (ECM), tumor stroma, transcriptomics

1 INTRODUCTION

Cutaneous squamous cell carcinoma (cSCC) is a prevalent non-melanoma skin cancer worldwide (1). As principally a disease of the sun-exposed skin, most notably in the head and neck, cSCC is particularly prevalent in regions with intensive sun exposure such as Australasia where it represents a significant health burden (2, 3). Metastasis to regional lymph nodes in the head neck occurs in <5% of cases but imparts significant morbidity and mortality (4). Notwithstanding conventional systemic treatment options such as chemotherapy and, more recently, epidermal growth factor receptor inhibitors or immunotherapy, for a substantial proportion of advanced cSCC patients there are still no valid second-line therapies (5), indicating a need for alternate targeted therapy options and strategies.

Conventional clinicopathologic prognostic markers in cSCC are unreliable predictors of lymph node metastasis (6–8). Recent studies assessing the genomic and transcriptomic landscape of cSCC have revealed heterogeneity of cellular subtypes in these cancers; however, tumor cell populations harboring potentially clinically useful gene signatures and/or therapeutic targets of metastatic risk in primary cSCC are evident (1, 9–16). These biomarkers or molecular signatures of invasion and metastasis are overwhelmingly related to cancer progression pathways encompassing extracellular matrix (ECM) interactions and remodeling, epithelial to mesenchymal transition (EMT), cellular motility, and survival.

Altered proteolysis and EMT programs are required for ECM remodeling and tumor cell escape (17–19). In particular, overexpression of the urokinase plasminogen activator (uPA, encoded by *PLAU*) and its cognate cell surface receptor (uPAR, encoded by *PLAUR*) (including downstream effector and upstream regulator molecules) is associated with EMT (20) and correlates with increased metastasis and/or poorer patient survival in many solid tumor types (21–23) including mucosal squamous cell carcinoma of the oral cavity (24–30).

These genes and their proteins are also overexpressed in advanced and metastatic cSCC (15, 31, 32) with uPAR mRNA shown to be localized to a subpopulation of invasive cells in primary cSCCs (33). Upon binding to uPAR, uPA efficiently activates co-localized plasminogen to the potent broad-spectrum protease plasmin, which initiates a cascade of pericellular proteolysis that directly and indirectly (through the activation of pro-metalloproteinases, pro-MMPs) degrades integral ECM molecules including fibronectin, laminins, elastins, and collagens, thus enabling tumor cell invasion and dissemination (18, 22). Plasmin and MMPs are also responsible for the release and activation of latent growth/angiogenic factors (such as EGF and VEGF) and chemokines from the ECM, which promotes cellular proliferation, survival, and motility (18, 22). Activated receptor tyrosine kinase pathways have also been shown to enhance uPA system expression in cancer (23).

While others have either specifically or coincidently explored the expression of the uPA system, MMPs, and ECM interactors in cSCC (summarized in **Table S1**), few have focused exclusively on the uPA system in UV-induced cSCC of the head and neck encompassing the spectrum of disease states. To this end, we performed gene expression analyses using a curated cancer progression-targeted gene set in non-metastasizing and metastasizing head and neck cSCC primary tumors, lymph node metastases, and matched sun-exposed skin (SES). This was then used for gene enrichment and pathway analyses. An integrated gene expression was also performed on relevant gene expression omnibus (GEO) datasets to strengthen our findings. Recognizing the *PLAUR* gene as an important mediator of proteolytic networks in the tumor microenvironment, we further investigated uPAR protein levels and association with metastatic disease. Finally, the predicted activating effects of EGF was assessed *in vitro* on EGFR-expressing human metastatic cSCC cell lines.

2 MATERIAL AND METHODS

2.1 Study Population and Sample Collection

The project was approved by the University of Wollongong Health and Medical Human Research Ethics Committee (Wollongong NSW, Australia, UOW/ISLHD HREC 14/397). Head and neck cSCC specimens from a total of 50 patients who underwent surgery with curative intent were retrieved from the Department of Tissue Pathology and Diagnostic Oncology at Royal Prince Alfred Hospital, Sydney NSW, Australia. Formalin-fixed paraffin-embedded (FFPE) specimens were derived from the head and neck region of 21 patients with primary tumors with no evidence of metastasis (PRI-), 14 patients with primary tumors that had metastasized (PRI+) (13 of which had available concurrent metastases), and an additional 15 patients with lymph node metastases, but with no available primary tumor. FFPE cores from SES were taken from the peripheral negative margins where available. The specimens used are summarized in **Supplementary Data Sheet 1**. High-risk disease was defined as

per criteria of the 7th edition of the American Joint Commission on Cancer Staging Manual (34). Patients in the non-metastatic group had to meet one or more of the following criteria: absence of metastases at the >24-month follow-up after resection of the primary; negative sentinel lymph node biopsy at the time of resection of the primary; or histologically negative prophylactic neck dissection. Clinical features, treatment, and follow-up were obtained from the Sydney Head and Neck Cancer Institute database. For comparisons between the cohorts, the Mann–Whitney-U test was applied for non-parametric continuous data, the Fisher's exact for categorical data in 2 × 2 contingency tables, and χ^2 test for larger contingency tables.

2.2 RNA Extraction

Specimens underwent histopathological review to select areas with high neoplastic content (>30%) and exclude areas containing necrosis, hemorrhage, high keratin content, or significant inflammation. Three to six tissue cores (2 mm diameter) were then obtained from FFPE blocks of these specimens for deparaffinization and homogenization prior to RNA extraction. Tumor nucleic acids from specimens were extracted using AllPrep DNA/RNA FFPE Kit (80234, Qiagen, Hilden, Germany) according to the manufacturer's instructions. RNA samples that met initial QC measures including high A260/280 (<1.8–2) and acceptable integrity (Invitrogen Qubit RNA IQ Assay, Thermo Fisher Scientific, Waltham, MA, USA) were utilized in gene expression assays.

2.3 Gene Expression Assays and Data Analysis

Up to 150 ng of purified RNA was run on the nCounter Sprint (NanoString Technologies, Seattle, WA, USA) platform using the nCounter PanCancer Progression Panel (NanoString; 740 target genes, 30 housekeeping genes) as per the manufacturer's instructions. nSolver Analysis Software 4.0 (NanoString) was used to remove specimens with low binding density or other technical QC flags. The raw data from the remaining specimens was then processed using the iterative RUVSeq normalization pipeline for QC, normalization, and data visualization/validation using NanoNormIter R package (35). After technical quality control steps, specimens SESP3, SESP29, and PRI+P7 were excluded from further analysis because of very low geometric mean of housekeeping gene expression. Housekeeping genes associated with phenotype were also excluded using the glm.nb function (Negative Binomial Generalized Linear Model) as specified in the RUVseq-based pipeline [refer to (35)]. The normalization step of all possible combinations of pairwise analyses was tested using different values of k (RUVg) and the different normalized expression datasets visualized using principal component analysis (PCA) and RLE plots to detect problematic samples for assessment of removal from further analysis. By this method, METP16 was flagged, assessed, and discarded. The final list of included specimens that underwent NanoString analyses are shown in **Supplementary Data Sheet 1**. After RUVg normalization of final specimens, differential expression analyses were performed using DESeq2. The top differentially expressed genes (DEGs) were selected based on both $\log_2$fold change between the compared groups and the p-values adjusted for multiple testing using the Benjamini–Hochberg method (36). **Supplementary Data Sheet 2** contains differential gene expression data for all cohort comparisons.

Where indicated, raw data from the retained specimens that passed these QC steps were also analyzed using the global significance score function within the nCounter Advanced Analysis 2.0 software (NanoString) which is derived using the most DEGs in gene sets representative of a particular cancer progression annotation.

2.4 Functional Enrichment Analysis

Ingenuity Pathway Analysis (IPA; Qiagen Inc., https://www.qiagenbioinformatics.com/products/ingenuitypathway-analysis) software was used to generate networks and functional analyses of gene expression datasets (37). IPA core analysis default settings were used, limited to the human knowledge base. We applied a global molecular network developed from information contained in the Ingenuity Pathways Knowledge Base incorporating DEGs from our study with log2 fold change (logFC) <-0.58, >0.58 (p-value < 0.05) for each comparison. Networks of these gene lists were then generated algorithmically based on their interrelationships. The significance of the association between lists of DEGs and the Diseases and Functions were assessed using (1) the ratio of DEGs (molecules) from the dataset that map to a specific cellular and molecular function category (in relation to the total number of molecules included in the particular disease and function) and (2) Fischer's exact test (to determine the likelihood of association between the molecules in the dataset and the disease and function).

IPA uses the activation z-score algorithm to make a prediction of activation or inhibition (or no prediction) as well as to reduce the chance that random data will generate significant predictions. Causal Network and Upstream Regulator analyses were used to identify regulators with a probability of being responsible for the changes in gene expression observed, by calculating an overlap p-value with Fisher's exact test and an activation z-score. Causal Networks are small hierarchical networks of regulators that control the expression of the dataset targets.

2.5 Integrative Gene Expression Meta-Analysis Using the Robust Rank Aggregation Approach

An expression meta-analysis study was performed on all available cSCC datasets in Gene Expression Omnibus (GEO) (38) containing normal skin from sun-exposed areas and cSCC cases classified as invasive or metastatic for comparison to our PRI+ vs. SES analyses. Using the detailed filtering criteria described in **Table S2**, only three datasets comprising 18 SES and 25 cSCC samples matched these criteria. In the first step, three separate differential expression analyses for each dataset was performed using the Limma (39) and GEOquery (40) packages. A universal threshold of p-value < 0.01 and logFC <-0.58, >0.58 was used for the collection of significantly DEG lists for each comparison. RankerGUI (41) ranked the DEG lists based on the logFC values, which were then used for a differential meta-analysis

using the Robust Rank Aggregation (RRA) method (42). Significant DEG lists of the meta-analysis were extracted using a p-value cutoff < 0.05. In addition, Reactome (43) functional enrichment analysis of significantly DEG was carried out using Bioconductor package-ReactomePA (44).

2.6 Immunohistochemistry

Immunohistochemical staining for uPAR was performed using FFPE tissues from primary and metastatic cSCC specimens (listed in **Supplementary Data Sheet 1**). Briefly, 4-µm sections were deparaffinized and uPAR detected (after antigen retrieval at 100°C in pH 9.0 solution) with anti-uPAR at either 1:100 dilution (clone R4; Dako, Glostrup, Denmark) or 1:500 (10925-T30; Sino Biological, Chesterbrook, PA, USA) using the Ventana BenchMark Ultra Automated Immunohistochemistry (IHC)/ISH slide staining system with diaminobenzidine (DAB) as chromogen, followed by counterstaining with hematoxylin. The confounder effect of using the two different sources of anti-uPAR in this study was not significant (data not shown). Slides containing neutrophils and macrophages as internal and external positive controls, respectively, accompanied all staining runs. The proportion of tumor cells demonstrating complete membranous staining with uPAR was initially recorded as a proportion of the total number of tumor cells at the advancing edge of the tumor. Complete membranous staining of any intensity of the tumor cells was then scored and used for statistical analyses in this study. Scores were analyzed in GraphPad Prism 8.4.3.

2.7 miRNA Analysis

Small RNA-Seq was performed using the Illumina HiSeq platform at the Australian Genome Research Facility Ltd., Westmead, NSW, Australia. The quality test of raw reads was assessed using the FastQC tool v0.11.9 (https://www.bioinformatics.babraham.ac.uk/projects/fastqc/). Poor-quality reads were trimmed using Cutadapt (version 2.8). Trimmed fastq sequences were mapped and annotated using sRNAbench (45). Next, a differential expression analysis based on negative binomial distribution was performed using the sRNAde tool (46), which integrates Deseq2 (47) and EdgeR (48). Further, significantly differentially expressed miRNAs were extracted based on $\log_2$FC ≥ ± 1 and p-values adjusted for multiple testing using the Benjamini–Hochberg method (36). In downstream analyses, miRDB (49, 50) was used to obtain putative targeted genes of statistically significant miRNAs. miRDB provides a collection of miRNA and mRNA interactions predicted by the Machine Learning Tool (MirTarget), which utilizes features related to miRNA binding and downregulated targets. miRNA–mRNA interactions having a score >75 were considered for further analysis. Finally, experimentally validated miRNA–mRNA interactions for *PLAUR* from the miRtarbase database (51) were explored. Two-tailed Spearman correlation coefficient between uPAR IHC and miRNA was calculated using GraphPad Prism 9.0.2.

2.8 Cell-Based Assays

The effect of EGF on cell migration was assessed in a scratch-wound assay using the IncuCyte® Zoom Kinetic Imaging System (Essen BioScience, Ann Arbor, MI, USA). Patient-derived metastatic cSCC cell line UW-CSCC2 [described in detail in (52)] was seeded onto collagen 1-coated 96-well ImageLock plates (Essen). After 24 h incubation in low serum containing media (DMEM supplemented with 1% FCS, no EGF), the cells were scratched according to manufacturer's instructions using the 96-pin Essen Woundmaker™. The cells were subsequently washed with serum-free media, then incubated with 0, 5, 10, or 20 ng/ml human EGF ± 1 µM gefitinib in low serum media at 37° C, 5% CO_2, and imaged over 24 h at ×10 objective to track cell motility and wound width. IncuCyte™ ZOOM software was used to analyze wound width reduction over time. Data were analyzed using GraphPad Prism 9.0.2.

For determination of uPAR levels, UW-CSCC2 cells were treated as above except that cells were lysed for total protein extraction and Western blotting 24 h after EGF ± 1 µM gefitinib treatment. Blots were incubated with anti-human uPAR rabbit polyclonal antibody (1:2,000; ab103791, Abcam) or anti-GAPDH mouse monoclonal antibody (1:5,000; G8795, Sigma-Aldrich, St. Louis, MO, USA) and detected using horseradish peroxidase-conjugated anti-rabbit IgG (7074S, Cell Signaling, Danvers, MA, USA) or anti-mouse IgG (ab205719, Abcam, Cambridge, MA, USA) both at 1:5,000 dilution. Chemiluminescence was generated using Pierce ECL Western Blotting Substrate (Thermo Fisher Scientific, Waltham, MA, USA) and visualized using a ChemiDoc MP Imaging System (Bio-Rad Laboratories). Densitometry was conducted using ImageJ (v1.53e, NIH, USA) and values normalized against the housekeeping protein GAPDH as protein loading control.

For detection of EGFR, cells were seeded into ibidi chamber slides (ibidi GmbH, Gräfelfing, Germany) and grown under regular culture conditions prior to staining with human anti-EGFR monoclonal antibody (1:1,000; MAB1095-100—R&D Systems, Minneapolis, MN, USA) followed by Alexa Fluor® 555-conjugated donkey anti-mouse IgG H&L (1:2,000; ab150106, Abcam). The cells were then counterstained with ActinRed 555 ready probes (Thermo Fisher) and RedDot2 Far-Red Nuclear Stain (Biotium, Inc., Fremont, CA, USA), and then imaged with a ×20 oil immersion objective and a TCS SP5 confocal microscope (Leica, Wetzlar, Germany).

3 RESULTS

3.1 Clinical and Demographic Characteristics

Clinical and demographic data are shown in **Table 1**. While the sex distribution was similar, patients suffering from metastasizing cSCC (PRI+ and/or MET) were significantly older than patients with non-metastasizing cSCC (PRI-; $p = 0.034$). This age difference may be subject to bias, since in patients with MET where the primary tumor was not known, the age was recorded at the time of treatment of the lymph node metastasis, which is at a later point of the course of the disease. The two groups differed significantly in TNM tumor stage at the time of surgery, which was expected since the presence of lymph node metastasis is the determinant of the N-stage ($p < 0.001$) and reflects in higher overall stage ($p < 0.001$). The validity of the

TABLE 1 | Demographic and clinical data of the cohort of 50 patients with cSCC with (cohorts PRI+, MET) or without lymph node metastasis (PRI-).

Variable	PRI+/MET (metastasizing tumors), n = 29	PRI- (locally confined tumors), n = 21	Total (n = 50)	p-value
Mean age, years (range)	74.8 (32 to 93)	68.2 (39 to 92)	72.1 (32 to 93)	0.034[c]
Sex, n (%)				
Female	2 (7)	4 (19)	6 (12)	0.22[d]
Male	27 (93)	17 (81)	44 (88)	
Site of primary tumor, n (%)				
Scalp	4 (14)	5 (24)	9 (18)	0.99e[e]
Ear and temple	5 (17)	7 (33)	12 (24)	
Nose and midface	3 (10)	5 (24)	8 (16)	
Lip	2 (7)	2 (10)	4 (8)	
Neck	1 (3)	2 (10)	3 (6)	
Unknown	14 (48)	0	14 (28)	
Recurrent tumor, n (%)[a]				
No	15 (52)	15 (71)	30 (60)	0.24[d]
Yes	14 (48)	6 (29)	20 (40)	
T-stage at surgery, n (%)[b]				
0 or unknown	12 (41)	1 (5)	13 (26)	0.039[e]
1	3 (10)	3 (14)	6 (12)	
2	6 (21)	4 (19)	10 (20)	
3	6 (21)	11 (52)	17 (34)	
4	2 (7)	2 (10)	4 (8)	
N-stage at surgery, n (%)[b]				
0	5 (17)	21 (100)	26 (52)	<0.001[e]
1	5 (17)	0	5 (10)	
2	4 (14)	0	4 (8)	
3	13 (45)	0	13 (26)	
Unknown	2 (7)	0	2 (4)	
Overall stage (AJCC 7th edition)[b]				
I	1 (3)	3 (14)	4 (8)	<0.001[e]
II	2 (7)	4 (19)	6 (12)	
III	5 (17)	11 (52)	16 (32)	
IV	20 (69)	2 (10)	22 (44)	
Unknown	1 (3)	1 (3)	2 (4)	
Histopathological grading, n (%)[b]				
1 (well differentiated)	2 (7)	2 (10)	4 (8)	0.13[e]
2 (moderately differentiated)	13 (45)	14 (67)	27 (54)	
3 (poorly differentiated)	14 (48)	4 (19)	18 (36)	
Unknown	0	1 (5)	1 (2)	
Lymph-vascular infiltration (LVI), n (%)[b]				
No	18 (62)	18 (86)	36 (72)	0.11[d]
Yes	10 (34)	3 (14)	13 (26)	
Unknown	1 (3)	0	1 (2)	
Perineural invasion (PNI), n (%)[b]				
No	11 (38)	11 (52)	22 (44)	0.56[d]
Yes	15 (52)	10 (48)	25 (50)	
Unknown	3 (10)	0	3 (6)	

[a]*Recurrent tumors at surgery. Recurrences after last surgery are not included.*
[b]*When multiple samples of a single patient from the primary (PRI+) and lymph node metastasis (MET) were analyzed, the index tumor (PRI+) was prioritized.*
[c]*Mann–Whitney U test.*
[d]*Fisher exact test.*
[e]*Chi-square test.*

difference in the T-stage is limited, since the primary was no longer present at the time of surgery in 12 MET samples and could not be retrospectively determined. Although not statistically significant, lympho-vascular infiltration (LVI) was more commonly seen in the metastatic cohort, which could be expected since LVI is a crucial step in the development of lymph node metastasis. The rate of perineural infiltration and histopathological grading did not significantly differ between the two groups. Full clinico-pathological data for each sample are listed in **Supplementary Data Sheet 1**.

3.2 Cancer Progression Pathways Involving ECM Remodeling and Cell Movement are Upregulated in a Stepwise Manner From SES to Non-Metastatic to Metastatic cSCC

3.2.1 Gene Expression Analyses in Tumors Versus SES

A principal component analysis (PCA) plot based on all the normalized data of all cohort comparisons clearly separate the

tumor cohorts (MET, PRI+, and PRI-) from SES (**Figure 1A**), with significant differential gene expression (log2FC ≥1 or ≤-1; adj*p*-value < 0.05) between all tumor cohorts and SES (**Figures 1B–D**). This included 229 DEGs in MET tumors vs. SES (147 up- and 82 downregulated), 214 in PRI+ (metastasizing primary tumors) vs. SES (133 up- and 81 downregulated), and 213 in PRI- (non-metastasizing primary tumors) vs. SES (124 up- and 89 downregulated) (refer to **Supplementary Data Sheet 2** for gene list). This highlights the striking differential gene expression in cSCC compared to SES despite the high mutational burden reported in SES (53). Fifty percent (148/295) of the DEGs between the three comparisons (i.e., between MET or PRI+ or PRI- vs. SES) were shared (**Figure 1E**; **Supplementary Data Sheet 2**). Of the top 20 upregulated shared DEGs (**Supplementary Data Sheet 2**), 12 are associated with MMP remodeling, cell motility, and ECM receptor interaction annotations (**Supplementary Image 1A**), indicating that these pathways are already dysregulated in non-metastasizing primary tumors. However, key MMP remodeling-associated genes *PLAU* and *MMP10* and basal cell marker *KRT19* were uniquely shared upregulated genes in metastatic tumors (MET and PRI+) (**Supplementary Image 1A**). Of the top 20 downregulated DEGs, 10 genes with varied functions such as keratinocyte differentiation (*KRT1*) and dysregulated tumor–microenvironment interactions were shared between all tumor cohorts and SES (**Supplementary Image 1B**). Four genes with disparate functions were among the top 20 downregulated genes uniquely shared by metastatic tumors compared to SES (**Supplementary Image 1B**). These unique shared up- and downregulated genes clustered the MET/PRI+ cohort together away from the PRI- cohort, which showed intermediate behavior between the metastatic tumors and SES (**Supplementary Image 1C**).

3.2.2 Pathway Analyses of Gene Expression Profiles in Tumors Versus SES

A gene set analysis of the differential gene expression profiles of tumor cohorts compared to SES confirmed that MMP remodeling followed by cell motility, collagen family, and ECM receptor interaction was the most differentially expressed cancer progression pathway (**Figure 2A**). Stepwise increases in expression from SES to PRI- to PRI+ and MET were most evident for MMP remodeling (**Figure 2B**) and cell motility (**Figure 2C**) annotations.

Ingenuity pathway analysis was then used to categorize the DEGs from the MET vs. SES, PRI+ vs. SES and PRI- vs. SES comparisons into canonical pathways. Significantly enriched canonical pathways [-log(p-value) >1.3, absolute value z-score >2, <-2] and the DEGs in each pathway are listed in **Supplementary Data Sheet 3**. In all tumor cohorts vs. SES, tumor microenvironment, leukocyte extravasation, hepatic fibrosis signaling pathway, and HIF1α signaling were among the top significantly activated CPs (**Figures 2D–F**). Significantly inhibited pathways included PTEN signaling (MET/PRI+ vs. SES only) and inhibition of matrix metalloproteinase (MET vs. SES only) (**Figure 2F**). Activation of leukocyte extravasation, which is the movement of leukocytes from the circulatory system toward a tumor [63], is in line with upregulated cell motility in tumors vs. SES found in our gene set analyses (**Figure 2C**). In line with other reports comparing cSCC vs. normal sun-exposed skin [64],

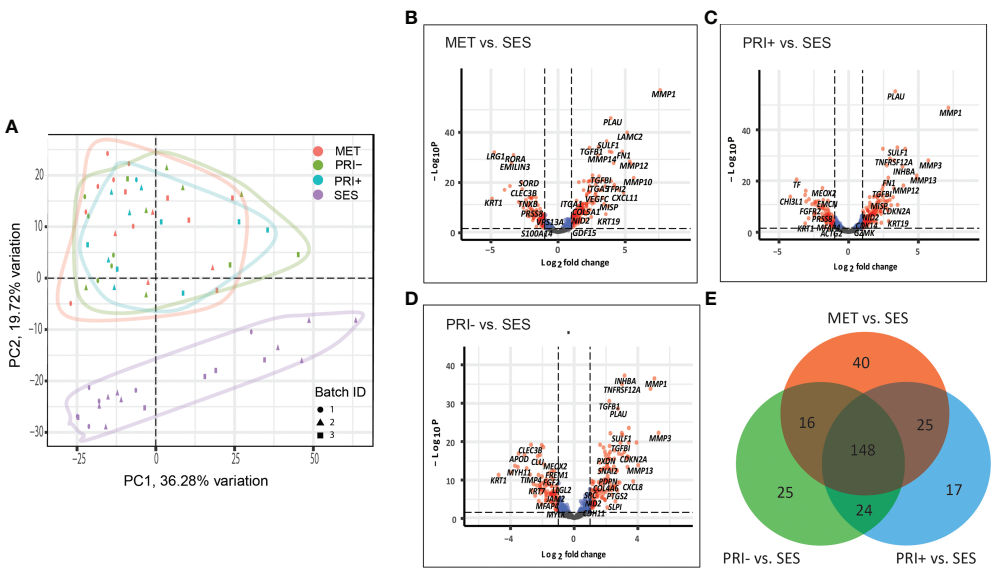


FIGURE 1 | Cancer progression gene expression patterns of sun-exposed skin (SES) and non-metastatic (PRI-) and metastatic (PRI+ and MET) cSCC. **(A)** Principle component plot of tumor cohorts and SES normalized gene expression data. The first and second principal components are plotted on the x- and y-axis, respectively. Batch ID symbols indicate different NanoString runs and show lack of batch effect. **(B–D)** Volcano plots illustrating gene expression differences (x-axis) and significance (y-axis) (dotted horizontal lines) of **(B)** MET vs. SES, **(C)** PRI+ vs. SES, and **(D)** PRI- vs. SES. Each dot represents a gene. **(E)** Venn diagram depicting DEGs with log2 fold changes of ≥1 or ≤-1 between MET vs. SES, PRI+ vs. SES, and PRI- vs. SES and adjusted *p*-value ≤ 0.05. The number of DEGs for each pairwise comparison is indicated in the circles of the Venn diagram. The overlap between the circles shows DEGs that occur in more than one comparison.

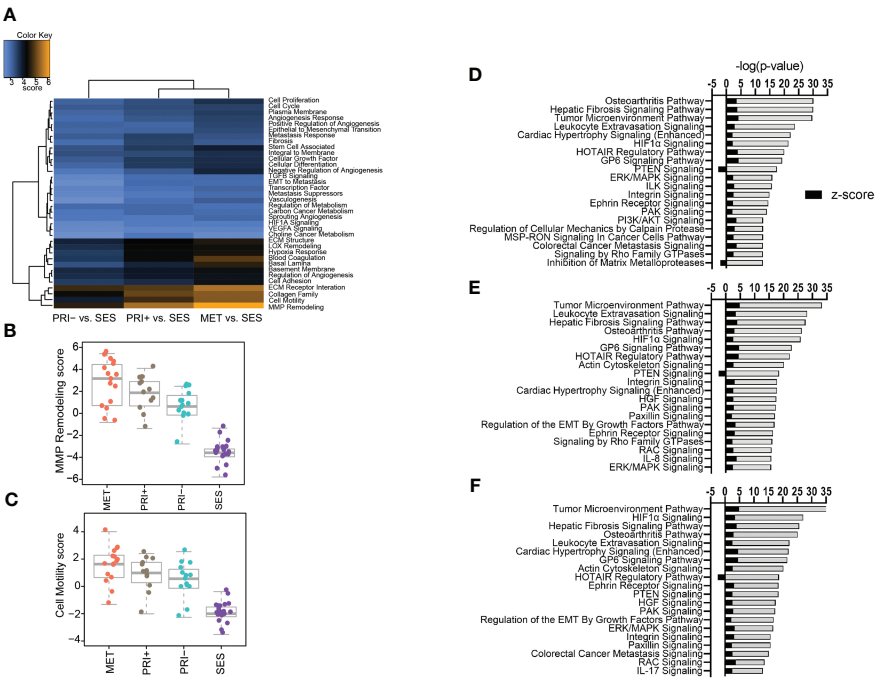


FIGURE 2 | Pathway analyses of tumors vs. SES. **(A)** Heatmap of global significance scores of cancer progression gene annotations generated using nSolver Advanced Analysis software 2.0 (orange denotes gene sets whose genes exhibit extensive differential expression with the covariate (SES), blue denotes less differential expression). **(B, C)** Boxplots showing pathway scores (y-axis; fit using the first principal component of each gene set's data) for two of the top differentially expressed cancer pathways specified in the heatmap. **(D–F)** Top 20 activated and inhibited canonical pathways (refer to **Supplementary Data File 3**) for **(D)** MET vs. SES, **(E)** PRI+ vs. SES, and **(F)** PRI- vs. SES showing significance level (-log (p-value)) along the x-axis and absolute activation z-score (<-2, >2) along the y-axis.

ECM receptor interaction and interleukin signaling and PI3K/AKT/mTOR signaling were also significantly activated canonical pathways in our analyses (**Figures 2D–F**).

Integrative gene expression meta-analysis of publicly available invasive/metastatic cSCC (n = 25) vs. normal skin from sun-exposed area (n = 18) array data on the GEO platform (see **Table S2** for detailed sample filtering criteria) revealed a total of 127 upregulated and 59 downregulated significant DEGs (**Supplementary Data Sheet 4**). Comparison of these significantly DEGs with our PRI+ vs. SES dataset found 33 DEGs genes in common (**Supplementary Image 2A**). Reactome pathway analysis using these shared genes again highlight enrichment of activated pathways affecting extracellular matrix interactions, organization or degradation, collagen family, and interleukin/chemokine signaling (**Supplementary Image 2B**) as per our independent analyses using nSolver and IPA.

3.3 Differential Gene Expression and Pathway Analysis Between Metastatic and Non-Metastatic cSCCs Identifies *VEGFA*, *EGF*, and *IL1RN* as Key Upstream Regulators of Metastasis

3.3.1 Gene Expression Analyses in Metastatic Versus Non-Metastatic Tumors

A progressive decrease in the number of significantly DEGs was found between the metastatic (PRI+) compared to non-metastatic (PRI-) tumors vs. MET (**Figure 3A**). The MET vs. PRI+ comparison revealed 8 significant DEGs while MET vs. PRI- revealed 58 significant DEGs (**Figure 3A**; **Supplementary Data Sheet 2**). At these stringent cutoffs, only 3 DEGs were found in the PRI+ vs. PRI- comparison (**Supplementary Data Sheet 2**) likely due to small sample size and bulk sampling (discussed further below). Using a less stringent cutoff for PRI+ vs. PRI- ($p < 0.01$ instead of adjp < 0.05), there were 16 significant DEGs (**Figure 3A**, gray circle). That there were few significant cancer progression gene expression differences between metastatic primaries and metastases suggested that the PRI+ tumors had acquired many of the activated pathways necessary for metastasis. In further support of this, pathway analysis of the six available patients' specimens with matched MET, PRI+, and SES samples showed that the tumor pairs by and large clustered together and away from SES (**Supplementary Image 3**).

Of the 8 significantly DEGs between MET and PRI+, only one (*TIMP1*) was not shared with the MET vs. PRI- grouped cohort comparison (**Figure 3A**). Although *TIMP1* encodes an inhibitor of MMPs, elevated expression of TIMP1 has been reported in head and neck SCCs (54–60) and has been shown to stimulate cell proliferation and prevent apoptosis (61). A PCA loading plot using these 8 significant DEGs (**Figure 3B**) indicates that *ANGPTL4* (encodes angiopoietin) and *TFPI2* (encodes tissue factor inhibitor 2) exert the largest effects on PC1 and PC2 (followed by *VEGFA*, *ITGA5*, *TIMP1*, and *RHOA*). These genes are involved

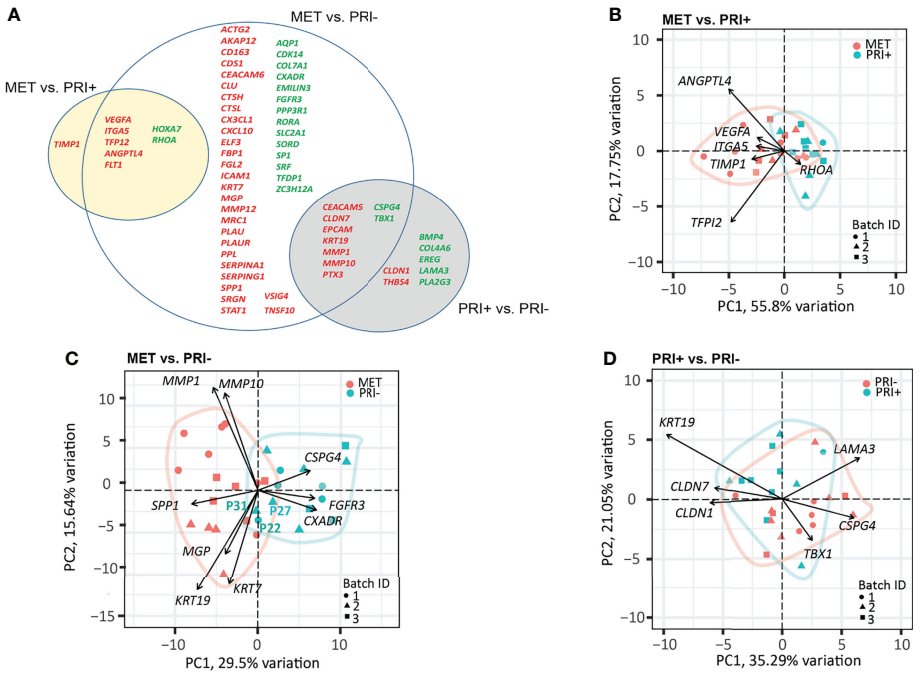


FIGURE 3 | Cancer progression gene panel differential expression analysis between tumor cohorts. **(A)** Venn diagram depicting DEGs with log2 fold change ≥1 or ≤-1 between MET vs. PRI+ and MET vs. PRI- (adjusted *p*-values <0.05), and PRI+ vs. PRI- (*p*-values <0.01). Upregulated (red) and downregulated (green) DEGs for each pairwise comparison are indicated. The overlap between the circles show DEGs genes that occur in more than one comparison. **(B–D)** PCA loading plots based on significant DEGs between **(B)** MET and PRI+ (8), **(C)** MET and PRI- (54), and **(D)** PRI+ and PRI (16). Each symbol corresponds to one sample. Ellipses represent the region where the majority of samples are expected to fall. Non-overlapping ellipses imply that gene expression profiles cluster groups apart based on their distinct principal component scores. Batch ID symbols indicate samples analyzed in different NanoString runs and show lack of batch effect.

in various functions that promote either angiogenesis, cell adhesions or motility, protection from anoikis, matrix remodeling, or epithelial–mesenchymal transition (EMT) and are known to play important roles in the metastatic process in several cancers (62). Interestingly, *ITGA5*, which is also a classic EMT marker enriched on tumor-specific keratinocyte (TSK) subsets of metastatic cSCC (9) and upregulated in various cancers (63), showed a stepwise increase in expression from SES to PRI, to PRI+ to MET (**Supplementary Image 4**).

Although the MET and PRI- cohorts could be separated using the 58 significant DEGs from the MET vs. PRI- comparison, a few PRI- specimens (P22 and P31 in particular) clustered with the MET cohort (**Figure 3C**). A closer examination of the clinicopathological characteristics of these specimens found these to be from patients with high-risk features such as either recurrences or PNI. PCA loadings show that the genes exerting the largest effects include *MMP1* and *MMP10*, *KRT7*, and *KRT19* (**Figure 3C**), high levels of which in other cancers have been associated with unfavorable prognosis (64). Another example is *SPP1*, which encodes a stromal cell ligand shown to interact with integrin receptors encoded by *ITGB1* and *ITGA5*, which are both enriched on TSKs (9).

Of the 16 significant DEGs between PRI+ vs. PRI-, the majority were shared with the MET vs. PRI- comparison (**Figure 3A**). These genes feature MMPs (*MMP10*), cell differentiation and adhesion markers (*KRT19*, *CEACAM5*), and cell polarity and signal transducers (*CLND7*). While these genes exerted the largest effects on PRI+ as assessed by PCA loadings (**Figure 3D**), these cohorts were not distinguishable, possibly due to intra-tumoral heterogeneity and/or the particular area of primary tumor sampled.

3.3.2 Pathway and Functional Analyses in Metastatic Versus Non-Metastatic Tumors

To further investigate the molecular mechanisms underlying cSCC progression, the IPA downstream effect analysis function was used to identify diseases and function activation status, given the observed differential gene expression data described above. A relatively small number of significantly activated functions (*p*-value > 9.89E-10, z-score > 2) were evident in MET vs. PRI+, and these were broadly associated with cellular movement (**Supplementary Image 5A; Supplementary Data Sheet 5**). Notably, functions associated with cell death and survival were either significantly decreased or inactivated (e.g., apoptosis/anoikis of tumor cell lines) or activated (e.g., cell viability). A larger number of significantly activated functions were found in MET vs. PRI- (**Supplementary Image 5B; Supplementary Data Sheet 5**) with top-scoring functional categories most strongly associated with cellular movement (inclusive of invasion/migration of cells, leucocyte migration, chemotaxis) and cell-to-cell signaling and interaction. Cellular movement was the main functional category predicted to be activated in the PRI+ vs.

PRI- comparison (inclusive of migration of keratinocytes and fibroblasts); however, functions related to inflammatory response was the top activated category (**Figure 5C; Supplementary Data Sheet 5**).

We then used the Upstream Analysis and Causal Network module of IPA to understand how the abovementioned functions might be regulated in our dataset by activated or inhibited upstream regulators. **Supplementary Data Sheet 6** lists all the predicted activated or inhibited master regulators (z-score >2, <-2) which are hypothesized to control the expression of our dataset molecules either directly or indirectly through other regulators. Of these, *IL1RN* (interleukin 1 receptor antagonist) is predicted to be a significantly inhibited master regulator contributing to the gene expression changes seen in MET vs. primary (PRI+ or PRI) tumors. *IL1RN* acts indirectly on downstream targets distinguishing MET from PRI+ by mediating the activity of intermediary regulators including *TGFB1* (an important TSK/EMT marker) and the inflammatory cytokines *TNF*, *IFNG*, and *IL1* (with high confidence of activation) (**Figure 4A**). This then leads to the upregulation *of VEGFA*, *TIMP1*, *SPP1*, *ITGA5*, and *CEACAM5*, all known to be associated with increased invasiveness (9, 56, 65), and downregulation of various genes including the tumor-suppressor *APC* (APC regulator of WNT signaling pathway). Altogether, this is predicted to increase the neoplasia of tumor cells, migration of tumor and leukocytes, and decrease apoptosis of tumor cell lines (**Figure 4A**). In MET vs. PRI-, *IL1RN* acts directly on downstream targets such as *VEGFA*, *TIMP1*, *SPP1*, and *MMP1* and the stem cell gene *CD44* (**Supplementary Data Sheet 6**).

VEGFA (vascular endothelial growth factor A) and *EGF* (epidermal growth factor) are predicted to be significantly activated master regulators driving differential gene expression in MET vs. PRI- (**Supplementary Data Sheet 6**). Both growth factors are known stimulators of uPAR mRNA expression (23). **Figure 4B** demonstrates the VEGFA-mediated upregulation of genes involved in ECM interaction and MMP remodeling (also TSK-specific genes (9)) such as *MMP1*, *MMP10*, *MMP12*, *PLAU*, and *CXCL10* in MET, as well as *FLT1* (encodes VEGFA receptor), which in turn promote metastatic functions such as angiogenesis, growth, migration and invasion, and evasion of apoptosis. **Figure 4C** demonstrates the EGF-mediated upregulation of genes of an overlapping subset of genes as well as *PLAUR*, *VEGFA*, and *KRT19* and a variety of transcription factors in MET. *EGFR* mRNA levels were high in all cohorts, and there was no significant differential expression in any of the tumor comparison or in tumor vs. SES (**Supplementary Data Sheet 2**).

In PRI+ vs. PRI- analysis, *JAG1* (encodes Jagged Canonical Notch Ligand 1) appeared as one of the main activated master regulators (z-score = 2.668, $p = 6.43E^{-10}$) predicted to act through *AKT*, *EGFR*, *ERK1/2*, *NOTCH1*, and *TCF7L2* leading to the expression of matrix remodeling genes *MMP1*, *MMP10*,

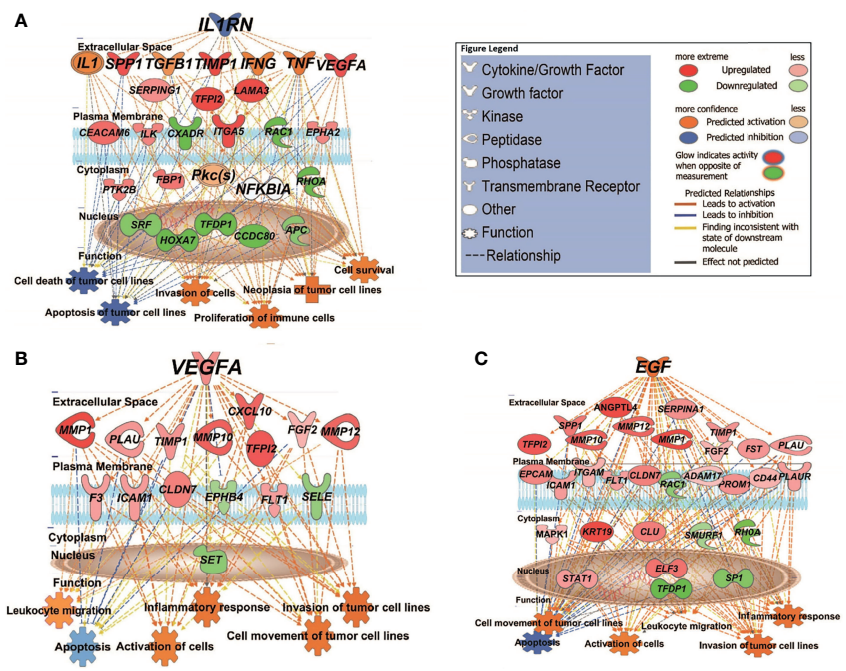


FIGURE 4 | IPA causal network analysis depicting the interactions between upstream regulators, downstream genes, and physiological functions in cSCC. **(A)** MET vs. PRI+ comparison showing effect of predicted master regulator *IL1RN* (depth: 2). **(B, C)** MET vs. PRI- comparison showing predicted master regulators *VEGFA* (depth: 1) and *EGF* (depth: 1). Master regulators were predicted based on the causal paths known to influence the expression of their target genes leading to the physiological functions shown. Regulators with depth of 2 influence the expression of target genes *via* other regulators. Figure legend indicates whether genes were upregulated or downregulated in MET relative to PRI tumors; the predicted activation state of the upstream regulators, and the predicted relationships between these and downstream genes and functions.

ICAM1, and *PLAUR* (**Supplementary Data Sheet 6**), possibly from TSKs sampled from the leading edge of PRI+ tumors.

3.4 uPAR Protein Levels Are Significantly Increased in Metastatic cSCC and Correlates With Downregulation of hsa-miR-340-5p and hsa-miR-377-3p

Given the upregulation of the genes for uPA and its receptor uPAR in metastatic tumors compared to PRI- and SES (see also **Supplementary Image 4**) and their contribution to tumor progression through different pathways and functions, we examined spatially localized uPAR protein levels in an extended cohort of cSCC tumors of the head and neck. **Figure 5A** shows an example of membranous staining typically found in MET specimens (from lymph node deposits). Interestingly, a positively stained tumor embolus was captured in-transit in a lymphatic vessel (**Figure 5B**), highlighting the upregulation of uPAR on invasive and metastatic tumor cells. uPAR was found to be highly tumor-specific, with increased staining in the tumor compartment, particularly at the leading edge of tumors, with absence of staining in SES (**Supplementary Image 6**). Analysis of the staining scores (**Table S3**) found significantly increased uPAR staining in MET tissues compared to PRI+ and PRI- ($p = 0.0255$ and <0.0001, respectively) (**Figure 5C**). The staining intensity was generally higher in PRI+ than in PRI-, but this was not statistically significant (**Figure 5C**) potentially due to the effects of an outlier in the PRI- group with high uPAR staining (Patient 37, **Table S3**). This specimen was characterized to be a highly invasive 160-mm-diameter × 70-mm-thick exophytic primary tumor in the scalp as opposed to other PRI- tumors with less than 20-mm depth of invasion (**Figure 5C**).

To assess the potential regulation of *PLAUR* expression by miRNAs in cSCC, we extracted *PLAUR* targeting miRNAs from the miRDB based on the target prediction score of >75 (high confidence; **Table S4**) and then from a list of experimentally confirmed miRNA-*PLAUR* interactions compiled from miRTARBASE (**Table S5**). Of these lists, only hsa-miR-340-5p and hsa-miR-377-3p from the miRDB list showed a statistically significant differential expression between MET and combined PRI tumor cohorts with both miRNAs being significantly downregulated in MET (**Table S6**). By computing two-tailed Pearson correlation coefficients, the strongest significant negative correlation was found between miR-340-5p and uPAR staining intensity for our dataset (**Figure 5D**). No significant correlation was found between miR-340-5p and *PLAUR* mRNA expression

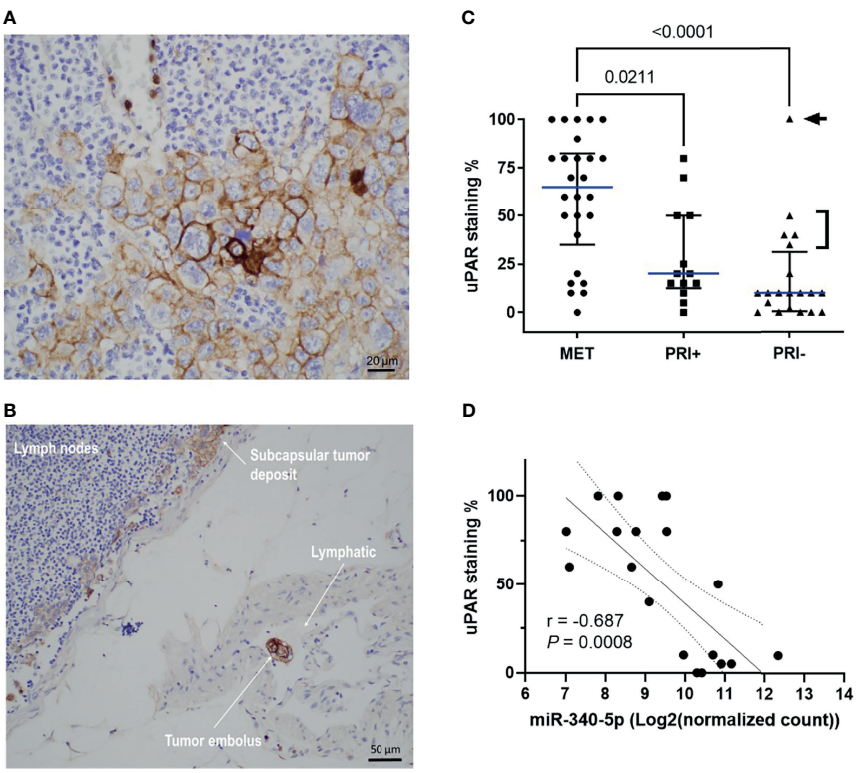


FIGURE 5 | uPAR protein expression is increased on metastatic tumors and correlates with miRNA-340-5p expression. Representative photomicrographs showing uPAR staining in **(A)** a metastatic deposit in the lymph node of Patient 2 and **(B)** a positively stained embolus as well as staining in the subcapsular tumor deposit from the lymphatic of patient 2. **(C)** Scatter plot of uPAR IHC scores of all patient specimens stained (n = 58 total) showing cohort median values (blue line) with interquartile ranges (refer to **Table S3** for individual patient values). *p*-values shown were derived using a Kruskal–Wallis test for multiple comparisons with uncorrected Dunn's posttest. Arrowhead denotes patient 37 who had a 160 mm diameter × 70 mm thick PRI-. Bracket denotes PRI- tumors with >50-mm diameter and PNI. **(D)** Scatter plot showing relationship between uPAR staining scores and hsa-miR-340-5p normalized gene count (n = 20 pairs; refer to **Table S6**) and show Rho (Spearman's) correlation, *p*-value, and interquartile range for the correlation.

(data not shown). Interestingly, the expression of both miRNAs and uPAR protein was much higher and lower, respectively, in MET04 than the remainder of the cohort (**Table S6**). In contrast, PRI+02, with 100% positivity for uPAR staining, expressed much lower levels of both miRNAs than the other primary tumors.

3.5 EGF Enhances cSCC Cell Motility and uPAR Expression

Given that uPAR levels were increased on metastatic vs. non metastatic tumors and that EGF was identified as a master regulator leading to *PLAUR* upregulation, we sought to confirm this relationship *in vitro* using a metastatic cSCC cell line derived from a lymph node deposit, UW-CSCC2 (Patient 40, **Table S3**) (52). These cells constitutively express EGFR (**Figure 6A**) (but did not harbor *EGFR* mutations or copy number variations, data not shown) and responded to exogenous 5–20 ng/ml EGF with increased cell migration (**Figure 6B**) and uPAR protein levels (**Figure 6C**) compared to untreated cells. Treatment with the EGFR tyrosine kinase inhibitor gefitinib, even in the presence of 20 ng/ml EGF, significantly inhibited wound closure with respect to both control and EGF-treated cells (**Figure 6B**). uPAR expression levels were also significantly decreased (**Figure 6C**). A second metastatic cSCC cell line (UW-CSCC1; Patient 17, **Table S3**) was found to be similarly affected by EGF/R stimulation and inhibition (data not shown).

4 DISCUSSION

Dysregulated activation of extracellular proteolytic networks is strongly linked to mechanisms that enable tumor invasion and metastasis. Our cSCC cohort gene expression and pathway enrichment analyses using various methodologies strongly implicate ECM remodeling and interactions allowing cell motility as among the most significant activated pathways and functions, with stepwise increases in activation from SES to metastatic cSCC. Further, we identified the growth factors EGF and VEGF-A as potential master regulators that concordantly upregulate the expression of ECM remodeling genes encoding uPA/R and MMPs—well-recognized metastasis driver proteases in many cancer types. **Figure 7** summarizes the key molecular alterations we found in MET/PRI+ compared to PRI-/SES which center on the urokinase plasminogen activation system.

The upregulation of plasminogen activation family members and MMPs has been reported in previous studies using squamous cell carcinomas, including those of the skin (33, 35, 51, 54, 57, 66–69) (**Table S1**). It was thus not surprising that *PLAU* and MMP genes were among the highest DEGs in all tumors vs. SES comparisons in our cSCC cohort. However, the quantifiable stepwise increase in expression from SES to PRI- to PRI+/MET has not been previously reported in cSCC derived exclusively from the head and neck. Correspondingly, uPAR protein levels were significantly increased in metastases and this was corroborated by our identification of a significant negative correlation (correlation coefficient <-0.60) between hsa-miR-340-5p and uPAR staining, suggesting that this miRNA plays a role in silencing *PLAUR* at a posttranscriptional level. While several miRNAs have been reported to modulate uPAR expression in a variety of diseases (**Tables S4, S5**), this particular miRNA–target interaction is a novel finding in cSCC and should be functionally validated in future studies. Interestingly, *SERPINE1* (encodes plasminogen activator inhibitor type 1, a potent inhibitor of uPAR-bound uPA) was also upregulated in all our tumor cohorts (refer to **Supplementary Data Sheet 2**). This is of note because combined upregulated *PLAU* and *SERPINE1* expression is strongly associated with poor cancer outcomes in various other cancers *via* mechanisms that affect cell adhesion, ECM remodeling, and signaling pathways leading to increased cell survival, migration, invasion, and angiogenesis (21, 23, 70–73).

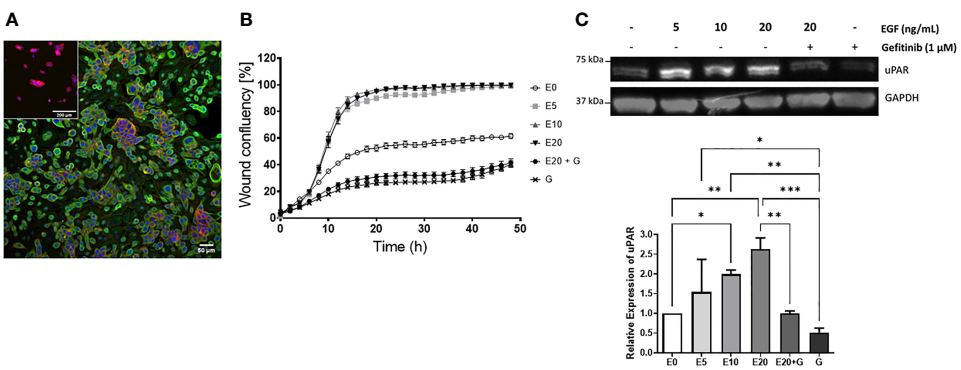


FIGURE 6 | EGF upregulation of cSCC cell line motility and uPAR expression. **(A)** Immunocytochemical image of UW-CSCC2 cells stained with anti-EGFR antibody (green) or anti-mouse IgG negative control (inset) and counterstained with RedDot (blue) and ActinRed 555 (red). **(B)** Representative *in vitro* scratch wound healing assay showing effect of EGF E ± EGFR inhibitor gefitinib G on simple migration of UW-CSCC2 cells. Values shown are mean ± SEM, n = 5; all treatment groups were significantly different from untreated controls p-value < 0.05, all gefitinib treatment groups significantly different to EGF only treatment groups p-value < 0.001; ordinary one-way ANOVA with Dunnett's post-test. **(C)** Representative Western blot (right panel) demonstrating UW-CSCC2 uPAR levels in response to 24-h pretreatment with EGF ± gefitinib, at concentrations shown. Panel below: densitometry analysis showing the ratios of uPAR/GAPDH (used as a total protein loading control) for each treatment relative to no EGF control. Significance values are shown with *p-value < 0.05; **p-value < 0.01; ***p-value < 0.001.

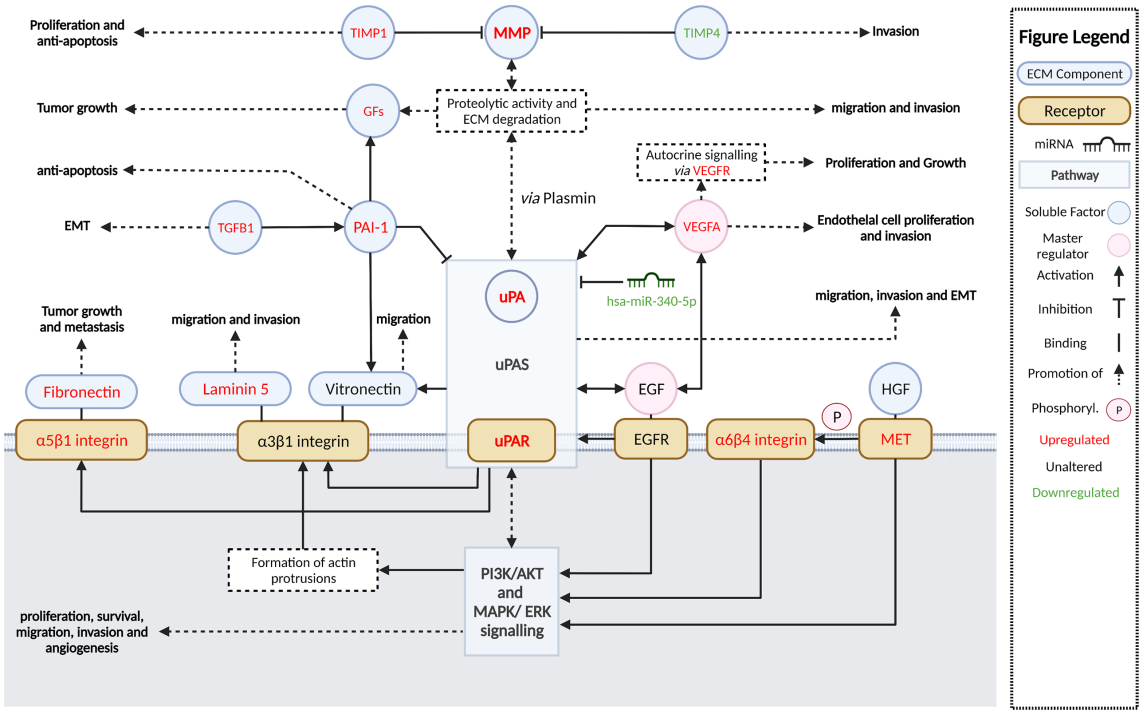


FIGURE 7 | Summary and schematic illustration of key pathways and regulators identified as up- or downregulated in metastatic versus non-metastatic tumors or SES in this study. The urokinase plasminogen activator system (uPAS) plays a central role in remodeling the extracellular matrix (ECM) promoting metastasis. The uPAS exerts its activity by enhanced uPA-mediated conversion of co-localized plasminogen to plasmin and subsequent activation of matrix metalloproteases (MMP). PAI-1 (*SERPINE1*) can inhibit uPA activity but is also upregulated and contributes to cell signaling. MMPs and plasmin cleave and remodel the ECM leading to the release of latent growth factors (GFs) such as EGF, VEGF-A, TGF-β, and HGF (hepatocyte growth factor). By binding to their cognate receptors, EGFR and VEGFR (encoded by *FLT1*), and c-MET, these growth factors in turn act as important upregulators of the uPAS (*via* uPAR) and other downstream effectors, which induce large-scale cellular changes that further promote ECM remodeling, cellular migration, and invasion and, ultimately, metastasis. A few of these growth factor receptors are themselves overexpressed (i.e., *MET*, *FLT1*) and can drive invasion and metastasis regardless of growth factor activation. Aberrant miRNA expression, such as downregulated has-miR-340-5p, is also associated with upregulated uPAR expression. Direct and indirect downstream effectors of the uPAS include vitronectin, focal adhesions *via* integrins and focal adhesion kinase (FAK), the proliferation, and survival pathways MAPK/ERK PI3K/Akt/mTOR and VEGF-A, which facilitate increased protection against apoptosis/anoikis, increased cell proliferation, and EMT and angiogenesis; these are also important for invasion and metastasis. Created with BioRender.com.

In a study by Ji et al., single-cell RNA sequencing with spatial transcriptomics identified four subpopulations of keratinocytes within primary cSCCs with a specific TSK subpopulation localized to the leading edge (9). The gene signature of the TSKs is uniquely linked to EMT, cellular movement, and extracellular matrix disassembly, suggestive of invasive behavior and that these cells are responsible for metastasis (9). The presence of these subpopulations may explain why our bulk tumor analysis of DEG in PRI+ vs. PRI- could not effectively distinguish the two groups, despite sampling from areas of high tumor cellularity at the leading edge. While bulk tumor analysis represents a limitation of our study, nonetheless we identified significant upregulation of key TSK signature genes, in particular *PLAU*, *MMP1* and *MMP10*, *ITGA5* in MET vs. PRI- and PRI+ vs. PRI-. Interestingly, of these important TSK genes only *MMP10* is included in a 40-gene expression profile test that was recently shown to identify cSCC patients' risk of metastasis (74). Nevertheless, these genes together with many other genes that were upregulated in MET/PRI+ vs. PRI- have known functions in ECM adhesion and remodeling (e.g., *PLAUR*, *SPP1*, *MMP12*) and/or cell proliferation and motility (e.g., *STAT1* and *CXCL10*). In concordance with the primary cytokine activation signature observed in our Reactome enrichment analyses, Ji *et al.* (9) and others (75) also identified elevated expression of key components of the JAK-STAT pathway (e.g., *STAT1*) and various inflammatory cytokine genes in invasive cSCC. We also identified upregulation of genes encoding the macrophage and CAF ligands, secreted phosphoprotein 1 (*SPP1*), and fibronectin (*FN1*) which have been shown to interact with the TSK receptors integrin subunit beta 1 (*ITGB1*) and subunit alpha 3 or 5 (*ITGA3*, *ITGA5*), respectively, in cSCC (9). This likely reflects the presence of stromal cells in our samples and aberrant tumor–stroma interactions. Notably, a high expression of *ITGB1* and *PLAU* has been shown to be associated with reduced progression-free survival in clinical trials of anti-PD-1 in lung and head and neck mucosal SCC (9, 76). As both genes were upregulated in metastatic cSCC, this suggests that a similar association may occur in cSCC.

We also found that the matrix metalloproteinase inhibitor genes, *TIMP1* and *TIMP4*, were differentially expressed in metastatic versus non-metastatic/SES tissues. Many studies

have reported on the elevated expression of *TIMP1* in non-cutaneous head and neck SCC (54–60), but only one of these (56) included any cSCC among their samples. While *TIMP4* has been previously reported to be downregulated in non-cutaneous head and neck SCCs (77), we are the first to report the downregulation of *TIMP4* in MET and PRI+ compared to SES in cSCC. Further, our finding of a positive and negative association with *TIMP1* and *TIMP4* expression, respectively, is in line with a previous study comparing their mRNA and protein expression in normal human brain and malignant gliomas (78). Silencing of *TIMP4 via* hypermethylation of its promoter has been reported in other human cancers (79), with reduced *TIMP4* associated with increased angiogenesis (55, 80–82). Epigenetic regulation of *TIMP4* might also possibly explain *TIMP4* downregulation in metastatic cSCC and should be further explored in future studies.

The activating effects of EGF and VEGF-A on downstream genes including *PLAU/R* highlights the potential for anti-EGFR- and/or anti-VEGF- with anti-uPA/uPAR-targeting approaches for metastatic cSCC. EGFR inhibition as monotherapy for metastatic cSCC has had moderate success (5), even though EGFR is often overexpressed in cSCC, with one study showing an association with EGFR levels and lymph node progression and tumor cell proliferation (83). In our study, *EGFR* mRNA counts were generally equally high across all tumor cohorts and SES suggesting no relationship with tumor status (data not shown) but rather that the presence of high levels of active EGF (and VEGF-A) in the pericellular space of metastatic tumors may be responsible for enhanced stimulation of EGFR-mediated signaling pathways (**Figure 7**). This would contribute to EGFR drug resistance mechanisms through stimulation of compensatory signaling pathways (5) in metastatic cSCC and drive overexpression of downstream targets, including *PLAU/R* and MMP genes, promoting functions linked to cell invasion such as cell motility. The latter was functionally validated in our EGFR-expressing cell line models. Notably, gefitinib significantly inhibited uPAR expression and cell migration, further supporting EGFR tyrosine kinase activation as a mechanism driving uPAR overexpression. Further, as *PLAUR* overexpression was shown to induce gefitinib resistance through the EGFR/p-AKT/surviving signaling pathway in cell models of human lung adenocarcinoma (84), strategies that downregulate *PLAUR* could also be explored to avoid EGFR-targeted resistance mechanisms.

In conclusion, our integrated analysis of the mRNA, miRNA, and uPAR protein expression in a well-characterized spectrum of disease states provides a comprehensive evaluation of the pathways that promote metastasis in cSCC of the head and neck (**Figure 7**). The central role of uPA/R as a biomarker of cSCC metastasis should be further explored using larger cohort studies and with functional studies using metastasis models of cSCC *in vivo*. Combinations of drugs targeting uPA/R and EGFR and/or angiogenesis could be novel therapeutic strategies for metastatic cSCC.

DATA AVAILABILITY STATEMENT

The original contributions presented in the study are included in the article/**Supplementary Material**. Further inquiries can be directed to the corresponding author.

ETHICS STATEMENT

The studies involving human participants were reviewed and approved by the University of Wollongong Health and Medical Human Research Ethics Committee. Written informed consent for participation was not required for this study in accordance with the national legislation and the institutional requirements.

AUTHOR CONTRIBUTIONS

EM, AT, BG, and JP performed and analyzed the gene expression and cell-based experiments and wrote drafts of the manuscripts. SM, JM, and RG compiled and analyzed the clinciopath data and provided specimens. RG performed and analyzed IHC data. BA, JC, and MR conceived and designed the project. MR revised and edited the manuscript and figures. BA and JC edited the finalized the manuscript. BA, JC, RG and MR acquired funding. All authors contributed to the article and approved the submitted version.

FUNDING

EM was supported by a CONCERT Translational Cancer Research Centre grant 13/TRC/1-01 to MR. The Sydney Head and Neck Cancer Institute contributed toward NanoString reagents. JP was supported by a NHMRC Ideas Grant APP1181179 awarded to MR, BA, and RG.

ACKNOWLEDGMENTS

We thank the Illawarra Cancer Carers for their generous donations that helped support this research and the Sydney Head and Neck Cancer Biobank.

SUPPLEMENTARY MATERIAL

The Supplementary Material for this article can be found online at: https://www.frontiersin.org/articles/10.3389/fonc.2022.835929/full#supplementary-material

REFERENCES

1. Ashford BG, Clark J, Gupta R, Iyer NG, Yu B, Ranson M. Reviewing the Genetic Alterations in High-Risk Cutaneous Squamous Cell Carcinoma: A Search for Prognostic Markers and Therapeutic Targets. *Head Neck* (2017) 39 (7):1462–9. doi: 10.1002/hed.24765
2. Perera E, Gnaneswaran N, Staines C, Win AK, Sinclair R. Incidence and Prevalence of Non-Melanoma Skin Cancer in Australia: A Systematic Review. *Australas J Dermatol* (2015) 56(4):258–67. doi: 10.1111/ajd.12282

3. Pondicherry A, Martin R, Meredith I, Rolfe J, Emanuel P, Elwood M. The Burden of Non-Melanoma Skin Cancers in Auckland, New Zealand. *Australas J Dermatol* (2018) 59(3):210–3. doi: 10.1111/ajd.12751
4. D'Souza J, Clark J. Management of the Neck in Metastatic Cutaneous Squamous Cell Carcinoma of the Head and Neck. *Curr Opin Otolaryngol Head Neck Surg* (2011) 19(2):99–105. doi: 10.1097/MOO.0b013e328343e811
5. Aboul-Fettouh N, Morse D, Patel J, Migden MR. Immunotherapy and Systemic Treatment of Cutaneous Squamous Cell Carcinoma. *Dermatol Pract Concept* (2021) 11(Suppl 2):e2021169S. doi: 10.5826/dpc.11S2a169S
6. Brunner M, Ng BC, Veness MJ, Clark JR. Assessment of the New Nodal Classification for Cutaneous Squamous Cell Carcinoma and Its Effect on Patient Stratification. *Head Neck* (2015) 37(3):336–9. doi: 10.1002/hed.23602
7. Gore SM, Shaw D, Martin RC, Kelder W, Roth K, Uren R, et al. Prospective Study of Sentinel Node Biopsy for High-Risk Cutaneous Squamous Cell Carcinoma of the Head and Neck. *Head Neck* (2016) 38(S1):E884–9. doi: 10.1002/hed.24120
8. Moeckelmann N, Ebrahimi A, Dirven R, Liu J, Low TH, Gupta R, et al. Analysis and Comparison of the 8th Edition American Joint Committee on Cancer (AJCC) Nodal Staging System in Cutaneous and Oral Squamous Cell Cancer of the Head and Neck. *Ann Surg Oncol* (2018) 25(6):1730–6. doi: 10.1245/s10434-018-6340-x
9. Ji AL, Rubin AJ, Thrane K, Jiang S, Reynolds DL, Meyers RM, et al. Multimodal Analysis of Composition and Spatial Architecture in Human Squamous Cell Carcinoma. *Cell* (2020) 182(2):497–514.e22. doi: 10.1016/j.cell.2020.05.039
10. Lazo de la Vega L, Bick N, Hu K, Rahrig SE, Silva CD, Matayoshi S, et al. Invasive Squamous Cell Carcinomas and Precursor Lesions on UV-Exposed Epithelia Demonstrate Concordant Genomic Complexity in Driver Genes. *Mod Pathol* (2020) 33(11):2280–94. doi: 10.1038/s41379-020-0571-7
11. Lobl MB, Clarey D, Higgins S, Sutton A, Hansen L, Wysong A. Targeted Next-Generation Sequencing of Matched Localized and Metastatic Primary High-Risk SCCs Identifies Driver and Co-Occurring Mutations and Novel Therapeutic Targets. *J Dermatol Sci* (2020) 99(1):30–43. doi: 10.1016/j.jdermsci.2020.05.007
12. Pickering CR, Zhou JH, Lee JJ, Drummond JA, Peng SA, Saade RE, et al. Mutational Landscape of Aggressive Cutaneous Squamous Cell Carcinoma. *Clin Cancer Res* (2014) 20(24):6582–92. doi: 10.1158/1078-0432.CCR-14-1768
13. Zehir A, Benayed R, Shah RH, Syed A, Middha S, Kim HR, et al. Mutational Landscape of Metastatic Cancer Revealed From Prospective Clinical Sequencing of 10,000 Patients. *Nat Med* (2017) 23(6):703–13. doi: 10.1038/nm.4333
14. Zilberg C, Lee MW, Kraitsek S, Ashford B, Ranson M, Shannon K, et al. Is High-Risk Cutaneous Squamous Cell Carcinoma of the Head and Neck a Suitable Candidate for Current Targeted Therapies? *J Clin Pathol* (2020) 73(1):17–22. doi: 10.1136/jclinpath-2019-206038
15. Zou D-D, Xu D, Deng Y-Y, Wu W-J, Zhang J, Huang L, et al. Identification of Key Genes in Cutaneous Squamous Cell Carcinoma: A Transcriptome Sequencing and Bioinformatics Profiling Study. *Ann Transl Med* (2021) 9(19):1497. doi: 10.21037/atm-21-3915
16. Zilberg C, Lee MW, Yu B, Ashford B, Kraitsek S, Ranson M, et al. Analysis of Clinically Relevant Somatic Mutations in High-Risk Head and Neck Cutaneous Squamous Cell Carcinoma. *Mod Pathol* (2018) 31(2):275–87. doi: 10.1038/modpathol.2017.128
17. Lu P, Weaver VM, Werb Z. The Extracellular Matrix: A Dynamic Niche in Cancer Progression. *J Cell Biol* (2012) 196(4):395–406. doi: 10.1083/jcb.201102147
18. Ranson M, Andronicos NM. Plasminogen Binding and Cancer: Promises and Pitfalls. *Front Biosci* (2003) 8:s294–304. doi: 10.2741/1044
19. Puram SV, Tirosh I, Parikh AS, Patel AP, Yizhak K, Gillespie S, et al. Single-Cell Transcriptomic Analysis of Primary and Metastatic Tumor Ecosystems in Head and Neck Cancer. *Cell* (2017) 171(7):1611–24.e24. doi: 10.1016/j.cell.2017.10.044
20. Pavón MA, Arroyo-Solera I, Céspedes MV, Casanova I, León X, Mangues R. uPA/uPAR and SERPINE1 in Head and Neck Cancer: Role in Tumor Resistance, Metastasis, Prognosis and Therapy. *Oncotarget* (2016) 7:57351–66 doi: 10.18632/oncotarget.10344
21. Brungs D, Chen J, Aghmesheh M, Vine KL, Becker TM, Carolan MG, et al. The Urokinase Plasminogen Activation System in Gastroesophageal Cancer: A Systematic Review and Meta-Analysis. *Oncotarget* (2017) 8(14):23099–109. doi: 10.18632/oncotarget.15485
22. Madunic J. The Urokinase Plasminogen Activator System in Human Cancers: An Overview of Its Prognostic and Predictive Role. *Thromb Haemost* (2018) 118(12):2020–36. doi: 10.1055/s-0038-1675399
23. Tincknell G, Piper AK, Aghmesheh M, Becker T, Vine KL, Brungs D, et al. Experimental and Clinical Evidence Supports the Use of Urokinase Plasminogen Activation System Components as Clinically Relevant Biomarkers in Gastroesophageal Adenocarcinoma. *Cancers* (2021) 13(16):4097. doi: 10.3390/cancers13164097
24. Hundsdorfer B, Zeilhofer HF, Bock KP, Dettmar P, Schmitt M, Kolk A, et al. Tumour-Associated Urokinase-Type Plasminogen Activator (uPA) and Its Inhibitor PAI-1 in Normal and Neoplastic Tissues of Patients With Squamous Cell Cancer of the Oral Cavity - Clinical Relevance and Prognostic Value. *J Craniomaxillofac Surg* (2005) 33(3):191–6. doi: 10.1016/j.jcms.2004.12.005
25. Shi Z, Stack MS. Urinary-Type Plasminogen Activator (uPA) and Its Receptor (uPAR) in Squamous Cell Carcinoma of the Oral Cavity. *Biochem J* (2007) 407(2):153–9. doi: 10.1042/BJ20071037
26. Ghosh S, Koblinski J, Johnson J, Liu Y, Ericsson A, Davis JW, et al. Urinary-Type Plasminogen Activator Receptor/Alpha 3 Beta 1 Integrin Signaling, Altered Gene Expression, and Oral Tumor Progression. *Mol Cancer Res* (2010) 8(2):145–58. doi: 10.1158/1541-7786.MCR-09-0045
27. Dhanda J, Triantafyllou A, Liloglou T, Kalirai H, Lloyd B, Hanlon R, et al. SERPINE1 and SMA Expression at the Invasive Front Predict Extracapsular Spread and Survival in Oral Squamous Cell Carcinoma. *Br J Cancer* (2014) 111(11):2114–21. doi: 10.1038/bjc.2014.500
28. Magnussen S, Rikardsen OG, Hadler-Olsen E, Uhlin-Hansen L, Steigen SE, Svineng G. Urokinase Plasminogen Activator Receptor (uPAR) and Plasminogen Activator Inhibitor-1 (PAI-1) Are Potential Predictive Biomarkers in Early Stage Oral Squamous Cell Carcinomas (OSCC). *PloS One* (2014) 9(7):e101895. doi: 10.1371/journal.pone.0101895
29. Christensen A, Kiss K, Lelkaitis G, Juhl K, Persson M, Charabi BW, et al. Urokinase-Type Plasminogen Activator Receptor (uPAR), Tissue Factor (TF) and Epidermal Growth Factor Receptor (EGFR): Tumor Expression Patterns and Prognostic Value in Oral Cancer. *BMC Cancer* (2017) 17(1):572. doi: 10.1186/s12885-017-3563-3
30. Zou B, Li J, Xu K, Liu JL, Yuan DY, Meng Z, et al. Identification of Key Candidate Genes and Pathways in Oral Squamous Cell Carcinoma by Integrated Bioinformatics Analysis. *Exp Ther Med* (2019) 17(5):4089–99. doi: 10.3892/etm.2019.7442
31. Garcia-Diez I, Hernandez-Munoz I, Hernandez-Ruiz E, Nonell L, Puigdecanet E, Bodalo-Torruella M, et al. Transcriptome and Cytogenetic Profiling Analysis of Matched in Situ/Invasive Cutaneous Squamous Cell Carcinomas From Immunocompetent Patients. *Genes Chromosomes Cancer* (2019) 58(3):164–74. doi: 10.1002/gcc.22712
32. Mitsui H, Suarez-Farinas M, Gulati N, Shah KR, Cannizzaro MV, Coats I, et al. Gene Expression Profiling of the Leading Edge of Cutaneous Squamous Cell Carcinoma: IL-24-Driven MMP-7. *J Invest Dermatol* (2014) 134(5):1418–27. doi: 10.1038/jid.2013.494
33. Romer J, Pyke C, Lund LR, Ralfkiaer E, Dano K. Cancer Cell Expression of Urokinase-Type Plasminogen Activator Receptor mRNA in Squamous Cell Carcinomas of the Skin. *J Invest Dermatol* (2001) 116(3):353–8. doi: 10.1046/j.1523-1747.2001.01241.x
34. Edge SB, Compton CC. The American Joint Committee on Cancer: The 7th Edition of the AJCC Cancer Staging Manual and the Future of TNM. *Ann Surg Oncol* (2010) 17(6):1471–4. doi: 10.1245/s10434-010-0985-4
35. Bhattacharya A, Hamilton AM, Furberg H, Pietzak E, Purdue MP, Troester MA, et al. An Approach for Normalization and Quality Control for NanoString RNA Expression Data. *Briefings Bioinf* (2021) 22(3):bbaa163. doi: 10.1093/bib/bbaa163
36. Benjamini Y, Hochberg Y. Controlling the False Discovery Rate: A Practical and Powerful Approach to Multiple Testing. *J R Stat Soc Ser B (Methodological)* (1995) 57(1):289–300. doi: 10.1111/j.2517-6161.1995.tb02031.x
37. Krämer A, Green J, Pollard JJr., Tugendreich S. Causal Analysis Approaches in Ingenuity Pathway Analysis. *Bioinformatics* (2014) 30(4):523–30. doi: 10.1093/bioinformatics/btt703
38. Edgar R, Domrachev M, Lash AE. Gene Expression Omnibus: NCBI Gene Expression and Hybridization Array Data Repository. *Nucleic Acids Res* (2002) 30(1):207–10. doi: 10.1093/nar/30.1.207

39. Ritchie ME, Phipson B, Wu D, Hu Y, Law CW, Shi W, et al. Limma Powers Differential Expression Analyses for RNA-Sequencing and Microarray Studies. *Nucleic Acids Res* (2015) 43(7):e47. doi: 10.1093/nar/gkv007
40. Davis S, Meltzer PS. GEOquery: A Bridge Between the Gene Expression Omnibus (GEO) and BioConductor. *Bioinformatics* (2007) 23(14):1846–7. doi: 10.1093/bioinformatics/btm254
41. Thind AS, Tripathi KP, Guarracino MR. RankerGUI: A Computational Framework to Compare Differential Gene Expression Profiles Using Rank Based Statistics. *Int J Mol Sci* (2019) 20(23):6098. doi: 10.3390/ijms20236098
42. Kolde R, Laur S, Adler P, Vilo J. Robust Rank Aggregation for Gene List Integration and Meta-Analysis. *Bioinformatics* (2012) 28(4):573–80. doi: 10.1093/bioinformatics/btr709
43. Jassal B, Matthews L, Viteri G, Gong C, Lorente P, Fabregat A, et al. The Reactome Pathway Knowledgebase. *Nucleic Acids Res* (2020) 48(D1):D498–503. doi: 10.1093/nar/gkz1031
44. Yu G, He Q-Y. ReactomePA: An R/Bioconductor Package for Reactome Pathway Analysis and Visualization. *Mol Biosyst* (2016) 12(2):477–9. doi: 10.1039/C5MB00663E
45. Martin M. Cutadapt Removes Adapter Sequences From High-Throughput Sequencing Reads. *EMBnet J* (2011) 17(1):10–2. doi: 10.14806/ej.17.1.200
46. Barturen G, Rueda A, Hamberg M, Alganza A, Lebron R, Kotsyfakis M, et al. sRNAbench: Profiling of Small RNAs and Its Sequence Variants in Single or Multi-Species High-Throughput Experiments. *Methods Next Generation Sequencing* (2014) 1(1):21–31. doi: 10.2478/mngs-2014-0001
47. Aparicio-Puerta E, Lebron R, Rueda A, Gomez-Martin C, Giannoukakos S, Jaspez D, et al. sRNAbench and Srnatoolbox 2019: Intuitive Fast Small RNA Profiling and Differential Expression. *Nucleic Acids Res* (2019) 47(W1): W530–5. doi: 10.1093/nar/gkz415
48. Love MI, Huber W, Anders S. Moderated Estimation of Fold Change and Dispersion for RNA-Seq Data With Deseq2. *Genome Biol* (2014) 15(12):1–21. doi: 10.1186/s13059-014-0550-8
49. McCarthy DJ, Chen Y, Smyth GK. Differential Expression Analysis of Multifactor RNA-Seq Experiments With Respect to Biological Variation. *Nucleic Acids Res* (2012) 40(10):4288–97. doi: 10.1093/nar/gks042
50. Chen Y, Wang X. miRDB: An Online Database for Prediction of Functional microRNA Targets. *Nucleic Acids Res* (2020) 48(D1):D127–D31. doi: 10.1093/nar/gkz757
51. Chou C-H, Shrestha S, Yang C-D, Chang N-W, Lin Y-L, Liao K-W, et al. miRTarBase Update 2018: A Resource for Experimentally Validated microRNA-Target Interactions. *Nucleic Acids Res* (2018) 46(D1):D296–302. doi: 10.1093/nar/gkx1067
52. Perry J, Ashford B, Thind AS, Gauthier ME, Minaei E, Major G, et al. Comprehensive Mutational and Phenotypic Characterization of New Metastatic Cutaneous Squamous Cell Carcinoma Cell Lines Reveal Novel Drug Susceptibilities. *Int J Mol Sci* (2020) 21(24):9536. doi: 10.3390/ijms21249536
53. Martincorena I, Campbell PJ. Somatic Mutation in Cancer and Normal Cells. *Science* (2015) 349(6255):1483–9. doi: 10.1126/science.aab4082
54. Ruokolainen H, Pääkkö P, Turpeenniemi-Hujanen T. Tissue Inhibitor of Matrix Metalloproteinase-1 Is Prognostic in Head and Neck Squamous Cell Carcinoma: Comparison of the Circulating and Tissue Immunoreactive Protein. *Clin Cancer Res* (2005) 11(9):3257–64. doi: 10.1158/1078-0432.CCR-04-2277
55. Cruz-Munoz W, Khokha R. The Role of Tissue Inhibitors of Metalloproteinases in Tumorigenesis and Metastasis. *Crit Rev Clin Lab Sci* (2008) 45(3):291–338. doi: 10.1080/10408360801973244
56. Culhaci N, Metin K, Copcu E, Dikicioglu E. Elevated Expression of MMP-13 and TIMP-1 in Head and Neck Squamous Cell Carcinomas may Reflect Increased Tumor Invasiveness. *BMC Cancer* (2004) 4(1):1–8. doi: 10.1186/1471-2407-4-42
57. Kurahara S, Shinohara M, Ikebe T, Nakamura S, Beppu M, Hiraki A, et al. Expression of MMPS, MT-MMP, and TIMPs in Squamous Cell Carcinoma of the Oral Cavity: Correlations With Tumor Invasion and Metastasis. *Head Neck* (1999) 21(7):627–38. doi: 10.1002/(SICI)1097-0347(199910)21:7<627::AID-HED7>3.0.CO;2-2
58. O-Charoenrat P, Rhys-Evans PH, Eccles SA. Expression of Matrix Metalloproteinases and Their Inhibitors Correlates With Invasion and Metastasis in Squamous Cell Carcinoma of the Head and Neck. *Arch Otolaryngol Head Neck Surg* (2001) 127(7):813–20.
59. Shimada T, Nakamura H, Yamashita K, Kawata R, Murakami Y, Fujimoto N, et al. Enhanced Production and Activation of Progelatinase A Mediated by Membrane-Type 1 Matrix Metalloproteinase in Human Oral Squamous Cell Carcinomas: Implications for Lymph Node Metastasis. *Clin Exp Metastasis* (2000) 18(2):179–88. doi: 10.1023/A:1006749501682
60. Singh RD, Nilayangode H, Patel JB, Shah FD, Shukla SN, Shah PM, et al. Combined Evaluation of Matrix Metalloproteinases and Their Inhibitors has Better Clinical Utility in Oral Cancer. *Int J Biol Markers* (2011) 26(1):27–36. doi: 10.5301/JBM.2011.6359
61. Ma Y, Pu Y, Peng L, Luo X, Xu J, Peng Y, et al. Identification of Potential Hub Genes Associated With the Pathogenesis and Prognosis of Pancreatic Duct Adenocarcinoma Using Bioinformatics Meta–Analysis of Multi–Platform Datasets. *Oncol Lett* (2019) 18(6):6741–51. doi: 10.3892/ol.2019.11042
62. Stelzer G, Rosen N, Plaschkes I, Zimmerman S, Twik M, Fishilevich S, et al. The GeneCards Suite: From Gene Data Mining to Disease Genome Sequence Analyses. *Curr Protoc Bioinf* (2016) 54(1):1.30.1–.33. doi: 10.1002/cpbi.5
63. Hou J, Yan D, Liu Y, Huang P, Cui H. The Roles of Integrin α5β1 in Human Cancer. *Onco Targets Ther* (2020) 13:13329–44. doi: 10.2147/OTT.S273803
64. Communal L, Roy N, Cahuzac M, Rahimi K, Köbel M, Provencher DM, et al. A Keratin 7 and E-Cadherin Signature Is Highly Predictive of Tubo-Ovarian High-Grade Serous Carcinoma Prognosis. *Int J Mol Sci* (2021) 22(10):5325. doi: 10.3390/ijms22105325
65. Lambert SR, Mladkova N, Gulati A, Hamoudi R, Purdie K, Cerio R, et al. Key Differences Identified Between Actinic Keratosis and Cutaneous Squamous Cell Carcinoma by Transcriptome Profiling. *Br J Cancer* (2014) 110(2):520–9. doi: 10.1038/bjc.2013.760
66. Mazzieri R, Pietrogrande G, Gerasi L, Gandelli A, Colombo P, Moi D, et al. Urokinase Receptor Promotes Skin Tumor Formation by Preventing Epithelial Cell Activation of Notch1. *Cancer Res* (2015) 75(22):4895–909. doi: 10.1158/0008-5472.CAN-15-0378
67. Jee BA, Lim H, Kwon SM, Jo Y, Park MC, Lee IJ, et al. Molecular Classification of Basal Cell Carcinoma of Skin by Gene Expression Profiling. *Mol Carcinog* (2015) 54(12):1605–12. doi: 10.1002/mc.22233
68. Marschall C, Lengyel E, Nobutoh T, Braungart E, Douwes K, Simon A, et al. UVB Increases Urokinase-Type Plasminogen Activator Receptor (uPAR) Expression. *J Invest Dermatol* (1999) 113(1):69–76. doi: 10.1046/j.1523-1747.1999.00631.x
69. Wu K, Mao Y-Y, Han N-N, Wu H, Zhang S. PLAU1 Facilitated Proliferation, Invasion, and Metastasis *via* Interaction With MMP1 in Head and Neck Squamous Carcinoma. *Front Oncol* (2021) 11:574260. doi: 10.3389/fonc.2021.574260
70. Ganesh S, Sier CM, Heerding M, Griffioen G, Lamers CH, Verspaget H. Urokinase Receptor and Colorectal Cancer Survival. *Lancet* (1994) 344 (8919):401–2. doi: 10.1016/S0140-6736(94)91427-3
71. Harbeck N, Kates RE, Look MP, Meijer-Van Gelder ME, Klijn JG, Kruger A, et al. Enhanced Benefit From Adjuvant Chemotherapy in Breast Cancer Patients Classified High-Risk According to Urokinase-Type Plasminogen Activator (uPA) and Plasminogen Activator Inhibitor Type 1 (N = 3424). *Cancer Res* (2002) 62(16):4617–22.
72. Kubala MH, DeClerck YA. The Plasminogen Activator Inhibitor-1 Paradox in Cancer: A Mechanistic Understanding. *Cancer Metastasis Rev* (2019) 38 (3):483–92. doi: 10.1007/s10555-019-09806-4
73. Pedersen H, Grondahl-Hansen J, Francis D, Osterlind K, Hansen HH, Dano K, et al. Urokinase and Plasminogen Activator Inhibitor Type 1 in Pulmonary Adenocarcinoma. *Cancer Res* (1994) 54(1):120–3.
74. Ibrahim SF, Kasprzak JM, Hall MA, Fitzgerald AL, Siegel JJ, Kurley SJ, et al. Enhanced Metastatic Risk Assessment in Cutaneous Squamous Cell Carcinoma With the 40-Gene Expression Profile Test. *Future Oncol* (2022) 18(7):833–47. doi: 10.2217/fon-2021-1277
75. Das Mahapatra K, Pasquali L, Sondergaard JN, Lapins J, Nemeth IB, Baltas E, et al. A Comprehensive Analysis of Coding and Non-Coding Transcriptomic Changes in Cutaneous Squamous Cell Carcinoma. *Sci Rep* (2020) 10(1):3637. doi: 10.1038/s41598-020-59660-6
76. Prat A, Navarro A, Paré L, Reguart N, Galván P, Pascual T, et al. Immune-Related Gene Expression Profiling After PD-1 Blockade in Non–Small Cell Lung Carcinoma, Head and Neck Squamous Cell Carcinoma, and Melanoma. *Cancer Res* (2017) 77(13):3540–50. doi: 10.1158/0008-5472.CAN-16-3556

77. Melendez-Zajgla J, Del Pozo L, Ceballos G, Maldonado V. Tissue Inhibitor of Metalloproteinases-4 The Road Less Traveled. *Mol Cancer* (2008) 7(1):85. doi: 10.1186/1476-4598-7-85
78. Groft L, Muzik H, Rewcastle N, Johnston R, Knäuper V, Lafleur M, et al. Differential Expression and Localization of TIMP-1 and TIMP-4 in Human Gliomas. *Br J Cancer* (2001) 85(1):55–63. doi: 10.1054/bjoc.2001.1854
79. Dammann R, Strunnikova M, Schagdarsurengin U, Rastetter M, Papritz M, Hattenhorst UE, et al. CpG Island Methylation and Expression of Tumour-Associated Genes in Lung Carcinoma. *Eur J Cancer* (2005) 41(8):1223–36. doi: 10.1016/j.ejca.2005.02.020
80. Bigg HF, Morrison CJ, Butler GS, Bogoyevitch MA, Wang Z, Soloway PD, et al. Tissue Inhibitor of Metalloproteinases-4 Inhibits But Does Not Support the Activation of Gelatinase A *via* Efficient Inhibition of Membrane Type 1-Matrix Metalloproteinase. *Cancer Res* (2001) 61(9):3610–8.
81. Chun T-H, Sabeh F, Ota I, Murphy H, McDonagh KT, Holmbeck K, et al. MT1-MMP–dependent Neovessel Formation Within the Confines of the Three-Dimensional Extracellular Matrix. *J Cell Biol* (2004) 167(4):757–67. doi: 10.1083/jcb.200405001
82. Hiraoka N, Allen E, Apel IJ, Gyetko MR, Weiss SJ. Matrix Metalloproteinases Regulate Neovascularization by Acting as Pericellular Fibrinolysins. *Cell* (1998) 95(3):365–77. doi: 10.1016/S0092-8674(00)81768-7
83. Canueto J, Cardenoso E, Garcia JL, Santos-Briz A, Castellanos-Martin A, Fernandez-Lopez E, et al. Epidermal Growth Factor Receptor Expression Is Associated With Poor Outcome in Cutaneous Squamous Cell Carcinoma. *Br J Dermatol* (2017) 176(5):1279–87. doi: 10.1111/bjd.14936
84. Zhou J, Kwak KJ, Wu Z, Yang D, Li J, Chang M, et al. PLAUR Confers Resistance to Gefitinib Through EGFR/P-AKT/Survivin Signaling Pathway. *Cell Physiol Biochem* (2018) 47(5):1909–24. doi: 10.1159/000491071

Conflict of Interest: The authors declare that the research was conducted in the absence of any commercial or financial relationships that could be construed as a potential conflict of interest.

Publisher's Note: All claims expressed in this article are solely those of the authors and do not necessarily represent those of their affiliated organizations, or those of the publisher, the editors and the reviewers. Any product that may be evaluated in this article, or claim that may be made by its manufacturer, is not guaranteed or endorsed by the publisher.

Copyright © 2022 Minaei, Mueller, Ashford, Thind, Mitchell, Perry, Genenger, Clark, Gupta and Ranson. This is an open-access article distributed under the terms of the Creative Commons Attribution License (CC BY). The use, distribution or reproduction in other forums is permitted, provided the original author(s) and the copyright owner(s) are credited and that the original publication in this journal is cited, in accordance with accepted academic practice. No use, distribution or reproduction is permitted which does not comply with these terms.

frontiers | Frontiers in Oncology

ORIGINAL RESEARCH
published: 28 April 2022
doi: 10.3389/fonc.2022.855782

Outcomes From Cytotoxic Chemotherapy Following Progression on Immunotherapy in Metastatic Melanoma: An Institutional Case-Series

Elizabeth M. Gaughan[1]* *and Bethany J. Horton*[2]

[1] Department of Medicine, Division of Hematology and Medical Oncology, University of Virginia, Charlottesville, VA, United States, [2] Department of Public Health Sciences, University of Virginia, Charlottesville, VA, United States

OPEN ACCESS

Edited by:
Sapna Patel,
University of Texas MD Anderson Cancer Center, United States

Reviewed by:
Lucy Kennedy,
Cleveland Clinic, United States
Evan Hall,
University of Washington, United States
Kevin Kim,
California Pacific Medical Center Research Institute, United States

***Correspondence:**
Elizabeth M. Gaughan
egaughan@virginia.edu

Specialty section:
This article was submitted to Skin Cancer, a section of the journal Frontiers in Oncology

Received: 16 January 2022
Accepted: 28 March 2022
Published: 28 April 2022

Citation:
Gaughan EM and Horton BJ (2022) Outcomes From Cytotoxic Chemotherapy Following Progression on Immunotherapy in Metastatic Melanoma: An Institutional Case-Series. Front. Oncol. 12:855782. doi: 10.3389/fonc.2022.855782

Introduction: The role of chemotherapy in the management of advanced melanoma is limited due to low response rates and short survival. Improved outcomes to chemotherapy administered after immunotherapy for metastatic melanoma and other solid tumors have been reported. We studied the outcomes of subjects treated at the University of Virginia (UVA) with chemotherapy following progression on prior systemic immunotherapy and compared the results with the existing literature.

Materials and Methods: Subjects were identified through an institutional database of patients treated with immunotherapy at UVA. Demographic, pathologic and clinical factors were collected, along with dates of therapy, investigator-assessed best response as per Response Evaluation Criteria for Solid Tumors version 1.1 and dates of death or last follow up. Kaplan-Meier survival estimates and log-rank tests were used to perform time to event analysis of progression free survival and overall survival.

Results: Forty-five patients were identified who met the inclusion criteria including 24 men and 21 women with a median age of 61 years. All patients had received at least one line of immunotherapy including 64.4% with prior anti-PD1 treatment. The cytotoxic chemotherapy regimens used included carboplatin with paclitaxel (55.6%), temozolomide (31.1%) and *nab*-paclitaxel (13.3%). The overall response rate for cytotoxic chemotherapy 22.2% and the disease control rate was 35.6%. The median progression-free survival was 1.7 months and median overall survival was 4.7 months. Nineteen (42.2%) patients survived greater than 6 months and seven (15.5%) patients survived over 12 months. Fourteen patients were able to proceed to further therapy.

Discussion: Our results reveal that receipt of immunotherapy prior to chemotherapy for metastatic melanoma does not appear to improve the benefit of chemotherapy. The palliation of symptoms, maintenance of performance status and disease control may be valuable for some patients during this time of robust research and discovery for metastatic melanoma.

Keywords: chemotherapy, immunotherapy, progression, metastatic melanoma, cancer

INTRODUCTION

Advances in immunotherapy and targeted therapy have revolutionized the management of metastatic melanoma. Despite the prolonged responses and improvements in survival seen with these treatments, many patients ultimately progress and seek additional therapy. The role of chemotherapy for melanoma remains limited and uncertain, with the agents often used in the late disease setting after failure of or ineligibility for other treatment. The relatively rapid pace of research and development of new and effective therapies for melanoma raises the value of disease control and the maintenance of performance status through palliation of cancer-related symptoms. Treatments that can offer these outcomes, such as chemotherapy, may help some patients in the salvage setting access emerging therapies.

Most data on chemotherapy for melanoma come from studies conducted before the widespread use of immune checkpoint inhibition and BRAF-targeted agents. There is a long history of utilizing the alkylating agents dacarbazine and temozolomide in this setting, with overall response rates (ORR) of 7.2-21%, median progression free survival (mPFS) of 1.5-2.3 months and overall survival (OS) of 5.5-10.8 months (1–5). More recently, *nab*-paclitaxel demonstrated single-agent activity in advanced melanoma patients with an ORR of 15-21.6% and mOS of 9.6-12.6 months (6, 7). The most common combination regimen is carboplatin and paclitaxel with an ORR of 11-20%, and mOS 8.6-11.3 months (8–10). Overall, these data indicate that chemotherapy can provide response in some patients with a limited impact on survival.

The effect of prior immunotherapy on the chemotherapy outcomes of patients with advanced melanoma has not been prospectively studied. Retrospective case series suggest the potential for improved responses and survival from chemotherapy treatment after immunotherapy for melanoma and other solid tumors (11–20). Our institutional experience also revealed some patients with unexpected and notable benefit to chemotherapy following progression on immunotherapy including patients who were able to access new melanoma therapy after disease stabilization. We studied the outcomes of patients treated at the University of Virginia (UVA) with chemotherapy after progression on prior systemic immunotherapy and compared the results with the existing literature.

MATERIALS AND METHODS

After obtaining UVA -Institutional Review Board (IRB) approval, subjects were identified through an IRB-approved institutional database of patients treated with immunotherapy. Patients were included if they received immunotherapy in the advanced disease setting (metastatic or unresectable melanoma), including interleukin-2, ipilimumab, ipilimumab and nivolumab combination, pembrolizumab and nivolumab, followed by the receipt of cytotoxic chemotherapy. Included patients may have received any number of regimens of immunotherapy and/or targeted therapy prior to chemotherapy administration. Any regimen of chemotherapy administered in the second line or beyond for advanced melanoma was allowed, including single-agent and combination treatments. For subjects that received multiple lines of chemotherapy, only data for the first line of chemotherapy were collected. For each subject, data on demographics, melanoma characteristics, staging per AJCC 7th edition and prior treatment history were obtained. The type of chemotherapy, treatment course, investigator-assessed best response to therapy *via* Response Evaluation Criteria in Solid Tumors version 1.1 criteria and date of progression were collected.

Kaplan-Meier survival estimates and log-rank tests were used to perform time to event analyses of progression free survival and overall survival. Standard descriptive statistics were used to summarize baseline patient characteristics. ORR is defined as the percentage of subjects experiencing a complete response (CR) or partial response (PR) as their best response at any time, reported by the investigator. Disease control rate (DCR) is defined as the percentage of patients with CR, PR or stable disease (SD) as their best response at any time, reported by the investigator. Progression-free survival (PFS) is calculated as time from the start of chemotherapy to progression. Overall survival (OS) is calculated as the time from the start of chemotherapy to either death or last follow-up date, if a date of death is unavailable. All analyses were performed using SAS 9.4 (Cary, NC).

RESULTS

Of the 549 patients with advanced melanoma treated at UVA with immunotherapy from 01/01/2011 through 04/05/2021, 45 met inclusion criteria. Of these, 53.3% were male, 95.6% were white and the median age at advanced melanoma diagnosis was 61 years (**Table 1**). Most patients, 31 (68.9%) had a cutaneous primary, while seven (15.6%) had a mucosal, six (13.3%) had uveal and one (2.2%) had conjunctival primary melanoma. Most, 31 (68.9%) had wild-type tumors, while seven patients had tumors with *BRAF* V600E mutation (15.6%). Twelve subjects (26.7%) had a history of brain metastases, 39 (86.7%) had M1c disease and 23 (51.1%) had an elevated lactate dehydrogenase.

All patients had received at least one line of immunotherapy prior to chemotherapy, including interleukin-2, ipilimumab monotherapy, anti-PD1 monotherapy, and ipilimumab and nivolumab combination (**Table 1**). The median time from diagnosis of metastatic disease to initiation of chemotherapy was 14.1 months. Patients received up to seven lines of prior treatment, including up to four lines of prior immunotherapy before chemotherapy administration. Twenty-nine (64.4%) subjects received at least one line of anti-PD1 monotherapy with pembrolizumab or nivolumab and 16 (35.6%) subjects received combination ipilimumab and nivolumab. There were 16 subjects in the cohort without prior exposure to anti-PD1

TABLE 1 | Patient characteristics.

DEMOGRAPHICS	N = 45 patients (percentage)
Gender	
Male	24 (53.3%)
Female	21 (46.7%)
Race	
White	43 (95.6%)
African American	1 (2.2%)
Other	1 (2.2%)
Median Age at Diagnosis	61 years (range 21-86 years)
DISEASE CHARACTERISTICS	
Type of Primary Melanoma	
Cutaneous	31 (68.9%)
Mucosal	7 (15.6%)
Ocular	6 (13.3%)
Conjunctival	1 (2.2%)
Mutation	
BRAF V600E	7 (15.6%)
NRAS	2 (4.4%)
c-KIT	1 (2.2%)
Wild-Type	31 (68.9%)
Not Reported	4 (8.9%)
Brain Metastases	
Yes	12 (26.7%)
No	33 (73.3%)
LDH ≥ than upper limit of normal	
Yes	23 (51.1%)
No	20 (44.4%)
Not Reported	2 (4.4%)
Stage (AJCC 7th Edition)	
Unresectable III	3 (6.7%)
M1a	1 (2.2%)
M1b	2 (4.4%)
M1c	39 (86.7%)
TREATMENT HISTORY	
Lines of Prior Therapy (1-7)	
1	9 (20.0%)
2	19 (42.2%)
3	10 (22.2%)
4	5 (11.1%)
5	1 (2.2%)
7	1 (2.2%)
Lines of Prior Immunotherapy (1-4)	
1	10 (22.2%)
2	21 (46.7%)
3	11 (24.4%)
4	3 (6.7%)
Types of Prior Immunotherapy	
Interleukin-2	20 (44.4%)
Ipilimumab monotherapy	21 (46.7%)
Combination	16 (35.6%)
Ipilimumab/Nivolumab	
Anti-PD1 monotherapy	29 (64.4%)
Other	5 (11.1%)
Prior Targeted Therapy	8 (17.8%)

therapy including three patients without any prior immune checkpoint inhibitor treatment. Twenty patients (44.4%) had received prior interleukin-2.

Patients received one of the following chemotherapy regimens: carboplatin with paclitaxel (55.6%), *nab*-paclitaxel (13.3%) or temozolomide (31.1%) (**Table 2**). No subject received concurrent chemotherapy and immunotherapy. For the overall cohort, ten subjects achieved a partial response to therapy (22.2%), while six subjects (13.3%) had stable disease, leading to an overall disease control rate (DCR) of 35.6%. The ORR to chemotherapy ranged 14.3% to 28%, and the DCR ranged 28.6% to 40% depending on the regimen administered with the highest response rates seen with carboplatin and paclitaxel. In this dataset, no patient experienced a complete response and all patients ultimately experienced disease progression. Three patients were censored at their last follow up date due to unavailable date of death (1 patient) and the patient being alive at the time of analysis (2 patients). The mPFS for the cohort was 1.7 months and mOS was 4.7 months (**Figure 1**). There was no statistically significant difference in mPFS or mOS observed across the different chemotherapy types (log-rank p-values 0.8366 and 0.1889, respectively). Nineteen (42.2%) patients survived greater than 6 months after starting chemotherapy and seven (15.5%) patients survived over 12 months. Fourteen subjects (31.1%) went onto subsequent lines of therapy. All of these 14 patients had received prior Ipilimumab either monotherapy or in combination with nivolumab and 12 had received both prior Ipilimumab and anti-PD1 therapy. Eleven of the 14 did not have brain metastases, 11 had *BRAF* wild-type tumors and 10 were treated with carboplatin and paclitaxel.

The response and survival outcomes based on clinical and pathologic features are outlined in **Table 2**. A history of anti-PD1 therapy prior to chemotherapy resulted in a marginally better overall survival versus those without prior anti-PD1 exposure (mOS 5.9 versus 3.4 months, p=0.0646) (**Figure 2**). Patients with *BRAF*-mutant tumors had numerically worse survival than those with *BRAF*-wild-type tumors or tumors of unknown *BRAF* mutation status (mOS 2.9 versus 5.5 months, p=0.4565), though not statistically significant. The ORR for subjects with primary cutaneous melanoma was numerically highest of the primary sites and within the cutaneous melanoma subgroup, there was slightly higher ORR and DCR for patients with prior anti-PD1 exposure versus no prior anti-PD1 treatment (27.8% vs 23.1% and 38.9% vs 30.8%, respectively) without a difference in survival.

DISCUSSION

Chemotherapy has long played a limited role in the management of melanoma, typically utilized in the resistant/refractory setting or for patients with contraindication to immunotherapy. Modern treatment options including immune checkpoint inhibitors and targeted therapy result in improved outcomes for most patients. Despite the durable responses experienced by some patients, many will progress and there is a continued need for additional therapy. The success of checkpoint inhibitors and targeted therapy, coupled with the relatively low toxicity burden, often results in patients with preserved performance status that permits further therapy. While clinical trial participation to test new therapies and combinations is a priority, access to these treatments is limited. Cytotoxic chemotherapy is often readily available and understanding

TABLE 2 | Chemotherapy outcomes.

	N	%	ORR (%)	DCR (%)	mPFS (months) (95% CI)	mOS (months) (95% CI)
OVERALL COHORT	45	100	22.2	35.6	1.7 (1.2, 3.0)	4.7 (3.0, 8.2)
CHEMOTHERAPY REGIMEN						
Carboplatin/Paclitaxel	25	55.6	28	40	1.5 (1.2,5.4)	5.9 (2.9,8.7)
nab-Paclitaxel	6	13.3	16.7	33.3	2.4 (0.9,6.1)	6.0 (2.8,–)
Temozolomide	14	31.1	14.3	28.6	2.0 (0.7,3.4)	3.4 (1.1,8.2)
BRAF MUTATION STATUS						
BRAF V600E positive	7	15.6	14.3	28.6	1.2 (0.2,5.4)	2.9 (0.3,6.8)
BRAF wild-type/not-reported	38	84.4	23.7	36.8	2.2 (1.2,3.4)	5.5 (3.0,8.4)
BRAIN METASTASIS						
Positive	12	26.7	33.3	50	2.9 (0.2,6.8)	4.4 (0.7,10.0)
Negative	33	73.3	18.2	30.3	1.5 (1.2,2.4)	4.7 (2.9,8.4)
TYPE OF PRIMARY LESION						
Cutaneous	31	68.9	25.8	35.5	1.7 (1.2,3.7)	4.3 (2.8,8.2)
Mucosal	7	15.6	14.3	28.6	0.9 (0.4,5.4)	4.6 (1.1,8.5)
Ocular	6	13.3	0.0	33.3	2.8 (1.0,6.0)	7.3 (3.0,–)
Conjunctival	1	2.2	100	100	3.0 (–)	5.1 (–)
PRIOR ANTI-PD1						
Positive	29	64.4	20.7	37.9	1.5 (1.2,3.5)	5.9 (3.0,8.7)
Negative	16	35.6	25.0	31.3	2.3 (0.7,3.7)	3.4 (1.1,8.2)

Response rate and survival results for the entire cohort and based on clinical and pathologic variables of interest.

optimal value of the agents can be useful for counseling patients and maximizing benefit.

Our own institutional experience, and others, reveals that some melanoma patients have an exceptional response to chemotherapy after progression on immunotherapy (11–15). Our observed clinical scenarios involve responses leading to significant palliation, disease control lasting sufficiently until a new agent became available and responses >1 year in some patients. Maeda et al, presented their retrospective analysis of seven melanoma patients that received at least two cycles of carboplatin and paclitaxel after progression on immune checkpoint inhibition in Japan. They showed a 29% ORR, 57% DCR, mean PFS of 5 months and mean OS of 7.6 months (12). In 2020, Hadash-Bengad et al, published their single-center retrospective assessment of patients treated with chemotherapy (dacarbazine, temozolomide or carboplatin with paclitaxel) after immunotherapy (n=11) versus those who received chemotherapy without prior immunotherapy (n=24) in Israel (11). The mPFS for the post-immunotherapy cohort was 5.2 months versus the 2.5 months in the no-prior immunotherapy cohort (p=0.039). The mOS result (11.8 months versus 8.6 months) and the response rate difference (36.4% versus 19%) were not statistically significant. Also in 2020, Saint-Jean et al. reported their institutional experience of 18 subjects who received chemotherapy (dacarbazine alone or in combination with carboplatin or fotemustine) after failure or limiting toxicity of prior immunotherapy in France (13). They showed a 19% ORR and 25% DCR, with a mPFS of 5.4 months and mOS of 12 months. Taken together, these reports are suggestive of higher response rate and slightly longer survival with chemotherapy than the prospective studies. The cohorts were small, and patients received a variety of chemotherapeutic agents, limiting interpretation of results.

While there were individual patients with notable benefit, the results for our cohort are similar to the historic experience with chemotherapy. Our ORRs ranging 14.3%-28% depending on the regimen used, are in line with prospective trials results with temozolomide and *nab*-paclitaxel and slightly higher than ORRs reported for combination carboplatin and paclitaxel (4–10). Our overall mPFS of 1.7 months and mOS of 4.7 months are numerically lower in comparison with historical controls (1–10). This cohort of patients included subjects with cutaneous, mucosal or uveal melanoma and any number of prior treatments in the advanced disease setting was permitted. Patients were identified through a clinical database of all patients treated with immunotherapy at UVA since 2011, and therefore, representative of the real-world, varied patient population seen over 10 years. Many of the comparison prospective studies excluded patients with uveal melanoma and limited the number of prior systemic agents. Only three subjects in our entire cohort had only received interleukin-2 and had no exposure to immune checkpoint inhibition prior to chemotherapy. Sixteen patients did not receive prior anti-PD1 therapy (either monotherapy or in combination with ipilimumab) before receipt of chemotherapy. While the response rate and mPFS were similar for those with and without prior anti-PD1 exposure, there was a marginally better mOS for patients with prior anti-PD1 treatment.

Forty-two percent of our cohort survived greater than 6 months after chemotherapy and 16% survived greater than 12 months. Fourteen patients were able to go onto subsequent treatment after progression on chemotherapy. Two subjects were alive past the data cutoff, 18 and 28 months after chemotherapy administration. Both subjects experienced partial response to chemotherapy and were able to access additional effective agents after progression. It is difficult to know if these subjects had greater benefit to chemotherapy because of their prior immunotherapy or if their tumors would have been sensitive to the chemotherapy regardless of prior treatment.

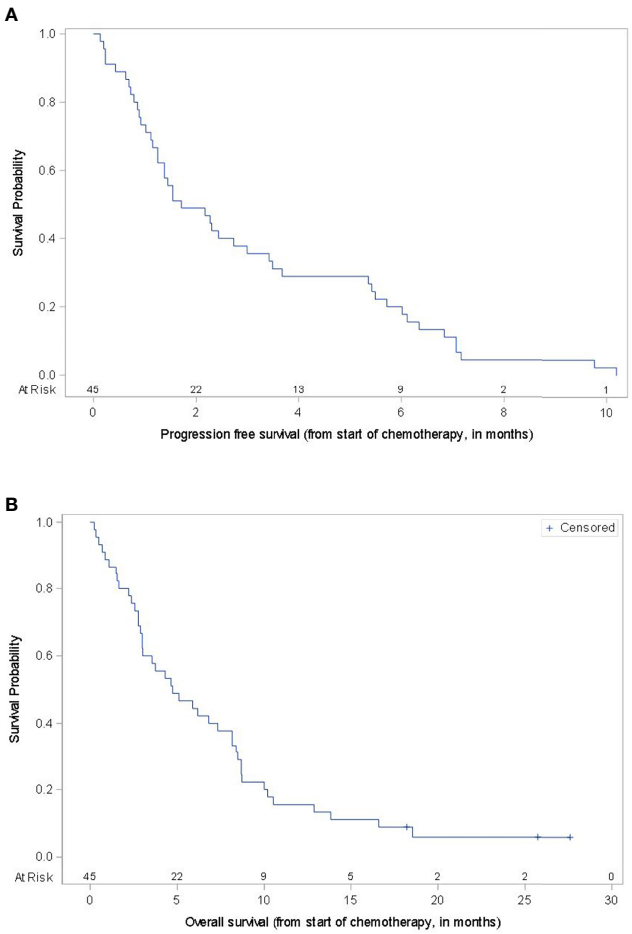


FIGURE 1 | Progression-Free Survival and Overall Survival. Kaplan-Meier survival curves for progression-free survival **(A)** and overall survival **(B)** for the entire cohort.

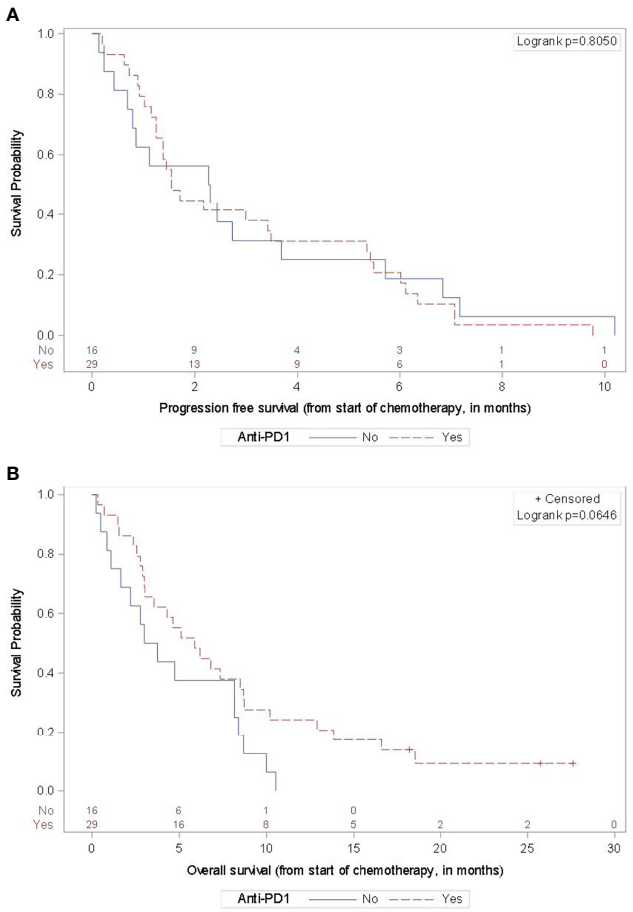


FIGURE 2 | Progression-Free and Overall Survival by Prior Anti-PD-1 Therapy. For the 29 subjects with any prior anti-PD1 therapy in the advanced disease setting, the mPFS **(A)** was 1.5 months (95% CI 1.2-3.5 months) and the mOS **(B)** was 5.9 months (95% CI 3.0-8.7). For the 16 subjects without prior anti-PD1 therapy, the mPFS was 2.3 months (95% CI 0.7-3.7 months) and the mOS was 3.4 months (95% CI 1.1-8.2 months).

The strengths of our analysis include the size and full scope of our single institution experience over the last 10 important years of melanoma therapy advancement. It provides a real-world population for analysis with various types of primary melanoma, presence of brain metastases and high-stage disease, and a variety of prior immunotherapy agents including cytokines, checkpoint inhibitors and investigational vaccine therapy. All clinical, pathologic and radiographic data was available to the investigators for review which standardized interpretation. The limitations of our data include the retrospective nature of the analysis and the lack of biologic correlates for the outcomes. There was no standard time to chemotherapy administration, with a range of 2.0 to 99.2 months after the diagnosis of metastatic disease. Subjects had up to seven lines of prior systemic therapy for advanced disease reflecting the biologic diversity of the tumors under evaluation.

Our results reveal that receipt of immunotherapy prior to chemotherapy for metastatic melanoma does not appear to improve the benefit of chemotherapy. The opportunity to palliate symptoms, maintain performance status and disease control can be valuable during this time of research and discovery for metastatic melanoma.

DATA AVAILABILITY STATEMENT

The raw data supporting the conclusions of this article will be made available by the authors, without undue reservation.

ETHICS STATEMENT

The studies involving human participants were reviewed and approved by University of Virginia Institutional Review Board.

Written informed consent for participation was not required for this study in accordance with the national legislation and the institutional requirements.

AUTHOR CONTRIBUTIONS

EG: study concept and design, subject identification, data collection, data interpretation and manuscript preparation. BH: study design and statistical data interpretation. All authors contributed to the article and approved the submitted version.

FUNDING

This work was supported by the UVA Cancer Center Support Grant P30CA044579.

REFERENCES

1. Middleton MR, Grob JJ, Aaronson N, Fierlbeck G, Tilgen W, Seiter S, et al. Randomized Phase III Study of Temozolomide Versus Dacarbazine in the Treatment of Patient With Advanced Metastatic Malignant Melanoma. *J Clin Oncol* (2000) 18(1):158–66. doi: 10.1200/JCO.2000.18.1.158
2. Robert C, Long GV, Brady B, Dutriaux C, Maio M, Mortier L, et al. Nivolumab in Previously Untreated Melanoma Without *BRAF* Mutation. *N Engl J Med* (2015) 372(4):320–30. doi: 10.1056/NEJMoa1412082
3. Avril MF, Aamdal S, Grob JJ, Hauschild A, Mohr P, Bonerandi JJ, et al. Fotemustine Compared With Dacarbazine in Patients With Disseminated Malignant Melanoma: A Phase III Study. *J Clin Oncol* (2004) 22(6):1118–25. doi: 10.1200/JCO.2004.04.165
4. Patel PM, Suciu S, Mortier L, Kruit WH, Robert C, Schdendorf D, et al. Extended Schedule, Escalated Dose Temozolomide Versus Dacarbazine in Stage IV Melanoma: Final Results of a Randomized Phase III Study (EORTC 18032). *Eur J Cancer* (2011) 47(10):1476–83. doi: 10.1016/j.ejca.2011.04.030
5. Bleehen NM, Newlands ES, Lee SM, Thatcher N, Selby P, Calvert AH, et al. Cancer Research Campaign Phase II Trial of Temozolomide in Metastatic Melanoma. *J Clin Oncol* (1995) 13(4):910–3. doi: 10.1200/JCO.1995.13.4.910
6. Hersh EM, O'Day SJ, Ribas A, Samlowski WE, Gordon MS, Shechter DE, et al. A Phase 2 Clinical Trial of Nab-Paclitaxel in Previously Treated and Chemotherapy-Naïve Patients With Metastatic Melanoma. *Cancer* (2010) 116(1):155–63. doi: 10.1002/cncr.24720
7. Hersh EM, Del Vecchio M, Brown MP, Kefford R, Loquai C, Testori A, et al. A Randomized, Controlled Phase III Trial of Nab-Paclitaxel Versus Dacarbazine in Chemotherapy-Naïve Patients With Metastatic Melanoma. *Ann Oncol* (2015) 26(11):2267–74. doi: 10.1093/annonc/mdv324
8. Hauschild A, Agarwala SS, Trefzer U, Hogg D, Robert C, Hersey P, et al. Results of a Phase III, Randomized, Placebo-Controlled Study of Sorafenib in Combination With Carboplatin and Paclitaxel as Second-Line Treatment in Patient With Unresectable Stage III or Stage IV Melanoma. *J Clin Oncol* (2009) 27(17):2823–30. doi: 10.1200/JCO.2007.15.7636
9. Flaherty KT, Lee SJ, Zhao F, Schuchter LM, Flaherty L, Kefford R, et al. Phase III Trial of Carboplatin and Paclitaxel With or Without Sorafenib in Metastatic Melanoma. *J Clin Oncol* (2013) 31(3):373–9. doi: 10.1200/JCO.2012.42.1529
10. Kim KB, Sosman JA, Fruehauf JP, Linette GP, Markovic SN, McDermott DF, et al. BEAM: A Randomized Phase II Study Evaluating the Activity of Bevacizumab in Combination With Carboplatin Plus Paclitaxel in Patients With Previously Untreated Advanced Melanoma. *J Clin Oncol* (2012) 30 (1):34–41. doi: 10.1200/JCO.2011.34.6270
11. Hadash-Bengad R, Hajaj E, Slein S, Merims S, Frank S, Eisenberg G, et al. Immunotherapy Potentials the Effect of Chemotherapy in Metastatic Melanoma – a Retrospective Study. *Front Oncol* (2020) 10:70. doi: 10.3389/fonc.2020.00070
12. Maeda T, Yoshino K, Nagai K, Oaku S, Kato M, Hiura A, et al. The Efficacy of Platinum-Based Chemotherapy for Immune Checkpoint Inhibitor-Resistant Advanced Melanoma. *Acta Oncol* (2019) 58(3):379–81. doi: 10.1080/0284186X.2018.1541252
13. Saint-Jean M, Fronteau C, Peuvrel L, Khammari A, Varey E, Quéreux G, et al. Chemotherapy Efficacy After First-Line Immunotherapy in 18 Advanced Melanoma Patients. *Med (Baltimore)* (2020) 99(29):e21329. doi: 10.1097/MD.0000000000021329
14. Swami U, Monga V, Freesmeier M, Zhang W, Bossler AD, Zakharia Y, et al. Exceptional Responses With Sequential Metronomic Temozolomide After Pembrolizumab Failure in Patients With Metastatic Melanoma. *Melanoma Res* (2019) 29(6):643–7. doi: 10.1097/CMR.0000000000000592
15. Simon A, Kourie HR, Kerger J. Is There Still a Role for Cytotoxic Chemotherapy After Targeted Therapy and Immunotherapy in Metastatic Melanoma? A Case Report and Literature Review. *Chin J Cancer* (2017) 36 (1):10. doi: 10.1186/s40880-017-0179-6
16. Schvartsman G, Peng SA, Bis G, Lee JJ, Benveniste MF, Zhang J, et al. Response Rates to Single-Agent Chemotherapy After Exposure to Immune Checkpoint Inhibitors in Advanced non-Small Cell Lung Cancer. *Lung Cancer* (2017) 112:90–5. doi: 10.1016/j.lungcan.2017.07.034
17. Park SE, Lee SH, Ahn JS, Ahn M-J, Park K, Sun JM, et al. Increased Response Rates to Salvage Chemotherapy Administered After PD-1/PD-L1 Inhibitors in Patients With non-Small Cell Lung Cancer. *J Thorac Oncol* (2018) 13:106–11. doi: 10.1016/j.jtho.2017.10.011
18. Saleh K, Daste A, Martin N, Pons-Tostivint E, Auperin A, Herrera-Gomez RG, et al. Response to Salvage Chemotherapy After Progression on Immune Checkpoint Inhibitors in Patients With Recurrent and/or Metastatic Squamous Cell Carcinoma of the Head and Neck. *Eur J Cancer* (2019) 121:123–9. doi: 10.1016/j.ejca.2019.08.026
19. Kacew AJ, Harris EJ, Lorch JH, Schoenfeld JD, Margalit DN, Kass JI, et al. Chemotherapy After Immune Checkpoint Blockade in Patients With Recurrent, Metastatic Squamous Cell Carcinoma of the Head and Neck. *Oral Oncol* (2020) 105:104676. doi: 10.1016/j.oraloncology.2020.104676
20. Dwary AD, Master S, Patel A, Cole C, Mansour R, Mills G, et al. Excellent Response to Chemotherapy Post Immunotherapy. *Oncotarget* (2017) 8 (53):91795–802. doi: 10.18632/oncotarget.20030

Conflict of Interest: The authors declare that the research was conducted in the absence of any commercial or financial relationships that could be construed as a potential conflict of interest.

The handling Editor declared a past co-authorship with one of the authors EG.

Publisher's Note: All claims expressed in this article are solely those of the authors and do not necessarily represent those of their affiliated organizations, or those of the publisher, the editors and the reviewers. Any product that may be evaluated in this article, or claim that may be made by its manufacturer, is not guaranteed or endorsed by the publisher.

Copyright © 2022 Gaughan and Horton. This is an open-access article distributed under the terms of the Creative Commons Attribution License (CC BY). The use, distribution or reproduction in other forums is permitted, provided the original author(s) and the copyright owner(s) are credited and that the original publication in this journal is cited, in accordance with accepted academic practice. No use, distribution or reproduction is permitted which does not comply with these terms.

frontiers | Frontiers in Oncology

CASE REPORT
published: 23 May 2022
doi: 10.3389/fonc.2022.846278

Neurotropic Cutaneous Malignancies: Case Report on Keratinocyte Derived Malignancies of the Head and Neck With Perineural Invasion

Grace Sora Ahn[1], Brian Hinds[1], Frederic Kolb[2], Amy K. Reisenauer[3], Seaver L. Soon[4], Ali R. Sepahdari[5], Kathryn B. Bollin[6] and Soo J. Park[7]*

[1] Department of Dermatology, University of California, San Diego, La Jolla, CA, United States, [2] Department of Plastic Surgery, University of California, San Diego, La Jolla, CA, United States, [3] Private Practitioner, Kihei, HI, United States, [4] Private Practitioner, San Diego, CA, United States, [5] Diagnostic Neuroradiology, Scripps Clinic Medical Group, La Jolla, CA, United States, [6] Division of Hematology and Oncology, Scripps MD Anderson Cancer Center, La Jolla, CA, United States, [7] Moores Cancer Center, University of California, San Diego, La Jolla, CA, United States

OPEN ACCESS

Edited by:
Sapna Patel,
University of Texas MD Anderson Cancer Center, United States

Reviewed by:
Joanne Jeter,
The Ohio State University, United States
Peter Parsons,
The University of Queensland, Australia

***Correspondence:**
Kathryn B. Bollin
Bollin.Kathryn@scrippshealth.org

Specialty section:
This article was submitted to Skin Cancer, a section of the journal Frontiers in Oncology

Received: 31 December 2021
Accepted: 16 March 2022
Published: 23 May 2022

Citation:
Ahn GS, Hinds B, Kolb F, Reisenauer AK, Soon SL, Sepahdari AR, Bollin KB and Park SJ (2022) Neurotropic Cutaneous Malignancies: Case Report on Keratinocyte Derived Malignancies of the Head and Neck With Perineural Invasion. Front. Oncol. 12:846278. doi: 10.3389/fonc.2022.846278

Background: The recent addition of immunotherapy as a treatment modality to surgery and radiation has vastly improved disease control for patients with keratinocyte-derived carcinomas (KCs) that are incurable with local therapies alone. With the advent of immune checkpoint inhibitors (ICPis) in non-melanoma skin cancers comes diagnostic and therapeutic challenges when considering treatment strategies for patients presenting with clinical perineural invasion (cPNI) of locally advanced KC of the head and neck.

Objectives: We report four cases that convey the diagnostic and therapeutic complexity of managing patients with neuropathic symptoms from cutaneous neurotropic carcinomas of the head and neck. We also discuss an updated review regarding immunotherapies and perineural invasion within KC management.

Conclusion: Patients presenting with symptoms suspicious for cPNI warrant an expanded diagnostic evaluation to correlate neurological findings with neurotropic spread of disease. While nerve biopsies can be precarious in sensitive areas, a history of skin cancer and clinical presentation suggestive of neurotropism may be enough to pursue timely management in the form of surgery, radiation, and/or systemic therapy given each patient's individual priorities, comorbidities, and prognosis. When adding ICPi as a treatment modality for patients with disease not amenable to local therapies, the potential for immune-related adverse events must be considered. A multi-disciplinary review and approach to the management of patients with KC and cPNI is essential for obtaining optimal patient outcomes.

Keywords: neurotropic cutaneous malignancies, non-melanoma skin cancer, cutaneous oncology, cutaneous squamous cell carcinoma, basal cell carcinoma, perineural invasion, immunotherapy, immune checkpoint inhibitors

INTRODUCTION

The revolutionary impact of immune checkpoint inhibitors on a wide range of malignancies has now expanded into the realm of advanced non-melanoma skin cancer. Achieving the impressive clinical benefits of immunotherapies for patients with high-risk and locally advanced cutaneous malignancies requires the engagement of surgical, radiation, and medical oncology specialists in highly complex decision making. Herein, we present four cases that highlight several diagnostic and therapeutic challenges when considering treatment strategies for locally advanced keratinocyte-derived malignancies of the head and neck with clinical perineural invasion.

Keratinocyte-derived carcinoma (KC) includes basal cell carcinoma (BCC) and cutaneous squamous cell carcinoma (CSCC)—ubiquitous cancers whose incidence is poorly documented due to exclusion from national and global tumor registries. While surgical excision of these cancers results in cure for most patients, in the setting of high-risk factors, such as >2 cm diameter, poorly differentiated histology, perineural invasion of nerves ≥0.1 mm, and tumor invasion beyond fat, there can be significant risk for local recurrence after surgery and/or radiation or for the development of locoregional metastases (1). Perineural invasion (PNI) is a rare complication of KC that involves tropism of tumor cells extending along the tissue stroma of the nerve sheath. Incidental PNI (iPNI) is found upon histological examination in the absence of symptoms. Clinical PNI (cPNI) is diagnosed radiographically and/or by the presence of sensory disturbances or motor deficits correlating with malignant neurotropism involving large caliber nerves. Radiographic definition of PNI involving the head and neck is described anatomically by a zonal classification system applied to magnetic resonance imaging (MRI) (2, 3). The mechanism of PNI involves migration along the nerve trunk within the perineural space that, in turn, activates numerous signaling pathways involving trophic factors, extracellular matrix adhesion proteins, and regulators of chemotaxis (4–9). In both BCC and SCC, for example, the presence of neural cell adhesion molecules may help determine such tumor aggression and increased levels of nerve growth factor, and TrkA, B, and C may reflect unique survival pathways (10). Emerging models of PNI suggest that interactions between tumor cells and nerves not only induce tumor migration but also stimulate axonogenesis and neurogenesis, which leads to both the enlargement and increased nerve density, respectively, around neurotropic malignancies (10–12).

Keratinocyte carcinomas with PNI are uncommon relative to the overall incidence of KC, with estimates of incidence rates of PNI in CSCC ranging from 2.5% to 14% and in BCC ranging from 0.18% to 10% (13–16). BCC with PNI independent of other high-risk features, including large diameter, aggressive histologic subtype, deep tumor invasion, and location on the face, does not appear to correlate with worse prognosis (17). However, CSCC with either iPNI or cPNI is associated with an increased risk for nodal and distant metastases, while patients with cPNI have worse recurrence-free and disease-specific survival with a 30% risk of death (18). Features associated with higher incidence of cPNI include male sex and previous history of skin cancer, whereas immunosuppression, lymph node involvement, and extranodal extension are independently associated with worse outcomes for patients with high stage primary CSCC (19, 20).

Diagnosis of PNI can be missed despite reliable techniques including histopathological examination, clinical examination evaluating neuropathic symptoms, and diagnostic imaging, such as high-resolution MRI (21–24). Recognizing the presence of PNI early may influence treatment decisions, which can in turn improve patient outcomes that have historically proven to be poor due to increased rates of disease recurrence and increased morbidity and mortality, especially in the setting of CSCC of the head and neck (HNCSCC) (18, 25–27). Location of cPNI can be inherently morbid, such as with perineural outgrowth into cerebral nerves resulting in severe pain or neurological disturbances such as cranial neuropathies (21, 22, 28). Invasive biopsies of neurologically sensitive areas present a diagnostic challenge; thus, a greater understanding of the association between neurotropism, symptomatic presentation, extent, and morbidity of disease is needed for physicians to best manage patients with the varying degrees of perineural spread. Treatment of patients with KC and PNI can include surgical excision, definitive and/or adjuvant radiation, concurrent chemoradiotherapy, hedgehog growth signaling pathway inhibitors for unresectable BCC, and, in the case of unresectable or advanced CSCC and BCC, immune checkpoint inhibition (ICPi) targeting the [programmed cell death protein 1 (PD-1) and its ligand L1 (PD-L1). For patients with cPNI and locally advanced KC of the head and neck, many of whom have had prior treatment with surgery and/or radiation, the potential for surgical disfigurement and/or exacerbation of underlying medical comorbidities with systemic therapies is a common confounding factor and should prompt multi-disciplinary review for individualized treatment planning.

In the four cases that follow, we seek to convey the complexity of therapeutic decision making for patients presenting with neuropathic symptoms from cPNI in KC of the head and neck and to highlight current gaps in knowledge that may warrant further research.

CASE PRESENTATIONS

Case 1

A 74-year-old man with a history of multiple cutaneous SCC of the head and neck presented to the clinic in June 2021 with severe neuropathic pain of the right neck and scalp. In October 2020, the patient noted gradually increasing pain in the right shoulder that did not improve with physical therapy. After 2 months of increasing numbness that extended to the right anterior upper chest wall and eventually to the jaw, MRI of the neck and shoulder in February 2021 showed asymmetric enhancement of the right C4 nerve just distal to the C3–C4 neural foramen (**Figure 1**). At this time, he was noted to have SCC of the right post-auricular region and vertex scalp and underwent Mohs microsurgery in February 2021. There was no histological evidence of PNI in the examined frozen sections. Neuropathy subsequently progressed further until the patient noted a right supraclavicular lump in April 2021. The right anterior deep neck mass was excised by head and neck surgery and diagnosed as a lymph node, associated with invasive SCC and without extranodal extension. MRI imaging in

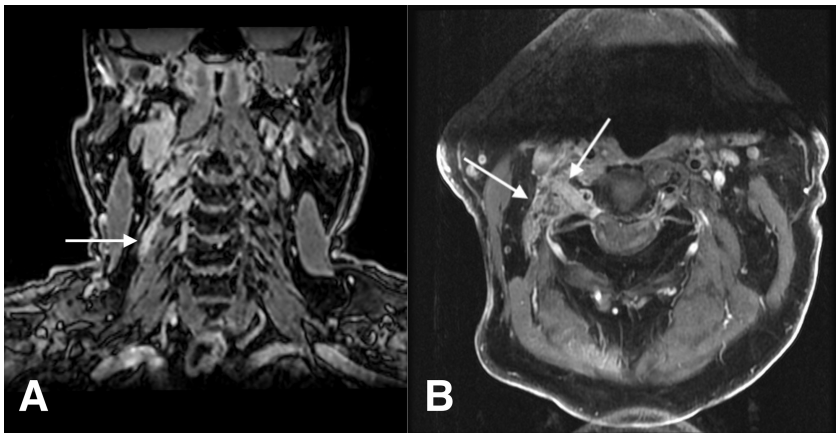


FIGURE 1 | Case 1: a 74-year-old man with squamous cell carcinoma. **(A)** Coronal fat-suppressed contrast-enhanced T1-weighted image shows a thickening, abnormally enhancing right C4 nerve (arrow). **(B)** Axial fat-suppressed contrast-enhanced T1-weighted image shows thickening and abnormal enhancement of the right C3 nerve, from the dorsal root ganglion through its course through the posterior cervical space (arrows).

May 2021 revealed thickening of the right C3 and C4 nerves, with asymmetric contrast enhancement. After hematology oncology consultation, the patient was referred to radiation oncology to consider adjuvant radiation and to neurosurgery for cervical spine nerve root biopsy for suspicion of PNI of SCC. Options for treatment of high-risk SCC in the absence of gross or radiographic disease initially included adjuvant radiation to the post-auricular and supraclavicular regions versus ICPi, but radiation was ultimately not recommended due to difficulty in delineating the radiation field after rapidly progressive neuropathy. In June 2021, the patient underwent biopsy of the C3 nerve root with pathology demonstrating perineural SCC. Pembrolizumab 400 mg intravenously (IV) every 6 weeks was initiated. After the first dose of immunotherapy, the patient's neuropathic pain worsened, and he developed clinical involvement of several right-sided cranial nerves, including the vagal and hypoglossal nerves, with vocal cord paralysis and aspiration. In August 2021, a gastrostomy tube was placed, and high-dose palliative radiation was delivered to the at-risk cervical spinal canal, involved neck, and all involved and at-risk cranial nerves up to the skull base. Pain of the right neck region improved until recurrence in October 2021, with CT neck revealing new right paravertebral and upper chest wall soft tissue masses. Carboplatin (AUC 5) IV and paclitaxel 80 mg/^{m2} IV were added to pembrolizumab. The patient tolerated three cycles of chemoimmunotherapy without clinical disease progression; however, he contracted severe acute respiratory syndrome coronavirus 2 (SARS-CoV-2) in January 2022 and died 1 month later from respiratory failure attributed to coronavirus disease 2019 (COVID-19) pneumonia.

Case 2

A 50-year-old woman presented to the clinic with headaches subsequent to the complete resection of a central left forehead BCC in April 2019. Histopathology was notable for admixed features including nodularity and a focal infiltrating proliferative pattern with one focus of PNI identified within a 0.05-mm caliber nerve fiber and negative margins. As the patient's headaches increased in severity, pain management strategies including lifestyle adjustment, acupuncture, and migraine therapy proved ineffective. She eventually developed intermittent severe pain above the left eyebrow followed by numbness extending inferiorly to the left upper eyelid. She was treated with antibiotics for a presumed infection when swelling and drainage were noted. Symptoms did not abate and ultimately a punch biopsy in August 2020 demonstrated invasive, well-differentiated, and partially cystic SCC, 1.2-mm deep without overt perineural, perineurium, endoneural, or angiolymphatic involvement identified. MRI of the face showed nodular enhancement along the course of the left V1 frontal nerve branch, while MRI of the brain noted concern for extensive perineural spread along the superior medial aspect of the left orbit. The perineural spread (PNS) along V1 seemed not to extend beyond zone 1. Nerve biopsy of the left supraorbital nerve identified multifocal PNI, and tertiary comprehensive pathology review rendered a diagnosis of basosquamous carcinoma. Multidisciplinary review was held at three separate cancer centers, with two favoring immunotherapy due to high response rates in CSCC and anticipated disfigurement from surgery, while the third favored surgery followed by radiation as a curative intent treatment plan that provided microscopic definition of the extent of disease. Ultimately, the patient decided upon surgery and radiation for its curative potential and against anti-PD-1 immunotherapy due to potential toxicity. Surgery involved wide margin resection of glabellar SCC with exhaustive selective neural microdissection to assess precisely the clinical and incidental neural invasion beyond the surgical resection. All small and large nerve branches were identified and tagged at the margins. Small branches were traced for at least 5 mm. Large V1 nerve trunks (bilateral supratrochlear and supraorbital nerves) were dissected for at least 3 cm in their intra-orbital cavity course. The right V1 and left supratrochlear branches had a normal macroscopic appearance, and their dissection was not continued

beyond the 3 cm. The left supra-orbital nerve was macroscopically enlarged in accordance with pre-operative MRI findings (**Figure 2**). Its selective microdissection was continued until its entrance in the superior orbital fissure. At this level, the nerve had a normal diameter. A sentinel node biopsy was included, and a total of four sentinel lymph nodes were resected. Histopathology revealed invasive poorly differentiated SCC, perineural spread (PNS) involving the supraorbital nerve with clear close margin, no PNI along the small nerve branches, and negative lymph nodes. Upon final histopathological assessment, she was diagnosed with basosquamous carcinoma of the forehead with macroscopic V1 neurotropism bilaterally. Following surgery, the patient was treated with intensity-modulated proton therapy (IMPT) to the left V1, including zone 1 and 2 and glabella to better spare optic structures. At 1-year follow-up, her typical trigeminal headaches were absent, and she remains disease free.

Case 3

An 81-year-old man without significant medical problems presented in March 2020 with a cutaneous nodule and severe pain above the left eyebrow at the site of four prior Mohs microsurgery procedures for SCC. Biopsy of the skin lesion revealed moderately to poorly differentiated squamous cell carcinoma with a residual nerve engulfed and surrounded by tumor. MRI of the brain demonstrated a 1.0-cm soft tissue mass at the left superior orbital rim with tumor perineural extension along V1 into the left supraorbital foramen, left orbit, and left cavernous sinus (**Figure 3**). After reviewing treatment options, he decided against surgery due to morbidity and need for enucleation in favor of the ICPi, cemiplimab 350 mg IV every 3 weeks, and by the third infusion, his neurotropic pain had resolved. Soon after the fourth infusion, he developed progressive shortness of breath, and a resting oxygen saturation of 97% decreased to 80% with ambulation. Computerized tomography (CT) scan showed extensive peribronchial parenchyma consolidation in all lung segments, and results of SARS-CoV-2 tests were repeatedly negative. He was initiated on high-dose corticosteroids and hospitalized out of concern for grade 3 immune-mediated pneumonitis. Bronchoalveolar lavage was negative for infection; however, his respiratory status failed to improve with steroids. Empiric antimicrobials and sequential immunosuppressive therapy with anti-tumor necrosis factor-alpha inhibitor and intravenous immune globulin (IVIG) were provided. Upon further clinical decline, the patient required intubation and mechanical ventilation with repeat bronchoalveolar lavage revealing infection with *Pneumocystis jirovecii*. The patient died several days later after his family elected for comfort-directed care.

Case 4

A 74-year-old man with a history of invasive well-differentiated cutaneous SCC of the nose underwent Mohs microsurgery in April 2016 with negative margins after four stages and no mention of PNI. In the fall of 2017, he started to notice some left facial numbness, but this was attributed to recent dental work. The left facial numbness persisted, and in May 2018, the patient presented with left facial droop and noted that the numbness had now spread to the right side of his face. MRI of the brain demonstrated perineural tumor spread along the left V2 segment extending from the premaxillary fat to the inferior cavernous sinus and along the left Vidian nerve (**Figure 4**). A 1.8-cm enhancing subcutaneous mass was also seen along the right infraorbital cheek. Subsequent biopsy of the left infraorbital nerve revealed peripheral nerve tissue with areas of moderately differentiated SCC and associated chronic inflammation. Excision of the right subcutaneous cheek nodule confirmed invasive moderately differentiated SCC with an infiltrative pattern and PNI. The patient declined definitive radiation therapy over concerns for significant toxicity and elected to

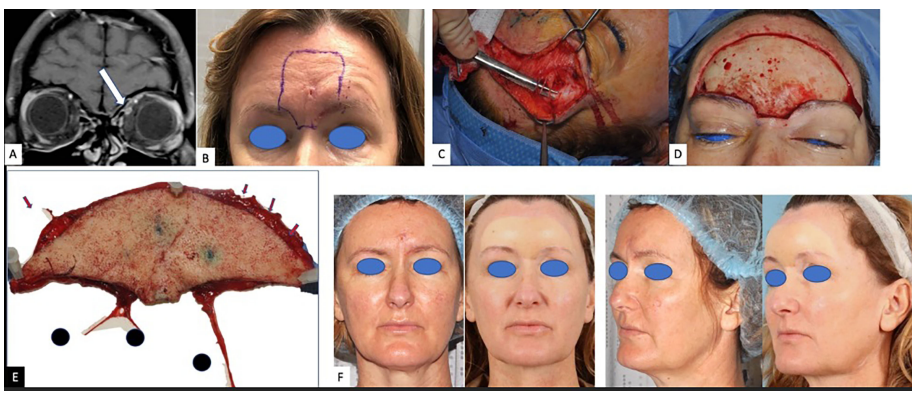


FIGURE 2 | Case 2: a 50-year-old woman with basosquamous carcinoma. **(A)** Coronal fat-suppressed contrast-enhanced T1-weighted image shows asymmetric enhancement along the superior orbit (arrow), adjacent to the superior rectus muscle. **(B)** Pre-operative forehead recurrence. **(C)** Intra-operative dissection of the distal sensitive branches of the forehead sensory nerves. **(D)** Defect of the forehead after resection of the recurrence with 2 cm margins. **(E)** Pathological sample. Red arrows showing the tagged distal sensory branches. 1 = right supraorbital nerve; 2 = right supratrochlear nerve; 3 = left supraorbital nerve dissected until its entrance in the superior orbital fissure. The left supratrochlear nerve is missing and was dissected separately as interrupted by a pre-operative biopsy. **(F)** Pre - and 14-month post-operative clinical photos. Post-operative proton radiotherapy spared the reconstructed forehead and focused on the retro-orbital and skull course of the supratrochlear nerve including the Gasser nerve.

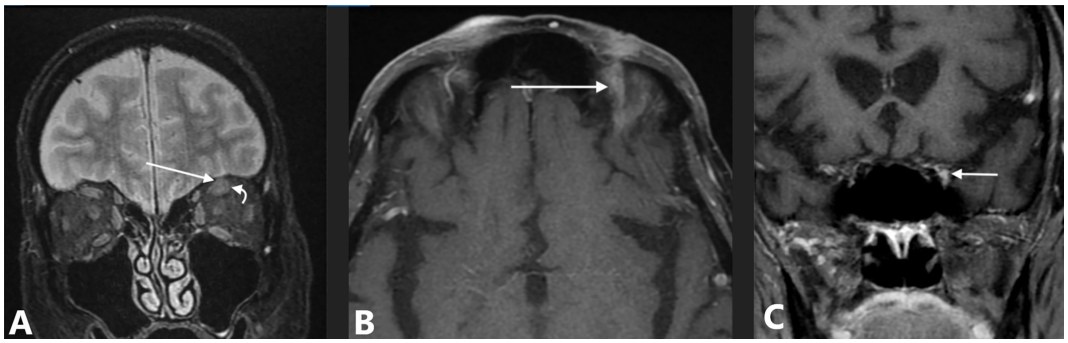


FIGURE 3 | Case 3: an 81-year-old man with squamous cell carcinoma and perineural spread along V1 to the cavernous sinus. **(A)** MRI with coronal fat-suppressed T2-weighted image shows intermediate signal intensity tumor involving V1 (straight arrow) adjacent to normal superior rectus muscle (curved arrow). **(B)** Axial fat-suppressed contrast-enhanced T1-weighted image shows abnormal enhancement in the superior orbit (arrow). **(C)** Coronal contrast-enhanced T1-weighted image, obtained just posterior to the superior orbital fissure, shows asymmetric enhancement and fullness along the lateral margin of the cavernous sinus (arrow).

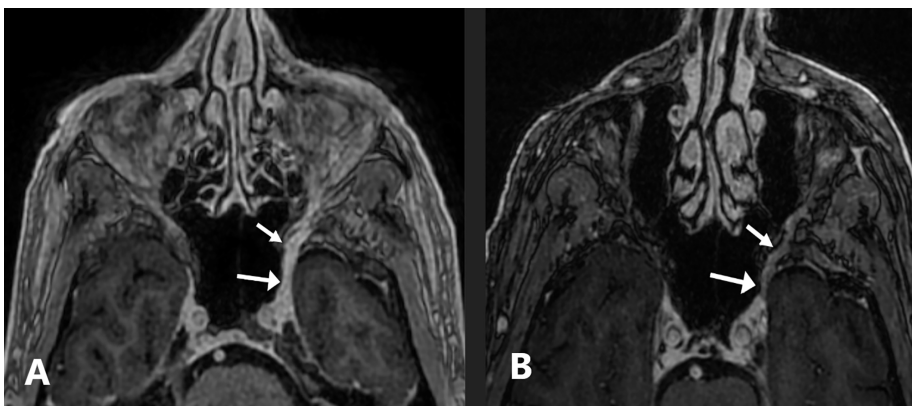


FIGURE 4 | Case 4: a 74-year-old-man with squamous cell carcinoma. **(A)** Axial fat-suppressed contrast-enhanced T1-weighted image shows a thickened, abnormally enhancing left V2 nerve extending from the premaxillary fat to the inferior cavernous sinus and along the left Vidian nerve (arrows). **(B)** Axial fat-suppressed contrast-enhanced T1-weighted image performed 6 months after permanently discontinuing pembrolizumab shows mild asymmetric enhancement of the left V2 nerve that is improved compared to pre-treatment (arrows).

pursue immunotherapy with pembrolizumab 200 mg IV every 3 weeks citing emphasis on quality of life. His facial numbness did not improve despite radiographic response. After 12 infusions, he developed severe diarrhea and was diagnosed with grade 3 immune-related colitis confirmed on colonoscopy. He was treated with high-dose corticosteroids with rapid resolution of symptoms. Shared decision-making led to immunotherapy rechallenge, but the patient had recurrence of colitis after four infusions, and thus, treatment was permanently discontinued. The patient completed 1 year of pembrolizumab and has been off therapy since September 2019 with clinically stable disease.

DISCUSSION

Endoneural and perineural metastasis is a common mechanism of aggressive tumor spread in which primary malignancies fan along the course of neural pathways. There is an estimated 1%–5% incidence of PNI in head and neck KCs with cPNI occurring most commonly along the facial and trigeminal nerves (29). Patients presenting with neuropathic symptoms in a region of previously treated KC should prompt clinicians to evaluate for recurrent disease along neural pathways. Patients presenting with facial palsy or trigeminal neuralgia are often misdiagnosed to have benign cranial neuropathies resulting in delayed treatment, increased morbidity, and decreased quality of life. MRI detects perineural spread with the highest specificity, whereas earlier PNI detection within the head and neck has been shown with high-resolution MR neurography protocols (30).

Historically, complete surgical excision of perineural and endoneural metastases was often limited in its success with the extent of surgical resection recommended to include the entire skin regions supplied by the affected nerve (31). Current literature detailing treatment modalities of KCs with PNI stems

mostly from treatment of cutaneous squamous cell carcinoma of the head and neck (CSCCHN). Surgical approaches and outcomes have improved since advances in MRI neurography for preoperatively defining the zonal distribution of disease, resulting in 5-year disease-free survival rates ranging between 50% and 75% following excision and post-operative radiation (32). This approach is superior to postoperative concurrent chemoradiotherapy, which has not been shown to provide statistical benefit in overall survival, disease-free survival, or even freedom from locoregional relapse when compared with surgery and postoperative radiotherapy alone (33). There may be a role for adjuvant proton radiotherapy where risk for toxicities following radiation therapy, including retinopathies, optic neuropathies, hearing loss, and brain or brainstem necrosis, may be mitigated (34).

Two ICPis, cemiplimab and pembrolizumab, are Food and Drug Administration (FDA)-approved and now considered the standard of care for locoregionally advanced or metastatic cutaneous SCC in patients who are not eligible for curative surgery or radiation. Data from the Phase II EMPOWER-CSCC-1 study with cemiplimab demonstrated clinically meaningful improvements with an overall response rate (ORR) of 46.1% and complete response (CR) rate of 16.1% at 3-year follow-up (35). The median time to a CR was 11.2 months, and both the duration of response (DOR) and overall survival had not yet been reached. *Post-hoc* exploratory analysis of this cemiplimab study also showed symptomatic benefit with improvements in health-related quality of life and pain control (36). Similarly, the Phase II KEYNOTE-629 study with pembrolizumab reported an ORR of 50% in the locally advanced cohort and 35.2% in the recurrent/metastatic cohort, including a 16.7% and 10.5% CR rate, respectively (37). The median DOR was not reached in either cohort. Both agents induce relatively high response rates with durable disease control. Early phase studies suggest that neoadjuvant immunotherapy may facilitate less extensive upfront treatment (38, 39). Cemiplimab was also recently FDA approved for locally advanced or metastatic BCC previously treated with or inappropriate for a hedgehog inhibitor and is the only ICPi with this indication where responses have shown early evidence of durability in the Phase II Study 1620 (40). The hedgehog inhibitor, vismodegib, has shown promising results as a neoadjuvant strategy in the Phase II VISMONEO study of locally advanced BCC, with ORR of 71% and 25 of 44 patients with pathological assessment of response demonstrating a complete response (41).

As we see through our four cases highlighting variable degrees of clinical PNI, management of patients with symptoms of PNI does not fit a single mold. While ICPi came to be clearly indicated in the first case, the patient's quality of life worsened during the period of diagnostic evaluation that delayed initiation of therapy. Ultimately, the multi-disciplinary provision of treatment including palliative radiation, ICPi, and chemotherapy provided symptom and disease control; however, he succumbed to infection in the setting of multiple comorbid conditions attributable to his cancer and treatments. The second case demonstrated a delicate balance between the risks and benefits of either intricate surgery or palliative immunotherapy. Due to the availability of extraordinary surgical expertise, the patient was able to undergo curative intent surgery and adjuvant proton radiation with success. The third case illustrates lethal sequelae of immunotherapy-related toxicity in a patient who was eligible for potentially curative resection but declined due to misalignment with his individual goals of care. The last case underscores the durability of response to immunotherapy in the absence of surgery or radiation, although again not without known toxicity risks. All cases bring into question the utility of neo-adjuvant and adjuvant systemic therapies to reduce surgical morbidity and recurrence for high-risk KC, both of which are currently being studied in clinical trials. Whether ICPi could be a practical treatment option for other neurotropic malignancies such as prostate and pancreatic adenocarcinomas remains underexplored. This is primarily due to the immunosuppressive tumor microenvironment that characterizes these "cold tumors" and hence predicts marginal response to ICPi without robust biomarkers. Here, PNI itself may mediate a cold immune microenvironment and signify the need for combinatorial ICPi strategies to overcome inherent treatment resistance (42).

In conclusion, patients presenting with symptoms suspicious for cPNI warrant an expanded diagnostic evaluation to precisely correlate neurological findings with neurotropic spread of disease. While nerve biopsies can be precarious in sensitive areas, a history of skin cancer and clinical presentation suggestive of neurotropism may be enough to pursue timely management in the form of surgery, radiation, and/or systemic therapy given each patient's individual priorities, comorbidities, and prognosis. It is imperative that the pathology laboratory properly process the nerve specimens and resection specimens to ensure sufficient sectioning that limits sampling error. Among patients considering immunotherapy instead of definitive local therapy, one must consider the potential for immune-related adverse events that may arise from ICPi. A multi-disciplinary review and approach to the management of patients with KC and cPNI is essential given the complexity of therapeutic decision making.

ETHICS STATEMENT

Written informed consent was obtained from the individual(s) for the publication of any potentially identifiable images or data included in this article.

AUTHOR CONTRIBUTIONS

Conception and design: GSA and KBB. (II) Administrative support: GSA and KBB. (III) Provision of study materials or patients: AKR, ARS, BH, FK, KBB, SLS, and SJP. (IV) Collection and assembly of data: ARS, BH, GSA, FK, KBB, and SJP. (V) Data analysis and interpretation: AKR, ARS, BH, FK, KBB, SLS,

and SJP. (VI) Manuscript writing: AKR, ARS, BH, FK, GSA, KBB, SLS, and SJP. (VII) Final approval of manuscript: AKR, ARS, BH, FK, GSA, KBB, SLS, and SJP. All authors contributed to the article and approved the submitted version.

FUNDING

Funding for this manuscript provided by Scripps MD Anderson Cancer Center.

REFERENCES

1. Karia PS, Jambusaria-Pahlajani A, Harrington DP, Murphy GF, Qureshi AA, Schmults CD. Evaluation of American Joint Committee on Cancer, International Union Against Cancer, and Brigham and Women's Hospital Tumor Staging for Cutaneous Squamous Cell Carcinoma. *J Clin Oncol* (2014) 32(4):327–34. doi: 10.1200/JCO.2012.48.5326
2. Williams LS, Mancuso A, Mendenhall WM. Perineural Spread of Cutaneous Squamous and Basal Cell Carcinoma: CT and MR Detection and Its Impact on Patient Management and Prognosis. *Int J Radiat Oncol Biol Phys* (2001) 49 (4):1061–9. doi: 10.1016/S0360-3016(00)01407-3
3. Gandhi MR, Panizza B, Kennedy D. Detecting and Defining the Anatomic Extent of Large Nerve Perineural Spread of Malignancy: Comparing "Targeted" MRI With the Histologic Findings Following Surgery. *Head Neck* (2011) 33(4):469–75. doi: 10.1002/hed.21470
4. Maroldi R, Farina D, Borghesi A, Marconi A, Gatti E. Perineural Tumor Spread. *Neuroimaging Clin North Am* (2008) 18(2):413–29. doi: 10.1016/j.nic.2008.01.001
5. Binmadi NO, Basile JR. Perineural Invasion in Oral Squamous Cell Carcinoma: A Discussion of Significance and Review of the Literature. *Oral Oncol* (2011) 47(11):1005–10. doi: 10.1016/j.oraloncology.2011.08.002
6. Koide N, Yamada T, Shibata R, Mori T, Fukuma M, Yamazaki K, et al. Establishment of Perineural Invasion Models and Analysis of Gene Expression Revealed an Invariant Chain (CD74) as a Possible Molecule Involved in Perineural Invasion in Pancreatic Cancer. *Clin Cancer Res* (2006) 12(8):2419–26. doi: 10.1158/1078-0432.CCR-05-1852
7. McLaughlin RB, Montone KT, Wall SJ, Chalian AA, Weinstein GS, Roberts SA, et al. Nerve Cell Adhesion Molecule Expression in Squamous Cell Carcinoma of the Head and Neck: A Predictor of Propensity Toward Perineural Spread. *Laryngoscope* (1999) 109(5):821–6. doi: 10.1097/00005537-199905000-00026
8. Maruya SI, Myers JN, Weber RS, Rosenthal DI, Lotan R, El-Naggar AK. ICAM-5 (Telencephalin) Gene Expression in Head and Neck Squamous Carcinoma Tumorigenesis and Perineural Invasion! *Oral Oncol* (2005) 41 (6):580–8. doi: 10.1016/j.oraloncology.2005.01.002
9. Anderson TD, Feldman M, Weber RS, Ziober AF, Ziober BL. Tumor Deposition of Laminin-5 and the Relationship With Perineural Invasion. *Laryngoscope* (2001) 111(12):2140–3. doi: 10.1097/00005537-200112000-00011
10. Chen-Tsai CP, Colome-Grimmer M, Wagner RF. Correlations Among Neural Cell Adhesion Molecule, Nerve Growth Factor, and Its Receptors, TrkA, TrkB, TrkC, and P75, in Perineural Invasion by Basal Cell and Cutaneous Squamous Cell Carcinomas. *Dermatol Surg* (2004) 30(7):1009–16. doi: 10.1111/j.1524-4725.2004.30306.x
11. Kanik AB, Yaar M, Bhawan J. P75 Nerve Growth Factor Receptor Staining Helps Identify Desmoplastic and Neurotropic Melanoma. *J Cutan Pathol* (1996) 23(3):205–10. doi: 10.1111/j.1600-0560.1996.tb01468.x
12. Ayala GE, Dai H, Powell M, Li R, Ding Y, Wheeler TM, et al. Cancer-Related Axonogenesis and Neurogenesis in Prostate Cancer. *Clin Cancer Res* (2008) 14 (23):7593–603. doi: 10.1158/1078-0432.CCR-08-1164
13. Cottel WI. Perineural Invasion by Squamous-Cell Carcinoma. *J Dermatol Surg Oncol* (1982) 8(7):589–600. doi: 10.1111/j.1524-4725.1982.tb00317.x
14. Johnson TM, Rowe DE, Nelson BR, Swanson NA. Squamous Cell Carcinoma of the Skin (Excluding Lip and Oral Mucosa). *J Am Acad Dermatol* (1992) 26 (3 Pt 2):467–84. doi: 10.1016/0190-9622(92)70074-p
15. Feasel AM, Brown TJ, Bogle MA, Tschen JA, Nelson BR. Perineural Invasion of Cutaneous Malignancies. *Dermatol Surg* (2001) 27(6):531–42. doi: 10.1046/j.1524-4725.2001.00330.x
16. Leibovitch I, Huilgol SC, Selva D, Richards S, Paver R. Basal Cell Carcinoma Treated With Mohs Surgery in Australia III. *Perineural Invasion J Am Acad Dermatol* (2005) 53(3):458–63. doi: 10.1016/j.jaad.2005.04.089
17. Massey PR, Morgan FC, Stamell Ruiz E, Schmults CD. Histologic Perineural Invasion of Unnamed Nerves Does Not Affect Basal Cell Carcinoma Outcomes. *JAAD* (2020) 82(6):1528–30. doi: 10.1016/j.jaad.2020.02.028
18. Karia PS, Morgan FC, Ruiz ES, Schmults CD. Clinical and Incidental Perineural Invasion of Cutaneous Squamous Cell Carcinoma: A Systematic Review and Pooled Analysis of Outcomes Data. *JAMA Dermatol* (2017) 153 (8):781–8. doi: 10.1001/jamadermatol.2017.1680
19. Warren TA, Nagle CM, Bowman J, Panizza BJ. The Natural History and Treatment Outcomes of Perineural Spread of Malignancy Within the Head and Neck. *J Neurol Surg B Skull Base* (2016) 77(2):107–12. doi: 10.1055/s-0036-1579777
20. Smile T, Ilori E, Varra V, Ruiz ES, Murad F, Wei D, et al. Predictors of Recurrence and Survival in High-Stage Primary Cutaneous Squamous Cell Carcinoma: A Recursive Partitioning Analysis. *Int J Radiat Oncol Biol Phys* (2021) 111(3):e417–8. doi: 10.1016/j.ijrobp.2021.07.1197
21. Ständer S, Ständer H, Kutzner H, Luger TA, Metze D. Squamous Epithelial Carcinomas of the Face With Neurotropic Growth. *Hautarzt* (2003) 54 (11):1087–94. doi: 10.1007/s00105-003-0555-9
22. Leach BC, Kulbersh JS, Day TA, Cook J. Cranial Neuropathy as a Presenting Sign of Recurrent Aggressive Skin Cancer. *Dermatol Surg* (2008) 34(4):483–97. doi: 10.1111/j.1524-4725.2007.34094.x
23. Chabaane M, Ayadi K, Rkhami M, Drissi C, Houimli S, Bahri K, et al. Management of a Recurrence of a Squamous Cell Carcinoma of the Scalp With Extension to the Brain: A Case Report and Literature Review. *Surg Neurol Int* (2020) 11:347. doi: 10.25259/SNI_356_2020
24. Gandhi M, Sommerville J. The Imaging of Large Nerve Perineural Spread. *J Neurol Surg B Skull Base* (2016) 77(2):113–23. doi: 10.1055/s-0036-1571836
25. Osguthorpe JD, Abel CG, Lang P, Hochman M. Neurotropic Cutaneous Tumors of the Head and Neck. *Arch Otolaryngol Head Neck Surg* (1997) 123 (8):871–6. doi: 10.1001/archotol.1997.01900080105013
26. Tang C, Fischbein NJ, Murphy JD, Chu KP, Bavan B, Dieterich S, et al. Stereotactic Radiosurgery for Retreatment of Gross Perineural Invasion in Recurrent Cutaneous Squamous Cell Carcinoma of the Head and Neck. *Am J Clin Oncol* (2013) 36(3):293–8. doi: 10.1097/COC.0b013e3182468019
27. Chatzistefanou I, Lubek J, Markou K, Ord RA. The Role of Perineural Invasion in Treatment Decisions for Oral Cancer Patients: A Review of the Literature. *J Craniomaxillofac Surg* (2017) 45(6):821–5. doi: 10.1016/j.jcms.2017.02.022
28. Clément C, Lebreuilly I, Stephan A, De Raucourt S, Dutriaux C, Comoz F, et al. Extension Intracrânienne D'un Carcinome Spinocellulaire De La Face: Implication De La Voie Neurotrope [Intracranial Extension of Cutaneous Facial Squamous Cell Carcinoma: Involvement of the Neurotropic Pathway]. *Ann Dermatol Venereol* (2010) 137(8-9):551–4. doi: 10.1016/j.annder.2010.04.018
29. Balamucki CJ, Mancuso AA, Amdur RJ, Kirwan JM, Morris CG, Flowers FP, et al. Skin Carcinoma of the Head and Neck With Perineural Invasion. *Am J Otolaryngol* (2012) 33:447–54. doi: 10.1016/j.amjoto.2011.11.004
30. Baulch J, Gandhi M, Sommerville J, Panizza B. 3t MRI Evaluation of Large Nerve Perineural Spread of Head and Neck Cancers. *J Med Imaging Radiat Oncol* (2015) 59:578–85. doi: 10.1111/1754-9485.12338
31. Terashi H, Kurata S, Tadokoro T, Ishii Y, Sato H, Kudo Y, et al. Perineural and Neural Involvement in Skin Cancers. *Dermatol Surg* (1997) 23(4):259–264; discussion 264-265. doi: 10.1111/j.1524-4725.1997.tb00040.x
32. Solares CA, Mason E, Panizza BJ. Surgical Management of Perineural Spread of Head and Neck Cancers. *J Neurol Surg B Skull Base* (2016) 77(2):140–9. doi: 10.1055/s-0036-1579751
33. Porceddu SV, Bressel M, Poulsen MG, Stoneley A, Veness MJ, Kenny LM, et al. Postoperative Concurrent Chemoradiotherapy Versus Postoperative Radiotherapy in High-Risk Cutaneous Squamous Cell Carcinoma of the Head and Neck: The Randomized Phase III TROG 05. *Trial J Clin Oncol* (2018) 36(13):1275–83. doi: 10.1200/JCO.2017.77.0941

34. Bryant CM, Dagan R, Holtzman AL, Fernandes R, Bunnell A, Mendenhall WM. Passively Scattered Proton Therapy for Nonmelanoma Skin Cancer With Clinical Perineural Invasion. *Int J Part Ther* (2021) 8(1):285–93. doi: 10.14338/IJPT-20-00062.1
35. Rischin D, Khushalani NI, Schmults CD, Guminski AD, Chang ALS, Lewis KD, et al. Phase II Study of Cemiplimab in Patients (Pts) With Advanced Cutaneous Squamous Cell Carcinoma (CSCC): Longer Follow-Up. *J Clin Oncol* (2020) 38(15):10018. doi: 10.1200/JCO.2020.38.15_suppl.10018
36. Migden MR, Rischin D, Sasane M, Mastey V, Pavlick A, Schmults CD, et al. Health-Related Quality of Life (HRQL) in Patients With Advanced Cutaneous Squamous Cell Carcinoma (CSCC) Treated With Cemiplimab: *Post Hoc* Exploratory Analyses of a Phase II Clinical Trial. *J Clin Oncol* (2020) 38 (15):10033. doi: 10.1200/JCO.2020.38.15_suppl.10033
37. Hughes BGM, Munoz-Couselo E, Mortier L, Bratland Å, Gutzmer R, Roshdy O, et al. Pembrolizumab for Locally Advanced and Recurrent/Metastatic Cutaneous Squamous Cell Carcinoma (KEYNOTE-629 Study): An Open-Label, Nonrandomized, Multicenter, Phase II Trial. *Ann Oncol* (2021) 32 (10):1276–85. doi: 10.1016/j.annonc.2021.07.008
38. Atlas JL, Kanos M, Symanowski JT, Brickman D, Forster M, Frenkel C, et al. Cemiplimab as First Intervention for Patients With Locally Advanced Cutaneous Squamous Cell Carcinoma. *J Clin Oncol* (2020) 38(15):10065. doi: 10.1200/JCO.2020.38.15_suppl.10065
39. Gross N, Ferrarotto R, Nagarajan P, Bell D, El-Naggar A, Johnson JM, et al. Hase II Study of Neoadjuvant Cemiplimab Prior to Surgery in Patients With Stage III/IV (M0) Cutaneous Squamous Cell Carcinoma of the Head and Neck (CSCC-HN). *Ann Oncol* (2019) 30(5):v851–934. doi: 10.1093/annonc/mdz394
40. Stratigos AJ, Sekulic A, Peris K, Bechter O, Prey S, Kaatz M, et al. Cemiplimab in Locally Advanced Basal Cell Carcinoma After Hedgehog Inhibitor Therapy: An Open-Label, Multi-Centre, Single-Arm, Phase 2 Trial. *Lancet Oncol* (2021) 22(6):848–57. doi: 10.1016/S1470-2045(21)00126-1
41. Bertrand N, Guerreschi P, Basset-Seguin N, Saiag P, Dupuy A, Dalac-Rat S, et al. Vismodegib in Neoadjuvant Treatment of Locally Advanced Basal Cell Carcinoma: First Results of a Multicenter, Open-Label, Phase 2 Trial (VISMONEO Study): Neoadjuvant Vismodegib in Locally Advanced Basal Cell Carcinoma. *EClinicalMedicine* (2021) 35:100844. doi: 10.1016/j.eclinm.2021.100844
42. Yang M, Tao L, Jiang Y, Yang J, Huo Y, Liu D, et al. Perineural Invasion Reprograms the Immune Microenvironment Through Cholinergic Signaling in Pancreatic Ductal Adenocarcinoma. *Cancer Res* (2020) 80(10):1991–2003. doi: 10.1158/0008-5472.CAN-19-2689

Conflict of Interest: The authors declare that the research was conducted in the absence of any commercial or financial relationships that could be construed as a potential conflict of interest.

Publisher's Note: All claims expressed in this article are solely those of the authors and do not necessarily represent those of their affiliated organizations, or those of the publisher, the editors and the reviewers. Any product that may be evaluated in this article, or claim that may be made by its manufacturer, is not guaranteed or endorsed by the publisher.

Copyright © 2022 Ahn, Hinds, Kolb, Reisenauer, Soon, Sepahdari, Bollin and Park. This is an open-access article distributed under the terms of the Creative Commons Attribution License (CC BY). The use, distribution or reproduction in other forums is permitted, provided the original author(s) and the copyright owner(s) are credited and that the original publication in this journal is cited, in accordance with accepted academic practice. No use, distribution or reproduction is permitted which does not comply with these terms.

frontiers | Frontiers in Oncology

CASE REPORT
published: 10 June 2022
doi: 10.3389/fonc.2022.846187

Circulating Tumor DNA Testing Supports Rapid Therapeutic Decision-Making in Metastatic Melanoma: A Case Report

*Tapas Ranjan Behera[1], Jung Min Song[1], Jennifer Ko[2], Donald Eicher[1], Joshua Arbesman[3], Brian Gastman[1], Daniel H. Farkas[4] and Pauline Funchain[1]**

[1] Taussig Cancer Institute, Cleveland Clinic, Cleveland, OH, United States, [2] Anatomic Pathology, Cleveland Clinic, Cleveland, OH, United States, [3] Dermatology & Plastic Surgery Institute, Cleveland Clinic, Cleveland, OH, United States, [4] Pathology and Laboratory Medicine Institute, Cleveland Clinic, Cleveland, OH, United States

Treatment of metastatic melanoma includes the option of targeted therapy in patients with driver *BRAF* mutations. BRAF-MEK inhibitor drugs improve survival in the approximately 50% of patients with melanoma that harbor *BRAF* mutations. As *BRAF* mutation detection in tissue often takes days to weeks, it is not always possible or timely to obtain *BRAF* status in tissue using immunohistochemistry or next generation sequencing. Plasma-derived circulating tumor DNA (ctDNA) is a potential alternative analyte in such treatment settings. We present a case of metastatic melanoma that was treated in an emergent setting using therapy supported by rapid PCR-based detection of ctDNA positive for a *BRAF* V600 mutation. In this rapidly deteriorating 53-year-old male with diffuse melanoma metastases and unknown *BRAF* mutation status requiring hospital admission, a plasma-based *BRAF* mutation detection supported treatment with targeted therapy, dabrafenib and trametinib. Same-day initiation of therapy resulted in swift amelioration allowing discharge within a week, followed by substantial clinical improvement over the following weeks. In cases requiring urgent clinical decision making, a plasma-based, near point-of-care detection system is useful in supporting targeted therapy decisions without the need for invasive and time-consuming biopsy.

Keywords: Rapid ctDNA test, ctDNA, *BRAF* mutation, rt-PCR, targeted therapy, melanoma

OPEN ACCESS

Edited by:
Sapna Patel, University of Texas MD Anderson Cancer Center, United States

Reviewed by:
Rodabe N. Amaria, University of Texas MD Anderson Cancer Center, United States
Stefano Calvieri, Sapienza University of Rome, Italy

***Correspondence:**
Pauline Funchain
funchap@ccf.org

Specialty section:
This article was submitted to Skin Cancer, a section of the journal Frontiers in Oncology

Received: *30 December 2021*
Accepted: *10 May 2022*
Published: *10 June 2022*

Citation:
Behera TR, Song JM, Ko J, Eicher D, Arbesman J, Gastman B, Farkas DH and Funchain P (2022) Circulating Tumor DNA Testing Supports Rapid Therapeutic Decision-Making in Metastatic Melanoma: A Case Report. Front. Oncol. 12:846187. doi: 10.3389/fonc.2022.846187

INTRODUCTION

Circulating tumor DNA (ctDNA) is a useful disease monitoring analyte in many cancers (1). Diagnosing cancer from evaluation of ctDNA has been reported in lung and trophoblastic tumors (2–4). Generally, definitive diagnosis employs early imaging-based identification and/or specific laboratory testing, or pathology investigation. ctDNA evaluation is not usually employed diagnostically. Furthermore, since ctDNA tends to appear in detectable levels in the peripheral blood in advanced disease, the utility of ctDNA for impactful characterization in advanced cancer is

Abbreviations: ICI, immune checkpoint inhibitor; PD-1, programmed cell death-1; PET-CT, positron emission tomography-CT.

clinically attractive, especially when detection of specific markers can affect therapy choice and thus clinical outcome.

Melanoma is a rapidly progressive cancer that, when detected at advanced stages, limits the efficacy of available treatment options. The identification of *BRAF* mutation status in melanoma offers the option for specific targeted therapy agents. Specifically, the combination of BRAF and MEK inhibitors in melanoma are highly effective in improving survival and often precipitate rapid symptom resolution (5). Typically, surgical resection of melanoma for histopathological diagnosis generates a specimen for evaluation of *BRAF* mutation status by tissue immunohistochemistry (IHC) or molecular diagnostic techniques, which is accomplished by next generation sequencing (NGS). Tissue-based *BRAF* detection may take days to weeks, depending on an institution's capabilities and whether tests are typically "sent out" to a reference laboratory. In patients where the primary site is occult, and sites of metastases are not accessible for tissue sampling, *BRAF* mutation status may be difficult to obtain and/or remain unknown. In advanced melanoma, ctDNA is generally higher in concentration compared to earlier stages (6). For patients needing urgent *BRAF* status evaluation to aid clinical decision-making regarding therapy choice(s), a PCR-based, near-point of care, rapid testing platform could be useful to detect *BRAF* variants in plasma-derived ctDNA (7).

CASE PRESENTATION

A 53-year-old male presented to an outside hospital with a three-week history of nausea, vomiting, and jaundice. On admission, he complained of abdominal discomfort, back pain, jaundice, and dark urine. He was afebrile, normotensive, with non-cholangitic pain. The patient was admitted for severe jaundice in face of a suspected metastatic process. On admission, creatinine was 1.38, and LFTs were elevated; total bilirubin was 21.9, ALP 359, ALT 211, AST 202, lipase normal, lactate 2.7 (**Table 1**). Chest X-ray redemonstrated a previously identified chest nodule of 3.5 x 2.5 cm in the mid to lower left lung without any consolidation or effusion. An abdominal radiograph did not show dilated bowel loops. CT scan of the abdomen identified widespread metastatic disease in the liver, a 2.5 cm renal mass in left lower pole, and a non-specific sclerotic focus in the right ileum (**Figure 2**). CT scan of the chest identified a lingular mass (**Figure 3**), bilateral pulmonary nodules, and a destructive lesion in the T3 vertebral body. Pathologic review of a liver biopsy from an outside hospital revealed metastatic melanoma. An MRI of the brain was negative for intracranial or leptomeningeal metastases. Due to the need for rapid assessment of BRAF status for therapeutic decision making, the patient underwent another liver biopsy for evaluation of *BRAF* mutation status. Simultaneously, a plasma sample was tested for ctDNA *BRAF* mutation status.

The plasma sample tested positive for ctDNA-based *BRAF*. Supported by this ctDNA finding, BRAF/MEK inhibitors, dabrafenib and trametinib, were initiated. Patient lab values improved within two weeks of treatment initiation; bilirubin levels decreased from 21.3 to 7.8 mg/dL. The patient's clinical condition improved and he was discharged from the hospital within a week of admission. The patient's treatment events during admission are represented in **Figure 1** (circle).

CT scans of the abdomen/pelvis and chest showed significant response to the therapy as shown in **Figures 2** and **3**. The imaging on day 104, compared to that of day one, demonstrated decreased size and number of innumerable hepatic masses. For example, a 1.6 x 1.3 cm right dome lesion, previously measured 5.1 x 4.0 cm. Lymph node sizes also decreased; left periaortic node from 1.7 x 1.2 to 1.4 x 0.8 cm; aortocaval node from 1.4 x 1.3 to 1.2 x 1.0 cm; and caval node from 1.8 x 1.5 to 1.9 x 1.3 cm. The sizes of the peritoneal implants also decreased from 1.5 x 1.1 cm to 1.2 x 0.7 cm. Chest imaging showed significant decreases in size and number of multiple scattered bilateral pulmonary nodules, suggestive of metastatic disease with favorable treatment response.

Serial ctDNA-based variant levels were assessed over time and remained consistently detectable. Three months after the initial admission, an MRI scan of the brain demonstrated multiple small lesions of the bilateral frontal lobes and left occipital lobe. Radiation therapy was initiated but the patient's condition deteriorated when multiple hemorrhagic metastases developed seven weeks after initial metastasis detection. The patient was initially intubated, and compassionately extubated when no medical options for improvement remained.

DISCUSSION

This is, to our knowledge, the first reported case where the clinical decision for treatment in melanoma was supported by the result of rapid ctDNA-based *BRAF* variant identification. The case demonstrates the impact rapid ctDNA-based variant

TABLE 1 | Patient laboratory values pre-treatment at admission (day 0) and post-treatment on day 6, 19, and 28.

Laboratory Parameter	DAY 0 admission	Day 6 discharge	Day 19 visit	Day 28 visit
BUN (9-24mg/dl)	50	47	11	13
Creatinine (0.73-1.22 mg/dl)	1.38	1.20	0.87	0.92
Bilirubin, Total (0.2-1.3 mg/dl)	21.9	21.3	7.8	5.1
Alkaline Phos. (38-113 U/l)	359	315	324	278
ALT (10-54 U/l)	211	158	64	36
AST (14-40 U/l)	202	142	69	46
Anion Gap (9-18 mmol/l)	15	11	5	9
LD (135-225 U/l)		2667 (on day 4)	1179	840 (on day 32)

Treatment with BRAF MEK inhibitors was initiated on day 5 from hospital admission.

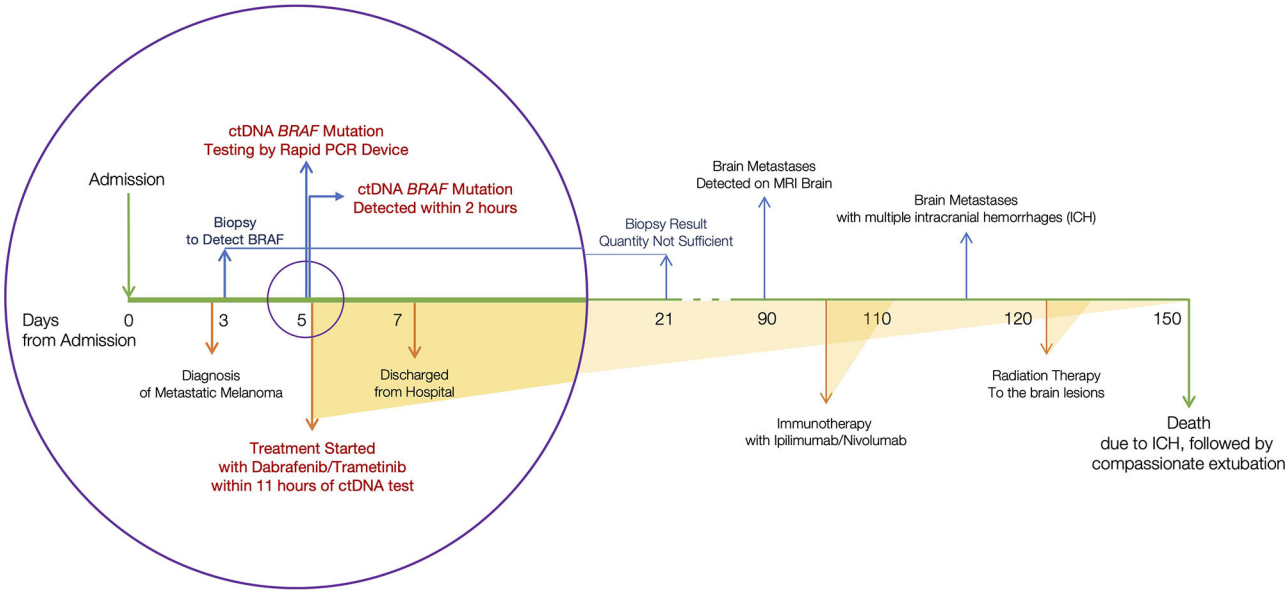


FIGURE 1 | Timeline of clinical events. Considering the day of admission as day 0, ctDNA *BRAF* variant was identified on day 5. Therapy was initiated the same day.

detection can make when a tissue biopsy is not available or when awaiting biopsy results can lead to treatment delay, particularly in a quickly declining, admitted patient. Combination BRAF/MEK inhibitors can result in very rapid amelioration of a patient's clinical condition. Immediate onset of positive drug effects can be seen in some clinical situations, thus, having access to a rapid test for *BRAF* variants in melanoma can dramatically affect time to treatment initiation, an important variable in progression-free and overall survival (8).

Tumor biopsy is the conventional source of tissue for *BRAF* variant interrogation in melanoma. Next Generation Sequencing (NGS) performed on the biopsy tissue is the gold standard for detecting BRAF mutation in patients diagnosed with melanoma. Tissue immunohistochemistry (IHC) is a sensitive and relatively

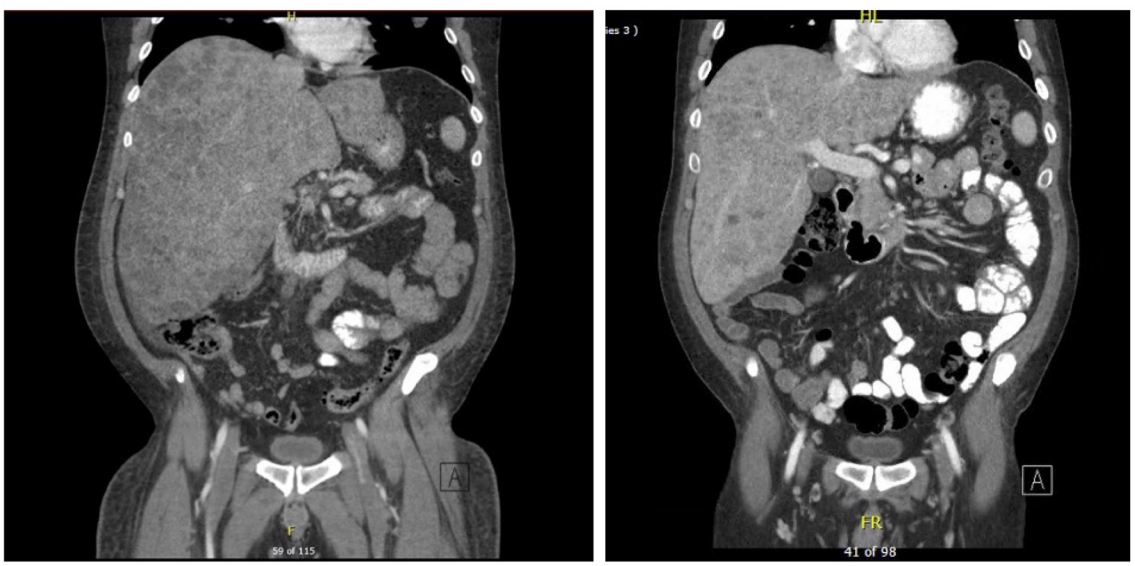


FIGURE 2 | CT scan of abdomen showing innumerable lesions throughout the liver consistent with metastatic disease on day 1 on the left vs day 104 on the right with improved lesion sizes.

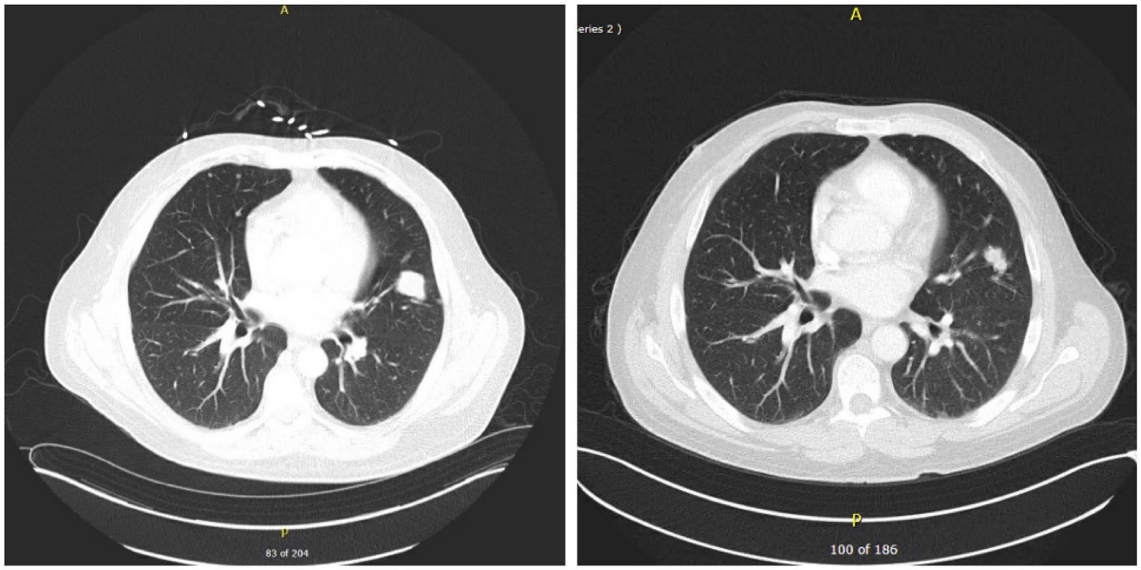


FIGURE 3 | CT scan of chest showing dominant lingular mass concerning for primary lung cancer or metastatic lesion. Multiple bilateral small pulmonary nodules and T3 vertebral body destructive lesion seen concerning for metastatic disease on day 1 on the left vs on day 104 on the right showing decrease in sizes and numbers of pulmonary nodules suggestive of favorable treatment response.

quicker alternative routinely employed to identify the presence of BRAF V600E mutations (9). While NGS and IHC rely on availability of biopsy tissue, a liquid biopsy, *i.e.*, examination of ctDNA in plasma specimens, may serve as an alternative when tissue specimens cannot be obtained, or when insufficient tumor tissue is available. Furthermore, liquid biopsy could provide a result in as early as an hour compared to days to weeks in tests employing NGS or IHC. In this case, we showed that liquid biopsy was useful when treatment decisions must be made quickly. It can take days to get relevant NGS or immunohistochemistry results, depending on laboratory case load, "send-out" logistics, etc. In this case, a real-time PCR-based, automated testing device (Idylla; Biocartis, Belgium) was employed to detect *BRAF* variants in plasma-derived ctDNA (10). The test requires very little sample input and minimal technical demand; one mL of plasma is introduced into a testing cartridge which is inserted into the instrument. The assay is semi-quantitative in nature; positive results are based on a minimum detectable variant threshold level. Test results are binary – positive or negative; V600E, V600E2, and V600D are simultaneously interrogated and not differentiated in the analysis. From the time blood reaches the lab, results are generated in ~90 minutes, thus clinical decisions requiring BRAF status may be made within hours.

As was the case with this patient, the clinical decision on the ability to use the preferred early therapeutic, ie, BRAF/MEK inhibition, was dependent on rapid acquisition of the patient's *BRAF* mutation status. Delay in identifying the presence of the relevant targetable variant would compel the clinician to choose the targetable therapy based on clinical judgement alone, as initiating conventional immunotherapy is in many cases financially impossible for admitted patients. Recent evidence from the DREAMseq trial, a phase III trial to compare the efficacy and toxicity of the sequence of ipilimumab/nivolumab (Ipi/Nivo) followed by dabrafenib/trametinib (Dab/Tram) to the converse sequence in treatment-naive BRAFV600-mutant patients with ECOG performance status 0 or 1 suggests that the treatment sequence beginning with the combination of Ipi/Nivo results in superior OS (11). The treatment decision made in this case predates the outcomes of the above trial to advocate beginning of treatment sequence with Ipi/Nivo followed by Dab/Tram. It is not clear from the DREAMseq data, which did not accrue patients of poor performance status, if the same survival benefit would be seen in a critically ill hospitalized patient with a immunotherapy first approach. In many centers there are administrative and financial obstacles to starting Ipi/Nivo in an inpatient setting. Given the clinical deterioration of the patient, early initiation of therapy was prudent. ctDNA-based detection of *BRAF* mutant status supported the decision to initiate targeted therapy with dabrafenib and trametinib. Of note, the patient also underwent an inpatient biopsy procedure on the same day as the peripheral blood sample for ctDNA testing was drawn. After 16 days, *BRAF* variant identification was indeterminate due to insufficient tumor in the liver biopsy. Ultimately, the ctDNA result was the only modality available to support the treatment decision, which allowed patient discharge and marked clinical improvement over the next 100 days.

Further, ctDNA-based *BRAF* variant detection has been reported to be a prognostic marker in patients with brain metastasis (12). Persistent, detectable *BRAF* variant in the patient's plasma supported subsequent further imaging that

revealed brain metastases three months after admission. The detection of new brain metastases precipitated initiation of immunotherapy with ipilimumab and nivolumab.

In conclusion, a rapid real-time PCR-based evaluation of peripheral blood could serve as a non-invasive, rapid tool to aid prompt treatment decision making in advanced melanoma in emergent situations where BRAF mutation detection utilizing NGS or IHC of the biopsy tissue is not feasible or could potentially delay clinical decision making.

DATA AVAILABILITY STATEMENT

The original contributions presented in the study are included in the article/supplementary material. Further inquiries can be directed to the corresponding author.

ETHICS STATEMENT

The studies involving human participants were reviewed and approved by Cleveland Clinic ethics committee. Written informed consent was obtained from the next of kin for the publication of any potentially identifiable images or data included in this article.

AUTHOR CONTRIBUTIONS

TB, JS, JK, DE, JA, BG, DF and PF contributed to conception and writing, DF and PF contributed to finalize the manuscript. All authors approved the submitted version.

FUNDING

This work and TB were partially supported by Gross Family Melanoma Registry.

ACKNOWLEDGMENTS

The authors are pleased to thank Biocartis for providing test equipment and reagents.

REFERENCES

1. Pessoa LS, Heringer M, Ferrer VP. ctDNA as a Cancer Biomarker: A Broad Overview. *Crit Rev Oncol Hemat* (2020) 155:103109. doi: 10.1016/j.critrevonc.2020.103109
2. Qian C, Dai N, Xu M, Luo H, Feng Y, Zhang M, et al. ctDNA Facilitated the Diagnosis of a Patient With Synchronous Urothelial Carcinoma and Non-Small Cell Lung Cancer: Case Report. *Ann Transl Med* (2020) 8:1323. doi: 10.21037/atm-20-6552
3. Openshaw MR, Harvey RA, Sebire NJ, Kaur B, Sarwar N, Seckl MJ, et al. Circulating Cell Free DNA in the Diagnosis of Trophoblastic Tumors. *Ebiomedicine* (2016) 4:146–52. doi: 10.1016/j.ebiom.2015.12.022
4. Dharajiya NG, Grosu DS, Farkas DH, McCullough RM, Almasri E, Sun Y, et al. Incidental Detection of Maternal Neoplasia in Noninvasive Prenatal Testing. *Clin Chem* (2018) 64:329–35. doi: 10.1373/clinchem.2017.277517
5. Khan M, Zheng T, Zhao Z, Arooj S, Liao G. Efficacy of BRAF Inhibitors in Combination With Stereotactic Radiosurgery for the Treatment of Melanoma Brain Metastases: A Systematic Review and Meta-Analysis. *Front Oncol* (2021) 10:586029. doi: 10.3389/fonc.2020.586029
6. Marczynski GT, Laus AC, dos Reis MB, Reis RM, de L Vazquez V. Circulating Tumor DNA (ctDNA) Detection Is Associated With Shorter Progression-Free Survival in Advanced Melanoma Patients. *Sci Rep UK* (2020) 10:18682. doi: 10.1038/s41598-020-75792-1
7. Uguen A, Troncone G. A Review on the Idylla Platform: Towards the Assessment of Actionable Genomic Alterations in One Day. *J Clin Pathol* (2018) 71:757. doi: 10.1136/jclinpath-2018-205189
8. Khorana AA, Tullio K, Elson P, Pennell NA, Grobmyer SR, Kalady MF, et al. Time to Initial Cancer Treatment in the United States and Association With Survival Over Time: An Observational Study. *PloS One* (2019) 14:e0213209. doi: 10.1371/journal.pone.0213209
9. Long GV, Wilmott JS, Capper D, Preusser M, Zhang YE, Thompson JF, et al. Immunohistochemistry Is Highly Sensitive and Specific for the Detection of V600E BRAF Mutation in Melanoma. *Am J Surg Pathol* (2013) 37:61–5. doi: 10.1097/PAS.0b013e31826485c0
10. Bisschop C, Elst At, Bosman LJ, Platteel I, Jalving M, Berg Avd. Rapid BRAF Mutation Tests in Patients With Advanced Melanoma. *Melanoma Res* (2018) 28:96–104. doi: 10.1097/CMR.0000000000000421
11. Atkins MB, Lee SJ, Chmielowski B, Ribas A, Tarhini AA, Truong T-G, et al. DREAMseq (Doublet, Randomized Evaluation in Advanced Melanoma Sequencing): A Phase III Trial—ECOG-ACRIN Ea6134. *J Clin Oncol* (2021) 39:356154–4. doi: 10.1200/JCO.2021.39.36_suppl.356154
12. Behera TR, Song JM, Eicher DM, Gastman B, Farkas DH, Funchain P, et al. Circulating Tumor DNA Mutation as a Prognostic Marker in Melanoma With Brain Metastasis. *J Clin Oncol* (2021) 39:e21560–0. doi: 10.1200/JCO.2021.39.15_suppl.e21560

Conflict of Interest: The authors declare that the research was conducted in the absence of any commercial or financial relationships that could be construed as a potential conflict of interest.

Publisher's Note: All claims expressed in this article are solely those of the authors and do not necessarily represent those of their affiliated organizations, or those of the publisher, the editors and the reviewers. Any product that may be evaluated in this article, or claim that may be made by its manufacturer, is not guaranteed or endorsed by the publisher.

Copyright © 2022 Behera, Song, Ko, Eicher, Arbesman, Gastman, Farkas and Funchain. This is an open-access article distributed under the terms of the Creative Commons Attribution License (CC BY). The use, distribution or reproduction in other forums is permitted, provided the original author(s) and the copyright owner(s) are credited and that the original publication in this journal is cited, in accordance with accepted academic practice. No use, distribution or reproduction is permitted which does not comply with these terms.

frontiers | Frontiers in Oncology

TYPE Brief Research Report
PUBLISHED 23 September 2022
DOI 10.3389/fonc.2022.855794

Check for updates

OPEN ACCESS

EDITED BY
Sapna Patel,
University of Texas MD Anderson Cancer Center, United States

REVIEWED BY
Lucy Kennedy,
Cleveland Clinic, United States
Sunil Reddy,
Stanford University, United States

*CORRESPONDENCE
Leslie A. Fecher
lfecher@med.umich.edu

†These authors have contributed equally to this work

SPECIALTY SECTION
This article was submitted to Skin Cancer, a section of the journal Frontiers in Oncology

RECEIVED 16 January 2022
ACCEPTED 16 August 2022
PUBLISHED 23 September 2022

CITATION
Homan M, Warrier G, Lao CD, Yentz S, Kraft S and Fecher LA (2022) Treatment related toxicities with combination BRAF and MEK inhibitor therapy in resected stage III melanoma.
Front. Oncol. 12:855794.
doi: 10.3389/fonc.2022.855794

COPYRIGHT
© 2022 Homan, Warrier, Lao, Yentz, Kraft and Fecher. This is an open-access article distributed under the terms of the Creative Commons Attribution License (CC BY). The use, distribution or reproduction in other forums is permitted, provided the original author(s) and the copyright owner(s) are credited and that the original publication in this journal is cited, in accordance with accepted academic practice. No use, distribution or reproduction is permitted which does not comply with these terms.

Treatment related toxicities with combination BRAF and MEK inhibitor therapy in resected stage III melanoma

Morgan Homan[1†], Govind Warrier[2†], Christopher D. Lao[3], Sarah Yentz[2], Shawna Kraft[1] and Leslie A. Fecher[3*]

[1]Department of Pharmacy, University of Michigan, Ann Arbor, MI, United States, [2]Department of Internal Medicine, University of Michigan, Ann Arbor, MI, United States, [3]Department of Internal Medicine and Dermatology, University of Michigan, Ann Arbor, MI, United States

Combination dabrafenib (D) and trametinib (T) is an FDA approved adjuvant therapy for patients with resected stage III BRAF-mutant melanoma. We describe treatment-related toxicities with adjuvant D+T in a real-world population through a retrospective case series. The primary endpoint was development of toxicities.

Results: Eighteen of the 20 patients (90%) required at least one treatment interruption due to adverse events (AEs), 11 patients (55%) required a dose reduction and 13 (65%) permanently discontinued therapy due to an AE. The nine patients who did not require dose reduction had been initiated on a lower starting dose of dabrafenib. The most common treatment-limiting AEs were recurrent pyrexia and chills (85%) and liver laboratory abnormalities (50%). The median total time on therapy was 148.5 days (range 19-383), 40.7% (range 5.2-100%) of the intended one-year duration.

Conclusion: Adjuvant treatment of melanoma with combination D+T is associated with treatment-limiting toxicities in the majority of this patient group. Patients should be carefully monitored throughout therapy.

KEYWORDS

BRAF, MEK, melanoma, pyrexia, toxicity, inhibitor

Introduction

Invasive melanoma represents approximately 1% of all skin cancers but accounts for the majority of skin cancer related deaths. For localized melanoma, surgical resection alone has been the standard of care with high 5-year melanoma specific survival rates for early stages. Patients with stage II and III disease are at higher risk for recurrence after

resection with some cases progressing to metastatic melanoma. 5-year survival rates for melanoma metastatic regionally and distantly are 66% and 27%, respectively (1).

In melanoma, mutations in BRAF are found in approximately 40% of cases and result in constitutive activation of the MAPK pathway (2). Mutant BRAF, and downstream kinase protein MEK, have proved viable targets for melanoma therapies. Three combinations of inhibitors of mutant BRAF and MEK have been approved by the FDA for treatment of advanced unresectable melanoma (3).

A study of adjuvant combination therapy with BRAF inhibitor, dabrafenib, and MEK inhibitor, trametinib, in patients with resected stage III BRAF V600E/K-mutant melanoma showed improved recurrence free survival benefit at 3 years with overall survival rate of 86% compared to 77% with placebo. This study was published in September 2017 and led to FDA approval in April 2018. The difference in 3 year overall survival was not considered statistically significant as it did not cross the prespecified interim analysis boundary of P=0.000019 for significance (4, 5). In the aforementioned study, adverse events led to dose interruption in 66% of patients, dose reduction in 38% of patients, and permanent discontinuation of therapy in 26% of patients. Common adverse events include fevers and chills, with any grade reported in 63% of patients. These data are greater than that reported in the metastatic setting (3). Subsequent analyses suggest the rate of adverse events decreased with increased duration of therapy (6, 7). Adjuvant therapy with dabrafenib and trametinib has an intended duration of one year (4, 5).

Here we present a retrospective case series of patients with resected stage III melanoma treated with adjuvant BRAF and MEK inhibition with the purpose of describing toxicities in a real-world population.

Methods

We reviewed medical records of patients treated at a single center with resected stage III melanoma who started treatment with adjuvant dabrafenib and trametinib by three independent academic medical oncologists between November 2017 and December 2019. Planned treatment was for a total of 1 year of dabrafenib and trametinib with full doses being dabrafenib 150 mg twice daily and trametinib 2 mg daily. Primary endpoint was development of toxicities. Using REDCap Data Management software, baseline patient characteristics were collected in addition to secondary endpoints including number of treatment interruptions, dose reductions, and total time on combination therapy. The study was performed according to a protocol approved by the institutional review board at the University of Michigan.

Results

Patient characteristics

Twenty patients were treated with adjuvant dabrafenib and trametinib during the study period (Supplementary Appendix 1). Stage at the time of initiation of adjuvant therapy is reported; in the event of relapse, this incorporates pathology from both the initial presentation and at relapse.

Individual patient treatment courses

Table 1 reviews the adjuvant treatment course for each patient. Eighteen patients (90%) required at least one treatment interruption due to adverse events. Fifteen patients required two or more interruptions (mean = 2). The median time to first interruption was 30.5 days (range 3-94 days). Eleven patients required a dose reduction, with median time to first reduction of 40 days (range 8-138 days). The nine patients who did not require a dose reduction had all been initiated on a lower dose of dabrafenib (75 mg BID) due to physician experience with toxicities in prior patients. Fourteen patients were started at a reduced dabrafenib dose of 75 mg twice daily. All patients except two patients were started on full dose of trametinib (2 mg daily). Patients were evaluated for uptitration of doses throughout their yearlong course. While no specific criteria for uptitration were used, if patients had good tolerance of current doses without recent need for holding or dose reduction, an increase in dose was considered. Five patients were uptitrated, two to the full dose of dabrafenib (150mg twice daily). Side effects prevented uptitration in the remaining nine patients. Additionally, two of the patients who were started at a lower dose of dabrafenib also required dose reduction of trametinib (0.5 mg once daily for one patient and 2 mg every other day for another patient). All patients have either completed or discontinued therapy.

Adverse events

The adverse events experienced by our patients are compared to phase III trial toxicity data in Table 2. Recurrent pyrexia and chills occurred in 17 patients (85%) and was the primary reason for treatment discontinuation in nine patients (45%). Ten patients (50%) experienced liver laboratory elevations, with median maximum values for the first reporting were AST of 81 (range: 44-550 IU/L), ALT of 95 (range: 27-470 IU/L), and alkaline phosphatase of 150 (range: 102-544 IU/L). This contributed to discontinuation in five patients (25%).

TABLE 1 Treatment summaries.

Pt	Age	Sex	Stage, AJCC 8th ed.	Starting Dabrafenib (D) Dose	Starting Trametinib (T) Dose	Max tolerated dose (D,T)[a]	Total time (days) on combination therapy	Percentage of time on intended therapy[b]	Time (days) to first hold	Time (days) to first dose reduction	Reason for discontinuation	Relapse after adjuvant theraphy	Days to Relapse[h]	Current Status; treatment
1	54	F	IIIC	150 mg BID	2 mg daily	150 mg BID, 2 mg daily	85	23.2%	27	32	pyrexia, chills, elevated liver labs	No	N/A	NED/Obs
2	40	M	IIIC	150 mg BID	2 mg daily	75 mg BID, 2 mg daily	40	11%	3	8	pyrexia, chills, elevated liver labs	unknown	N/A	Lost to follow up
3	40	F	IIIC	150 mg BID	2 mg daily	75 mg BID, 2 mg daily	57	15.6%	13	15	pyrexia, chills, elevated liver labs	No	N/A	Ned/Obs
4	73	F	IIIC	75 mg BID	2 mg daily	75 mg BID, 2 mg daily	67	18.4%	49	N/A	pyrexia, chills, demand ischemia[c]	Yes -In scar and LN	550	Additional relapse, Systemic treatment
5	62	F	IIIB	75 mg BID	2 mg daily	75 mg BID, 2 mg daily	333	91.2%	49	62	Recurrent URI requiring holds-attributed to tobacco/ pulmonary status	Yes -lung	427	Systemic therapy
6	50	F	IIIB	75 mg BID	2 mg daily	150 mg qam 75 mg qpm, 2 mg daily	184	50.4%	18	22	decrease in RV function[d]	No	N/A	NED/Obs
7	64	M	IIIC	75 mg BID	2 mg daily	75 mg BID, 2 mg daily	38	10.4%	9	N/A	Poor tolerance, patient preference, dilated right atrium[e]	No	N/A	NED/Obs
8	68	F	IIIB	150 mg BID	2 mg daily	Not reached	19	5.2%	5	10	pyrexia, chills, elevated liver labs, thrombocytopenia, arthralgias	No	N/A	NED/Obs
9	58	M	IIIC	150 mg BID	2 mg daily	150 mg qam 75 mg qhs, 2 mg daily	365	100%	55	67	Completed course	Yes brain	28	DOD
10	46	M	IIIC	75 mg BID	2 mg daily	150 mg qam 75 mg qhs, 2 mg daily	366	100%	29	40	Completed course	Yes -lung and LNs	142	Systemic therapy
11	32	F	IIIA	75 mg BID	2 mg daily	75 mg BID, 2 mg daily	64	17.5%	37	N/A	pyrexia, diarrhea, abdominal pain	Yes -LN	444	NED; s/p systemic therapy and surgery
12	29	M	IIIC	75 mg BID	2 mg daily	150 mg qam 75 mg qhs, 2 mg daily	373	100%	62	N/A	Compled course	No	N/A	NED/Obs
13[f]	43	M	IIIC	75 mg BID	2 mg QOD	75 mg BID, 2 mg QOD	50	13.7%	26	49	Pyrexia, chills	No	N/A	NED/Obs
14	21	F	IIIC	75 mg BID	2 mg QOD	75 mg BID, 2 mg QOD	113	31%	25	N/A	Pyrexia, chills	No	N/A	NED/Obs

(Continued)

10.3389/fonc.2022.855794

TABLE 1 Continued

Pt	Age	Sex	Stage, AJCC 8th ed.	Starting Dabrafenib (D) Dose	Starting Trametinib (T) Dose	Max tolerated dose (D,T)[a]	Total time (days) on combination therapy	Percentage of time on intended therapy[b]	Time (days) to first hold	Time (days) to first dose reduction	Reason for discontinuation	Relapse after adjuvant theraphy	Days to Relapse[h]	Current Status; treatment
15	47	M	IIIB	75 mg BID	2 mg daily	75 mg BID, 2 mg daily	32	8.8%	32	N/A	RA and RV dilation dizziness, nausea, fatigue	No	N/A	NED/Obs
16[f]	62	M	IIID	75 mg BID	2 mg daily	150 mg BID, 2 mg daily	195	53.4%	N/A	N/A	Disease progression	Disease progression	N/A	s/p Systemic therapy/ CR
17	34	IIIC	M	75 mg BID	2 mg daily	150 mg BID, 2 mg daily	377	100%	N/A	N/A	Completed course; simultaneous relapse	Yes -local	N/A	Systemic treatment for additional relapse
18	38	F	IIIB	150 mg BID	2 mg daily	150 mg BID, 2 mg daily	363	99.4%	94	115	Completed course	No	N/A	NED/Obs
19	40	M	IIIC	75 mg BID	2 mg daily	75 mg BID, 2 mg daily	352[g]	96.4%	38	N/A	Pyrexia, chills, elevated liver labs	Yes -brain	1167	Surgery, radiation, systemic therapy
20	40	M	IIIA	75 mg BID	2 mg QOD	75 mg BID, 2 mg QOD	383	100%	60	138	Completed course	No	N/A	NED/Obs

Patients 3,4,7,9,17,18,19, and 20 did not have CLND.

N/A, Not Applicable.

[a]Max tolerated dose: Stable on dose for 14 days without adverse events.

[b]Intended therapy: one year of combination therapy at any doses; Percentage of time on intended therapy: number of days on combination therapy out of 365 days 100% is maximum.

[c]Demand ischemia secondary to pyrexia and chills.

[d]RV function normalized on repeat imaging off medication.

[e]Initial determination of right atrium dilation was found to be unchanged from baseline after review by a second provider.

BID, twice daily; NED, no evidence of disease; Obs., close observation; D + T, dabrafenib and trametinib; RA, right atria; RV, right ventricle.

[f]Received adjuvant radiation.

[g]includes 45 day hold required for elevated liver enzymes.

[h]Days to relapse = time relapse first occurred from day of last dose of adjuvant therapy.

10.3389/fonc.2022.855794

TABLE 2 Select adverse events.

	Long et al. (4)		Study population		
	N = 435		N = 20		
	Patients, n (%)				
Adverse Event	**Total (Any Grade)**	**Grade 3-4**	**Total (Any Grade)**	**Grade 1-2**	**Grade 3-4**
Liver laboratory Abnormalities	ALT: 67 (15%) AST: 63 (14%)	16 (4%)	10 (50%)	8 (40%)	2 (10%)
Pyrexia	273 (63%)	23 (5%)	17 (85%)	16 (80%)	1 (5%)[a]
Chills/Rigors	161 (37%)	6 (1%)	17 (85%)	17 (85%)	0
Nausea	172 (40%)	4 (1%)	12 (60%)	12 (60%)	0
Arthralgias	120 (28%)	4 (1%)	9 (45%)	9 (45%)	0
Rash	106 (24%)	0	9 (45%)[b]	9 (45%)	0
Vomiting	122 (28%)	4 (1%)	4 (20%)	4 (20%)	0
Cardiac abnormalities	Not reported	Not reported	4 (20%)	4 (20%)	0
Vision complaint	Not reported	Not reported	1 (5%)[c]	1 (5%)	0

Grading with CTCAE v5.0 where applicable.
[a]Grade 3 pyrexia = >40°C.
[b]Including panniculitis vs. erythema nodosum and maculopapular rash.
[c]Patient described vision change as an inability to see the end of a word during the process of reading because the word"looked bright". Similar concerns were not subsequently described.

Ten patients (50%) had a hospitalization, ED visit, or oncology urgent care visit during their treatment course. Initial visits in seven patients (35%) were for pyrexia, ultimately attributed to treatment. Four patients (20%) had two or more visits, two for liver laboratory abnormalities, which were not associated with acetaminophen, statin use, or alcohol. All presentations were potentially related to treatment.

Discussion

Our study offers a novel examination of a real-world population with resected stage III melanoma treated with adjuvant combination BRAF and MEK inhibition. In our experience, adjuvant combination BRAF and MEK inhibition was associated with clinically significant treatment related toxicities with the rate of adverse events exceeding what has been reported in the literature. Specifically, in the COMBI-AD trial, fevers and chills of all grades occurred in 63% of patients. Dose interruption in 66% of patients, dose reduction in 38% of patients, and permanent discontinuation of therapy in 26% of patients (4). The median time to onset of pyrexia was 23 days with median duration of 3 days. Of the patients who experienced pyrexia, 72% had recurrence (≥ 2 episodes) (8). Interestingly, there was no difference in patient reported quality of life between those receiving treatment and those receiving placebos.

In our population, 90% of patients experienced adverse effects prompting treatment interruption, 55% required at least one dose reduction, and 65% permanently discontinued therapy due to an adverse event. For the 20 patients who completed or discontinued therapy, the median total time on therapy was 148.5 days, 40.7% of the intended duration. The majority of these patients never tolerated the FDA labeled combination doses.

Our systematic approach to BRAF/MEK therapy includes obtaining baseline labs including complete blood count (CBC), comprehensive metabolic panel (CMP), lactate dehydrogenase (LDH), EKG for QTc assessment, echocardiogram to evaluate cardiac function, ophthalmologic evaluation, and standard cross-sectional imaging to assess disease at baseline. Cardiovascular testing (EKG and echocardiogram) is repeated every 3-6 months or with change in clinical status given potential cardiovascular adverse events (9). History and physical exams with laboratory testing are repeated every 4 weeks, however, additional 2 week appointments have been necessary due to symptoms and lab abnormalities. Specific attention is given to changes in liver labs which have been seen in several patients despite the relative infrequency reported in advanced melanoma patients. It is possible that use of acetaminophen could have contributed to these liver laboratory abnormalities. Combination therapy was initially started at doses of dabrafenib 150 mg BID and trametinib 2 mg daily. High rates of poor tolerance often related to pyrexia and chills leading to need for treatment interruptions, re-evaluations within days and weeks of starting treatment, some emergency department evaluations, as well as multiple dose reductions, and early termination of treatment were frequently observed regardless of disease and/or patient characteristics, or treating physician. This physician group discussed these issues and elected to decrease the starting dose of dabrafenib to 75 mg BID with the intent of minimizing initial treatment related adverse events, minimizing treatment interruptions, with the intent of uptitrating to the goal dose of 150 mg BID. This generally allowed improved

adherence and fewer toxicities although uptitration was not tolerated in most cases.

Recommended management of common side effects with combination BRAF and MEK inhibition has been described in metastatic melanoma and are being used in the adjuvant setting as well (10–12). As in clinical trials, dose interruptions and dose reductions of one or both medications, as well as supportive medications, were used in the management of adverse events. In this patient cohort, premedication for pyrexia/chills with acetaminophen, ibuprofen, or low dose prednisone (n=2) were typically used for recurrent episodes of pyrexia/chills. The majority of patients used both acetaminophen and NSAIDs. This permitted some patients to tolerate the desired dose of therapy. In the two patients who received prednisone 5mg daily, this did not permit tolerance and both discontinued treatment prematurely. To date, eight of the 20 patients have relapsed with only one death. Two of these relapsed on therapy. The impact of dose interruptions and/or dose reductions on outcomes remains to be determined in the adjuvant setting. Data in advanced melanoma have shown inferior outcomes with intermittent dosing of BRAF and MEK combination therapy (13, 14).

There are few other reports of patient groups treated with adjuvant dabrafenib and trametinib. One report of 36 patients had incidences of fevers or chills of all grades of 36% and 2.8%, respectively (15). This group also reported liver adverse events in 11% as well as SAEs in 22.2% and a 'protocol completion rate' of 64.3%. There was no comment on cardiac side effects. Another report of 65 patients reported a discontinuation rate due to treatment related adverse events of only 9% and only one patient stopped treatment due to pyrexia (16). Forty-three patients completed treatment as scheduled. The median time to discontinuation was 9 months. The incidence of chills was very low at 1.5% and of fever at 35.4%. There was no specific comment on liver or cardiac toxicities, nor on dosages or dose reductions or interruptions. It is not known as to the reason for the differences seen in the few papers published on real world experience with dabrafenib/trametinib for melanoma in the adjuvant setting however it is possible that there is a geographical factor. Dabrafenib can cause hemolytic anemia in patients who have G6PD deficiency and it is known that there are geographic differences worldwide in percent of patients who are G6PD deficient (17, 18). While no patients at our institution experienced hemolytic anemia, this is one example of possible geographic differences in medication tolerance.

Oncologists continuously face the difficult task of balancing benefits and toxicities associated with cancer treatment. We report our findings of the side effects of adjuvant combination BRAF and MEK inhibition to demonstrate the frequency and severity of toxicities. Adjuvant combination BRAF and MEK inhibition is an approved treatment for resected stage III melanoma but requires diligent toxicity assessment and management.

Limitations

There were some limitations to our study. First, this study was performed at a single academic center. Second, this study was retrospective and information bias must be considered. Third, practice pattern variation among physicians in dosing, management of toxicities, and decisions to hold therapy or dose reduce is probable.

Conclusions

Our findings indicate that adjuvant combination dabrafenib and trametinib in the treatment of resected stage III melanoma can be associated with treatment limiting toxicities. We support a comprehensive approach to adjuvant treatment including a thorough initial evaluation, close monitoring for toxicities, and prompt interventions with the goal of completing therapy with tolerable adverse events. Additional studies with larger numbers of patients are needed to validate our findings.

Data availability statement

The original contributions presented in the study are included in the article/Supplementary Material. Further inquiries can be directed to the corresponding author.

Ethics statement

The studies involving human participants were reviewed and approved by University of Michigan IRB. Written informed consent for participation was not required for this study in accordance with the national legislation and the institutional requirements.

Author contributions

MH, GW, SK, and LF contributed to conception and design and manuscript drafting. MH, GW, SK and LAF performed data collection. All authors provided substantial contribution to data analysis, editing, and final approval of the manuscript.

Conflict of interest

LF: institutional funding for clinical trials (site PI) from Array/Pfizer, Bristol Myers Squibb, EMD Serono, Kartos. Consultant for Elsevier. Array/Pfizer funding of ECOG-ACRIN clinical trial (national PI) for LAF.

The remaining authors declare that the research was conducted in the absence of any commercial or financial relationships that could be construed as a potential conflict of interest.

Publisher's note

All claims expressed in this article are solely those of the authors and do not necessarily represent those of their affiliated organizations, or those of the publisher, the editors and the reviewers. Any product that may be evaluated in this article, or claim that may be made by its manufacturer, is not guaranteed or endorsed by the publisher.

Supplementary material

The Supplementary Material for this article can be found online at: https://www.frontiersin.org/articles/10.3389/fonc.2022.855794/full#supplementary-material

References

1. *Cancer facts & figures* (2021). Available at: https://www.cancer.org/content/dam/cancer-org/research/cancer-facts-and-statistics/annual-cancer-facts-and-figures/2019/cancer-facts-and-figures-2021.pdf.

2. Davies H, Bignell GR, Cox C, Stephens P, Edkins S, Clegg S, et al. Mutations of the BRAF gene in human cancer. *Nature* (2002) 417(6892):949–54. doi: 10.1038/nature00766

3. Robert C, Grob JJ, Stroyakovskiy D, Karaszewska B, Hauschild A, Levchenko E, et al. Five-year outcomes with dabrafenib plus trametinib in metastatic melanoma. *N Engl J Med* (2019) 381(7):626–36. doi: 10.1056/NEJMoa1904059

4. Long GV, Hauschild A, Santinami M, Atkinson V, Mandalà M, Chiarion-Sileni V, et al. Adjuvant dabrafenib plus trametinib in stage III BRAF-mutated melanoma. *N Engl J Med* (2017) 377(19):1813–23. doi: 10.1056/NEJMoa1708539

5. Hauschild A, Dummer R, Schadendorf D, Santinami M, Atkinson V, Mandalà M, et al. Longer follow-up confirms relapse-free survival benefit with adjuvant dabrafenib plus trametinib in patients with resected BRAF V600-mutant stage III melanoma. *J Clin Oncol* (2018) 36(35):3441–9. doi: 10.1200/JCO.18.01219

6. OncologyPRO. *Adverse events (AEs) over time in patients (pts) treated with adjuvant dabrafenib plus trametinib (D + T) or placebo (Pbo) in the COMBI-AD trial* . Available at: https://oncologypro.esmo.org/Meeting-Resources/ESMO-2018-Congress/Adverse-events-AEs-over-time-in-patients-pts-treated-with-adjuvant-dabrafenib-plus-trametinib-D-T-or-placebo-Pbo-in-the-COMBI-AD-trial (Accessed January 13, 2020). OncologyPRO.

7. OncologyPRO. *Adverse event (AE) kinetics in patients (pts) treated with dabrafenib + trametinib (D + T) in the metastatic and adjuvant setting* . Available at: https://oncologypro.esmo.org/Meeting-Resources/ESMO-2019-Congress/Adverse-event-AE-kinetics-in-patients-pts-treated-with-dabrafenib-trametinib-D-T-in-the-metastatic-and-adjuvant-setting (Accessed January 13, 2020). OncologyPRO.

8. Schadendorf D, Hauschild A, Santinami M, Atkinson V, Mandalà M, Chiarion-Sileni V, et al. Patient reported outcomes in patients with resected, high-risk melanoma with BRAFV600E or BRAFV600K mutations treated with adjuvant dabrafenib plus trametinib (COMBI-AD): a randomized, placebo-controlled, phase 3 trial. *Lancet Oncol* (2019) 20:701–10. doi: 10.1016/S1470-2045(18)30940-9

9. Mincu RI, Mahabadi AA, Michel L, Mrotzek SM, Schadendorf D, Rassaf T, et al. Cardiovascular adverse events associated with BRAF and MEK inhibitors: A systematic review and meta-analysis. *JAMA Netw Open* (2019) 2(8):e198890. doi: 10.1001/jamanetworkopen.2019.8890

10. Chalmers A, Cannon L, Akerley W. Adverse event management in patients with BRAF V600E-mutant non-small cell lung cancer treated with dabrafenib plus trametinib. *Oncologist* (2018) 24(7):963–72. doi: 10.1634/theoncologist.2018-0296

11. Welsh SJ, Corrie PG. Management of BRAF and MEK inhibitor toxicities in patients with metastatic melanoma. *Ther Adv Med Oncol* (2015) 7(2):122–36. doi: 10.1177/1758834014566428

12. Atkinson V, Robert C, Grob JJ, Gogas H, Dutriaux C, Demidov L, et al. Improved pyrexia-related outcomes associated with an adapted pyrexia adverse event management algorithm in patients treated with adjuvant dabrafenib plus trametinib: primary results of COMBI-aplus. *Eur J Cancer* (2022) 163:79–87. doi: 10.1016/j.ejca.2021.12.015

13. Algazi AP, Othus M, Daud AI, Lo RS, Mehnert JM, Truong TG, et al. Continuous versus intermittent BRAF and MEK inhibition in patients with BRAF-mutated melanoma: a randomized phase 2 trial. *Nat Med* (2020) 26(10):1564–8. doi: 10.1038/s41591-020-1060-8

14. Gonzalez-Cao M, Mayo de Las Casas C, Oramas J, Berciano-Guerrero MA, de la Cruz L, Cerezuela P, et al. Intermittent BRAF inhibition in advanced BRAF mutated melanoma results a phase II randomized trial. *Nat Commun* (2021) 12 (1):7008. doi: 10.1038/s41467-021-26572-6

15. Amagai R, Muto Y, Kato H, Matsushita S, Maekawa T, Fukushima S, et al. Retrospective analysis of adjuvant therapy using dabrafenib plus trametinib in Japanese patients with advanced melanoma: analysis of 36 cases. *Mel Res* (2021) 31:575–8. doi: 10.1097/CMR.0000000000000770

16. Manzano JL, Martin-Liberal J, Fernandez-Morales LA, Benitez G, Medina J, Quindos M, et al. Adjuvant dabrafenib plus trametinib (DT) treatment completion in patients with resected melanoma in spain; a retrospecitve observational study (GEM 1901-DESCRIBE-AD). *Ann Oncol* (2021) 32(supp 5):S900–1. 1088P. doi: 10.1016/j.annonc.2021.08.1473

17. Tafinlar. Package insert. *Novartis Pharmceuticals* (2022).

18. Nkhoma ET, Poole C, Vannappagari V, Hall SA, Beutler E. The global prevalence of glucose-6-phosphate dehydrogenase deficiency: a systematic review and meta-analysis. *Blood Cells Mol Dis* (2009) 42(3):267–78. doi: 10.1016/j.bcmd.2008.12.005

Advantages of publishing in Frontiers

OPEN ACCESS
Articles are free to read for greatest visibility and readership

FAST PUBLICATION
Around 90 days from submission to decision

HIGH QUALITY PEER-REVIEW
Rigorous, collaborative, and constructive peer-review

TRANSPARENT PEER-REVIEW
Editors and reviewers acknowledged by name on published articles

Frontiers
Avenue du Tribunal-Fédéral 34
1005 Lausanne | Switzerland

Visit us: www.frontiersin.org
Contact us: frontiersin.org/about/contact

REPRODUCIBILITY OF RESEARCH
Support open data and methods to enhance research reproducibility

DIGITAL PUBLISHING
Articles designed for optimal readership across devices

FOLLOW US
@frontiersin

IMPACT METRICS
Advanced article metrics track visibility across digital media

EXTENSIVE PROMOTION
Marketing and promotion of impactful research

LOOP RESEARCH NETWORK
Our network increases your article's readership